Issue 5 2015 ISSN 2053-9681

TOS forum

Contents

Proceedings of the 7th World Conference on Sampling and Blending

Edited by Kim H. Esbensen and Claas Wagner

Innovative Process Sampling Solutions for the Mining Industry

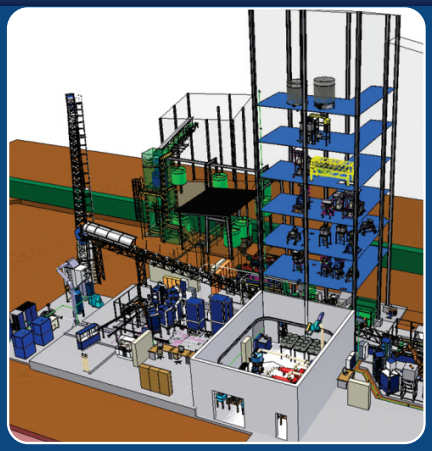

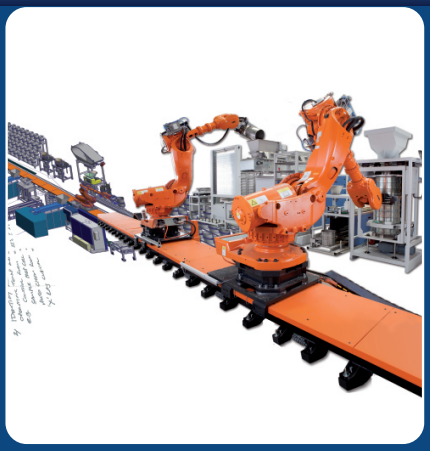

IMP has been providing complete solutions from sampling to analysis for the mining and metallurgical industries since 1987

IMP

Innovative Solutions

doi: 10.1255/tosf.81

Editorial

This issue number 5 of *TOS forum* is dedicated to publishing the Proceedings of the 7th World Conference on Sampling and Blending, WCSB7. The process that ends with the publication in your hands (or on your PC/tablet screen) started at the previous WCSB6 (2013, Lima, Chile) when it was realised that the world economic depression would likely mean that sponsorship would be much more difficult to obtain (something that was an under-estimate as the last two years have proved). So, a radically different strategy for the publication of the proceedings was called for. The present Editor offered to shoulder this responsibility, aiming at a dramatically small, but effective production setup (an editorial staff of two, and IM Publications).

The entire editorial process—abstract submission, grading (naturally this was the job for the full scientific committee) and subsequent ranking of the 56 submissions, peer reviews, revisions, rebuttals, second reviews... ending with 38 finally accepted manuscripts—had to be conducted under severe time pressure due to the 2015 Easter holiday season interacting with an unmerciful vengeance, and was for these reasons very intense. THANK YOU VERY MUCH to Claas Wagner for keeping meticulous order in the organisation of this complex process (from his remote "web post office" in Athens). Most importantly, the Editorial staff extends a very big THANK YOU to ALL the reviewers involved: Francis Pitard, Rolf Steinhaus, Richard Minnitt, Pentti Minkkinen, Stéphane Brochot, Dominique François-Bongarçon, Ana Carolina Chieregati, Claudia Paoletti, the Editors themselves, Simon Dominey, Ralph Holmes. The Editor would like to acknowledge the excellent collaboration with IM Publications. THANK YOU VERY MUCH, Ian, Sara, Katie!

As soon as the conference is over, the WCSB7 Proceedings will be the main lasting physical documentation that will be available to posterity. In this context, we owe a great debt of gratitude to IM Publications for the creative suggestion to publish the proceedings both as the conventional printed issue, as an accompanying USB stick, as well as freely available on the Internet as an Open Access publication. The latter is likely to be the most important dissemination option in the broader historical view. With all of the above the Editor can be fully satisfied with these contributions to the evolution of the by now well-established WCSB tradition.

Historical comparison: Another small organising committee: WCSB1, 19–22 August 2003, Esbjerg, Denmark.

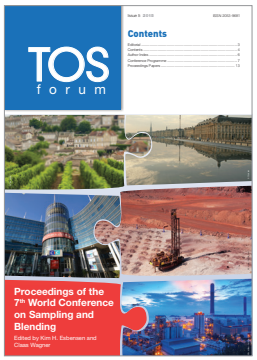

This issue comprises the Proceedings of the 7th World Conference on Sampling and Blending, held from 10 to 12 June in Bordeaux, France. Cover image with kind permission of the organisers.

Proceedings of the 7th World Conference on Sampling and Blending

EDITORS
Kim H. Esbensen (Geological Survey of Denmark and Greenland (GEUS), Copenhagen, and ACABS research group, Aalborg University, campus Esbjerg, Denmark; ke@geus.dk)

Claas Wagner (Sampling Consultant; cw@wagnerconsultants.com)

www.impublications.com/wcsb7

TOS forum

EDITOR
Kim H. Esbensen (Geological Survey of Denmark and Greenland (GEUS), Copenhagen, and ACABS research group, Aalborg University, campus Esbjerg, Denmark; ke@geus.dk)

PUBLISHER
Ian Michael (ian@impublications.com)

6 Charlton Mill, Charlton, Chichester, West Sussex PO18 0HY, UK.
Tel: +44-1243-811334;
Fax: +44-1243-811711;
E-mail: subs@impublications.com

TOS forum is currently available free-of-charge. Visit www.impublications.com/tos-forum for details.

Editorial correspondence to Kim Esbensen, ke@geus.dk. All production correspondence should be sent to *TOS forum*, 6 Charlton Mill, Charlton, Chichester, West Sussex PO18 0HY, UK, Tel: +44(0)1243–811334, Fax: +44(0)1243–811711, e-mail: ian@impublications.com.

contents

author index

Technical Program

Wednesday, June 10 Opening Session		Amphithéâtre BRISBANE
08:30	Opening Ceremony	
08:50	Program update and general information	

Wednesday, June 10 Session 1 – Theory of sampling		Amphithéâtre BRISBANE
Chair:		
09:00	**Keynote** The Advantages and Pitfalls of Conventional Heterogeneity Tests and a Suggested Alternative **Pitard, Francis F.**, Francis Pitard Sampling Consultants, LLC	
09:40	Applications of Sampling Theory in Bulk Commodities: An Iron Ore Case Study **Dominguez, Oscar R.**, BHP Billiton Iron Ore; **Smith, Kathleen**, BHP Billiton Iron Ore	
10:00	Proper TOS Sampling, Variographic Analysis, Total Measurement Uncertainty & Fit-for-Purpose Acceptance Levels for Pharmaceutical Mixing Processes Monitoring – A Call for a Paradigm Shift **Esbensen, Kim H.**, Geological Survey of Denmark and Greenland (GEUS); **Romañach, Rodolfo J.**, Recinto Universitario de Mayaguez	
10:20	**Poster Session and Coffee Break**, Espace BAMAKO	

Wednesday, June 10 Session 2 – Theory of sampling and blending		Amphithéâtre BRISBANE
Chair:		
11:00	Comparison Between Samples With Constant Mass And Samples With Constant Fragment Population Size (and calculation of their sampling variances) **Matheron, Georges** – Presented by **Dominique François-Bongarçon** and **Francis Pitard**	
11:20	The Decision Unit – A Lot with Objectives **Ramsey, Charles A.**, EnviroStat, Inc.	
11:40	Pre-Crusher Stockpile Modelling to Minimise Grade Variability **Everett, Jim E.**, The University of Western Australia; **Howard, T.J.; Jupp, K.**	
12:00	Placer gold sampling – The overall measurement error when using gravity concentration on particle size ranges during sample treatment **Brochot, Stéphane**, Caspeo; **Mounié, François**, IDM Guyane	
12:20	**Lunch**, Salle JEFFERSON	

Wednesday, June 10 Session 3 – Sampling for food	Amphithéâtre BRISBANE
Chair:	
14:00	**Keynote** Food and Feed Safety Assessment: Proper sampling is imperative **Paoletti, Claudia**, European Food Safety Authority (EFSA); **Kuiper, Harry A.**, Institute of Food Safety (RIKILT) Wageningen UR
14:40	Sampling for mycotoxins in feed - heterogeneity characterization **Wagner, Claas**, Energy and environmental consultant
15:00	Sampling of cereals: development of a protocol for mycotoxins analysis **Mahaut, Brigitte**, ARVALIS – Institut du vegetal; **Veron Delor, Guislaine**, ARVALIS – Institut du vegetal
15:20	The Role of Inference in Food Safety **Ramsey, Charles A.**, EnviroStat, Inc.
15:40	**Poster Session and Coffee Break**, Espace BAMAKO

Wednesday, June 10 Session 4 – Sampling for pharmacy and metal production	Amphithéâtre BRISBANE
Chair:	
16:20	When “homogeneity” is expected – TOS in Pharmaceutical Manufacturing **Romañach, Rodolfo J.**, Recinto Universitario de Mayaguez; **Sánchez Paternina, Adriluz**; **Román Ospino, Andres**; **Alvaro, Barbara**; **Esbensen, Kim H.**, Geological Survey of Denmark and Greenland (GEUS)
16:40	TOS to the Rescue: Estimating TSE for Near Infrared Spectroscopic Analysis of Pharmaceutical Blends **Romañach, Rodolfo J.**, Recinto Universitario de Mayaguez; **Alvarado, Barbara**; **Román Ospino, Andres**; **Esbensen, Kim H.**, Geological Survey of Denmark and Greenland (GEUS)
17:00	Practical use of variographics to identify losses and evaluate investment profitability in industrial processes **Tellesbø, Hilde**, Saint-Gobain Byggevarer AS; **Esbensen, Kim H.**, Geological Survey of Denmark and Greenland (GEUS)
17:20	The overall measurement error – TOS and uncertainty budget in metal accounting **Brochot, Stéphane**, Caspeo
17:40	End of the day

Thursday, June 11	Amphithéâtre BRISBANE
08:50	Program update and general information

Thursday, June 11 Session 5 – Theory of sampling	Amphithéâtre BRISBANE
Chair:	
09:00	**Keynote** Complete Sampling Distribution for Primary Sampling, Sample Preparation and Analysis **Lyman, Geoffrey J.**, Materials Sampling & Consulting
09:40	The added-value of sampling **Bourgeois, Florent**, Université de Toulouse / Materials Sampling & Consulting; **Lyman, Geoffrey J.**, Materials Sampling & Consulting
10:00	Building Confidence Intervals Around the Obtained Value of a Sample **François-Bongarçon, Dominique**, Agoratek International Consultants Inc.
10:20	**Poster Session and Coffee Break**, Espace BAMAKO

Thursday, June 11 Session 6 – Sampling for exploration and grade control	Amphithéâtre BRISBANE
Chair:	
11:00	Comparing different heterogeneity tests for gold **Chieregati, Ana Carolina**; **Senefonte, Rafael**, University of Sao Paulo; **de Oliveira Nunan, Thiago**, Mineração Serra Grande S.A.
11:20	Blast hole sampling in two areas of the same deposit **Alfaro, Marco**, Catholic University of Valparaíso
11:40	Validation of reverse circulation drilling rig for reconciliation purposes **Chieregati, Ana Carolina**; **El Hajj, Thammiris**, University of Sao Paulo; **Imoto, Carla Fernanda**, MultiGeo
12:00	Determination of the precision of sampling systems and on-line analysers **Lyman, Geoffrey J.**, Materials Sampling & Consulting; **Asbury, James**, Realtime Group Limited
12:20	**Lunch**, Salle JEFFERSON

Thursday, June 11 Session 7 – Sampling equipment efficiency	Amphithéâtre BRISBANE
Chair:	
14:00	**Keynote** Sample Station Design and Operation **Holmes, Ralph J.**, Mineral Resources Flagship, CSIRO
14:40	Review of a Non-Probabilistic Sampler versus a Vezin Sampler on Low Weight Percent Solids Slurries **Kelly, Steve E.**, Washington River Protection Solutions; **Pitard, Francis F.**, Francis Pitard Sampling Consultants, LLC
15:00	A method to evaluate the possible sampling error of a multiple cutter metallurgical sampler **Loimi, Janne**, Outotec; **Minkkinen, Pentti**, Lappeenranta University of Technology; **von Alfthan, Christian**; **Lohilahti, Jarmo**; **Korpela, Tapio**, Outotec
15:20	Design advances and operational studies for the True Pipe® Sampler: A symmetry based unit for reliable sampling of pressurised particulate streams **Steinhaus, Rolf H.**; **Fouchee, Annelize**, Multotec Process Equipment (Pty.) Ltd
15:40	**Poster Session and Coffee Break**, Espace BAMAKO

Thursday, June 11 Session 8 – Sampling and in-situ analysis	Amphithéâtre BRISBANE
Chair:	
16:20	The application of an integrated software library for controlling and monitoring ISO sampling systems **Adams, Craig S.W.**; **Neidel, Tore T.**, FLSmidth
16:40	PFTNA logging tool and its contributions for boreholes in situ elemental analysis **Jeanneau, Philippe**; **Flahaut, Vincent**, Sodern
17:00	General information about Conference Dinner

Thursday, June 11 Conference Dinner	Museum
18:30	Cocktail and Conference Dinner
	Pierre Gy's gold medal ceremony

Friday, June 12	Amphithéâtre BRISBANE
08:50	Program update and general information

Friday, June 12 Session 9 – Theory of sampling	Amphithéâtre BRISBANE
Chair:	
09:00	**Keynote** The first ever rigorous derivation of liberation factor – a problem finally solved **François-Bongarçon, Dominique**, Agoratek International Consultants Inc.
09:40	A multi-parameters approach for process variograms **Dehaine, Quentin**; **Filippov, Lev O.**, GeoRessources, Université de Lorraine
10:00	Comparison of sampling methods by using size distribution analysis **Minkkinen, Pentti**, Lappeenranta University of Technology; **Auranen, Ilpo**, IMA Engineering; **Ruotsalainen, Lari**; **Auranen, Jesse**, Mine On-Line Service
10:20	**Poster Session and Coffee Break**, Espace BAMAKO

Friday, June 12 Session 10 – Sampling and geostatistics	Amphithéâtre BRISBANE
Chair:	
11:00	Geostatistical Comparison Between Blast and Drill Holes in a Porphyry Copper Deposit **Séguret, Serge Antoine**, Paris School of Mine
11:20	Sampling considerations for characterization of radioactive contamination using geostatistics **Desnoyers, Yvon**, Geovariances
11:40	Conference conclusion and presentation of the next WCSB
12:00	Closing Ceremony
12:20	**Lunch**, Salle JEFFERSON

Poster Session
Analysis of granite's roughness using stratified random sampling for the evaluation of radon gas emanation **El Hajj, Thammiris**; **Delboni, Homero**; **Chieregati, Ana Carolina**, University of Sao Paulo; **Gandolla, Mauro**, Università della Svizzera Italiana
Proper field sampling and laboratory processing for archæometric discrimination between cultivated and fallow Bronze-age fields on Bornholm, Denmark – TOS meets Chemometrics meets Archeology **Germundsson, Bastian**, Copenhagen University; **Pihl, Anders**, Bornholm Museum; **Esbensen, Kim H.**, Geological Survey of Denmark and Greenland (GEUS)
Improved counteracting soil heterogeneity sampling designs for environmental studies – TOS meets chemometrics **Kardanpour, Zahra**, Aalborg University; **Jacobsen, Ole Stig**; **Esbensen, Kim H.**, Geological Survey of Denmark and Greenland (GEUS)
Distributional assumptions in food and feed commodities: how to develop fit-for-purpose sampling protocols? **Paoletti, Claudia**, European Food Safety Authority (EFSA); **Esbensen, Kim H.**, Geological Survey of Denmark and Greenland (GEUS)
Practical Case: Representative Sampling for Full-scale Incineration Plant Test **Pedersen, Peter Bøgh**; **Jensen, Jan Hinnerskov**, Danish Technological Institute
Sample System Designs for the new NSPS Standards **Ponthieu, Dewey**, TRIAD Control Systems
Sampling for Food and Feed materials' safety **Thiex, Nancy**, Thiex Laboratory Solutions LLC; **Paoletti, Claudia**, European Food Safety Authority (EFSA); **Esbensen, Kim H.**, Geological Survey of Denmark and Greenland (GEUS)
A European Standard for sampling of waste materials: EN 14899 **Wavrer, Philippe**, Caspeo; **Morvan, Bernard**, Traidema; **Louis-Rose, Sébastien**, AFNOR
Innovative Sampling Solutions for the Mining Industry **Wicks, Maurice**, IMP Group P/L

doi: 10.1255/tosf.47

The advantages and pitfalls of conventional heterogeneity tests and a suggested alternative

Francis F. Pitard
Francis Pitard Sampling Consultants, 14800 Tejon Street, Broomfield, CO 80023, USA. E-mail: fpsc@aol.com

Heterogeneity Tests have been very popular for the last 30 years and there are several versions of them such as the method of choice used by François-Bongarçon to quantify and minimize QFE_1 which is a combination of the Fundamental Sampling Error and the Grouping and Segregation Error and sometimes Analytical Error. A more recent version called "segregation free analysis for calibrating the constants *K* and *x*" is used by Minnitt, and an older, obsolete version using fragments collected one by one at random from several size fractions to calibrate the constant *K* was used a long time ago by Gy and Pitard. All these methods have their merits and pitfalls. The common pitfall is that they all depend on the collection of a representative composite sample consisting of about half a ton of material. In Mineral Processing it is well known how difficult it is for geologists to provide a representative sample from a given geological unit to perform reliable metallurgical testing; the same difficulties are encountered in performing Heterogeneity Tests. Furthermore, experience clearly shows that for trace constituents such as gold, many tons should be collected to obtain a reliable composite. Perhaps there is a more representative way to collect the information necessary to calculate the variance of the Fundamental Sampling Error *FSE*, which can support and complement the method of choice referred to earlier. This paper suggests that all the necessary information can be obtained by slightly modifying the logging practices of geologists. From such observations, reliable histograms of the size distribution of particles of the mineral of interest can be made representing the properties of an entire geological unit. Such information can be obtained at an early phase of exploration leading to an unmistakable definition of the sampling constant *K*, and possibly an accurate definition of the mathematical model of the liberation factor leading to the constant *x*; using modern microscopy the mineralogist can define the evolution of the liberation factor as a function of increasing comminution better than anyone else. Furthermore, this paper suggests that the determination of the liberation factor is no longer a critical factor, though most certainly useful, if using the information from modified logging practices and two old formulas suggested by Gy in the 50's instead of his famous formula using the liberation factor.

Introduction

The following material should not be perceived as a replacement for the method of choice to estimate constants *K* and *x* in a formula suggested by François-Bongarçon to quantify the variance of the short-range Quality Fluctuation Error QFE_1 affecting splitting processes in routine sampling and subsampling protocols. The suggested calibration was approved as a method of choice in a common publication by Pitard and François-Bongarçon (2011)[1] and should remain so as far as sampling practitioners are concerned. However, Heterogeneity Tests are far from perfect and no matter how careful practitioners are, there are pitfalls that can be prevented by paying attention to arguments presented in this paper. Therefore the only objective is to suggest to geologists and mineralogists that early on they can provide valuable information by adding the necessary observations on the drilling log and by making simple mineralogical tests. The added information can help to prevent great mistakes in the ways exploration and grade control data are looked at. But first some paradigms that are well accepted by sampling experts should be eliminated.

Poisson Processes and liberation issues

In the mind of many people a Poisson Process cannot take place unless the constituent of interest particles (e.g., gold particles) are liberated from their rock matrix; there is nothing that can be so far from the truth. Such belief is based on the fact that gold particles should be randomly distributed, but obviously they are not. There are plenty of geological explanations for in-situ gold particles to be distributed in a certain area of a small ore block (e.g., 15 × 15 × 15 meters). Therefore, someone may rightly object to using a Poisson model which is the simplest possible and most random way in which we may explain why the gold particles are where they are. However, all this assumes some a priori knowledge of the regionalization within that little block. We may have some of that knowledge between blocks, but not necessarily within any given block.

Therefore, before going any further, we must elaborate on the paradigm of being an observer, since the observer has no idea where the gold in that block is. He may know there is gold, but he does not know where. The resulting effect is that when he drills that block, and within that block there may be 1, 2, 3, or more clusters of gold particles somewhere, the location to drill chosen by the observer who knows nothing ahead of time is a random process of its own, even if the gold is not strictly distributed at random. So, the resulting gold content of that core, within that block, can be assimilated to a random process, not because of the way it is distributed in the deposit, but because of what the observer is doing with the selected location and selected basic volume of the support of observation as he becomes a participant; there is a subtle difference. It is exactly the same thing for coarse fragments in which the gold is not necessarily liberated.

For the purist who rightly insists that random variables be defined by reference to an appropriate probability block it is not much of a loss to take the Poisson model as a good tool to help us, especially when the observer is personally responsible for introducing the Poisson Process in the first place (i.e., no a priori knowledge and an extremely small support volume).

For anyone who may have the desire to better understand what is meant by "Poisson Process" Kingman's book, 1993, is an excellent one[2].

With this knowledge in mind it is not difficult to demonstrate that collected data for most trace constituents, and gold is one of them, are affected by a Poisson Process of some kind that was originally introduced because of the limited volume of the drilling support. This has huge implications in the collection of representative samples to perform Heterogeneity Tests and ultimately calibrate constants *K* and *x*.

Poisson Processes and trace constituent size-grade trends

To simplify the discussion let's take the example of gold as a trace constituent, keeping in mind it is applicable to any trace constituent. When there is a large in-situ nugget effect combined with a clustering effect of the gold particles that don't like to be alone, the distance between clusters within mineralization increases. Many samples do not contain coarse gold as they should. Later on, when split duplicates are taken, and ultimately fire assay duplicates are taken, since they had no coarse gold to begin with, they give the illusion that low grade samples represent areas where no coarse gold is present, even though it is true for samples coming from areas where indeed there is no coarse gold. Again, the observer will not know the difference. So, let's not feel safe by saying the low grade material does not contain coarse gold; it most certainly will in a substantial amount of cases! This deserves further thinking from geologists, grade control engineers, and geostatisticians. The author became sure of such a property in several projects where grade control vastly underestimated the gold grade going to the plant for no apparent, good reason. The same problem was clearly observed for arsenic, molybdenum and cobalt minerals. It was even observed for impurities such as silica and aluminum in iron ore, for sulfur in coal, for silica in bauxite, etc… Basically, the problem is not rare.

Indirect implications for heterogeneity tests

The appropriate approach for conducting Heterogeneity Tests for major and some minor constituents has been well established and the objective of this paper is not to question this at all. However, for low grade gold deposits for example, the conventional approach may indeed work well for deposits with finely disseminated gold, but it may be misleading when gold particles are large (e.g., superior to a few hundred microns, or when fine gold or any other trace constituent is clustering). The author witnessed many such cases and clearly there is a need to suggest a strategy to make sure sampling practitioners are not reaching over-optimistic conclusions. Again, without understanding how Poisson Processes may take place, the following material may seem bizarre for the reader.

In a letter criticizing François-Bongarçon's work Smee and Stanley (2005)[3] said "Gy's formula is based on and derivable from the binomial theorem. Consequently, Gy's formula doesn't apply to samples containing very low concentrations of elements contained in rare grains (e.g., Au, PGE, diamonds, etc.), where a Poisson relation is applicable. Our avoidance in referencing Gy stems directly from the fact that we consider samples containing nuggets to be a scenario that is inconsistent with Gy's approach." This statement shows sampling practitioners in the world of Measurement Uncertainty vastly misunderstand Gy's work and have no idea about the many subtleties of his propositions and therefore they are in no position to criticize those who apply his work in a wise and knowledgeable way.

First, the Poisson model is a limit case of the Binomial Model use by Gy, and therefore a close "cousin" and Gy was perfectly aware of nugget problems. Nobody who is knowledgeable enough would use Gy's general formula to calculate the variance of *FSE* for a sample mass that is too small by several orders of magnitude. However, anyone can turn the formula around and calculate the necessary sample mass that is required to prevent the introduction of a Poisson Process, a domain for which the formula is perfectly applicable. This is exactly what Gy always did and it is what is suggested in this paper.

Cardinal Rule #1 in sampling

Biases in sampling are the worse misfortune that may take place, and were the driving force to establish the many rules of sampling correctness, so theoretical developments of equi-probable sampling made by Gy and Matheron could apply in practice. This led to the many advances to minimize Increment Delimitation Error, Increment Extraction Error, Increment Preparation Errors and Increment Weighting Error which are the biggest contribution of Gy's theory by far according to his own words. Is this sufficient to prevent sampling biases? The answer is no. For example, it is well known that the content of a constituent of interest may drastically change from one size fraction to another. Then, plain logic would suggest the following Cardinal Rule in sampling should never be broken up: a sample mass that is too small to well represent all size fractions cannot provide a sample representative of anything else; this has huge implications for any kind of Heterogeneity Test.

Successive stages of sampling and sub-sampling may each require compliance with a pre-established limit that highly depends on the practitioner's objectives as suggested by Pitard (2013)[4]. But, the most difficult size fraction to properly represent in the sample is obviously the one containing the largest fragments. This strongly suggests some long forgotten formulas from Pierre Gy should be brought back to the rescue and a careful discussion should follow. Let's be clear, without a good understanding of these formulas there is no possible understanding of Gy's subtle work.

Gy (1971)[5] and Pitard (1993)[6] derived the following formula to calculate the variance of Fundamental Sampling Error to be used to make sure a given size fraction is well represented in collected samples.

$$s^2_{FSE} = \left[\frac{1}{M_S} - \frac{1}{M_L}\right] f \cdot \rho \left[\left(\frac{1}{a_{Lc}} - 2\right) d^3_{FLc} + \sum_x d^3_{FLx} \cdot a_{Lx}\right] \qquad (1)$$

Notations are:

L_C a size fraction of interest
a_{Lc} the proportion of L_C in the lot L
M_S the mass of the collected sample
M_L the mass of the lot to be sampled
F_{Lc} the average fragment of the size fraction L_C
d_{FLc} the size of the average fragments in the size fraction of interest
d_{FLx} the size of the fragments in the other size fractions besides the one of interest
f a fragment shape factor
ρ the average density of the fragments

This formula can often be simplified for many applications:

- If $M_L > 10\ M_S$
- If d_{FLc} is not much different from d defined as the size opening of a screen that would retain 5% of the material by weight.

- If a_{Lc} is small, then

$$s^2_{FSE} = \frac{f \cdot \rho}{M_S}\left[\frac{1}{a_{Lc}} - 2\right] d^3_{FLc} \quad (2)$$

and if $d_{FLc} = d$

$$s^2_{FSE} = \frac{18 \cdot f \cdot \rho \cdot d^3}{M_S} \quad (3)$$

This convenient formula provides a filter to make sure the exponent x for d is not abused when used in a formula like one suggested by François-Bongarçon:

$$s^2_{QFE1} = \left[\frac{1}{M_S} - \frac{1}{M_L}\right] K \cdot d^x \quad (4)$$

where:

$$K = f \cdot g \cdot c \cdot (d_l)^r \text{ and } x = 2 - r$$

K and x are the key factors to quantify in various experiments. If $x < 3$, clearly it is not an issue when the values for d are below 1 cm, however it can indeed become an issue for large values of d such as for sampling run off mine material.

Example of application

If a run off mine material has a value of 10 cm for d and a 1-ton sample is required to represent the coarsest fragments with an uncertainty of 15% (1s), it would be unfortunate to recommend a much smaller mass on the basis that x is much smaller than 3. Obviously, the value used for K has a big influence on the outcome of this discussion; indeed if K is very high it is likely that there is no problem.

Cardinal Rule #2 in sampling

The size d_M of the grains of mineral of interest, liberated or not, must play an important role in the necessary sample mass. d_M can also be a cluster equivalent when several of those grains are very close to one another within a core sample or within a larger fragment. Gy corrected for this problem in an elegant way, not always well understood by practitioners, with his liberation factor. In other words, in his original formula with $x = 3$, both concepts d and d_M were preserved; be aware it is no longer the case with formula [4].

Often, especially for trace constituents, it is difficult and impractical to determine the liberation factor with sufficient accuracy, and this makes some formulas vulnerable. Enormous literature has been written on this subject, the best one by François-Bongarçon (2000, 2001)[9,10]. However, it is not a must to use the conventional, favorite approach suggested by Gy's general and well-known formula. The following suggestion is pragmatic, accurate, and falls in line with Ingamells' approach; it is summarized in the three following statements:

- Use Gy's suggested approach for liberated gold when d_M, which is d_{Au} in formula [5], becomes the dominant factor; it can be generalized to many other components of interest.

$$s^2_{FSE} = \left[\frac{1}{M_S} - \frac{1}{M_L}\right] \frac{f_{Au} \cdot g_{Au} \cdot \rho_{Au}}{a_L} d^3_{Au} \quad (5)$$

- Verify that the sample mass suggested by the generalized version of equation [4] is compatible with the mass necessary to represent all size fractions in the lot by using equation [1], or [3].
- The largest required sample mass for a pre-selected precision, obtained by equation [1] or [3] (i.e., using d) and equation [5] (i.e., using d_M defined below) necessarily takes priority on deciding what the sampling protocol should be.

Generalization of equation [5] by defining new notations:

f_M the shape factor of the constituent of interest

g_M the particle size distribution factor of the constituent of interest

ρ_M the density of the constituent of interest

d_M the maximum size of the constituent of interest particle, liberated or not, or cluster of such particles contained in a single fragment of the surrounding matrix; d_M is defined as the size of a screen that would retain no more than 5% by weight of all the particles of the constituent of interest.

Thus, we obtain the very useful simplified formula:

$$IH_L = f_M \cdot g_M \cdot d^3_M \cdot \frac{\rho_M}{a_L} \quad (6)$$

Useful sampling nomographs can be calculated with the following formula:

$$s^2_{FSE} = \left[\frac{1}{M_S} - \frac{1}{M_L}\right] \frac{f_M \cdot g_M \cdot \rho_M \cdot d^3_M}{a_L} \quad (7)$$

The great advantage of this approach is its accuracy and the easiness to collect the relevant and necessary information through microscopic observations, and it should somewhat reconcile Gy, Ingamells, and François-Bongarçon. In the event reconciliation is not possible it should be a clear indication some heterogeneity properties of the constituent of interest are still unknown and further investigation is needed. This debate naturally leads to Cardinal Rule #3.

Another advantage of equation [7] is for subsampling finely ground material, as some constituents such as soft ones like gold, molybdenite, galena and many more do not comminute well. Very hard minerals like chromite may show the same problem. For example a sample pulverized to 99% minus 106 microns may still contain a 300-micron gold particle making all other formulas weak and perhaps misleading.

Cardinal Rule #3 in sampling

As Pierre Gy said many times, especially when criticizing the work of Richard (1908)[15], when deciding what the exponent of d should be, and therefore the constant x, there is a confusion between *FSE*, QFE_1, and even the Analytical Error *AE* poorly defined by non-chemists and TOS experts. This confusion has been responsible for over a century for total chaos, and still remains an issue today. Problems are:

1) For very fine material the variance of *FSE* rapidly becomes a negligible factor unless unrecognized delayed comminution takes place for the constituent of interest.
2) The segregation error can be huge as the constituent of interest is liberated and possibly of a very different density than the rest of the material.
3) Taking the optimistic assumption that analytical increments are taken perfectly at random (an absolute requisite for Gy's definition

of *GSE*), which is rarely the case at the balance room of a laboratory, the variance of *GSE* can become small indeed; however it takes work an analytical chemist is not willing to spend the time on. As a result, the segregation error which is no longer *GSE*, may become vastly underestimated because it no longer obeys rules set by the TOS.

4) The Analytical Error *AE* cannot be estimated by doing replicate assays that include the last *FSE* and last *GSE*. Let's assume the chemist takes a 30-g analytical subsample for fire assay; the taking of that sample has nothing to do with the Analytical Error which includes fusion, cupellation, acid digestion of a bead, contamination, losses, spectrometer calibration or use of a precision balance, additive and proportional interferences, etc… In other word it is very hard, if not impossible in some cases to appreciate what *AE* really is. Furthermore, *AE* is extremely operator dependent. There is no such things as a bad analytical method, there are only incompetent analysts who apply it for the wrong conditions.
5) There is no such thing as a segregation free analysis when taking replicate samples in a given size fraction as particles segregate even if they are all the same size. They will most certainly segregate because of density, shape, electrostatic property differences, etc…

All this is clearly summarized in the sketch illustrated in Figure 1 and very familiar to Visman, Ingamells and Gy through verbal conversations, and many others who were wise enough to admit that what they measured with replicate samples or replicate assays may have nothing to do with the variance of *FSE*. It can be noticed as well that in this figure when segregation is mentioned it is not necessarily referring to *GSE* as defined in the TOS; the subtle difference depends on what the operator may do. The only thing the author asks is not much to comply with: call variance sources by their respective name instead of calibrating *x* to compensate for things that are not clearly defined or understood. An example is appropriate: an operator shakes a laboratory pulp to collect a tiny analytical sample, then makes the assumption there is no longer any significant segregation in the pulp, and finally takes one or two tiny increments with no respect to the TOS. The resulting variance, after guessing what the analytical variance should be and removing it is found to be large. The operator put the blame on a large variance of *FSE* when it is clear that he was introducing a massive segregation variance because of the way he collected the increments. In this particular case he was introducing a variance that has nothing to do with FSE, nor GSE, because all the subtle principles clearly defined in TOS were completely ignored therefore prohibit the segregation variance to be a random one as it should be.

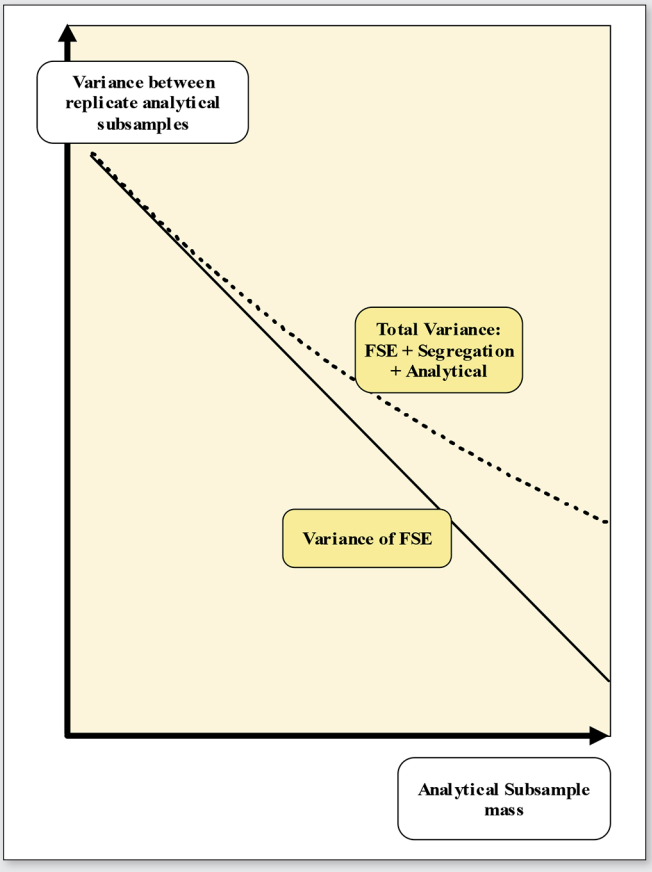

Figure 1. Replicate assays variance and its components.

Suggesting a new integrated iterative approach

Iteration is the word of wisdom in sampling. The following three steps are not necessarily suggested in chronological order. Rather, each step can be taken simultaneously which ultimately will provide confidence that no stone has been left unturned.

Step #1: The mandatory calibration of *K* and *x*

The calibration of constants *K* and *x* in equation [4] as suggested by François-Bongarçon is a mandatory step that is non-negotiable; please notice notations in that formula very carefully. Indeed, the use of the notation QFE_1 is valid only if the operator has been collecting many increments in full compliance with sampling correctness, which is a very optimistic assumption as experience proves. If not in full compliance, then the resulting variance is anyone's guess because there is no longer any theoretical development possible as demonstrated by Gy and Matheron. Such calibration allows minimizing the variance of the Fundamental Sampling Error and also measures the leftover effect of the Grouping and Segregation Error depending on the equipment used to split samples at the sample preparation room and at the laboratory, and on the operator's training which can be a huge factor. For the details of such procedure the reader is referred to François-Bongarçon's publications (2000 and 2001)[9,10].

Step #2: The geologist to the rescue

It is necessary to better log the properties of gold in each geological unit. With minor modifications the same list may easily apply to other constituents of interest in iron ore, in coal, in porphyry copper deposits, and others, gold being only a convenient example. For each core sample within substantial mineralization the following information should be carefully logged:

- Where is the gold?
- What are the associations of gold?
- How much gold is finely disseminated within sulfides, such as pyrite or other minerals?
- How much gold is coarse and perhaps nearby other minerals?
- Are gold and pyrite or other mineral occurrences associated with narrow or large quartz veins? If so, are there several quartz events?
- Study size distribution of gold particles. A good histogram is needed for each geological unit. After observing several thousand

samples within mineralization it should be possible to roughly estimate the size d_M above which only 5% of the gold can report.

- Equally important, study the size distribution of gold particle clusters; in other words when you see one gold particle (measure it), how many more gold particles are in the immediate vicinities? e.g., 10 or more within 100 cm^3? After observing several thousand samples within mineralization it should be possible to roughly estimate the size $d¢_M$ above which only 5% of the gold can report as cluster equivalents.
- Etc…

Step #3: The mineralogist to the rescue

Suarez and Carrasco (2011)[13] demonstrated in an unambiguous way that careful mineralogical studies can provide valuable information to model the variability of the liberation factor as a function of comminution stage. It is very unfortunate such study does not generate more interest. The same study suggests that the maximum content model suggested many years ago by Gy is a very reliable model that was used all the time in a mineral processing research laboratory (Minemet); see Gy (1956)[11] and Pitard (1993[6] and 2009[14]).

Step #4: The selected sample or subsample mass must fairly represent the coarsest fragments

This task is easily done by using formulas [1] or [3].

Step #5: The selected sample or subsample mass must fairly represent the largest particles of a given constituent of interest

This task is done by using formula [7]. This is critically important for constituents showing delayed comminution. Usually, soft minerals such as gold, galena, molybdenite and very hard minerals such as chromite can show such problem. As a good example, the coarse gold case shown by Pitard and Lyman (2013)[12] clearly shows that a Heterogeneity Test performed by using conventional 30-g fire assays would most likely have led to very misleading conclusions; the test is not the problem, but the completely inappropriate 30-g subsample is the issue, in other words the operators would have used the wrong tools.

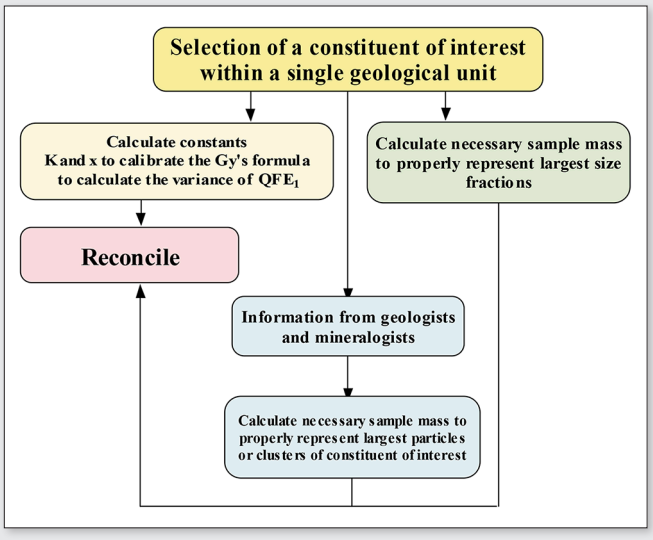

Figure 2. Logical Heterogeneity Test Flow Sheet.

Step #6: A logical flow sheet to perform Heterogeneity Tests

Figure 2 summarizes the necessary steps to perform a reliable Heterogeneity Test for various constituents of interest during exploration and grade control; the approach can easily be extended to other materials in other industries. The reconciliation box has a very important mission in cases where conclusions are grossly different: a logical explanation must be found that may lead to important decisions concerning the selection of fully optimized sampling and subsampling protocols.

References

1. Pitard F., and François-Bongarçon, D. Demystifying the Fundamental Sampling Error and the Grouping and Segregation Errors for Practitioners. Fifth World Conference on Sampling and Blending. Proceedings printed by Gecamin. 25-28 October 2011, Santiago, Chile, pp 39-55.
2. Kingman J.F.C. Poisson Processes. Oxford Studies in Probability.3. University of Bristol. Clarenton Press. Oxford, 1993.
3. Smee B.W. and Stanley C.R. Reply to Dr. Dominique François-Bongarçon, - Publication Type in a journal article: Explore - Association of Exploration Geochemists Newsletter, Volume 127, p.19-23 (2005)
4. Pitard F. Guidelines for acceptable allotted sampling uncertainty. Sixth World Conference on Sampling and Blending. Proceedings printed by Gecamin. November 19-2, 2013, Lima, Peru, chapter 2, paper 41.
5. Gy, P.M., L'Echantillonage des Minerais en Vrac (Sampling of particulate materials). Volume 2. Revue de l'Industrie Minerale, St. Etienne, France. Numero Special (Special issue, September 15, 1971, chapter 19).
6. Pitard, F.F., Pierre Gy's Sampling Theory and Sampling Practice. *Textbook published by CRC Press*, Inc., 2000 Corporate Blvd., N.W. Boca Raton, Florida 33431. Second edition, July 1993.
7. Ingamells, C.O, and Pitard F., Applied Geochemical Analysis. Wiley Interscience Division, John Wiley and Sons, Inc., New York, 1986. 733 pages textbook
8. François-Bongarçon, D. Fishy samples: how big a sample to avoid the infamous "Poisson effect"? Fourth World Conference on Sampling and Blending. The Southern African Institute of Mining and Metallurgy, 2009.
9. François-Bongarçon, D. (2000). The most common error in applying Gy's formula in the Theory of Mineral Sampling, and the history of the liberation factor. *monograph "Toward 2000", AusIMM*.
10. François-Bongarçon, D and Gy, P (2001). The most common error in applying 'Gy's Formula' in the theory of mineral sampling and the history of the Liberation factor, *in Mineral Resource and Ore Reserve Estimation – The AusIMM Guide to Good Practice*, pp 67-72 (The Australasian Institute of Mining and Metallurgy: Melbourne).
11. Gy, P.M., Poids a Donner a un Echantillon – Abaques d'Echantillonage. French edition of a former paper in German. Revue de l'Industrie Minerale, 1956, pp. 1-30.
12. Pitard F.F. and Lyman, G.J., Single and multi-stage Poisson processes: A case study for gold exploration. 6th World Conference on Sampling and Blending. Proceedings printed by Gecamin. 19-22 November 2013, Lima, Peru.
13. Suarez, E.V., and Carrasco P., Numerical studies of texture and liberation in microscopic images, Fifth World Conference on Sampling and Blending", 25-28 October 2011, Santiago, Chile. Proceedings printed by Gecamin.

14. Pitard, F.F. “Pierre Gy’s Theory of Sampling and C.O. Ingamells’ Poisson Process Approach, pathways to representative sampling and appropriate industrial standards”, doctoral thesis in technologies, Aalborg University, campus Esbjerg, Niels Bohrs Vej 8, DK-67 Esbjerg, Denmark, 2009.
15. Richard, R.H., Ore dressing, sampling. Vol.2: pp. 813-884, Vol. 3: pp. 1571 1578, Vol. 4: pp. 2031-2033. Mc Graw-Hill. New York (1908).

doi: 10.1255/tosf.62

Good sampling is good business: reconciling economic drivers of productivity and quality using fundamentals of sampling theory

O. Dominguez[a] and K. Smith[b]
[a]Oscar.R.Dominguez@bhpbilliton.com
[b]Kathleen.Smith@bhpbilliton.com

Iron Ore supply is outpacing global demand, reinforcing the importance of product quality and reliability as critical factors that distinguish Iron Ore producers in a competitive market. This expectation calls for a shift in industry attitudes toward sampling in bulk commodities, beginning with a greater emphasis on optimisation of sampling processes from Exploration to Port. Business initiatives aimed at optimising processes often call upon technological innovation, such as mobile sampling and analysis modules at the drill rig. Such technologies indeed represent an exciting frontier in the business of minerals exploration; however their merits must be critically compared to existing sampling protocols before implementation if sample quality is to be maintained. Quantifying the Fundamental Sampling Error (FSE) of the sampling protocol is a minimum requirement to achieve this and should be preceded by experimental calibration of the sampling constant K and the exponent alpha. Here, we present a case study in which the Segregation Free Analysis (SFA) calibration methodology proposed by Minnitt et al.[3] was used to determine K and alpha for a Channel Iron Deposit (CID) and a Brockman Iron Formation-hosted Bedded Iron Deposit (BID) from the Pilbara region of Western Australia. Following three experimental calibrations of K and alpha, liberation size was calculated for iron oxides and deleterious minerals using Gy's formula. Validation of liberation size is critical if the resulting FSE calculation is to inform business decisions. Electron beam instruments such as QEMSCAN have been proposed as a relatively quick and low cost way to estimate liberation size[2]. An "off-the-shelf" QEMSCAN analysis was trialled as a validation method against the SFA calibration results. Good agreement was achieved between liberation sizes determined by the SFA calibration method and the QEMSCAN analysis. Furthermore, the QEMSCAN results proved to be a beneficial source of supplementary information, in the form of particle size analysis, which indicates the degree of aggregation that persisted in the calibration material despite best efforts to eliminate it, as well as mineral abundance analyses, which either confirmed or highlighted uncertainty around critical mineralogical assumptions made in the calibrations. These observations emphasise the importance of validation when assessing FSE. The case study presents an industry perspective on the applications of sampling theory in response to an increasingly competitive Iron Ore market.

Introduction: economic drivers of technology, productivity and product quality

Commodity prices have fallen in recent times, leaving mining companies with an imperative to cut costs, improve productivity, innovate technological solutions, all whilst improving the quality of their product. Iron Ore in particular is an increasingly competitive market as global supply outpaces demand; thus product quality and reliability are becoming increasingly relevant factors that distinguish iron ore producers in the marketplace. Such economic conditions indeed necessitate challenging the status quo and looking to optimisation of processes aimed at lowering cost and raising productivity; however this must be done with great care where technical considerations such as sampling protocols are involved. Furthermore, adopting new technologies designed to streamline processes – such as mobile sample preparation and analysis equipment at the drill rig – must be carefully measured against traditional sampling and analytical methods; otherwise mining companies may find initiatives geared towards productivity in direct conflict with initiatives geared towards improving product quality.

To critically compare a conventional sampling protocol against a novel, technologically innovative protocol, one must first determine some measure of error which can be critically compared. Gy's Theory of Sampling (1979)[1] suggests that the single most influential error is the Fundamental Sampling Error (FSE) of the sampling design, and application of Gy's formula to calculate FSE must be preceded by experimental calibration of the sampling constants K and alpha for the particular ore type (Minnitt et al., 2011)[3]. Here we present a case study in which the BHP Billiton Iron Ore Exploration group, in collaboration with Dominique Francois-Bongarcon of Agoratek International, conducted three experimental calibrations of K and alpha in order to quantify the FSE of our sampling protocol. The determinations of K and alpha were ultimately used to calculate the liberation size of deleterious materials present in iron ores, chiefly alumina, silica, and phosphorous. For proprietary reasons, iron results will not be published.

As an influential variable in the FSE calculation, it was critical to validate the liberation sizes generated by the calibration experiments. QEMSCAN technology has been suggested as a novel approach to heterogeneity in the past (Lyman, 2011)[2] and was trialled as a validation technique using an "off-the-shelf" suite of analyses provided by Bureau Veritas Australia. The use of QEMSCAN proved to be a beneficial source of supplementary information, including particle size distribution analyses, which appear to confirm that aggregation persisted in the material used in the calibration experiments despite best efforts to eliminate it. Furthermore, the QEMSCAN work confirmed some mineralogical assumptions, which influences the FSE calculation as the density input associated with the sampling

constant K. In light of achieving good agreement between experimental and QEMSCAN liberation sizes, the QEMSCAN analysis is considered to be worthwhile.

Experimental calibration of k and alpha

Three calibration experiments were conducted according to the Segregation Free Analysis methodology proposed by Minnitt et al.[3]. These experiments will be referred to as Experiment 1, Experiment 2 and Experiment 3. Each experiment utilised high-grade iron ore sourced from BHP Billiton exploration projects or active mines. Two calibrations were conducted for Brockman hosted bedded iron formation; the first sourced bulk sampled material from Reverse Circulation (RC) drilling and the second sourced material from coarse-crushed diamond core, previously used for metallurgical test work. The third experiment assessed blasted Channel Iron Deposit (CID) material sourced directly from an active pit at the BHP Billiton Yandi mine. Details of sample collection and preparation for each experiment are presented below. All samples were assayed by XRF at the SGS Newburn Laboratory in Perth.

Experiment 1: RC sourced Brockman ore

The first calibration experiment utilised approximately 100 kg of high-grade Brockman ore generated by Reverse Circulation (RC) drilling from a BHP Billiton exploration project in the Pilbara. RC sourced bulk material was chosen for the initial trial for its easy availability and low cost. The bulk material was de-aggregated using a steel roller and split into four lots using a rotary splitter for easier handling. Approximately one half of the original 200 kg lot was run through a nest of sieves in geometric progression (r = 2); however, due to the destructive nature of the RC drilling method, the maximum grain size was smaller than anticipated with a dmax of 0.95 cm. This constrained the first calibration experiment to four size fractions and a pulp series, which is used to approximate analytical variance (Minnitt et al., 2011)[3]. A total of 30 samples were collected from each fraction by spooning approximately 100 g of sieved material into a sample bag. Each sample weighed approximately 100 g.

Experiment 2: Diamond sourced Brockman Ore

The second calibration experiment utilised approximately 100 kg of high-grade Brockman ore sourced from coarse-crushed diamond core from a BHP Billiton exploration project in the Pilbara. Partially mineralised shale material contained within the lot was highly subject to aggregation. Following de-aggregation using a steel roller, the diamond sourced material yielded a dmax of 1.9 cm. The material was then rotary split for easier handling, and run through the nest of sieves as per experiment 1, resulting in five size fractions and a pulp series. Between 16 and 32 samples were collected from each size fraction as per experiment 1, depending on the volume of material generated in that fraction during sieving. Each sample was approximately 120 g.

Experiment 3: Mine sourced CID

The third calibration experiment utilised approximately 100 kg of high-grade CID ore sourced from an active pit of the BHP Billiton Yandi mine. Aggregation was not apparent upon visual inspection; however the material was subject to de-aggregation with the steel roller as a precaution, followed by rotary splitting and sieving as per experiments 1 and 2. The mine material yielded a dmax of 3.8 cm, resulting in six size fractions and a pulp series. A total of 32 samples were collected from each size fraction as per experiments 1 and 2 at approximately 130 g per sample.

Data processing

Data processing was conducted according to the procedure outlined by Minnitt et al.[3]; thus the data reduction process by which a single-stage variance is calculated for each series will not be discussed in detail here. Perhaps of greater interest to the calibration is the removal of outliers. Outliers were removed according to the "Outlier Modes" method discussed in Minnitt et al.[3], under the supervision of Agoratek International. Using this approach, a total of 46 outliers were removed from a data-set of 584 assays; over half of these were observed in Experiment 2, perhaps due to the substantial aggregation observed in this material. Following outlier removal, calibration curves with slope alpha and intercept K were compiled according to the procedure outlined by Minnitt et al.[3] (Figure 1).

Liberation size was then calculated according to the formula (from Minnit et al.[3], p. 144):

$$d_\ell = \left(\frac{K}{c.f.g'}\right)^{\frac{1}{3-\alpha}}$$

Where K is given by the intercept of the calibration curve, composition factor *c* is given by the density (as grade has been normalised

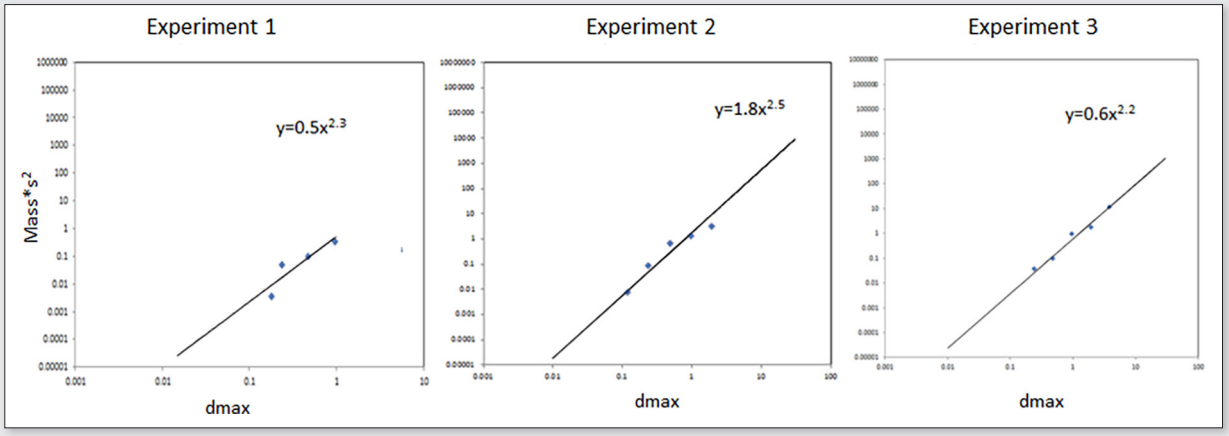

Figure 1. Al_2O_3 calibration curves for each SFA experiment

Table 1. Experimental alpha and liberation size (dL) for key analytes as determined by the SFA calibration experiments

SFA Experiment	Analyte	alpha	dL SFA (µm)
Experiment 1	Al_2O_3	2.3	8
	SiO_2	2.3	17
	P	2	2
Experiment 2	Al_2O_3	2.5	14
	SiO_2	2.4	21
	P	1.8	16
Experiment 3	Al_2O_3	1.8	25
	SiO_2	2	2
	P	1.8	3

to 1 according to the data processing procedure), shape factor *f* is assumed to be 0.5 and granulometric factor *g'* is equal to 0.44 according to the relationship of *g'* and the ratio of sieve sizes dmax/dmin (Minnitt et al.[3], p. 139). Experimental alphas and calculated liberation sizes are given in Table 1.

Results validated by QEMSCAN

QEMSCAN analysis was conducted primarily as means of validating liberation size, but also as a supplementary source of information regarding mineral abundance, particle size distribution and mineralogical associations related to liberation and locking. The QEMSCAN package also incorporated QXRD work as an additional validation method. Three samples from the calibration experiments were selected for QEMSCAN analysis, each representing a different size fraction. Two were selected from Brockman ores used in Experiment 2 and one was selected from the CID ore used in Experiment 3.

Fundamental to the work was validating mineralogical assumptions. The initial assumption considered alumina as kaolinite, which was confirmed to be the norm in the Brockman ores (Figure 2). However the QEMSCAN analysis, in addition to QXRD, suggests that no kaolinite is present in the CID material used in Experiment 3, but rather is entirely hosted by Goethite as intergrowths (Figure 3). Likewise, all silica was initially assumed to be quartz, however silica was found to be hosted primarily by kaolinite, and to a lesser degree in goethite, in the Brockman ores. While the QEMSCAN package was effective in definitively confirming some assumptions, it raised uncertainty around others; such was the case with Phosphorous hosting minerals. First, the presence of Xenotime (YPO4) as a phosphorous-host in the Brockman ores, as detected by the supplementary QXRD work, was not anticipated. Second, the presence of phosphorous was largely underestimated by QEMSCAN. While this is partly due to the fact that the system had not been programmed to detect Yttrium, it is surprising that Phosphorous hosted in Goethite was not detected; at 5x5 µm resolution, the bulk of phosphorous containing pixels were found to contain <20% Phosphorous, suggesting that either Phosphorous is present in very fine grained minerals or in mixture with other phases.

Further to this, particle distribution size analyses appear to indicate that aggregation persisted in some size fractions of the sieved calibration material, despite best efforts to remove it. For example, material from the 1.18 mm to 2.36 mm size fraction was found to be 80% passing 0.94 mm according to the QEMSCAN analysis, suggesting that the majority of material was actually smaller in size than the minimum sieve size. Size distribution analyses were conducted both on heterogeneous particles and individual mineral grains.

The QEMSCAN analysis reported liberation data for iron oxides, silicates (primarily existing as kaolinite) and intergrowths, or intimate mixtures of iron oxides and Al and Si. Liberation data for quartz was not provided. A mineral is considered liberated where area percent is greater than 90%; therefore liberation in this context is reported as the mass percent of mineral grains between 90% and 100%

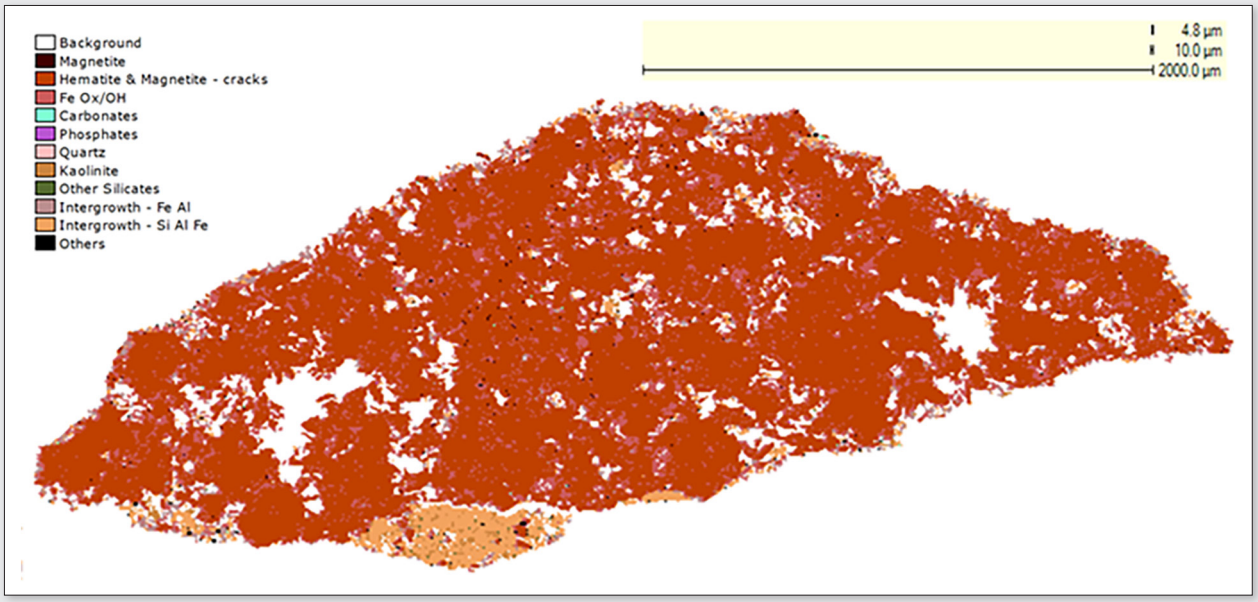

Figure 2. QEMSCAN image from a Brockman ore particle from Experiment 2 showing kaolinite grains (dark yellow) intermixed within siliceous intergrowth (light orange), interlocked with hematite grains (dark orange)

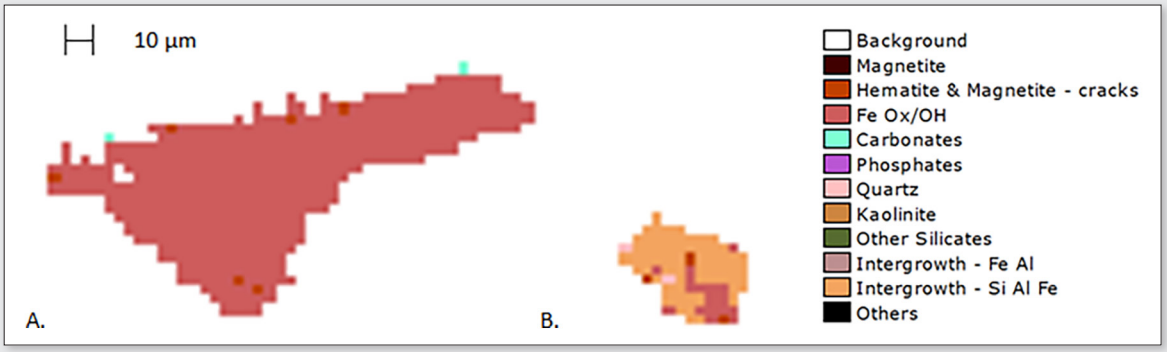

Figure 3. A. QEMSCAN image from a CID ore particle consisting primarily of goethite (dark pink) B. Intergrowth with quartz (light pink) from a CID ore showing typical size difference between goethite grains and intergrowths

liberated at a given P80, as determined by the size distribution analyses. In this way, an exact liberation size is not given, but can only be inferred based on the degree of liberation at a certain grain size. In spite of this constraint, the QEMSCAN results did not conflict with the liberation sizes calculated in the SFA calibration experiments except in a single instance. Combined results of the SFA experiments and the QEMSCAN analyses are compared in Table 2. Given that phosphorous bearing minerals were not detected at a 5x5 µm resolution in the QEMSCAN analysis, here we assume phosphorous is liberated at <5 µm. For proprietary reasons, iron results have been excluded.

Discussion

The purpose of this work was to determine the Fundamental Sampling Error of the exploration sampling protocol, firstly because it is an essential metric to confidently ensure product quality, and secondly, as a measure of comparison against future at-rig sampling technologies. It is therefore critical that the calculation of FSE is done correctly as it may ultimately inform business decisions. The QEMSCAN validation was found to be beneficial to ensuring that the mineralogical input parameters are as accurate as reasonably possible.

None of the experimental liberation sizes were in direct conflict with the QEMSCAN analysis, except in a singular instance with the phosphorous calibration in Experiment 2. The persistent aggregation confirmed by the particle size analyses may indeed point to a lesser degree of confidence in this experiment, however it must also be noted that phosphorous liberation is only assumed from the QEMSCAN analysis; a slight disagreement between SFA and QEMSCAN is not overly surprising given this degree of uncertainty.

As a mining company focused on productivity and cost, it is pertinent to discuss some practical matters associated with this work. Despite generating fewer size fractions and, consequently, fewer points with which to fit the calibration curve, we found that the RC sourced bulk material produced an experimental result which was no less reliable than the diamond core or mine sourced material. Given that most iron ore exploration primarily relies on RC drilling, this material is likely to be readily available, in addition to being low cost. Furthermore, a bulk sample can be taken from an RC rig without interrupting the standard collection of a primary sample, and it does not require interrupting production activities to collect material from an active pit. It is therefore suggested that RC sourced material is a reasonable place to start when conducting calibration experiments for K and alpha using the SFA method.

This work was conducted as the conversation about product quality, and therefore sample quality, becomes increasingly widespread in our business. In the context of this economic environment, the authors consider this most basic understanding of one's sampling protocol invaluable. With this, BHP Billiton Iron Ore reinforces the market imperative to deliver a consistent and high quality product to its customers by optimising sampling processes through the entire supply chain.

Table 2. Comparison of SFA and QEMSCAN calibration results, including assumed mineralogy as per QEMSCAN

SFA Experiment	Analyte	alpha	dL SFA (µm)	dL QEMSCAN (µm)	Assumed Mineral	Density (g/cm^3)
Experiment 1	Al_2O_3	2.3	8	<30	Kaolinite	2.4
	SiO_2	2.3	17	<30	Kaolinite	2.4
	P	2	2	<5	Xenotime	4.75
Experiment 2	Al_2O_3	2.5	14	<30	Kaolinite	2.4
	SiO_2	2.4	21	<30	Kaolinite	2.4
	P	1.8	16	<5	Xenotime	4.75
Experiment 3	Al_2O_3	1.8	25	<25	Al-Goethite	3.3
	SiO_2	2	2	Unknown	Quartz	2.6
	P	1.8	3	<5	Unknown	Unknown

References

1. Gy, P M, "*Sampling of Particulate Materials: Theory and Practice".* Elsevier, Amsterdam (1979).
2. Lyman, G J and Shouwstra, R, "Use of the scanning electron microscope to determine the sampling constant and liberation factor for fine minerals", *in Proceedings from the 5th World Conference of Sampling and Blending (WCSB5).* Gecamin, pp. 90-103 (2011).
3. Minnitt, R, Francois-Bongarcon, D and Pitard, F F, "Segregation Free Analysis for Calibrating the Constants K and alpha For Use in Gy's Formula", *in Proceedings from the 5th World Conference of Sampling and Blending (WCSB5).* Gecamin, pp. 134-150 (2011).

doi: 10.1255/tosf.68

Proper sampling, total measurement uncertainty, variographic analysis & fit-for-purpose acceptance levels for pharmaceutical mixing monitoring

K.H. Esbensen[a,b] and R.J. Romañach[c]
[a]Geological Survey of Denmark and Greenland (GEUS). Copenhagen. Denmark. E-mail: ke@geus.dk
[b]ACABS research group, Department of Chemistry and Bioscience, University of Aalborg, campus Esbjerg (AAUE), Denmark
[c]University of Puerto Rico, Department of Chemistry, Mayagüez, PR. E-mail: rodolfoj.romanach@upr.edu

Process monitoring in technology and industry in general, in pharmaceutical batch and continuous manufacturing in particular, is *incomplete* without full understanding of all sources of variation. Pharmaceutical mixture heterogeneity interacts with the particular sampling process involved (by physical extraction or by Process Analytical Technology (PAT) signal acquisition) potentially creating four Incorrect Sampling Errors (ISE), two Correct Sampling Errors (CSE) in addition to the Total Analytical Error (TAE). In the highly regulated pharmaceutical production context it is essential to eliminate, or reduce maximally, all unnecessary contributions to the Total Sampling Error (TSE) to the Measurement Uncertainty (MU_{total}) in order to be able to meet stringent regulatory blend and dose uniformity requirements. Current problems mainly stem from inadequate understanding of the challenges regarding sampling of powder blends. In this endeavor the Theory of Sampling (TOS) forms the only reliable scientific framework from which to seek resolution. We here present the variographic approach with an aim to conduct TSE error variance identification and to show how to develop *fit-for-purpose* acceptance levels in critical powder blending process monitoring. The key issue regards the nugget effect, which contains all non-optimised [ISE, CSE] plus TAE contributions to MU_{total}. A large nugget effect w.r.t. the sill is a warning that the measurement system is far from fit-for-purpose, and must be improved. Regulatory guidances have hitherto called for physical sampling from within blenders, leading to significant ISE associated with the insertion of sample thieves (sampling spears). Instead of self-crippling spear sampling we here call for a paradigm shift, very much from the TOS regimen, in the form of alternative on-line variographic characterisation of 1-D blender outflow streams. Practical illustrations and case histories are described in parallel contributions to WCSB7.

Introduction

Process monitoring in technology and industry in general, in pharmaceutical batch and continuous manufacturing in particular, is incomplete without full understanding of all sources of variation. Pharmaceutical mixture heterogeneity interacts with the particular sampling process involved, either by physical extraction or by PAT signal acquisition, potentially creating four Incorrect Sampling Errors (ISE), two Correct Sampling errors (CSE), and two process sampling errors (PSE) – in addition to the analytical error (TAE). In the highly regulated pharmaceutical production context it is essential to eliminate, or reduce maximally, all unnecessary contributions to the total measurement uncertainty MU_{total} when developing scientifically justifiable monitoring procedures. For the present overview, focus is on the effectiveness of mixer blending which is the last active processing step before tableting, i.e. how can it be ascertained that a particular blend has reached a mixing level that complies with the required 'homogeneity' and uniformity limits. The specific pharmaceutical manufacturing background was introduced to the TOS community by Romañach & Esbensen.[1] TOS provides the necessary tools to separate sampling errors from process variation, critically needed for full understanding of all sources of the sum-total of process, sampling and analytical variation.

Heterogeneity – also at the endpoint of mixing

Blending of fine-grained powders may be considered at both macro and micro-mixing scales. The proportion of a single Active Pharmaceutical Ingredient (API) may, or may not, be well distributed throughout the blend. The blend also includes other components, called excipients, that are important for various reasons. The blending process seeks to break up drug aggregates present at the beginning of the process. However, there is always a possibility that some aggregates will not respond completely if they are mainly located in an "inactive" location within the blender. Sampling methods have been developed to try to target material from such "dead spots" with an aim to protect patients from a potential drug overdose. Thus, differences in drug distribution within blends have been extensively investigated in the pharmaceutical industry, using a wide variety of analytical techniques (but largely without proper understanding of the associated sampling errors effects), and all have shown a significant scale-hierarchy of blend heterogeneity, ranging from a single dose (e.g. tablet) to the entire blender volume (mg-g-kg realm).

Heterogeneity in the framework of TOS focus on the central notion that all types of materials are heterogeneous at two fundamentally different scales, which gives rise to the two essential features: Constitutional Heterogeneity (CH) (heterogeneity between the fundamental compositional units) and Distributional Heterogeneity (DH) (heterogeneity between all virtual sampling increments throughout the lot). In the pharmaceutical realm, the focus has been to achieve "homogeneity" after the blending process (e.g. an API and several excipients) is completed. The term "homogeneous" is here not used to indicate when all units making up the lot are identical (TOS' definition), but refers to a blend with an acceptable low level of drug distribution variability, i.e. a fit-for-purpose homogeneity. The acceptable threshold drug distribution variability has been a

relative standard deviation (RSD) of less than 5% in many contexts. It is worth noting that this is identical to the demand in material balance operations, but considerably lower than requirement for commercial sampling (1%).

When a sampling process interacts with a lot with a specific heterogeneity, two sampling errors arise, the Fundamental Sampling Error (FSE) and the Grouping and Segregation Error (GSE) which influences the total MU. This is of course a trivial concept in TOS, but not in pharma: it bears noting that the differentiation into CH and DH is virtually unknown here, which is one of the reasons that a fully comprehensive theory of mixing has been very long in the making (50-60 years), and first is beginning to show a final conceptualization in the two first decades after the millennium. Sampling errors have been recognized in pharmaceutical studies, although not characterized in the same way and to the same level of comprehension as within TOS. A recently withdrawn guidance on sampling of powder blends indicated: "Sampling errors may occur in some powder blends, sampling devices, and techniques that make it impractical to evaluate adequacy of mix using only the blend data. In such cases, we recommend that you use in-process unit data in conjunction with blend sample data to evaluate blend uniformity."[2] The same document also indicated that: "If blend sampling error is detected, more sophisticated, statistical analyses should be applied to assess the situation".

However, such statistical evaluations are post fact, complex and do not give indications of how to eliminate the causative problem(s). The best approach, in pharma as everywhere else in science, technology and industry, is to completely avoid unnecessary and controllable sampling errors in the monitoring of manufacturing processes in the first place as stipulated by TOS. We here outline a radical way out of the blender sampling predicament in pharma, which amounts to a paradigm shift with respect to the current traditional situation.

Theory of mixing – does it help reducing MU_{total}?

A mixing theory is all very well – but does it help in reducing the adverse effects of sampling errors, the latter a notion that has just begun to be acknowledged in the pharmaceutical realm? The history of the evolution of a theory of mixing is presented elsewhere; only a few key aspects are necessary for the present overview.

1) It has always been assumed that effective mixing will lead to a perfect *random mixture*, and most theoretical analysis has been carried out on this background. This has a serious impact on how to address real-world mixing end-products however. It turns out that this is not a realistic end-point understanding (see further below regarding residual heterogeneity).
2) A very influential misunderstanding is that there has been only very little recognition that sampling processes suffer from significant errors inflicted by the processes themselves, i.e. Incorrect Sampling Errors (ISE). The one notable exception is that of Muzzio et al.,[3] which analysed in considerable detail the effects of using thieves for sampling of pharmaceutical mixtures, and which must be credited for pointing out the highly adverse effects resulting from forcing thieves through an in-homogenous medium ('clumped', segregated, layered) as well as casting a first empirical light on differential flow characteristics for API's and excipients respectively. API's and excipients are often of significantly different crystal/particle size and forms which can lead to markedly different flowability with resulting different mixability consequences, significantly hindering terminal mixing efforts.

How to sample from *within* a container – that is the question!

Pharmaceutical companies are extracting powder mixtures directly from blenders to check blend uniformity, and this is almost universally carried out using sampling thieves (sampling spears).

Figure 1 shows the recommended approach for what is currently considered to be adequate sampling from a V-blender. Note that

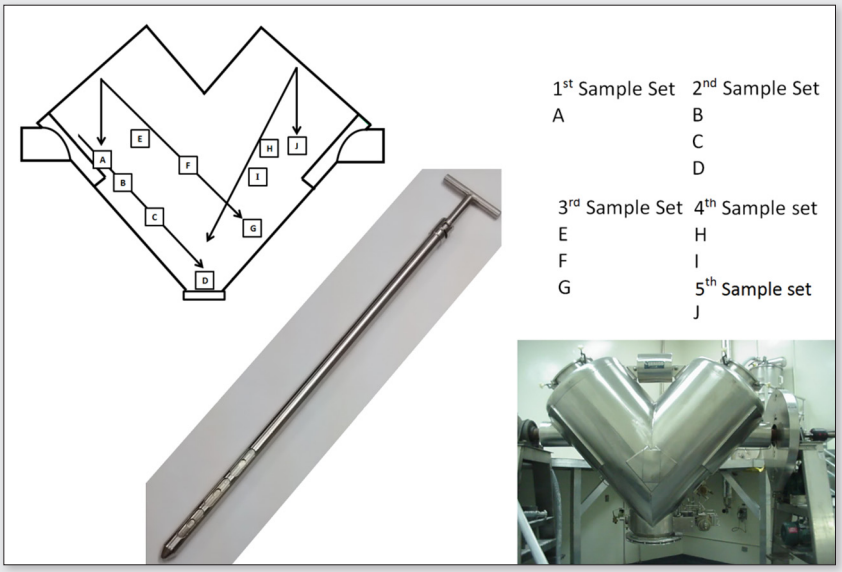

Figure 1. Traditional thief sampling (spear sampling) from *within* pharmaceutical mixing blenders (here a tumbling V-blender) recommends using 10 fixed locations organised in a certain order intended to minimize 'drag down' of powder from higher locations.[4] The fundamental assumption is that these locations (including replication at a few locations) represent the "most in-homogenous" parts of *any* blend, for *all* types of mixtures, in *all* types of blenders. Alas this assumption is untenable in the industrial practice.

each sample obtained from this geometrical scheme is analysed individually, there is specifically no requirement to aggregate these 10 singular samples into composite samples, because the objective is to estimate the residual heterogeneity present *after* mixing. This scheme is therefore forcing what is fundamentally a grab sampling approach, which has resulted in numerous difficulties w.r.t. the accuracy and precision of the desired quality check of the final blended mixtures. The sample thieves employ small, pre-set cavities to assure that the samples extracted has approximately the mass of a single dose unit, which from a 'consumer' point of view is a reasonable demand and a cogent solution: the analytical result must pertain to the dose unit the patient receives. The operation of pharma sampling thieves is otherwise standard: the cavities are closed when the metal rod is inserted into the blender and first opened for powder to flow into the cavity when reaching the appropriate location in the blender, and then closed again to remove the extracted material from the specific location targeted. However such a small sample size unavoidably forces the attending FSE to be at a maximum.

It is on this basis that a recommended geometrical set of fixed locations is assumed to be able to render a reliable quantification of the residual heterogeneity in the entire blender volume. From a TOS perspective, this is clearly an unsustainable assumption however. Sample thieves are unable to furnish representative samples under almost all circumstances – except regarding exceedingly uniform mixtures, which is of only little help when trying to monitor an ongoing mixing process, or trying to verify whether a mixing endpoint satisfies a regulation threshold, i.e. most of the times this sampling approach is used, the mixture will not be at its lowest heterogeneity near 'uniformity'. The fixed geometrical scheme sets the order in which the mixture is to be sampled with an aim to minimize the effect of disturbance of the powder bed (N.B. not to eliminate, but only to minimize this disturbance). Thief sampling is not an easy task in practice since blenders are quite large and accessibility is often restricted in the industrial practice. Thus, typically only 6 to 10 grab samples are removed from blenders following only minor variations of the master plan as illustrated, Figure 1.[4] Also, recent publications indicate that regulatory agencies want to understand the local sample-sample variation at specific locations, e.g. Reference 5. Multiple insertions of the sample thief at a specific, or a few pre-selected location(s) will only complicate the evaluation of mixing – this is just more disturbance of the final product caused by biased sampling unit operations.

Any set of fixed locations will not be able to target the worst "hidden zones" that is supposed to be associated with maximum variations in drug concentration in a comparable manner - for *all* types of compositionally different mixtures, for the *range* of different dimensions in current industrial and experimental blenders (very serious scale-up issues abound). TOS' Fundamental Sampling Principle (FSP) is systematically broken in all fixed location sampling plans, e.g. six fixed locations,[6] or 10 fixed locations in the conventional V-blender geometry,[4,7] resulting in a virtual certainty for non-representative sampling, DS 3077.[8] Thief sampling is very nearly always unable to deliver "correct sampling" in practice, which forces one to accept a sampling bias, as has been demonstrated in many practical studies in the TOS realm and also within pharma.[3] But no sampling bias can ever be estimated, nor can it ever be corrected for - with any means. In other words, the current paradigm in pharma is structurally and fatally flawed.

This state of affairs is critically serious but may not necessarily be unavoidable – TOS to the fore.

The starting task is therefore to discontinue efforts to demonstrate the adverse effects from biased sampling processes; the objective is directly the opposite: to embark on a program with an aim to eliminate all bias-prone sampling procedures, equipment and programs within pharma, i.e. to eliminate all that has to do with ISE. TOS offers a suite of practical solutions on how to eliminate or reduce the effects from the full complement of sampling errors [ISE, CSE] not in need to be iterated in detail here, suffice to point to References 9–12 and further references herein.

An iconoclastic solution – Do not sample from *within* a container!

We here propose a radical way out of the current situation in pharma - do *not* sample from within blenders!

All mixing products (with or without sampling-for-quality control) will eventually be discharged from the mixing container and transported to the tableting/encapsulating equipment immediately upon termination of the mixing stage. This process will unavoidably add to the material heterogeneity due to an assured impact of flow-segregation (pouring segregation); it is only a matter of how much additional flow/pouring segregation is heaped upon the carefully mixed product. This added heterogeneity will not be observed, or accounted for, until quality control of the final product units (tablets, capsules), i.e. any such heterogeneity is left unobserved. If the final product variability is found to be exceeding the pertinent regulatory threshold the whole batch will have to be discarded. It would have been far better if this case had been established *before* tableting and packaging, i.e. *en route* to the tableting unit, preferentially just before this last unit operation commences.

Romañach & Esbensen indicate an alternative, indeed optimal quality inspection location is on the blender output stream (obviously after the added outflow segregation impact).[1] For the sake of argument, picture the flow en route to the tableting unit as a mini conveyor belt, or similar.[13–16] The argument is that the length extension of this flow is a *linear mapping of the entire container volume* now allowing complete insight into the residual material heterogeneity after termination of mixing (plus whatever level of added flow-age segregation variability) – in stark contrast to today's situation characterized by the impossibility of adequate sampling from within the blender.

This proposal is a simple rectification that eliminates all errors associated with sampling thieves while acknowledging that the mixture is always also impacted by some level of segregation upon leaving the blender vessel. Blender sampling is to be discontinued and replaced by on-line process sampling of the output stream at a suitable location. With TOS competence, it is an easy matter to establish an effective, un-biased sampling and/or PAT signal acquisition situation on a flowing stream of matter with a small cross-sectional dimension and thus reap the full benefits of process sampling.[9–11,17,18]

Variographic characterisation of mixing processes – a new twist

Perhaps the most important issue in current pharmaceutical blending is: How to be able to recognize, identify and estimate the magnitude of the sum-total of sampling + analytical error effects influencing the total Measurement Uncertainty (MU_{total}) in current system

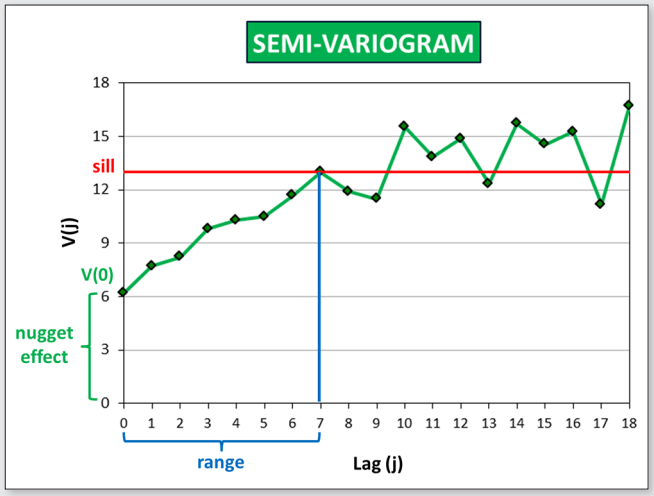

Figure 2. Generic variogram characterized by its three principal parameters: range, sill and nugget effect

implementations? TOS shows that there are many opportunities for process monitoring through the use of variographic analysis a.o. providing estimates of the nugget effect (n.e.) and the sill (MU_{total}).[8–12,17] The only necessary-and-sufficient condition is to be able to set up a TOS-correct variographic experiment, a task that will be easy to perform in the well regulated manufacturing and processing environments in pharma. N.B. All variograhic characterisation must be based on unbiased sampling processes and data (see further below).

All variograms are characterised by three principal parameters: the range, the sill and the nugget effect.

A powerful TOS insight concerns the variogram nugget effect as the magnitude made up of the sum-total of all sampling and analysis error effects contributing to the MU_{total}, i.e. [TAE, CSE, ISE]. Thus the degree to which efforts have not been fully successful in either eliminating the incorrect sampling errors, or reduce them optimally [leaving only CSE], will unavoidably show up as factors increasing the magnitude of the nugget effect.

TOS outlines that the nugget effect variance can also be viewed as the Minimum Possible Error (MPE), and how it is always possible, in principle as well as in practice, to reduce MPE either by sampling at an increased rate and/or by compositing more increments. If/when MPE is found to be "high", this is a sign that the current measurement system is marred by unacceptably high error contributions and that something must be done about it.

While these facts regarding the variogram are well-known in the TOS realm, they are virtually unknown in pharma! There is here a very fertile opportunity to introduce variographic analysis.

The variogram monitors the mixing process and at the same time characterizes the measurement system. Regarding the latter objective, it is only necessary to relate the nugget effect to the sill both as estimated by the experimental variogram. The sampling standard, DS 3077 (2013) a.o. established a generic measurement system quality index, termed $RSV_{1\text{-}dim}$, defined as the n.e./sill (expressed as a %-age). The smaller the $RSV_{1\text{-}dim}$ index, the better the measurement system will allow insight into the true process variation, as unencumbered by MU_{total} as possible.

Figure 3 shows the principal difference between an acceptable measurement system $RSV_{1\text{-}dim}$ ~30% (while appearing high this measurement system will still be able to "see" all pertinent process/product variations) and its unacceptable counterpart ($RSV_{1\text{-}dim}$ > 85%) as revealed by these simple variogram characteristics.[8]

For a perfectly mixed material, the variogram must appear flat. Any vestiges of imperfect mixing will be revealed by the form and level of the sill of the output variogram. Any significantly irregular sill 'morphology' will signify less than perfect mixing. The more a variogram represents the final state of a well-mixed blend, the smaller the overall sill.

It is never an issue to ascertain significant deviation from a flat variogram; neither is locating the lowest sill level, as shown in Figure 4 where, as an example, four alternative mixing processes variants are compared. Note that even for the lowest of the four variograms

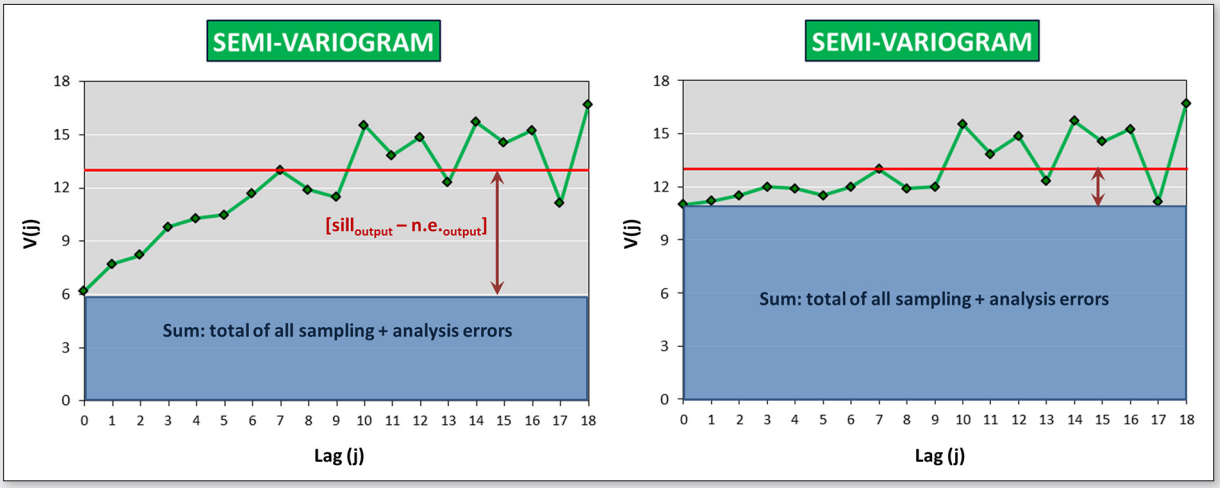

Figure 3. Principal difference between an acceptable measurement system (left) and its unacceptable counterpart (right); $RSV_{1\text{-}D}$ is ~30% (left), but >85% (right). The situation illustrated represents variographic analysis of a pharmaceutical blender output streams with identical sill levels for comparison, i.e. with similar total process variability. Resolving adverse sampling issues (reducing the nugget effect) may result in a significantly lower overall sill as well, see Figure 4.

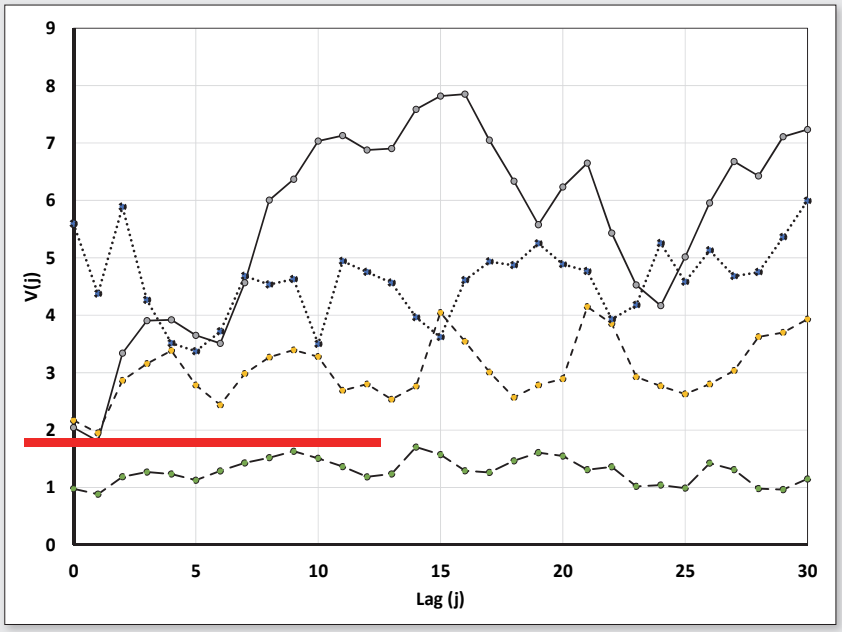

Figure 4. Schematic illustration of variograms of four alternative mixing process variants in pharmaceutical formulation development. The process represented by the bottom variogram is optimal because of its lowest sill level and least deviations from a flat variogram. All variograms reveal one form or other of feeder periodicity inheritance, only sufficiently dampened in the bottom one. Note regulator threshold criterion (horizontal line). Even though the optimal variogram is not flat the fact that it falls exclusively below the regulator threshold allows the blending process to be declared *fit-for-purpose*.

there is a minor, residual deviation for intermediate lags. Figure 4 also shows how the variograms relate to a regulator threshold translated into a variance level. As soon as when the sill is below the threshold, the mixing/blending process can be declared "fit-for-purpose".

For a blender output variogram (indeed for all process variograms) the 'true' process variation, i.e. the effective material residual variability after termination of mixing, is not the sill itself but the *corrected* sill: $sill_{output} - n.e._{output}$, arrived at by subtracting the effective MU_{total}. Thus a flat variogram does not necessarily signify a perfect, ideal mixture. Non-zero corrected sill levels: $sill_{output} - n.e._{output}$ represents *residual mixture heterogeneity* which never vanishes completely for all naturally occurring or technological mixtures, e.g. Reference 19. Thus it is the flat, low-level variogram with a non-zero corrected sill: $sill_{output} - n.e._{output}$ that represents the realistic, real-world end-point of all mixing processes.

Once embarking on a process using variographic characterization, the road is open, also for pharma, for progressing rapidly to be able to make use of the more advanced facilities, e.g. complete identification, decomposition and estimation of all process variance contributions, V(0), V(1), V(cyclic),V(trend), e.g. Pitard.[10]

Discussion

It would appear that current Federal Drug Administration (USA) demands, which has led to extensive thief sampling, to a large degree is in contradiction to its own objectives. The bias incurred by thief sampling will always cover up a non-trivial fraction (perhaps a significant, or a fatally large) fraction of the product heterogeneity manifestation (or process heterogeneity), thus effectively disallowing it to be validly observed and interpreted.

In the case of the critical pharmaceutical blending process this is an unacceptable situation. What is needed is guaranteed full observability giving optimal possibility for critical compliance testing.

Esbensen & Romañach are currently developing the variogram approach for pharmaceutical mixing quality control directed at the blender output stream in full detail.[16,20] Focus is both on the overall sill level as well as on the corrected sill: silloutput – n.e.output. This opens up for addressing regulator threshold compliance based on a dynamic, self-correcting measurement system. When a blender output variogram lies below this threshold, e.g. Figure 4, the blending product can be declared fit-for-purpose, which is all that is needed in the given regulation context. It is then not necessary to carry on with further mixing – the product is verified ready for tableting.

In the situation where it has been demonstrated that no further heterogeneity is added during tableting, variographic characterization of the blender output stream may in fact be all that is needed in order to prove to the regulator's satisfaction that also the dual final product inspection is in fact already tested and found acceptable.[21]

The proposed variographic outflow approach provides a clear alternative to current and other proposed methods that involve sampling from within the blender.[22]

The authors are in the process of outlining the present new concept in an official whitepaper format.

For the record: all valid variographic analysis must be carried out on unbiased process data. TOS is replete with warnings, elucidations and solutions regarding this stipulation.[8–12,17–19]

Conclusion—a call for a paradigm shift

There are many opportunities for TOS to be involved in significant TSE improvements in pharma, notably w.r.t. eliminating sampling bias in the primary blender sampling stage. It is here proposed to introduce a systematic variographic approach on blender outflow streams for determining the characteristics of both the product and the monitoring system itself, whether based on physical sampling

or on on-line PAT analysers. All that is needed is the availability of relevant blender output data. Variography is a highly favourable alternative to today's practice because of its self-checking MU_{total} features, i.e. the $RSV_{1\text{-}dim}$ [%] quality index, and because it can be based on routine monitoring outflow data which can be obtained as part of the on-line manufacturing process monitoring anyway.

For measurement systems in which a successful effort has been made to eliminate ISE, i.e. unbiased systems, the nugget effect (MPE) is a reliable estimate of the remaining MU_{total} precision. In the situation where the bias issue has not been fully resolved, an increased nugget effect compared to the sill is a critical and reliable warning of an inferior or a degraded measurement system. Even in this case the corrected sill: $sill_{output}$ – $n.e._{output}$ may still be able to characterize the mixing end-result although with decreased fidelity as this difference shrinks (for worse and worse total measurement systems).

Acknowledgements

This collaboration has been possible thanks to the support of the National Science Foundation (ERC research grant EEC-054085) to RR. Andres Roman Ospino and Ana Carolina Chieregati are thanked for help with figure preparation.

References

1. R. J. Romañach and K. H. Esbensen, "Sampling in pharmaceutical manufacturing - Many opportunities to improve today's practice through the Theory of Sampling (TOS).", *TOS Forum* **4,** 4-5 (2015). doi: 10.1255/tosf.37
2. Guidance for Industry Powder Blends and Finished Dosage Units-Stratified In-Process Dosage Unit Sampling and Assessment, (2003)
3. F. J. Muzzio, P. Robinson, C. Wightman and D. Brone, "Sampling practices in powder blending", *International Journal of Pharmaceutics*. **155,** 153-178 (1997). 10.1016/s0378-5173(97)04865-5
4. S. Bozzone, "Solid Oral Dosage Forms Powder Blending ", *IKEV Meeting Presentation*. (2001).
5. J. S. Bergum, J. K. Prescott, R. W. Tekwani, T. P. Garcia, J. Clark and W. Brown, "Current Events in Blend and Content Uniformity", *Pharmaceutical Engineering*. **34,** 28-39 (2014).
6. J. Berman and J. A. Planchard, "Blend Uniformity and Unit Dose Sampling", *Drug Development and Industrial Pharmacy*. **21,** 1257-1283 (1995). doi: 10.3109/03639049509063017
7. R. C. Hwang, M. K. Gemoules and D. K. Ramlose, "A Systematic Approach for Optimizing the Blending Process of a Direct-Compression Tablet Formulation", *Pharmaceutical Technology*. **22,** 158-170 (1998).
8. DS 3077, "Representative sampling - Horizontal Standard". Danish Standards Foundation, (2013)
9. P. Gy, *Sampling for Analytical Purposes*, 1st. Ed. Wiley, New York (1998) ISBN 0-471-97956-2
10. F. F. Pitard, *Pierre Gy's Sampling Theory and Sampling Practice. Heterogeneity, Sampling Correctness, and Statistical Process Control*, CRC Press, (1993) ISBN 0-8493-8917-8
11. K. H. Esbensen and L. P. Julius, "Representative Sampling, Data Quality, Validation - A Necessary Trinity in Chemometrics", *Comprehensive Chemometrics: Chemical and Biochemical Data Analysis, Vols 1-4*. C1-C20 (2009).
12. K. H. Esbensen & P.Minkkinen (Eds), "Special issue: 50 years of Pierre Gy's theory of Sampling - Proceedings: First World Conference on Sampling and Blending (WCSB1) - Tutorials on Sampling: Theory and Practice", *Chemometrics and Intelligent Laboratory Systems*. **74,** 1-1 (2004). 10.1016/j.chemolab.2004.07.001
13. A. U. Vanarase, M. Alcalà, J. I. Jerez Rozo, F. J. Muzzio and R. J. Romañach, "Real-time monitoring of drug concentration in a continuous powder mixing process using NIR spectroscopy", *Chemical Engineering Science*. **65,** 5728-5733 (2010). http://dx.doi.org/10.1016/j.ces.2010.01.036
14. M. Popo, S. Romero-Torres, C. Conde and R. J. Romanach, "Blend uniformity analysis using stream sampling and near infrared spectroscopy", *AAPS PharmSciTech*. **3,** E24 (2002). 10.1208/pt030324
15. Y. Colón, M. Florian, D. Acevedo, R. Méndez and R. Romañach, "Near Infrared Method Development for a Continuous Manufacturing Blending Process", *Journal of Pharmaceutical Innovation*. **9,** 291-301 (2014). 10.1007/s12247-014-9194-1
16. R. J. Romañach and K. H. Esbensen, "Estimating total sampling error for near infrared spectroscopic analysis of pharmaceutical blends—theory of sampling to the rescue", in Esbensen, K.H. & Wagner, C. (Eds), *Proceedings: 7th World Conference on Sampling and Blending (WCSB7)* pp 71–75 (2015). *TOS forum Special Issue* IM Publications (2015). doi: 10.1255/tosf.66
17. K. H. Esbensen and P. Paasch-Mortensen, "Theory of Sampling - The missing link in PAT" in Bakeev, K. (Ed.) *Process Analytical Technology,* chap. 3. (John Wiley & Sons, Ltd, 2010) 37-80 ISBN 978-0-470-72207-7
18. F. F. Pitard, *Pierre Gy's Theory of Sampling and C.O. Ingarell's Poission process approach, pathways to representative sampling and appropriate industrial standards* (Dr. Techn. thesis), Aalborg University,Campus Esbjerg, Denmark, 2009, ISBN 978-87-7606-032-9
19. F. F. Pitard and D. Francois-Bongarcon, "Demystifying the Fundamental Sampling Error and the Grouping and Segregation Error for Practitioners", in Alfaro, M, Magri, E, Pitard, F (Eds) *Proceedings: 5.th World Conference on Sampling and Blending*, pp 39-56 GECAMIN Publ. (2011) ISBN 978-956-8504-59-5
20. A. Sánchez Paternina, A. Roman Ospino, B. Alvarado, K. H. Esbensen and R. J. Romanach, "When "homogeneity" is expected – Theory of Sampling in pharmaceutical manufacturing", in Esbensen, K.H. & Wagner, C. (Eds) *Proceedings: 7th World Conference on Sampling and Blending (WCSB7)* pp 67–70 (2015). *TOS forum Special Issue* IM Publications. doi: 10.1255/tosf.61
21. J. Bergum, T. Parks, J. Prescott, R. Tejwani, J. Clark, W. Brown, F. Muzzio, S. Patel and C. Hoiberg, "Assessment of Blend and Content Uniformity. Technical Discussion of Sampling Plans and Application of ASTM E2709/E2810", *Journal of Pharmaceutical Innovation*. **10,** 84-97 (2015). 10.1007/s12247-014-9208-z
22. T. Garcia, J. Bergum, J. Prescott, R. Tejwani, T. Parks, J. Clark, W. Brown, F. Muzzio, S. Patel and C. Hoiberg, "Recommendations for the Assessment of Blend and Content Uniformity: Modifications to Withdrawn FDA Draft Stratified Sampling Guidance", *Journal of Pharmaceutical Innovation*. **10,** 76-83 (2015). 10.1007/s12247-014-9207-0

doi: 10.1255/tosf.75

The decision unit—a lot with objectives

Charles A. Ramsey
EnviroStat, Inc., PO Box 657, Windsor, CO 80550, USA chuck@envirostat.org

Sampling is more than shoveling material into a bucket. It is even more than using adequate mass, increments, and tools. Sampling is a systematic process that incorporates everything from development of objectives through final decision-making. Many sampling protocols currently in use focus only on the physical sample collection and ignore the preceding steps in the sampling process. The ignored steps include development of the critical decision objectives, integration of sufficient quality control, inferences from test portions to lots, and final decision making, statistical or otherwise. Without this supporting framework, it is impossible to ascertain the validity of the sampling protocols when needs or objectives change. Often, the same sampling protocol is implemented year after year without any consideration to its appropriateness.Proper Sample Quality Criteria (or Data Quality Objectives) are determined from the objectives of the project and must be an integral part of any sampling campaign. The major components of the Sample Quality Criteria are: 1) Question, 2) Decision Unit, and 3) Confidence. The Decision Unit is the specific material to which an inference from the analytical result is made and ultimately to which a decision is made. If the Decision Unit is not precisely determined and integrated into the development of the sampling protocol, the resulting decisions will be incorrect or, at a minimum, will not be cost effective. This contribution addresses development and integration of the Decision Unit into the sampling protocol framework.

Introduction

The physical process of sample collection is a very complex endeavor. It entails the consideration of appropriate mass, number of increments, correct tools, randomness, maintaining sample integrity, etc. However, physical sampling is only a part of the entire process of making decisions with analytical data regarding a specific unit of material. The complete process includes developing objectives, understanding the nature of the material sampled, developing the sampling protocol, physical sampling (including sample processing and subsampling in the laboratory), interpreting the data, and final decision-making regarding the material in question, Figure 1.

The steps in the process (Figure 1) are briefly described below:

Sample quality criteria

There are three parts of the Sample Quality Criteria (SQC)[1]

- Determination of the analyte(s) of interest and analyte concentration of concern. This is required to maintain analyte integrity and ensure proper care is taken during the sampling process not to contaminate the sample.
- Determination of the Decision Unit(s)[2]—the scale of decision-making. This will be addressed below.
- Determination of the confidence that the final decision is correct. This is a function of the error from the sampling process, how the analytical data will be used to make inference, and the consequences of an incorrect decision.

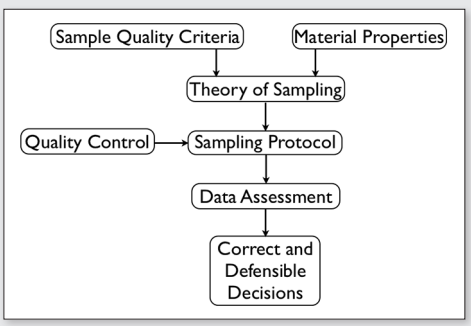

Figure 1. The comprehensive scientific, systematic process for defensible decision-making.

Material properties

There are two primary material properties

- The nature of the elements. The elements may be finite (common with attribute type sampling schemes) or infinite (sometimes referred to as bulk materials). The Theory of Sampling (TOS) covers both types of elements though most effort is on the infinite element materials.
- The nature of the heterogeneity. This includes both the constitutional (compositional) heterogeneity and the distributional heterogeneity (in time and space).

Theory of sampling (TOS)

The scientific principles that must be followed to develop a sampling protocol to ensure the samples meet the SQC.

Quality control

The specific samples collected for the determination of error. Replicate samples are generally collected to measure precision (reproducibility). A variety of other quality control samples are collected (e.g., blanks to measure contamination) to ensure the sampling process is not introducing error.

Sampling protocol

The specific instructions that must be followed to collect a representative sample (i.e., a sample that meets the SQC). It would address, among other items, sample mass, number of increments, selection and use of sampling tools, randomness, quality control, sample containers, necessary sample preservation, holding times, etc.

Data assessment

The process of analyzing the data to determine if the criteria in the SQC are met—if the data is useful for decision making. A major component of data assessment is the estimation of the actual sampling error (from the quality control samples) and comparison of this

error to the error that can be tolerated. This is inversely proportional to the confidence desired.

Correct and defensible decision

Once the data meets the SQC, they can be used to make *inference* (estimate the true concentration) to the Decision Unit. Once the true concentration is estimated, decisions can be made regarding the Decision Unit(s). These decisions could be to accept the Decision Unit as within specification, dispose of the Decision Unit (e.g. because it is contaminated), evaluate the Decision Unit further, etc. The list of potential decisions is almost infinite.

The objectives are as critical to the decision-making process as the physical sampling itself. Establishment of objectives is often overlooked. While Pitard addresses objectives[3,4] they are seldom developed by practitioners (at least in a manner suitable for the process of sampling). The objective that is most often overlooked and least understood is the scale of decision-making. The scale of decision-making, or the scale of observation, determines the specific material that needs to be included in the sample and the specific material the analytical results apply to. This scale of decision-making or observation is termed the Decision Unit (DU).

However, not all sampling objectives are related to making decisions regarding specific Decision Units. For instance, some sampling is performed for process control. However, in many fields including environmental, food, feed, pharmaceutical, chemical etc., testing products to determine if they meet specification or regulatory limits is very common. For this type of testing the Decision Unit must be established prior to sampling to determine if a limit is met. The Theory of Sampling uses the term "lot" to identify the material being sampled. Some common TOS definitions of the term "lot" are:

- The object to be evaluated[5]
- Batch of material from which increments and samples are selected[3]
- Sampling target, the specified material subjected to the sampling[6]
- All the material of interest[7]

Terminology is the cause of many disagreements and much frustration. It is therefore critical that terminology be very specific and precise so there is no room for misinterpretation. In the Theory of Sampling, the term "lot" is used to describe the material under investigation. However, this term (and the term population[8]) may not always be precise enough for development of sampling protocols and effective decision-making. In some cases, lot (and population) describes all the material under investigation, not the smaller amount of material that the decision is actually based on.

While these terms (lot, population, Decision Unit) appear very similar and descriptive, the following examples are given to demonstrate the limitation of how the term "lot" can be misused when making decisions.[†]

Dog food example

A small pet food manufacturer is making dog food by mixing ingredients in a vessel (batch) that can hold 2,000 kilograms (kg) of dog food. The pet food is formed into kibbles. The manufacturer makes five such batches each day they produce this type of dog food. This type of dog food is manufactured approximately 20 days each year; therefore, approximately 100 batches of dog food are produced annually. The batches of dog food are placed in 10 kg bags for sale to retail customers. Depending on the size of the dog (and how many treats she gets!), a single bag of dog food may last one month.

In this scenario what is the lot? Is it the 100 batches, individual 2,000 kilogram batches, individual 10 kilogram bags, individual serving size or something else? The reader may already have an idea of what the lot is or may state: "that depends." If so, what does it depend on? The lot cannot be determined until the reasons for sampling (objectives) are developed. Incorrectly identifying the lot, or not indentifying a lot prior to sampling at all, are two very common sampling mistakes that must be discontinued!

The question that begins the Decision Unit discussion is the reason for testing the dog food. One reason may be to determine if the actual nutritional value of the dog food is the same as the nutritional value listed on the bag of dog food. In this case, the Decision Unit would be a bag of dog food. Another reason may be to determine if each batch has the same concentration (within a specified error) of some specific ingredient. In this case, the Decision Unit would be individual batches of dog food. Yet another reason may be exposure to potential toxins in the dog food. If one serving of dog food contains toxins above a certain level, the dog may develop a health issue. In this case the Decision Unit is a serving of dog food. In all cases it is the same dog food, but the scale of decision-making is different and therefore the sampling protocol would be different. What can complicate this even more is that not all analytes have the same Decision Unit. It could be for some analytes that an average over a 10 kilogram bag is compared to a nutritional limit and for a prohibited toxin, every piece of dog food (kibble) must be safe. The lot (or population) may thus be quite different than the Decision Unit.

The discussion of why the dog food needs to be tested determines what analytes to analyze the dog food for and what levels may be of concern, the Decision Unit, how the data will be used in the decision-making process, i.a. It is imperative that these discussions take place before the sampling protocol is developed, not after (which is common).

While the material in question may be a single 2,000 kilogram batch (should the batch be accepted or rejected), it may not be the average of the entire batch that is of concern but the percent of bags from the batch that have a specific characteristic. For instance, the batch may be deemed acceptable if 95% of the individual bags are within a certain specification limit. In this case, the Decision Unit is the individual 10 kg bags because decisions are made on the individual bags. This obviously has a large impact on the sampling

[†]The author is not advocating a change in terminology but rather an awareness of the use of the term in compliance (regulatory, specification, etc.) sampling. If the term lot is used with the same meaning as the term Decision Unit there is no conflict. In some industries, however, the term lot is used to define a specific amount of material with similar characteristics produced under like conditions. The lot number is very important for identification and trace-back of unacceptable goods in the food and feed realms for example. When working in such industries, it is very important to have a term different than lot for the material being sampled as the term lot has already been defined (many times in actual regulations). If not, confusion will result. The term this author and others have adopted for clarity and distinction from other terms is Decision Unit.[1,2,9]

Table 1. OSHA permissible noise levels.

Duration per day, hours	Sound level dBA slow responses
8	90
6	92
4	95
3	97
2	100
1.5	102
1	105
0.5	110
0.25 or less	115

protocol. Any sample collected must represent an individual bag. If a sample is collected that represents the entire batch, it would be impossible to determine if the batch is acceptable because the percent of individual bags that meet the specification limit cannot be determined. In this case the 2,000 kg batch (material in question) may be viewed by some as a lot or population, but it is not the proper Decision Unit.

For a toxin, it may be a serving size (or daily amount) of dog food that is of concern. In other words, if a dog eats a serving of dog food that contains a toxin above a certain concentration, the dog may suffer some undesirable effect. In this case each and every serving of dog food must have a concentration of the toxin of concern below a certain level. In many cases this level would be the analytical detection limit. The Decision Unit is therefore each serving and there are many servings in each 10 kg bag. A sample that represents the entire 2,000 kg batch or even the 10 kg bag would not be sufficient to make a decision regarding the serving size.

Noise level example

The US Occupational and Safety Health Administration has developed noise guidelines for worker exposures[10]. These guidelines state permissible average noise levels for specific length of exposure. For noise guidelines, the time of exposure is the Decision Unit. As with most exposure scenarios, the longer the exposure the lower the amount to which a receptor can be exposed. The eight-hour limit is 90 dBA, but the 30-minute limit is 110 dBA (Table 1). There are different Decision Units with different limits for each. If a reading is 100 dBA, is there a problem? There is no way to know unless the Decision Unit (time in this example) is specified as part of the measurement. Without a specification of the Decision Unit, it is impossible to interpret the data. If the value of 100 dBA represents a 30-minute Decision Unit, there is not a problem. If the value of 100 dBA represents a 4-hour Decision Unit, there is a problem. Would it be possible to determine worker safety unless information is known about all the Decision Units (nine of them) that exist?

Coffee bean example

Coffee beans for import to the United States are regulated for mold. The current process to determine acceptance (conformance to the mold requirement) is to take 300 individual beans at random from the "lot" of coffee beans (usually beans are shipped in large sacks or containers). These beans are visually inspected individually for mold. If more than 25% of an individual bean is covered in mold, the bean is counted as moldy. If 21 or more of the 300 beans are moldy, the "lot" is submitted to the laboratory for further analysis. Otherwise the "lot" of coffee beans is accepted[11]. In this case, the Decision Unit is the individual bean and there are millions of these Decision Units. The analytical data (in this case a visual observation) applies to the individual bean. If a certain number (percentage) of these individual bean Decision Units meets a criteria, then the entire "lot" can be accepted.

The distinction of Decision Units and lot in this case is critically important. What if we have exactly the same testing and compliance scenario above, but the analyte of interest is not mold (attribute) but is some toxic compound (concentration)? This compound cannot be analyzed visually in the field, and a sample of 300 beans (minimum) is sent to the laboratory for analysis. Suppose the concept of Decision Units is ignored (forgotten, or never determined), and the laboratory decides to grind the entire sample so that a small portion can be selected for analysis (following the principles of TOS). In this case the analytical result represents the average of all 300 beans. This data could not be used to determine the percent of beans that have a certain threshold concentration, correct TOS or not. The result will be that a decision cannot be made, or the data will be used to make a decision, but that decision will be wrong (perhaps the correct decision will be made by dumb luck, but it would not be *defensible*). Determination of compliance is impossible without the concept of Decision Units.

Exposure to toxic analytes

Exposure to toxic chemicals must also specify a Decision Unit (or Exposure Unit). Sometimes an upper concentration limit is stated for toxic analytes, and this limit is incorrectly used to determine future health risks without consideration of Decision Units (a very common scenario). An example may be lead exposure. Limits for lead in soil for residential areas are typically in the hundred parts per million range. For this example, we will assume a limit of 100 mg/kg (part per million) as the limit to determine if the soil is "safe" (the specific language varies from agency to agency) for residential use. The obvious question should be "what Decision Unit does this 100 mg/kg apply to?" Is the Decision Unit every gram of soil in the residential area, or all the soil the receptor is exposed to? The scale of the Decision Unit has large consequences in the design of the sampling protocol and the interpretation of the analytical results. In order to determine the scale of the Decision Unit, the model that was used to develop the 100 mg/kg limit must be understood. Does lead exposure come from a single gram that is over the limit or from all the soil the receptor is exposed to on a daily or annual basis. In the case of long term (chronic) exposure, it would be all the soil the receptor is exposed to during that time. For the case of short term/one time (acute) exposure, the Decision Unit would be smaller.

The sampling protocol must consider the Decision Unit or erroneous decisions will be made regarding the exposure of lead. For example, what if the sampling protocol is to collect one or more discrete (grab, specimen) samples and then subsample 1.0 gram for metals analysis? Can this approach determine the daily or annual exposure of lead to the receptor? The answer is obviously a resounding NO. The correct sampling protocol would be to collect increments (following the principles of TOS) across the same exposure area (could be space or time or both) used to develop the 100 mg/kg limit. Collecting samples from Decision Units that are smaller

than or larger than the Decision Unit used to establish the 100 mg/kg standard would be inappropriate.

Summary of lessons from examples

- Decision Unit must be specified prior to the development of a sampling protocol.
- The Decision Unit may be specified in the case of compliance determination (regulatory or specification limits), or it may have to be developed (or determined) as in the case of exposure.
- The Decision Unit is the scale of decision-making which may be different than all the material in question. The material in question may be comprised of only one Decision Unit or many Decision Units.

Conclusion

Development of the Sample Quality Criteria is critical for effective decision-making. Of all the components of the SQC, the determination of the Decision Unit is the least understood, yet it has the largest impact on the design of sampling protocols. The Decision Unit determines the scale of sampling, the scale of inference, and how data will be used to make decisions. Without a specified Decision Unit (which may or may not be synonymous with how the term "lot" is used), it is impossible to develop a defensible sampling protocol or to correctly interpret analytical data. Without knowledge and proper application of Decision Units, many incorrect decisions will be made.

The concept of Decision Unit is critical for the development of proper sampling protocols used to determine compliance (e.g., specification limits, regulations) as has been illustrated in the examples above. There are other terms used to identify the material under investigation, including lot, population, target material, etc. Sometimes these terms are not specific enough to indentify the specific material that the decision must be made on. The term Decision Unit identifies the specific material the increments are collected from and the specific material the results and decisions apply to.

References

1. Ramsey, Charles A., Wagner, Claas, *Sample Quality Criteria*, Journal of AOAC International, Vol. 98, No. 2, March/April, 265-268 (2015).
2. Ramsey, Charles A., Hewitt, Alan D., *A Methodology for Assessing Sample Representativeness*, Environmental Forensics, 6:71-75, 2005.
3. Pitard, Francis F., *Pierre Gy's Sampling Theory and Sampling Practice* 2nd ed., CRC Press, 1993.
4. Pitard, Francis F., *Pierre Gy's Theory of Sampling and C.O. Ingamells' Poisson Process Approach*, Doctoral Thesis, Aalborg University, Denmark, 2009.
5. Gy, Pierre, *Sampling for Analytical Purposes*, Wiley, 1998.
6. *DS 3077 (2013) Representative Sampling– Horizontal Standard*, Danish Standards. www.ds.dk
7. Smith, Patricia L., *A Primer for Sampling Solids Liquids, and Gases,* ASA-SIAM, 2001.
8. Walpole, Ronald E., and Myers, Raymond H., *Probability and Statistics for Engineers and Scientists* 3rd ed., 1985.
9. Hawaii Department of Health, Office of Hazard Evaluation and Emergency Response, *Technical Guidance Manual for the Implementation of the Hawai'i State Contingency Plan*, 2009. http://www.hawaiidoh.org/tgm.aspx
10. U.S. Code Federal Regulations 29CFR1910.95(b)(2).
11. U.S., Food and Drug Administration, *Investigations Operations Manual*. http://www.fda.gov/ICECI/Inspections/IOM/default.htm

doi: 10.1255/tosf.50

Pre-crusher stockpile modelling to minimise grade variability

J.E. Everett[a], T.J. Howard[b] and K.F. Jupp[c]
[a] Emeritus Professor, Centre for Exploration Targeting, University of Western Australia, Nedlands WA 6009, Email: jim.everett@uwa.edu.au
[b] Director, Ore Quality Pty Ltd, PO Box 2579, Warwick, WA 6024, Australia. Email: orequality@bigpond.com
[c] Director, Georesphere, PO Box 443, Hillarys, WA 6923, Australia. Email: karl@georesphere.com

The use of pre-crusher stockpiles to store ore and buffer short-term fluctuations in production processes is generally well recognised and accepted. However, the potential to reduce short-term grade variation of ore entering the crusher is rarely recognised and generally poorly understood. Pre-crusher stockpiles are commonly built and reclaimed in an *ad-hoc* manner whereas well-designed and disciplined build and reclaim procedures can reduce variability into the crusher at low cost. Design options for pre-crusher stockpiling should consider the four competing roles of storage, buffering, blending and grade control, to produce predictable and uniform crusher feed grades. The selection of alternative grade allocation methods requires careful consideration, as decisions at this early stage of the production process have been shown to flow on to shipping and to the customer. This paper reports conclusions from studies simulating the reduction of grade variability for a range of alternative pre-crusher stockpiling configurations and grade allocation methods. The benefits achievable in reducing grade variance by systematically building stockpiles of appropriate dimension are quantified.

Introduction

Iron ore is used to feed blast furnaces to make steel. Steelmakers purchase and blend ore from multiple suppliers to create a consistent feed to the furnaces. A reliable long-term supplier of ore must satisfy three criteria to be an acceptable contributor of quality ore to the furnace feed blend. First the ore must be of an acceptable quality with suitably low level of contaminants, such as silica, alumina and phosphorus: this depends on the *in situ* resource and any subsequent upgrading process. Secondly, the supplier must maintain consistent average grades over time. Thirdly, there must be minimum grade variability from shipment to shipment. If these criteria can be satisfied, an iron ore supplier may remain a long-term preferred supplier, subject of course to satisfactory pricing.

Miners must therefore understand the grade variability of their delivered ore and have in place measures to control this variability.

Normally ore is hauled by haul trucks from the blasted mine face to an ore pad in front of a crusher, where it is dumped into some form of pre-crusher stockpile. When required for crushing, the stockpiled ore is picked up by a front-end loader and dumped into the crusher. Following crushing the ore is stacked onto post-crusher stockpiles, storing it ready for transportation to the port, where it is again stockpiled by automatic stacking. Finally the ore is reclaimed and shipped to customers. On some occasions the ore is dumped from the train and goes direct to the ship. Figure 1 shows a schematic of key steps in the mining process for reducing short-term grade variability[4]. The precrusher stockpiling step is highlighted.

In large operations the reduction of short-term grade variability can be achieved through capital intense methods, such as large stockpiles built by automatic stackers and reclaimers at the mines and ports. These stockpiles are essential for logistic purposes in large operations and so advantage is taken of their presence to reduce grade variability, for example by chevron ply stacking and pilgrim step reclaiming with bucket wheel reclaimers. Most of the effort put into understanding the control of short-term variability has been on these systems downstream of the crusher.[1,2,3] To date there has been little detailed study on the effect of pre-crusher stockpiling on short-term grade variability. These pre-crusher stockpiles are commonly built in an undisciplined manner and to a design that best suits the operations buffering requirements with scant regard for grade variation reduction and reconciliation.

A study has therefore been carried out into all aspects of the pre-crusher stockpile operations and the effect on short-term grade variability control. Simulation has been used to study the most effective ways to maximise the reduction of variability during crushing, through separating ore into various grade stockpiles and the design and manner of build and reclaim of these stockpiles.

The purpose of this paper is to highlight the importance of pre-crusher stockpile design and operation and to demonstrate their potential effectiveness in reducing short-term grade variability if designed and operated correctly.[4]

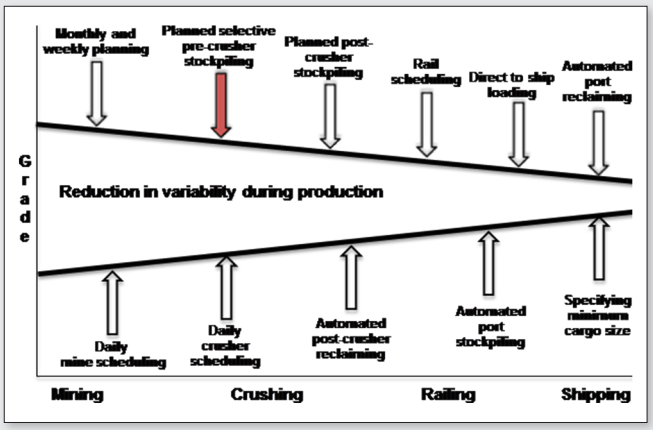

Figure 1. A schematic of key steps in the mining process in reducing short-term grade variability[8]. The precrusher stockpiling step is highlighted.

Roles of pre-crusher stockpiles

Pre-crusher stockpiles carry out the usual roles attributed to stockpiles, of buffering, storage and blending but they also have a role in grade control. Each role is summarised below:

Buffering

- Maintain sufficient tonnages to adequately decouple the mining extraction and crushing operations to maximise production, *i.e.* no bottlenecking of production.
- Allow ore to be stacked from the mine and recovered to the crusher simultaneously in a safe manner.

Storage

- When necessary, hold ore with grade that does not fit into the monthly plan but is too valuable to dispose of as waste. These stockpiles are usually referred to as long-term stockpiles. This function is outside the scope of this paper except to say that if stockpiles are used for this purpose they should not be seen as part of the normal production process.

Blending

- Break up as much of the grade serial correlation coming from the mine as practical (discussed in more detail below). It should be noted that, because of the nature of the building process, there is limited blending opportunity within the stockpile. Significant blending depends on the relationship between the stacking and reclaiming methods.
- Provide a highly predictable and uniform grade when ore is recovered from the stockpile in relatively small quantities for crusher feed.

Grade Control

- Contain adequate tonnage to allow compensation for natural grade fluctuations during a monthly plan.
- Allow ore to be traced back to floorstocks for tonnes and grade reconciliation, to examine grade bias, enable truck factor calculations and allow algorithm generation in the case of lump and fines product.
- Maximise grade separation of critical analytes to enhance the effectiveness of the daily scheduling system by providing diverse grade ore sources for the daily crusher plan (discussed in more detail below).

To satisfy all of these requirements a compromise in design is necessary. We suggest that the ideal pre-crusher stockpiling system requires:

- blended-in blended-out stockpiles (BIBO) which are paddock dumped from haul trucks in rows in one direction and then reclaimed across the build direction by front end loader for feed into the crusher;
- building to a width that facilitates full face reclaim over a period of 24 hours;[4]

Figure 2. A well designed system of paired BIBO precrusher stockpiles.

Figure 3. Building of pre-crusher stockpiles.

Figure 4. Reclaiming of pre-crusher stockpile for transport to the crusher.

- always pairing stockpiles of comparable grade, with one being built while the other is reclaimed;
- building sets of stockpiles (usually up to three pairs; high, medium and low grade) with maximum grade differential (described in detail below);
- adopting a grade separation method suited to the nature of the ore and the customer quality requirements to give maximum effectiveness when they are being blended back together to form the daily crusher product;
- allocating uniform tonnages to each set of stockpiles over a month to maximise the tonnage capacity of the pre-crusher pad;
- building to a maximum tonnage that can cover grade fluctuations within the month, so as to decouple delays in mining or crushing: *i.e.* maintain continuous sites for building and reclaiming;
- building to a minimum tonnage that satisfies the above requirements so that ore can be reliably traced back to original floorstocks for reconciliation purposes;
- building and reclaiming to completion: *i.e.* once a BIBO stockpile build commences it continues uninterrupted until it reaches the specified tonnage. It then changes to reclaim mode and is reclaimed until it is empty. This is essential to maintain grade knowledge of the stockpile as well as for reconciliation purposes.

Typical well-designed pre-crusher stockpiles are shown in Figure 2 while the building and reclaiming method is shown in Figure 3 and 4.

Grade correlations in iron ores

Iron ore being extracted from a pit exhibits two types of grade correlations.

Table 1. Typical correlations (r) values between key analytes in iron ore.

Correlations between the key analytes typical in iron ore					
	Fe	Al_2O_3	SiO_2	P	LOI
Fe	1.000	-0.572	-0.868	-0.328	-0.699
Al_2O_3		1.000	0.429	-0.008	0.122
SiO_2			1.000	0.219	0.357
P				1.000	1.000
LOI					

Firstly, there is strong cross correlations between iron and the contaminants. Typical correlations of the analytes are shown in Table1.

As can be seen there are very strong correlations between iron, silica and LOI (loss of ignition) and to a slightly lesser extent alumina. The square of the correlation coefficient is the proportion of variance shared between two variables. The -0.868 correlation between silica and iron means that they share more than 75% of variance, so that low silica is a very strong predictor of high iron content, and *vice versa*. (Since each measurement includes random error variance, the true correlations are probably even larger). There are also weaker but statistically significant correlations between alumina and silica, and between phosphorus and LOI. These types of correlations exist in most iron ores and must be considered when establishing a grade control system. Blending does not alter these correlations.

The second type of correlation is the serial correlation evident in ore sequentially extracted direct from a pit. For example if a haul truck of ore from the pit is high in silica then there is a high probability that the next truckload from the same source will be similarly high in silica. This reflects the trends evident in floorstocks and again is dependent on the process used for mining. For example the serial correlation observed when one large digging unit is working on one floorstock will be much higher than the serial correlation observed when multiple small digging units are extracting ore from various parts of the same pit. Figure 5 shows the serial correlation in the major analytes in the data used for the simulations described later in the paper.

The grades for the analytes of interest (iron, silica, alumina and phosphorus) show strongly positive serial correlation, giving short-term grade variations. This type of correlation can be reduced through the processing stream.

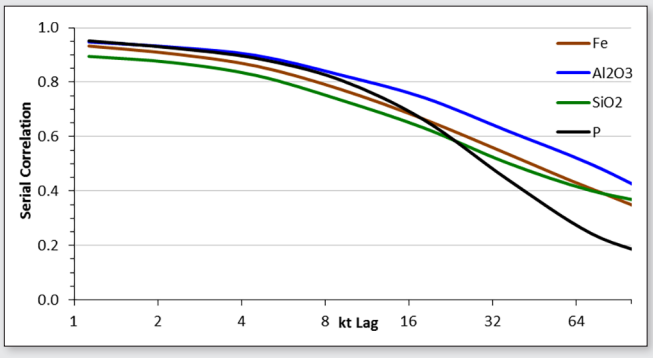

Figure 5. Serial correlation of each analyte for extracted blast blocks up to a lag of 100 kt.

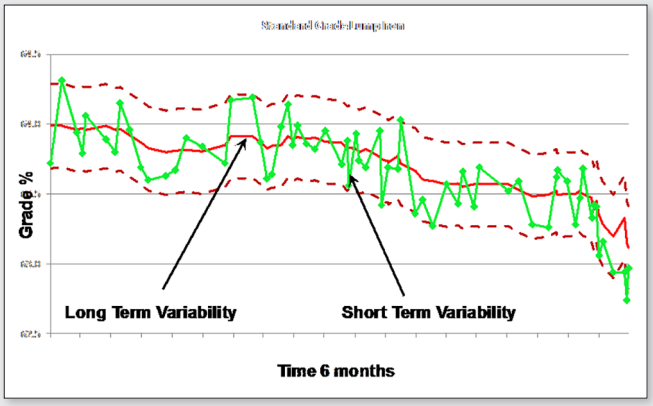

Figure 6. Typical variability coming from a mine.

Mined ore variability

An example of typical grade variability of mined ore is shown in Figure 6.

To appreciate the role of pre-crusher stockpiles in controlling variability in mining it is necessary to understand the various types and associated concepts of variability.

Wills, Jupp and Howard [5] explain the two types of variability (long-term and short-term), which are shown in Figure 6. We take their definition given to short-term variability and apply it to the variability in the run of mine ore that is delivered to the crusher for processing.

Long-term variability

Long-term variability (Figure 6) represents the trends that occur in average grade over extended time periods longer than a month and up to the life of mine. This is due to geological trends in the ore bodies as the mining progresses, or changes to the blend ratio between pits as resources are depleted and new pits come on line. The acceptable level of long-term variability is determined through the trade-offs between customer goals and the economics of the mine and resource. This type of variability is only controlled through the long-term planning process and, if unacceptable, necessitates potential changes to the mining sequence. It has no impact on the design and utilisation of pre-crusher stockpiles and as such is outside the scope of this paper.

Short-term variability

Short-term variability in the mining extraction process relates to the grade variation of the mined ore over time periods of up to a month. It is a reflection of the process capability that is embedded in the mining operations which includes the system of mining over the month and the natural variability of the ore deposit. For example, short-term variability coming from a single large digging unit that works its way through a floorstock and is then moved to another is very different from the short-term variability experienced from having multiple small mobile digging units moving around the pit. Short-term variability necessitates the design of the downstream process to reduce it to an acceptable level by the time the cargoes are produced.

Pre-crusher stockpiles play a critical role in the control of this short-term variability by one of two mechanisms. Firstly, some control is achieved by the allocation criteria on which extracted ore is directed to one of several grade separated pre-crusher stockpiles and then later blending back into the crusher blend. Secondly,

blending also occurs through the systematic building and reclaiming of pre-crusher stockpiles[4]. Both mechanisms play an important role in minimising the ship-to-ship grade variability seen by customers.

Short-term grade variability minimisation

Several simulation models were constructed in Excel using Visual Basic to examine different aspects of the short-term variability and its effect on variability of shipments.

The total data input for simulations was twelve months of data taken from the mining plan, based on the kriged block models of a planned iron ore mine located in Western Australia's Pilbara region[4]. The data were from five individual ore sources (pits) over three separate mining hub areas where pre-crusher stockpiles were used to collect ore ready for transport to the crusher. The distance between the various pits necessitated this design. Long-term variability was removed from the data to avoid clouding the short-term variability.

Ore allocation methods for pre-crusher stockpiles using floorstock grades

As previously stated, the ideal pre-crusher stockpiling system sends similar tonnages through each set of paired stockpiles, maintaining a maximum spread of grade to allow flexibility in the grade control system so as to smooth mined grades over a monthly period. This was modelled using a simulation that took an annual mine plan and simulated the flow of ore from the pit into pre-crusher stockpiles and then through the process to shipping. The simulation collected data on the effects of the different allocation methods on daily crushing grades, and on mine, port stockpiling and shipping grades which were later analysed.

A crusher decision support system based on the Continuous Stockpile Management System was incorporated to create the daily crusher feed plan, taking ore from the three hubs to maintain the daily target grade.

Nine alternative grade allocation criteria were simulated and their effectiveness determined by comparing the standard deviation of grade into the crusher, into post-crusher stockpiles, and at shipping, both with and without direct ship-to-train unloading. The best ore allocation criteria would achieve ore allocations generating pre-crusher stockpiles having maximum practical differences of all grades to give flexibility to smooth out the grades at crushing. The daily grade control system concentrated on smoothing silica and alumina: because of the high cross-correlations it also controlled iron.

A data set was developed for a twelve-month mining period that contained all of the typical ore characteristics evident in mining operations. The long-term trend was removed from these data so the results would be directly comparable to a normal monthly production run, but with the statistical power provided by the extra data across the twelve-month duration. As is normal practice for iron ore, the daily grade control simulation software emphasised silica and alumina and to a lesser extent phosphorus, with only a slight emphasis on iron.

The following alternative allocation criteria were included in the investigation:

1) **Principal components**: the calculation of principal components of each floorstock grade[6] takes into account all analytes in maximizing the separation of grades. Theoretically this method would provide the best compromise of maximum spread of all analytes over all stockpiles.
2) **Each key analyte alone**: individual analytes iron, alumina, silica, phosphorus and LOI were used as allocation methods.
3) **Silica plus alumina**: similar to above but representing the majority of gangue in the ore.
4) **Random**: blocks were allocated in a totally random manner, independent of grade, to each of the pre-crusher stockpile sets available. The allocation of incoming ore was based on which paired build stockpile had the lowest current tonnage, with no

Table 2. Distribution of grades achieved in the simulation for various separation criteria. Grey background indicates the analytes used to select in the particular allocation criteria. The absolute differences between the stockpiles (highlighted) are a proxy for the 'most effective' analyte grade separated in the stockpiles.

Allocation critria	Pile Distribution	Average BIBO Stockpile Grades						Absolute Difference in Average Stockpile Grades					
		Fe	Al_2O_3	SiO_2	P	LOI	SiO_2+Al_2O_3	Fe	Al_2O_3	SiO_2	P	LOI	SiO_2+Al_2O_3
Principal Component	Low	56.64	3.63	6.58	.113	8.06	10.22	1.65	0.49	1.54	0.007	0.30	2.03
	High	58.29	3.14	5.04	.120	7.76	8.18						
Fe	Low	56.55	3.56	6.48	.120	8.37	10.04	1.84	0.34	1.34	0.006	0.94	1.68
	High	58.39	3.22	5.14	.113	7.44	8.36						
Alumina	Low	56.94	3.68	6.31	.109	7.85	10.00	1.06	0.59	1.00	0.016	0.11	1.59
	High	58.00	3.09	5.31	.125	7.96	8.40						
Silica	Low	56.65	3.61	6.61	.113	8.04	10.22	1.62	0.44	1.58	0.008	0.27	2.03
	High	58.27	3.17	5.03	.120	7.77	8.19						
Phosphorus	Low	57.17	3.31	5.84	.142	8.30	9.15	0.60	0.15	0.05	0.091	0.78	0.10
	High	57.77	3.46	5.79	.091	7.52	9.25						
LOI	Low	56.86	3.36	6.00	.125	8.62	9.36	1.23	0.06	0.38	0.02	1.44	0.32
	High	58.09	3.42	5.62	.108	7.18	9.04						
SiO_2 + Al_2O_3	Low	56.69	3.65	6.59	0.11	7.96	10.24	1.54	0.51	1.54	0.012	0.11	2.05
	High	58.23	3.14	5.05	0.12	7.85	8.19						
Random	Low	57.45	3.39	5.83	.118	7.90	9.22	0.03	0.01	0.03	0.003	0.02	0.04
	High	57.49	3.38	5.80	.115	7.91	9.18						
Value	Low	56.59	3.62	6.57	.117	8.16	10.18	1.74	0.46	1.50	0.000	0.50	1.96
	High	58.34	3.16	5.06	.116	7.66	8.22						

reference to grade. This would represent a practice of stockpiling with no grade control objective or the ultimate situation for a poorly executed grade control regime.

5) **Value**: this criterion was developed to allocate the ore coming from the pits based on the "value" to customers; for example; high iron, low silica, alumina and phosphorus are of greater value than ore of low iron, high silica, alumina and phosphorus. The exact calculation is:

$$\text{Value} = \sum\text{Stress}[i] = P[i].\sum(\text{Grade}[i]-\text{Target}[i])/\text{Tolerance}[i],$$

where: X[i] = the relevant number for Fe, Al_2O_3, SiO_2 and P

P[i] = 1 for Fe and -1 for Al_2O_3, SiO_2 and P, categorising their value to the customer.

The average grades achieved using the alternative allocation criteria for two sets of pre-crusher stockpiles, *i.e.* low and high grade at one of the mine sites using the nine alternative criteria, are shown in Table 2. Note the cut-offs to each high and low stockpile set were determined so as to facilitate uniform tonnes into each stockpile set at each hub.

The results show the analyte specific allocation criterion gives the maximum separation of that analyte, as expected. The cross correlations complicate but also complement the allocation criteria based on a single analyte. While it appears that it is only one analyte that is being used to allocate ore, other analytes are also being separated, because of the cross correlations. For example when alumina is used as the separation criteria, a reasonable separation of iron and silica also occurs. This cross correlation is obviously not destroyed during the allocation criteria for single analytes and is the reason for success of these apparently simple allocation methods.

The principal components have an averaging effect on the grades in the stockpiles and are not as effective in utilising the natural cross correlations within the ore. Hence the principle component and value do not achieve as large a separation of any individual analyte overall when compared to the single analyte methods of separation.

Random allocation presented no significant grade separation, as expected.

These stockpiles from all pits were then run through the simulation, allocating a constant tonnage to be crushed each shift. The standard deviations of the daily crusher grades for each analyte produced over the year are shown in Figure 7. However, the standard deviations do not provide comparable measures of quality, since each analyte has a different dimension.

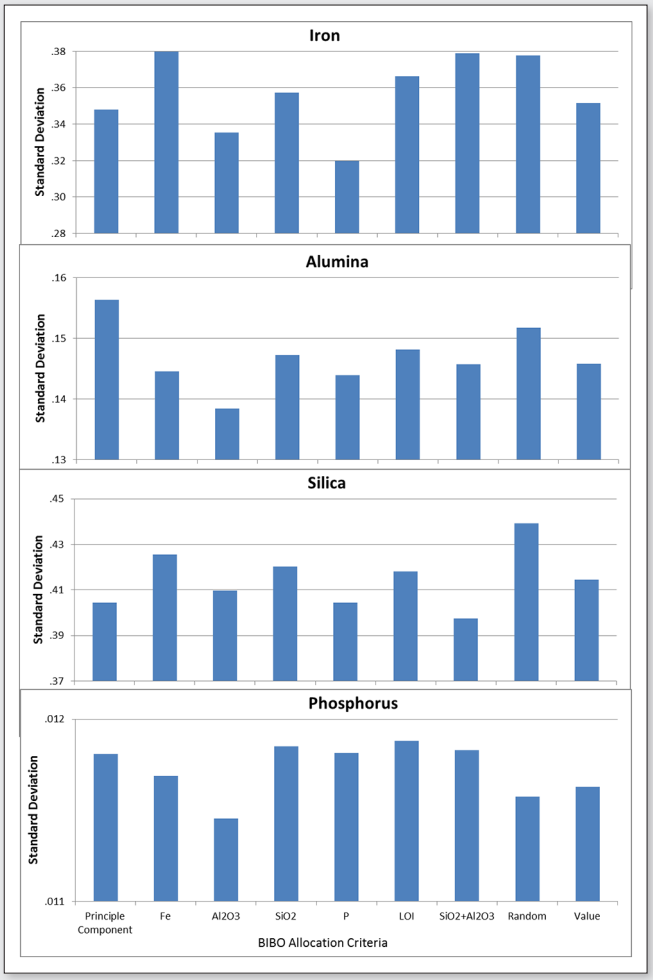

Figure 7. Shows standard deviations of the daily crusher grades for each allocation alternative.

Figure 8 shows the average daily total grade stress for the alternative allocation criteria. As we saw earlier, the stress for each analyte is its deviation from target grade, divided by the tolerance. Each analyte stress is dimensionless. Squaring each stress component and adding them together gives the total grade stress. The total grade stress is thus a dimensionless measure of overall departure

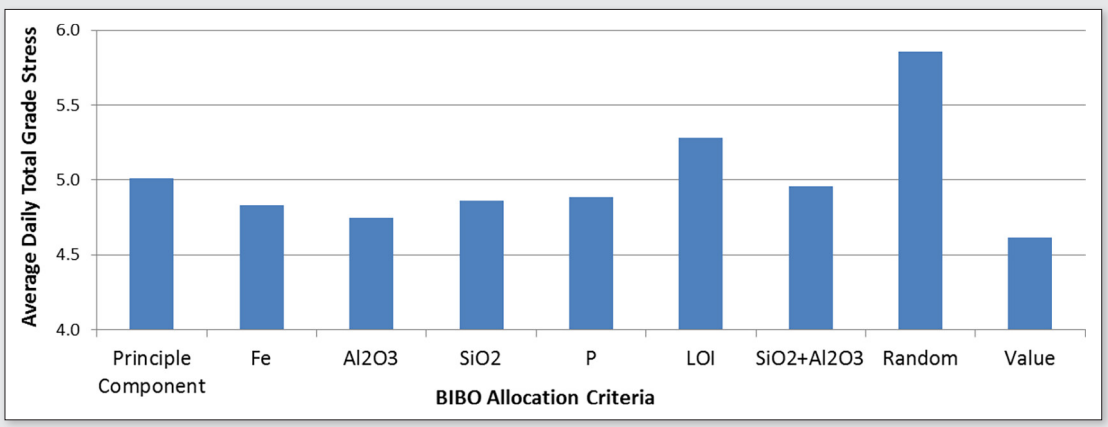

Figure 8. Average daily crusher total grade stress for alternative allocation criteria.

from target grade, appropriately weighted for each analyte. A total grade stress of zero would mean that the target grade has been exactly met for each analyte.

The average crusher total grade stress can thus be used as a measure of success in achieving target on all analytes during each daily grade scheduling process. From Figure 8, it appears that the alumina allocation criterion gave near to the best result, *i.e.* lowest standard deviation overall for all analytes. For total grade stress, the value criterion was slightly better, but its complicated nature makes it less attractive for the normal production process.

The effects of various ore grade allocation methods on shipping variability

The reclaimed BIBO stockpile data from each allocation method were finally used as input data for the overall process simulation that took the ore from pre-crusher BIBO stockpiles through crushing, onto 130 kt post-crusher stockpiles. The ore was then railed to the port and stacked onto 200 kt stockpiles, or as an alternative it was loaded direct to ship 33% of the time simulating the normal potential for such an activity (a method to reduce serial correlation). Finally the ore was loaded as 90 kt ship cargoes.

The standard deviations for each key analyte for a selected number of the allocation criteria are shown in Figure 9.

While there is a significant reduction in variability as a result of the post-crusher and port stockpiling, the influence of the allocation method for pre-crusher stockpiles is still evident with the alumina allocation criteria giving the lowest overall shipment standard deviations. Even when direct to ship is employed to reduce variability, the effect of pre-crusher allocation criteria can still be seen.

Mechanism of grade reduction in grade separated pre-crusher stockpiles

The relationship between the variation in grade over a month coming out of the pits and the ore movement tonnage in the pre-crusher stockpiles was studied in more detail at one of the mine hubs to better understand the mechanisms at play in the pre-crusher stockpiles which are reducing the serial correlation and hence the variability. Alumina was used as the allocation criteria.

Note that ore was coming out of the pit at the grade shown but was moved from the stockpiles to the crusher so as to maintain the average grade for all the analytes, taking into account the other hub contributors as well. The results are shown in Figure 10 with the grades on the left for iron, alumina and silica and the percentage of the total tonnes on the pre-crusher pad in each of the high, medium and low alumina stockpile sets on the right. The red lines represent the average grade and percentage tonnes. What can be seen is the build-up of tonnes in the high alumina stockpile set when the pit is running high in alumina and decreasing when the pit is running low in alumina. The effect of the cross correlations are also evident in the fluctuations in iron and silica. In the early period of the month it is evident that the low alumina stockpile pair were fully depleted of ore because the pit was running high alumina and there were insufficient tonnes in the stockpiles. The resulting crusher grades cannot be shown because these stockpiles are blended with stockpiles from other hubs as they go through the crusher to achieve the desired target grade, taking into account the variability coming out of these pits.

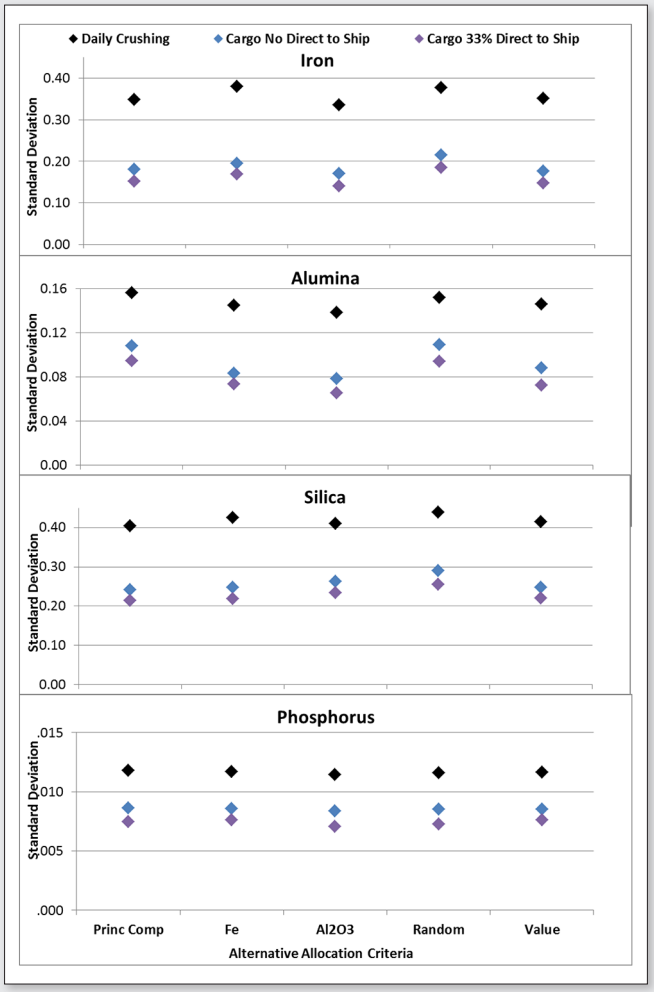

Figure 9. The standard deviation of daily crushing and shipping showing influence of the various pre–crusher allocation methods on the finished product.

We can conclude that, if the pre-crusher stockpiles are managed correctly and built to the correct size, they can provide a significant opportunity for reducing grade variability and serial correlation. However, this is dependent on using the correct allocation criteria to separate the stockpile pairs.

Conclusion

There is a low-cost opportunity to maximise the effectiveness of pre-crusher stockpiling to assist in controlling short-term grade variability. The benefit of variability reduction into the crusher will flow through the production process and eventually to the customer.

A significant reduction in short-term variability can be achieved by the use of adequately sized BIBO paired stockpiles using a grade differentiation system that best matches the grade and cross correlations characteristics of the ore. The ideal size of the stockpiles is dependent on the serial correlation of the extracted ore as well as the crusher and shipping variability requirements on a monthly basis. Simulation modelling can assist in determining the most appropriate stockpile sizes and grade allocation methods to meet operational and organisational requirements.

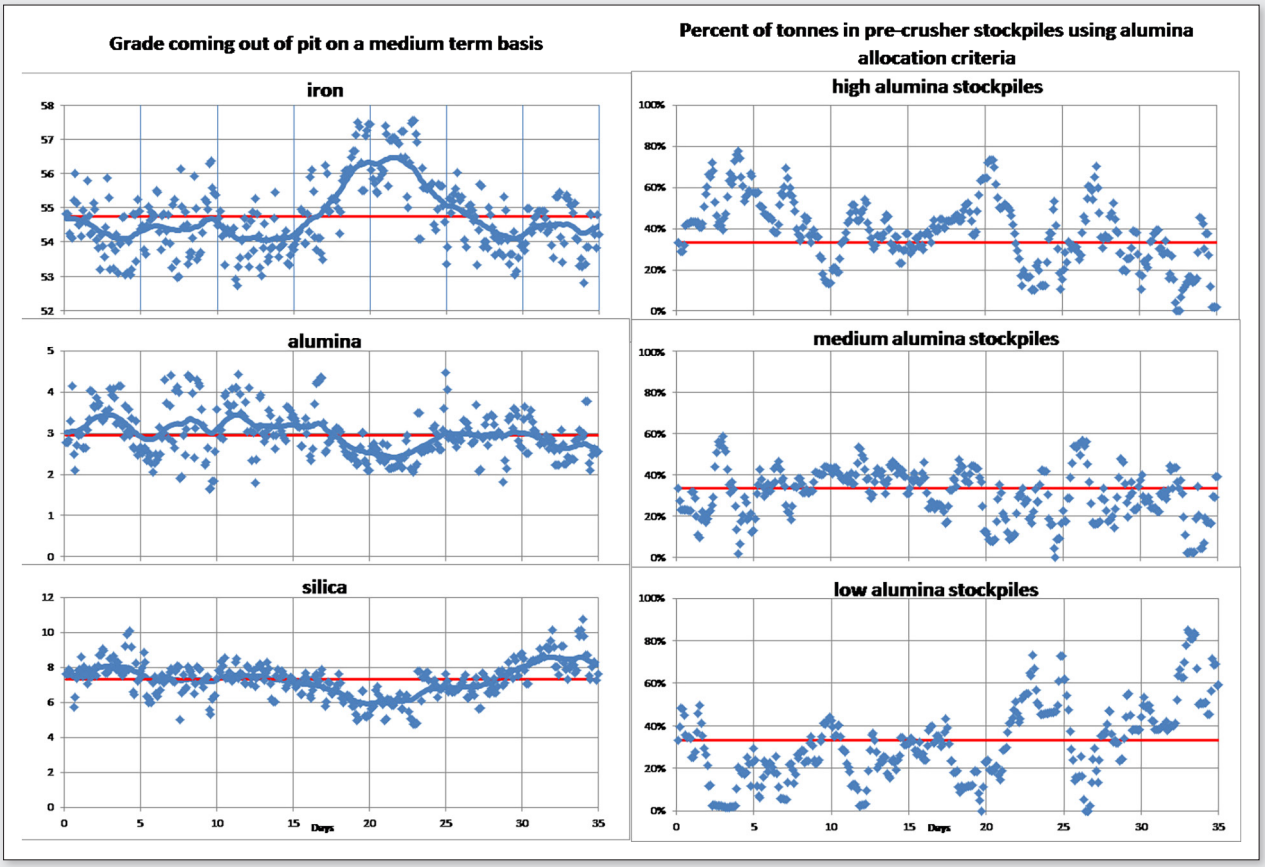

Figure 10. Grades coming out of a pit on the left hand side and pre-crusher stockpile tonnage distribution in response to ore coming from pit and requirement to crush ore to attain target grade for all analytes. Red lines are average grade and average percent ore distribution.

References

1. Gy, P.M. A new theory of bed-blending derived from the theory of sampling-development and full-scale experimental check, *Int. J. Miner. Process*., 8/3, 201–238 (1981).
2. Benndorf, J. Investigating in situ variability and homogenisation of key quality parameters in continuous mining operations, *Min. Technol*., 122/2, 78–85 (2013).
3. Robinson, G. K. How much would a blending stockpile reduce variation, *Chemometr. Intell. Lab*., 74, (1), 121–133 (2004).
4. Jupp K., Howard T.J. & Everett J.E The Role of Precrusher Stockpiling for Grade Control in Mining, *Applied Earth Science*, 122/4, 242-255 (2013).
5. Wills, A., Jupp, K.F. and Howard, T.J. The product quality system at Cliffs Natural Resources – Koolyanobbing Iron Ore Operations, *Proceedings Iron Ore 2011*, 563–574 (2011), Melbourne, The Australasian Institute of Mining and Metallurgy.
6. Everett, J.E., Howard, T.J. and Jupp, K. Simulation modelling of grade variability for iron ore mining, crushing, stockpiling and ship loading operations, *Min. Technol*., 119/1, 22–30 (2010).

doi: 10.1255/tosf.65

Placer gold sampling—the overall measurement error using gravity concentration on particle size ranges during sample treatment

Stéphane Brochot[a]* and François Mounié[b]
[a]Caspeo, 3 avenue Claude Guillemin BP36009, Orléans CEDEX 2, France. E-mail: s.brochot@caspeo.net
[b]IDM Guyane, Rémire Montjoly, Guyane Française. E-mail: idmguyane@hotmail.fr

Placer deposits are generally characterized by low grade of free gold. This is the case in French Guiana where the main placer deposits are in the river bed. Most have already been exploited by very small mining companies using sluices. If this technology is efficient for coarse gold, it releases fine gold in the tailings. During the last years, studies have been performed on various sites and recoveries have been estimated between 40 and 60% depending on the size distribution of gold particles and of the quality of the sluice configuration. Many recent or ancient tailings are available with a non-negligible quantity of remaining gold, offering retreatment opportunities. They are generally found in the form of sand heaps with the shape of an alluvial fan originating at the sluice discharge. Due to the resulting large distribution heterogeneity it is necessary to take many samples at many strategically deployed locations. These samples have to be large enough to be representative of the local material. As gold is mainly liberated in this type of lot, traditional sample treatment with successive size reductions and sub-samplings is not efficient and can be very expensive. Another approach using sieving and gravity concentration per particle range is preferred and presented here. After presentation of the sampling and measurement protocol used, this paper focuses on estimation of the overall sampling error. Various tailing cases are presented for which retreatment decision depends on the level of confidence obtained for the estimate of the quantity of recoverable gold.

Introduction

Most of the historical gold production in French Guiana came from placer deposits. It is still the situation case today even though more and more primary gold deposits are also exploited. The main technology used for gold recovery has been the sluice approach which is efficient for coarse free gold but less so for fine free gold and remaining embedded gold associated with minerals coming from the primary deposit sources. This is why sluice rejection lots contains a non-negligible quantity of gold, which can be valuable when the gold price is high enough as it is the case today. During the years 2006 and 2007, measurement campaigns have been performed on several production sites to estimate the remaining gold in the sluice residues and the technical and economic feasibility of their retreatment.

The objectives of the sampling campaigns were:

- Estimate the quantity of gold remaining in sluice rejects;
- Design of the retreatment process and estimation of its profitability;
- Design of a processing plant for placer gold deposit able to maximise the recovery and minimise the quantity of gold losses in the tailings.

Knowing the accuracy of the measurements (or, conversely, designing the measurement procedures to achieve the Data Quality Objective) is a key step in the financial risk assessment.

The preparation method of such placer samples using screening and gravity concentration has been used since the beginning of the gold deposit sampling. Ancient miners were just using the pan[1]. The last century has seen the emergence of heavier sample preparation plants using various technologies from sluice to centrifugal concentrators[2]. If these techniques have been mentioned in the theory of sampling[4, 5], their advantage in terms of overall measurement error has been rarely treated.

This paper describes the sampling and measurement protocol with a detailed presentation of the procedures for sample collection, sample preparation and various measurements performed on it. From this well-structured process, it is possible to estimate the sampling and analytical errors through the moments of their calculable components (such as fundamental sampling error, grouping and segregation error or direct measurement error linked to devices). In addition to the objective of material characterisation for processing, the results obtained from this sampling campaign are used to design a sampling plan for the sole measurement of gold. Then a general procedure is proposed for the measurement of the gold content of such placer deposits or tailings.

Sampling and measurement procedures

The set of studies presented here have been performed at the demand of several Small and Medium Enterprises (SME) producing gold from small alluvial placer deposits or primary gold ore bodies in the department of French Guiana situated between Brazil and Surinam. It mainly concerns permits of exploitation of small areas in the middle of the rain forest only accessible by air or river, rarely by road.

In this context, the means for sample collection and preparation are limited on mine site. It is why, in the following description of the procedures, we define four different locations:

- The site: location of the sluice reject or placer deposit;
- The camp: close to the site where the personnel is living and where some means are available for sample preparation;
- The preparation laboratory: situated in the main city with available equipment for concentration, sieving and water management;
- The analysis laboratory: subcontractor performing fine sieving, pulverisation and analysis by Fire Assay.

Some mine sites were sufficiently equipped to perform at the camp the work normally done in the preparation laboratory. In addition to the objective of obtaining accurate measurements, these campaigns allowed to optimise the procedures in order to minimize the material handling and to reduce the number and masses of samples and sub-samples to carry between the site and the camp and between the camp and the laboratory. Indeed, the cost of transportation by air can be too high and the risk of sample contamination or losses is not negligible when carried by river or other land transportation.

The material characteristics required for this study are: the particle size distribution of sand and the gold content per size class, from which gold particle size distribution and global gold content are deducted. The measurements performed on each sample are then: mass of sample, masses of each size fraction after sieving, gold assaying on each size fraction for finest size classes.

Gold concentration process and rejection heap description

The mainly used concentration technique for alluvial placer deposit in French Guiana is the sluice. The sand is extracted from a production cell by mechanical shovel feeding an inclined hopper where water is added for scrubbing. Some hoppers are equipped by a grate (20 to 35 mm opening) for scalping allowing a better concentration efficiency of the sluice. The oversized particles are stored in a heap close to the sluice. The slurry is then feeding a nugget box where very coarse gold can be caught. Slurry is then passing through the sluice channels where gold flakes and heavy minerals are concentrated. Overflowing barren slurry is discharged in a previously exploited cell in which sand particles constitute a sandbank as an alluvial fan. Fine gold flakes and fine heavy minerals that have not been recovered by the sluice mainly report in this heap. Very fine and colloidal particles of clay are entrained with water up to the decantation pond with some very fine gold flakes that float.

The objective of the sampling campaign was to estimate the quantity of gold remaining in these rejection heaps and select the more appropriate process for their retreatment. Figure 1 shows a typical shape of such heap with a symmetry axis in the direction of the sluice channel. As they are constituted by accumulation of layers corresponding to different parts of the production cell (with variability in head content), one can suspect a vertical stratification. The cycles of concentrate recovery are also sources of this vertical distribution heterogeneity. Nevertheless, the kinetics of gold particle settling will generate a higher heterogeneity of distribution in the horizontal plan where coarsest gold particles are accumulated just after the sluice discharge, the finer the gold particles are the farer they are deposited. The gold content in tailings is then decreasing from the top to the toe.

Due to the relative constant regime of the water flowing on the surface of the sandbank, the size distribution of the sand particles appears the same everywhere except close to the sluice discharge where coarsest gravels are retained.

Sample taking of sluice reject

Due to the heterogeneity of distribution in the horizontal direction, it can be necessary to take several samples on each heap to estimate the gold content distribution and the associated volumes to be able to calculate the weighted average of the various measured parameters. Figure 1 shows a case where two samples, R1 and R2,

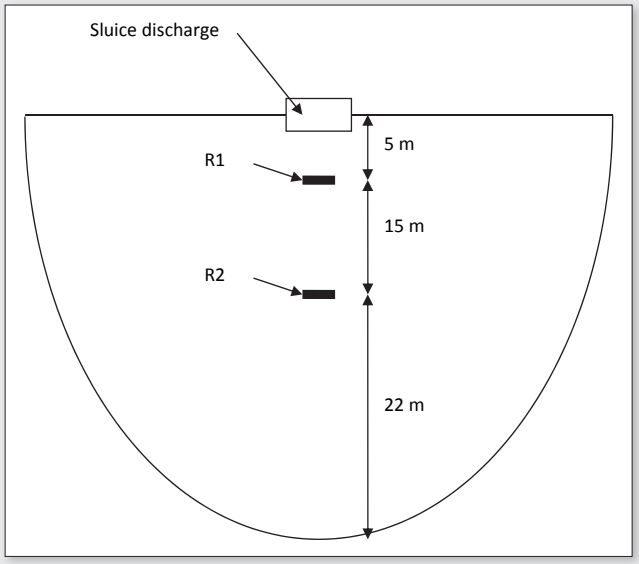

Figure 1. Overview of the typical shape of a sluice rejection heap and location of samples R1 and R2.

have been taken. A preliminary study has been performed by taking many samples along the symmetry axis and on both sides. The most untypical sample was the one taken at the sluice discharge where the remaining coarse particles of gold are concentrated. It is only representative of itself. After few meters, the distribution is less heterogeneous. It has been observed that the samples taken between 5 and 10 m from the sluice discharge on the symmetry axis have characteristics (sand size distribution and gold content) close to the average ones. In order to limit the number of samples to manage, and then the sampling campaign costs, only one primary sample has been taken for some rejection heaps.

The heterogeneity of distribution in the vertical direction suggests to take a sample on the entire height of the heap. But, as explained above, this heterogeneity is certainly smaller than the horizontal one. It is why it has been decided to limit the depth of sample taking to several tens of centimetres. When sampling ancient rejection heaps, the superficial layer can be considered as altered by weather (such as entrainment of fine particles of sand with rain and wind, or migration of gold particles with rain water infiltration) or by working activity. A superficial layer of 30 cm is then systematically removed before taking a parallelepiped-shape sample in one operation using a mechanical shovel. The bucket is then unloaded into a container constituting the primary sample with a mass between 140 and 320 kg depending on the sand fineness. Depending on the transportation conditions, it can be decided to perform some sample preparation tasks on site to reduce the quantity of material to carry to the camp.

Coarse size distribution

For such sluice rejects, there is no chance to have gold particles larger than 1 mm. The sample mass can then be reduced just by sieving. It can be performed on site or in the camp to beneficiate of better conditions for sample preparation. Sample sieving also allows the measurement of the proportions of the coarsest size classes of the sand size distribution.

The sieve series used here was: 50 mm, 25 mm, 10 mm and 2.5 mm. If a grate is used before sluicing, the 50 mm sieve is not used. Otherwise, a larger sample is taken and the passing fraction can be divided by riffle splitter after each sieving. Up to 10 mm, dry sieving is performed. If the sand is sufficiently dry, the oversize particles are clean and the retained fractions can be directly weighed and subject to a visual inspection to detect presence of coarse particles of gold or of potentially-bearing minerals. If the sand is wet, involving sticking of fine particles on the coarse ones, the retained fractions are washed with a minimum volume of clear water into a vessel, then dried and weighed. The washing water is clarified by decantation, gently siphoned off before to mix the recovered sediments (after rough drying) with the passing fraction. Wet sieving is performed for 2.5 mm, generally just before concentration in the preparation laboratory. The +2.5 mm fraction is dried and visually inspected to verify the absence of coarse gold particles or potentially-bearing minerals. In two specific cases, an additional sieving has been performed respectively at 1100 µm and 500 µm before concentration. The 1100–2500 µm and the 500–2500 µm have been washed by panning and the heavy particles have been visually inspected to verify the absence of coarse gold or potentially-bearing minerals.

In all studied cases, the retained fractions were free of coarse gold or of bearing minerals. It is then supposed all the remaining gold in the sluice rejects is concentrated in the –2.5 mm fraction which represents between 20% and 60% of the tailings, rarely more. Sieving allows to divide the sample mass by a factor between 2 and 5 keeping more or less the same fundamental sampling error regarding the gold content. A simple calculation using theory of sampling approach shows that sand crushing to produce –2.5 mm has practically no effect on the Constant Factor of Constitution Heterogeneity. That is to say crushing, conversely to sieving, is unable to reduce the sample mass and, for such low grade materials, subsampling can be affected by the Poisson process.

Gold concentration using shaking table

Considering that finer sieving is more difficult to perform and that size classes under 2.5 mm can contain gold particles, gravity concentration is another way to reduce the mass of sample by concentrating most of the gold in a small fraction of the sample. All the –2.5 mm sub-samples have been entirely treated by a Gemini shaking table well adapted for free gold and heavy minerals recovery; such heavy minerals potentially being gold-bearing minerals. The operating conditions have been tuned visually to recover the black minerals into the concentrate output. The dry mass of the –2.5 mm material subjects to concentration has to be known as accurately as possible. For that, the passing –2.5 mm has to be drained as much as possible before wet weighing and a small sample has to be taken for moisture content measurement.

The Gemini shaking tables have three outputs: heavy, mid and light products. Here, the heavy and mid products have been combined as “concentrate” and light product reports as “tailings”. The concentrate yield varies between 1.2% and 78.5%. This corresponds to a concentration factor between 1.3 and 82. Most of the treated samples have their concentrate yield between 5% and 20% (concentration factor between 5 and 20). Great attention has been paid to reduce flotation of fine gold particles, specifically in the container receiving the products of the table from which water is overflowing and not recovered. Fortunately, sluice rejects don’t contain very fine and colloidal particles which have been reporting into the decantation pond during primary treatment.

Size distribution and gold contents of table concentrates and tailings

The table concentrate is screened at 500 µm in the preparation laboratory. The +500 µm fraction is dried, weighed, washed by panning and the heavy particles are visually inspected to verify the absence of coarse gold or potentially-bearing minerals. In case of presence, this pan concentrate can be dried, weighed and then sent to laboratory for assaying. The –500 µm fraction is dried, weighed and sent to the analysis laboratory for fine sieving at 250 µm, 125 µm and 63 µm. In rare cases, the –500 µm fraction has been divided to perform sieving on a smaller quantity; a sub-sample has been then taken from the second part for a direct assaying. The 250–500 µm and 125–250 µm size classes are pulverised to –125 µm. The four size classes are divided to obtain 50 g of pulp for Fire Assay.

The table tailings are entirely recovered as wet material and drained as much as possible taking care to not lose the fine and light particles. They are homogenized (as segregation took place in the reception vessels) and spread onto a plastic sheet to obtain a sub-sample by many increments. This sub-sample is sent to the analysis laboratory to be dried, weighed, pulverised and divided to obtain 50 g for Fire Assay.

Calculation of sampling and measurement errors

The main objective of the following demonstration is the calculation of the overall measurement error of the mean gold content of the sluice rejection heap. The calculation of the measurement error of the size distribution has been discussed in previous papers[6,7]. As the aim of this paper is to show the advantage to use screening and gravity concentration to increase the sampling accuracy, for the sake of simplification, the rejection heap is supposed to be homogeneous in distribution or, as we know it is not the case, the part of the heap around the sample location is supposed to be homogenous and constitutes a lot sufficiently large compared to the sample mass. To summarize, the only error taken into account at the primary sampling stage will be the fundamental sampling error.

Heterogeneity model

The base formulae of the theory of sampling[3,4,5,8,9], such as the heterogeneity of constitution, are considering particles individually with their key parameters: unit mass (mass of one particle) and content of critical component. As it is impossible to have such a fine description, particles are classified in numerous families in which they are supposed identical. Each family is then characterised by three parameters: the mean unit mass and the mean critical component content of the member particles, and the mass proportion of that family into the lot. These families have to be as homogenous as possible but in a reasonable number. Their parameters have to be obtained by measurement through specific experiments. It is why the first approach used in the field of ore sampling has been the classification in terms of size and density[5,8,9,10]. It is the more relevant approach as the unit mass is mainly dependant on the particle size and density, and the critical content is linked to the density. If it is not the case, specific experiments have to be performed to classify the particles of the same size class regarding their critical content[11]. In some cases, sources of heterogeneity are suspected

Table 1. Heterogeneity model.

Family name	Size range	Mean size	Unit mass	Gold content	Density (g/cm^3)	Shape factor
+50 mm sand	50–100 mm	76 mm	591 g	0%	2.7	0.5
+25 mm sand	25–50 mm	38 mm	73.8 g	0%	2.7	0.5
+10 mm sand	10–25 mm	17.7 mm	7.47 g	0%	2.7	0.5
+2.5 mm sand	2.5–10 mm	6.3 mm	332 mg	0%	2.7	0.5
+500 µm sand	0.5–2.5 mm	1.5 mm	4.5 mg	0%	2.7	0.5
+500 µm gold	0.5–2.5 mm	1.5 mm	10.7 mg	100%	16	0.2
+250 µm sand	250–500 µm	380 µm	73.8 µg	0%	2.7	0.5
+250 µm gold	250–500 µm	380 µm	175 µg	100%	16	0.2
+125 µm sand	125–250 µm	190 µm	9.23 µg	0%	2.7	0.5
+125 µm gold	125–250 µm	190 µm	21.9 µg	100%	16	0.2
+63 µm sand	63–125 µm	95 µm	1.16 µg	0%	2.7	0.5
+63 µm gold	63–125 µm	95 µm	4.13 µg	100%	16	0.2
–63 µm sand	–63 µm	35 µm	0.056 µg	0%	2.7	0.5
–63 µm gold	–63 µm	35 µm	0.266 µg	100%	16	0.2

but no measurement method exists or the technique is not available or too expensive regarding the study challenge. Hypothesis can then be done and a sensitivity analysis can be performed to estimate the impact of such assumptions[7].

Generally, the size classes used as primary family description are the ones coming from the sieve series used for the size distribution measurement. The opening ratio between two successive sieves is too large to consider a uniform particle size in such a range. The choice of the mean unit size has to be conservative but preventing excessive overestimate of the sampling variance[7]. Table 1 gives the used size ranges and the associated mean particle size for unit mass calculation. Gold is supposed to be present only in liberated pure gold particles. If some bearing minerals can contain a small content of gold, the proportion of such locked gold compared to total gold is sufficiently low to not have large effect on the sampling error estimate. In addition, the assumption of only liberated gold is conservative. As no gold or bearing minerals have been observed in the +500 µm size classes during this study, only the size classes below 500 µm have been divided into two families: sand and gold. Unfortunately, only the size distribution of the shaking table concentrate has been measured, not the one of the tailings, which is certainly different. As this difference has a low effect on the estimate of the fundamental sampling error, the size distribution of the concentrate will be used for the size distribution of the –2.5 mm sand. The gold content per size class of the concentrate gives the size distribution of the gold particles. The size distribution of gold particles in the tailings cannot be deducted without the sand size distribution and the gold content per size class. It is then assumed that only fine gold reports to the tailings as observed in many cases[12], that is to say in the –63 µm class. The set of families listed in Table 1 is used for the various heterogeneity models corresponding to the different stages of the sampling and measurement protocol. A special attention has to be paid in the number of selected particles in each family, specifically for coarse gold particles, to verify the validity of the Normal distribution assumption, and when there is a risk to be confronted to a Poisson process[5].

Fundamental sampling error of the primary sample

The relative variance of the fundamental sampling error (FSE) for the measurement of the content a_L of the critical component in the lot is given by the equation (1).

$$\sigma^2(a_L) = \left(\frac{1}{M_S} - \frac{1}{M_L}\right) \sum_{i \in I_F} m_i t_i \left(\frac{a_i - a_L}{a_L}\right)^2 \quad (1)$$

In this formula, M_S is the mass of sample and M_L the mass of the lot. The N_F families, numbered with index $i \in I_F = \{1...N_F\}$, should be as homogenous as possible, meaning that all the particles in one family have more or less the same unit mass, m_i, and the same critical component content, a_i. t_i is the mass proportion of the family in the lot. The mass of lot being significantly larger than the mass of sample, the second term of the difference is negligible.

In the case of only free gold, the gold particles are distributed in a set of families, with indexes in the subset $I_G \subset I_F$, following their size and shape. These families are characterised by a gold content $a_i = 1$ and the sum of their mass proportions is the gold content in the lot:

$$\sum_{i \in I_G} t_i = a_L$$

The other ore particles are distributed in the other families following their size, density and shape. These families are characterised by a null gold content. Taking into account this heterogeneity model and considering that the gold content in the lot is very small compared to unity, the equation (1) becomes[5,10]

$$\sigma^2(FE) = \left(\frac{1}{M_S} - \frac{1}{M_L}\right)\left[\frac{\bar{m}_G}{a_L} + \sum_{i \notin I_G} m_i t_i\right] \quad (2)$$

where the mean mass of gold particles is defined by:

Table 2. FSE for primary sampling of various sluice rejection heaps.

Sample	Sample mass (kg)	Proportion of –25 mm	Proportion of –2.5 mm	Proportion of gold + 250 µm	Proportion of gold –63 µm	Variance ($\times 10^{-6}$)	Error	Proportion of IH_{golg} [a]
#1	220	83%	49%	61.8%	4.8%	738	5.4%	83%
#2	209	89%	50%	0.7%	93.6%	52	1.5%	14%
#3	220	92%	44%	0%	71.8%	52	1.5%	33%
#4	242	95%	49%	6.6%	77.5%	59	1.5%	65%
#5	300	67%	21%	21.3%	18.3%	1084	6.5%	86%
#6	180	99%	65%	10.9%	74.1%	242	3.1%	96%
#7	190	99%	67%	6.4%	66.4%	294	3.1%	98%
#8	220	99%	55%	13.7%	50.0%	431	4.1%	98%
#9	200	98%	78%	17.6%	52.8%	1615	7.9%	99%
#10	240	97%	56%	15.7%	15.5%	425	4.1%	97%
#11	200	88%	68%	5.8%	73.8%	452	4.2%	90%
#12	15	100%	57%	19.3%	3.6%	1293	7.1%	99%
#13	40	81%	37%	17.3%	32.2%	9294	18.9%	96%

[a]Proportion of the first term of the sum of equation (2) in the sum of the constant factor of constitution heterogeneity IH.

$$\bar{m}_G = \frac{\sum_{i \in I_G} m_i t_i}{\sum_{i \in I_G} t_i}$$

Table 2 gives the variance and the error (approximately two times the standard deviation corresponding to a 95% confidence interval) of the FSE for various samples treated during this campaign. The mass of the lot is supposed to be very large compared to the mass of sample.

If the ratio between the largest sand particles and the largest gold particles is sufficiently small, the second term in the sum of the equation (2) is negligible and the simplified formula for free gold can be applied[3–5]. As shown in Table 2, it is not always the case when the proportion of the first term, the heterogeneity carried by the gold particles, is less than 95% of the constitution heterogeneity. In some cases, the number of particles of one family in the sample is too small. It mainly concerns the coarsest size class of sand or the coarsest size class of gold. In the first case, the impact on gold content variability is low. In the second case, it can be worst and the sample size has to be increased.

The calculation of the FSE for the primary sampling allows to specify the sample mass to achieve a desired level of confidence. From this primary sample, various preparation procedures can be proposed. The current study was using scalping of coarse sand particles to reduce the mass of sample to analyse and then gravity concentration. In the following sections, more conventional procedures, using sample crushing and grinding, are compared in terms of overall measurement error.

Sample screening

It has been observed that the size classes larger than 2.5 mm in the sluice rejection heap are free of gold. Removing the +2.5 mm has the effect to reduce the quantity of sample for subsequent preparation without generating fundamental sampling error. Naturally, preparation errors can take place but can be avoided by good practice.

Following the formalism proposed by Pierre Gy[9] for the general case of probabilistic sampling, the sample screening can be considered as a secondary sampling without equiprobability. The limit of non-probabilistic selection is achieved for perfect classification during sieving for which the probability of a particle coarser than 2.5 mm to be selected is 0 whereas it is 1 for finer particles. Such "sampling stage" has the particular property to have a null variance but a large bias which is absolutely manageable as it gives the link between the primary sample content and the scalped sample content. If $t_<$ is the proportion of sample passing the 2.5 mm sieve and $a_<$ the gold content in this passing fraction, the content in the primary sample is $a_S = t_< a_<$ and

$$t_< = \sum_{i \in I_<} t_i$$

where $I_< \subset I_F$ is the subset of the indexes of the families of particles finer than 2.5 mm.

The variance of the measurement error of the gold content in the primary sample is then given by the rule of error propagation:

$$\sigma^2(a_S) = \sigma^2(t_<) + \sigma^2(a_<) \quad (3)$$

providing the measurements of the proportion $t_<$ and the gold content $a_<$ have a small variance and are independent. It is true concerning the analytical error even though weighing (to obtain proportion) and subsequent processing (to obtain gold content) are performed on the same passing material. The proportion of passing material and the gold content are both subject to FSE as measured from the primary sample. If one suppose all the sample can be analysed, the gold content is then calculated by the ratio between the measured mass of gold and the mass of sample. As in first approximation the mass of sample is considered as a constant, the variance of the gold content is the variance of the mass of gold in the sample. As this mass of gold is the same in the primary sample and in the screened primary sample, the variance of the FSE is well the one calculated by equation (2).

Considering a reduction of 50% of the sample mass after sieving, an alternative procedure can be done with crushing of the primary sample up to –2.5 mm followed by a division to produce a secondary sample. During crushing, there is no chance to have size reduction of gold particles. It is then supposed that the size distribution of gold particles is conserved and the crushed sand has the same size distribution under –2.5 mm as the one of the table concentrate. In that case, the variance of the FSE of the secondary sampling has to be added to the previous one. As it is of the same order of magnitude than the primary one, the advantage of screening is largely demonstrated.

After screening, the heterogeneity model is limited to the 10 last families of Table 1. Their proportion in the scalped sample is:

$$t_{<i} = t_{<} t_i \quad i \in I_{<}$$

If the passing material is divided before concentration, the secondary sampling generates a FSE for which the variance is given by the equation (1) using the new heterogeneity model and the mass of passing material as lot mass. For the cases treated here, when dividing by 2, the variance is of the same order, but when dividing by 4, it is generally larger than the one of the primary sampling. If the sample is divided between two screening stages, intermediate FSE has to be considered for the proportion of undersize[7].

Sample concentration

After screening and division (if required), the sample is passing through a shaking table to concentrate gold. The gold content is then measured size by size for the concentrate and globally for the tailings. The separation cannot be considered as perfect and fine gold particles are reporting to the table tailings. As the shaking table is operating more to maximize the recovery than for concentration, only very fine gold particles, less than 63 µm, can be rejected with tailings as it has been observed in some concentration plants[12]. In absence of gold assaying size by size for the tailings, this observation is used as assumption in the current case. The separation is then considered as perfect for gold particles coarser than 63 µm and there are only –63 µm gold particles in the tailings. The other particles reporting to concentrate are heavy minerals (mainly black minerals) which can be gold bearing minerals. Nevertheless, in such alluvial placer, the proportion of locked gold is very small compared to the free gold. This effect can then be neglected. Some coarse particles of sand are also reporting to the concentrate. For simplification, we consider a mean density for all minerals other than pure gold. As the size distribution has not been measured for the tailings, it is supposed to be identical to the one of the concentrate.

If Y_c is the mass proportion of the secondary sample recovered into the concentrate, and a_c and a_t the gold content in the concentrate and in the tailings respectively, the content in the secondary sample is $a_{<} = Y_c a_c + (1 - Y_c) a_t$. Y_c being a constant regarding sampling error (it is a measurement with an analysis error given by weighing accuracy but negligible compared to the sampling errors), the variance of the sampling error is given by

$$\sigma^2(a_{<}) = \left(\frac{Y_c a_c}{a_{<}}\right)^2 \sigma^2(a_c) + \left(\frac{(1-Y_c) a_t}{a_{<}}\right)^2 \sigma^2(a_t) \qquad (4)$$

The heterogeneity model used for the concentrate is then limited to the 10 last families of Table 1. The one of the tailings is limited to the 5 last sand families and the –63 µm gold family. After drying, the concentrate can be divided before pulverisation, depending on the quantity of concentrate and the laboratory milling capacity. Similarly, the tailings are drained, then quartered to reduce the quantity to be dried and then divided before pulverisation.

Concentrate and tailings analysis

Pulverisation of concentrate and tailings are done up to have 100% passing 125 µm. If coarse gold appears retained by the sieve, then a Screen Fire Assay (SFA) is performed: Fire Assay (FA) of the oversize up to extinction, division of the passing material to obtain 50 g of analytical sample for FA. If there is no retained material in the sieve, a simple FA is performed. The advantage of SFA in case of presence of coarse gold has been proved and discussed in a previous paper[13]. To simplify the calculation, only a simple FA is presently considered. To take into account the fact that gold particles have difficulties to be ground, all gold particles larger than 125 µm in the concentrate are supposed to report into the 63–125 µm size class during pulverisation. The size distribution of pulverised sand is the one of the –125 µm fraction of the concentrate. The similar assumption is done for the tailings, all the gold particles remaining in the –63 µm size class.

The heterogeneity model used for the pulverised products is limited to the 4 last families of Table 1. As shown in Table 3, it is difficult to have low FSE variances for tailings sampling before and after pulverisation. The FSE component of the variance for the reconstituted content of the –2.5 mm material is calculated following the equation (4). It depends on the individual variances for concentrate and tailings assaying, but also on the gold split between concentrate and tailings and gold size distribution. For example, the bad level of confidence in the tailings assaying can have low effect as for sample #1 or dramatic consequences as for sample #5. In contrary, apparent better level of confidence for concentrate and tailings assaying (sample #2 compared to #1) generates a larger error.

As for screening, the advantage of using concentration, compared to a more conventional procedure using grinding and sample mass reduction, can be easily demonstrated by calculating the overall FSE variance for this method.

Proposed procedure for sampling and measurement of placer gold content

In conclusion to these calculations concerning various types of sluice rejection material, it appears difficult to propose a general procedure for sampling which can be applied whatever the size distribution of sand and, principally, the size distribution of gold. Nevertheless, it appears necessary to improve the last stages of the sampling procedure—the sampling of concentrate and tailings for assaying—in order to reduce the variance of the FSE components for the measurement of the gold content of the undersize fraction of the material. The use of SFA with a finer sieve (106 µm or 75 µm in place of 125 µm) seems absolutely necessary. In addition, the use of a more efficient concentrator, such as centrifugal concentrator, can reduce the proportion of gold in the tailings (then its impact on the overall error) as well as the quantity of concentrate allowing its entire pulverisation.

Determining the required mass of primary sample has to be conducted by the size distribution of sand. It can be easily adjusted as the size and proportion of the coarsest particles can be visually estimated. The effect of the gold content and gold particle size

Table 3. FSE for sub-sampling after screening and concentration of various sluice rejection heaps.

	Sample #1	Sample #2	Sample #5	Sample #6
Sampling of screened material				
Mass of –2.5 mm (kg)	109	104	61.6	117
Mass for concentration (kg)	27.1	25.9	15.4	29.3
Variance ($\times 10^{-6}$)	1840	21	2800	698
Sampling of concentrate				
Mass of concentrate (kg)	0.60	0.31	1.32	2.4
Mass for pulverisation (kg)	0.60	0.31	1	1
Variance ($\times 10^{-6}$)	0	0	1610	2470
Sampling for concentrate FA[a]				
Variance ($\times 10^{-6}$)	988	80	8840	4460
Sampling of tailings				
Mass of tailings (kg)	26.5	25.6	14.1	27.0
Mass for pulverisation (kg)	1	1	1	1
Variance ($\times 10^{-6}$)	36100	47100	52700	33600
Sampling for tailings FA[a]				
Variance ($\times 10^{-6}$)	368000	16700	171000	92400
FSE of equation (4)				
Variance ($\times 10^{-6}$)	5710	46860	287000	31200
Overall FSE variance[b]				
Variance ($\times 10^{-6}$)	8290	46930	291000	32200
Error (95% confidence)	17.9%	42.5%	106%	35.2%

[a]The mass of sample for FA is 50 g.

[b]Includes the variance of the FSE of the primary sampling as given in Table 2.

distribution is more difficult to appreciate before measurements. Only assumptions can be done at the light of what is known concerning process generating the tailings. A mass of 200 kg seems sufficient when a grate has been used before sluicing and the material is finer than 25 mm. If particles larger than 50 mm appear, it is preferable to increase the mass up to 500 kg. In that case, screening can be done with intermediate division of passing product.

Screening at 2.5 mm seems a good compromise between the maximum feed size to have a good efficiency of the concentration using shaking table and the difficulty to screen a large amount of material with finer sieves. Nevertheless, if the proportion of undersize material is larger than 50%, screening can be performed at 1 mm to reduce the quantity of material for concentration. The same 1 mm screening has to be done to use centrifugal concentrator. The size class 1–2.5 mm has to be washed by panning to verify the absence of coarse gold. The passing material can be divided but the secondary sample for concentration has to be between 30 and 60 kg. If coarse gold (larger than 500 µm) is suspected, this amount can be increased.

As many mine sites are equipped with shaking table, this is preferable. In this case, operating conditions have to maximize the recovery more than the concentration. The objective is to minimize the number of gold particles reporting to tailings. If the quantity of concentrate is too large, it can be reprocessed, then favouring the concentration. The second tailings have to be assayed separately. Concentration operation has to be carefully observed to detect the presence of coarse gold particles (+250 µm) and if fine gold particles are misclassified into the tailings.

The first tailings (as well as the second tailings in case of reprocessing of first concentrate) has to be screened at 1 mm and maybe at 500 µm if it can drastically reduce the mass to be analysed. The retained sand has to be washed by panning to verify the absence of coarse gold. Then the passing is divided and a second screening can be performed at 500 µm or 250 µm with similar treatment of retained sand. Last passing can be dried and divided to obtain between 1 and 2 kg for pulverisation at –106 µm. If gold particles are retained in the sieve, SFA is required. The passing powder is then divided to take 30 to 50 g for FA.

The concentrate (the second one in case of reprocessing of first concentrate) has to be screened at 500 µm. The retained particles have to be washed by panning to verify the absence of coarse gold or bearing minerals. In case of presence, the pan product is weighed and assayed. The passing 500 µm is dried and divided only if its mass exceeds 4 kg. It is then pulverised at –106 µm for a SFA.

Conclusion

Estimating gold content in a low grade placer deposit, or in tailings remaining after sluice treatment, makes it necessary to collect numerous large samples. As these samples cannot be processed

in toto by grinding, it is necessary to use concentration stages (by screening or gravity concentration) to be able to reduce the quantity of material for final analysis.

The measurements performed during this study were with the objective of placer deposit treatment or tailings retreatment. The obtained material characteristics have been used to build heterogeneity models in order to calculate the components of the variance of the overall fundamental sampling error. The results showed, a posteriori, a relatively low accuracy for the estimate of the global gold content. Considering the local conditions of work, this level appears satisfactory and the reprocessing performed after this study gave the expected gold recovery. Nevertheless, at the light of the results of this study, an enhanced procedure is proposed. It has now to be verified and the variance of the overall measurement quantified.

Acknowledgements

The authors would like to acknowledge the mining companies of French Guiana which have contracted IDM Guyane and Caspeo to perform such studies: SARL SOMIRAL, SARL SM5°, Entreprise Henrique Costa, SARL COTMIG, Compagnie Minière Boulanger and SARL SGEA. The authors would like to acknowledge also Jean-François Thomassin who was promoting this kind of study when he was in charge of the mining sector at the Trade and Industrial Chamber of Guyane.

References

1. J.M. West, *How to Mine and Prospect for Placer Gold*. Information Circular 8517, US Bureau of Mines, Washington (1971).
2. G. Beaudoin, “Gold Test on the Toson Terrace Placer, Zaamar Goldfield of Mongolia”, *World Placer Journal*. **1**, 1–9 (2000). http://www.mine.mn/WPJ1_1_1–9_placer_test.pdf
3. P. Gy, *L’échantillonnage des minerais en vrac. Tome 1 – Théorie générale*. Mémoires du BRGM, N°56, Paris (1967).
4. P. Gy, *L’échantillonnage des minerais en vrac. Tome 2 – Théorie générale, erreurs opératoires, compléments*. Mémoires du BRGM, N°67, Paris (1971).
5. F.F. Pitard, *Pierre Gy’s Theory of Sampling and C.O. Ingamells’ Poisson Process Approach, pathways to representative sampling and appropriate industrial standards*. Doctoral thesis, Aalborg University, Denmark (2009).
6. S. Brochot, “Sampling for grinding pilot plant test: the effect of size distribution variability”, in *Proceedings of the Sampling2012 Conference*, AusIMM, Perth, Western Australia, Australia, 27–28 August, pp. 127–134 (2012).
7. S. Brochot, “Application of sampling theory to optimal design of size distribution measurement procedures”, in *Proceedings of the Sixth World Conference on Sampling and Blending*, Ed by J. Beniscelli, J. Felipe Costa, O. Domínguez, S. Duggan, K. Esbensen, G. Lyman, B. Sanfurgo. Gecamin, Santiago de Chile, pp. 129–140 (2013).
8. P. Gy, *Sampling of Particulate Materials, Theory and Practice*. Elsevier, Amsterdam (1979).
9. P. Gy, *Hétérogénéité, Echantillonnage, Homogénéisation, Ensemble cohérent de théories*. Masson, Paris (1988).
10. F.F. Pitard and D. Stevens, “The development of a solution to the sample preparation of coarse gold samples”, in *Proceedings Fifth World Conference on Sampling and Blending*, Ed by M. Alfaro, E. Magri, F. Pitard. Gecamin, Santiago de Chile, pp. 331–344 (2011).
11. Ph. Wavrer, P. Botane and S. Brochot, “Sampling protocol design for characterization of plastics from small WEEE”, in *Proceedings of the Sixth World Conference on Sampling and Blending*, Ed by J. Beniscelli, J. Felipe Costa, O. Domínguez, S. Duggan, K. Esbensen, G. Lyman, B. Sanfurgo. Gecamin, Santiago de Chile, pp. 143–152 (2013).
12. G. Wardell-Johnson, A. Bax, W.P. Staunton, J. McGrath and J.J. Eksteen, “A Decade of Gravity Gold Recovery”, in *Proceedings of the World gold Conference*, AusIMM, Brisbane, Queensland, Australia, 26–29 September, pp. 225–232 (2013).
13. S. Brochot, “Standard Fire Assay or Screen Fire Assay? Application of the overall measurement error approach to choose the most appropriate method”, in *Proceedings of the Sampling2012 Conference*. AusIMM, Perth, Western Australia, Australia, pp. 135–142 (2012).

doi: 10.1255/tosf.72

The crucial role of proper sampling in food and feed safety assessment

C. Paoletti[a], K.H. Esbensen[b] and H.A. Kuiper[c]
[a]European Food Safety Authority (EFSA), Parma, Italy. E-mail: paolecl@efsa.europa.eu
[b]National Geological Surveys of Denmark and Greenland, Copenhagen and Department of Biotechnology, Chemistry and Environmental Engineering, Aalborg University campus Esbjerg (AAUE), Denmark. E-mail: ke@geus.dk
[c]formerly Institute of Food Safety (RIKILT) Wageningen UR, Wageningen, The Netherlands. E-mail: harry.kuiper@wur.nl

The general principles for safety and nutritional evaluation of foods and feed and potential health risks associated with hazardous compounds have been developed by FAO and WHO[1] and further elaborated in the EU funded project Safe Foods, where specific attention was given to a coherent scientific analysis of health and environmental risk-benefits and impacts on economics, social and ethical aspects[2]. Nevertheless, the crucial role that sampling has in foods/feed safety assessment has never been explicitly recognized. High quality sampling should always be applied to ensure the use of adequate and representative samples as test materials for all the steps of food/feed safety assessment: hazard identification, toxicological and nutritional characterization of identified hazards, as well as estimation of quantitative and reliable exposure levels of foods/feed or related compounds of concern for humans and animals[3]. The different types of substances under study which are present in food/feed matrices and commodities, raw or semi- processed, pose both general and specific challenges to the development of appropriate sampling strategies and analytical detection methods. Although it is well recognized that both sampling and analytical errors affect the reliability of any final risk estimation, traditionally much more attention has been devoted to the development and improvement of analytical methods, as compared to the development of appropriate sampling plans. But the reality is that analytical results are of low or no value, no matter the quality of the method used, if the sampling process is not representative of the entire field-to-aliquot pathway.

The Theory of Sampling (TOS) has developed over the last six decades a complete theory of heterogeneity, sampling procedures and sampling equipment assessment, the importance of which was first recognized in the mining and geological sectors, but since transgressed nearly all boundaries between science, technology and industry[4,5]. Over the course of the last 10-15 years the universality of TOS principles has been proven thoroughly, demonstrating that all sampling processes, irrespective of the nature of their target lots, need to be structurally correct (unbiased) in order to ensure a sufficient degree of accuracy and precision[6]. This is true also when assessing foods and feed safety, including food/feed contaminants, additives, naturally occurring toxins/ anti-nutrients, or contaminating micro-organisms, and whole foods/feed derived from genetically modified plants/animals.

More specifically, TOS allows estimating the variability remaining after all sources of sampling bias have been removed, i.e. the variability intrinsic to the specific material under investigation for both stationary as well as dynamic lots. From a food and feed safety perspective, this constitutes the level of unavoidable risk associated with any given survey. No other sampling framework allows objective quantification of the risk as a direct function of the specific heterogeneity properties of the test material. On the contrary: all other sampling frameworks rely on *specific* distributional assumptions, do *not* characterize heterogeneity patterns stemming from the specific properties of the test material, and do *not* include an estimation of the risk associated with sampling surveys[7]. For these reasons we consider that only TOS provides a complete framework to ensure accuracy and precision of all sampling steps involved in any given scenario, starting from the primary sampling all the way to the subsequent secondary sampling steps involved in the field-to-fork continuum necessary to monitor foods and feed safety[3].

Therefore we propose to explicitly recognize the central role of sampling in foods and feed safety assessment and to integrate TOS in the well-established FAO/WHO risk assessment approach in order to guarantee a transparent and correct frame for the safety assessment of foods and feed and the many steps of the subsequent decision making process. A key example of successful implementation of this approach regarding GMO detection and quantification was published recently[8,9,10].

References

1. FAO and WHO, *Food Safety Risk Analysis, a guide for national food safety authorities*. Geneva: World Health Organization (2006).
2. A. König, H. A. Kuiper, H.J.P. Marvin, P.E. Boon, L. Busk, F. Cnudde, S. Cope, H.V. Davies, M. Dreyer, L.J. Frewer, M. Kaiser, G.A. Kleter, I. Knudsen, G. Pascal, A. Prandini, O. Renn, M.R. Smith, B.W. Traill, H. Van der Voet, H. Van Trijp, E. Vos and M.T.A. Wentholt, in: Safe Foods - towards a New Risk Analysis Framework for Food Safety. Special Issue Food Control 21 (2010).
3. H. A. Kuiper and C. Paoletti, Food and feed safety assessment: proper sampling is imperative. *J. AOAC Int*. 98 (2015).
4. P. Gy, Sampling for Analytical Purposes. Wiley. ISBN 0-471-97956-2 (1998).
5. K.H. Esbensen and P. Minkkinen, Special Issue: 50 years of Pierre Gy's Theory of Sampling. Proceedings: First World Conference on Sampling and Blending (WCSB1). Tutorials on Sampling: Theory and Practise. Chemometrics and Intelligent Laboratory Systems 74, 236 (2004).
6. DS 3077- Horizontal Standard: Representative Sampling. www.ds.dk
7. C. Paoletti and K.H. Esbensen, Distributional assumptions in food and feed commodities – development of fit-for-purpose sampling protocols. *J. AOAC Int*. 98 (2015).
8. K.H. Esbensen, C. Paoletti and P. Minkkinen, Representative sampling of large kernel lots I. Theory of sampling and variographic analysis. *Trends in Analytical Chemistry* (TrAC) 32, 154-164 (2012).
9. P. Minkkinen, K.H. Esbensen and C. Paoletti, Representative sampling of large kernel lots II. Application to soybean sampling for GMO control. *Trends in Analytical Chemistry* (TrAC) 32, 165-177 (2012).

10. K.H. Esbensen, C. Paoletti and P. Minkkinen, Representative sampling of large kernel lots III. General considerations on sampling heterogeneous foods. *Trends in Analytical Chemistry* (TrAC) 32, 178-184 (2012).

doi: 10.1255/tosf.53

Sampling for mycotoxins in feed — heterogeneity characterization

Claas Wagner
Sampling Consultant, www.wagnerconsultants.com **E-mail:** cw@wagnerconsultants.com

The presence of mycotoxins, in particular aflatoxin B1, can cause significant health problems as well as severe societal economic losses, and is therefore regulated with respect to maximum acceptable concentration in various feed- and foodstuffs. International regulatory authorities have begun to recognize the importance of representative sampling, but sampling guidelines are only partly in compliance with the Theory of Sampling (TOS). In particular, practical guidance regarding sampling, including correct design and operation of sampling devices, including explanation on how to develop sufficient sampling protocols are lacking in current guidelines. These are critical practicalities of main importance, especially when dealing with trace concentrations and/or concentrations that are irregularly distributed - as is the case for mycotoxins. Furthermore, heterogeneity characterization, which is a necessary requirement to be able to develop valid sampling protocols or validation assessments of existing sampling operations, is currently not mentioned in the existing guidelines. The present paper focuses on heterogeneity characterization with respect to sampling of mycotoxins for 1-D and 3-D feed lots (a full analysis of all critical practicalities in sampling mycotoxins is published elsewhere). Structural guidelines for correctly designing experimental heterogeneity characterizations are presented, allowing evaluation of sampling representativeness and determination of optimal number of increments per composite sample.

Background

Mycotoxins are toxic secondary metabolites of moulds, which can occur during plant growth and during storage and processing. Among various mycotoxin types, aflatoxins are of major concern due to potential impact on human and animal health. The food and feed industry has set a special focus on aflatoxin B1, which occurs most frequently and is the most toxic aflatoxin, since it has been directly correlated to adverse health affects.[1] Mycotoxins can occur within a concentration range of µg/kg to mg/kg. The Food and Agriculture Organization of the United Nations (FAO) has estimated that approximately 25% of the world's agricultural production is contaminated with mycotoxins, resulting in significant economic loss due to their impact on human health, trade and animal productivity.[2] Due to the fact that the presence of mycotoxins in food- and feedstuffs cannot be avoided, valid testing is demanded, and therefore, sampling methods for raw and processed materials are a critical necessity. The U.S. Department of Agriculture (USDA) and its Grain Inspection, Packers & Stockyards Administration (GIPSA) has estimated that non-representative sampling accounts for nearly 90% of the error associated with aflatoxin detection,[3] mainly due to non-random spatial distribution throughout materials when occurring in the trace concentration range (mg/kg or ug/kg).

In the following critical practicalities with focus on heterogeneity characterization required for developing sampling protocols for determining mycotoxins in feed (equally applicable to food) are presented. Results are substantiated with data from field trials. The real-world data used here have been redacted and serve specifically to strengthen the general arguments and not to represent specific results of the studied field trials, which are proprietary.

Critical sampling practicalities

The reason for all sampling errors is *lot heterogeneity*, causing material to vary irregularly throughout the lot on spatial but also a compositional dimensions and scales. Increasing the number of correctly extracted increments in a composite sample is the most effective way to decrease primary sampling errors, and will lead to results, which are closer to the true lot value. The difficultly is to determine the 'optimal number of increments', since this depends on heterogeneity, the analyte concentration level, and the size and lot geometry. In practice, sampling is often a compromise between the desired levels of accuracy/precision and labour/cost deemed necessary. The only criterion that must never be up for negotiation is representativity, which needs to be based on sampling correctness. In particular when dealing with trace concentrations, or highly heterogeneous distributions, as it is the case for mycotoxins, the sampling variance is by far the dominating source of uncertainty, due to the characteristically skewed, polymodal, highly irregular 'distribution' of these analytes.[4,5]

In the following tools for determining optimal number of increments and minimizing errors at each sampling and mass reduction step are presented. Examples are based on a real-world field trial performed on various materials used as animal feedstuff for determining aflatoxin B1 levels within each feed component, as well as within the total feed mixture (also termed 'total mixed ration', TMR).

Sampling stages

In the present field trials, all total mixed ration components are stored in piles and could only be sampled once unloaded (3-D sampling situation). The feed components are mixed in a predetermined ratio to form the total mixed ration (TMR), which is spread out in elongated feed bunks (1-D sampling situation). For each feed component, as well as the TMR, an individual sampling strategy determining the optimal number of increments has been developed, based on preceding material heterogeneity characterizations. All individual feed components have been analysed for aflatoxin B1 including pre-set control variables (protein, fibre and moisture). Samples collected from the feed mixture (TMR) have also been analysed for the same analytes, allowing a comparison of the TMR results with the analytical results of the individual TMR components.

For developing an appropriate aflatoxin sampling plan the following steps have been undertaken:

Figure 1. TMR 'sampling box' covering entire depth and width of target material, which is spread out in the longitudinal (horizontal) direction.

- Assessment of optimal sampling location (preferentially sampling in a 1-D sampling situation)
- Selection of appropriate sampling devices and mass reduction procedures for each material and lot type
- Design of experiments for characterizing material heterogeneity
- Determination of optimal sampling frequency based on empirical experimental outcomes

As stated above, only the total mixed ration can be considered as a 1-D sampling situation, while all individual feed components are piled up in 3-D lots, which were regrettably not able to be sampled during unloading.

Primary sampling

Before presenting the experimental design for the required material heterogeneity characterizations, the sampling tools used for the elongated TMR, the individual TMR components, as well as applied mass reduction procedures are presented.

The total mixed ration is pre-mixed and spread out in elongated feed bunks. Such a sampling situation (one-dimensional lot) allows extraction of increments covering the entire depth and width of the material, while a fully comprehensive spatial distribution of the increments is covered in the longitudinal direction of the lot (distance in-between increments as well as total number of increment is based on experimental design). In order to correctly delineate and extract the increments a 'sampling box' has been designed, suitable for the relevant lot dimensions and material characteristics, as depicted in Figure 1.

For individual TMR components (three-dimensional lots), the use of sampling spears is claimed to allow the best accessibility for all lot dimensions. Various types of sampling spears exist in the market; but they are seldom designed in compliance with TOS. The most important aspects with respect to sampling spear design are its length, width, aperture positions and opening width, as well as the closing mechanism. In the optimal case the length of the sampling spear should cover the entire depth of the lot, which allows insertion of the sampling spear vertically at every position within the lot (as indicated by the arrows in figure 2, left side). However, due to the fact that some of the TMR component piles exceeded the maximum available length of sampling spears, positioning and inserting direction were carefully considered. On the right hand side of figure 2, a pile is depicted that exceeds the length of the sampling spear. In order to cover all lot dimensions, i.e. also the lower and bottom parts of the lot at its highest level (row 3), the sampling spear was inserted horizontally in row 2 at the lowest accessible inserting point. It is emphasized that this spear sampling procedure is a result of a compromise based on the factual situation that the individual TMR components could not be sampled during unloading (1-D sampling situation). Muzzio et al. have published a particularly illuminating expose of the deficiencies in spear sampling for powders and granular mixtures.[6]

Mass reduction

Correct mass reduction procedures needs to be applied or sampling errors will adversely impact the secondary, tertiary etc. sampling stages and inflate the total measurement uncertainty.[7] Petersen et al. have performed an extensive study on various

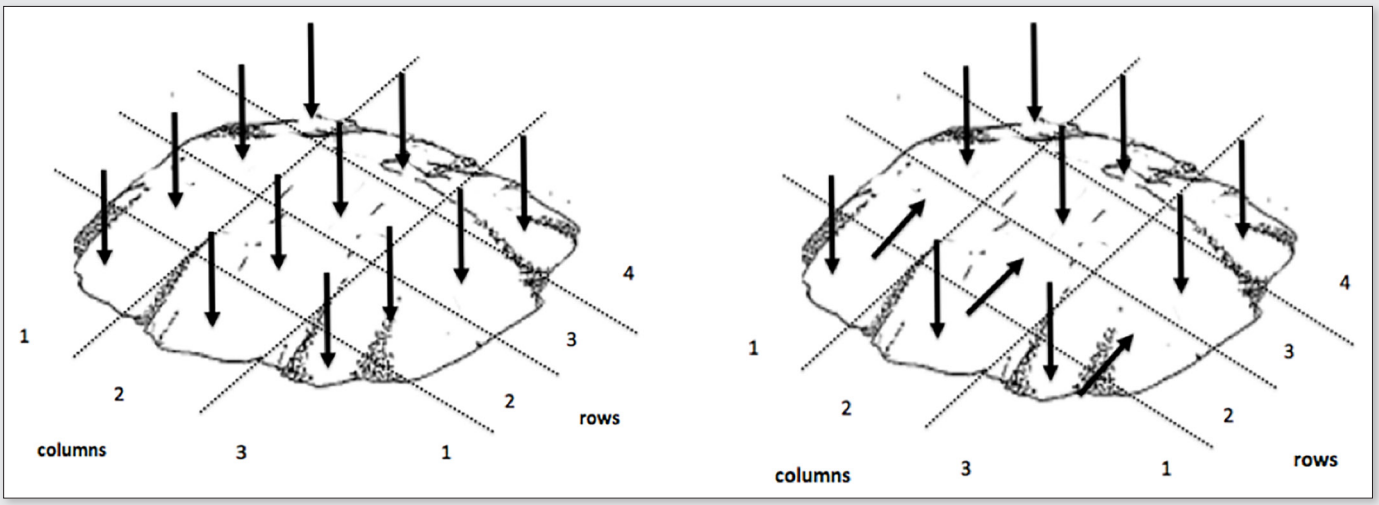

Figure 2. Illustrating stratified composite sampling of non-equal height 3-D storage piles. Sampling spear length versus pile height – spear inserting directions.

available mass reduction procedures and have rated them according to their representativeness, with the conclusion that only riffle splitters and rotational splitters allow correct mass reduction.[8]. For the majority of the TMR components riffle splitters with appropriate chute opening widths have been used, while for some fibrous, very light and wet materials the primary samples have been mass reduced using a circular cutting device, dividing the primary sample in eight equal sectorial cuts (increments). Four of the eight cuts have been used in the secondary sampling stage, while the other four cuts were discarded. All primary samples were mass reduced and further processed in the laboratory, including comminution and mass reduction to analytical sample size. Also in the final analytical mass reduction stage riffle splitters and bed-blending technique have been used to avoid sampling errors, especially important since dealing with a trace concentration range of aflatoxins, ibid.

Design of experiments for characterizing material heterogeneity

Following the proposed outline for developing an appropriate aflatoxin sampling protocol, the steps are (1) assessment and decision on optimal sampling location (3D vs. 1D), (2) selection of appropriate sampling devices and mass reduction procedures, (3) the design of experiments for material heterogeneity characterisation in order to determine (4) the optimal sampling frequency for each material.

Depending on the lot type, the sampling variance associated with the final sampling protocol and the heterogeneity distribution of the targeted analyte (e.g. aflatoxin B1) can be quantified using two different procedures: the replication experiment (stationary 3-D decision units) and variographic analysis (dynamic or stationary 1-D decision units). These assessment methods can also be applied to incorrect sampling procedures, for which the result would reflect the material heterogeneity plus the significantly inflated sampling errors. For the present field trials, sampling errors have been minimized by selection of appropriate increment sampling location and procedures allowing to characterize the sampling variability of the heterogeneity of the target analyte in the lot; based on that the optimal number of increments for the final composite sample has been determined.

The replication experiment was applied to all TMR components (3-D sampling situations), while a variographic experiment was applied to the sampling variance for the TMR in a 1-D sampling situation.

For the replication experiments ten primary samples were collected from every TMR component, each time repeating the full lot-to-test portion sampling pathway in completely identical fashion, DS 3077 (2013). Each primary sample consists of 30-40 increments depending on the lot dimensions. The minimum requirement is that the entire spatial geometry of the target material is fully covered by the sampling tool and the selected number of increments. It is important that all sampling operations, particularly at the primary sampling stage, are fully realistic during the replication experiment, meaning for example that the replicates should not be extracted at the exact same locations. In the described experimental field trial, different sampling operators collected the replicate primary samples in order to reflect all possible variation also that caused by individual differences regarding operating the sampling and mass reduction devices. For each replication experiment, the 'relative sampling variation (RSV)', the statistical relative 'coefficient of variation ($CV_{\%}$)', has been calculated, giving a measure of the specific heterogeneity of the target material (e.g. aflatoxin distribution), as expressed by the specific sampling procedure applied.

Heterogeneity characterization of the TMR is based on a variographic experiment, for which 60 equally spaced increments have been extracted from the feeding lane using the described TMR sampling procedure (see section 2.2). The main objective of the variographic experiment is similar to the replication experiment, meaning to determine the RSV (here called $RSV_{1\text{-}dim}$). Additionally, the influence of different sampling rates (i.e. distance between extracted increments) has been evaluated, allowing determination of the optimal sampling frequency or the optimal sampling interval.

Results and discussion of heterogeneity characterizations

The following section explains how results gained from heterogeneity characterization experiments have been interpreted to correctly determine aflatoxin levels in feed. The results have been redacted, rather serving to explain general features and interpretation possibilities than to present the actual values of the studied field trial, which are proprietary.

Results of individual TMR components

In addition to aflatoxin B1, all materials have also been analysed for protein, dietary fibre and moisture content, which serve as control variables to evaluate the applied sampling methods. For TMR components containing no detectable aflatoxin, protein, dietary fibre and moisture are used as control variables to determine required sampling frequency for reflecting inherent material heterogeneity.

The replication experiments used for characterizing 3-D lots also allow comparison of the sampling variances originating at different sampling stages (i.e. primary sampling, secondary sampling, tertiary sampling etc.). Figure 3 shows a result of the sampling variances in the different sampling stages for one of the TMR components, protein content. For nearly all materials and analytes in the study, similar results established the primary sampling variance as completely dominating over the secondary and tertiary sampling variance. This also confirmed the correctness of the mass reduction procedures used.

In contrast to figure 3, figure 4 shows the sampling variance of dietary fibre for a different TMR component (proprietary), revealing that the sampling variance decreases from primary to secondary sampling stage, but actually increases in magnitude in the tertiary sampling stage. This latter is a clear indication that an incorrect sampling procedure was used at this stage. This example demonstrates how a replication experiment allows detection of 'hidden'

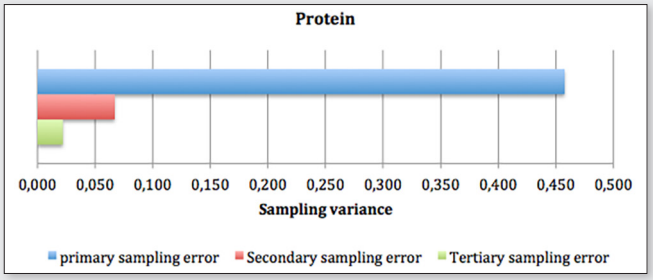

Figure 3. Typical example of comparison of sampling variances from different sampling stages. Dominance of primary sampling variance over secondary and tertiary sampling variance is the typical case.

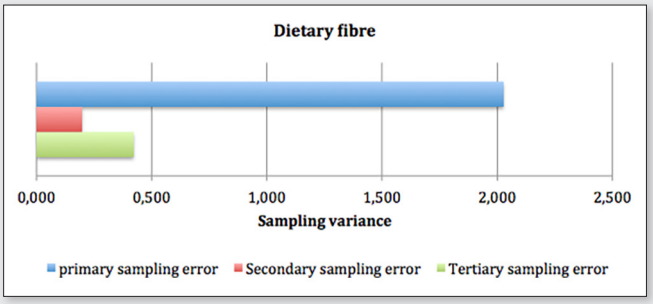

Figure 4. Typical example of comparison of sampling variances from different sampling stages, revealing an incorrect mass reduction procedure in the tertiary sampling stage (see text for details).

sampling errors. In this particular case, it was discovered that grab samples were extracted to gain the final test portion (despite the pre-designed, correct mass reduction steps), disobeying TOS' principles of sampling correctness. After correction of this incorrect procedure (replacement by a bed-blending technique), the sampling variance of the tertiary sampling stage decreased to a level below the secondary sampling variance, confirming reduction, or elimination of the incorrect mass reduction procedure.

The replication experiments of the field trial have also been used to quantify the heterogeneity of each TMR component, in particular with respect to the aflatoxin concentration. For all TMR components containing aflatoxin, the pertinent distributions are significantly skewed to the right; a characteristic of aflatoxin which has also been confirmed by various other studies.[9,10] The relative sampling variation (RSV) confirms this observation, ranging from around 50% to above 300% for the analysed materials. Since sampling errors have been minimized by means of the experimental design, the determined RSV values measure the total empirical sampling variance influenced by the aflatoxin heterogeneity of the target material. The RSV values for the control variables for all TMR components ranges between 2% and 15%, confirming that the comparatively high RSV values for materials containing aflatoxin is dominantly caused by the irregular, non-normal distribution of aflatoxin, rather than by incorrect sampling procedures. In order to lower the sampling variance for aflatoxin (if required by quality specifications), the number of increments per composite sample would need to be increased.

Results of TMR mixture

The total mixed ration (mixture of all individual feed components) is the last point at which aflatoxins can be detected before being fed to the animals and potentially causing dangerous health effects. The high RSV values determined for the various TMR components with respect to aflatoxin B1 indicate that despite elimination of potential incorrect sampling errors, the overall uncertainty on aflatoxin concentration is still uncomfortably high. For the field trials a specific uncertainty level on aflatoxin level in the TMR was pre-set, requiring that the sampling method and sampling frequency guarantee this uncertainty level. A variographic analysis also allows determining the influence of different sampling rates on the overall uncertainty, which has also been assessed for the present field trial.

Figure 5 shows the variographic results of the control variables for the TMR, comparing the number of increments used for final composite sample with the corresponding relative uncertainty incurred. The exact numerical values of the corresponding uncertainty are again not shown here due to confidentiality reasons.

Adding the variographic results for aflatoxin B1 to the same graph (see figure 6), it is obvious that the corresponding uncertainty for aflatoxin is dramatically higher (~10 times higher) compared to the control analytes, as also concluded from the assessment of the RSV values of the individual TMR components. The steepest decrease of uncertainty can be observed increasing the number of increments from one to two and from six to ten for the final composite sample. For this field trial the pre-set acceptable uncertainty level has been reached combining 10 increments to a final composite sample. In

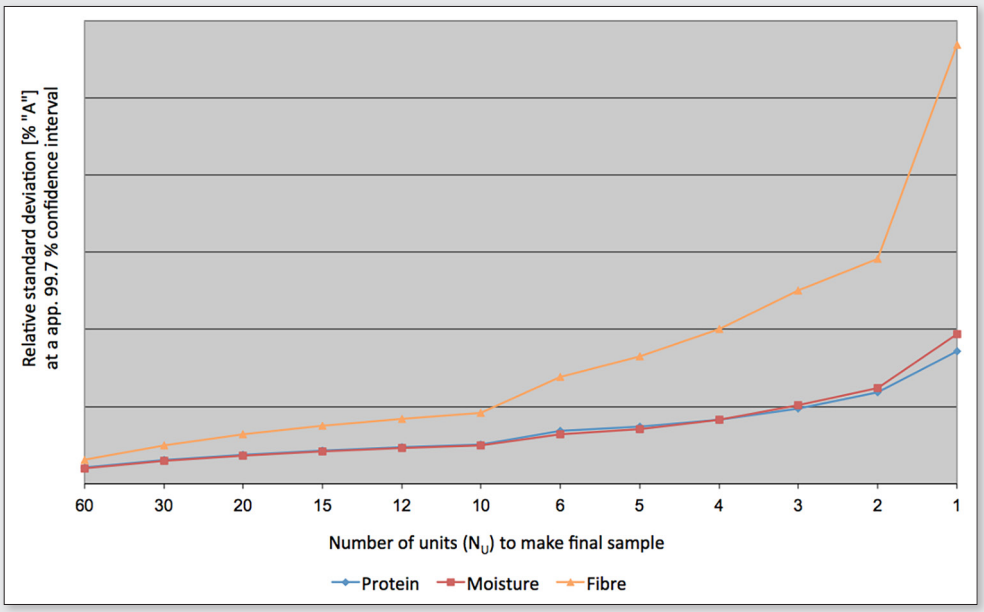

Figure 5. Variographic result for TMR (excluding aflatoxin) for a varying number of increments in a composite sample and the corresponding rel. total sampling-plus-analysis uncertainty. Values of y-axis have been removed due to confidentiality reasons without any loss of generality. Results are calculated for a systematic sampling mode.

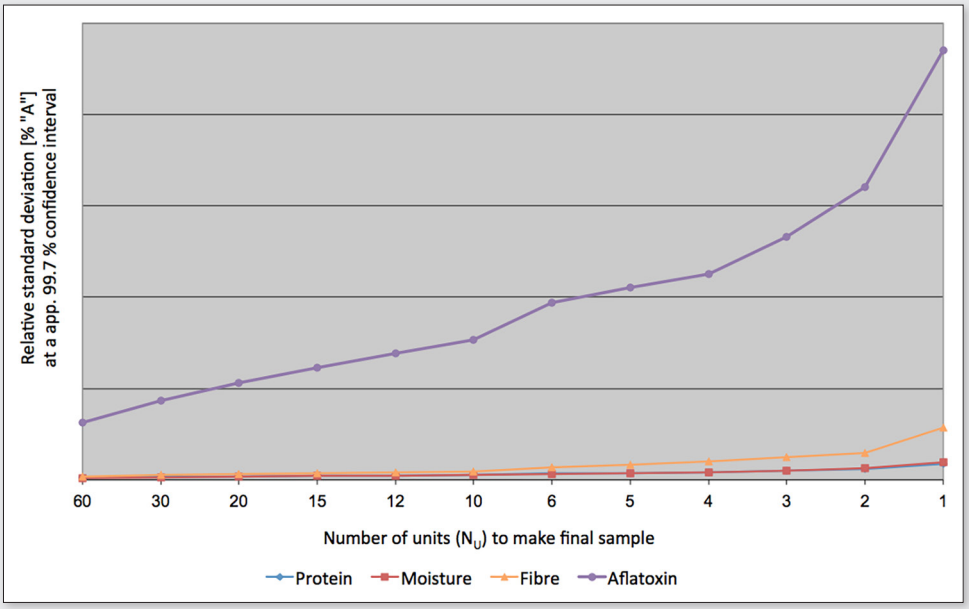

Figure 6. Variographic result for TMR (including aflatoxin) for a number of increments in a composite sample and their corresponding rel. uncertainty. Values of y-axis have been removed due to confidentiality without any loss of generality. Results are calculated for systematic sampling mode.

case a lower uncertainty level is required in the future, the appropriate number of increments can be selected directly from these variographic results, allowing full detection and uncertainty control of the aflatoxin concentration present in the TMR.

Conclusions

Critical practicalities in feed sampling for mycotoxins have been presented, which are currently not considered in the relevant sampling guidelines. The main problem for detection of mycotoxins, and especially aflatoxin in feed, is their decidedly irregular, non-normal distribution in the target feed/food materials. 'Hot spot' characteristics and low trace concentration ranges and distributions make representative sampling critical for valid mycotoxins concentration control. Assessment of optimal sampling locations as well as selection of the appropriate sampling and mass reduction devices forms the basis for representative sampling. A primary consideration is to determine the optimal number of increments, since practical sampling is a trade-off between labour/economic efforts and sample quality. When the empirical effect from increasing the number of increments is known, an educated decision can be made. Replication experiments for 3-D decision units and variographic analysis for 1-D decision units serve as a basis for the mandatory initial material heterogeneity characterization; and can be used to derive an optimal number of increments. Examples of an industrial field trial were presented including heterogeneity characterizations for various total mixed ration components, as well as for mixed feed itself. Interpretation guidelines were given on how to assess applied sampling methods on the basis of these experimental designs and how to determine an optimal increment number and location. It was highlighted how variography can be used to compare various sampling strategies based on their corresponding total uncertainty levels. The developed criteria regarding sampling practicalities can be transferred to many other feed- and foodstuffs and other commodities with similar characteristics regarding trace concentrations or concentrations which are irregularly distributed throughout the target material.

References

1. FAO 1993, Food and Agriculture Organization of the United Nations. *Sampling plans for aflatoxin analysis in peanuts and corn*, Rome – Italy, ISBN 92-5-103395-1.
2. FAO 2014a, Food and Agriculture Organization of the United Nations: http://www.fao.org/food/food-safety-quality/a-z-index/ mycotoxins/en/, accessed February 2015.
3. USDA 2014: U.S. Department of Agriculture - Grain Inspection, Packers & Stockyards Administration, http://www.gipsa.usda.gov/, accessed February 2015.
4. FAO 2014b: Food and Agriculture Organization of the United Nations. *Mycotoxin Sampling Tool – User guide.* http://www.fstools.org/mycotoxins/Documents/UserGuide.pdf, accessed February 2015.
5. T. B. Whitaker, J. W. Dickens, R. J. Monroe, E.H. Wiser, E.H., 1972. *Comparison of the Observed Distribution of Aflatoxin in Shelled Peanuts to the Negative Binomial Distribution*. Journal of the American Oil Chemists' Society, 49:590-593.
6. F.J. Muzzio, P. Robinson, C. Wightman, D. Brone, 1997. *Sampling practices in powder blending*. International Journal of Pharmaceutics 155 (1997) 153-178.
7. K.H. Esbensen, C. Wagner, 2014. *Theory of Sampling (TOS) vs. Measurement Uncertainty (MU) – a call for integration*. Trends in Analytical Chemistry, Volume 57, May 2014, Pages 93–106, http://dx.doi.org/10.1016/j.trac.2014.02.007
8. L. Petersen, C.K. Dahl, K.H. Esbensen, 2004. *Representative mass reduction: a critical survey of techniques and hardware*, Chemometr. Intell. Lab. Syst. 2004 (74) (2004) 95–114.
9. T.B. Whitaker, 2003. *Standardisation of Mycotoxin Sampling Procedures: an urgent necessity*, Food Control 14 (4) 233–237.
10. T.F. Schatzki, 2000: *Distribution of aflatoxin in pistachios*. Sequential sampling, Journal of Agricultural and Food Chemistry 48 (9) 4365–4368.

doi: 10.1255/tosf.59

Sampling of cereals: assessment of alternative protocols for mycotoxin analysis

Brigitte Mahaut and Guislaine Veron Delor
ARVALIS-Institut du végétal, Station Expérimentale, 91720 Boigneville, France. E-mail: b.mahaut@arvalisinstitutduvegetal.fr

Context and objectives

European directives[1,2] for official controls of some contaminants in cereals such as mycotoxins set methods for sampling and analysis. The sampling protocols are strict and not very practical.

The composition of batches of cereals is rarely homogeneous and, in particular, certain contaminants like Fusarium-mycotoxins are distributed in a non-uniform way. Sampling is therefore a procedure which requires a great deal of care; it is necessary to get a guaranteed representative sample before initiating analysis.

For four years, studies have been undertaken by a French working group of associated storage organizations and suppliers of sampling devices in order to:

- evaluate mycotoxin distributions in cereal batches,
- compare different sampling protocols, including the European directive (reference method),
- determine the relationship between the number of increments and the total analysis uncertainty, and
- define an acceptable sample weight for laboratory analysis.

Evaluation of the distribution of mycotoxins

Three wheat batches of 500T were selected and 100 increments are taken from each. The DON content is determined on each sample by an Elisa test.

Nine maïze batches of 500T to 1500T are selected and 25-150 elementary samples are taken. Fumonisins B1,B2 contents are measured for seven batches, Zearalenone content for three batches and DON content for one batch. Measurements are performed by chromatographic analyses[3,4,5].

The levels of mycotoxins span a wide range of contamination that cover the regulatory thresholds in human food.

For wheat, grids were drawn on the top of the silos in order to ensure a consistent sampling plan across the whole batch. An example of static sampling plan is given Figure 1.

Each of 100 increments are homogenized and ground before being analysed. Mappings are developed based on the results; these all show strong heterogeneity in the silo. This heterogeneity results from the field variability (wheat heterogeneity study conducted by ARVALIS over four years). The silo can be considered as a stack of plots. One level of the silo is made up from different field plots; the observed silo variability is similar to that noted as intra-plot field variability.

The level and the variability of DON contents are very different between silos. The higher the silo's average content, the greater the dispersion.

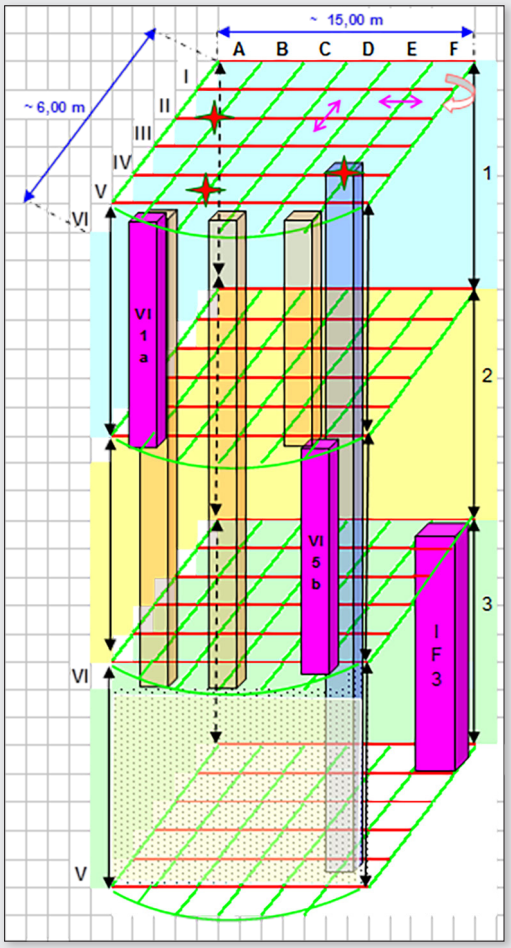

Figure 1. Silo sampling plan.

Table 1. *Mycotoxin* contamination levels

Fusariotoxin	Cereal	Number of silos	Mean silo value (µg/kg)	Food regulatory threshold (µg/kg)
DON	Common wheat	5	477 to 1988	1250
	Maize	1	2633	1750
Fumonisins B1 + B2	Maize	7	534 to 7132	4000
Zearalenone	Maize	3	139 to 683	350

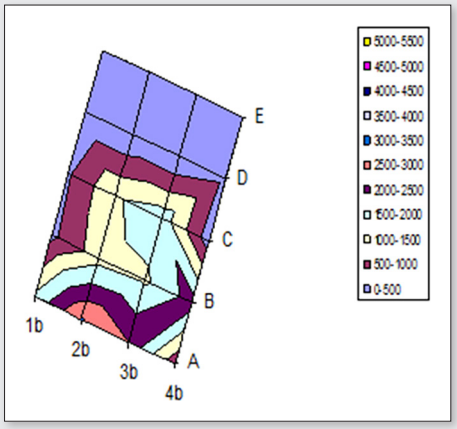

Figure 2. Heterogeneity measured at 4 m depth (DON)

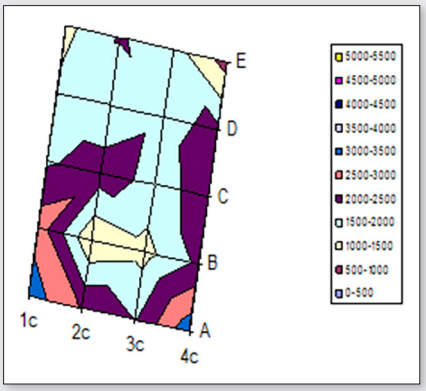

Figure 3. Heterogeneity measured at 6 m depth (DON)

The trials on maize are conducted on flowing grain streams. An increment is taken every 20 to 25 tons. As for wheat, the dispersion of the samples is different depending on the silo. The results recorded for Fumonisins in seven silos show a relationship between average contents and variability.

The higher the mycotoxin contents, the higher the variability between samples. The heterogeneity of batches depends on the level of contamination. The distribution of mycotoxins is not uniform and in addition varies according to the content levels.

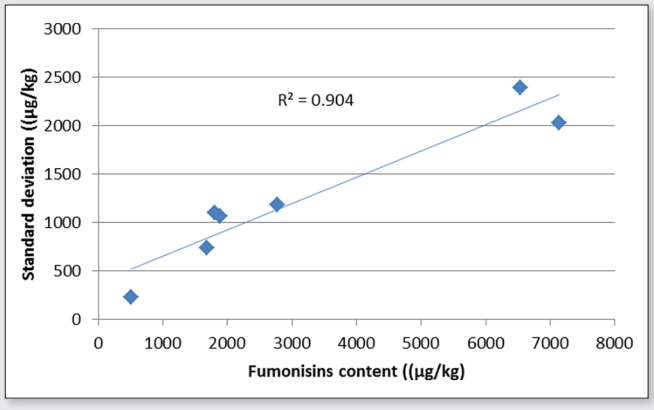

Figure 4. Between-sample standard deviation variability vs. Fumonisin content.

Table 2. Number of increments in alternative sampling protocols

	Reglementary protocol	Normative protocol	Routine protocol
Flowing – 500T	100	25	10
Static – lorry	100	10	3
Static - 500T	100	50	10

Comparison of alternative sampling protocols

The official control of mycotoxins is to be performed on an average sample of the grain batches. Three different protocols for arriving at this average sample are studied here:

- the protocol corresponding to regulation n°401/2006 for fusarium toxins. This is considered as a reference.
- the "normative" protocol drafted by the standardisation working group (EN ISO 24333 standard).This method is adapted to certain situations experienced by cereal operators (e.g. intervention scheme)
- the "routine" protocol with a smaller number of increments than the two alternatives. This protocol is suited to the practical and economic conditions encountered on the daily controls by the cereal industry operators.

Two different grain sampling situations have been taken into account: flowing cereal streams (transfer from one silo to another one, discharge and Redler samplings or train discharge) and static batches (lorries, flat or vertical silos). A total of 22 tests were conducted with a large range of devices. The number of increments for each type of situation is shown in Table 2.

The mycotoxin used for estimation is DON for wheat and maize.

The average DON content of the different batches of grains investigated ranges between 477 and 6,275µg/kg. These values frame the regulatory limits or recommendations well. Statistical analysis of the results (Student's T-test) showed that there is no significant difference between the three protocols. It should be noted however that in the case of lorries, the routine protocol may sometimes misjudge the level of contamination (2 cases out of 14).

A comparison between sampling methods (manual vs automatic sampling) indicated there was no statistically significant difference.

Thus the alternative protocols (normative and routine) *may* be used for estimating the average mycotoxin content of a batch of grain instead of regulatory protocol. A sampling protocol based on a smaller but sufficient number of increments does not lead to an underestimation of the average mycotoxin content of the batch. Use of the regulatory protocol lead to higher, perhaps unjustified costs.

Estimation of the impact of a sampling protocol on accuracy

All test data were used to estimate the error of the estimation of the average mycotoxin content (accuracy).

The global variability observed, characterized by a coefficient of variation (CV), seems to be *independent* of the average content of the silo; it is about 45%.

This variability has two origins: the variability due to sampling errors and that due to the analytical error.

When producing a composite sample obtained from n increments, the sampling variability can be reduced if based on an increased number of individual increments (N.B. covering the full lot volume). By contrast, the analytical error component is constant.

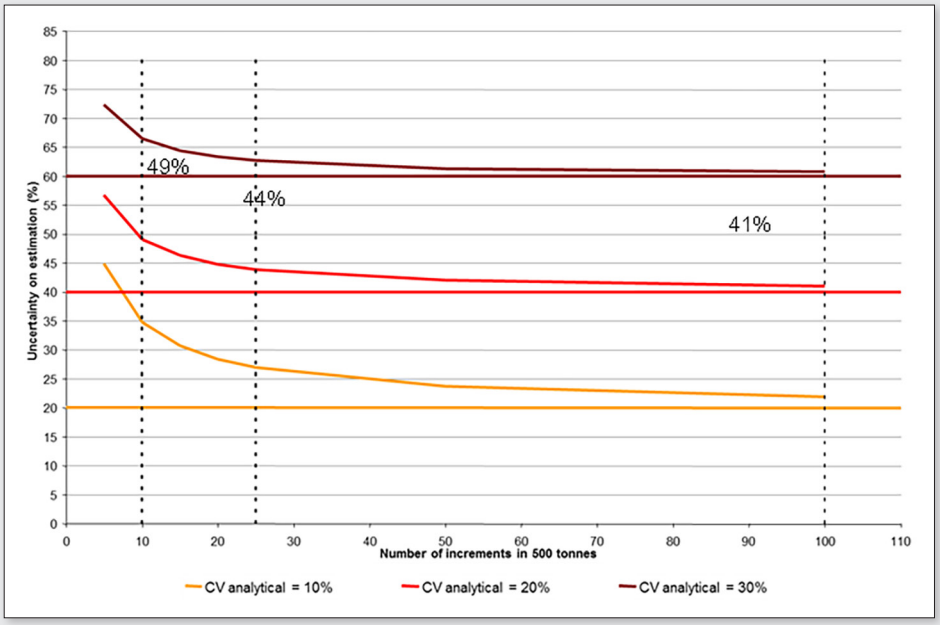

Figure 5. Uncertainty of estimated average mycotoxin content as a function of the number of increments from a 500 T lot.

Statistical simulations were carried out to define the degree of variability due to sampling over that of the chromatographic analysis. For this, three hypothetical levels were considered for the analytical error (CV = 10%, CV = 20% and CV = 30%). The variability due to sampling error can be estimated in relation to the number of individual increments, see Figure 5. Here it can be observed that after a certain number of increments, the reduction of the overall uncertainty of the result generated by an additional increments becomes negligible.

Thus the benefit of a higher sampling intensity is low. By increasing the number of increments from 10 to 100, the total accuracy improves only 8% for an analytical uncertainty equal to 40% (CV analytical = 20%). These models are applicable for wheat and maize contaminated with DON, Zearalenone and Fumonisins.

Influence of the reduction of the size of the laboratory sample

The regulation (EC) defines a total sample mass as the result of aggregation of all the increments taken from the lot or batch, specifying its weight to be 10 kg. But no specification is given for the laboratory sample mass. A mass of 10 kg is too big for the laboratory and causes different problems associated with sub-sampling (division), grinding, storage.

Our trials consisted of reducing a 20 kg sample to ≈500g by using a conical divider, see Figure 6. All the split off fractions were ground and analysed by chromatographic methods. Two wheat samples were characterized for DON while two samples of maize were analysed for for Fumonisins B1, B2.

For this study, the averages obtained at each step of division (sub-sampling) are compared to the average calculated using all available data. This latter corresponds to the initial sample of 20 kg (called “reference”).

Two modes of interpretation of the results were applied:

- comparing the means with the reference, using the critical difference (CD) as defined in the standard NF ISO 5725 – 6 [6];
- Assessing the uncertainty that characterizes the dispersion of values around the reference.

The critical difference was estimated from the standard deviation of repeatability specified in the standard used.

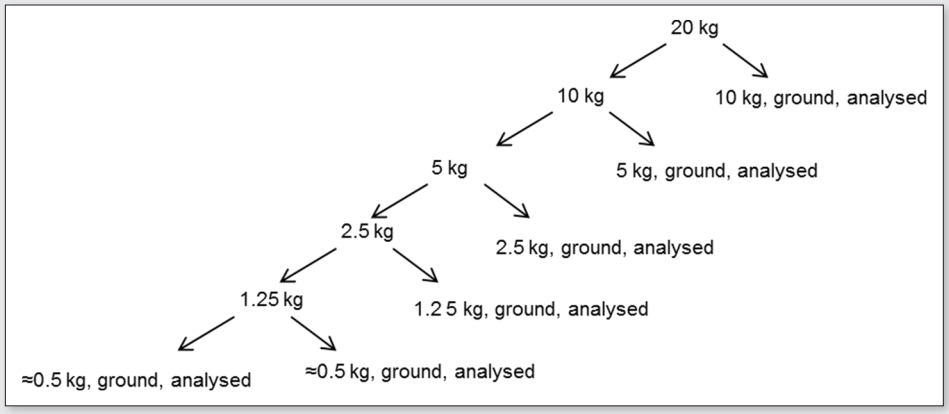

Figure 6. Sub-sampling (division) flow chart.

For DON, only one batch corresponding to a mass of 1kg for one sample showed a greater difference than the DC. For Fumonisins, some differences were observed for fractions less than or equal to 2.5kg.

An uncertainty, Ue, equal to 2 standard deviations of reproducibility from standards was assigned to each reference:

- 39% for DON;
- 34% for Fumonisin B1;
- 39% for Fumonisin B2.

The averages obtained at each step of sub-sampling, for each sample and each level, are included in the intervals of uncertainty associated with references, except for the fraction of 1kg for the 2 maize samples.

The results of this study show that it is possible to suggest the laboratory sample mass as low as 3kg without affecting the estimation of the average level of contamination. It should be noted that it appears possible to reduce this mass to 1kg for the analyte DON.

Conclusions

These studies confirm the significantly high spatial variability of mycotoxin distributions.

They also showed that an average sample composed by a smaller number of increments than that stated in the regulation, may still representative of the target grain lot. The results regarding Fusarium-mycotoxin contents are similar. This means that it is possible to reduce the sampling intensity.

The results were included in the data that supported the drafting EN ISO 24333. This standard, published in 2009[7], has received positive feedback from users. During the review of regulation 401/2006 in 2014[8], the EN ISO 24333 standard has been recognized to sample lots ≥500T and thus reduces the resources devoted to sampling.

The mass of the sample sent to the laboratory for mycotoxin analysis is reduced from 10 to 3kg.

Acknowledgments

These studies have been coordinated and undertaken by IRTAC, FranceAgriMer and ARVALIS-Institut du végétal.

References

1. Commission Regulation (EU) No 401/2006 of 23 February 2006 laying down the methods of sampling and analysis for the official control of the levels of mycotoxins in foodstuffs. *Official Journal of the European Union (9.3.2006)*, L 70: 12-34
2. Commission Regulation (EU) No 691/2013 of 19 July 2013 amending Regulation (EC) No 152/2009 as regards methods of sampling and analysis
3. EN 13585:2002, Foodstuffs - Determination of fumonisins B1and B2 in maize - HPLC method with solid phase extraction clean-up
4. ISO 17372:2008 Animal feeding stuffs - Determination of zearalenone by immunoaffinity column chromatography and high performance liquid chromatography
5. EN 15891:2010, Foodstuffs - Determination of Deoxynivalenol in cereals, cereal products and cereal based foods for infants and young children - HPLC method with Immunoaffinity Column Cleanup and UV Detection
6. ISO 5725-6: 1994, Accuracy (trueness and precision) of measurement methods and results. Part 6: use in practice of accuracy values

7 EN ISO 24333:2009, Cereals and cereal products - Sampling

8 Commission Regulation (EU) No 519/2014 of 16 May 2014 amending Regulation (EC) No 401/2006 as regards methods of sampling of large lots, spices and food supplements, performance criteria for T-2, HT-2 toxin and citrinin and screening methods of analysis.

doi: 10.1255/tosf.77

The role of inference in food safety

Charles A. Ramsey
EnviroStat, Inc., PO Box 657, Windsor, CO 80550, USA chuck@envirostat.org

Concerned individuals have been trying to determine the safety of their food since ancient times. In ancient times, people themselves were the ultimate test of food safety, but as human evolution progressed, other techniques such as sensory perception and experimentation on animals were used. Today sophisticated analytical techniques and models are available to measure and predict food safety. These sophisticated techniques and models are dependent not only on the quality of samples that are collected and analyzed but also on how inferences are made from the analytical results to the food being sampled. Unfortunately, the Theory of Sampling and the role of inference have not been fully integrated into prediction of food safety.The basis for many "modern" food sampling protocols was developed prior to the development of the Theory of Sampling. Many of these sampling protocols were based on concepts of acceptance sampling procedures and associated inference. The Theory of Sampling enables the representative sampling of bulk materials and eliminates the reliance of acceptance sampling as the only method for the characterization of food and utilizes a different type of inference than for acceptance sampling. This contribution addresses the differences between inference for acceptance sampling and inference for the sampling of bulk materials and the implications of these differences for food safety.

Introduction

The testing of food for poison has occurred since ancient times. Until recently (and even some today), most food testing was performed by having someone taste the food and waiting to see if there were any ill effects. This process worked for fast acting poisons but was ineffective for slower acting poisons. Through the use of sophisticated analytical techniques and better understanding of toxins, the use of humans to make inference regarding the safety of food has greatly diminished. However, it has been reported that several notable people, including Vladimir Putin[1] and Barack Obama[2] have recently used food tasters to ensure their food is not poisoned.

Food safety today is mostly dependent on manufacturing practices that focus on critical contamination points in the manufacturing process. These are Hazard Analysis and Critical Control Points (HACCP) conceived in the 1960s when Pillsbury developed food for the first space flights[3] and Good Manufacturing Practices (GMP). However, there is still a need for inspection of food to determine the adequacy of HACCP and GMP, assess contamination after manufacturing, respond to outbreaks and a variety of other reasons. Since the amount of food produced is very large compared to the number of samples collected, it is critical that sampling protocols be very efficient. Because the consequences of contaminated food are extreme, it is also critical that inferences are correct and that correct decisions are made.

Inference is the process of estimating parameters of a Decision Unit[4] based on analytical results of samples from the Decision Unit[5]. The most common parameter estimated is the true mean concentration of an analyte of interest. The requirement to enable inference is that the sample is from an equiprobabilistic (random) selection of the elements within the Decision Unit. The error (closeness of the estimation to the true value) in the inference is controlled through the application of principles of the Theory of Sampling[6,7] (TOS). See Figure 1.

In cases where multiple Decision Units exist, inference can also be used to estimate the percent (portion) of Decision Units that possess a specific concentration or characteristic. Equi-probabilistic (random) selection is also required for this type of inference, but it is random selection of the Decision Units, not random selection of the elements within the Decision Unit as above, that must be equiprobable. Figure 2.

These two inferences (to an individual Decision Unit and to unsampled Decision Units) are sometimes used individually and sometimes combined, depending on the Sample Quality Criteria (SQC)[8]. Understanding of the differences in the types of inference is critical for the design of sampling protocols as well as for the interpretation of analytical results and final decision-making. In both types of inference, inference is made from what is sampled (collected) to what is not sampled (not collected). While this paper focuses on food safety, the inference principles are generic and applicable to all sampling and analysis.

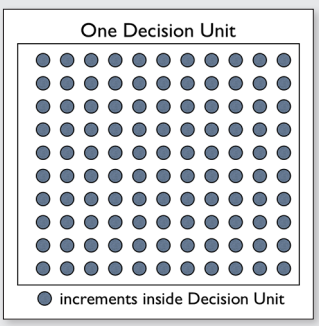

Figure1. Sampling from within a Decision Unit allows inferences to be made with respect to the entire Decision Unit.

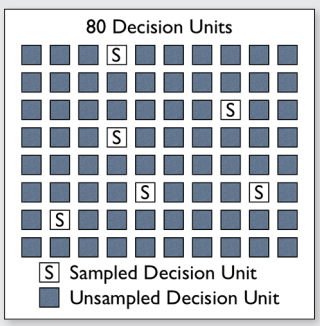

Figure 2. Sampling individual Decision Units allows inferences to be made with respect to all the Decision Units.

Inference to a single decision unit

A Decision Unit may be small in size/mass or it may be quite large. There are no size or geometric constraints on a Decision Unit. In the case of a small Decision Unit, it may be possible to collect the entire Decision Unit (DU) as the primary sample. This may be the case for a loaf of bread DU or a cantaloupe DU. However, in most cases the Decision Unit it too large to practically collect in its entirety as a primary sample. This would be the case for a warehouse of bread DU or a truck of cantaloupes DU. In some cases, even if the entire Decision Unit can be collected in its entirety that may not be desired as there would be nothing left.

In the laboratory, it is also possible to analyze the entire primary sample as received or it may be necessary to collect a smaller test portion from the primary sample for subsequent analysis. The possible sampling situations in the field and in the laboratory are very similar, either the entire DU (primary sample) can be taken or the DU (primary sample) must be representatively sampled according to the principles of TOS. In total there are four possibilities:

- Take entire DU in the field, analyze entire primary sample in the laboratory
- Take entire DU in the field, subsample primary sample in the laboratory
- Sample DU in the field, analyze entire primary sample in the laboratory
- Sample DU in the field, subsample primary sample in the laboratory

Each and every one of these possibilities exists in food safety. Inference for each of these possibilities is discussed below.

Take entire DU in the field, analyze entire primary sample in the laboratory

Inference is the simplest in this case. The result from the laboratory is the true concentration of the analyte of interest in the primary sample (except for analytical uncertainty, which will not be discussed). The primary sample in this case is the Decision Unit. No inference is required as everything is taken and analyzed.

Take entire DU in the field, subsample primary sample in the laboratory

The result from the laboratory is used to estimate the true concentration of the analyte of interest in the primary sample. Since the entire primary sample was not analyzed, an inference must be made from the analytical result to the concentration of the analyte of interest in the primary sample. The entire DU in the field was collected as the primary sample, so no inference is required from the primary sample to the DU.

Sample DU in the field, analyze entire primary sample in the laboratory

The result from the laboratory is the true concentration of the analyte of interest in the primary sample. The entire primary sample was analyzed in the laboratory, so there is no inference required from the analytical result to the primary sample. However, the entire DU was not collected in the field as the primary sample, so there will be an inference from the analytical result of the primary sample to the DU.

Sample DU in the field, subsample primary sample in the laboratory

The result from the laboratory is used to estimate the true concentration of the analyte of interest in the primary sample. The primary sample was sampled in the laboratory, so there is an inference from the analytical result to the primary sample. However, the DU was also sampled so there will be another inference from the primary sample to the DU. In this case there are two inferences being made. One inference from the analytical result to the primary sample and one inference from the primary sample to the Decision Unit.

Inference for each of these situations can be made directly or through some type of statistical calculation. Direct inference occurs when an individual analytical result is used to estimate the concentration in the primary sample and/or to the entire Decision Unit. This is very common. Alternatively, several measurements can be made and a statistical calculation used for inference to either the primary sample or to the DU. Examples may be an average or a 95% upper confidence interval of the mean. The type of inference desired (direct or statistical calculation) therefore has an impact on the sampling protocol. For each type of inference it must be determined how that inference is going to be made and the error associated with each inference.

Inference from sampled to unsampled decision units

In some cases the amount of material in the Decision Unit is very small compared to the total amount of material under investigation. In other words, there are many, many Decision Units; so many, in fact, they cannot all be sampled. Even if all the DUs could be sampled, it may be desired not to sample all of them since there would be no Decision Units left for consumption! If every can of tuna fish was tested for mercury or every nut tested for aflatoxin, there would be no canned tuna or nuts left to eat. This type of sampling is actually common, not only in food but in other industries as well. It is commonly known as attribute (or acceptance) sampling[9]. This is the type of sampling used in surveys and quality control. The premise is that if enough Decision Units are sampled, claims can be made about all the Decision Units (especially those not sampled). The claim made is typically based on the percent (or portion) of individual Decision Units that have some specific characteristic or attribute. This characteristic or attribute can also be concentration related as in the case of detection limits.

Survey example to illustrate concepts

Many companies and governments survey (or poll) to determine the percentage of the population that has some opinion, belief, owns a product, etc. For many of these surveys, only several hundred to several thousand people are contacted. The percent of people contacted that have the opinion, belief, product, etc. is used to make an inference to a larger number of people, which can be millions or billions. Surveys can be very accurate even though only a very small amount of people are actually surveyed. The only criteria to make inference from the surveyed people to all the people is that the surveyed people are selected at random (specific types of random are not addressed). The more people surveyed, the better the estimate of the true percentage of people that have that opinion, belief, product, etc. For this example, the individual is the Decision Unit. It is the individual that is “sampled” and information is obtained on the individual. This type of sampling is common and is applicable to food safety where the conditions for implementation are met.

In some cases there are multiple Decision Units, but they can all be sampled. There may be three trucks (Decision Units) of grain, and it is possible and desirable to sample all three, obtaining

specific information on each truck. The amount of material taken for the samples is negligible compared to the total mass of the three trucks. However, if these three trucks each contained 5,000 packages (Decision Units), it may be impractical to collect 15,000 primary samples. Even if it was practical, there would be little material left.

Inference to unsampled Decision Units is a function of only the number of Decision Units sampled, not about mass, increments, tools, etc. as in the case of inference to a DU (where mass, increments, tools, etc. are critical for primary sample collection). Inference to unsampled Decision Units assumes the attribute, characteristic, or concentration of the Decision Unit is known (or can be known) and all that is required is random selection of enough Decision Units to meet a specified confidence. Inference to unsampled DUs is based solely on probability (the reason random selection of Decision Units is required). The importance of random selection of Decision Units cannot be over stressed. Since the entire inference scheme is based on randomness, no compromises can be made. Attitudes like "This looks random to me," and "I can't get to those Decision Units so I will skip them" are unacceptable.

A special case of attribute sampling exists when the desire is to claim the absence of a particular attribute or characteristic. While it is impossible to determine for certain that no DUs have a specified attribute or characteristic, if enough DUs are sampled and the characteristic or attribute is absent from each DU, an inference can be made that there is a XX% confidence that no more than YY% of the DUs have a particular characteristic or attribute. The details of the calculations are addressed in most introductory texts on statistics[9-12].

Example

Lima beans are sold in a variety of packaging including frozen, bagged, bulk, and canned. Two packaging examples, one frozen and the other bulk, will be considered to illustrate the two different types of inference.

Frozen lima beans

Lima beans can be sold in frozen packages. For some reason (e.g., routine surveillance, customer complaint) it was decided to test frozen packages of lima beans to see if a certain contaminant is present above a specified detection limit in any of the packages of lima beans. If any of the packages contains a detectable concentration of the contaminant, one course of action will follow. If none of the packages contain a detectable concentration of contamination, another course of action (no action) will follow. In this case the individual package would be the Decision Unit. It would be easy (and desirable) to select an entire package (DU) as the primary sample and send it to the laboratory. This is a perfect primary sample as no sampling error exists (as long as the sample integrity is maintained). The laboratory, however, cannot analyze the entire primary sample. Instead, the laboratory will have to process the primary sample and remove a small portion (subsampling) for analysis. The act of sample processing and subsampling will contain some error. An inference will have to be made from the analytical result to the primary sample. This inference may be performed with just one analysis (direct), or there could be multiple analysis and some type of statistical calculation could be used for inference. These details would be addressed during the SQC process. For this example direct inference will be used.

The obvious next question is which packages of lima beans are of concern. Just one package, all the packages at the local grocery store, all the packages in the warehouse, all the packages in Europe or something else? From a sampling and inference point of view, it does not matter (as long as random selection is achieved). For this example the choice will be a specific warehouse at a specific point in time. In the case of surveillance sampling or exposure assessment, the packages of lima beans could be sampled over the course of a year or some other time frame.

There will be two types of inference in this example: one will be from the analytical result to the package of lima beans and one will be from sampled packages of lima beans in the warehouse to all the packages of lima beans in the warehouse. The quality of the inference to the package is a function of the error in the sample processing and subsampling. The quality of the inference to all the packages in the warehouse is a function of how many packages (DUs) are sampled. There is no set number for quality. It should be a function of the consequences of an incorrect inference (and resulting incorrect decision). This would be addressed in the SQC process.

It is important to understand these inferences and their impact on the sampling protocol. For instance, the laboratory may receive 300 packages of lima beans and decide to combine them in groups of ten and only perform 30 analysis to save money. If this happened, information would be lost on the individual Decision Units and it would be impossible to determine a course of action.

Bulk lima beans

This example is the same as above except the lima beans are in 10 kg bulk containers (Decision Unit). In this case the entire DU cannot be taken as a primary sample, so the DUs (individual 10 kg bulk containers) will have to be sampled and an inference made from the primary sample back to the DU. In this example there are many DUs (more than can be sampled) and information is required on all the DUs, therefore another inference must be made from the sampled DUs to the unsampled DUs. In other words several, but not all, of the 10 kg packages will be sampled using the principles of TOS. The results from the sampled DUs will be used to infer (estimate) the percent of all the DUs in the warehouse that have a detectable concentration of the specified contaminant. If none of the 10 kg packages have a detectable concentration, one course of action will follow, and if any of the 10 kg packages have a detectable concentration, then another course of action will follow.

As in the frozen package example, understanding of these inferences is critical for developing the sampling protocol. It would be incorrect to select increments from different bulk containers and combine them into a primary sample because information will be lost on the individual bulk containers. For bulk containers, an overall error for both primary sampling and for the sample processing/subsampling in the laboratory need to be established.

Issues

In many cases a single sample can be used to represent a Decision Unit. This is always desirable. However, in some cases it may require multiple samples. If the desire is to estimate the exposure risk from pesticides on tomatoes to all individuals in a country, one could theoretically collect a single sample from tomatoes in time and space (across the entire country for a 30 year period), but this could never happen. In a situation such as this multiple samples

of tomatoes within the Decision Unit (entire country for 30 years) would have to be collected.

It is typically not appropriate to combine increments across Decision Units as this will dilute the concentration of the individual Decision Units. There is, however, an exception to this. It is acceptable to combine multiple increments (from different Decision Units) for analytical efficiency (a composite sample) as long as information regarding the individual Decision Units is not lost. A common example is the presence of some prohibited attribute or characteristic that can be detected/measured (analyte is not diluted out) in the composite sample. In this case composting (as described above) is a viable strategy to reduce analytical cost and still achieve the objectives.

Inference to unsampled Decision Units can be made using attributes and concentrations. There are many, many statistical approaches to estimate both attributes and concentrations that are not addressed in this paper. The purpose of this paper is to identify the types of inferences and how they are used, not how the inferences are calculated.

In some cases the average of the Decision Units is calculated for decision-making purposes. In this case, the Decision Unit was incorrectly chosen. There should have been only one Decision Unit that contained all of the material. While it could be argued that the same average result is achieved, it would be more cost effective to treat all the material as one Decision Unit.

Conclusion

Knowledge of inference to Decision Units and to unsampled Decision Units is critical when applying the Theory of Sampling to food safety to make correct and defensible decisions. The sampling protocols for inference to a Decision Unit and to unsampled Decision Units are very different. Inference within a Decision Unit is based on the sampling errors incurred, sample processing and analysis. This error is mitigated and controlled through correct application of the principles of TOS. Confidence is indirectly related to the total sampling plus analysis error. Inference to unsampled Decision Units is based on the number of Decision Units sampled. This number is based on the probability of finding all the Decision Units that possess or lack a specific attribute or characteristic. Confidence in this case is directly related to the number of Decision Units sampled.

As TOS becomes more widely adopted in the food industry, it is imperative that practitioners understand and apply the principles of inference correctly in the development of sampling protocols. This is critical to ensure that defensible and cost effective decisions are made regarding food safety.

References

1. Walsh, John, *Vladimir Putin employs a full-time food taster to ensure his meals aren't poisoned*, The Independent, July 23, 2014.
2. Luthern, Ashley, *Testing for Poison Still a Profession for Some*, Smithsonian.com, June 26, 2009.
3. Ross-Nazzal, Jennifer, *Farm to Fork: How Space Food Standards Impacted the Food Industry and Changed Food Safety Standards*, In Dick, Steven J. and Launius, Roger D. (eds.), Societal Impact of Spaceflight, US Government Printing Office, 2007.
4. Ramsey, Charles A., The decision unit—a lot with objectives, in Proceedings of the 7th *International Conference on Sampling and Blending*, *TOS forum* **Issue 5,** 31–34 (2015). doi: 10.1255/tosf.75
5. Ramsey, Charles A., *Considerations for Inference to Decision Units*, Journal of AOAC International, Vol. 98, No.2, 288-294, 2015.
6. Pitard, Francis F., *Pierre Gy's Sampling Theory and Sampling Practice* 2nd ed., CRC Press, 1993.
7. *DS 3077 (2013) Representative Sampling– Horizontal Standard*, Danish Standards. www.ds.dk
8. Ramsey, Charles A., Wagner, Claas, *Sample Quality Criteria*, Journal of AOAC International, Vol 98, No. 2, 265-268 (2015)
9. Schilling, Edward G., Neubauer, Dean V., *Acceptance Sampling in Quality Control*, CRC, 2009.
10. Montgomery, Douglas C., *Introduction to Statistical Quality Control,* 2nd ed., Wiley, 1991.
11. ANSI/ASQ Z1.4: *Sampling Procedures and Tables for Inspection by Attributes*, American Society for Quality.
12. Walpole, Ronald E., and Myers, Raymond H., *Probability and Statistics for Engineers and Scientists,* 3rd ed., 1985.

doi: 10.1255/tosf.61

When "homogeneity" is expected—Theory of Sampling in pharmaceutical manufacturing

A. Sánchez-Paternina,[a] A. Román-Ospino,[a] C. Ortega-Zuñiga,[a] B. Alvarado,[a] Kim H. Esbensen[b] and R.J. Romañach[a,*]
[a]Department of Chemistry, University of Puerto Rico at Mayagüez, PO Box 9000, Mayagüez Campus, Mayagüez 00682, Puerto Rico. E-mails: rodolfoj.romanach@upr.edu, adriluz.sanchez@upr.edu, andres.roman@upr.edu, carlos.ortega4@upr.edu, barbara.alvarado@upr.edu
[b]Geological Survey of Denmark and Greenland (GEUS), Copenhagen, Denmark, ACABS research group, University of Aalborg, campus Esbjerg (AAUE), Denmark and Telemark University College, Porsgrunn, Norway. E-mail: ke@geus.dk

A stream sampling method has been developed to facilitate implementation of variographic analysis and use of replication experiments in the development of pharmaceutical formulations. These methods are thoroughly developed in the Theory of Sampling but are not currently used in pharma. Pharmaceutical formulations have very strict requirements as drug products are expected to deliver a specific drug content to patients and are required to avoid possible consequences of over-dosing or under-dosing. Formulation developers currently rely on grab sampling, the use of a sample thief (spear) to extract material from areas suspected of having incomplete mixing ("dead spots"). This study applies an alternative stream sampling approach based on the Theory of Sampling in connection with testing two alternative mixing processes.

The mixing process based on vibration and tumbling can be shown to provide a significantly lower end-point heterogeneity. The results show the usefulness of the variographic approach in combination with replication experiments; both are effective in identifying areas of unacceptable heterogeneity in pharmaceutical blends, and point to the need to continue improving the mixing processes described in this study.

Background

Pharmaceutical manufacturing contains an expectation, indeed a regulatory demand that powder blends that precede tablets and capsules be "homogeneous".

This term is a first collision between Theory of Sampling (TOS) and pharmaceutical industry quality control (QC) practices.[1] Here "homogeneous" does not imply a perfect mixture where the distribution of particles is strictly identical throughout the lot however, but is used to communicate that heterogeneity is sufficiently low that patients will receive a product with the strength "it purports or is represented to possess". These "homogeneous" unit doses are usually required a relative standard deviation (RSD) of less than 5%.[2,3] Quality control units in pharmaceutical manufacturing have a strong interest both in determining the average concentration of a blend, and an equally strong interest in determining how the drug varies throughout a lot (so much for homogeneity in TOS' fashion).

In this study two different methods are evaluated for mixing the active pharmaceutical ingredient (API) and excipients in a pharmaceutical blend. The first mixing procedure involves only tumble mixing. The second procedure involves a vibration mixing step to break the agglomerates of the cohesive acetaminophen particles, and a second tumble blending step.[5,6] Variographic analysis and replication experiments were then used to compare the effectiveness of the two mixing procedures. We show that variographic analysis and TOS could be very valuable in the development of pharmaceutical formulations in combination with near infrared (NIR) spectroscopy. This preliminary work is performed at lab scale but the same approach could be used by personnel at a pharmaceutical company.

Experimental

Materials: The blends were prepared from lactose monohydrate Granulac (Meggle Pharma), microcrystalline cellulose Vivapur 102 (JRS Pharma) and semi-fine acetaminophen (APAP) received from Mallinckrodt Inc. (Raleigh, NC). The lactose monohydrate was passed through a U.S. Standard Sieve 60 (250 µm opening) before mixing.

Calibration Model: An experimental design was followed to minimize correlation between components and obtain a robust NIR calibration model. Three components blends were prepared, (correlation between majority components is unavoidable, and this process reduces the other two), using the experimental design software MODDE 8.0.0.0 Umetrics (Umeå, Sweden). Settings were 14 runs, objective: screening, in a D-optimal design linear model. The concentration range was 50% (relative) above and below the 15.0% w/w (target concentration), resulting in a calibration set spanning 7.5%–22.5% w/w. The experimental design is thoroughly described by Roman et.al.[7]

Preparation of Blends: for the validation of sampling method three blends were prepared, two of 1.5 kg and one of 400 g. The blends consisted of 15% (w/w) acetaminophen (APAP), 66.67% (w/w) microcrystalline cellulose (MCC), and 18.33% (w/w) lactose (LAC). Two mixing procedures were evaluated: 1. mixing in tumble blender for one hour – this was called the T process; 2. 30 minutes of vibration and 90 minutes of tumble blending –- called the VT process. A test set blend (400 g) to challenge the calibration model was prepared with a mixing time of 30 min in each blender.

Description of FT-NIR system and software to develop the calibration model: A Bruker Optics (Billerica, MA) Matrix Fourier Transform (FT)-NIR spectrometer was used to obtain spectra. Calibration and test set spectra were obtained at a spectral resolution of 8 cm^{-1} and a total of 32 scans were averaged. Each spectrum (average of 32 scans) requires about 4.4 seconds. All spectra were obtained as the powder moved at a linear velocity of 10 mm/s, except for the static repeatability test (see below). Under these conditions each spectrum can be estimated to represent approximately 180 mg of powder mixture, based on a depth of penetration of 1.2 mm measured for this spectroscopic system.[7,8] Calibration models were developed in SIMCA 13.0 Umetrics (Umeå, Sweden), partial least squares algorithm (PLS). NIR spectra were pre-treated with a

Table 1. Results of prediction of test set blend (tumble + vibration blender) by the FT-NIR calibration model.

Validation Blend prepared with tumble mixer + vibration mixer, mixed by one hour (T + V)					
Deposition	Average % (w/w) APAP	Std. Dev	RSD (%)	RMSEP	RSEP (%)
n = 1	15.58	0.46	2.93	0.54	4.71
Spectra (#)			68		

standard normal variate transformation and a first derivative based on 17 points. The chemometric model was performed on the 9100 – 5000 cm^{-1} NIR spectral range. The performance of the calibration model was evaluated with independent test blends, aka test set validation.[9–11] Table 1 shows the results obtained in the prediction of an independent test set.

A sampling system was designed to deposit blends over a laboratory conveyor belt for simulating a 1-dim industrial blender outflow sampling/analysis system: Each powder mixture (both calibration – and validation blends) was deposited in a 3 m long, 4 cm wide and 3 cm deep rig by the use of an in-house developed screw feeder.[7] The feeder was operated so as to provide a thick powder bed on the rig. FT-NIR spectra were obtained along the entire 3 m length rig corresponded to approximately 250 g of the 1.5 kg lot powder mixture. The powder surface was left uneven and no attempt was made to obtain a flat surface of powder in the recipient, aiming to produce a highly realistic industrial situation.

Results and Discussion

Real-time analysis of drug concentration was performed by near infrared spectroscopy, as a non-destructive analytical method applied to blender output streams.[8,12] Figure 1 shows the stream sampling system used to obtain the NIR spectra. The drug concentration associated with each spectrum was predicted with the validated PLS calibration model and are shown in Figure 2 for three different blends.[13] The blend marked VT involved both vibration and tumbling mixing as described in the Experimental section, and the blends marked T1 and T2 only included tumble mixing.

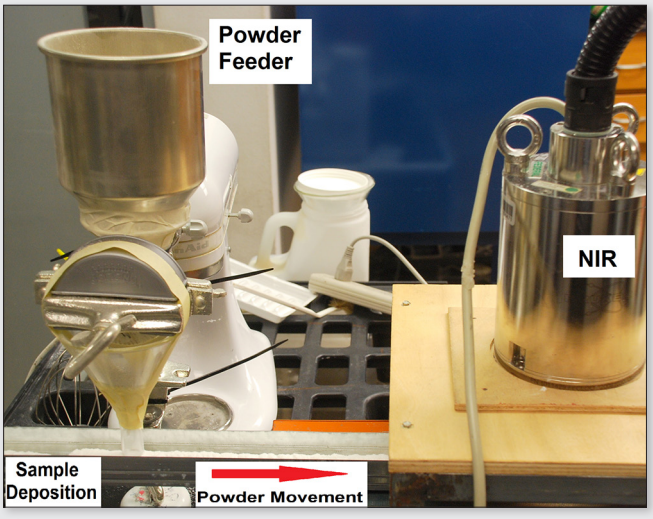

Figure 1. Powder deposition into the 3 meter rig used for moving the powder at 10 mm/sec towards the FT-NIR spectrometer.

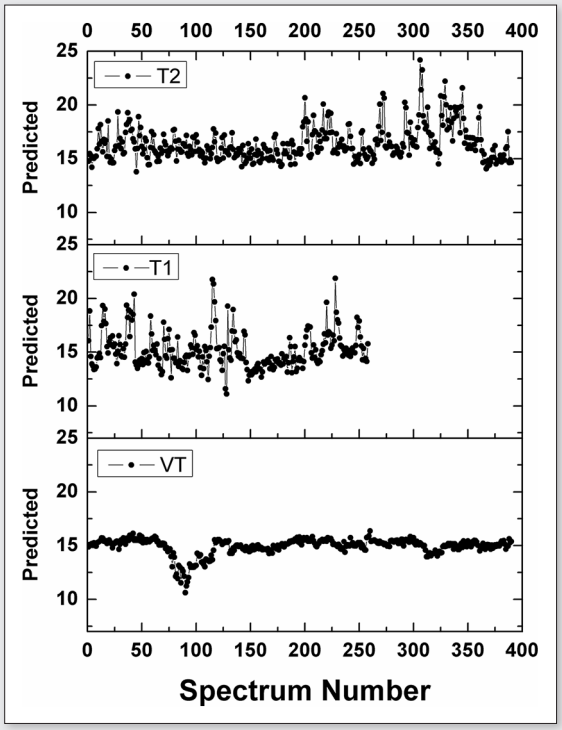

Figure 2. Prediction of drug concentration in three different blends using NIR spectroscopy and the rig shown in Figure 1.

The stream sampling approach also facilitates the use of variographic analysis and the replication experiment[9–11,14], which are virtually new in pharmaceutical blending.[7,8] The Replication Experiment was performed with the three blends (six successive rig depositions, 10 times to-and-fro over just one deposition), and the results are shown in Table 2. Figure 2 shows drug concentration results from a replication experiment where six depositions of 250 g are made onto the 3 m rig shown in Figure 1.

Figure 2 clearly shows that the VT process was superior in mixing to obtain concentrations near the 15.0% (w/w) APAP target level. Particle breaking due to vibration also improved the flow properties of the powder mixture. The central graph (T1) shows less drug concentration results due to difficulties in powder flow and deposition onto the 3 m rig. The VT process showed the lowest standard deviation (0.78% w/w APAP) as shown in Table 2, at least half of those obtained for the T process. The VT process should still be improved due to a drop in concentration observed from spectra #78–116.[7]

Table 2 also shows that the T process has a much higher standard deviation in the replication experiment (n = 10) for a single deposition. The standard deviation of the VT process is 0.34% (w/w) APAP, while the T process blends show standard deviations of 1.06 and 2.02. This replication experiment shows the significant differences in heterogeneity observed. Table 2 also shows similar repeatability study for all blends, since this study is a measurement of instrument (measurement) performance. The repeatability study was conducted by obtaining six consecutive spectra of the same static powder.

The results shown in Figure 2 are important because of the novelty of stream sampling in pharmaceutical blending[15] since most processes have been developed with sample thief ("spear") extracts.[16] Thief sampling has been used to find "dead spots"

Table 2. Comparison of the two mixing methods

	Deposition n = 6 % (w/w) APAP			Replicate of single deposition n = 10 % (w/w) APAP			Repeatability study (n = 6, at 10 points) % (w/w) APAP		
	VT	T1	T2	VT	T1	T2	VT (n = 6)	T1 (n = 10)	T2 (n = 10)
Average	14.93	15.17	16.39	15.21	14.63	16.24	15.78	15.82	15.54
Std.Dev	0.78	1.74	1.58	0.34	1.06	2.02	0.14	0.14	0.17
RSD(%)	5.20	11.46	9.62	2.23	7.25	12.46	1.3	0.88	1.12
Spectra (#)	390	258	390	647	570	650	36	60	60

– areas of incomplete mixing within the blender. The stream sampling approach is effective in showing areas of heterogeneity as shown in this study. The use of NIR spectroscopy to develop pharmaceutical processes is also increasing but most NIR spectroscopic methods are based on a NIR spectrometer installed at a single point (interface) to a blender.[17,18]

Figure 3 shows the variograms obtained for the three processes.[19,20] The three variograms show the very clear differences between the blending processes. The T process shows a significantly higher sill and nugget effect, demonstrating a very high heterogeneity of the outflow material, i.e. the least effective blending. Comparison indicate that the VT process provides a superior mixed-in distribution of the drug in the blend. However, even the best of these tentative processes would not meet pharmaceutical regulatory expectations - yet. A recently withdrawn draft guidance required: 1) a relative standard deviation ≤ 5%, and 2) all individual results within 10.0 percent (relative) of the mean drug concentration.[3] Thus, the stream sampling is clearly effective in finding areas of heterogeneity in the powder blend and simply cannot hide any presence hereof.

The VT process shows a nugget effect - minimum practical error (MPE) of only 0.04% as shown in Figure 3. Thus, the sampling and analysis system is indeed capable of providing a satisfactory very low MPE (the sum of all correct and incorrect sampling errors plus the analytical error, TAE). MPE still depends critically on the heterogeneity of the blend: MPE is greater for the less mixed, more heterogeneous blends.

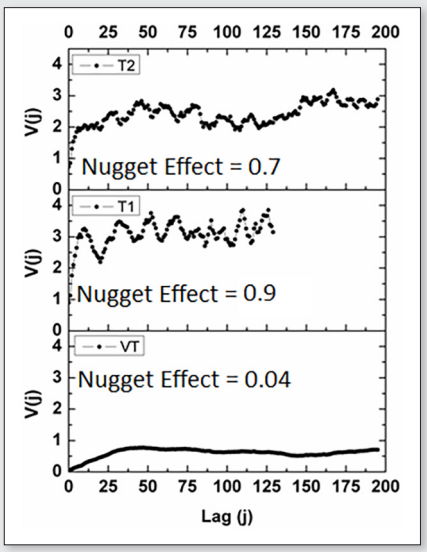

Figure 3. Variograms for the three blending procedures.

Conclusions

The stream sampling method was effective in identifying areas of significant heterogeneity in the powder blends and the need to continue improving both the mixing process, as well as the monitoring approach itself. We regard the present results as very encouraging. This pilot study indicates the way forward for a possible blending process-and-measurement-system development in the laboratory before industrial deployment, i.e. up-scaling, which will always constitute a specific issue to be tackled on a case-by-case basis.

Acknowledgements

This collaboration has been possible thanks to the support of the National Science Foundation (ERC research grant EEC-054085).

References

1. A. Ghaderi, "On characterization of continuous mixing of particulate materials", *Particulate Science and Technology.* **21,** 271-282 (2003). 10.1080/02726350390223303
2. G. Boehm, J. Clark, J. Dietrick, L. Foust, T. Garcia, M. Gavini, L. Gelber, J.-M. Geoffroy, J. Hoblitzell, P. Jimenez, G. Mergen, F. Muzzio, J. Planchard, J. Prescott, J. Timmermans and N. Takiar, "The Use of Stratified Sampling of Blend and Dosage Units to Demonstrate Adequacy of Mix for Powder Blends1", *PDA Journal of Pharmaceutical Science and Technology.* **57,** 64-74 (2003).
3. Guidance for Industry Powder Blends and Finished Dosage Units-Stratified In-Process Dosage Unit Sampling and Assessment, (2003)
4. J. H. Timmermans, "A Report of the PQRI Workshop on Blend Uniformity", *Pharmaceutical Technology.* **25,** 76-76-84 (2001).
5. J. G. Osorio, G. Stuessy, G. J. Kemeny and F. J. Muzzio, "Characterization of pharmaceutical powder blends using in situ near-infrared chemical imaging", *Chemical Engineering Science.* **108,** 244-257 (2014). 10.1016/j.ces.2013.12.027
6. J. G. Osorio and F. J. Muzzio, "Evaluation of Resonant Acoustic Mixing Performance", *Powder Technology.* http://dx.doi.org/10.1016/j.powtec.2015.02.033
7. A. Roman Ospino, C. Ortega, A. Sanchez, S. Ortiz, R. J. Romañach and K. H. Esbensen, "Estimating total sampling error for near infrared spectroscopic analysis of pharmaceutical blends—theory of sampling to the rescue", in *Proceedings of the 7th International Conference on Sampling and Blending*, *TOS forum* **Issue 5**, 71–75 (2015). doi: 10.1255/tosf.66

8. Y. Colón, M. Florian, D. Acevedo, R. Méndez and R. Romañach, "Near Infrared Method Development for a Continuous Manufacturing Blending Process", *Journal of Pharmaceutical Innovation.* **9,** 291-301 (2014). 10.1007/s12247-014-9194-1
9. K. Esbensen, P. Geladi and A. Larsen, "The Replication Myth 1", *NIR news.* **24,** 17-20 (2013).
10. K. Esbensen, P. Geladi and A. Larsen, "The Replication Myth 2: Quantifying empirical sampling plus analysis variability", *NIR news.* **24,** 15-19 (2013).
11. K. H. Esbensen and P. Geladi, "Principles of Proper Validation: use and abuse of re-sampling for validation", *Journal of Chemometrics.* **24,** 168-187 (2010). 10.1002/cem.1310
12. A. U. Vanarase, M. Alcalà, J. I. Jerez Rozo, F. J. Muzzio and R. J. Romañach, "Real-time monitoring of drug concentration in a continuous powder mixing process using NIR spectroscopy", *Chemical Engineering Science.* **65,** 5728-5733 (2010). http://dx.doi.org/10.1016/j.ces.2010.01.036
13. H. Martens and T. Naes, *Multivariate Calibration*, Wiley, (1992)
14. DS 3077, Danish Standards Foundation, (2013)
15. M. Popo, S. Romero-Torres, C. Conde and R. J. Romanach, "Blend uniformity analysis using stream sampling and near infrared spectroscopy", *AAPS PharmSciTech.* **3,** E24 (2002). 10.1208/pt030324
16. R. C. Hwang, M. K. Gemoules and D. K. Ramlose, "A Systematic Approach for Optimizing the Blending Process of a Direct-Compression Tablet Formulation", *Pharmaceutical Technology.* **22,** 158-170 (1998).
17. Y. Sulub, B. Wabuyele, P. Gargiulo, J. Pazdan, J. Cheney, J. Berry, A. Gupta, R. Shah, H. Wu and M. Khan, "Real-time on-line blend uniformity monitoring using near-infrared reflectance spectrometry: a noninvasive off-line calibration approach", *J Pharm Biomed Anal.* **49,** 48-54 (2009). 10.1016/j.jpba.2008.10.001
18. M. Alcala, M. Blanco, M. Bautista and J. M. Gonzalez, "On-line monitoring of a granulation process by NIR spectroscopy", *Journal of Pharmaceutical Sciences.* **99,** 336-45 (2010). 10.1002/jps.21818
19. K. H. Esbensen and P. Paasch-Mortensen, in *Process Analytical Technology* (John Wiley & Sons, Ltd, 2010) 37-80
20. K. H. Esbensen and L. P. Julius, "Representative Sampling, Data Quality, Validation - A Necessary Trinity in Chemometrics", *Comprehensive Chemometrics: Chemical and Biochemical Data Analysis, Vols 1-4.* C1-C20 (2009).

doi: 10.1255/tosf.66

Estimating total sampling error for near infrared spectroscopic analysis of pharmaceutical blends—theory of sampling to the rescue

A. Roman-Ospino[a], C. Ortega-Zuñiga[a], A. Sanchez-Paternina[a], S. Ortiz[a], K. Esbensen[b] and R.J. Romañach[a]
[a]andres.roman@upr.edu, [a]carlos.ortega4@upr.edu, [a]adriluz.sanchez@upr.edu, [a]stephanie.ortiz10@upr.edu, [b]ke@geus.dk, [a]rodolfoj.romanach@upr.edu

A replication experiment was performed to validate a stream sampling method for a pharmaceutical powder blend. A 1.5 kg powder blend was prepared and an in-house developed feeder was used to divide into six sub-samples of approximately 250 g. Each 250 g sub-sample (1/6 total blender lot volume) was deposited along a rig of 3 meter length. A validated near infrared (NIR) spectroscopic method was used to determine the drug concentration as the powder deposited in the rig moved at a linear velocity of 10 mm/sec. The depth of penetration of the NIR radiation was 1.2 mm and the sample volume analysed was approximately 180 mg. The MPE (minimum practical error) obtained with the system was 0.04% w/w acetaminophen (APAP), which was considered excellent for the system. The replicate analysis of the powder deposition provided 390 measurements of drug concentration, with a mean APAP concentration of 14.93% (w/w) and a relative standard deviation (RSD) of 5.20%. Replicate measurements (n = 650) of the powder deposited along a single rig of 3 m length ×10 provided an RSD of 2.23%, attributable to deposition (outflow) heterogeneity. Finally, static replicate analysis of the measurement error alone amounted to an RSD of 0.14%. The embedded replicate experiments elucidated all sources of variation in a sampling system for pharmaceutical powder blends, and proved reliable and highly sensitive in identifying areas of non-acceptable residual heterogeneity (dead zones).

Background

The analysis of drug concentration in pharmaceutical blends is mostly done through grab sampling where a sampling spear (called sampling thief in the pharmaceutical industry) is frequently inserted into a blender to extract 6–10 samples.[1,2] The extracted material is then taken to a laboratory where the drug concentration of the powder blend is determined. The sample thief is used to extract powder mixture from specific locations and transects through the blender volume, which based on previous studies, have shown a greater likelihood to represent "dead spots" (areas of residual incomplete mixing).[3] Thus, all the components of the blender volume, the lot, do not have the same probability of being extracted for analysis. This is a structural fault of the sampling system. If the areas of incomplete mixing are not those selected with this fixed location approach the sampling approach will fail to do what it is supposed to do and volumes with larger residual heterogeneities will go undetected. This is the exact opposite of the objective of end-of-mixing sampling and analysis.[1–3]

These flawed approaches are currently being complemented by non-destructive near infrared (NIR) spectroscopic methods developed to analyse the drug concentration within the blender (in-line), or at-line/off-line. The non-destructive spectroscopic methods are so far usually interfaced at a single location within the blending vessel (or interacting through a window in the vessel wall).[4] If powder moves in and out of the sampling interface there is a greater likelihood that larger parts of the lot will be analysed than with a powder thief, depending on the specific combination of analysis volume w.r.t. material through-flow in relation to the full vessel volume. But such solutions, despite having a clear potential of being significantly better than thief sampling, are by no means a complete solution for the desired blender material characterisation based on the full blender volume. To the degree that this is not achieved (yet), the present verification approaches cannot be said to be comprehensive.

However the powder mixture can alternatively be sampled after it leaves the blender, either using a physical sampling approach or by invoking the rapid, and more efficient NIR spectroscopic method for analysis.[1,2] In this approach the powder flows down a chute, or is ducted via a mini-conveyor belt, from which a NIR spectrometer can obtain spectra of the mixture. This is a Process Analytical Technology (PAT) approach, of great potential and considerable proved merit.[5–7] Based on a chemometrics multivariate calibration model it is possible to predict the drug concentration in the NIR-beam analytical volume.[8] This stream sampling approach has been followed experimentally in a limited number of pilot studies.[9–11]

We here report on pioneering laboratory validation of a PAT stream sampling approach where the active drug concentration is determined by NIR spectroscopy. Previous studies have involved thorough validations of NIR analytical methods obtaining accurate estimates of the Total Analytical Error (TAE), but have not addressed the accompanying sampling errors.[4] This study describes the result of a first systematic Replication Experiment approach[12] in a realistic laboratory setting. The systematic replication experiments represent a new approach to the analysis of blends and to estimating the *effective* sampling and measurement uncertainty within pharma.[12–14] We are aware of only two other forays within pharma, in which TOS is also an important element, both focusing on product analysis uncertainty[17,18]

Experimental

Materials: The blends were prepared from lactose monohydrate Granulac (Meggle Pharma), microcrystalline cellulose Vivapur 102 (JRS Pharma) and semi-fine acetaminophen (APAP) from Mallinckrodt Inc. (Raleigh, NC). The lactose monohydrate was passed through a U.S. Standard Sieve 60 (250 µm opening) before mixing.

Calibration Model: An experimental design was followed to minimize correlation between components and obtain a robust

Table 1. Composition of calibration and test set blends for NIR calibration model.

Blend	1	2	3	4	5	6	7	8	Test set
APAP (% w/w)	7.50	7.50	7.50	14.00	15.00	16.25	22.50	22.50	15.0
MCC (% w/w)	30.00	90.00	60.00	63.50	30.00	83.75	77.50	30.00	66.67
LAC (% w/w)	62.50	2.50	32.50	22.50	55.00	0.00	0.00	47.50	18.33

calibration model. Three component blends were prepared (correlation between majority components is unavoidable, and this process reduces the other two). The experimental design software MODDE 8.0.0.0 Umetrics (Umeå, Sweden) was used. Settings were 14 runs, objective: screening, in a D-optimal design linear model. The concentration range was 50% above and below the 15.0% w/w APAP target concentration, resulting in a calibration set spanning 7.5–22.5% w/w. Table 1 shows the concentrations of the eight calibration blends prepared.

Preparation of Test Set Blend: A 1.5 kg blend with an APAP concentration of 15.0% (w/w) was prepared as shown in Table 1. This blend was used for the entire replicate study.

Description of Fourier Transform Near Infrared (FT-NIR) system and software to develop the calibration model: A Bruker Optics (Billerica, MA) Matrix FT-NIR spectrometer was used to obtain spectra. Calibration and test set spectra were obtained at a spectral resolution of 8 cm^{-1} and a total of 32 scans were averaged. Each spectrum (average of 32 scans) requires about 4.4 seconds. All spectra were obtained as the powder moved at a linear velocity of 10 mm/s, except for the static repeatability test (see below). Under these conditions, each spectrum can be estimated to represent approximately 180 mg of powder mixture as shown in Figure 1.[11] Calibration models were developed in SIMCA 13.0 Umetrics (Umeå, Sweden), partial least squares algorithm. NIR spectra were pre-treated with a standard normal variate transformation and a first derivative based on 17 points. The chemometric model was performed on the 9100–5000 cm^{-1} NIR spectral range. The performance of the calibration model was evaluated with independent test blends, aka test set validation.[13–15]

A sampling system was designed to deposit blends over the conveyor belt for simulating a 1-dim industrial blender outflow sampling/analysis system. Each powder mixture (both calibration – and validation blends) was deposited in a 3 m long, 4 cm wide and 3 cm deep rig by the use of an in-house developed screw feeder, as shown in Figure 2. The feeder was operated so as to provide a thick powder bed on the rig. FT-NIR spectra were obtained along the entire 3 m length rig corresponded to approximately 250 g of the 1.5 kg lot powder mixture. The powder surface was left uneven and no attempt was made to obtain a flat surface of powder in the recipient, aiming to produce a highly realistic industrial situation.

Figure 2 shows a photograph of the system for Replication Experiment studies (six successive rig depositions, 10 times to-and-fro over just one outflow. The Matrix FT-NIR spectrometer is situated at a height ~10 cm to obtain spectra as the rig moves at 10 mm/sec. The replicate experiment was first conducted by performing 6 outflow depositions each of approximately 250 g along the 3 m rig. This setup yielded approximately 65 spectra per outflow stream. The APAP drug concentration was predicted for each spectrum using the validated FT-NIR calibration model (multivariate calibration prediction).[8]

The second replication experiment consisted of moving one of the full length outflow deposition over the conveyor belt to and fro 10 times, obtaining spectra from one end to the other. The final part consisted of a repeatability study, where six consecutive spectra were obtained at one fixed location without moving the powder mixture or the spectrometer. This repeatability study was itself performed a total of 6 times. All replication experiment results are shown in Table 2.

Results and Discussion

The above replication experiment was performed to validate a specific PAT sampling/analysis facility for a realistic 1.5 kg powder blend

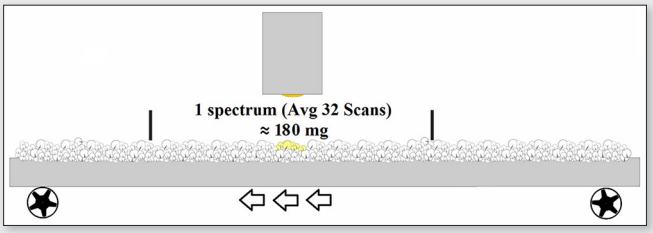

Figure 1. Schematic rig illustration of PAT sampling by a NIR spectrometer along conveyor belt material stream. Observe how the NIR beam only interacts with the top layers of the material stream, giving rise to structural IDE/IME contributions to the total measurement system error in the vertical direction[depth of penetration is 1.2 mm]. The estimated analytical mass is about 180 mg.

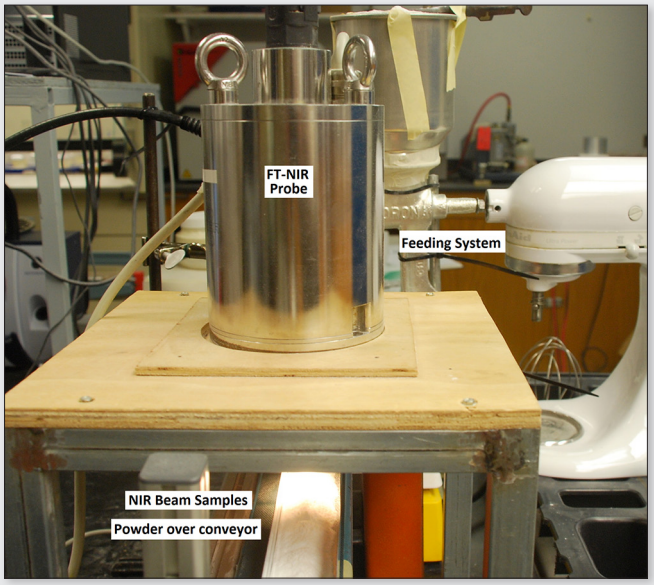

Figure 2. Conveyor belt assembly (total length 3 m) with FT-NIR spectrometer positioned at a height of 10 cm and powder feeding system (background). Note that the NIR beam covers the entire width of the conveyor belt, suppressing a potential IDE contribution to the total measurement system error in the cross-stream direction.

Table 2. Results of Replication Experiments.

	Deposition[a] (n = 6)	Replicates[b] of Single Deposition (n = 10)	Repeatability Study[c] (n = 6)
Ave.	14.93	15.21	15.78
Std. Dev.	0.78	0.34	0.14
RSD (%)	5.20	2.23	1.3
Spectra (#)	390	647	36

[a]Deposition = one deposition length (3 m)

[b]Spectra were collected 10 times along the complete length of the rig for a total of 647 spectra

[c]Static NIR beam footprint on unmoving rig; six replicated NIR spectra acquisition

prepared with a 15.0% (w/w) APAP concentration. The lot in question was the full 1.5 kg prepared blend, from which the six repetitions of a full length (3 m) 250 g rig experiment could be performed. Each 250 gram sub-sample (1/6 total blender lot volume) allowed about 65 analyses (based on NIR spectra) to be made along the rig length, Figures 1 and 2. This enables evaluation of both full and partial blender outflow analysis performance.

Table 2 shows that the grand average concentration predicted by the NIR calibration model was 14.93% (w/w), based on all 390 analyses performed for the lot, i.e. a situation in which the *entire* outflow material stream has been analysed. The relative standard deviation of this complete lot volume results was 5.20%. These results must be considered excellent as these involve the maximal combined variation effects stemming from i) the outflow deposition (flow segregation), ii) residual blend heterogeneity and iii) TAE of the PAT NIR analytical method. The relative standard deviation is termed the relative sampling variability (RSV) for the replication experiment approach.[12]

Table 2 also shows the results from replicate analysis of a single deposition (i.e. a single conveyor belt pass but repeated to-fro 10 times). This experiment addresses the specific blend heterogeneity in one 1/6 total lot stream only (including the attendant TAE). As expected, this RSV variation is significantly lower, 2.23%. The average drug concentration is here 15.21% (w/w). Thus, the average concentration is different from that when the entire lot was analysed. There is thus a difference of +0.28% APAP, due to that only 1/6 part of the lot is being analysed.

The static analytical repeatability studies results (the NIR beam was focused on a single unmoving area of the powder blend and six consecutive spectra were acquired) are also shown in Table 2. The relative standard deviation in the repeatability study is approximately 0.2%, attesting to TAE only.

Variability larger than this analytical baseline represents i) residual blend heterogeneity (imperfect mixing), ii) specific outflow variability ("deposition" above) as well as iii) possible process sampling errors for the PAT sensor system. The variance of this analytical repeatability study $(0.2)^2$ may be subtracted from the square of the standard deviation of the replicate analysis of the single deposition to obtain a measure of the blend heterogeneity. The replicates of single deposition show a standard deviation of 0.34, and after subtracting the measurement repeatability the blend heterogeneity is

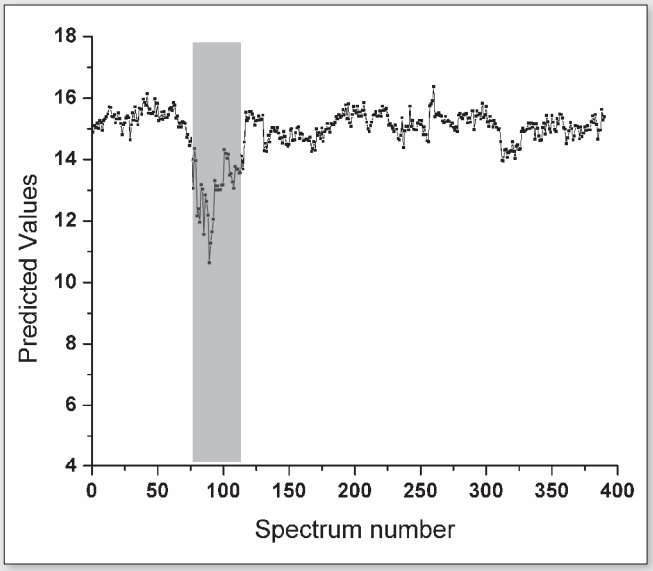

Figure 3. Prediction of drug concentration for the 390 individual analysis of the complete lot (six ×3 m rig lengths).

0.31. These values could be used as baseline level to improvement the sampling and measurement systems.

Figure 3 shows the plot of the drug concentration values throughout the entire run, revealing a significant drop in drug concentration from approximately spectrum #78 to 116. This simple plot is crucial in showing that a certain part of the blend was responsible for the overwhelming part the heterogeneity observed—a dead spot. The drug concentration from spectrum #81 to 100 averaged 12.5% instead of the 15.0% target level. Thus, the stream sampling approach was very capable to identify incomplete mixing process without the use of sampling spear.

The main feature of the replication experiment studies concerns the possibility to apply a variographic characterisation of the outflow stream. The variogram function V(j) was determined based on the drug concentration values predicted by the NIR calibration model. A lag of 1 was based on consecutive predictions of drug concentration, each concentration corresponding to approximately 180 mg as shown in in Figure 1. The maximum lag shown in the variogram is 190, since the total number of drug concentration predictions was ~390. From Figure 4 it is obvious that the total PAT measurement system error is very small (nugget effect) compared to the level of drug content variance (sill) along the full 3m outflow stream. The range is approx. 30–36, i.e. the distance within each predicted drug concentration is increasingly auto-correlated for smaller lags than this.

This run also allows a simulation of the variographic outflow approach for NOC (normal operation conditions), by excluding the samples in the interval #78–116 (resulting in a seamless outflow only characterised by the NOC residual heterogeneity). A renewed variogram for this data series is presented in Figure 4 (right), in which can be seen that the nugget effect is identical, while there is a very notable reduction of the sill level – both features as expected. Renewed estimation of the $RSV_{1\text{-}dim}$ results in 2.6%. This run is fully realistic w.r.t. to its industrial counterpart to the degree that the blender used is reasonably up-scalable; all other system elements

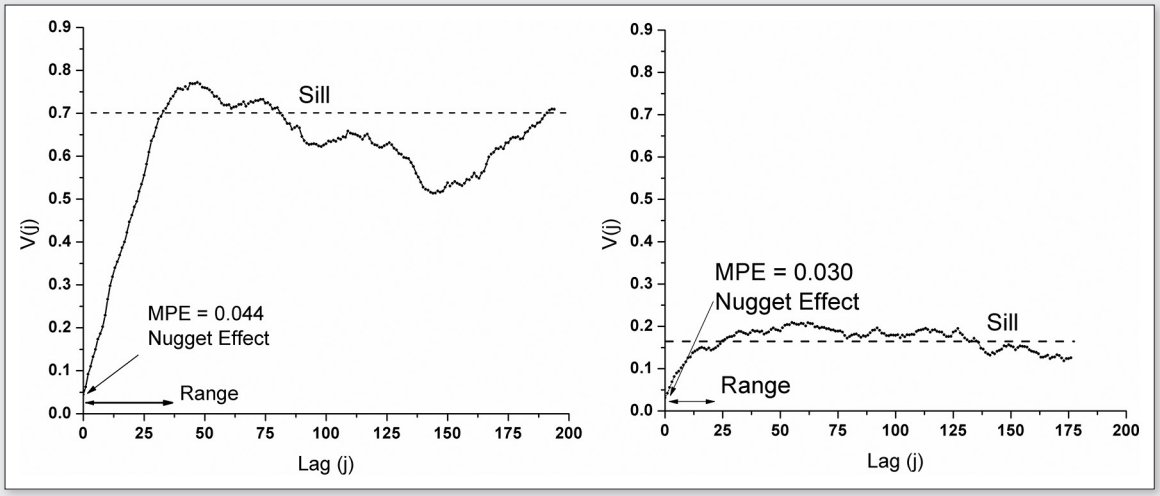

Figure 4. Left: Variogram based on the total of 390 individual analyses of the complete lot (six ×3 m rig lengths). The range is ~30-36; nugget effect = 0.04; sill = 0.7. The total measurement system uncertainty, $RSV_{1\text{-}dim}$, is therefore ~5.2% (rel).[12] Right: Same variogram excluding shaded area in Figure 3.

would be identical: outflow facility, NIR spectrometer, chemometric prediction model.

A recently withdrawn draft guidance which describes the analysis of powder blends by thief sampling requires the analysis of drug concentration for at least 10 blends from a tumble blender with: 1) a relative standard deviation ≤5%, and 2) all individual results within 10.0 percent (relative) of the mean drug concentration.[16] The 390 determinations of drug concentration display a RSD of 5.20% slightly exceeding the first requirement and did not meet the second requirement due to the dead spot drop in concentration shown in Figure 3. Thus, the outflow stream sampling system is eminently capable of finding areas of heterogeneity in the entire blend lot. If the blending process were improved by eliminating the sudden drug concentration drop shown in Figure 3, then the RSD in drug concentration reduces to approximately 2.6% and all values are now within 10% of the mean drug concentration stipulation.

To the degree that a complete, up-scalable measurement system can be established in the laboratory, the present approach will be able to guide rational product development, to some considerable degree without pilot—or full scale plant demonstration—until the manufacturing process has been brought into complete statistical control in the laboratory.

The value of an outflow variographic facility has been demonstrated and its merits exemplified. This is the first time a TOS-based approach (variographic and replication experiment) for the characterisation of a pharmaceutical manufacturing process has been applied with illustrative and highly satisfactory results.

Acknowledgements

This collaboration has been possible thanks to the support of the National Science Foundation (ERC research grant EEC-054085).

References

1. R. J. Romañach and K. H. Esbensen, “Sampling in pharmaceutical manufacturing - Many opportunities to improve today’s practice through the Theory of Sampling (TOS).”, *TOS Forum.* **4,** 5-9 (2015).
2. K. H. Esbensen and R. J. Romañach, “Proper sampling, total measurement uncertainty, variographic analysis & fit-for-purpose acceptance levels for pharmaceutical mixing monitoring”, in *Proceedings of the 7th International Conference on Sampling and Blending*, *TOS forum* **Issue 5,** 25–30 (2015). doi: 10.1255/tosf.68
3. G. Boehm, J. Clark, J. Dietrick, L. Foust, T. Garcia, M. Gavini, L. Gelber, J.-M. Geoffroy, J. Hoblitzell, P. Jimenez, G. Mergen, F. Muzzio, J. Planchard, J. Prescott, J. Timmermans and N. Takiar, “The Use of Stratified Sampling of Blend and Dosage Units to Demonstrate Adequacy of Mix for Powder Blends1”, *PDA Journal of Pharmaceutical Science and Technology.* **57,** 64-74 (2003).
4. C. V. Liew, A. D. Karande and P. W. S. Heng, “In-line quantification of drug and excipients in cohesive powder blends by near infrared spectroscopy”, *International Journal of Pharmaceutics.* **386,** 138-148 (2010). http://dx.doi.org/10.1016/j.ijpharm.2009.11.011
5. K. A. Bakeev, *Process Analytical Technology: Spectroscopic Tools and Implementation Strategies for the Chemical and Pharmaceutical Industries*, Second. Wiley, (2010)
6. K. H. Esbensen and P. Paasch-Mortensen, in *Process Analytical Technology* (John Wiley & Sons, Ltd, 2010) 37-80
7. K. H. Esbensen and L. P. Julius, “Representative Sampling, Data Quality, Validation - A Necessary Trinity in Chemometrics”, *Comprehensive Chemometrics: Chemical and Biochemical Data Analysis, Vols 1-4.* C1-C20 (2009).
8. H. Martens and T. Naes, *Multivariate Calibration*, Wiley, (1992)
9. M. Popo, S. Romero-Torres, C. Conde and R. J. Romanach, “Blend uniformity analysis using stream sampling and near infrared spectroscopy”, *AAPS PharmSciTech.* **3,** E24 (2002). 10.1208/pt030324
10. A. U. Vanarase, M. Alcalà, J. I. Jerez Rozo, F. J. Muzzio and R. J. Romañach, “Real-time monitoring of drug concentration in a continuous powder mixing process using NIR spectroscopy”, *Chemical Engineering Science.* **65,** 5728-5733 (2010). http://dx.doi.org/10.1016/j.ces.2010.01.036
11. Y. Colón, M. Florian, D. Acevedo, R. Méndez and R. Romañach, “Near Infrared Method Development for a Continuous Manufacturing Blending Process”, *Journal of Pharmaceutical Innovation.* **9,** 291-301 (2014). 10.1007/s12247-014-9194-1
12. DS 3077, Danish Standards Foundation, (2013)

13. K. Esbensen, P. Geladi and A. Larsen, “The Replication Myth 1”, *NIR news.* **24,** 17-20 (2013).
14. K. Esbensen, P. Geladi and A. Larsen, “The Replication Myth 2: Quantifying empirical sampling plus analysis variability”, *NIR news.* **24,** 15-19 (2013).
15. K. H. Esbensen and P. Geladi, “Principles of Proper Validation: use and abuse of re-sampling for validation”, *Journal of Chemometrics.* **24,** 168-187 (2010). 10.1002/cem.1310
16. Guidance for Industry Powder Blends and Finished Dosage Units-Stratified In-Process Dosage Unit Sampling and Assessment, (2003)
17. M. Paakkunainen, S. Matero, J. Ketolainen, M. Lahtela-Kakkonen, A. Poso and S. P. Reinikainen, “Uncertainty in dissolution test of drug release”, *Chemometrics and Intelligent Laboratory Systems*. **97,** 82-90 (2009).
18. M. Paakkunainen, J. Kohonen and S. P. Reinikainen, “Measurement uncertainty of lactase-containing tablets analyzed with FTIR”, *Journal of Pharmaceutical and Biomedical Analysis*. **88,** 513-518 (2014).

doi: 10.1255/tosf.71

Practical use of variographics to identify losses and evaluate investment profitability in industrial processes

Hilde S. Tellesbø[a], Helle Fossheim[b] and Kim H. Esbensen[c]
[a] Weber Leca Rælingen, Saint-Gobain Byggevarer AS, Rælingen, Norway. E-mail: hilde.tellesbo@weber-norge.no
[b]Saint-Gobain Byggevarer AS, Oslo, Norway. E-mail: helle.fossheim@weber-norge.no
[c]ACABS research group, Institute of Chemistry and Biology, Aalborg University, campus Esbjerg. Denmark. E-mail: kes@bio.aau.dk

This work illustrates variographic analysis applied to industrial production processes to identify and reduce adverse production deviations (over-specification, loss) and evaluate profitability. A first example concerns production of light-weight expanded clay aggregates (Exclay), produced in cement-like rotary kilns. Clay raw material is heated to 1150 ºC to be expanded. An adverse periodicity was observed in a specific plant cooler manifested as fluctuations in the material volume (height level) causing a periodic variance in the production output from the kiln. This problem must be resolved by instigating a more stable cooler, which could in fact be engineered by a very small investment of about 5,000 Euro. A variogram characterization was carried out to evaluate the amplitude of the periodicity, and the quantities involved (losses), which information was used to calculate the investment pay-back time. From the variogram it was observed that the reduced kiln output volume was at least 0.7%. During one year with improved cooler level control, this translates into savings of about 100,000 Euro, i.e. a pay-back time will be less than one month. A second example is from a LRM-project (Loss and Reduction Model) at a plant producing bagged pre-mixed mortars, in which the variance of the weight of the produced bags was found to be consistently too large. A pilot variographic analysis was applied with an aim to identify the root causes of this problem (three filling stations at the same line were investigated, all with identical filling systems and scales): Two stations were found to have a total material loss of 1.2%, while the third was running perfectly well (low V(0) and low sill), but with a too high set point. The technical resolution shows that it is possible to reduce material loss with existing equipment by improved monitoring/recording routines but no need to acquire new expensive belt scales a.o. For two of the stations V(0) (MPE) was in fact at a level almost identical to the sill making it structurally impossible to keep bag weight within specifications. Recurrent monitoring of V(0) and moving average smoothing should be evaluated at the very many similar production lines in the multinational corporation involved to gain improved process control to reduce overfilling. While relatively small on the basis of an individual filling line, the potential accumulated corporate savings take on a quite different economic significance. Variographic analysis is a powerful tool for industrial technicians and process engineers to improve processes – and in the present cases for industrial managers as well for evaluating ultimate investment profitability in industrial processes.

Introduction

To illustrate systematic application of variographic analysis in process industry, two examples from the multi-national Saint-Gobain Weber corporation are presented. The first example, from production of expanded clay aggregate building material, shows how variografic analysis can be used to calculate investment pay-back time with better accuracy than by use of standard statistical methods. The other example concerns bagging of premixed mortars are in fact typical for a variety of industrial bagging processes in general. This example shows how variographic analysis can be used to identify the main reasons for adverse product variances (here bag weight) and how to reduce such deviations and thereby reduce production costs.

Example from Exclay industry

The first example concerns production of light-weight expanded clay aggregates (Exclay), produced in cement-like rotary kilns. Clay raw material is heated to 1150ºC to be expanded. A periodicity was observed in a specific plant cooler regarding fluctuations in the material level. This influences the amount of air passing through the cooler and thereby amount of air and the pressure in the kiln. Periodicities in the pressure in the kiln cause periodicities in the level of expansion and thereby in the output from the kiln. A lower expansion means a smaller volume produced from the same amount of raw material, i.e. higher production costs (sales are valued by m3 produced). There is a lower limit to an acceptable product density. Also, if the temperature/pressure is raised too high, a point will be reached where the material will sinter and sizable lumps in the kiln will cause severe problems. The operators always try to burn as hard as possible to optimise the m3 output from the kiln. However the maximum level of hard burning is limited by the material with lowest densities, if a cyclic short term periodicity is manifested. Periodicities in the densities will then reduce the output of the kiln.

The unstable level in the cooler could be improved by a small investment of about 5,000 Euro. Earlier the level in the cooler has been measured by use of a radioactive isotopes. This has been found not to be precise enough however (besides being a serious environmental issue). By replacing this approach with a modern radar measurement system, the precision is increased satisfactorily. Variographic analysis was carried out to evaluate the pay-back time of the investment. Figure 1 shows a photo and schematic drawings of the Niems cooler used at the plant.

Example from pre-mix industry

The other example is from a LRM-project (Loss and Reduction Model) at a plant producing pre-mixed mortars. LRM enables manufactures to evaluate four modules: material, machine, distribution and maintenance, that each may require improvement. The losses in each module are identified by breaking down the process in its part elements, allowing a simplified, focused improvement

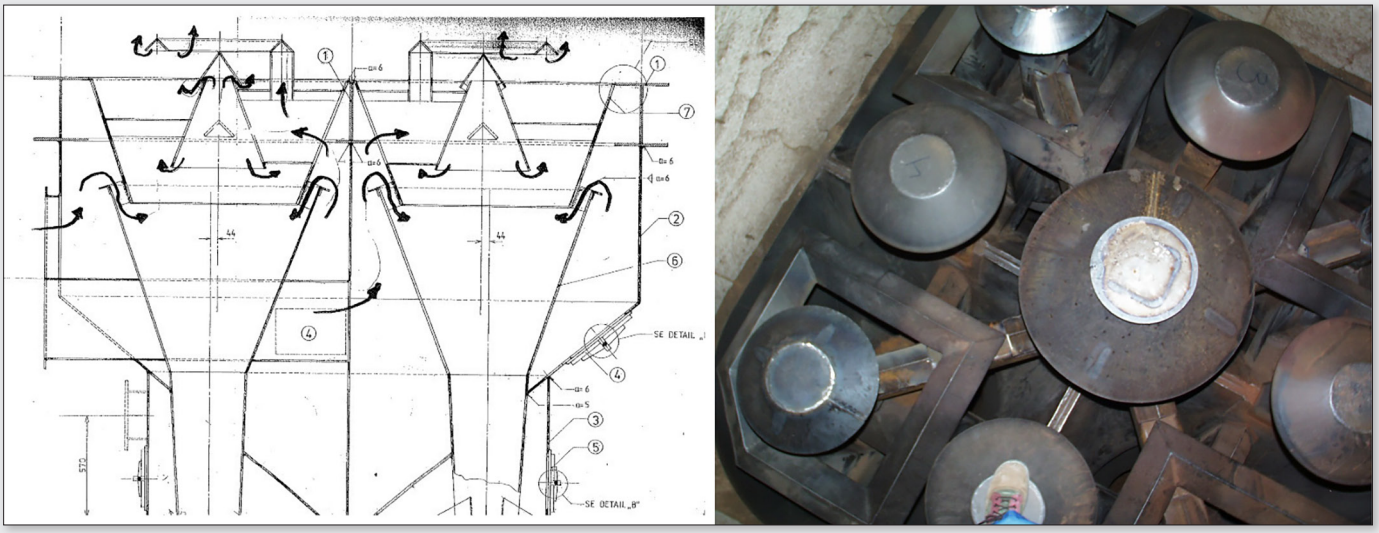

Figure 1. Schematic drawing and photo of a Niems shaft cooler. Material falls from the kiln head into the top of the cooler. Cooling air is blown in from below as shown in the drawing (left).

approach. Variographic analysis is not included in LRM today, but the present contribution suggests how this may be introduced with significant advantage.

The LRM project identified a material loss by weighing pallets of bagged material. The bags on the pallet originated from three filling stations at a specific line as a pilot study. The bags shall have a nominal weight of 25 kg. The lower and upper acceptance limits are stipulated to 24.5 and 25.5 respectively. The pallets were too heavy and indicated material losses. Variographic analysis together with traditional statistics was used to try to identify the root causes and suggestions for further progress on reduction of material losses. Variographic analysis has earlier shown to be a powerful tool to separate the different potential factors contributing to this variance[2]. Investment caution rules the day, e.g. it would be futile to invest in new expensive equipment to level the filling degree, if the main problem f.ex. turned out to be caused by inaccurate scale measurements.

The bags are filled by using air-pressure from two nozzles into a transportation air-tube. One of the nozzles sets the packing chamber under pressure to force the material through an opening, with a connecting tube that leads into the filling-bag. The second nozzle delivers the conducting airstream. Adjustment of the differential air-pressure between these two streams controls the filling of the bags. The nozzles get their regulatory input from the scales, which are stipulated to operate according to a specification of 25 ± 0.5 kg. Outside these limits the filling station is stopped. The scales are normally put on 'auto-correct' which is able to perform corrections with a magnitude of ±0.1–0.2 kg. If the weight of a particular bag is registered as above 25 kg, the weight of the next bag is reduced with 0.1 kg – and conversely if the weight is below 25 kg, the weight of the next bag is increased with 0.1 kg.

Methodology

A variogram can be used to break down the contributing elements together making up the overall variance into their separate component sources. This is of critical interest in industrial processes. The variogram can be divided into three different components[1]:

$$V(j) = V_1(j) + V_2(j) + V_3(j) \quad (1)^1$$

Where:

V(j) is the overall variance (total observed process variance), i.e. the variogram

$V_1(j)$ is the short-range random, discontinuous contribution

$V_2(j)$ is the long-range, non-random continuous contribution (trend errors)

$V_3(j)$ is the periodic continuous contribution (periodic error)

j – is the sampling inter-distance, aka the lag

$V_1(j = 1)$ describes the overall variance contribution reflecting the uncertainty introduced because measurements are only made at discrete intervals[1]. This is of course always of interest, but even more interesting is $V_1(j = 0)$. This is a back-extrapolation made from the variogram indicating the variance to be obtained, if one would be able to sample at the exact same location twice (repeated sampling). This estimate (the 'nugget effect') quantifies the quality of the total sampling and measuring systems used. Thus V(0) includes all the correct and incorrect sampling errors (CSE + ISE) in addition to TAE. For this reason V(0) is also termed the Minimum Possible Error (MPE) for a process monitoring system. V(0) will never be zero due to Fundamental Sampling Errors (FSE), but in the practical industrial use V(0) is never dominated by FSE alone, but will always be significantly higher. Thus a high V(0) usually indicates significant contributions from the Incorrect Sampling Errors and or GSE. A significantly high V(0) (with respect to the sill) is a critical warning of a serious total measurement system problem, which must be rectified. If V(0) is too high in this sense, it will not be possible to control the process in a satisfactory way, since this disallows insight into the real process variations. The closer V(0) is to the sill the more the real process variation signals are drowned out by a structurally flawed measurement system, a situation which will unavoidably lead to faulty decisions and actions.

$V_2(j)$ reflects underlying process trends, important in any industrial production process, but easily spotted already in the raw time series process monitoring data. It is preferable to deal with this type of process deviations before applying variographic analysis.

$V_3(j)$ reflects cyclic process behaviours, of critical interest in production and manufacturing process. A variogram will easily detect a periodicity and its apparent amplitude, indicating how much it contributes to the overall variance. The associated costs can thereby also be estimated with relative ease. This is an area that requires some insight and experience.

The overall variance V(j) at high j (large sampling distances) reflects the total process variance beyond the range, i.e. the sill.

It has been found useful to relate the magnitude of V(0), the process measurement system error (MPE), to the level of the sill, as a%-age, and to use this as a *quality index* for the total process measurement system[6]. The higher this index w.r.t. its maximum value (100% – at which level it would be equal to the sill), the worse the performance of the measurement system. Indices over 50% run a severe risk of deceiving process monitoring proper; in general this index should be below 33% or so to be acceptable *ibid*.

Estimation of cyclic amplitudes

Considering a sine curve, $h_x(T)$, with an amplitude h_3 and a period T, one can calculate the corresponding variogram

$$h_{3t} = h_3 \sin\left(\frac{2\pi t}{T}\right) \quad (2)^1$$

$$V_3(j) = (h_3^2)/2(1-\cos(2\pi j/T)) \quad (3)^1$$

Thus the amplitude of a cyclic variogram is:

$$V_3(j) = \frac{h_3^2}{2} \quad (4)^1$$

i.e. half the distance from minimum to maximum in the relevant cyclic part variogram[1].

The amplitude of the cycle h_3 can thus be calcualted as follows:

$$h_3^2 = 2 \times V_3(j) \quad (5)$$

Leading to:

$$h_3 = \sqrt{2 \times V_3(j)} \quad (6)$$

i.e the square root of the cyclic contribution variance estimated from the variogram.The amplitude of a cyclic periodicity is found by first defining V(0). Thereafter is a line drawn from the minimum in the cycle to V(0) on the y-axes (see Figure 6). A parallel line is drawn from the maximum point to the y-axis (see Figure 6). The value of the cyclic contribution of the variance is read/measured/calculated by subtracting the minimum value of crossing from the maximum value. This furthers a basis for estimating cost savings from reducing or eliminating a cyclic contribution.

Exclay industry

Samples for loose bulk density measurements were taken after the cooler unit every 90 seconds for close to two hours. The samples were taken from a falling stream with a customized collector. See Figure 2. This sampling equipment is not in full accordance with Theory of Sampling (TOS), but has earlier been evaluated to be fit-for-purpose[3]. This earlier work also concluded that loose bulk density is an informative parameter regarding instability

Figure 2. Sampling equipment for loose bulk density measurements (while not 100% TOS compliant, the manual cross-stream sampler at least covers the entire width of the falling stream).

control in the production process[3]. Density measurements were carried out continuously by a Thaulow bucket in accordance with EN1097-3[4].

Pre-mix industry

Since bag weights are not recorded in the present plant setup, a continuous film recording was made of the bagging line showing the display of all three filling lines. The weights were extracted from this documentation variographic analysis was carried out on this basis.

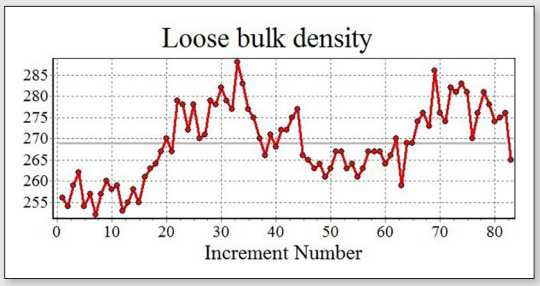

Figure 3. All 83 single measurements from the Exclay experimental campaign.

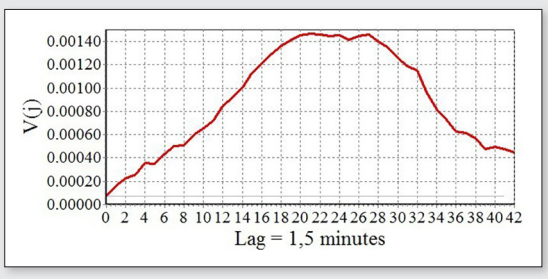

Figure 4. Variogram of the 83 measurements in Fig. 3.

Results and discussion

Exclay industry

All 83 single measurements of the loose bulk densities and the corresponding variogram are shown in Figures 3 and 4.

A major long term periodicity is observed, showing an unstable production period, interpreted as probably caused by changes in clay and/or coal feeding. It is important to follow up on this variance contribution[3,5], but this is not a part of the present study. In order to assess the contribution from the level in the cooler better, the long term periodicity has to be eliminated from the variogram. The first part of the period measured is from a period with an increasing trend and unstable production. This part is not included in the final analysis. In addition there is a dip in the densities between measurements 45 and 65 of about 10 kg/m^3. This is typically what happens when the operator adjust the coal feeding to the burner. These densities are therefore increased by 10 kg/m^3 to eliminate this long term contribution. One outlier (measurement no 63) was also adjusted.

The adjusted measurements and the corresponding variogram are shown in Figures 5 and 6.

After these process-experience dependent adjustments, a periodicity with a frequency of lag = 5 emerges, i.e. 7.5 minutes. This corresponds well with the experience of seasoned process operators. This strong periodicity makes it difficult to estimate V(0), but from Figure 6 it can be seen that the V(0) probably lies between 0.000067 and 0.00010. A conservative estimate of the contribution to the variance from the cyclic periodicity, would therefore be ~0.00005 (see Figure 6). The amplitude of the recorded data is then calculated from equation 6 to be 0.0071 or 0.71%. With an average density of 276 kg/m^3 this equals 2.0 kg/m^3. This may appear as but a small effect, but when accumulated equals savings of approximately 100,000 Euro per year. On this bases pay-back time of the investment of 5,000 Euro will be less than one month. It will likely even be shorter since short term cycles often confuse operators to decide to take action where they in fact should have remained passive.

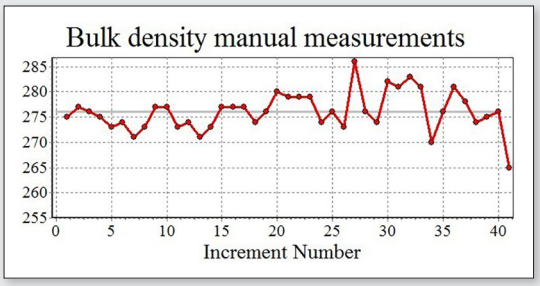

Figure 5. Single measurements of loose bulk density (see text for details)

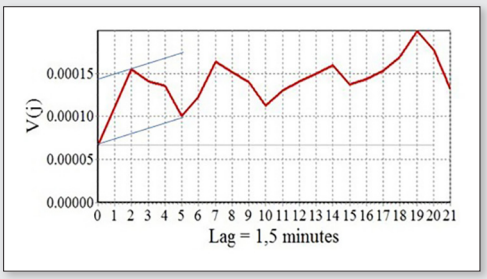

Figure 6. Variogram of the last part of the measured period (see text for details).

Pre-mix industry

For each filling station 23 (24) bags are included in the analysis. This is absolutely at the lower end to give a fully satisfactory data base upon which to arrive at fully credible conclusions, but the results may still point to real-world problems and may certainly help to illustrate how variografic analysis can be used to identify root causes and to propose an action plan at a bagging line.

Figures 7– 9 show the results of the three filling stations of the bagging line investigated. Figures 10–12 show the corresponding variograms. It is easily seen that the three filling stations behave very different at the pilot study campaign time.

The overall overfilling was 1.2% in the period analysed, i.e. 1.2% unnecessarily increased raw material costs.

Bagging station 1 was found to be the one best tuned. The overall variance (sill) is low, and almost the whole contribution to

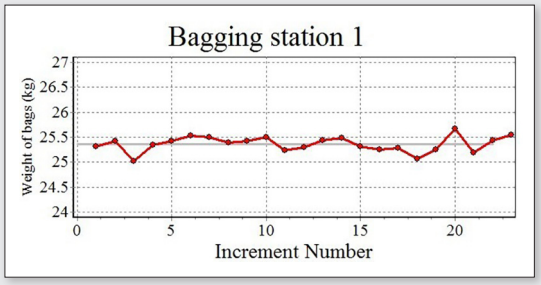

Figure 7. Weight measurements at bagging station 1.

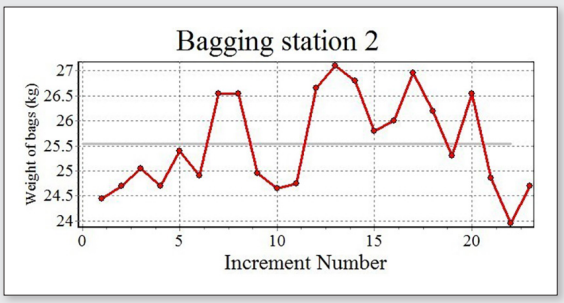

Figure 8. Weight measurements at bagging station 2.

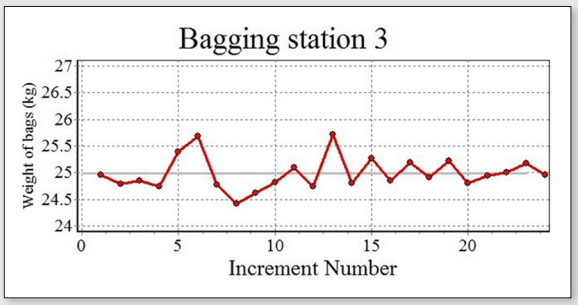

Figure 9. Weight measurements at bagging station 3.

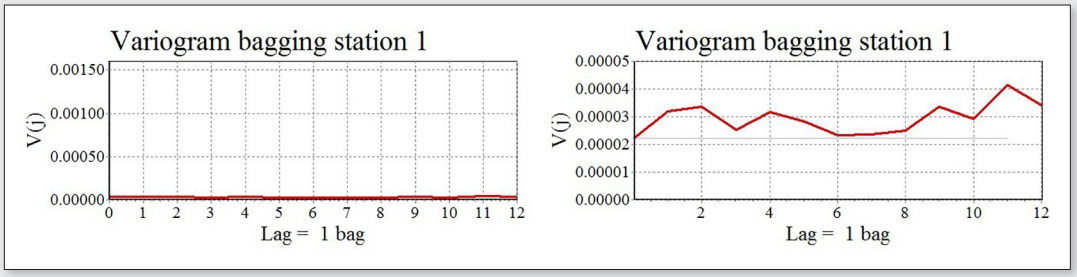

Figure 10. Variogram of data from bagging station 1, (left) for comparison of all stations; (right) for close-up evaluation.

the variance comes from V(0). This means that most of the variance observed stems the measurement system. The variance of the bags from this station is well inside the limits of ±0.5 kg from the average. There was one notable issue however; the average is 25.36, i.e. an overconsumption of 1.5% of raw material. This will of course increase the production costs. The explanation for the high average was probably that the autocorrect of the weight was found to be turned off, in combination with slightly too high pressure.

Bagging station 2 has a serious problem, displaying extremely high variations. The sill (overall variance) is 100 times higher than for bagging station 1. One bag is even above 27 kg. The average weight is 25.55 kg which corresponds to an overconsumption of 2.2%. V(0) is higher than for bagging station 1. The different bagging lines are using the same type of scale, but there could be other factors contributing to the higher V(0) value, such as vibrations, dust on the scales etc. V(0) is presently at the limit to give bag weights just within the ±0.5 kg specifications. Two STD (95% confidence level) interval around V(0) is 0.44 kg, meaning that the scales will measure 5% of the bags above 25.44 kg or below 24.56 kg – even if all bags had a weight of 25 kg on statistical average. This will make it very difficult to adjust the filling to 25 kg when the remaining part

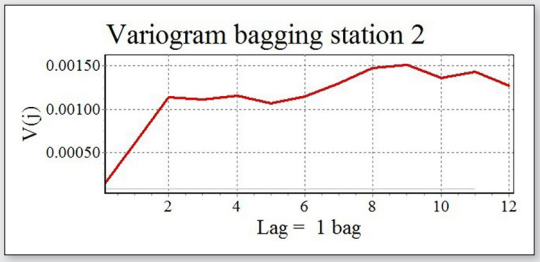

Figure 11. Variogram of data from bagging station 2; same Y-axis variance units as Fig. 10 (left).

of the variance is also considered. The tolerance limit has probably been *increased* by the plant personal to avoid an uncomfortably high occurrence rate in the production. In addition the high variance indicates an air-leakage influencing the filling. Could it be that the air-leakage influences the scale causing a high V(0) as well as a high overall variance due to bad filling control? If this is the case the air-leakage simply doubles-up the problems, in practise making it virtually impossible to control the process. The last 'explanations' are only speculative at the present, but show how detailed interpretation of experimental variograms is of great help for process control in pointing out both problems as well as possible solutions.

Bagging station 3 has an accurate, correct set point; 24.99 kg, but both the sill (total variance) and V(0) is significantly higher compared to bagging station 1, bagging station 3: 0.00015 compared with 0.00003 for bagging station 1. The difference is more or less explained by higher V(0) and a contribution from a strong cyclic periodicity with lag = 2. V(0) is again at the limit to deliver the bags within the spec of ±0.5 kg. The two STD (95% confidence level) around the V(0) is here 0.43 kg. By a similar argument as above, this means that the scales will measure 5% of the bags above 25.43 kg or below 24.57 kg solely as a function of the quality of the measurement system. Combined with the cyclic periodicity, this gives 3 bags out of spec, even if the material consumption is perfect. The cyclic periodicity again comes from the auto-correction facility. This is deemed acceptable, but a high v(0) will probably cause the auto-correction occasionally to go in the wrong direction, and again make it almost impossible to keep all the bags inside the limits of ±0.5 kg. Investigations will be carried out as to why the scale has such a high variance. It also must be pointed out that the periodicity makes the estimation of V(0) difficult.

It is important to realise that a high V(0) is a function of an inferior (TSE + TAE), which will occasionally indicate bags out of spec, which are in fact not. Such a measurement system is not acceptable in the industrial practise as it disturbs proper process control.

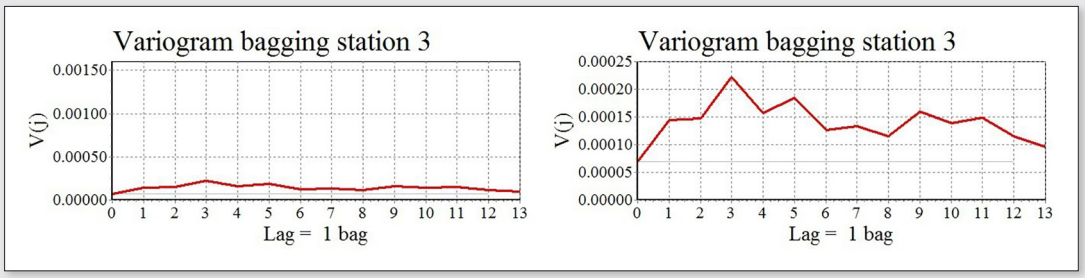

Figure 12. Variogram of data from bagging station 3, (left) for comparison of all stations; (right) for close-up evaluation.

To reduce material losses at the production line, the first step should be to evaluate the weight measurement system. This will make it much easier to eliminate or to reduce real losses. It will be important to monitor and keep V(0) low. Bagging line 1 had an acceptable V(0), and since all the station use the same system it should be possible to achieve the same system quality at the other two stations as well. Further analysis to find the root causes of the differences has to be carried out, e.g. is there influencing dust contamination, air-flow or other, not yet identified agents? Can operator adjustment influence V(0)?

As an important aside, it is worthy of considerable note (and concern) that all scales were newly calibrated before this experiment.

It is likely that operators have been under time pressure during the experimental campaign, possibly substantiated in their choice to increase the specification limits instead of stopping the bagging equipment to solve the problems. There is always a balance between the costs (and time pressure) of non-production time and the costs of increased raw material consumption. On-line recording using moving average smoothing and V (0) monitoring could ease the decision of when to stop or not. Specific routines of when to take action, related to specific limits could be worked out depending of type of product and raw material costs. Even if the producer chooses to continue without correction, for example due to high demand, they will now be fully aware of the potential costs of doing so.

Conclusions

A periodicity with a frequency of lag equal 5, i.e. 7.5 minutes arises from cooler level fluctuations in the case of production of Exclay. This corresponds to a conservative estimate of a loss of 0.71% of output of the kiln, leading to a yearly loss of 100,000 Euro. An investment of 5,000 Euro will have a pay-back time of less than 1 month. This is but a modest economic result but shows the power of variografic analysis as a strong strategic tool for industry in general.

Bag overfilling in the analysed period was 1.2%, originating from two stations with an overfilling of 1.5 and 2.2% respectively and one perfectly run station. It seems that the plant focus has been on time and not on costs, since an auto-correction facility was deliberately turned off on one of the weighing stations and the specification limits of another were manually increased – leading to weights far off from the ±0.5 kg specification. The existing equipment used to fill and weigh the bags is likely good enough, based on the fact that the acceptable filling station shows completely acceptable levels of V(0) and sill, resulting in bags well within the limit of ±0.5 kg . It is necessary to pay more attention and awareness to the costs of overfilling – at the very least, data from the scales must be recorded. On-line moving average smoothing with set limits of action depending on product should also be introduced. On-line monitoring of V(0) is also a new feature to be implemented, since two of the bagging stations show such a high V(0) that it is in practise structurally impossible to keep the measured weight of the bags within the stipulated specifications. By the unavoidable addition of even small process variances, e.g. periodicity stemming from the auto-correction, the whole process monitoring is bound to get out of control. At all times a special focus must be on keeping V(0) low, indicated the need, and the significant return from, proper education of the plant operators/supervisors. This example shows the usefulness of variographic analysis in industrial LRM analysis.

The power of using variograms to untangle and separate different contributors to the total process and measurement system variances in industry is ‘priceless’ in more ways than one.

References

1. F. Pitard, “PIERRE GY’S SAMPLING THEORY and SAMPLING PRACTICE. Hetrogeneity, Sampling Correctness, and Satatistical Process Control, 2nd edition, chap. 7, *CRC Press. ISBN 0-8493-8917-8* (1993).
2. H.Tellesbø and K.H. Esbensen, “Practical use of Variography to find root causes to high variances in industrial production processes II” *WCSB7 (2013)*.
3. EN 1097-3, “Tests for mechanical and physical properties of aggregates, Determination of loose bulk density and voids.”
4. H.Tellesbø and K.H. Esbensen, “Corporate Exclay process and process quality control – Variographic analysis of kiln bulk density” *Proceedings WCSB4, pp. 259-2676 SAIMM Publ. (Southern African Institute of Mining and Metallurgy)*. ISBN 978-1-920211-29-5 (2009).
5. H.Tellesbø and K.H. Esbensen, “Practical use of Variography to find root causes to high variances in industrial production processes I” *WCSB7 (2013)*.
6. DS 3077 (2013) Representative Sampling – Horizontal Standard. Danish Standardisation Authority (DS) www.ds.dk

doi: 10.1255/tosf.73

The overall measurement error—TOS and uncertainty budget in metal accounting

Stéphane Brochot
Caspeo, 3 avenue Claude Guillemin BP36009, Orléans CEDEX 2, France. E-mail: s.brochot@caspeo.net

Metal accounting is one of the main tools for financial and technical management of metal production industry. It is based on measurements and has to manage the uncertainty inherent to the measurement process. The uncertainty in the metal accounting generates financial risk. The accuracy of the metal accounting results is directly linked to the accuracy of the material balance and then to the accuracy of the mass and content measurements. Estimate the overall measurement error, through its probability distribution or its first and second moments (mean and variance), can contribute to the enterprise decision making.

The overall measurement error can be calculated and analysed by establishing the uncertainty budget. If this approach has been mainly introduced to calculate the analytical error (cf. ISO GUM), it has to take into account the sampling procedure. Even though it is not explicitly named "uncertainty budget", the same approach is proposed in the Pierre Gy's Theory of Sampling (TOS), where the various components of the overall error are well identified and described with their properties and their relative weights.

The present paper proposes a methodology to build such uncertainty budgets in the frame of the implementation of a metal accounting system. It can be applied to an existing measurement system, analysing the results in order to find some ways for improving the measurement accuracy. In addition, it can be used to define a new measurement procedure with an objective of accuracy. Various real examples illustrate both applications.

Introduction

If "Metal accounting is the estimation of (saleable) metal produced by the mine and carried in subsequent process streams over a defined period of time"[1], it has become widely used to quantify the performances of production plants (metal recovery, losses, environmental impact) and to establish an accurate estimation for the metal inventory (stock taking and work in progress estimation). A large discrepancy between the estimated and actual inventory can have significant financial consequences. Similarly, poor estimation of metal recovery and losses can hide process issues and give inappropriate production planning. This is why "metal accounting provides interface between technical and financial performance measurement"[1]. These two cultures have two very different points of view and have difficulties to conciliate them. The main topic of disagreement is the uncertainty of measurement which implies uncertainty in the estimation of production and inventories.

The measurement uncertainty and the methods of reducing it have been largely discussed in many papers[2,3,4,5,6]. The objective of the current paper is to propose a method to be able to quantify the uncertainty with the establishment of the uncertainty budget of any measurement useable for metal accounting. An audit of the measurement system has to take place in order to examine the current situation, collect all information necessary for uncertainty budget and make recommendations for measurement accuracy improvements.

Metal accounting implementation

Metal accounting is a component of the general enterprise accounting[7,8]. It constitutes a powerful tool to manage metal producing companies at their various stages: mine and mill, concentrator, smelter or hydrometallurgical plant, refinery, or a combination of these stages. It is the bridge between the technical and the financial point of views of the process. The process data generated to manage the production performances are used to valuate the products and stocks into financial data.

The main objective of a metallurgical accounting system is to help the company in managing process data to generate a material balance in order to obtain a metal accounting report. The secondary objective is to use the material balance to accurately calculate the process performances and help the process manager in optimising it. The metal accounting is generally established for a period of production. This period can be defined by a regular time period or by the period of production of a material batch. In accordance with the financial and accounting rules, the regular time period is generally a month.

In the life time of a company we can consider three life cycle levels for metal accounting[9]:

- Metal accounting system life cycle: this begins with the decision to implement the metal accounting system in a company and finishes with the decision to end it.
- Production evolution life cycle: this regards the adjustments of the metal accounting system due to production evolutions such as a process change, a new production unit, or new products.
- Metal accounting life cycle: this groups the periodical tasks to obtain a regular metal accounting report.

From the moment a company decides to implement a metal accounting system to the time the system reaches completion, three periods can be identified. The "implementation" groups all tasks to obtain an operational and efficient metal accounting system. The "production" groups all tasks to regularly generate metal accounting reports and update the system according to notable evolutions. The "closing" groups all tasks to finalize the last metal accounting taking into account the plant dismantlement.

The implementation of a metal accounting system is a company project mobilising all staff: general management, financial, accounting, production, laboratory, metrology, information technology, purchasing, sales staff… Depending on the initial level of development of the company many tasks have to be taken into consideration[9]. The ones concerning the present paper are: a review of the existing measurement system; the design and implementation of necessary

additional measurements; the establishment of the measurement uncertainty budget[6] involving the identification and implementation of some improvements; the standardisation of the measurement system.

Measurements at the basis of metal accounting

The metallurgical accounting is based on the calculation of the material balance of the considered system. This calculation necessitates raw data, such as masses, moisture contents or assays, which are obtained by measurements. As the measurement is a random process, it is subject to uncertainty which can be quantified with its associated "measurement error"[2]. It concerns also the measurements of mass[3], moisture or metal content, percentage of solids or density… These last measurements generally necessitate sampling which is the main source of uncertainty[4,5]. All efforts have to be done to obtain correct sampling and measurement to avoid any bias. This bias would produce discrepancies between metal accounting and real production with the risk of unacceptable financial consequences. Nevertheless, the variance of the overall measurement error cannot be avoided and its calculation necessitates the establishment of its uncertainty budget[6].

The quantity of material managed during the considered period of metal accounting is generally given by the sum of many mass measurements such as truck loads or production weights per shift. Similarly, the mean moisture or metal contents are calculated by the weighted average of the contents of many samples. The aggregation of this raw data gives the "basis data" which is the sum of the total masses or the average contents of the material during the accounting period. A measurement error can then be attached to the basis data using the error propagation calculation rules[10].

Measurement error and data reconciliation

Due to the measurement uncertainty, the basis data are incoherent regarding the material conservation laws[11,12]. The incoherence can be observed when there is data redundancy: when there is more data than the required minimum to calculate the material balance. The objective of data reconciliation by material balance is to find a set of estimates for the measured values which are as close as possible to the measurements and verify the material conservation laws. Sometimes, balancing behaviour reveals non-stationary processes or bad accuracy estimation. The information redundancy allows delivering coherent estimators more accurate than the initial measurements[13,14]. This approach allows for the detection of aberrant values and to reduce error due to sampling and measurement.

Overall measurement error

The relative measurement error is defined as the difference between the value of a parameter obtained by a measurement protocol and the true value which is, by definition, unknown, the whole divided by the true value. Due to the natural variability occurring in any measurement protocol, the measurement error is a random variable following a probability law which can be obtained using different approaches. For the statistical approach, the same measurement is performed a large number of times and statistics are done on the set of results. This approach, referring to evaluation of type A, is called a posteriori as it is necessary to do the measurements to be able to evaluate the probability law. The probabilistic approach, evaluation of type B, is called a priori because it is based on theories such as the sampling theory. A combination of these two approaches can be used to evaluate the overall measurement error. The moments of the probability distribution are used to characterise the measurement error. The first moment, the mean, gives an evaluation of the bias, a systematic deviation between the measurements and the true value. It measures the accuracy of the measurement. The second moment, the variance, quantifies the reproducibility (or precision) of the measurement.

Components of the measurement error

The overall measurement error (OE) includes a lot of components which can be divided, following the Pierre Gy's classification[15, 16, 17], into two main components: the total sampling error (TE) and the analytical error (AE).

The analysis error is due to the imperfection of the protocols and devices used for analytical operations[19]. When concerning assaying or moisture content, the analysis is performed on the sample obtained from the last sampling stage, which is generally taken in the laboratory. The evaluation of the analysis error needs the decomposition of the protocols and procedures to find all sources of error. Calculation rules and metrological approach are used to calculate the total analysis error. Another approach, mainly used in QAQC procedures, is based on the variance analysis of a large number of performed measurements[18].

The total sampling error has to take into account the succession of particle size and bulk reductions. It is then the sum of the total sampling errors at each stage (TEn). The sample preparation operations generate the increment preparation error (IPE) due to contamination, loss, chemical or physical alteration, unintentional or intentional mistakes. The operation of taking a small amount of material in a lot in order to obtain a sample generates: the fundamental sampling error (FSE), the grouping and segregation error (GSE), all together called short-range process integration error (PIE_1), result from the heterogeneity of constitution, while the long-range (PIE_2) and periodic (PIE_3) process integration errors, and the increment weighing error (IWE) comes from the heterogeneity of distribution in the space or in the time. The increment delimitation error (IDE) and the increment extraction error (IEE) constitute the materialisation error.

Uncertainty budget

The evaluation of the overall measurement error necessitates listing all the sources of error along the entire process, from the original lot, subject to the measurement, to the use of the analytical results. The inventory of the sources of errors is obtained from a preliminary diagnostic phase of the plant measurement system. This phase has a double objective: calculate the variance of the overall measurement error and improve the measurement process, everywhere it is possible, in order to reduce this error in terms of bias and variance.

The uncertainty budget lists all the components of the overall measurement error with their respective weights. The analysis of the repartition of the components allows focussing on the improvement of the main components. The establishment of such a list necessitates an a priori approach of type B. Indeed, it is very difficult to extract the error components from the variance analysis of a large number of measurements in the frame of an a posteriori approach of type A. Nevertheless, some components can be obtained from such type A approach such as the device repeatability or, concerning sampling, the process integration errors obtained from chronostatistics[15,16].

Audit of the measurement system

The term "Measurement System" refers to all aspects of the measurements:

- All pieces of equipment used for measurements including sample taking and preparation, and laboratory;
- Their documentation: manuals, maintenance log-sheets, calibration log-sheets and certificates, inventory;
- The measurement procedures including sample taking and preparation, analysis;
- The measurement results management and storage;
- The Quality Assurance / Quality Control (QA/QC) documentation: procedures, reports;
- The uncertainty budget for all relevant measurements;
- Information and data repository.

The first step of the audit is to examine the current situation of the measurement system. It starts with an inventory of all the measurements required for metal accounting. This list is confronted with the inventory of the currently performed measurements. A special attention has to be paid at this level. Indeed, the definition of the material flow diagram[9] (including material movements and stocks which are accounted) and its level of details is commonly conducted by the availability of measurements, while common sense would dictate the contrary: define the material flow diagram with the objective of accurate metal accounting and then locate, design and implement the measurements. The comparison between the inventories of the expected and actual measurements gives a first idea of the "cost" for the measurement system upgrading.

The already performed measurements are then analysed in details one by one. An on-site visit is absolutely necessary to observe the measurement process in operation: true location of the measurement or of the sampling point, material subject to measurement, operating conditions of the equipment, operator practice, operating environment… All the documentation concerning equipment (such as user's guide, technical sheets, and maintenance and calibration log-sheets), procedures (for sampling taking and preparation, analysis and safety rules), QA/QC (procedures and reports) and material are collected. Results of already performed measurements have to be collected from databases (historians) or log-sheets for subsequent statistical analysis.

The technical documentation of the equipment allows to list its inherent sources of error and to collect the quantitative values used to estimate their components in form of variances (such as readability or temperature sensitivity). The procedures give the detailed description of the measurement process with all its steps and the sources of error arising at each stage. The list of items to account in the uncertainty budget is deducted from these both kinds of documentation. If documentation is missing, operator interview is absolutely required. Even though the documentation is available, such interview is always rewarding as there is always a gap between the documentation and the real practice.

Material characterisation for heterogeneity model

The theory of sampling gives guidance how to calculate the fundamental sampling error starting from the description of the heterogeneity of the material regarding the parameter to measure (moisture content, assay, slurry density). A detailed description of the heterogeneity can be deducted from various sources of information: mineralogical studies including quantitative mineralogy using image analysis, size and density distribution analysis, processing test results and process data. Such a model of heterogeneity has to be developed for each stage of the sampling plan. Indeed, the material being ground before sub-sampling, the heterogeneity changes in terms of size distribution and mineral liberation. Generally, most of the required information are available in the collected documentation. If there are missing data, specific experiments can be conducted to refine the material characterisation.

The variographic analysis is the better way to estimate the components of the process integration error (PIE) and mainly the ones associated to the distribution heterogeneity[15,16,20]. Such studies are rarely available before the audit. Sometimes, the historical data are sufficient to have a first idea of the process variability. But the required operating conditions to conduct such a study are not the one of the routine measurements. It is why it has to be performed for the more relevant sampling points, that is to say where the benefit will cover the cost.

A multi-disciplinary approach is absolutely necessary during this task. Indeed, the heterogeneity model is built by inference from a great diversity of information sources. In addition, it is generally necessary to do, and justify, some realistic assumptions.

Audit report

The main part of the audit report concerns the uncertainty budget. It allows to associate a quantitative error to each measurement, what is the basis of data reconciliation. The uncertainty budget highlights the main components of the overall error pointing out the possible improvements. Recommendations can then be done at the light of these results.

Conclusion

A metallurgical accounting system has to conciliate two points of view: the technical point of view for which the material balance is the product of a statistical approach of the reality and the financial point of view for which the metal balance refers to an exact and coherent economic value in the accounting system. Nevertheless, the material balance is based on measurements which are random processes. The measurement error has to be considered when corrections take place during the data reconciliation process. If the data reconciliation is based on a statistical coherent material balance, the obtained estimated values are the more probable ones.

In the implementation of a Metal Accounting system, the initial diagnostic of the existing measurement system has to be carefully conducted to have a good quantification of the overall measurement error. This error is directly used by the data reconciliation system and gives the accuracy of the key point indicators. In addition, the analysis of the uncertainty budget of the overall error indicates the main components on which the efforts of improvement have to be done.

References

1. R.D. Morrison, "Motivation for and benefits of accurate metal accounting", in *An Introduction to Metal Balancing and Reconciliation*, Ed by R.D. Morrison. Julius Kruttschmitt Mineral Research Centre, Indooroopilly, Australia, pp. 3-23 (2008).
2. R.D. Morrison, "Basic statistical concepts for measurement and sampling", in *An Introduction to Metal Balancing and Reconciliation*, Ed by R.D. Morrison. Julius Kruttschmitt Mineral Research Centre, Indooroopilly, Australia, pp. 27-75 (2008).

3. M. Wortley, “Mass measurement”, in *An Introduction to Metal Balancing and Reconciliation*, Ed by R.D. Morrison. Julius Kruttschmitt Mineral Research Centre, Indooroopilly, Australia, pp. 77-139 (2008).
4. R.J. Holmes, “Correct sampling and measurement the foundation of accurate metallurgical accounting”, *Chemometrics and Intelligent Laboratory Systems*. **74**, 71-83 (2004).
5. R.J. Holmes, “Sampling”, in *An Introduction to Metal Balancing and Reconciliation*, Ed by R.D. Morrison. Julius Kruttschmitt Mineral Research Centre, Indooroopilly, Australia, pp. 141-170 (2008).
6. S. Brochot, “The application of sampling theory in metallurgical accounting process – Inventeo methodology implementation”, in *Proceedings Fifth World Conference on Sampling and Blending*, Ed by M. Alfaro, E. Magri, F. Pitard. Gecamin, Santiago de Chile, pp. 185-193 (2011).
7. AMIRA P754, *Metal accounting, code of practice and guidelines: Release 3* (2007).
8. R.D. Morrison and P.G. Gaylard, “Applying the AMIRA P754 code of practice for metal accounting”, in *Proceedings MetPlant 2008*, AusIMM, Melbourne, Australia, pp. 3-22 (2008).
9. S. Brochot and M.V. Durance, “A New Approach to Metallurgical Accounting”, in *Proceedings 11th Mill Operators’ Conference*. AusIMM, Hobart, Tasmania, Australia, pp. 217-223 (2012).
10. Z. Xiao and A. Vien, “Limitations of variance analysis using propagation of variance”, *Minerals Engineering*. **16**, 455-462 (2003).
11. D. Hodouin and M.D. Everell, “A hierarchical procedure for adjustment and material balancing of mineral process data”, *International Journal of Mineral Processing*. **7**, 91-116 (1980).
12. J.A. Herbst, R.K. Mehta and W.T. Pate, “A hierarchical procedure for mass balance closure and parameter estimation: application to ball mill grinding”, in *Proceedings XVI International Mineral Processing Congress*, Ed by K.S.E. Forssberg, Elsevier, Amsterdam, pp. 1719-1732 (1988).
13. J. Ragot, M. Darouach, D. Maquin and G. Bloch, *Validation de Données et Diagnostique*, Hermes, Paris (1990).
14. J. Ragot and D. Maquin, “Validation et réconciliation de données. Approche conventionnelle, difficultés et développements”, *Les Techniques de l’Industrie Minérale*, La SIM, Paris. **29**, 22-30 (2006).
15. P. Gy, *Sampling of Particulate Materials, Theory and Practice*. Elsevier, Amsterdam (1979).
16. F.F. Pitard, *Pierre Gy’s Theory of Sampling and C.O. Ingamells’ Poisson Process Approach, pathways to representative sampling and appropriate industrial standards*. Doctoral thesis, Aalborg University, Denmark (2009).
17. P. Minkkinen, “Practical application of sampling theory”, *Chemometrics and Intelligent Laboratory Systems*. **74**, 85-94 (2004).
18. P. Minkkinen, “Estimation of variance components from the results of interlaboratory comparisons”, *Chemometrics and Intelligent Laboratory Systems*. **29**, 263-270 (1995).
19. JCGM/WG 1, *Evaluation of measurement data – Guide to the expression of uncertainty in measurement*. BIPM, Paris (2008).
20. P. Minkkinen and K.H. Esbensen, “Multivariate variographic versus bilinear data modeling”, *Journal of Chemometrics*. **28**, 395-410 (2014).

doi: 10.1255/tosf.44

Complete sampling distribution for primary sampling, sample preparation and analysis

Geoffrey J. Lyman
Materials Sampling & Consulting, Southport, Queensland, Australia 4215. E-mail: glyman@iprimus.com.au

Following from the author's recent paper at Sampling 2014 which presented a method for calculation of the sampling probability density function due to the particulate heterogeneity (density function of the fundamental sampling uncertainty), it is possible to apply the same characteristic function method to arrive at the overall sampling distribution for any sampling protocol and analysis method. This paper develops the application of the method of characteristic functions to the overall sampling problem including the uncertainty which derives from the primary sampling from a process stream. The assay distribution in a process stream or of impurities in the flow of a final product can be governed by non-Gaussian, serially correlated distributions. The paper shows how such circumstances can be dealt with to arrive at robust solutions. The paper represents an end-point in the theory of sampling as it provides a means of determining the entire distribution function for a sampling system. Such a determination has not previously been possible and having determined the entire distribution function, the statistics of the sampling process are completely determined.

Introduction

One cannot say too much about the theory of sampling put forward by Pierre Gy. Gy consolidated the elements of sampling theory that had been proposed over the years leading up to his definitive works in the 50s and 60s. For the English-speaking world, the theory of sampling arrived in 1979 with his book published by Elsevier.

This was close to the time when I first began to take an interest in sampling theory so that I could design plant tests intended to reveal the performance of unit operations in coal processing, with which I was then involved. There was always in mind that party A claims an increase in yield of *X* percent while party B claims an increase of *Y* percent. Who was correct? How were the trials carried out? Is it possible to assess the uncertainty involved in the claims of improved performance? If everyone who carried out trials was correct, the yield of product would be 120% of the feed content.

The resolution of this conundrum is found in the provision of estimates of uncertainty to be attached to each of the quantities measured in the test work and to have those uncertainties propagated through to the final figure for recovery, yield or whatever performance indicator is preferred. Unlike the physicists who were working at the time when I was an undergraduate and graduate engineer learning my trade, I found that the mineral processors never provided error bars on their results in the same way that the physicists and chemists did. I found this to be an unscientific approach and to be rather political in nature. An engineering or physical quantity has no validity until there is a reasonably accurate estimate of its uncertainty that is stated along with the figure.

Pierre Gy waged a campaign to bring the mineral processors into the world of modern science by focussing on the uncertainties that we experience when doing test work or running a plant. While a number of investigators had made estimates of sampling variance due to the particulate nature of a mineral mixture, Gy created a mathematical structure that could be used in a coherent fashion to describe the variance of sampling due not just to the particulate nature of the mineral but also to the process variance in the flow in the plant that was being sampled. His recognition that he could borrow from the nascent theory of geostatistics to describe the variance due to grade variation in a process stream was a unique and brilliant step forward. This very important component of sampling variance had been ignored up to that point in time.

The mineral processing world is still struggling to come to terms with the power of Gy's work. The full power of his theory is often neglected in the design of sampling systems. We have new analytical tools to look at fine particle compositions that permit the implementation of the detail of Gy's work; we don't have to guess at a liberation constant any more or postulate how that value may vary with the top size of the sample.

I have recently been lucky enough to come across some work by a skilled statistician that lead me to develop a means of estimating the entire sampling distribution, due to all factors. This paper presents the outline of how these calculations are made.

I respectfully dedicate this presentation to Pierre whose work has been a constant inspiration since I learned of it and met him many years ago in Sydney.

The paper will briefly recall the mathematical method by which the calculations can be made and will then provide an example of the outcome of the calculations, for a gold ore.

Mathematical background

The method of calculation of the entire sampling distribution is based on the fact that given a set of random variables that are statistically independent and each have arbitrary probability density functions, the characteristic function for the probability density of a weighted sum of the random variables is determined from the product of the characteristic functions for each of the random variables. This is a fundamental relationship of mathematical statistics. In fact, the probability density function and the characteristic function are Fourier transform pairs. Knowledge of the characteristic function for a random variable is equivalent to knowledge of the probability density function.

For every probability density function, $p(x)$, the characteristic function is defined as

$$\varphi_X(u) = \mathrm{E}\left\{e^{iuX}\right\} = \int_{-\infty}^{\infty} e^{iux} p(x)\,dx = \int_{-\infty}^{\infty} \left[\cos(ux) + i\sin(ux)\right] p(x)\,dx \quad (1)$$

where, $i = \sqrt{-1}$ so it is a complex-valued function and is a Fourier transform of the density function. Given the characteristic function

of a density function, the density function can be recovered as an inverse transform yielding a real-valued function

$$p(x) = \frac{1}{2\pi} \int_{-\infty}^{\infty} e^{-iux} \varphi(u) du \tag{2}$$

The characteristic function has the following properties

$$\begin{aligned} \varphi(0) &= 1 \\ |\varphi(u)| &\leq 1 \\ \varphi(-u) &= \bar{\varphi}(u) \end{aligned} \tag{3}$$

where $\bar{\varphi}(u)$ is the complex conjugate of $\varphi(u)$.

It is also possible to calculate the non-central moments of the density function directly from the characteristic function without making the inversion, as

$$\mu_r' = i^{-r} \left. \frac{\partial^r \varphi(u)}{\partial u^r} \right|_{u=0} \tag{4}$$

This last relationship is very useful as one can find the sampling variance without having to make an inversion.

In sampling a process stream for a particular critical content, when the sampling is carried out in a mechanically correct manner, there are only three sources of variance:

- variance due to the time variation of the critical content of the process stream
- variance due to the intrinsic (particulate) heterogeneity of the primary increments and the subsamples retained in the sample preparation protocol, including that of the analytical aliquot
- variance due to the final analysis of the aliquot by some appropriate means

It is usual to base the calculation of the variance due to intrinsic heterogeneity on an average composition of the material being sampled, although this is not mandatory. It is then implicit that the variance due to intrinsic heterogeneity depends only on the particular state of comminution of the material being sampled. Indeed, the distribution of the uncertainty due to intrinsic heterogeneity is taken to be dependent only on the average grade and the state of comminution of the material.

In such a case, it is possible to state that the three sources of uncertainty are statistically independent. Consequently, if it is possible to determine the probability density functions for each of the three sources of uncertainty, it will be possible to calculate the probability density function for the sampling protocol as a whole by finding the characteristic functions for each of the sources of uncertainty, taking their product and inverting this product. Even if the probability density function varies with the state of comminution of the subsample within the sampling protocol, that change can be accommodated within the procedure by introducing additional independent density functions into the calculation.

The first source of variance, due to time variation of grade in the stream is something about which we know very little in practical terms as it is very rare to undertake sampling campaigns in which frequent increments are taken with preparation and analysis of individual increments. Such information as we have usually comes from on-line analysis systems. For the purpose of this analysis, the grade variation in the process stream under examination will be simulated on a very fine time scale (all potential increments will be created) and the stream will be sampled at an appropriate frequency over an 8 hour shift.

We know more about the second source of variance if an appropriate investigation of the ore is undertaken to determine the size distribution of the gold grains. This information is absolutely fundamental to the sampling of the material and development of sampling protocols. The required information can be developed in conjunction with gravity recoverable gold studies.

The final source of uncertainty, the analytical uncertainty can be determined from laboratory duplicate assay information. It is important that such information be uncensored (all assays made must be captured by the laboratory information management system). This distribution should be Gaussian if the protocol and method is correct.

Example

The calculations will be illustrated by considering a variable feed to a gold plant that is treating ore from two different sources, one of

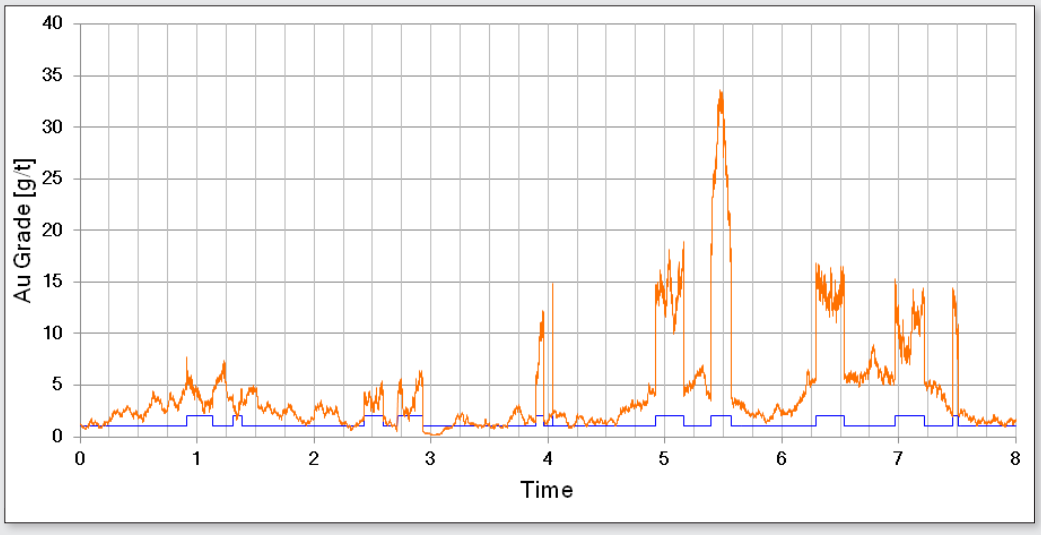

Figure 1. Typical simulated variation of feed gold grade, showing the switching between the two feed types (bottom trace).

which has a higher grade than the other and a different size distribution of gold in the ore. We take the following case:

- Ore A is treated 25% of the time and is the higher grade material
- The switching of the feed between the two sources is random in that the duration for which each ore is treated follows an exponential distribution with an expected duration of 10 minutes (high grade) and 30 minutes (low grade).
- Both ores carry gold with two distributions of grain sizes to explore the impact of 'coarse gold'.

Feed variation and primary sampling density function

A typical trace of the feed gold grade is shown in Figure 1. Both the low grade and the high grade material are taken to follow gamma distributions of grade. The low grade material has an average of 2 g/t and the high grade material, 10 g/t. Both distributions have an order of two. Their density functions are shown in Figure 2.

The time variations of the grade for both ore types are taken to follow random functions with an exponential covariance functions with a range of about 70 minutes and are used in such a way that the variation in an ore type remains correlated even when interrupted by feeding of the other ore type. This simulates feeding alternately from one of the two ore sources.

The simulated trace of grade as a function of time is sampled at a 15 minute period (32 increments per shift) and the grade of the accumulated sample is compared to the true grade for the time period. The sampling is of course unbiased. The quantity of interest is the distribution of the difference between the true unknown grade and the grade of the sample as that is the sampling uncertainty. It is essentially impossible to calculate this distribution *a priori*, so the simulation method must suffice.

The simulations were run 5000 times, simulating 5000, 8 hour periods on a time base of 1 second (28800 points in the simulation) Such large simulations require special methods to ensure that the simulation is exact. Methods such as sequential Gaussian simulations are not exact. The histogram of differences was extracted and was recognised to follow a Laplace distribution very closely (double sided exponential distribution). The distribution parameters were extracted by a fitting method. The result is shown in Figure 3 and the Laplacian model is very good indeed (could this be a general result for the sampling distribution?).

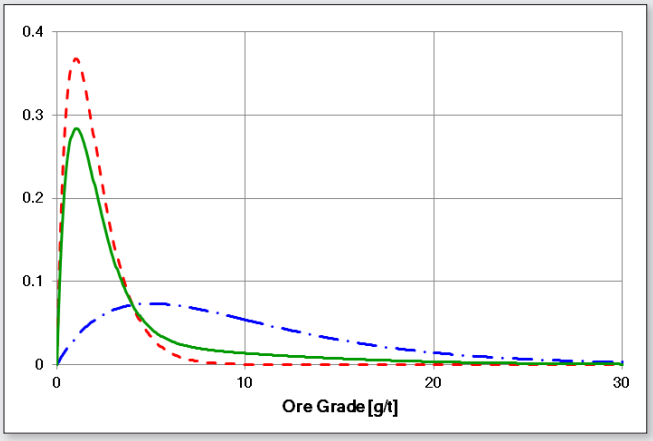

Figure 2. Probability density functions for the low grade (- - -), high grade (- . - .) and average grade (solid line).

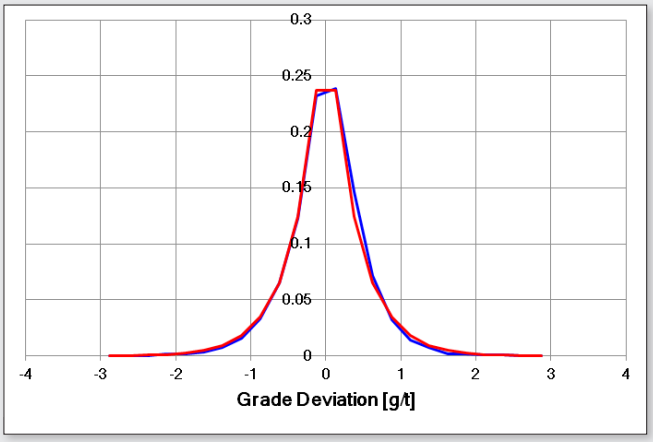

Figure 3. Fit of the Laplacian density function to the histogram on an interval of 0.1 g/t for the difference between true and sampled shift grade. 5000 simulations. Density function parameter = 0.389 g/t.

The Laplace density function centred on zero is given by

$$p(x)=\frac{1}{2\alpha}e^{-\frac{|x|}{\alpha}}\ ;\ -\infty<x<\infty \tag{5}$$

The tails of the Laplacian distribution are much heavier than a normal distribution. The variance of the distribution is $2\alpha^2$, so the standard deviation of the sampling distribution is 0.550 g/t and a 95% confidence interval is ±1.17 g/t (±2.12σ).

Intrinsic heterogeneity of the sampled ore and density function

To correctly evaluate the sampling distribution for the plant feed, it is necessary to consider the two ore types and possible dilution by barren material. The methodology for doing this was provided by Lyman.[1]

For the case at hand, the intrinsic heterogeneity of the ore will be based on a 75:25 mix of the two ores and dilution will be ignored (dilution would further broaden the distribution described above).

The plant feed is considered to have a 95% passing size of 200 mm and to be fed at 1000 tph. The cutter has an aperture of 0.6 m and a speed of 0.6 m/s, leading to a primary increment mass of 277 kg, which is numerically equal to the feed rate in kg/s. The increment therefore represents 1 second of plant feed (hence the simulation of the feed on a 1 second basis). The sampling interval is 15 minutes, providing 32 increments, as noted above.

The two ores are taken to carry both fine and coarse gold. For convenience, the mass distributions of the gold particles are taken to follow Weibull (Rosin-Rammler) distributions. The mass fraction passing at a sieve size d is given by

$$w(d)=1-\exp\left[-\left(\frac{d}{\tilde{d}}\right)^n\right] \tag{6}$$

where $\tilde{d}$ is the size at which 0.632 of the sample passes.

The distributions are shown in Figure 4.

In sampling gold ores, it is very important to recognise that the objective of sampling is to collect an adequate number of gold particles in order to control the variance and distribution of sampling. When there is no dilution, the uncertainty in the grade of the sample derives only from the Poisson distribution of the number of

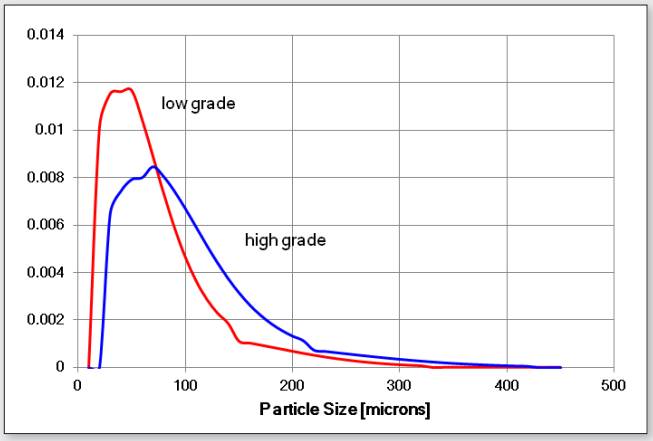

Figure 4. Gold particle size distributions, each a weighted sum of Weibull distributions, for low and high grade ore.

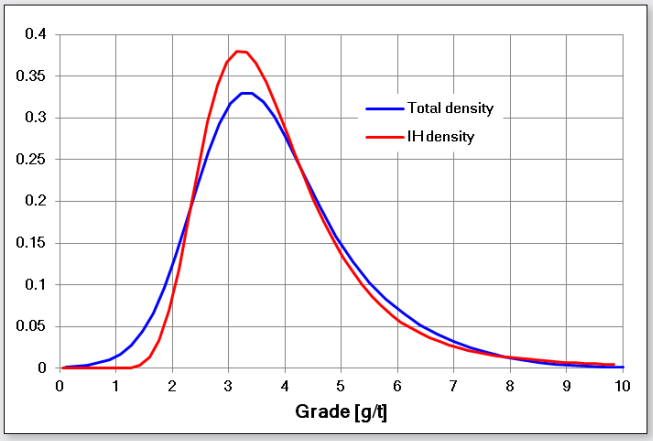

Figure 6. Total sampling distribution, with distribution due to sample intrinsic heterogeneity for comparison.

gold grains arriving in the sample. It does not matter whether these grains are contained in large or small particles of the host rock. The link between the number of particles of gold and the grade of the sample is the distribution by mass of the gold particles: their size distribution. Once the size distribution (or better still, the mass distribution if the gold is present in particles of a complex structure) is defined, the sampling distribution can be calculated.

If a sampling constant, K_s, for the gold is defined such that

$$\frac{\sigma}{\bar{x}} = \sqrt{\frac{K_S}{M_S}} \qquad (7)$$

where σ is the variance of sampling and $\bar{x}$ is the mean grade and M_S is the mass of the sample, the value of the sampling constant for the gold will not change until the comminution of the ore is such that the number of gold particles increases due to the breaking of the particles. It is not enough to 'liberate' or flatten the particles, they must break. When a subsample is taken at any stage in the sample preparation protocol, the only impact is the expected number of gold particles in the subsample. With the smaller mass being retained, the sampling variance will increase, but the sampling constant will not change unless the gold particles have been broken.

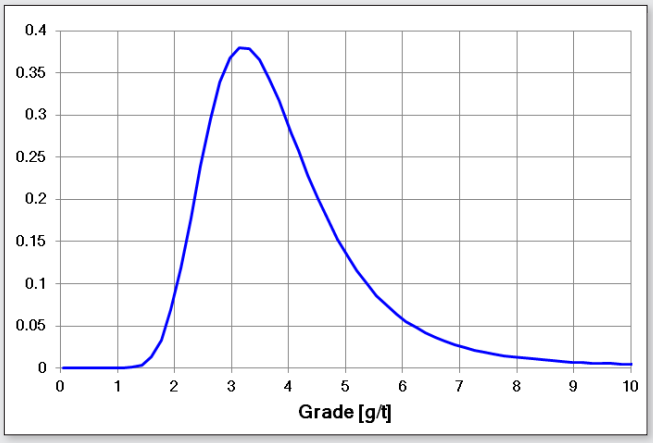

Figure 5. Grade distribution of 30 g aliquots of the ore.

The situation differs when there are totally barren fragments as these will impact on the sampling constant, but this is not the case in this example.

For the purpose of illustration of the calculation of the total sampling distribution, we will take the sampling to the stage at which we have 30 g of comminuted material for fire assay. We will assume that the gold particles have not been broken, but simple flattened by the sample pulverisation. The grade distribution of 30 g aliquots is shown in Figure 5 and has an expected value of 4 g/t.

Analytical density function

Given that the expected grade is 4 g/t, it is not unreasonable to assume that the uncertainty attached to the fire assay procedure itself is normally distributed. Note that this uncertainty does not include the intrinsic heterogeneity of the analytical aliquot. If this factor were to be included, the distribution might be skewed. The SD is taken to be 0.2 g/t, for the purpose of illustration.

Total sampling distribution

To determine the total sampling distribution, it is necessary to take the total uncertainty to be the sum of three random variables: the uncertainty due to distributional heterogeneity and a fixed number of increments per shift (a Laplace distribution), the uncertainty due to the intrinsic heterogeneity of the ore (a skewed distribution) and the uncertainty due to the analytical procedure (a normal distribution). The total distribution is shown in Figure 6.

Discussion

Up to this point in time, assessment of sampling uncertainty has been limited to knowledge of the variance of sampling without being able to assess whether the sampling distribution is skewed or, worse, bimodal.

In the realm of geostatistics, some practitioners have indulged in the practice of 'top cutting', that is, the discarding or reduction of grade values that seem to be too high. These high values destroy the 'normality' of the data and have adverse effects on the estimation of the variogram. The methods presented here, in combination with a full knowledge of the mineralogy of the ore under scrutiny, have the ability to determine precisely the distribution of the grades of samples, permitting assessment of the probability of observing

high grade results. At the start of evaluation of a potential orebody, one of the first steps should be the determination of the heterogeneity of the ore and ore samples so that the exploration samples collected are of sufficient mass to yield assay results of a precision that are fit for purpose, that is to say, representative. The tools presented here permit a full assessment for the first time.

In process sampling, especially in sampling a feed or product material where metallurgical accounting or product valuation is involved, the assumption that grade values follow a Gaussian (normal) distribution carries significant financial risk. In the metallurgical accounting setting, skewed grade distributions for assays can invalidate the reconciliation of the material balance. The classical example of this is the weighted least squares adjustment of assays, to arrive at a material balance that closes exactly, that produces adjusted tailings grades that are negative. Failure to take non-normality of tailings (or other process flows) grades into account distorts the entire material balance leading to bias in the adjusted balance.

In the sale of any commodity, or the valuation of a raw ore for toll treatment, knowledge of the sampling distribution is vital to the construction of the contract of sale and the development of quality reconciliation agreements between the seller and buyer. It is not uncommon to see agreements that involve unrealistically narrow splitting limits let alone ones that do not take possible skewness of grades into account. Responsible development of contracts must be based on knowledge of the full sampling distribution of a product or ore, so that an operational characteristic curve can be drawn up that reveals the financial risk to both seller and buyer.[2,3]

Conclusion

The foregoing example demonstrates that it is possible to develop a full statistical model of all sources of variance impacting the sampling of a process stream. The method also has potential application in geostatistical studies. The method for dealing with ore heterogeneity has been dealt with in detail by Lyman.[1] A key to the advances made here is the recognition that the distribution of the uncertainty due to the extraction of primary increments from a process flow can be estimated by simulation and that that distribution can be modelled by any suitable means.

The combination of the three sources of uncertainty can be combined using the characteristic function method to arrive at a total sampling distributions.

The value of the method is particularly evident when sampling ores of precious metals where the material may be nuggetty leading to skewed distributions due to the intrinsic heterogeneity of the ore. Knowledge of the full sampling distribution is of great value in the case wherein an operation is toll treating a gold ore for a client. The contract and sampling protocol can be developed with full knowledge of the financial risk involved through the use of an operational characteristic curve which depends entirely and directly on the full sampling distribution. The fact that the full sampling distribution is known is also reassuring to the client.

The statistical basis of the theory of sampling can now be considered to be complete.

References

1. G. J. Lyman, “Determination of the Complete Sampling Distribution for a Particulate Material”, Proceedings of Sampling 2014, 29-30 July 2014, Perth, Australia, AusIMM, Publication series No 5/2014, pp. 17-24.
2. F. S. Bourgeois and G. J. Lyman, “Getting high added-value from sampling”, in *Proceedings of the 7th International Conference on Sampling and Blending*, Ed by K.H. Esbensen and C. Wagner, *TOS forum* **Issue 5,** 95–100 (2015). doi: 10.1255/tosf.46
3. G.J. Lyman and F. S. Bourgeois, “Sampling, Corporate Governance and Risk Analysis”, to be presented at MetPlant 2015, Perth, Australia, in press.

doi: 10.1255/tosf.46

Getting high added-value from sampling

F.S. Bourgeois[a,b] and G.J. Lyman[b]
[a]Université de Toulouse, Laboratoire de Génie Chimique, Toulouse, France. E-mail: florent.bourgeois@inp-toulouse.fr
[b]Materials Sampling & Consulting Pty Ltd, Southport, Queensland, Australia. E-mail: glyman@iprimus.com.au

Determination of the complete sampling distribution (Lyman, 2014), as opposed to estimation of the sampling variance, represents a significant advance in sampling theory. This is one link that has been missing for sampling results to be used to their full potential. In particular, access to the complete sampling distribution provides opportunities to bring all the concepts and risk assessment tools from statistical process control (SPC) into the production and trading of mineral commodities, giving sampling investments and results their full added-value. The paper focuses on the way by which sampling theory, via the complete sampling distribution, interfaces with production and statistical process control theory and practice. The paper evaluates specifically the effect of using the full sampling distribution on the Operating Characteristic curve and control charts' Run Length distributions, two SPC cornerstones that are essential for quality assurance and quality control analysis and decision-making. It is shown that departure from normality of the sampling distribution has a strong effect on SPC analyses. Analysis of the Operating Characteristic curve for example shows that assumption of normality may lead to erroneous risk assessment of the conformity of commercial lots. It is concluded that the actual sampling distribution should be used for quality control and quality assurance in order to derive the highest value from sampling.

Introduction

Any engineering, quality or business analysis that deals with a real situation seeks to quantify a performance indicator and its associated uncertainty. This uncertainty comes from the propagation of the uncertainties associated with all the variables that contribute to the analysis. Sampling is concerned with providing the user with the uncertainty about any property of a commercial lot that cannot be observed fully.

Sampling is the starting point for anything that has to do with analysis and improvement of engineering, quality and commerce in the production and trading of minerals. The added-value of sampling comes not from the sampling itself, but from the use to which sampling data are put. Of course, the added-value of sampling is entirely dictated by the quality of sampling.

While estimation of sampling variance for the grade of a commercial lot is one important objective pursued by sampling theory, it must be remembered that sampling grade is a random variable. Tracking the variance only of this random variable implies that one assumes normality, which could lead to erroneous analyses and decisions once sampling data are put to the purpose for which they have been acquired should such an assumption be untrue. At any rate, it is always preferable to use the full sampling distribution over the sampling variance. The sole objective of this paper is to illustrate this point, through examples related to production control, quality assurance and quality control.

The assumption one has to make in order to use sampling data to any practical end, once sampling variance has been estimated using accepted sampling theory, is that the underlying full sampling distribution is Gaussian. It is difficult to ascertain whether this assumption is sound, and one may claim that it is perhaps so 80% of the time. In some situations, it is not the case (Venter, 1982). Recently, Lyman (2014, 2015) has shown that it is possible to estimate the full sampling distribution from sampling measurements, so that the limitation associated with the normality assumption can now be lifted altogether.

Figure 1 gives four distributions with identical mean μ = 42% and standard deviation σ = 0.5%, which will be used throughout the paper. These distributions represent realistic sampling distributions, some of which exhibit skewness and bimodality. Standard sampling theory would state that these distributions are one and the same as their variances are equal, which implies that they should yield identical downstream analysis and decision-making.

The results presented in this paper show that not only it is imperative that the full sampling distribution be estimated and used in order to get the maximum added-value from sampling, but that assuming a Gaussian sampling distribution can lead to erroneous and damaging analysis and decision-making.

The paper makes compelling arguments for using the actual full sampling distribution to get the full added-value of sampling, by examining three major uses of sampling data:

1. Production control, by looking at grade variation during the making of a commercial lot.
2. Quality assurance, with the Operating Characteristic curve (OC curve) as a risk analysis and decision-making tool for the conformity of commercial lots.

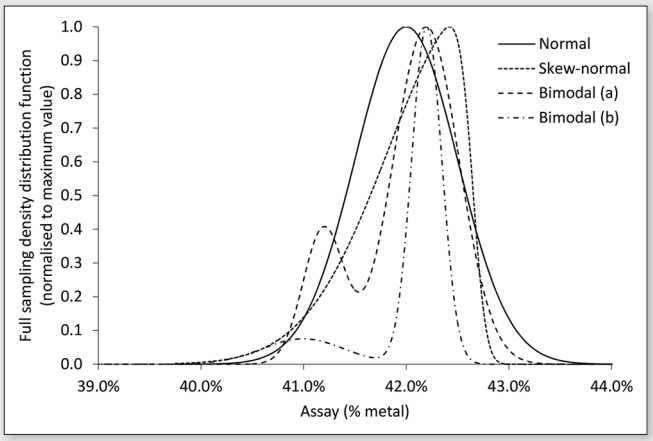

Figure 1. Four distributions with identical mean μ = 42% and standard deviation σ = 0.5%. The skew-normal distribution has parameters α = –8, ξ = 42.65%, ω = 0.82%. The bimodal (a) and (b) distributions have parameters α = 0.2, μ_1 = 41.20%, σ_1 = 0.20%, μ_2 = 42.20%, σ_2 = 0.32% and α = 0.17, μ_1 = 41.00%, σ_1 = 0.40%, μ_2 = 42.20%, σ_2 = 0.15% respectively (see appendix for details).

3. Quality control, with the Run Length (RL) distribution of control charts used for monitoring quality during production or in the laboratory.

Full sampling distribution and production control

Sampling can be used for optimising the revenue during production of a lot. In particular, sampling should be used to optimise shipment grade during production of metal concentrates, by ensuring that commercial lots contain the maximum amount of valueless material acceptable under the terms of the client's contract. This optimization requires knowledge of the full sampling distribution.

Figure 2 shows the 95% confidence interval for a 50000 t shipment loaded at a rate of 500 tph, sampled every 250 t for all four sampling distributions from Figure 1. The sampling distributions are assumed not to change during the making of the commercial lot.

In all cases, the narrowing confidence interval is a direct consequence of the propagation of variance from one sample to the next. Given that 200 samples are taken during the making of the lot, all four sampling distributions yield the same final sampling uncertainty, as per the central limit theorem. With the example shown, the 95% confidence interval of the lot assay is ±1.96(0.5%/ $\sqrt{200}$) = 0.07% absolute. The 95% confidence intervals differ between the sampling distributions only at the start of the making of the lot. The differences are small with the example chosen, whose RSD = (0.5% / 42%) = 0.12% only. As expected, after approximately n = 50 sampling assays, all four sampling distributions converge toward

$$\aleph\left(\mu = 42\%, \sigma = \frac{0.5\%}{\sqrt{n}}\right)$$

It is worth noting that the width of the confidence interval, as well as the rate at which it narrows during the making of a lot, can be improved by improving sampling precision and increasing sampling frequency respectively.

From the point of view of production control during the making of a lot, the data that have been presented indicate that knowledge of the full sampling distribution is not necessary for quantifying the precision of the final lot assay, provided a sufficient number of samples (more than 50) are taken during the making of the lot. If one wants to use a small number of samples during the making of a lot, and yet make a correct estimation of the precision of the final lot assay, knowledge of the actual sampling distribution would be necessary.

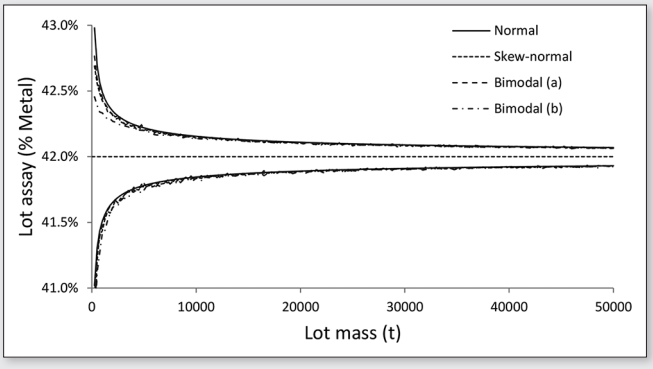

Figure 2. Evolution of grade during the making of a commercial lot, with the sampling distributions from Figure 1.

When considering that the loading of a commercial shipment may involve say 200 increments that are combined into 1 to 10 partial samples, using the full sampling distribution for assessment of shipment grade uncertainty is significant. Knowledge of the full sampling distribution would also prove useful should one want to optimise grade control during the making of a lot, since different sampling distributions will yield a different grade confidence interval at the beginning of the making of the lot.

Full sampling distribution and quality assurance

The Operating Characteristic curve, or OC curve, is the main risk analysis tool for practical acceptance sampling (Shmueli, 2014). It quantifies the conformity of a lot, by putting a number on the probability of accepting (alt. rejecting) a lot as a function of the true (unknown) assay of the lot and an Acceptance Quality Level (AQL). The OC curve truly is a sampling plan's fingerprint, in that two distinct sampling schemes yield different OC curves. The OC curve is relevant to both the consumer and the producer, and it is widely used throughout the manufacturing industry and the food industry. The minerals industry however does not appear to make much use of the concept at the present time.

The OC curve has been accepted and is being used by the food industry as a key food safety risk analysis tool for mycotoxins in cereal grains (FAO, 2014; Bourgeois and Lyman, 2012; Lyman et al., 2011). The similarities between sampling mycotoxins in cereal grains in the food industry and sampling valuable metals in mineral concentrates in the minerals industry implies that the OC curve should also be of significant value to the trading of mineral commodities, and ought to be developed as a minerals trading risk analysis tool.

The link between sampling and the OC curve

Construction of the OC curve, for a given sampling plan, requires access to the full sampling distribution. This may partially explain why it has not been developed in the minerals industry, as it is only recently that a solution for estimating the full sampling distribution has been published (Lyman, 2014). This however is a partial explanation only, as it is possible to estimate the OC curve from estimation of sampling variance from standard sampling theory, under the assumption of normality of the sampling distribution.

The basic elements for constructing and interpreting an OC curve are briefly presented hereafter. Quantifying the risk of accepting or rejecting a lot with a true (unknown) assay requires that one defines an Acceptance Quality Level (AQL), which may be a Lower Acceptance Quality Level (LAQL), an Lower Acceptance Quality Level (UAQL) or both. A supplier may want for example to produce a shipment of metal-bearing concentrate that bears no less than 41% metal, and no more than 43% metal. Depending on the AQL levels, the probability P_a of accepting the lot from sampling is calculated from the cumulative sampling distribution Φ_X according to:

$$LAQL \leq X \leq UAQL: P_a = \Phi_X(x = UAQL) - \Phi_X(x = LAQL)$$
$$X \geq LAQL \text{ only}: P_a = 1 - \Phi_X(x = LAQL)$$
$$X \leq UAQL \text{ only}: P_a = \Phi_X(x = UAQL)$$

Let us assume that the lot, whose true (unknown) assay is 42%, is characterized by a full sampling distribution $\Phi_X = \aleph(\mu = 42\%, \sigma = 0.5\%)$, and that LAQL = 41% is the quality acceptance level criterion of interest. The probability of accepting the lot is then

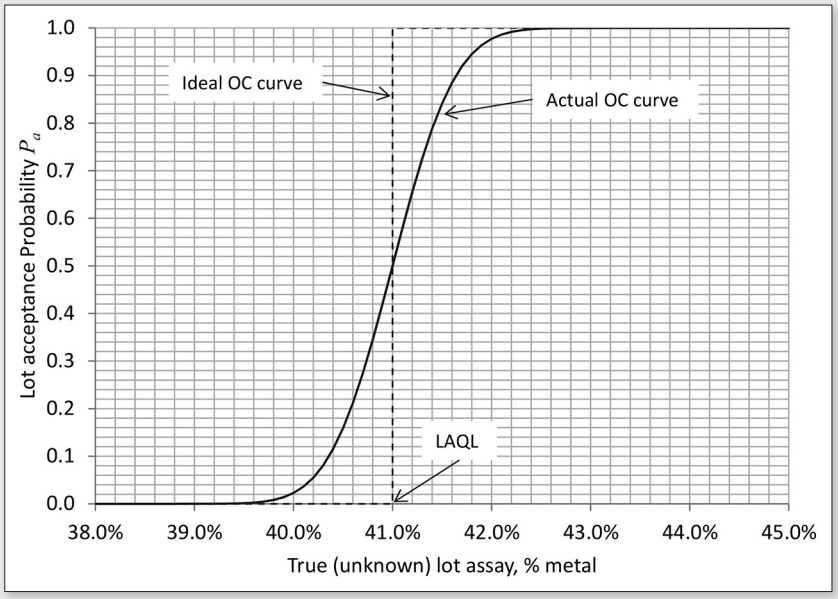

Figure 3. Example of OC curve for a Gaussian sampling distribution $\Phi_X = \aleph(42\%, 0.5\%)$, with LAQL = 41%.

$P_a = 1 - \aleph(X = 41\% \mid \mu = 42\%,\ \sigma = 0.5\%) = 97.73\%$. The acceptance probability can be calculated for any true (unknown) value μ of the lot assay, which yields the OC curve.

The dotted line in Figure 3 is the ideal OC curve, which corresponds to a sampling distribution with a variance equal to zero. This ideal case yields a lot acceptance probability strictly equal to 0 or 1 on either side of the AQL. In practice, there will always be a finite probability of accepting a non-conforming lot, or rejecting a conforming lot, for any true (unknown) assay of the lot. The steepness of the OC curve is entirely dictated by the nature of the sampling distribution, in particular its skewness, and by its variance, which is a measure of sampling precision. The effect of sampling variance σ^2 on the steepness of the OC curve is illustrated in Figure 4, for $\Phi_X = \aleph(42\%, \sigma\%)$.

The OC curve gives the actual value of the acceptance probability, which in turn quantifies the risk of accepting a non-conforming lot or rejecting a conforming lot. The OC curve is therefore a powerful risk management and decision making tool, whose construction relies entirely on the full sampling distribution.

The full sampling distribution and the OC curve

Figure 5 shows the OC curves obtained with the sampling distributions of Figure 1. It is recalled that all four sampling distributions share the same mean $\mu = 42\%$ and standard deviation $\sigma = 0.5\%$. In all cases, the acceptance quality level used to calculate the OC curves is set to LAQL = 41%.

The first observation is that the OC curves calculated using the non-Gaussian sampling distributions are all different from the one

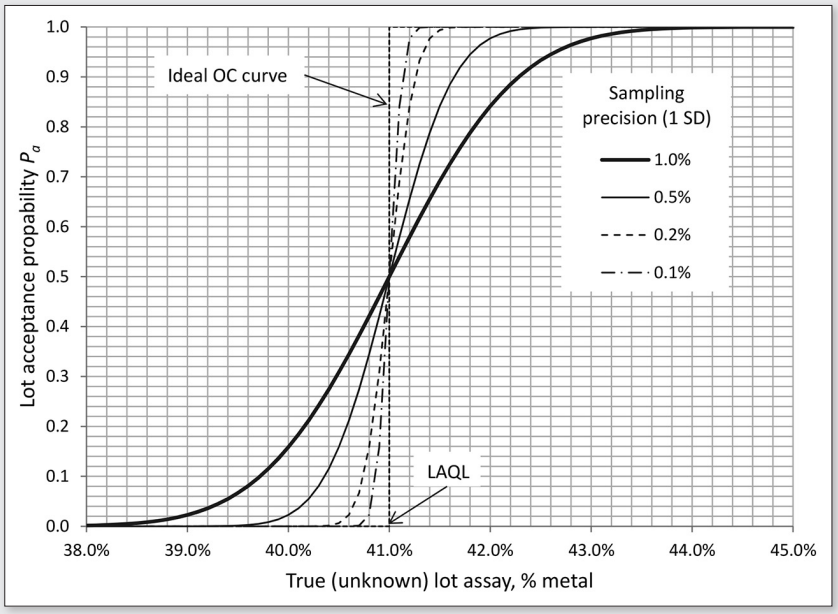

Figure 4. Illustration of the effect of sampling precision (values are 1 standard deviation σ of the full sampling distribution) on the steepness of the OC curve. The OC curves are calculated for $\Phi_X = \aleph(42\%, \sigma\%)$ with LAQL = 41%.

obtained with the Gaussian sampling distribution. The OC curve being the basis for quality assurance, it is concluded that the actual full sampling distribution must be used whenever sampling results are to be used for quality assurance purposes.

It is found that both the skewness and the bimodality of the sampling distributions have a significant effect on the OC curve. For the sake of clarity, Table 1 gives acceptance probabilities that are extracted from Figure 5 for lots whose true (unknown) assays are in the range 40% to 42%, for all four sampling distributions considered in the paper.

Let us first consider the nonconforming 40% and 40.5% cases from Table 1, which correspond to lots whose true (unknown) grade is less than LAQL. The buyer wants any such lot to be rejected 100% of the time. The 40% lot would be rejected 97.7% of the time under the Gaussian assumption, whereas all three other sampling distributions would yield a rejection rate significantly closer to 100%. Using the Gaussian sampling distribution would disadvantage the buyer. With the examples chosen, the bimodal (b) distribution yields the lowest acceptance rate for nonconforming lots. This indicates that the stronger the departure from normality of the sampling distribution, the more important it is to use the actual full sampling distribution in order to make the best decision about conformity of the lot.

With a just conforming lot whose true grade is equal to LAQL, the acceptance probability is precisely 50% with the Gaussian sampling distribution, which, of all four sampling distributions, is the most unfavourable value for the producer. Here again, the highest acceptance probability is obtained with the bimodal (b) distribution, which departs the most from the Gaussian distribution.

With conforming lots whose true grade is above LAQL, the producer expects the lot to be accepted 100% of the time. The acceptance probabilities with all four sampling distributions do not differ significantly, even though the numbers used indicate that the Gaussian assumption would in this case be better for the producer.

The examples presented have demonstrated the value of using the full sampling distribution, over that of assuming a Gaussian distribution, for assessing the conformity of a commercial lot. It is concluded that, for decision making about lot conformity and estimation of the associated risks, which are of significant importance in trading of minerals, it is important to determine and use the actual full sampling distribution.

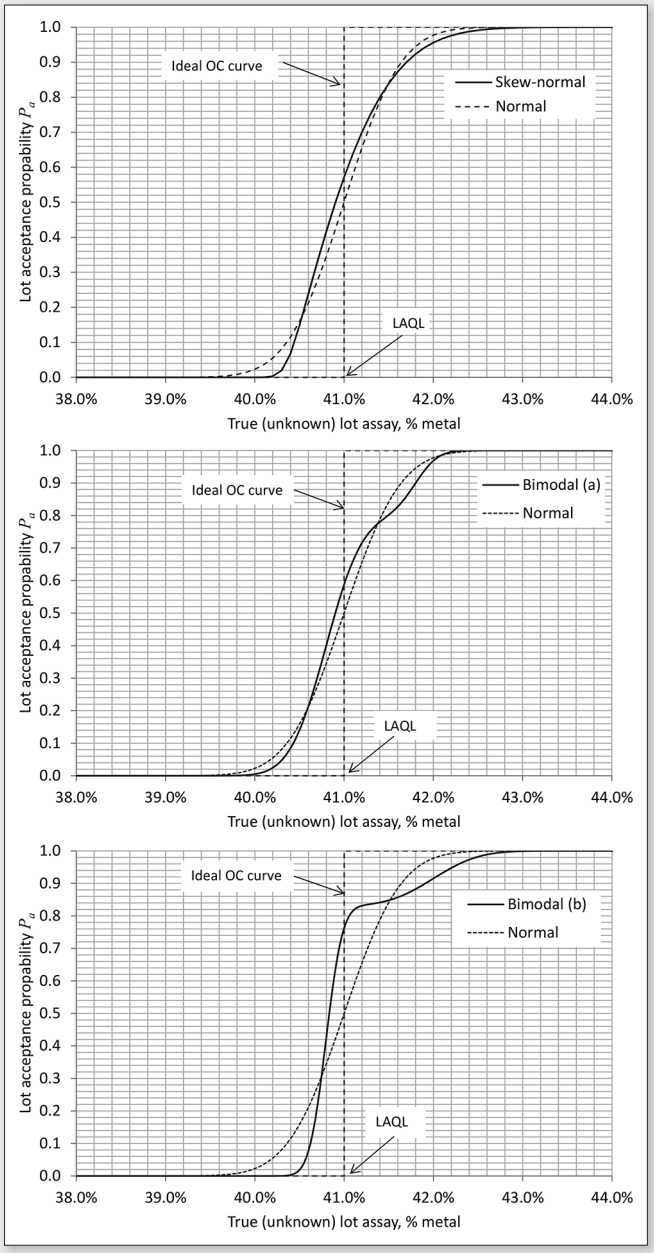

Figure 5. Illustration of the effect of the full sampling distribution on the estimation of the OC curve.

Full sampling distribution and quality control

Control charts are the power tools of the statistical process control toolkit used for quality control in any industry that seeks to guarantee quantitative quality criteria. Anything to do with control charts, from their construction to their interpretation, is built entirely upon sampling results. Indeed, the value of the control chart variable is calculated directly from sampling measurements, and the control limits of a control chart from which process quality is judged are also derived from the full sampling distribution.

Table 1. Values of acceptance probabilities for lots whose true (unknown) assays are in the range 40% to 42% with all four sampling distributions considered. Shaded columns represent conforming lots (true assay ≥LAQL), and unshaded columns nonconforming lots.

Sampling distributions from Figure 1	True (unknown) lot assay				
	40%	40.5%	41%	41.5%	42%
Normal	2.2750%	15.87%	50.00%	84.13%	97.72%
Skew-normal	0.0007%	14.68%	57.14%	83.92%	95.59%
Bimodal (a)	0.4985%	13.95%	58.71%	80.18%	96.82%
Bimodal (b)	0.0000%	1.87%	76.30%	84.80%	91.50%

The link between sampling and control charts

The purpose of a control chart is to record the value of a quality criterion, obtained by sampling, and assess its shift, or departure, from a target value. From *n* independent sampling measurements of the property of interest, the value of the control chart variable is calculated and placed on the associated control chart. Depending on the position of the value with respect to the control limits of the control chart, it can be found readily with known risks whether the process is in-control or out-of-control. If the value is inside the control limits, the process is said to be in-control, with an associated risk β that it is not the case (false negative). If the value is outside the control limits, the process is said to be out-of-control, with the probability $(1 - \beta)$ that this is indeed the case, and a risk α that this is not so (false positive). The higher the value the probability $(1 - \beta)$, also known as statistical power, the greater one's certainty that the process is out of control when a point is outside the control chart's control limits. The settings of a control chart are such that the probability $(1 - \beta)$ is as high as possible for a given situation.

There are a number of control charts that can be used depending on the nature of the shift that is being monitored, as control charts are more or less efficient in their capacity to detect a given shift. Perhaps the most relevant ones are Shewhart and Cusum control charts. Every time a sample is taken whose value is placed onto the control chart, there is a probability β that an out-of-control situation remains undetected. As successive samples are being collected and placed on the control chart, the probability that an out-of-control situation remains undetected decreases. The number of samples necessary to signal an out-of-control situation defines the Run Length (RL). It is a random variable whose distribution, referred to as the RL distribution, is the basis upon which one control chart is selected and tuned to control any given quality variable that is observed by sampling.

The RL distribution is derived from the full sampling distribution. Let us define the event E_k as "the k^{th} sample has control chart property X greater than UCL or less than LCL", where LCL and UCL are the control chart's Lower and Upper Control Limits respectively. Such an event, which defines an out-of-control situation, may occur for sample $k = 1$, $k = 2\ldots$ The probability p of such an event, for all $k \geq 1$ is given by:

$$\begin{aligned} P(E_k) &= p \\ &= P(X < LCL \text{ or } X > UCL) \\ &= P(X < LCL) + P(X > UCL). \end{aligned}$$

Both events are mutually exclusive so that their probabilities are additive. The value of p is derived from the complete sampling distribution.

In the case of Shewhart control charts, the points reported onto the control chart are independent. Hence, the event E_k corresponds precisely to a Bernoulli trial whose probability of success is p and that of failure is $q = 1 - p$. This Bernoulli trial is defined for $k = 1$, $k = 2\ldots$ but not for $k = 0$. It follows that the probability of $k - 1$ failures (in-control variable) followed by one success (out-of-control variable) obeys a geometric distribution with parameter p, defined for $k \geq 1$. The run length (RL) is defined as the number of samples that yields the first event E_k. Useful properties of the geometric distribution of RL are summarized hereafter:

- Parameter $p = P(X < \text{LCL or } X > \text{UCL})$, defined for all events $K \geq 1$. The parameter p is derived from the sampling distribution.

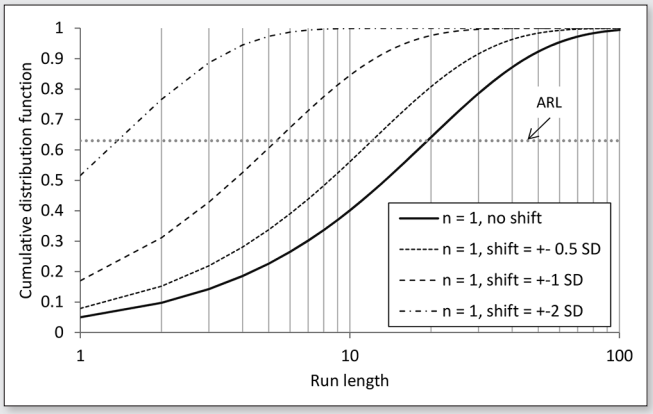

Figure 6. RL distribution for a Gaussian sampling distribution with shift $\delta = 0, \pm 0.5, \pm 1$ and ± 2 standard deviation, for $\alpha = 5\%$ and n = 1. Average run lengths (ARL) are read at the probability 0.63.

- Cumulative Distribution Function: $P(\text{RL} \leq k) = 1 - (1 - p)^k$
- Density Distribution Function: $P(\text{RL} = k) = p(1 - p)^{k-1}$
- Average run length (ARL): ARL = E(ARL) = 1 / P
- 95% RL limit: $\text{RL}_{max} = [\ln(1 - 0.95)] / [\ln(1 - p)]$

The probability p is the property which makes the RL distributions different. Once the control limits UCL and LCL have been derived for the initial in-control sampling distribution, it is a simple matter to shift the sampling distribution any amount δ and calculate the associated probability p of the RL distribution that results.

It is important to note that the shift δ can be either positive or negative, which corresponds to a sampling distribution that shifts to the right or to the left of the initial in-control sampling distribution. For a Gaussian sampling distribution, since it is symmetrical, the value of p is the same whether the distribution shifts right or left. The assumption of normality leads the control limits of an x-bar Shewhart chart to be set to $\pm$ 3 standard deviation of the sampling distribution for a risk $\alpha = 0.27\%$ (Minnitt and Pitard, 2008).

Figure 6 shows the RL distribution for a Gaussian sampling distribution with shift δ equal to 0, $\pm$ 1 and $\pm$ 2 standard deviation, using a risk $\alpha = 5\%$ and sample size $n = 1$.

Full sampling distribution and control charts

The effect of departure from normality on control charts has led to a number of publications in relation to quality control (Borror et al., 1999), and yet, the effect is not fully recognised by industry. The distribution of run lengths is shown in Figure 7 for the bimodal (b) distribution. The first and most important observation is that the RL distributions are not the same for positive and negative shifts of the mean. This result, which is due to the asymmetry of the sampling distribution, does not appear to have been reported elsewhere as it is not common for asymmetrical sampling distributions to be used in Statistical Process Control.

Figure 8 provides a graphical explanation as to why the RL distributions are not equal for left and right shift of the mean for asymmetrical sampling distributions. From one single sample measurement ($n = 1$), it is apparent that a positive (right) shift will be detected significantly faster than a negative (left) shift of equal magnitude. For an absolute 1% shift of the mean of the bimodal (b) sampling distribution, the type II error β for the left shifted distribution is 83.95%

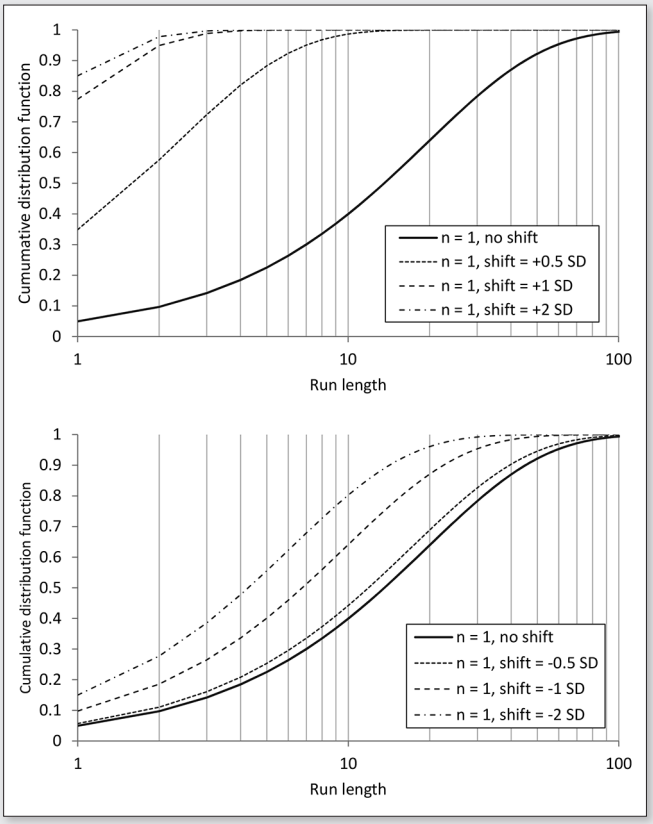

Figure 7. RL distribution for the bimodal (b) sampling distribution, for α = 5% and n = 1. The upper Figure is for positive shifts of the mean, and the lower Figure for negative shifts of the mean.

versus 14.83% only for the right shifted distribution, as highlighted by the shaded areas in Figure 8.

At any rate, whether left or right shifts occur, the RL distributions for the bimodal (b) sampling distribution are all different from those of the normal distribution for shifts of the same magnitude.

It can be concluded that assuming normality in setting up and applying control charts for quality control will yield erroneous decision making for non-Gaussian sampling distributions. Even though the above analysis was carried out for Shewhart X-bar charts only for the sake of conciseness and clarity, the same conclusions are expected to apply to any type of control charts.

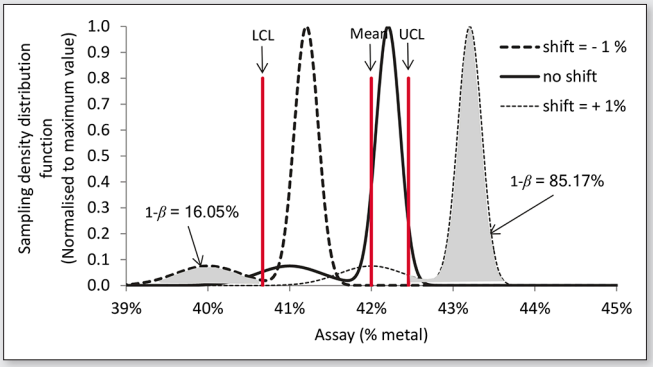

Figure 8. Full sampling distributions – bimodal (b) – with mean assay 41% (shift = –1%), 42% (no shift) and 43% (shift = + 1%) from left to right. The vertical lines show the lower (LCL) and upper (UCL) control limits at the 95% confidence level.

Conclusions

Lyman (2014) has shown that it is now possible to estimate the actual full sampling distribution from sampling data, as opposed to estimating the sampling variance and assuming a Gaussian sampling distribution. The aim of this paper was to assess the benefit of using the actual full sampling distribution for some of the important uses to which sampling results are put, namely production control, quality assurance and quality control. Through a number of illustrative examples, it was demonstrated that the actual sampling distribution should be used in order to apply sampling data to their full potential in production control, quality assurance and quality control. A corollary to that statement is that using sampling variance under the assumption of normality of the sampling distribution could yield erroneous analyses, which could lead to wrong decision-making related to Quality Assurance and Quality Control (QAQC).

- For production control during the making of a lot, it was found that knowledge of the full sampling distribution is not necessary for quantifying the precision of the final lot assay, provided a sufficient number of samples are taken during the constitution of the lot. However, knowledge of the actual sampling distribution is imperative if a few samples only are used to quantify the assay of a lot. Since different sampling distributions yield different confidence intervals at the beginning of the making of the lot, using the full sampling distribution is deemed necessary for grade control optimization during production of a commercial lot.
- Assuming normality of the sampling distribution for quality assurance can be to the advantage of the seller or the buyer, however there is no way to know without knowledge of the actual sampling distribution; hence it is necessary to use the actual sampling distribution for quality assurance. These conclusions were obtained by studying the effect of sampling distribution on the OC curve, one key decision-making tool in quality assurance. It was further observed that the greater the departure from normality, the more important it is to use the actual sampling distribution for accepting conforming and rejecting nonconforming lots.
- For quality control, the effect of using the actual sampling distribution on the RL distribution for Shewhart X-bar charts was investigated. It was found that the RL distribution, which encapsulates the efficiency of control charts for detecting shifts in quality in any production process, was highly sensitive to the nature of the full sampling distribution. The conclusion is that the actual sampling distribution must be used for application of control charts in quality control. Interestingly, it was observed that asymmetrical sampling distributions, which are likely to occur with particulates, yield RL distributions that are sensitive to the sign of the shift.

References

1. Lyman, G., Determination of the complete sampling distribution for a particulate material, in *Proceedings of Sampling 2014*, 29-30 July 2014, Perth, Australia, AusIMM, Publications series No 5/2014, pp. 17-24 (2014).
2. Lyman, G., "Complete sampling distribution for primary sampling, sample preparation and analysis", in *Proceedings of the 7th International Conference on Sampling and Blending*, Ed by K.H. Esbensen and C. Wagner, *TOS forum* **Issue 5,** 87–91 (2015). doi: 10.1255/tosf.44

3. Venter, J.H., A model for the distribution of concentrations of trace analytes in samples from particulate materials, *Technometrics*, 24(1), pp. 19-27 (1984).
4. Shmueli, G., *Practical acceptance sampling – A hands-on guide*, 2nd Edition (2014). ISBN 978-1-463-78904-6.
5. FAO - Food and Agriculture Organization of the United Nations. Mycotoxin Sampling Tool – User Guide, http://www.fstools.org/mycotoxins/, Sections 1.2 and 2.3 (2014).
6. Bourgeois, F.S., and Lyman, G.J., Quantitative estimation of sampling uncertainties for mycotoxins in cereal shipments, *Food Additives & Contaminants: Part A: Chemistry, Analysis, Control, Exposure & Risk Assessment*, 29:7, 1141-1156 (2012).
7. Lyman, G. J., Bourgeois, F.S., and Tittlemier, S., Use of OC curves in quality control with an example of sampling for mycotoxins, in *Proceedings 5th World Conference on Sampling and Blending (WCSB5)*, Santiago, Chile, 25-28 October 2011, pp. 431-443 (2011).
8. Minnitt, R.C.A. and Pitard, F., Application of variography to the control of species in material process streams: %Fe in an iron ore product, The Journal of the Southern African Institute of Mining and Metallurgy, 108, 109-122.
9. Borror, C.M., Montgomery, D.C., and Runger, G.C., Robustness of the EWMA control chart to non-normality, Journal of Quality Technology, 31, pp. 309-316 (1999).

Appendix

Skew-normal distribution

The skew-normal distribution is a useful distribution for simulating a skewed Gaussian looking distribution. It is a three parameter distribution whose density distribution function is defined by:

$$f(x) = \frac{2}{\omega}\phi\left(\frac{x-\xi}{\omega}\right)\phi\left(\alpha\left(\frac{x-\xi}{\omega}\right)\right)$$

where ϕ is the density distribution function of the standard normal distribution. The parameter α defines the skewness of the distribution. The mean and variance of the distribution are:

$$\mu = \xi + \omega\delta\sqrt{\frac{2}{\pi}} \text{ where } \delta = \frac{\alpha}{\sqrt{1+\alpha^2}}$$

$$\sigma^2 = \omega^2\left(1-\frac{2\delta^2}{\pi}\right)$$

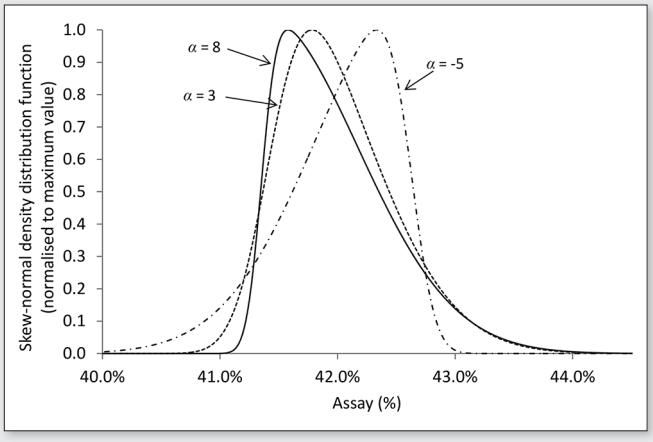

Figure 9. Examples of skew-normal distributions with mean μ = 42% and standard deviation σ = 0.5%. A negative skewness parameter α yields a left-skewed distribution, whereas a positive parameter yields a right-skewed distribution. α = 0 yields the normal distribution.

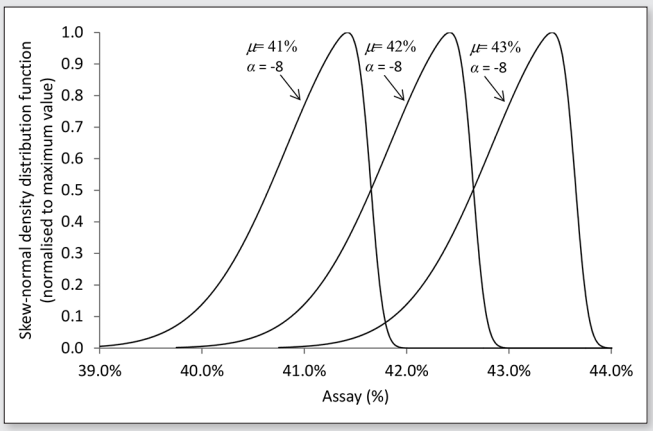

Figure 10. Examples of skew-normal distributions with variable mean and standard deviation σ = 0.5%, as used in the OC-curve section. The parameters used are:

μ = 41%, σ = 0.5% ⇒ α = -8, ξ = 41.65%, ω = 0.82%
μ = 42%, σ = 0.5% ⇒ α = -8, ξ = 42.65%, ω = 0.82%
μ = 43%, σ = 0.5% ⇒ α = -8, ξ = 43.65%, ω = 0.82%

The skew-normal distribution, with set skewness parameter α, is set to any true (unknown) mean μ and variance σ^2 of the lot using the following parameters:

$$\omega = \frac{\sigma^2}{\left(1-\frac{2\delta^2}{\pi}\right)}$$

$$\xi = \mu - \frac{\sigma^2}{\left(1-\frac{2\delta^2}{\pi}\right)}\delta\sqrt{\frac{2}{\pi}}$$

Figure 9 shows the flexibility of the skew-normal distribution, which provides a mean for simulating left and right skewed distributions.

Figure 10 gives an example of shifted skew-normal distributions with a shift in mean value only, as used in the section about the OC-curve. It suffices to shift the parameter ζ to shift the mean of the skew-normal distribution without changing its shape.

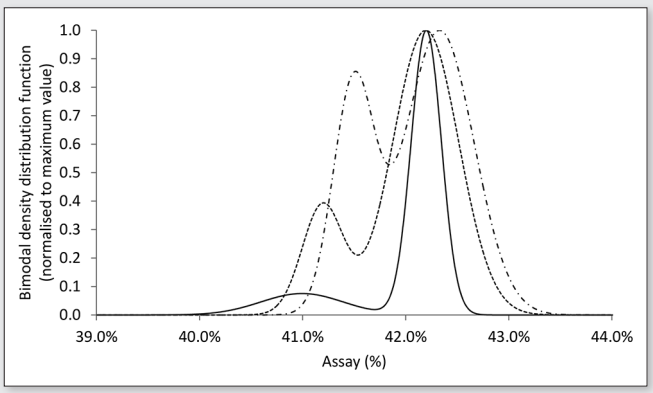

Figure 11. Examples of bimodal distributions with mean μ = 42% and standard deviation σ = 0.5%.

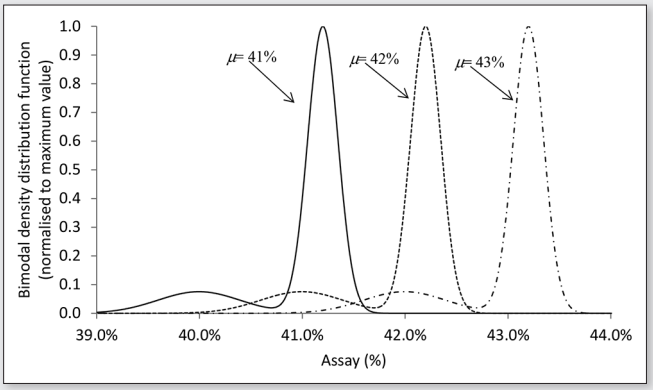

Figure 12. Examples of bimodal distributions with variable mean and standard deviation σ = 0.5%, as used in the OC-curve section. The values of the parameters used are:

$\mu = 41\%, \sigma = 0.5\% \Rightarrow \alpha = 0.4, \mu_1 = 40.00\%, \sigma_1 = 0.40\%, \mu_2 = 41.20\%, \sigma_2 = 0.15\%$
$\mu = 42\%, \sigma = 0.5\% \Rightarrow \alpha = 0.4, \mu_1 = 41.00\%, \sigma_1 = 0.40\%, \mu_2 = 42.20\%, \sigma_2 = 0.15\%$
$\mu = 43\%, \sigma = 0.5\% \Rightarrow \alpha = 0.4, \mu_1 = 42.00\%, \sigma_1 = 0.40\%, \mu_2 = 43.20\%, \sigma_2 = 0.15\%$

Bimodal distribution

The bimodal distribution used in this work, with mean μ and variance σ^2, is a mixture of two Gaussian random variables as shown in Figure 11. It is a five parameter distribution whose parameters are defined as:

$$\mu = \alpha\mu_1 + (1-\alpha)\mu_2$$
$$\sigma^2 = \alpha\left(\sigma_1^2 + \delta_1^2\right) + (1-\alpha)\left(\sigma_2^2 + \delta_2^2\right) \text{ where } \delta_i = \mu_i - \mu$$

The parameters μ_1 and μ_2 are the modes of the distribution, whereas the variances σ_1^2 and σ_2^2 define the spread of both peaks. The parameter α is a weighting factor for the mixture of distributions. Figure 12 gives an example of shifted bimodal distributions with a shift in mean value only, as used in the OC-curve section of the paper. It suffices to shift the parameters μ_1 and μ_2 by the same amount in order to shift the mean of the bimodal distribution without changing its shape.

doi: 10.1255/tosf.48

Building confidence intervals around the obtained value of a sample

Dominique M. Francois-Bongarcon, PhD
Agoratek International Consultants Inc., North Vancouver, Canada. E-mail: dfbgn2@gmail.com

Common practice in sampling for the TOS erudite consists of using the sampling variance obtained from Gy's numerical theory to build confidence intervals around the true sample value. This is usually done to characterise the 'precision' of the sample, and, by centring that interval on the sampled value, one states for instance that "the true value has 95% chances of being between values x and y", those two values usually being centred on the sampled value". The somewhat naïve rationale behind this practice is reviewed in some details and criticised. It is suggested the confidence interval of real interest to the user of the sampled value, is more difficult to define and more delicate and indirect to build. Some methods for doing so are examined and a methodology is recommended.

Introduction

Gy's Theory of Sampling[1] (TOS) has a powerful numerical section that gives us a wealth of information about the behaviour of a sample, provided we know enough about some physical characteristics of the matter being sampled and basic parameters about the sample such as its mass. Armed with it, we can in particular predict the variance we are likely to encounter should the sample be taken many times, i.e. characteristics about the distribution of the possible sample values. That predicted variance, which measures the dispersion of that sample distribution, allows for a characterisation what is often termed the 'precision' of the sample, or in other words, its goodness.

It is not uncommon then to use that variance to build some kind of a confidence interval around the obtained sample value to state where the true value of the variable to be measured may lie. Indeed, what is the use of the sampled value if we have no notion of what it really means regarding the unknown, true value we are trying to best guess? Building this confidence interval also clearly requires, implicitly or not, not only the variance, but also an idea of the distribution type or shape.

This practice, however, can often be applied quite naively, as we are going to see, starting with the fundamental question: "What distribution exactly are we speaking about?"

Better definition of the problem

So, here we are, with a sample value in hand, and the ability to predict the dispersion variance attached to it. Now, experience and knowledge also give us an idea of the shape of the sample distribution:

- Normal-like if the variance is relatively small (and the sample 'precision relatively good); this is a consequence of the symmetrisation of such distributions when their variances diminish, itself deeply and implicitly rooted in the general mechanism underlying the famed Central Limit Theorem.
- Lognormal-like or binomial-like in the opposite case.

We can therefore predict a 'histogram of sorts' of the possible sample values. And this, in practice, may not be hugely rigorous, but in reality, experience shows it works well enough: when that histogram is built experimentally as the result of repeated sampling, this method is usually reasonably validated. But there lies an often unseen difficulty: we then need to define very clearly the nature and full range of what it is, exactly, we are trying to guess.

When a sample is taken, hopefully in a representative fashion, we are obviously hoping to be able to use its value in lieu of the unknown, true value of the variable measured/estimated by that sampling operation, and we would like to know how imperfect doing so can eventually be. That is where a confidence interval may come into play: a very explanatory view to it consists of trying to attach probabilities to the unknown value underlying the sampling, saying for instance that there are 95% chances that it is in a specific, known interval around the obtained sample value.

To quickly understand/illustrate why using the sample distribution shape to do so is a rather naive idea, and for the sake of the exercise, let us assume a true value T and that the sample distribution around it is skewed towards high values ('to the right') like in the 3-bar histogram of Figure 1 where the true value is the centre value of the 3 possible sample outcomes. When we take a sample, we do not know the true value, and in this simplistic case, all we know is that the sample is one of the possible outcomes, in this case one of three, but we do not know which one.

Going in turn to every possible sample value in the distribution, and looking where the true value lies in each case with respect to that sample value, i.e. on which side of the sample value and how often this will happen, the histogram of the possible true values that could generate this sample can be drawn (Figure 2). Clearly, this is not the distribution of the sample values, it is, at best its mirror image. Skewed distributions calling for asymmetric confidence intervals, it becomes clear using the sample distribution directly would be very wrong in this case.

It does not mean, however, the solution lies in symmetry. This example was simple but also itself quite naive. The models of TOS tell us that the variance of the sample distribution is heteroscedastic, meaning it changes with the true value being sampled, i.e. it is concentration-dependent. In this example, we had ignored this important fact.

It is nevertheless possible to reach the following conclusions:

- The distribution of sample values around a given true value is not the same (in dispersion and shape) as the underlying distribution of potential true values around a known sample.
- The first one is usually simple and fairly well known (to a good enough degree in practical terms), the latter, conversely, is not readily known, and its determination would be very complex.
- For confidence intervals characterising the unknown true value, unfortunately it is that second, problematic one that really counts.

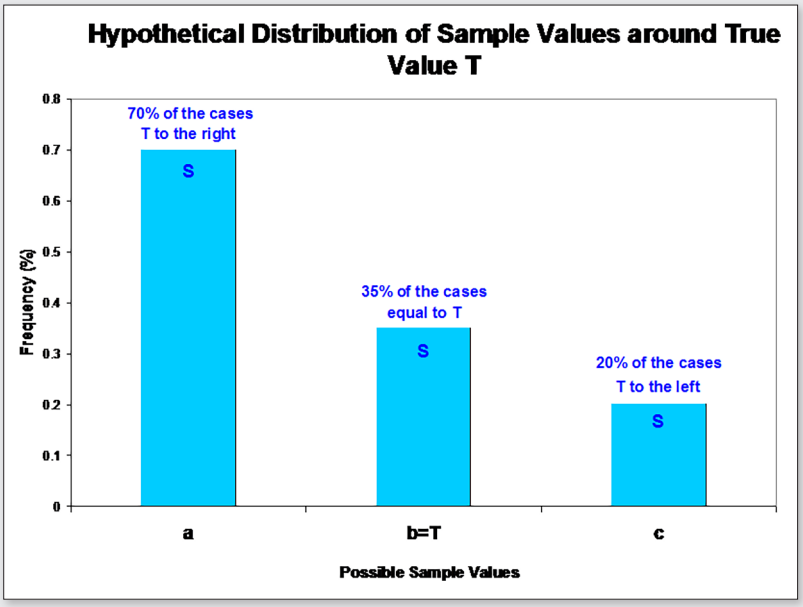

Figure 1. Hypothetical distribution of sample values around true value T

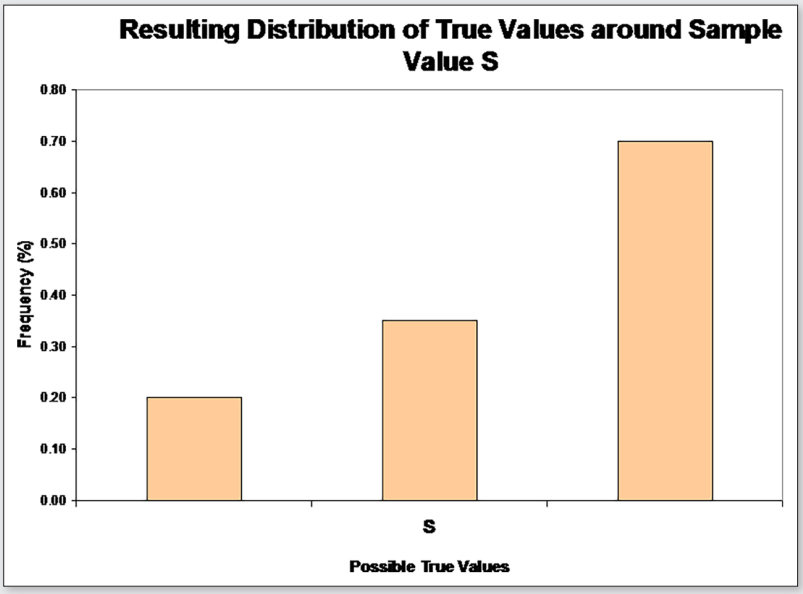

Figure 2. Resulting distribution of true values around sample value S

The lookup method

The ignorance in which we are of the underlying distribution of the possible true values that are able to give raise to a known sample value (obtained experimentally), indeed makes the problem of building a proper confidence interval around the sample value, a rather complex one. A method sometimes used is the lookup method, based on the likelihood concept. In this method, each possible true value (concentration) is considered in turn, and a confidence interval (e.g. 95% confidence as an example) is built around it for the sample values, based on what is known of the sample distribution, including its concentration-dependent variance. By definition each interval contains the 95% most likely sample values for a given true value. These intervals are plotted on a diagram. The upper and lower limits of these intervals define a region in the [True Value, Sample Value] space, containing all the sample values belonging to their respective 95% confidence intervals around their true values (in the example of Figure 3, the sample distributions were assumed to be binomial). We will call it the '95% Domain'.

Then, when considering a specific sample value, it defines a horizontal line on the diagram. The intersection of the line with the 95% Domain is then used as a confidence interval (the red segment on Figure 3). It is assumed (intuitive, but not demonstrated) that this interval contains approximately the 95% most likely true values able to generate that specific sample value.

Testing

The proportion selected by the lookup method was therefore put to a test by spreadsheet simulation of sample binomial distributions,

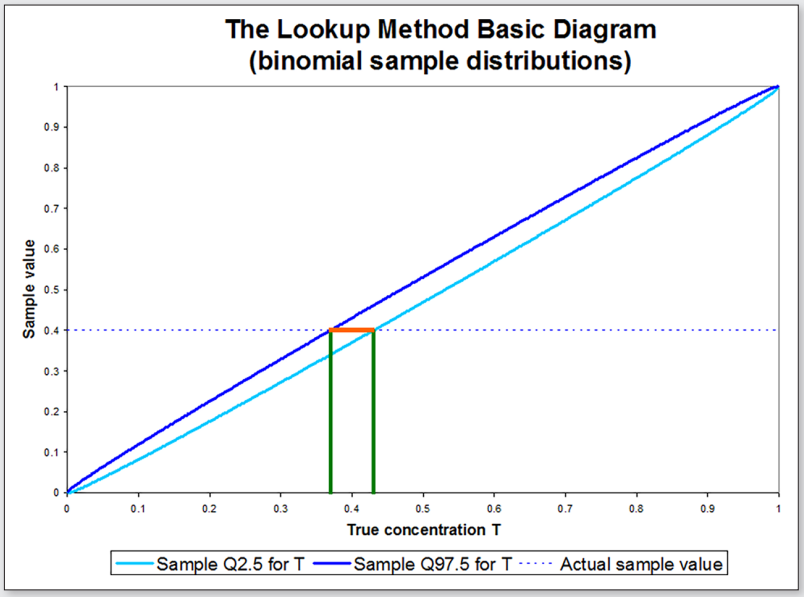

Figure 3. The lookup method basic diagram

for a full range of true values (concentrations) varying between the minimum of 0 and the maximum of 1, using 1,000 binomial trials for each. For numbers of success draws lesser than 5, i.e. concentrations lesser than 0.005, numerical stability problems altered the results to some degree. As kindly pointed out by a reviewer, the discrete nature of the binomial distribution is a significant factor in this observation. In any case, for these low numbers, the proportion of values within the lookup interval averaged to 95%, but with large variations, between 90.4% and 98.8%, with no pattern. Above these, the variations around 95% tend to become increasingly smaller, still without pattern, and still averaging to 95%. Given the numerical limitations imposed by the spreadsheet precision, the method was therefore reasonably validated, in conformity with our initial intuition.

Method comparisons

The simulation, however, is too heavy a process for routine applications, and as mentioned, of imperfect numerical stability. Using it as a benchmark, simpler - initially considered naive - methods were compared to it, namely:

- Gaussian confidence interval around the experimental sample value using the estimated binomial sampling variance.
- Lognormal and binomial confidence interval variants of the latter.
- Mirror images of the above two variants (skewed the other way).

As a comparison score, the maximum, relative, unsigned difference obtained for the two limits of the interval was used, along with an eyeball examination.

The following was observed:

- Surprisingly, the mirror images did not perform well, as the lookup interval was always slightly skewed to the right, likely a consequence of the variance heteroscedasticity we had previously ignored.
- The binomial intervals fared very erratically, possibly due solely to numerical problems. Where they seemed to behave properly, their results were however rather poor.

Table 1. Comparison of 95% Confidence Intervals on Simulated Sample Distributions

Sample Concentration	Lookup		Lognormal		Normal	
	LL	UL	LL	UL	LL	UL
0.005	0.002	0.010	0.002	0.011	0.001	0.009
0.010	0.005	0.017	0.005	0.017	0.004	0.016
0.050	0.038	0.064	0.038	0.065	0.036	0.064
0.100	0.083	0.119	0.083	0.120	0.081	0.119
0.250	0.224	0.277	0.224	0.278	0.223	0.277
0.270	0.243	0.297	0.244	0.299	0.242	0.298
0.350	0.321	0.379	0.321	0.380	0.320	0.380
0.500	0.469	0.530	0.470	0.532	0.469	0.531
0.900	0.880	0.916	0.882	0.919	0.881	0.919

- The normal and lognormal intervals both performed well at concentrations of 0.005 and above. Below these, numerical problems made the comparison unreliable.
- An approximate concentration threshold of 0.26 on the concentration was found to exist, that differentiated their performances: below 0.26 the lognormal intervals worked best, with the normal intervals performing better above 0.26.

A selection of these results is offered in Table 1.

Conclusion

In the case of binomial-like sample distributions, the lognormal and normal confidence intervals can be used, lognormal below concentrations of 0.26, normal ones above. When normal distribution are simulated instead, the normal confidence intervals are winning over lognormal at all concentrations, which is not surprising, but violates the expected distribution shapes at low concentrations. The simple rule described above and its concentration threshold of 0.26, should heuristically give good results in all practical cases.

Acknowledgments

An anonymous reviewer is hereby acknowledged for a very valuable suggestion.

Reference

1. Gy, P. M. (1998) *Sampling for Analytical Purposes*, John Wiley & Sons Ltd, Chichester, England.

doi: 10.1255/tosf.58

Validation of reverse circulation drilling rig for reconciliation purposes

A.C. Chieregati[a], T.M. El Hajj[b], C.F. Imoto[c] and L.E.C. Pignatari[d]
[a,b] Dept. of Mining and Petroleum Engineering, University of Sao Paulo, Av. Prof. Mello Moraes 2373, 05508-030, Sao Paulo, Brazil. E-mail: ana.chieregati@usp.br; thammiris.poli@usp.br
[c] MultiGeo, R. Funchal 19, 8th floor, 04451-060, São Paulo, Brazil. E-mail: carla.imoto@gmail.com
[d] Yamana Gold, R. Funchal 411, 04451-060, São Paulo, Brazil. E-mail: lpignatari@yamana.com

Representative samples of ore containing precious metals is a difficult task. The lower the grade and the higher the nugget and/or cluster effect, the more complex and difficult extracting samples that are both accurate and precise. Reconciliation practices can be used as an effective tool to evaluate sampling accuracy throughout grade control processes. However, a proper reconciliation system must be based on reliable data and, therefore, optimisation of sampling techniques is a must for development of a reliable reconciliation system. This paper is a result of an extensive reconciliation study carried out at a copper and gold mine in Brazil, where a significant reconciliation problem took place while using manual sampling for grade control and short-term modeling. After analysing several sampling equipment/sample selection techniques, the authors suggested the use of a reverse circulation drilling rig with an automatic sampling system for grade control sampling. The samples generated by this automatic system were compared with the manual samples collected from the piles generated by the previous percussion rotary air blast drilling rig. Also, three pairs of twin holes were drilled in order to validate the new reverse circulation approach. Results allowed estimation of the bias related to the increment weighting error (IWE) generated by manual sampling, and show that the reverse circulation rig eliminates significant sampling biases, thus improving the general sample representativeness by increasing both sample accuracy and precision.

Introduction

Sampling is an essential operation performed in many stages of a mining project: before its implementation, during mineral exploration for resources and reserves evaluation, and after its implementation, during mining and minerals processing for short-term planning, process control and reconciliation. Sampling is defined as a sequence of operations that aims to take a significant part, or sample, of a given lot[1]. Reconciliation, in turn, consists of comparing the tonnages and grades estimated by the geological models with the tonnages and grades obtained in the processing plant.

The main objective of this work was to optimise sampling procedures of a copper and gold mine in Brazil, where sampling for reconciliation purposes traditionally has been performed using a blast-hole drilling rig, model HCR1500 by Furukawa. After drilling, samples were manually collected from the coarse material pile using shovels.

According to Pitard[2], the main problems related to blast-hole sampling are: upward and downward contamination during drilling, upward losses during drilling, refluxing during drilling, sub-drill material disposal at the top of the pile, poor recovery of the former sub-drill, pile segregation, pile shape irregularity, loss of fines, deterministic and operator-dependent sampling, sampling interfering with mining productivity, and a too small sample mass (not enough for representativeness), resulting in massive misclassification of ore and waste. The same author lists the many advantages of separate drilling campaigns using reverse circulation drilling rigs, which includes: absence of a sub-drill, possibility to drill several benches at once, possibility to drill at an appropriate angle (perpendicular to the mineralisation structure), limited contamination and losses, no interferences with mining productivity, possibility of drilling many months ahead of mining time, smaller representative sample masses (since the chips are usually smaller than the ones generated by blast-hole drilling rigs), better mining logistics, easier automation of sampling, more accurate and precise grade control.

In 2013[3], the authors presented the results of a sampling campaign in the same mine, which demonstrated the tendency of the Furukawa to overestimate both gold and copper grades, especially due to poor recovery (only 80%) coupled with segregation between fines and coarse material. Therefore, a reverse circulation (RC) drilling rig with automatic sampling system (recovery of up to 99%) was recommended, in order to minimise the errors generated by manual sampling, such as the increment delimitation error, the increment extraction error, the increment weighting error and the grouping and segregation error (IDE, IEE, IWE, GSE).

This paper presents the results of sampling optimization for reconciliation purposes, based on the validation of the RC ROC L8 drilling rig with an automatic sampling system by Atlas Copco. The advantages of working with this type of rig offset the cost of acquisition, especially when dealing with very heterogeneous and geologically complex deposits.

Methodology

The mine selected for this study has a very complex geology. Gold and copper do not correlate with one another and are not preferably associated with any of the geological structures, requiring a versatile and appropriate sampling system to determine the limits between ore and waste. In addition, low grades and variable rock type occurrences make sampling even more difficult.

Earlier sampling procedure

The previous sampling approach was carried out using a Furukawa HCR1500, a percussion rotary air blast drilling rig with a 3.5” drill bit. This rig has two outputs originating from the cyclone underflow (front discharge: coarse and medium fragments) and overflow (rear discharge: fine fragments). The rig also has 5 filters, through

which all fine material passes before being discharged, constituting one of the likely sources of contamination, as part of the material is retained in the filters and is first eliminated later together with material from the next hole.

The previous method consisted in manual collection of 12 increments from the medium and coarse pile, using a shovel. The fines were discarded because (according to the sampling team): "the fines 'salt' the sample, which does not reconcile with the plant"[*sic*].

The previous work[3] proved that this drilling rig is not able to recover all the material from the hole, especially the coarse and consequently lower grade material. Thus, the fragments sent to the surface piles (finer fragments) are richer than the original lot (all fragments composing the drill hole: fines, medium and coarse). It was observed that in a 10 m drill hole, approximately 2 m of material could remain in the hole. Over time, incorrect sampling of coarser material has been compensating the error due to the Furukawa's low recovery, generating excellent, but illusory, reconciliations[4].

New sampling procedure

The new equipment acquired for short and medium-term sampling is an RC Atlas Copco ROC L8, equipped with a 5.5" drill bit and which is capable of recovering up to 99% of the drilled material. The RC drilling rod has a lining inside which the fragments are lifted, minimizing the material loss inside fractures and avoiding contamination with fragments from the wall of the drill hole. The fragments are then sent directly to the automatic sampling system, where they are split by a riffle splitter. Figure 1 shows the drilling rig with the automatic sampling system.

Compressed air moves between the drill pipes, recovering the material and sending it to a ceramic baffle to reduce the speed of the particles. Upon reaching the desired depth, the drilling is interrupted and the material is discharged through the automatic quartering system, consisting of three sets of riffle splitters which generate the sample and the waste (Figure 2).

In order to validate the new sampling system and compare it to the old, three twin holes were executed. The samples were taken every 5 m, resulting in a total of 10 samples altogether: two from hole #1, four from hole #2 and four from hole #3. The remaining material was also collected: for the Furukawa, this was composed of the fines and the remaining part of the coarse pile; for the RC ROC L8, the remaining material was composed of the rejects of the riffle splitters and the material deposited on the top surrounding the hole.

Figure 1. RC ROC L8 drilling rig with automatic sampling system.

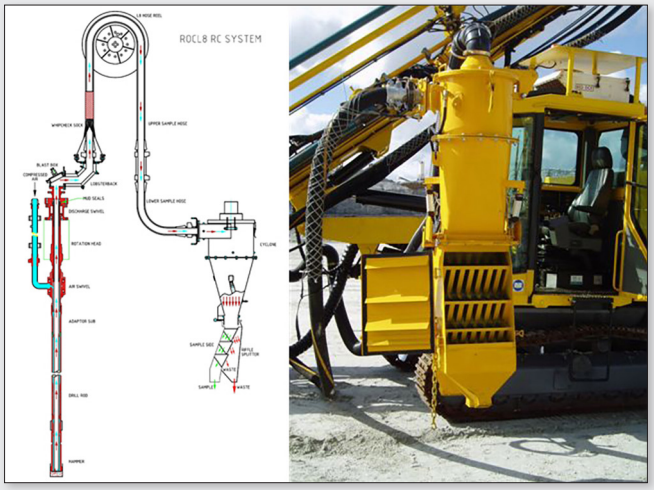

Figure 2. Drill hole material pathway until reaching the automatic sampling system, consisting of three sets of riffle splitters.

The twin holes sampling procedure is described as follows:

- Drilling (Furukawa), stopping every 5 meters.
- Collection of 12 increments sample using a shovel.
- Collection of the remaining material.
- Drilling (RC ROC L8), stopping every 5 meters.
- Collection of the sample generated by the automatic sampling system.
- Collection of the remaining material.

Results

The data processing is designed to perform the following analyses:

- Accuracy of the Furukawa drilling rig for sampling purposes.
- Quality of samples generated by each sampling method.

Accuracy of the Furukawa drilling rig

Comparing the results of this study with those of the previous study[3] showed that the Furukawa tends to overestimate the actual gold and copper grades, with an average relative error of +57.6% and

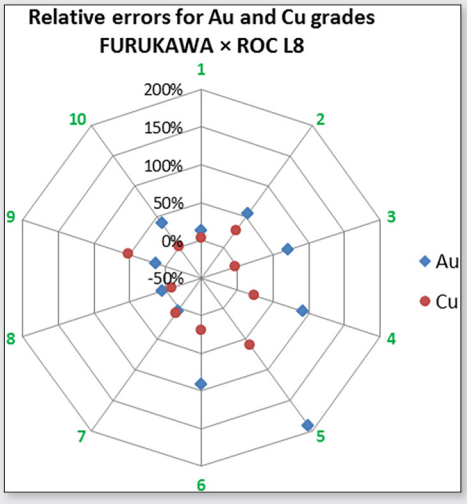

Figure 3. Furukawa relative errors for copper and gold grades compared to RC ROC L8 twin holes.

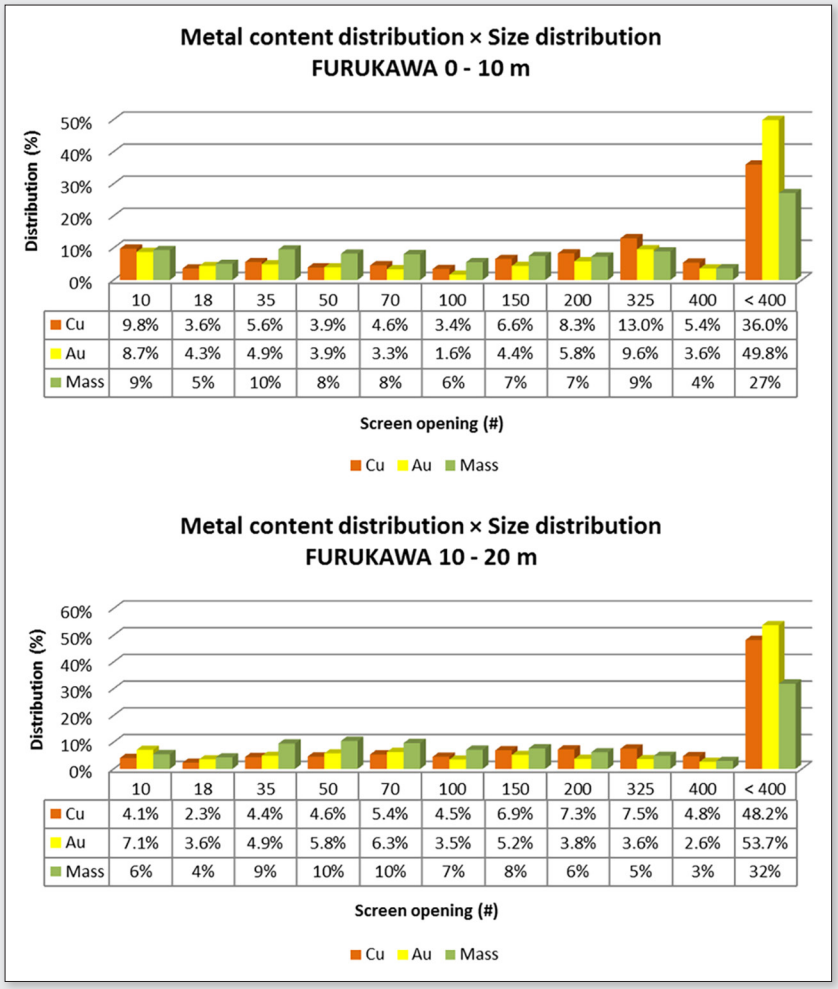

Figure 4. Distribution of gold and copper content, and mass retained, for 11 size fractions. Calculations are based on size distribution and chemical analysis for all material recovered by the Furukawa rig from hole #3 (0 to 10 m and 10 to 20 m).

+18.3% respectively. These errors were calculated relatively to the corresponding grades of the material from the twin holes recovered by the RC ROC L8. Figure 3 (related to Table 3) shows the gold and copper relative errors for all 10 individual samples.

This figure shows that the error dispersion related to gold is much higher than the one related to copper, and indeed that all samples were overestimated for gold while 80% of the samples were overestimated for copper.

Quality of samples – Furukawa

The quality of manual samples taken from the material recovered by the Furukawa can be characterised in two ways:

- Comparing the grades of manual samples with the grades of all the material recovered by the Furukawa.
- Comparing the grades of manual samples with the grades of all the material recovered by the RC ROC L8 (twin holes).

Figure 4 shows that both copper and gold are concentrated in the finest size fraction, since most of the contained gold (49.8% Au and 53.7% Au) and the contained copper (36.0% Cu and 48.2% Cu) is in the -400# fraction. Thus, samples taken from the coarse fragments pile will underestimate the grades, due to the increment weighting error (IWE).

Table 1 shows the errors associated with manual sampling relative to the grades calculated for all the material recovered by the Furukawa, showing a clear pattern of underestimation.

Table 2 shows the errors associated with manual sampling relative to the grades calculated for all the material recovered by the RC ROC L8, showing a pattern of overestimation.

Interestingly, unlike to the results shown in Table 1, in this case manual sampling leads to an overestimation of the hole grades. This can be explained by the fact that the Furukawa doesn't recover the coarser/poorer fragments and thus overestimates the gold grades in 57.6% and the copper grades in 18.3% (see relative error means in Table 3). Even though the samples have an underestimation trend (–12.6% for gold and –7.1% for copper: see relative error means in Table 1), this is not enough to compensate the error induced by the drilling rig. It's important to note that, if increments were collected from the fines pile as well, the overestimation trend of manual samples would be even greater.

Since one error compensates another in the earlier approach, it was often possible to obtain what *appeared* as excellent reconciliations – even with very poor and biased samples. The fact that reconciliation results were deceptively satisfactory did not allow, for years, proper recognition of the errors involved and the optimization of sampling procedures in order to ensure the

Table 1. Absolute and relative errors for Cu and Au grades comparing Furukawa samples (Sample) with all the material recovered by Furukawa (Total)

g/t Au (FURUKAWA)				
Hole/Depth	Total	Sample	ABS Error	REL Error
H1/0-5 m	0.345	0.294	-0.051	-14.7%
H1/5-10 m	0.110	0.081	-0.029	-26.5%
H2/0-5 m	0.907	0.825	-0.082	-9.0%
H2/5-10 m	0.185	0.131	-0.054	-29.0%
H2/10-15 m	0.081	0.060	-0.021	-25.8%
H2/15-20 m	0.048	0.037	-0.011	-22.9%
H3/0-5 m	0.294	0.282	-0.012	-3.9%
H3/5-10 m	0.100	0.111	0.011	10.8%
H3/10-15 m	0.045	0.047	0.002	4.6%
H3/15-20 m	0.043	0.038	-0.005	-11.7%

Mean	-0.022	-12.6%
Variance	0.00085	
Standard deviation	0.029	
Representativeness ($r^2 = m^2 + s^2$)	0.0013	

%Cu (FURUKAWA)				
Hole/Depth	Total	Sample	ABS Error	REL Error
H1/0-5 m	0.435	0.408	-0.027	-6.2%
H1/5-10 m	0.179	0.141	-0.038	-21.1%
H2/0-5 m	0.522	0.503	-0.019	-3.6%
H2/5-10 m	0.205	0.188	-0.017	-8.2%
H2/10-15 m	0.138	0.128	-0.010	-7.5%
H2/15-20 m	0.115	0.111	-0.004	-3.8%
H3/0-5 m	0.483	0.506	0.023	4.8%
H3/5-10 m	0.172	0.193	0.021	12.4%
H3/10-15 m	0.155	0.102	-0.053	-34.3%
H3/15-20 m	0.105	0.102	-0.003	-2.8%

Mean	-0.011	-7.1%
Variance	0.00061	
Standard deviation	0.025	
Representativeness ($r^2 = m^2 + s^2$)	0.00074	

Table 2. Absolute and relative errors for Cu and Au grades comparing Furukawa samples (Sample FK) with all the material recovered by RC ROC L8 (Total L8)

g/t Au (ROC L8 × FURUKAWA)				
Hole/Depth	Total L8	Sample FK	ABS Error	REL Error
H1/0-5 m	0.306	0.294	-0.012	-4.0%
H1/5-10 m	0.071	0.081	0.010	14.3%
H2/0-5 m	0.532	0.825	0.293	55.2%
H2/5-10 m	0.096	0.131	0.035	36.0%
H2/10-15 m	0.028	0.060	0.032	116.8%
H2/15-20 m	0.025	0.037	0.012	47.7%
H3/0-5 m	0.282	0.282	0.000	-0.1%
H3/5-10 m	0.095	0.111	0.016	16.9%
H3/10-15 m	0.040	0.047	0.007	18.6%
H3/15-20 m	0.031	0.038	0.007	23.1%

Mean	0.040	32.5%
Variance	0.0081	
Standard deviation	0.090	
Representativeness ($r^2 = m^2 + s^2$)	0.010	

%Cu (ROC L8 × FURUKAWA)				
Hole/Depth	Total L8	Sample FK	ABS Error	REL Error
H1/0-5 m	0.425	0.408	-0.017	-4.0%
H1/5-10 m	0.140	0.141	0.001	0.7%
H2/0-5 m	0.538	0.503	-0.035	-6.4%
H2/5-10 m	0.166	0.188	0.022	13.3%
H2/10-15 m	0.086	0.128	0.042	48.2%
H2/15-20 m	0.096	0.111	0.015	15.1%
H3/0-5 m	0.446	0.506	0.060	13.4%
H3/5-10 m	0.187	0.193	0.006	3.2%
H3/10-15 m	0.102	0.102	0.000	-0.3%
H3/15-20 m	0.104	0.102	-0.002	-2.1%

Média	0.009	8.1%
Variância	0.00075	
Desvio Padrão	0.027	
Representatividade ($r^2 = me^2 + se^2$)	0.00083	

representativeness of samples and hence the reliability of reconciliation results[4].

Quality of samples – RC ROC L8

Table 4 shows the errors estimates associated with the automated sampling system of RC ROC L8 relative to the grades calculated for all the material recovered by the same drilling rig. An important aspect is the absence of a systematic error, or bias, i.e., the samples do not have a tendency to underestimate or overestimate the grades (50% of the samples underestimate gold grades and 60% of the samples underestimate copper grades).

Figure 5 shows a comparison between the particle size distributions of the RC ROC L8 sample and the particle size distribution of all the material recovered by the RC ROC L8. This figure also shows the same comparison for the Furukawa, which presents very different distributions, proving the observed bias.

This display proves beyond any doubt that the RC ROC L8 distributions are fully compatible and that there's no selection of a particular size fraction at the expense of others. Knowing that if one wants to represent the grades, the imperative is to represent the complete particle size distribution, it can be stated that the RC ROC L8 automatic sampling system generates samples that are fully representative of the original lot.

Conclusions

Based on the presented results, the following conclusions can be made:

- The Furukawa overestimates both copper and gold grades, mainly because of the upward losses during drilling.

Table 3. Absolute and relative errors for Cu and Au grades comparing all material recovered by Furukawa (Total FK) with all the material recovered by RC ROC L8 (Total L8)

g/t Au (ROC L8 × FURUKAWA)				
Hole/Depth	Total L8	Total FK	ABS Error	REL Error
H1/0-5 m	0.306	0.345	0.038	12.5%
H1/5-10 m	0.071	0.110	0.039	55.6%
H2/0-5 m	0.532	0.907	0.375	70.5%
H2/5-10 m	0.096	0.185	0.088	91.7%
H2/10-15 m	0.028	0.081	0.053	192.2%
H2/15-20 m	0.025	0.048	0.023	91.7%
H3/0-5 m	0.282	0.294	0.011	4.0%
H3/5-10 m	0.095	0.100	0.005	5.5%
H3/10-15 m	0.040	0.045	0.005	13.4%
H3/15-20 m	0.031	0.043	0.012	39.4%

Mean	0.065	57.6%
Variance	0.013	
Standard deviation	0.112	
Representativeness ($r^2 = m^2 + s^2$)	0.017	

%Cu (ROC L8 × FURUKAWA)				
Hole/Depth	Total L8	Total FK	ABS Error	REL Error
H1/0-5 m	0.425	0.435	0.010	2.3%
H1/5-10 m	0.140	0.179	0.039	27.7%
H2/0-5 m	0.538	0.522	-0.016	-2.9%
H2/5-10 m	0.166	0.205	0.039	23.4%
H2/10-15 m	0.086	0.138	0.052	60.2%
H2/15-20 m	0.096	0.115	0.019	19.7%
H3/0-5 m	0.446	0.483	0.037	8.2%
H3/5-10 m	0.187	0.172	-0.015	-8.2%
H3/10-15 m	0.102	0.155	0.053	51.7%
H3/15-20 m	0.104	0.105	0.001	0.8%

Mean	0.022	18.3%
Variance	0.00067	
Standard deviation	0.026	
Representativeness ($r^2 = m^2 + s^2$)	0.0011	

Table 4. Absolute and relative errors for Cu and Au grades comparing RC ROC L8 samples (Sample) with all the material recovered by the RC ROC L8 (Total)

g/t Au (ROC L8)				
Hole/Depth	Total	Sample	ABS Error	REL Error
H1/0-5 m	0.306	0.282	-0.024	-8.0%
H1/5-10 m	0.071	0.069	-0.002	-2.6%
H2/0-5 m	0.532	0.578	0.046	8.7%
H2/5-10 m	0.096	0.121	0.025	25.6%
H2/10-15 m	0.028	0.025	-0.003	-9.7%
H2/15-20 m	0.025	0.037	0.012	47.7%
H3/0-5 m	0.282	0.277	-0.005	-1.8%
H3/5-10 m	0.095	0.082	-0.013	-13.6%
H3/10-15 m	0.040	0.044	0.004	11.1%
H3/15-20 m	0.031	0.036	0.005	16.6%

Mean	0.0046	7.4%
Variance	0.00039	
Standard deviation	0.020	
Representativeness ($r^2 = m^2 + s^2$)	0.00041	

%Cu (ROC L8)				
Hole/Depth	Total	Sample	ABS Error	REL Error
H1/0-5 m	0.425	0.320	-0.105	-24.7%
H1/5-10 m	0.140	0.140	0.000	0.0%
H2/0-5 m	0.538	0.551	0.013	2.5%
H2/5-10 m	0.166	0.166	0.000	0.0%
H2/10-15 m	0.086	0.081	-0.005	-6.2%
H2/15-20 m	0.096	0.093	-0.003	-3.5%
H3/0-5 m	0.446	0.422	-0.024	-5.4%
H3/5-10 m	0.187	0.168	-0.019	-10.1%
H3/10-15 m	0.102	0.097	-0.005	-5.1%
H3/15-20 m	0.104	0.105	0.001	0.8%

Mean	-0.015	-5.2%
Variance	0.0011	
Standard deviation	0.033	
Representativeness ($r^2 = m^2 + s^2$)	0.0013	

- The earlier manual sampling procedure tends to select only the coarser particles, thereby underestimating gold and copper grades – but this trend has been masked by an overestimation tendency by the drilling rig.
- The fines discard from the manual sampling procedure is incorrect. However, its positive results were due to a particular compensation of errors that led to a completely illusory reconciliation.
- Comparing with the grades of all the material recovered by the RC ROC L8, the samples generated by its automatic sampling system do not result in any systematic errors. This new system is unbiased.
- The samples generated by the RC ROC L8 are representative with respect to both total particle size distribution and to the gold and copper grades for individual particle size fractions.
- Knowing that the reliability of the reconciliation results depends on the quality of the input data, the authors conclude that the RC ROC L8 sampling system has been validated for reconciliation purposes.

The economic impact generated by incorrect sampling procedures should never be underestimated. In this study, the intrinsic errors in the process were being masked by compensations, and may have eventually led to erroneous interpretation of the reconciliation results, from which significant ore losses and ore dilution take place. These problems are amplified when production reaches poorer or more heterogeneous regions of the deposit.

Knowing that errors are amplified for lower grades, and considering the high geological complexity of the deposit, implementation of the new automatic sampling system is the only logical solution for effective control of mining operations. The new RC drilling rig

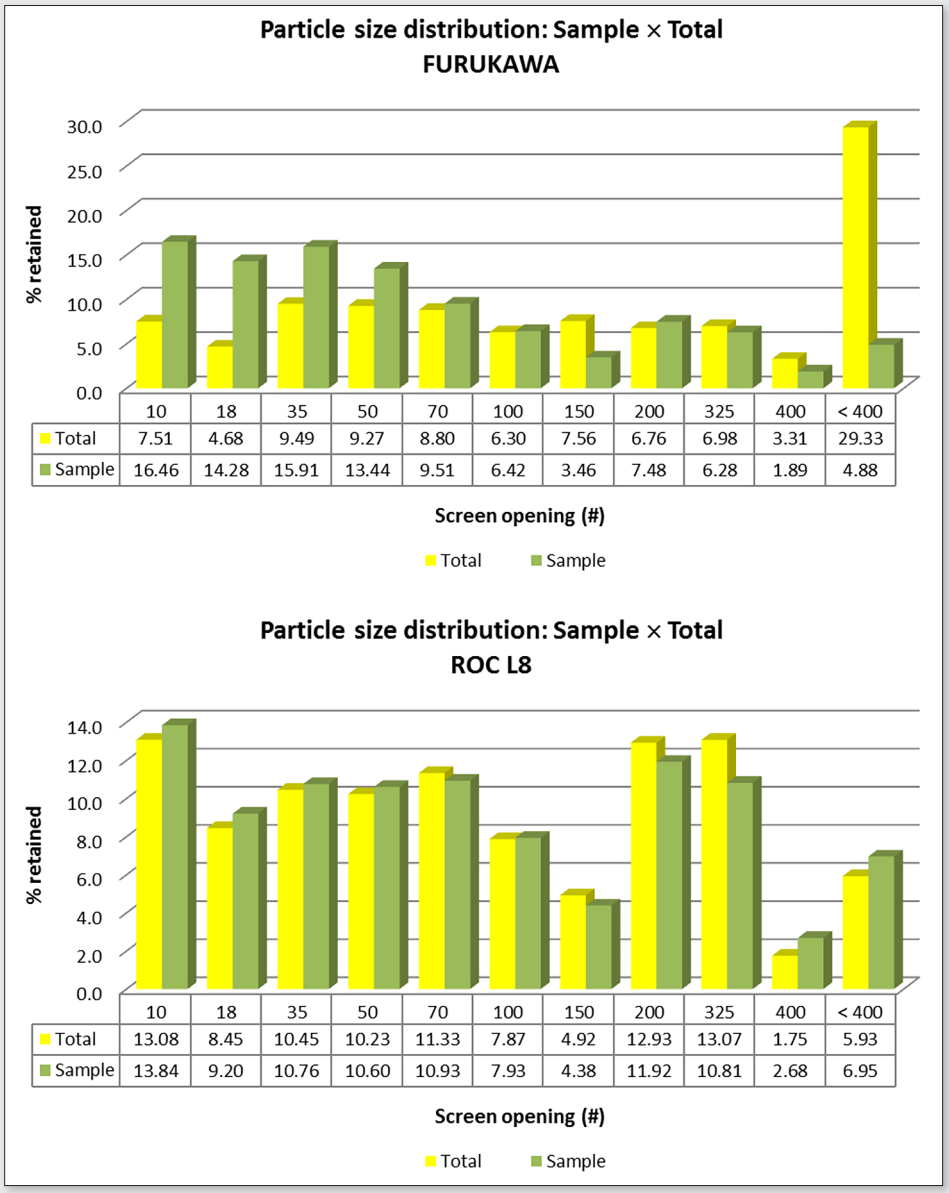

Figure 5. Particle size distributions comparing the samples with the total recovered material for Furukawa and RC ROC L8.

showed very encouraging results with respect to sample representativeness and significantly increased reconciliation reliability.

References

1. A.C. Chieregati and F.F. Pitard, "Fundamentos teóricos da amostragem", in *Teoria e prática do tratamento de minérios: manuseio de sólidos granulados*. Chaves, A.P. (Org.), Signus Ed., Sao Paulo (2011), pp. 299–338.
2. F.F. Pitard, "Blasthole sampling for grade control – the many problems and solutions", in *Proceedings of Sampling Conference*, AusIMM, Perth (2008), pp. 15–21.
3. T.M. El Hajj; A.C. Chieregati and L.E.C. Pignatari, "Illusory reconciliation – compensation of errors by manual sampling", in *Proceedings of 6th World Conference on Samplig and Blending*, Gecamin, Lima (2013), pp. 227–237.
4. T.M. El Hajj; A.C. Chieregati and L.E.C. Pignatari, "Illusory reconciliation: compensation of manual sampling errors", in *TOS Forum*, Issue 3 (2014), pp. 7–9.

doi: 10.1255/tosf.45

Determination of the precision of sampling systems and on-line analysers

Geoffrey J Lyman[a] and James Asbury[b]
[a]Materials Sampling & Consulting, 1902 / 4 Como Crescent, Southport, Queensland, Australia 4215. E-mail: glyman@iprimus.com.au
[b]Realtime Group Limited, Lot J Mackay Marina Village, Mulherin Drive, Mackay QLD 4740, PO Box 9117, Slade Point QLD 4740.
E-mail: james.asbury@rtiaustralia.com

There is a simple and relatively inexpensive way of determining the precision of sampling systems and on-line analysers when a data base of output values from the sampling system or on-line analyser can be accessed and there exists serial correlation in the data sets. For a sampling system, if it is possible to construct a variogram from the routine data collected, it is possible to extract the component of the precision estimate due to material intrinsic heterogeneity, preparation and analysis as this variance is simply given by the intercept (nugget variance) of the variogram. To determine the last component of uncertainty, a punctual variogram determined from a sampling campaign is necessary. The method is much superior to interleaved sampling, which gives incorrect estimates of the precision when serial correlation exists. It is rare to find that there is no serial correlation in plant data. For on-line analysers that interrogate a process stream continuously, the variogram constructed from the gauge output for short time intervals can be used to determine the precision with no additional effort. The gauge ideally should be operated in such a way that the output is not smoothed by some statistical procedure. This paper outlines the methods and illustrates the procedure with data sets from a coal washery.

Introduction

It is very useful to be able to determine the precision with which a sampling system operates. The ISO Standards say that this precision can be found by a process of interleaved sampling, but this statement is incorrect when the assays in the process stream from which the samples are taken show a serial correlation in time (Lyman[1]). Interleaved sampling also demands that sampling be carried out at double the rate of the routine sampling. Building this capability into a sampling system increases the system cost.

What is desired is a simple and cost-effective means of estimating sampling system precision. This can be done by taking advantage of the serial correlation in time that is present in virtually all process streams.

Similarly, it is of great importance to be able to estimate the precision of an output value from an on-line analyser which is interrogating a process stream continuously. A variogram constructed from unfiltered output from the gauge will provide the precision estimate.

This paper provides the mathematical background behind the methods of precision determination and illustrates the method using data from a coal washery.

Mathematical development

When a process stream is observed by intermittently taking increments of material from the process stream and analysing them, the assay of the increment can be modelled as the sum of a random function and a random variable. The random function describes the true value of the assays as a function of time and the random variable describes the uncertainty introduced in the determination of the assay as a result of the intrinsic heterogeneity of the increment and the sample preparation and analysis uncertainties. The relationship can be described as

$$Y(t) = X(t) + \varepsilon \tag{1}$$

where $X(t)$ is the random function describing the true value of the process stream assay at time t and ε is a uncorrelated random variable having a distribution corresponding to that of the intrinsic heterogeneity of the increment plus the distributions due to the sample preparation and analysis. The random variable is statistically independent from the random function.

The random function can be characterised by a covariance function or variogram. Consider increments taken at a set of times $\{t_i\}$ giving rise to a set of measurements $\{y(t_i)\}$. The covariance function of these measurements is then

$$\begin{aligned}\operatorname{cov}\left\{Y(t_i), Y(t_j)\right\} &= \mathrm{E}\left\{\left[X(t_i) - X_0 + \varepsilon_i - \varepsilon_0\right]\left[X(t_j) - X_0 + \varepsilon_j - \varepsilon_0\right]\right\} \\ &= \mathrm{E}\left\{\left[X(t_i) - X_0\right]\left[X(t_j) - X_0\right]\right\} + \mathrm{E}\left\{\left[\varepsilon_i - \varepsilon_0\right]\left[\varepsilon_j - \varepsilon_0\right]\right\}\end{aligned} \tag{2}$$

where X_0 and ε_0 are the expected values of the random function and random variable. Note that the cross-terms between the random function and the random variable vanish due to the independence of the two statistical quantities. Taking the expectations above, those involving the random variable are zero except when $i = j$, that is the covariance is the variance of the random function plus that of the random variable. We have

$$\operatorname{cov}\left\{Y(t_i), Y(t_i)\right\} = \operatorname{var}\left\{Y(t)\right\} = \operatorname{var}\left\{X(t)\right\} + \operatorname{var}\left\{\varepsilon\right\} \tag{3}$$

If the random function is stationary, the value above is the value of the covariance function for Y at the origin, which can be denoted as $C(0)$. The variogram or covariance function estimation will provide a picture of the rest of the function, $C(t)$ which in fact now depends only on the properties of the random function $X(t)$. The covariance function will have the form as shown in Figure 1. The corresponding variogram function is shown at the right of Figure 1.

The relationship between the (semi)variogram and the covariance function is

$$\gamma(t) = C(0) - C(t) \tag{4}$$

so the variogram starts at zero and rises to a sill value equal to the value of the covariance function at the origin.

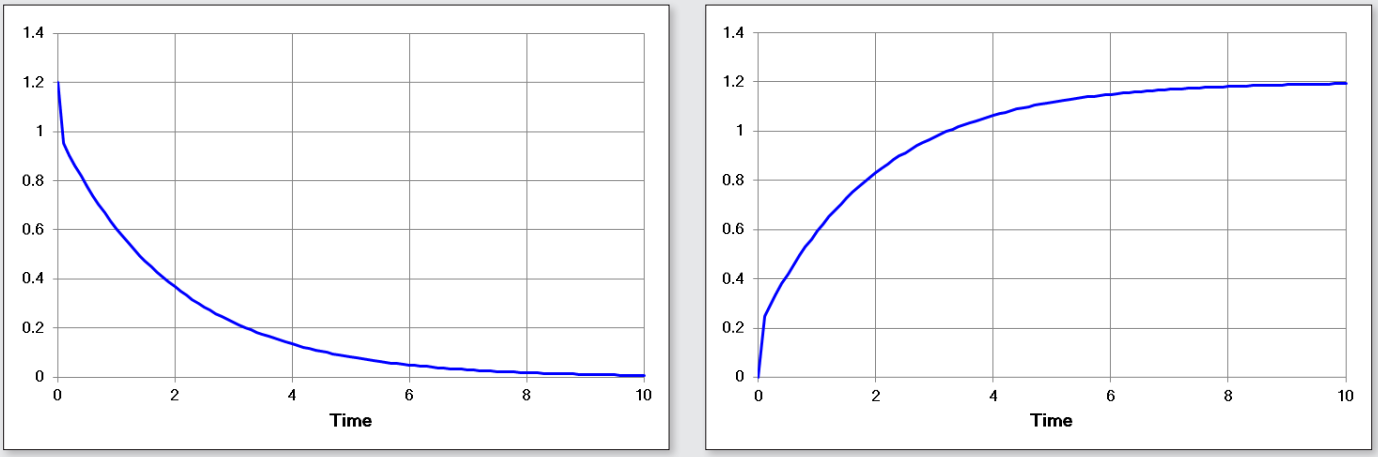

Figure 1. Covariance (left) and variogram (right) functions in the presence of measurement error.

In the operation of an on-line gauge, which may be of the nuclear type (prompt gamma neutron activation), gamma ray (transmission gauges) or x-ray fluorescence, the gauge interrogates the process stream and periodically provides an output which is an estimate of the composition of the stream with respect to one or more analytes. The output of the gauge can be modelled statistically in the same way as above, where $X(t)$ is the true analyte content averaged over some relatively short time period τ and ε is a random measurement error which is uncorrelated from one output value to the next. Some caution must be exercised here as the output from on-line gauges can involve the application of an exponentially weighted moving average process to the raw signals, or some other methodology that smoothes the output values. The use of such smoothing methods will cause serial correlation of the measurement error component of the output and well as modifying the covariance function of the component due to the changing analyte content of the stream.

The last circumstance to be considered is that in which increments are collected from a process stream over a period of time (a shift or day) and then analysed together as a whole. When values from this data stream are analysed variographically, the variogram observed is not the punctual variogram but a punctual variogram which has been regularised (a change of support having been made from single points to a set of points) over the period of sampling. This has important implications for the determination of the total sampling uncertainty as the punctual variogram is obscured.

Application to sampling of process streams

When a sampling system for a process stream is designed and the sampling is mechanically correct, there are three components of uncertainty that must be considered:

- the component due to the fact that there is a difference between the true average analysis of the increments extracted and the true average analysis of the process stream over the entire sampling period
- the component due to the intrinsic heterogeneity of the increments collected and that introduced within the sample preparation protocol
- the final analytical uncertainty

The first component is due to the distributional heterogeneity of the process stream, the second due to intrinsic heterogeneity of the material as sampled and at various stages in the sample preparation protocol and the last due to random error in the analysis procedure be it classical or instrumental.

The first component of uncertainty is determined by the shape and range of the variogram, that is by the time-wise serial correlation of the target analyte content of the stream. The second and third components are uncorrelated with the time variation and together are a measurement uncertainty. With a punctual variogram determined from the analysis of individual increments, the variogram can be extrapolated back to zero to make an estimate of the size of the jump after the origin, as in Figure 2.

The magnitude of the jump is equal to the measurement variance. This determines the sum of the last two components of uncertainty in sampling. The first component can be calculated from the shape of the variogram, providing an estimate of the total sampling uncertainty. There is a potential issue, however, with this procedure, namely that the sample preparation protocol for the individual increments may differ in a significant manner from that for the usual shift or daily sample. While the analytical variance will be the same as for the shift or daily sample (unless multiple assays are routinely carried out and only single assays applied to the individual increment), the second variance component due to the intrinsic heterogeneity of the material sampled may not match that involved in the preparation of the daily sample due to differences in the protocol.

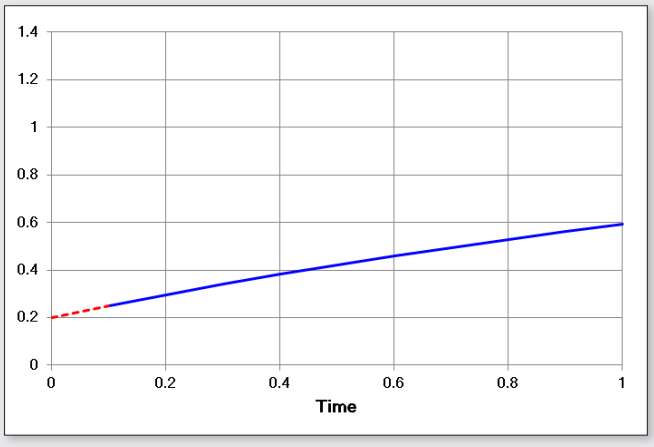

Figure 2. Backward extrapolation of a variogram to estimate the measurement variance.

When dealing with relatively small data sets, as is common when a special sampling program has been carried out, estimation of the value of the variogram and intercept can be made by maximum likelihood methods (Lyman[2]) which are very effective especially when the increments have not been extracted on a strictly constant time base. In such a case, the variance of the estimate of the measurements variance can be calculated as well.

When dealing with a variogram estimated from shift or daily samples, it is still possible to find a variogram and fit or extrapolate to find a measurement variance. However, this variogram cannot be used to find the sampling variance due to distributional heterogeneity as the compositing of the increments taken into a single sample has obscured the original punctual variogram. In particular, the sill of the variogram found will be lower than that for the punctual variogram and the range of the variogram will be longer as a result of the averaging process. It is not possible to work backwards to find a unique variogram that, when regularised using the actual sampling pattern, will match the observed variogram. There are many possible punctual variograms that will match the observed variogram after regularisation. But the intercept of this variogram is equal to the variance due to sample preparation and analysis for the protocol used routinely. This variance can be combined with the variance due to distributional heterogeneity determined from the punctual variogram to arrive at the correct estimate of the sampling system precision.

Therefore the analysis of the data set for shift or daily samples can be combined with the punctual variogram to provide the correct answer for the total sampling variance.

Note that it is an estimation of precision that is made, not an estimation of accuracy; bias cannot be detected in this way.

Application to on-line analysers

If the output from the on-line analyser has not been interfered with by averaging methods, the precision of the analyser on a punctual basis can be estimated. Note again that it is precision that is being estimated, not accuracy.

The current practice in the estimation of the precision of on-line analysers usually rests with the use of the Grubbs estimator (Lyman *et al.*[3]), which requires the use of two reference measurements in addition to the data from the gauge. It is necessary to coordinate the recording of signals from the gauge and the collection of physical samples of the material analysed in two independent ways in order to put this method into place. It is also desirable to ensure that the precision of the two reference measurements are better than that of the gauge; this can be difficult, given sampling problems.

By contrast the variogram approach for estimating analyser precision requires no additional effort. The estimate is derived directly from the gauge output. It is therefore very inexpensive and effective. On-line analysers produce a large volume of data as they generally produce an output value at any desired interval. A largest source of measurement variance may be the counting statistics for nucleonic systems, which ensures that the component of measurement error is independent from one reading to the next.

As for sampling, the estimate of measurement variance involves only the estimation of a variogram with backward extrapolation to the origin to find the intercept. With the large data sets from on-line analysers, the maximum likelihood method of variogram estimation is not practical.

Example

This example is drawn from data collected both from an on-line analyser and a conventional sampling system producing assays about every 6 hours. The operation of the conventional sampling system is somewhat erratic. The washery in question treats a number of types of coal with widely varying ash content. The on-line analyser interrogates all these feed coals on the same belt.

The conventional sampling system data was analysed on a per coal type basis in order to pick up the serial correlation for those coal streams. Figure 3 shows the data for coal type A as a function of tonnes of coal sampled.

The upper trace in Figure 3 is the actual coal ash content as sampled and the solid dark line is the trend line through the data determined by locally weighted regression. The lower trace is the deviation from this trend line. De-trending of the data is mandatory before calculating a variogram as this method can be applied only to stationary data. It is also desirable to apply the method to data that follows a Gaussian distribution as all theory and tools attached to variogram estimation assumes normality of the data. Figure 4 shows the deviation data after having been transformed to z-scores (standard Gaussian deviates of zero mean and unit variance). The

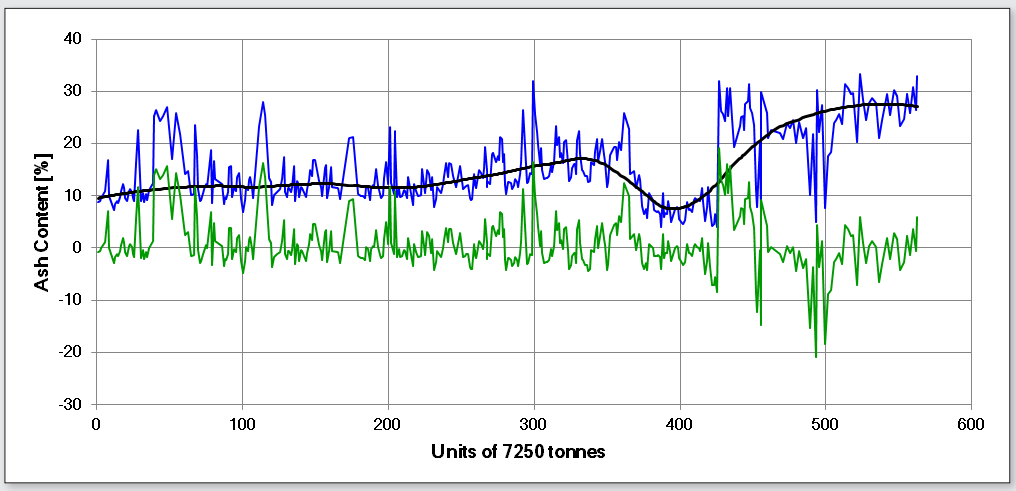

Figure 3. Ash content of coal type A as a function of tonnes of coal sampled. Lower curve shows deviations from trend (black).

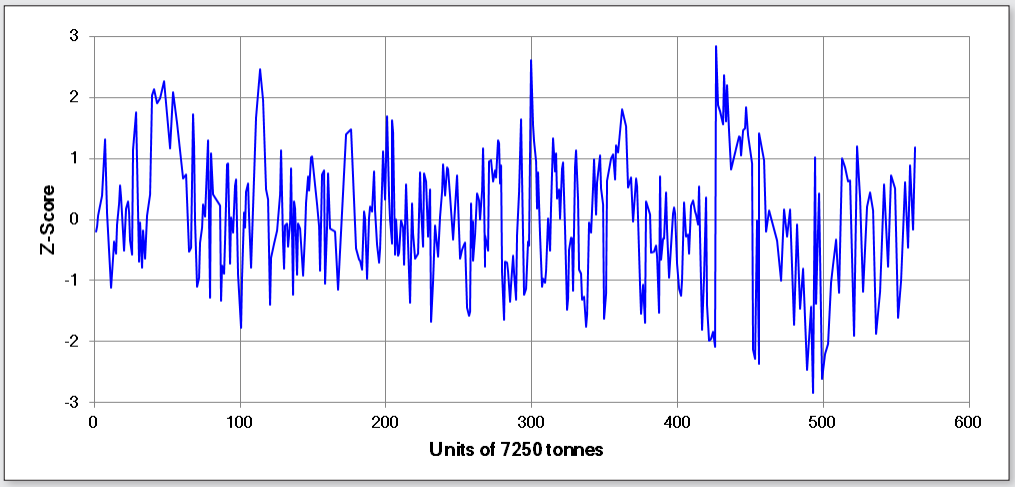

Figure 4. Z-scores for the deviation data of Figure 3.

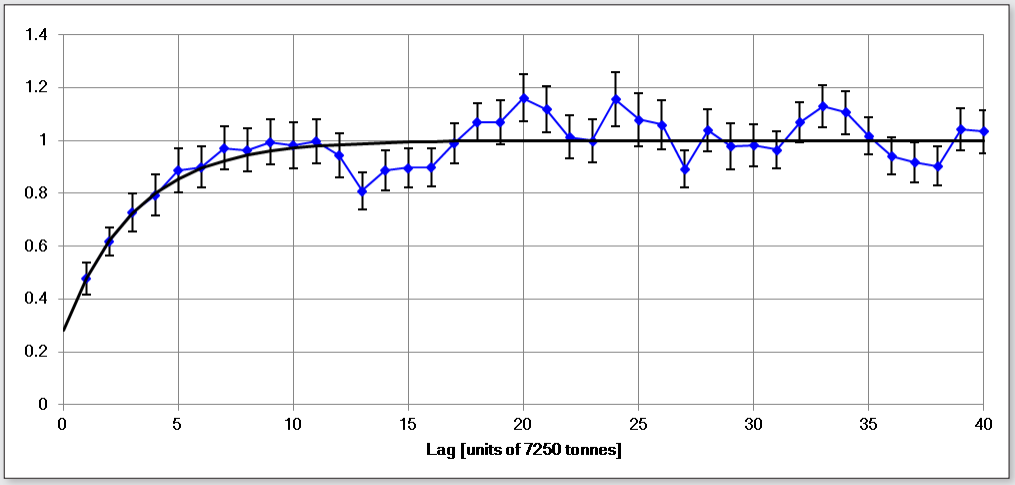

Figure 5. Variogram for coal A as sampled using z-score values, with a fitted exponential variogram. The intercept value is 0.284 from the fit.

variogram is calculated using this transformed data using the conventional Matheron estimator. Note that the variogram is based on actual assay results rather than a measure of heterogeneity as is often done when following Gy's methodology. The interest here is in the assay uncertainty and not a measure of heterogeneity. The error bars on the variogram represent a ±1 SD interval for the variogram estimate at the given lag. The variogram derived from the data of Figure 4 is shown in Figure 5.

The intercept of the z-score variogram can be found either using the first two points on the variogram or by fitting an admissible variogram function to the data. The intercept value is rescaled using the variance of the untransformed deviation data about their mean. Dividing the square root of the scaled intercept value by the mean ash content of the un-detrended data then provides a relative standard deviation for the measurement uncertainty. In this case the RSD is 17.2% ash. This indicates that there are serious problems with the sampling system or the manner in which the sample is prepared and analysed.

The corresponding data for coals B and C are shown in Figures 6 and 7. The RSD for coal B is 14.3% and for coal C 16.0%. The consistency of the estimates of the RSD underlines their validity, given that they are passing through the same sampling system. The ranges of the variograms are similar for coals A and B; that for coal C is longer. However, the last data set is relatively small and the variogram less well-defined.

The analysis of the gauge precision is based on one month of outputs at two minute intervals. The gauge is a prompt gamma neutron activation type (Realtime Group Allscan gauge).

The data for low ash coal is shown in Figure 8; there are just over 7000 data points in the data set. The z-score variogram is shown in Figure 9. The right hand frame shows a closer view of the behaviour of the variogram near the origin. The SD of a two minute reading is 2.12% ash or 23.7% relative.

The corresponding data for high ash coal is shown in Figure 10 with the z-score variogram in Figure 11. The SD of a two-minute reading is 3.04% ash or 12.0% relative.

It is interesting to consider the gauge measurement uncertainty over a period longer than 2 minutes. Because the gauge is measuring continuously, there is no uncertainty due to distributional heterogeneity such as would arise if punctual increments were

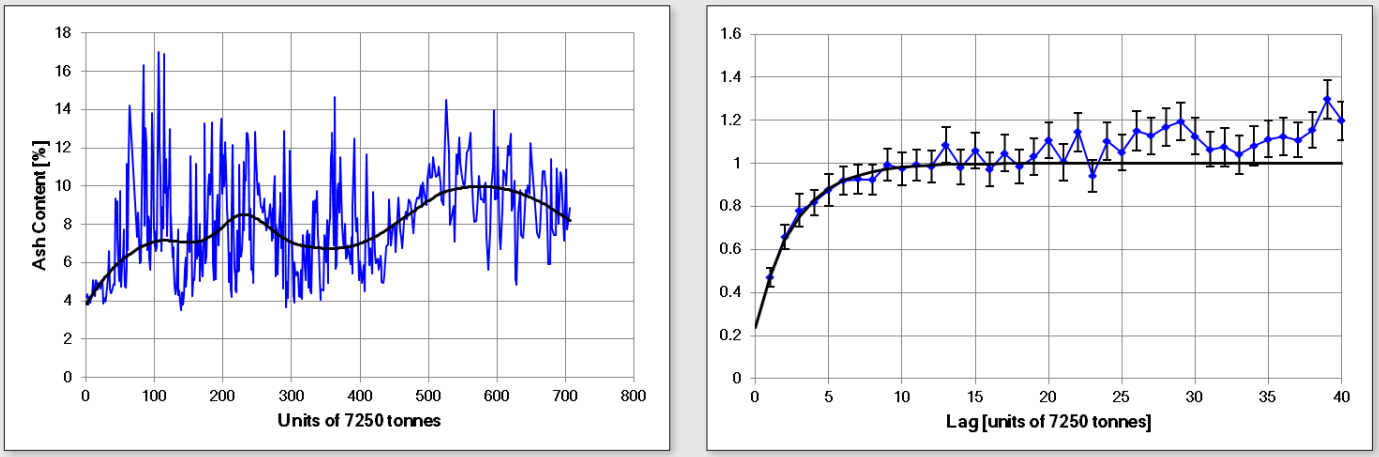

Figure 6. Data, detrending and z-score variogram for coal B.

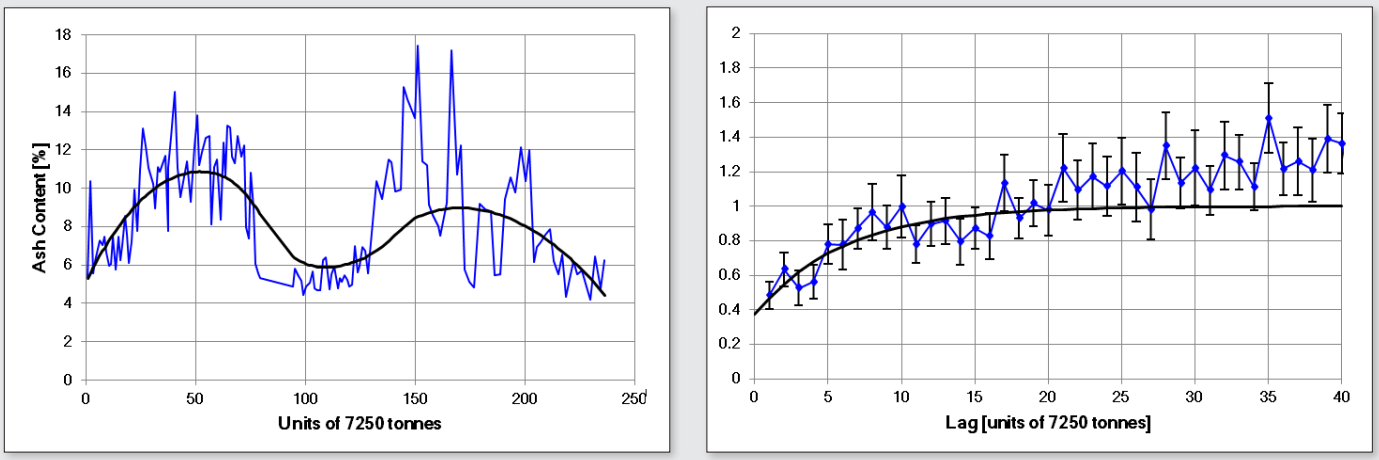

Figure 7. Data, detrending and z-score variogram for coal C.

being taken as in conventional sampling (the gauge misses nothing). Consequently, the measurement variance is simply inversely proportional to the number of two minute readings that are averaged. For a 6 hour period, there are 180 readings so the RSDs are reduced to 1.77% (SD = 0.158% ash) for the low ash coal and 0.894% (SD = 0.227% ash) for the high ash coal. As long as there is no bias in the gauging system, the gauge accuracy over a 6 hour period is extremely good. Over a daily period, the figures above

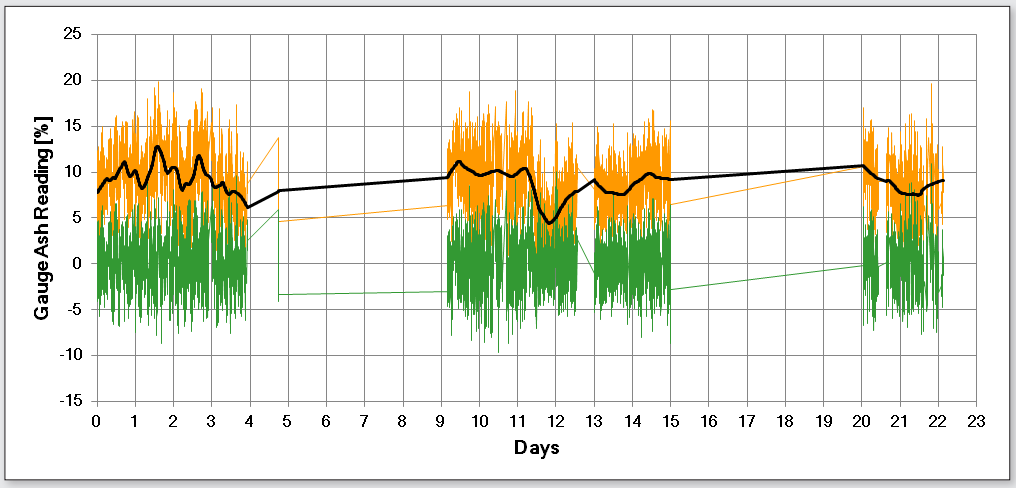

Figure 8. On-line analyser data for low ash coal (yellow) showing de-trending (black) and deviation values from the trend (green).

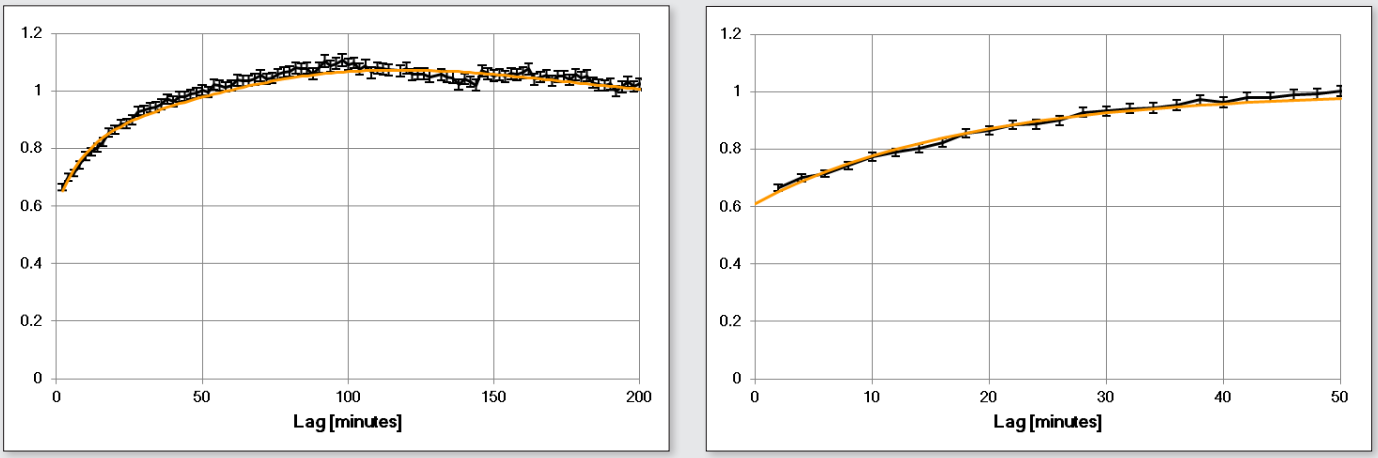

Figure 9. Variogram for low ash coal derived from on-line analyser z-score data. The right hand frame shows a closer view of the behaviour of the variogram near the origin.

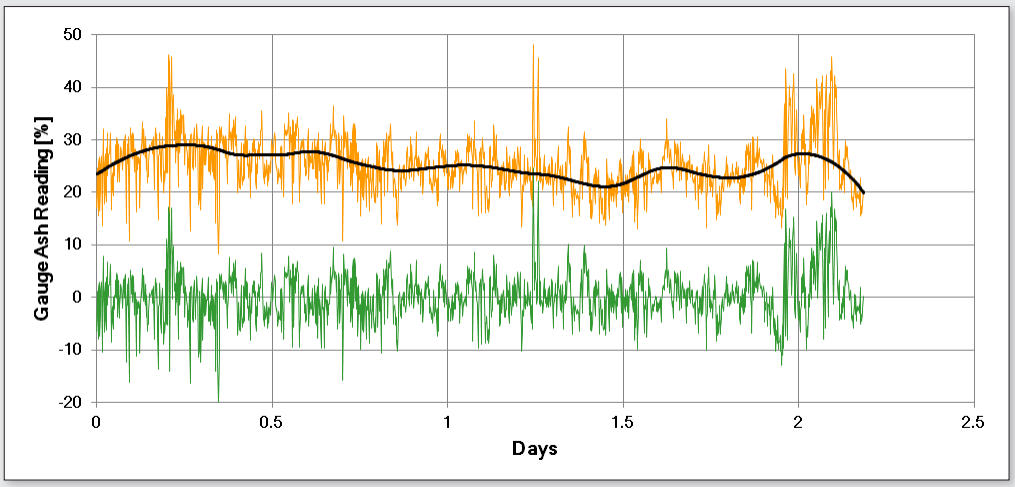

Figure 10. On-line analyser data for high ash coal showing de-trending and deviation values from the trend.

are reduced by half to deliver standard deviations of 0.076% ash and 0.114% ash respectively. These figures can be compared to the standard deviations of a single ash determination by Australian Standard 1038 of 0.05% ash and 0.085% ash.

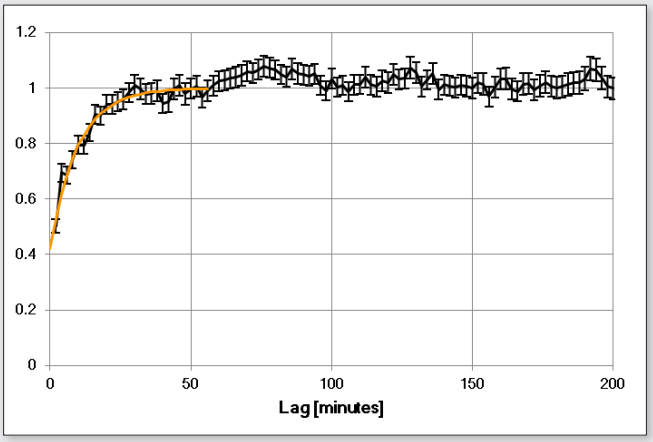

Figure 11. Variogram for high ash coal derived from on-line analyser z-score data.

By comparison, as long as the gauge is bias free (and the sampling system as well), the sampling system performance leaves a great deal to be desired.

This example points up the problems of attempting to calibrate an on-line gauge for coal ash and coal ash constituents against routine samples taken over the measurement period. To be of value in this setting, the sampling system must be unbiased and very precise. Conventional sampling systems rarely deliver this accuracy, so calibration against such sampling systems is impractical. A gauge manufacturer must offer a robust factory calibration procedure and this must be accepted by the buyer.

Conclusions

The determination of the precision of a sampling system requires that the punctual variogram for the process stream be known with some accuracy and that the variance due to the intrinsic heterogeneity of the primary increments as well as the variance added during sample preparation and analysis be known. The latter measurement uncertainty can be determined from analysis of a variogram based on consecutive samples (not increments) taken by the sampling system. With both these sources of information, the total sampling variance can be calculated.

The precision of an on-line analyser can be determined from a variographic analysis of the gauge output, as long as the gauge has not been set up to smooth the output by some statistical procedure such as a moving average. The unadulterated output on a small time interval must be available for construction of the variogram. The precision of the gauge over longer measurement time intervals is not affected by the time variation of the analyte content in the process stream because the gauge 'sees' all of the stream all of the time; there is no error due to distributional heterogeneity. Therefore the precision over longer time intervals can be determined by the classical formula for the standard deviation of the mean of independent quantities. If there are N measurements in the gauging period, the final precision is simply $1/\sqrt{N}$ times the precision determined from the variogram.

References

1. G. J. Lyman, "Estimation of sampling variance and quality variance about the mean by interleaved sampling", Proceedings of the 5th World Conference on Sampling & Blending, Santiago, Chile, Gecamin, 2011, pp 175-184
2. G. J. Lyman, "Variograms: properties and estimation", Proceedings of the 6th World Conference on Sampling & Blending, Lima, Peru, Gecamin, 2013, pp 185-206
3. G. J. Lyman, F. Lombard, D. Edward, and C.J. Clarkson, "Determination of the precision of on-line coal analysers – Theory and practice", Proceedings of the 7th Australian Coal Preparation Conference, J. Smitham (ed), Australian Coal Preparation Society, 1995, pp 324-355.

doi: 10.1255/tosf.57

Sample station design and operation

Ralph J Holmes
CSIRO Mineral Resources Flagship, Private Mailbag 10, Clayton South, Victoria 3169, Australia. E-mail: ralph.holmes@csiro.au

Accurate sampling practices in the mineral industry are critical for determining the chemical, mineralogical and physical characteristics of ores and mineral products for resource evaluation and utilisation, feasibility studies, process design and optimisation, quality control, metallurgical accounting, and ultimately commercial sales. Sampling is the first step in the measurement chain and is where the measurement process all begins, so if the sample that is collected is not representative, then the whole measurement chain is compromised at the outset. However, frequently the responsibility for sampling is entrusted to personnel who do not fully appreciate the significance and importance of collecting representative samples for analysis, and quite often everyone seems satisfied as long as some material is collected and returned to the laboratory for analysis. In the case of sample stations, cost is often the main consideration rather than sampling correctness (unbiasedness), which is unacceptable and needs to change. It is important that sampling experts are involved in the design stage at the outset to avoid structural design flaws and the subsequent need for expensive retrofits to address major and sometimes even fatal problems. Furthermore, ongoing audits of performance need to be conducted to ensure sample stations are adequately maintained and continue to conform to correct sampling principles. Provision also needs to be made for duplicate sampling to monitor the precision achieved in practice on an ongoing basis for quality assurance purposes. The examples used and commented upon here relate to one of the more difficult industry sectors with respect to correct sampling practices, material and constituent type (e.g. ores, concentrates and mineral aggregates), tonnages, process stream flow rates, and wear and tear, and as such provides the ideal showcase for the intended message which applies essentially to all technologies and industries.

Introduction

Samples are taken from many different locations in the mineral industry for optimising resource utilisation, process and grade control, metallurgical accounting and ultimately commercial transactions[1,2]. These locations include diamond and percussion drill holes, blast holes, feed and product streams, conveyor belts, trucks, railway wagons and stockpiles, a number of which present major, if not impossible, problems in extracting representative samples, e.g. in-situ sampling from a large stockpile. Notwithstanding this, it is surprising how frequently sampling is left to personnel who do not understand its critical importance in providing representative samples for analysis, and quite often everyone is happy as long as just *some* material is collected and sent back to the laboratory for analysis. This approach is totally wrong and completely unacceptable. Representative samples are essential to obtaining meaningful analyses that can be relied upon to make correct resource and quality control decisions and ensure equitable payment for the sale of mineral commodities. Sampling is where the measurement chain begins and the whole measurement process is corrupted at the outset if all samples are not representative. Furthermore, accurate analysis of non-representative samples submitted to the laboratory can very often be a waste of time, leading to reduced mine life, poor recovery in processing plans, and loss of sales revenue. It is therefore critical to ensure that the samples collected are free of significant bias and that the overall precision of the final analyses is appropriate for the required task, both of which are important in the design and operation of sample stations, which is the focus of this paper.

The "golden rule" for correct sampling is that "all parts of the material being sampled must have an equal probability of being collected and becoming part of the final sample for analysis", i.e. the Fundamental Sampling Principle (FSP in the Theory of Sampling).[1-7] If this golden rule is respected at the outset, then extraction of representative samples is largely assured. Otherwise, a sampling bias is easily introduced, which is particularly serious because no amount of replicate sampling and analysis is able to reduce bias once it is present, far less eliminate it[1]. There is no point in being "precisely" incorrect. As pointed out by Gy[4], the sources of bias that can be eliminated include incorrect delimitation of sample "increments" (i.e. incorrect cutter geometry), incomplete extraction of sample increments, preferential exclusion of specific size fractions, sample loss and sample contamination, while other errors due to the fundamental, grouping, segregation, long-range quality fluctuation, periodic quality fluctuation and weighting errors can never be totally eliminated, but they can be minimised or at the very least reduced to acceptable levels. Unfortunately, many of these requirements are frequently ignored in the design of sample stations to reduce capital costs, which is a dangerous false economy because the samples taken are likely to be seriously biased, the precision may be compromised, and the subsequent cost of retrofitting a correct sampling system can be large. The design of subsequent sampling stages is also very important, particularly in terms of the relationship between particle size and the sample mass that needs to be retained to achieve acceptable precision.

Sample station design

While samples are taken from many locations in mineral processing plants, by far the best method is to sample a moving stream at the discharge point at the end of a conveyor belt or at the end of a slurry pipe.[1-3, 8, 9] Here the process stream can be intersected at random or regular times or tonnages, and sample "increments" can be collected by taking a full cross-section of the stream with a sample cutter such as shown in Figure 1, and subsequently combining them into representative composite samples for specified time periods or tonnages of material passing through the processing plant. This is guaranteed to satisfy the Fundamental Sampling Principle. Having satisfied this requirement, the sample mass collected then needs to be large enough taking into account the particle size of the

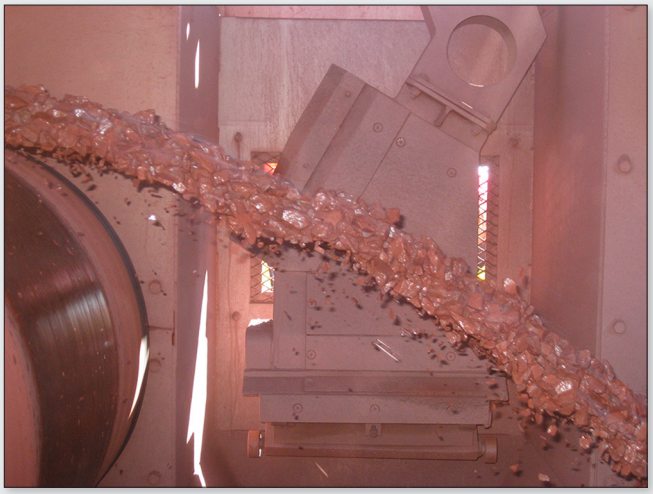

Figure 1. Cross-stream sample cutter (background) designed for taking a full cross-section of an ore stream at the discharge point of a conveyor belt.

Figure 3. Manual sampling from the top of a conveyor belt most emphatically does not sample the complete ore stream and raises serious safety concerns.

material being sampled to reduce the fundamental, grouping and segregation errors to acceptable levels and sufficient increments need to be taken to reduce the long-range quality fluctuation error to an acceptable level. In addition, the sampling location should be selected to avoid the presence of periodic variations in quality due to equipment such a bucket wheel reclaimers and centrifugal pumps. Clearly, accessory errors[4] such as sample contamination, sample spillage, particle degradation and operator mistakes also need to be eliminated at the outset. An example of such an error is shown in Figure 2, where the sample mass collected exceeded the minimum mass requirement by a large margin, and, instead of using a rotary sample divider or a riffle to reduce the sample mass, the operator simply tipped out part of the sample on the ground. Such practices are clearly unacceptable in the context of representative sampling, but it does indicate the need to design the sampling regime to generate samples of manageable mass for operators and provide lifting aids if required.

Figure 2. Accessory error caused by an operator tipping out part of a sample on the ground instead of using a rotary sample divider or a riffle to reduce its mass. The supervisor is not doing his/her job.

In contrast to full cross-stream sampling, examples of poor plant sampling practices include *scooping* material from the surface of a conveyor belt (see Figure 3), intercepting only part of a falling ore stream (see Figure 4), taking cuts from a fixed location within a launder or extracting slurry from a fixed position within a pipe as shown in Figure 5. Segregation occurs both vertically and horizontally across a conveyor belt due to the action of the idlers and the manner in which the material is fed onto the conveyor, and particles suspended in a slurry segregate under the effects of gravity and centrifugal forces. Consequently, partial stream cuts or extracting only part of the stream are structurally unable to provide representative samples. In Figure 4, the primary cutter is pivoted on the side of the head chute. Consequently, when the cutter is rotated into the ore stream, it does not traverse the complete ore stream and hence increments are extracted from only part of the falling stream, which is clearly incorrect.

Focussing on sampling at the discharge point of a conveyor belt or chute where the complete stream can be intersected with comparable ease at regular intervals, an important consideration is the design of the sample cutter, which must satisfy a number of requirements to eliminate both increment delimitation and extraction errors.[4]

Figure 4. Example of a poorly designed sample cutter that does not traverse the full ore stream.

Figure 5. Pressure pipe samplers do not extract a full cross-section of the slurry stream so the samples collected can never be representative.

Figure 7. Vezin cutter aperture that is no longer radial due to poor maintenance.

Correct increment delimitation

One of most important requirements for correct *increment delimitation* is that the sample cutter must take a complete cross-section of the process stream with both the leading and trailing edges of the cutter completely clearing the stream at the end of each traverse. Furthermore, the length of the cutter aperture must be large enough to intercept all the material in the stream, including particles that bounce off the inside edges of the cutter aperture in the direction of its long axis.

The cutter aperture must also be designed so that the cutting time at each point in the stream is equal. To achieve this, the cutter lips must be parallel for linear-path cutters, while the cutter lips must be radial for cutters travelling in an arc such as "Arcual" and "Vezin" cutters, where Arcual cutters rotate about their axis back and forth through the stream being sampled with the leading and trailing edges of the cutter completely clearing the stream at the end of each traverse while Vezin cutters rotate continuously in the one direction only. A correctly designed Vezin cutter with radial cutter lips is shown in Figure 6, while the original correct design of the Vezin cutter shown in Figure 7 has been compromised through poor maintenance practices, i.e. the cutter lips closer to the axis of rotation are no longer radial. An alternative radial cutter design that is also acceptable is the "rotating tube sampler", which consists of a tubular distributor rotating around a vertical axis that feeds the material being sampled across a stationary radial cutter aperture as shown in Figure 8. In contrast, flap or diverter type cutters that divert one side of the stream for a longer period of time than the other do not satisfy the requirement that the cutting time at each point in the stream is equal and hence are also structurally unable to provide representative samples.

A further requirement is that the cutter must travel through the stream at a uniform speed, accelerating up to its cutting speed before entering the stream and decelerating to a stop only after

Figure 6. Example of a correctly designed radial Vezin cutter aperture just before interacting with the vertical falling stream of ore.

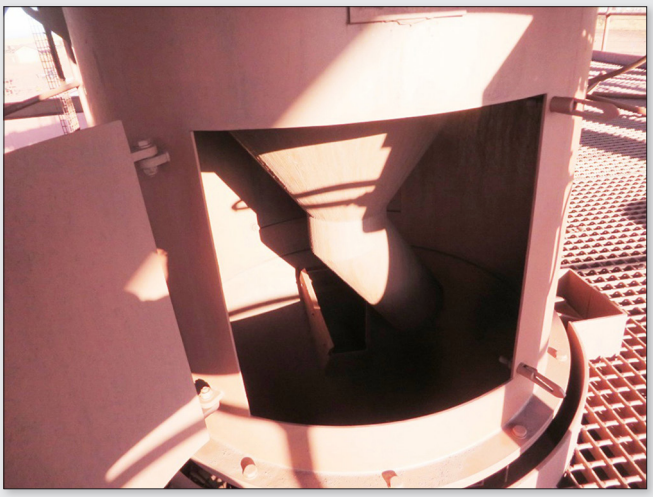

Figure 8. Example of a rotating tube sampler.

Figure 9. Belt scraper on a head pulley. The primary cutter needs to be moved closer to the head pulley or the cutter aperture extended to intersect all the belt scrapings.

Figure 10. Massive reflux from a poorly designed primary cutter aperture at high flow rates.

leaving the stream cross-section, thereby ensuring that the cutting time at each point in the ore stream is equal. Consequently, the cutter drive must have sufficient power to ensure that the cutter does not slow down as it enters the stream and/or speed up as it leaves the stream. Electric cutter drives are best for ensuring uniform cutter speed, although hydraulic drives can also be satisfactory provided they are well maintained. Pneumatic drives are not recommended, because gas is compressible and hence it is usually impossible to adequately control the cutter speed.

If a belt scraper is required to remove material adhering to the belt, the scraped material must fall within the area traversed by the cutter, although in many instances the amount of material removed by belt scrapers is negligible, particularly for dry materials. A belt scraper installed on the head pulley in an iron ore sample station is shown in Figure 9. In this case the belt scrapings are quite significant and the primary cutter needs to be moved closer to the head pulley or alternatively the length of the cutter aperture extended to intersect all the belt scrapings.

Correct increment extraction

A key requirement for correct *increment extraction* is that the sample cutter must be non-restrictive and self-clearing, discharging completely each increment without any reflux, overflow or hang-up in the cutter aperture. This is particularly important for so-called "reverse spoon" type cutters, where the material being sampled has to change direction as it strikes the back of the cutter body, which can cause sample reflux at high flow rates if the cutter does not have sufficient capacity. Furthermore, fine material that is damp has a tendency to hang-up in the cutter aperture, resulting in blockages and subsequent sample reflux. A bad case of sample reflux from a primary cutter in an iron ore sample station is shown in Figure 10. This problem can be overcome by incorporating generously large cutter bodies and chutes in the sample station design as well as setting the angle of the back of the cutter to deflect material down and away from the incoming stream (see Figure 11), thereby avoiding sample reflux and overflow from the cutter aperture. It should be noted, however, that the material removed by the belt scraper in Figure 11 is not sampled by the cutter in this case, so there is still room for improvement in this particular design. For sticky materials, steep chute angles (>60°) and stainless steel or polythene chute linings are generally used to reduce adhesion, and the cutter aperture is often increased above the minimum to prevent bridging of the aperture.

An additional important requirement is that the cutter aperture must be at least 3 times the nominal top size (d) of the material being sampled, i.e. 3d, to prevent preferential loss of the larger particles, subject to a minimum of 10 mm for fine dry solids[4]. However, the cutter aperture is often significantly increased above this minimum to make absolutely sure that no large particles are excluded from the sample. In addition, the cutter should intersect the stream either in a plane normal to, or along an arc normal to, the mean trajectory of the stream to reduce the distance that particles bounce along the length of the cutter aperture after striking the inside edge of the cutter lips and consequently need to be collected as part of the sample. Notwithstanding this, the plane of the cutter aperture must not be vertical or near vertical, because particles that strike the inside edge of the cutter aperture and which should therefore end up in the sample are deflected downwards and away from the

Figure 11. Cross-stream cutter with a large cutter body to eliminate sample reflux at high flow rates.

cutter aperture by gravity into the reject stream, resulting in sample loss[1,2,6].

The cutter speed is also an important consideration and according to Gy[4] must not exceed 0.6 m/s unless the cutter aperture exceeds 3d, because the "effective" cutter aperture decreases as the cutter speed increases, leading to the preferential exclusion of the coarser particles and hence the introduction of bias. However, Gy and Marin[10] showed experimentally on a sample of calcined bauxite at low flow rates that when the cutter aperture (w) is increased above the minimum cutter aperture w_0 (i.e. 3d or 10 mm, whichever is the greater), the maximum cutter speed (v_c) could be increased as follows, subject to an absolute maximum of 1.2 m/s:

$$v_c = 0.3\,(1 + \frac{w}{w_0}) \quad (1)$$

Notwithstanding the above relationship, the maximum cutter speed is usually limited to 0.6 m/s in the design of sample stations to allow for the high ore flow rates now routinely encountered and provide a reasonable safety margin.

Recently a few criticisms have appeared in the literature, and at World Sampling and Blending conferences, that the above cutter speed stipulations developed by Gy[4] may not always apply as the variety and type of materials sampled around the world increases. Needless to say there may be exceptions for some materials and flow regimes, but the above cutter speed guidelines are designed to provide a safe approach to sample station design for the majority of materials and applications.

While cutter-chute type sample cutters need to be designed to be non-restrictive and self-clearing, bucket-type cutters must have sufficient capacity to accommodate the entire increment mass extracted at the maximum flow rate of the stream without any reflux or overflow of sample from the cutter aperture. In addition, care needs to be taken to ensure that the gate on the bottom of the cutter bucket does not jam in the open position while traversing the stream or in the closed position when parked, and that no sample is lost from the bucket during each traverse. An example of a poorly designed and maintained bucket-type cutter used for secondary sampling in shown in Figure 12. The gap between the gate and the bottom of the cutter is much too large and part of the sample collected is lost while traversing the stream.

Figure 12. Poorly designed and maintained secondary cross-stream bucket cutter resulting in sample loss during its traverse.

The final design requirement for sample cutters is that no materials other than the sample must be introduced into the cutter or the sample delivery chute, and there must be no loss of sample from the sample delivery chute(s) or change in quality of the sample. If necessary, the sample cutter needs to be covered in the parked position between increments to prevent ingress of dust or spillage from within the sample station. Furthermore, possible sample loss due to the action of wind and air currents in sample stations needs to be eliminated by sealing and/or covering feeders, crushers, sample transfer conveyors and chutes, particularly when fine particles are being sampled, and any holes in chutes need to be rectified without delay to eliminate sample loss.

Cross-belt cutters

The sample cutters discussed so far have been cross-stream cutters where the cutter passes through a falling stream at the discharge point of a conveyor belt, chute or pipe. Provided suitable access is provided, it is reasonably straightforward to visually check that the cutter intercepts the complete stream and that increment delimitation and extraction are correct, thereby providing confidence that the samples collected are representative.

On the other hand, cross-belt cutters that take samples directly off conveyor belts are also used in the mineral industry. However, it is virtually impossible to check visually whether cross-belt cutters are operating correctly and remove a complete and correctly delimited cross-section of material from the conveyor belt. Consequently, while they may be less expensive to install than cross-stream cutters, cross-belt cutters have major deficiencies and are not recommended for the following reasons, particularly for high capacity streams:

- Cross-belt cutters tend to leave a layer of material on the conveyor belt if the profile of the conveyor belt is not matched to the path of the tip of the cutter or the skirts at the bottom of the cutter are not correctly adjusted as they gradually wear out. Furthermore, the wear of the skirts may not be uniform, resulting in gaps between the tip of the cutter and the conveyor belt, and maintenance staff often deliberately increase the gap between the cutter skirts and the conveyor for fear of damaging the conveyor belt. In each case the increment extraction is incorrect. Consequently, cross-belt cutters can be seriously biased, because the material on the bottom of the belt can be different in grade from the bulk of the material on the conveyor belt.
- As already pointed out above, it is virtually impossible to check visually whether a cross-belt cutter is performing correctly in terms of correct increment delimitation and increment extraction.

A typical example of a cross-belt cutter installation is shown in Figure 13. For safety reasons the cutter is fully enclosed, so it is impossible to visually check its operation. Figure 14 shows an ore stream after taking a cross-belt sample cut using a similar cutter to that in Figure 13, which indicates that almost certainly the cutter did not remove a full cross-section of ore from the conveyor belt, while Figure 15 is a photograph of an actual cross-belt cutter showing the poor condition of the rubber skirt on the bottom of the cutter. The sample cut shown in Figure 14 is clearly unsatisfactory. Cross-stream cutters must therefore be recommended in preference to cross-belt cutters to be sure of obtaining representative samples.

Figure 13. Typical fully enclosed cross-belt sampler installation. While 'hidden' from view, the very poor sampling performance with respect to extraction of a complete cross-section of the stream remains.

Figure 14. Sample cut taken by a cross-belt sampler indicating that a full cross-section of ore was not removed from the conveyor belt.

Figure 15. Poor condition of the rubber skirt on the bottom of a cross-belt cutter.

Increment mass

Returning to cross-stream cutters, the increment mass m_I (kg) collected by such cutters is determined by the cutter aperture A (m), the cutter speed v_c (m/s), and the flow rate of the stream G (tonnes/hr) as follows:[8,11]

$$m_I = \frac{GA}{3.6\, v_c} \qquad (2)$$

Consequently, for a given flow rate, the smallest increment mass that can be taken and conform to correct sampling principles is determined by the minimum cutter aperture (3d) and the maximum cutter speed (usually limited to 0.6 m/s). While increments of larger mass can be taken using a larger cutter aperture and/or a lower cutter speed, it is not possible to take unbiased increments of smaller mass unless the flow rate is reduced or the material being sampled in crushed prior to sampling so that the cutter aperture can be safely reduced. Sample stations therefore need to be designed taking into account these important requirements. Contrary to what may be found in a number of old national and international sampling standards, there is no absolute minimum increment mass for a given particle size, just the correct increment mass determined by the flow rate, cutter aperture and cutter speed.

The "extraction ratio" is a very useful parameter for checking the design and operation of sample cutters,[12] ie, the ratio of the actual increment mass collected to the calculated increment mass using equation (2). If this ratio is significantly less than one, then the cause needs to be identified and corrective action taken to rectify the problem. Possible problems include reflux from the cutter aperture, hang-up in the cutter chute due to capacity problems or blockages in the cutter chute. The extraction ratio should be determined as a function of flow rate, because problems with reflux and hang-up in cutters become more serious as the flow rate increases.

Minimum sample mass

In contrast to increment mass, there is a minimum sample mass that needs to be extracted and retained for a given particle size to control the fundamental error variance[4], which is determined by the particulate nature of the material being sampled, in particular the variation in quality between individual particles. Clearly, the fundamental error variance can be progressively reduced by including more and more particles in the sample that is collected, i.e. by increasing the sample mass. This is a very important sampling requirement, *which applies and needs to be checked at every stage of the sampling flowsheet,* i.e. at the primary, secondary, tertiary and if necessary quaternary stages of sampling, to ensure that the total sample mass collected at each stage meets the minimum requirement for the particle size at that stage.

However, unfortunately the minimum sample mass requirements are often ignored in the design of sample stations to reduce the masses that sampling personnel need to carry back to the sample preparation laboratory. While this might be desirable from the occupational health and safety perspective, it will seriously compromise the integrity of the sample. The correct approach is to crush the sample to a smaller particle size, thereby enabling the sample mass to be reduced by correct sample division (sub-sampling). An alternative is to provide mechanical lifting aids for sampling personnel to avoid the appalling situation shown earlier in Figure 2 where part of the sample is tipped out on the ground before taking the remaining sample material back to the laboratory for analysis.

There are several ways of determining the minimum sample mass that needs to be retained for a given particle size. One approach is to experimentally determine the precision by analysing replicate samples for a range of sample masses and particle sizes.[11] The relationship between sample mass and particle size that provides the required precision can then be plotted. An example of this approach may be found in ISO 3082 (Iron ores – Sampling and sample preparation procedures),[14] where an equation and a table are provided for determining the minimum mass of divided sample as a function of nominal top size and division precision. While not as rigorous as for iron ore, the minimum sample mass requirements as a function of particle size for other commodities are specified in their respective national and international (ISO) standards, e.g. ISO 13909 (Hard coal and coke – Mechanical sampling – Part 2: Coal – Sampling from moving streams)[16], and these mass requirements must be observed when designing sample stations. The alternative is to estimate the minimum sample mass from the well-known fundamental error (σ_{FE}) equation first derived by Gy[4] and subsequently expanded on by Pitard[6], ie, for a "binary" type ore when the divided sample mass is much less that the initial sample mass:

$$m_S = \frac{c\,\ell\,f\,g\,d^3\,a^2}{\sigma_{FE}^2} \qquad (3)$$

where m_S = divided sample mass (g)
σ_{FE} = fundamental error as a fractional concentration
c = mineralogical composition factor
ℓ = liberation factor
f = particle shape factor, which can usually be taken to be 0.5
g = size range factor, usually between 0.25 and 1.0.
d = nominal top size of the material (cm)
a = fractional concentration of the component of interest.

Further details on this approach together with worked examples are provided in text books by Gy[4] and Pitard,[6] as well as publications by other authors such as François-Bongarçon[15] and Holmes.[1,3]

Number of increments

Assuming the sample cutters have been designed to eliminate increment delimitation and extraction errors, and that the minimum sample mass requirements have been determined to reduce the fundamental error variance to acceptable levels, a sufficient number of increments now need to be taken to reduce the long-range quality fluctuation error variance to the desired level. A number of methods are used to determine the required number of increments.

For iron ores, the standard deviation of individual primary increments within strata is determined experimentally using ISO 3084 (Iron ores – Experimental methods for evaluation of quality variation).[17] This parameter is known as the quality variation σ_W, and the number of increments n required to achieve the desired primary sampling precision β_S, i.e. $2\sigma_S$, is calculated using the following equation:

$$n = \left(\frac{2\sigma_w}{\beta_s}\right)^2 \qquad (4)$$

The ISO standard for sampling iron ore (ISO 3082)[14] also provides a table specifying the minimum number of primary increments required to achieve the required sampling precision for large, medium and small quality variation, which is reproduced in Table 1.

On the other hand, the required number of increments for sampling coal is determined experimentally from the variance V_I of successive primary increments using the method specified in ISO 13909-2.[16] The number of primary increments n to be taken from each sub-lot is then calculated for the desired overall precision P_L (95% confidence limit) after correcting for the sample preparation and analysis variance V_{PT} using the following equation:

$$n = \frac{4V_I}{mP_L^2 - 4V_{PT}} \qquad (5)$$

where m is the number of sub-lots in the lot
V_{PT} is the preparation and analysis variance

While the above methods for determining the number of increments differ in detail, the general approach is similar, i.e. the required number of increments is determined by dividing the variance between individual increments by the required sampling variance.

In principle, the same approach can be used at the secondary, tertiary and quaternary sampling stages, and this approach is described in detail in ISO 12743 (Copper, lead, zinc and nickel concentrates – Sampling procedures for determination of metal and moisture content),[18] but the variance of individual cuts is hardly ever determined. Instead, the number of cuts is usually set at a minimum

Table 1. Example from ISO 3082 of the minimum number primary of increments required to achieve specific sampling precisions (sS) for iron ore14.

Mass of lot (1000 t)		Sampling precision (σ_S)			Number of primary increments		
					Quality variation Large (L), Medium (M) or Small (S)		
Over	Up to	Fe, SiO_2 or moisture content	Al_2O_3 content	P content	L	M	S
270		0.155	0.045	0.00115	260	130	65
210	270	0.16	0.045	0.0012	240	120	60
150	210	0.17	0.05	0.00125	220	110	55
100	150	0.175	0.05	0.0013	200	100	50
70	100	0.185	0.055	0.00135	180	90	45
45	70	0.195	0.055	0.00145	160	80	40
30	45	0.21	0.06	0.00155	140	70	35
15	30	0.225	0.065	0.0017	120	60	30
0	15	0.25	0.07	0.00185	100	50	25

of approximately four, although in many cases Vezin dividers are used for subsequent sampling stages, particularly at the tertiary and quaternary stages, and hence in practice a much larger number of cuts are taken.

Sampling regime

Assuming that the sample cutters to be used are correctly designed, that the relationship between particle size and minimum sample mass has been established for the desired fundamental error has been established for sample division, and that the number of increments required to achieve the required sampling precision has been determined, there are usually a range of sampling regimes that can be successfully used in sample station design.

The usual strategy after collecting the primary increments is to crush the increments first so that they can then be safely divided down to a smaller sample mass. However, it may be beneficial to divide primary increments down to a smaller sample mass first, particularly when sampling high capacity streams where the primary increment mass can be quite large (possibly as much as 1,000 kg or more), provided of course that the minimum sample mass requirement for the composite sample comprising all increments is respected. This approach can be beneficial in reducing the load on crushers in the sample station, thereby reducing wear and tear and significantly reducing the need to adjust crusher gaps to ensure that the required particle size of crusher products meets design specifications. This is particularly important in sample stations, because if the particle size of the crusher product increases due to wear and tear and is not re-adjusted, then the sample mass retained after crushing and subsequent division will almost certainly not meet the minimum sample mass requirements for the larger particle size. This is a common fault in sample stations, so crushers need to be selected that can comfortably perform their duty and their performance needs to be carefully monitored and adjustments made if required.

As alluded to above, it is critical that the minimum sample mass requirements be respected at all subsequent sampling stages as well, e.g. that the sum of the masses of all secondary increments collected to constitute an analysis sample meets the minimum sample mass requirements for the particle size of the material at that stage which may be preceded by a crushing step so that the sample mass can be safely reduced. It is also good practice to ensure that the secondary, tertiary and if required quaternary cutters are triggered to take their first cut independent of the timing of operation of the preceding cutter.

Example. As an example of the design of a sampling regime, assume that a 180,000 tonne shipment of iron ore lump is being sampled according to ISO 3082.[14] The particle size of the ore is -31.5 + 6.3 mm and the quality variation is assumed to be “small”. Hence, according to Table 1, 55 primary increments are required.

(a) Primary stage

The primary cutter is a cross-stream sample cutter

Flowrate = 12,000 tonnes/hr

Cutter aperture = 0.15 m

Cutter speed = 0.4 m/s

From equation 2, the primary increment mass = 1,250 kg

Consequently, the total sample mass collected at the primary stage = 1,250 × 55 = 68,750 kg, which far exceeds the minimum sample mass of 180 kg in ISO 3082[14] for a division precision of 0.1% Fe (see Table 2).

Table 2. Examples from ISO 3082 of minimum mass of divided gross sample for moisture and/or chemical analysis of iron ore[14].

Nominal top size (mm)	Minimum mass of divided gross sample (kg)	
	σ_D = 0.1% Fe	σ_D = 0.05% Fe
40	325	1,300
31.5	180	710
22.4	75	300
10	10	40
6.3	3.2	13
2.8	0.5	1.7
1.4	0.5	0.5
0.50	0.5	0.5
0.25	0.5	0.5

(b) Secondary stage

Because the primary sample mass is very large, use a cross-stream sample cutter taking 5 cuts from each primary increment to reduce the sample mass without crushing.

Flowrate = 10 t/hr to completely clear the sample station between primary increments

Cutter aperture = 0.15 m

Cutter speed = 0.4 m/s

From equation 2, the secondary increment mass = 1.04 kg

Consequently, the total sample mass collected at the secondary stage = 1.04 × 5 × 55 = 286 kg, which safely exceeds the minimum sample mass of 180 kg for a nominal top size of 31.5 mm in ISO 3082[14] for a division precision of 0.1% Fe (see Table 2).

(c) Tertiary stage

Because the sample mass cannot be reduced much below 286 kg at a nominal top size of 31.5 mm, a cone crusher is used to reduce the nominal top size of the lump ore to 6.3 mm prior to division using a Vezin divider with a single radial cutter dimensioned to extract 5% of the sample fed to the divider.

Total secondary sample mass = 286 kg

Nominal top size after crushing = 6.3 mm

Consequently, the total divided sample mass at the tertiary stage = 286 × 0.05 = 14.3 kg, which safely exceeds the minimum sample mass of 3.2 kg for a nominal top size of 6.3 mm in ISO 3082[14] (see Table 2).

This sample mass is also suitable for transfer to the laboratory for subsequent sample preparation and analysis.

Performance verification

Verification of the correct performance of sample stations is an important part of initial and ongoing quality assurance. For this purpose, comprehensive check lists are available,[12] including in a number of ISO standards, eg, for iron ore[14] and coal and coke.[19] Consequently, as pointed out by Pitard,[7] large and readily accessible inspection ports are required to enable inspection of sample cutters to ensure that they intercept the whole stream and are in good condition and free of build-up and blockages. Unfortunately, practical experience indicates that this is not always the case and inspection ports are often non-existent, inconveniently and/or inappropriately located, or bolted shut on safety grounds. However,

Figure 16. Excessive sample build-up and partial blockage of a secondary cutter aperture.

Figure 17. Duplicate sampling system installed in a sample station.

safety concerns associated with inspection ports can be overcome by installing steel mesh on the inside of inspection ports behind the access doors to prevent physical access. This enables inspection of cutters "live" as they intercept the stream to validate correct operation, provided of course that the steel mesh provides good visibility of cutter operation. Inspection ports should also be provided for checking chutes, crushers and sample dividers, such as Vezin dividers and rotating tube samplers, for blockages and maintained condition. An example of excessive sample build-up and partial blockage of a bucket cutter is shown in Figure 16. Furthermore, the ability to monitor increment mass and/or the extraction ratio also provides valuable information for checking performance.

When conducting routine inspections and verifying the performance of sample stations, the key items that need to be checked include the following:

- The size and geometry of cutter apertures, including checking that cutters take a complete cross-section of the stream being sampled
- The cutter speed and its uniformity while cutting the ore stream
- The condition of cutter lips, including identifying any missing cutter lips
- The presence of build-up on cutter lips and/or blockages in cutter apertures and chutes
- Sample reflux from cutter apertures, particularly at high flow rates and for fine moist materials
- Ingress of extraneous material into the cutter aperture when the cutter is parked
- The location of belt scrapers and whether material removed by belt scrapers is significant and if so intercepted by the sample cutter
- The increment mass and whether it corresponds with the calculated increment mass
- The number of primary, secondary and tertiary cuts depending on the number of sampling stages
- Holes in cutters, chutes and bins, as well as the action of excessive air currents or wind, resulting in sample loss
- Crusher performance, in particular blockages and whether the product particle size conforms to specification
- The condition of vibratory feeders
- Sample mass as a function of particle size at each sampling stage to ensure that it conforms to minimum sample mass requirements.

Overall precision

The overall precision of sampling, sample preparation and analysis must be appropriate for the required task and decided at the outset so that an appropriate sampling regime can be designed. For example, it is impossible to control plant, stockpile or shipment grades to high precision if the overall precision of measurement is poor and instances of plant operators responding to apparent changes in grade that are no more than measurement "noise" are not uncommon. Furthermore, target grades can be moved closer to contract specifications without incurring penalties if the overall precision of grade measurements is high, thereby significantly improving resource utilisation.

The actual precision achieved in practice can be determined via duplicate "interleaved" sampling, where alternate primary increments are directed to duplicate samples A and B, which are subsequently prepared and analysed in duplicate under strictly identical conditions.[20] This enables separate estimates of the precision of sampling, sample preparation and analysis to be obtained. Consequently, duplicate sampling facilities should be incorporated into sample stations at the outset (see Figure 17) so that the precision achieved in practice can be determined and monitored on an ongoing basis. A number of well-designed, efficient and user-friendly approaches to this type of "agreement analysis" are available[21], which enable a full range of precision assessments to be made for quality control purposes.

Conclusion

Accurate sampling practices are critical for characterising ores and mineral products in the mineral industry for resource evaluation, resource utilisation, feasibility studies, process design and optimisation, quality control, metallurgical accounting, and ultimately commercial sales. Sampling is the first step in the measurement chain, so if the sample that is collected is not representative, the whole measurement chain is compromised at the outset. On the other hand, it is still surprising how often sampling is entrusted to personnel who are not appropriately trained or do not fully

appreciate its importance, and everyone seems satisfied as long as just *some* material is collected and dispatched to the laboratory for analysis. Cost is often the overriding consideration instead of sampling correctness (unbiasedness) when designing sample stations, which is unacceptable. Sampling experts need to be fully involved in the design of sample stations and have the final sign-off to avoid structural flaws and the subsequent need for expensive retrofits to address major problems. Provision also needs to be made for duplicate sampling to monitor the precision achieved in practice on an ongoing basis for comprehensive quality assurance. After commissioning sample stations, regular performance audits need to be conducted to ensure they are adequately maintained and continue to conform to correct sampling principles. It is high time that sampling is given the necessary attention by company management right through to sample station operators as the first critical step in the quality measurement chain.

References

1. R.J. Holmes, "Correct sampling and measurement – The foundation of metallurgical accounting", *Chemometrics and Intelligent Laboratory Systems*, **74**: 71-83 (2004).
2. R.J. Holmes, "Sampling mineral commodities – the good, the bad, and the ugly", *Journal of the Southern African Institute or Mining and Metallurgy*, **110**: 1-8 (2010).
3. R.J. Holmes, "Design of sample plants – Getting it right first time", in *Proceedings Second World Conference on Sampling and Blending (WCSB2)*, Sunshine Coast, Australia, pp.103-110 (The Australasian Institute of Mining and Metallurgy: Melbourne) (2005).
4. P.M. Gy, *Sampling of Particulate Materials - Theory and Practice*, 2nd Edition (Elsevier: Amsterdam) (1982).
5. P.M. Gy, "Sampling from high capacity streams", in *Proceedings First Australian International Bulk Materials Conference*, Sydney, Australia, pp 407-423 (1982).
6. F.F. Pitard, *Pierre Gy's Sampling Theory and Sampling Practice*, 2nd Edition (CRC Press Inc: Florida) (1993).
7. F.F. Pitard, "Sampling correctness – A comprehensive guideline", in *Proceedings Second World Conference on Sampling and Blending (WCSB2)*, Sunshine Coast, Australia, pp. 55-66 (The Australasian Institute of Mining and Metallurgy: Melbourne) (2005).
8. R.J. Holmes, "Sampling", Chapter 4 of "An Introduction to Metal Balancing and Reconciliation", pp. 141-170 (Julius Kruttschnitt Mineral Research Centre, The University of Queensland) (2008).
9. R.J. Holmes, "The Importance of Sampling in the Mineral Industry", in *Proceedings MetPlant 2013*, Perth, Australia, pp. 34-49 (The Australasian Institute of Mining and Metallurgy: Melbourne) (2013).
10. P.M. Gy and L. Marin, L, "Unbiased sampling from a falling stream of particulate material", *International Journal of Mineral Processing*, **5**: 297-315 (1978).
11. R.J. Holmes, "Best Practice in Sampling Iron Ore", in *Proceedings Third World Conference on Sampling and Blending (WCSB3)*, Porto Alegre, Brazil, pp.416-429 (2007).
12. J. Docherty, "Mechanical sample plants", in *Proceedings Second World Conference on Sampling and Blending (WCSB2)*, Sunshine Coast, Australia, pp. 83-93 (The Australasian Institute of Mining and Metallurgy: Melbourne) (2005).
13. G.K. Robinson and R.J. Holmes, "Iron ores – Results of testwork on sample division for iron ores", ISO/TC 102 – Iron ores and direct reduced iron, *TC 102 Technical Committee Report No. 9*.
14. ISO 3082, Iron ores – Sampling and sample preparation procedures (ISO: Geneva) (2009).
15. D. François-Bongarçon, "The modelling of the liberation factor and its calibration", in *Proceedings Second World Conference on Sampling and Blending (WCSB2)*, Sunshine Coast, Australia, pp. 11-13 (The Australasian Institute of Mining and Metallurgy: Melbourne) (2005).
16. ISO 13909, Hard coal and coke – Mechanical sampling – Part 2: Coal – Sampling from moving streams (ISO: Geneva) (2009).
17. ISO 3084, Iron ores – Experimental methods for evaluation of quality variation (ISO: Geneva) (1998).
18. ISO 12743, Copper, lead, zinc and nickel concentrates – Sampling procedures for determination of metal and moisture content (ISO: Geneva) (1996).
19. ISO 21398, Hard coal and coke – Guide to the maintenance and inspection of sampling systems (ISO: Geneva) (2006).
20. ISO 3085, Iron ores – Experimental methods for checking the precision of sampling (ISO: Geneva) (2002).
21. M. Pitard, "Agreement analysis – Testing the boundaries between producers and consumers", TOS Forum Issue 2, pp. 12-15 (2014).

doi: 10.1255/tosf.49

Review of a non-probabilistic sampler versus a Vezin sampler on low weight percent solids slurries

Steven E. Kelly[a] and Francis F. Pitard[b]
[a]2425 Stevens Center Pl, MSN-H0-55, Richland, WA 99354 USA. E-mail: steven_e_kelly@rl.gov
[b]14800 Tejon Street, Broomfield, CO 80023 USA. E-mail: fpsc@aol.com

The Hanford Tank Operations Contractor (TOC) and the Hanford Waste Treatment and Immobilization Plant (WTP) contractor are both engaged in demonstrating mixing, sampling, and transfer system capability using simulated Hanford High-Level Radioactive Waste (HLW) formulations. This work represents one of the remaining technical issues with the high-level waste treatment mission at Hanford – the TOC's ability to adequately sample high-level waste feed to meet the Waste Treatment and Immobilization Plant (WTP) Waste Acceptance Criteria Data Quality Objectives. A full-scale sampling loop was used at a cold test facility to evaluate sampler capability. The sampler under investigation for deployment is non-probabilistic but radioactive environment friendly. A Vezin sampler (probabilistic) was used to obtain reference samples and accurately characterize the simulant as it flowed through the test loop. The two samplers are located in series, allowing for multiple samples to be taken from both samplers over the same time period (sample pairs) and direct sample comparison. The Vezin sampler was modified to minimize material build up allowing for steady-state operation. This report discusses modifications made to the Vezin sampler and the results of sampler comparison.

Introduction

The U.S. Department of Energy, Office of River Protection manages the River Protection Project. The River Protection Project mission is to retrieve and treat Hanford's tank waste and close the tank farms to protect the Columbia River. As a result, the Office of River Protection is responsible for the retrieval, treatment and disposal of approximately 208 million litres of radioactive waste contained in the Hanford Site waste tanks.

The Waste Treatment and Immobilization Plant will process the waste feed it receives from the Tank Operations Contractor into its final disposal form. Waste staged as feed will be sampled to ensure it meets Waste Treatment and Immobilization Plant – Tank Operations Contractor interface agreements. The Tank Operations Contractor's Waste Feed Delivery Mixing and Sampling Program is tasked with developing and demonstrating waste feed capabilities.

Implementation of the sampling concept on a Hanford million gallon double-shell tank will utilize the tank's transfer pump for recirculating waste feed through a sample loop where a small portion of the waste will be captured before the waste is returned to the tank. Sampling will occur while the tank is being mixed by two rotating jet mixer pumps. The sampling method must minimize contamination and be remotely operated to minimize operator exposure to radiation—. The total amount of material to be sampled for qualification of a feed tank will be between four and ten litres (most of the sampled material will be used for process evaluation, not analytical analysis). Sample container volume will be between 250 mL and 1000 mL; most likely 500 mL to best utilize current transportation systems.

A modified Isolok® MSE sampler, by Sentry, is the sampler of choice to meet safety, handling, and volume flexibility requirements. Because mixing cannot be assumed to produce a consistent homogenous feed the test loop, a custom two stage Vezin sampler, manufactured by FLSmidth USA Inc., was used to obtain reference samples during the same time period as the Isolok® samples were taken. A sketch of the test loop is below in Figure 1.

The test loop is primarily 3" schedule 40 pipe which is prototypic and allows for visual measurement of critical velocity through two clear sections; the method was developed during prototype testing for an ultrasonic pulse echo method for determine critical velocity.[1] A Coriolis meter was used to monitor flow rate. Temperature of slurry was control to approximately 21 °C using a chiller. The Isolok® is located ten pipe diameters above a 90° elbow and transition from 80 mm schedule 40 pipe to 50 mm schedule 40 pipe. The Isolok® captures a fixed sample volume using a plunger and cylinder which are each independently controlled pneumatically. A cut away figure of the Isolok® sampler for testing is show in Figure 2, and an animation of the Liquid Isolok® MSE sampler can be found at http://sentry-equip.com/Resources/Sentry-product-videos.htm. Each Isolok® sample was comprised of 115 increments; the final volume was ~630 mL. The two-stage Vezin sampler used is shown in Figure 3. The primary stage took approximately 77 cuts, and the secondary Vezin took approximately 170 cuts of the primary's sample; the final volume was ~1900 mL.

Two simulants (slurries) were used for testing.[2,3] Both slurries utilized the same carrier fluid, 31 % thiosulfate in water having a density of 1.29 g/mL and a viscosity of 3.3 cP. Six undissolved solids were used in the proportions outlined in Table 1. The typical

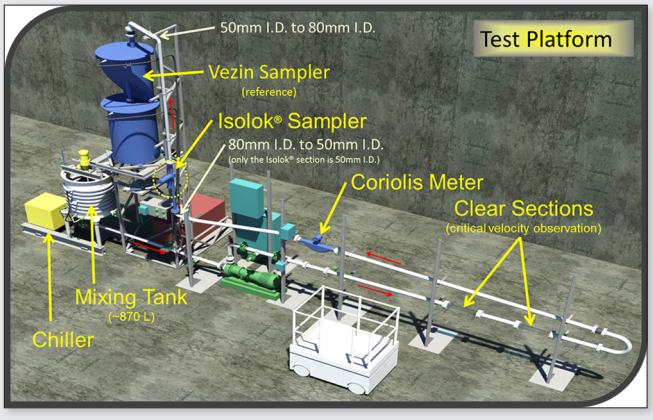

Figure 1. Test Loop

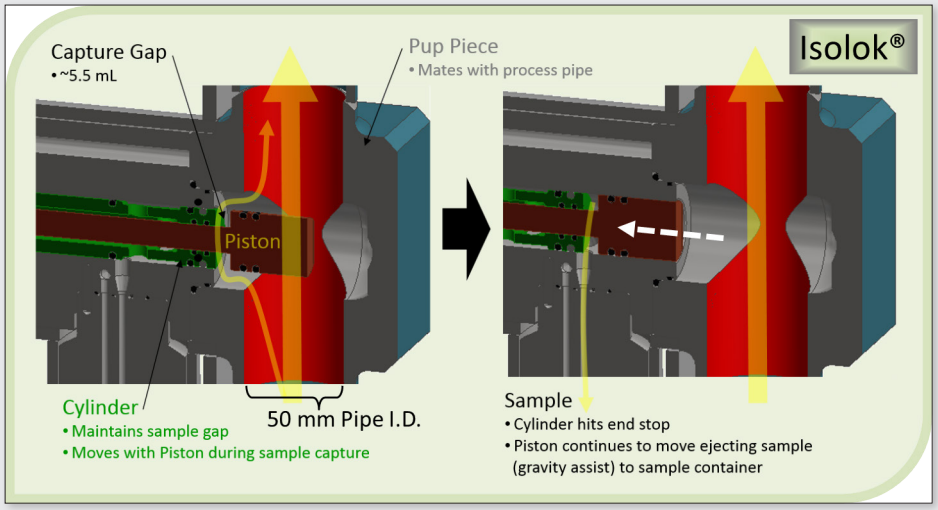

Figure 2. Isolok® Sampler

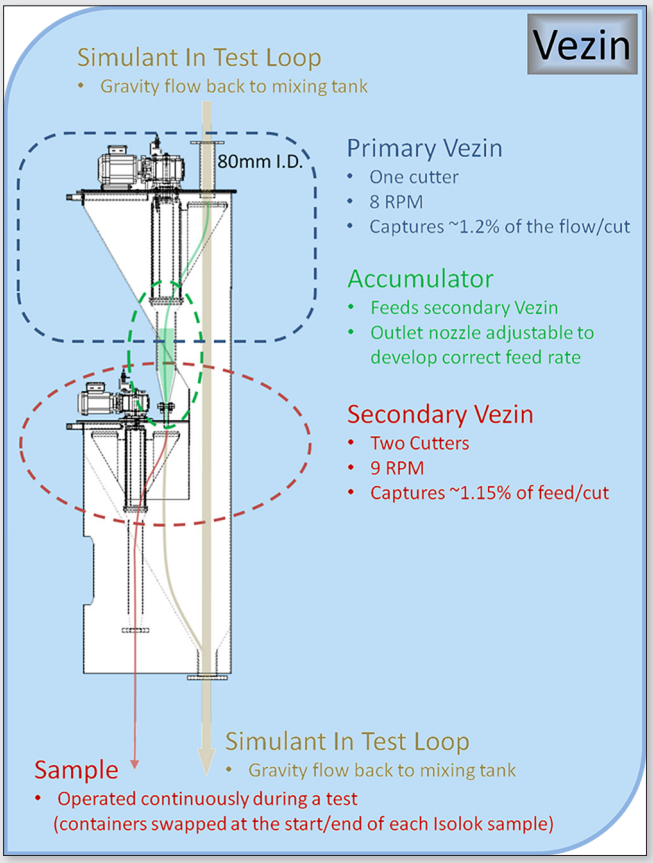

Figure 3. Two Stage Vezin Sampler

simulant recipe is primarily fine particulate, less than 75 µm, with a minor amount of fast settling solids – solids >75 µm. The high simulant recipe is a conservative (at the upper limit of fast settling solids relative to planned WTP feed) mix with a higher percentage of fast settling particles. Only the fast settling solids were targeted for analysis by sieving; large sand <710 µm (25 mesh) and >180 µm (80 mesh) and stainless steel <180 µm and >75 µm (170 mesh). All analytical sieves were American Society for Testing and Materials (ASTM) E161-12

Break-in and final test operations

Testing was performed in two phases[3] – a break-in test using the high simulant followed by final testing where both simulants were sampled and formal analytical data obtained. The break-in test was designed to allow the operators to practice sampling (capturing Isolok® and Vezin samples simultaneously) and work out any issues with the system. Two issues were resolved.

Accurate capture of Vezin samples for this type of test typically requires flushing of the cutters to make sure all material cut by the Vezin is included with the sample. Flushing the Vezin sampler is both time-consuming and has many steps, which increases the likelihood of operator error. The first goal of the break-in test was to determine if steady-state sampling could be performed. Material build up in the Vezin over time was estimated and modifications to the sampler were made to reduce material build up. Inspections showed that little, to no, material was left in the primary Vezin. Since only about 2.3% of the primary cutter material would be expected to be caught by the secondary Vezin, no changes were made to the primary Vezin.

Material did build up in the secondary Vezin. Rinsing the cutter and the flow path between the cutters and sample container separately resulted in an estimate that 40% of the material that was held up in the Vezin was held up by the cutters and 60% in the flow path. The cutters were modified to remove a lip at the bottom of the cutter where build up was most visible. The flow path was modified by reducing the size of the last section of pipe between the rotating cutters and sample container. See Figures 4 and 5 for photos and sketches of modifications made to the sampler.

Based on data review, the sampler was allowed to run 40 minutes before test samples were taken, and the modifications to the sampler reduced material build up during one sampling period (~9.5 minutes) from about 1 gram to less than 0.34 grams. Ideally, for sampling of slurries where concentration of material is the goal, the flow paths through the Vezin should be sized appropriately to the flow that they will carry. In the case presented here the secondary Vezin was sized identically to the primary Vezin, resulting in excess surface area along the flow path.

The second issue found during break-in testing was foaming caused by the free fall of slurry through the Vezin sampler. The

Table 1. Simulant Solids Components.

Component	Particle Density g/cm^3	Particle Size (d_{50}) µm	Mass Fraction of Undissolved Solids By Simulant	
			Typical	High
Small Gibbsite[a]	2.42	2.2	0.27	0
Large Gibbsite[b]	2.42	9.9	0.44	0.053
Small Sand[b]	2.65	20.8	0.09	0.616
Large Sand[c]	2.65	414.3	0.04	0.074
Zirconium Oxide[a]	5.7	17.6	0.10	0.141
Stainless Steel[d]	8.0	122.3	0.06	0.116
Bulk Solids Density (g/cm^3)			2.7	3.1
Solids Loading in Slurry (wt %)			9.0	5.3

[a] Verified to be less than 63 µm.

[b] Pre-sieved through a 63 µm mesh.

[c] Pre-sieved, passed 710 µm and captured on 210 µm mesh.

[d] Pre-sieved, passed 150 µm and captured on 90 µm mesh.

Note: All pre-sieving was performed with sieves having 70% of the tolerances specified in ASTM E11-13.

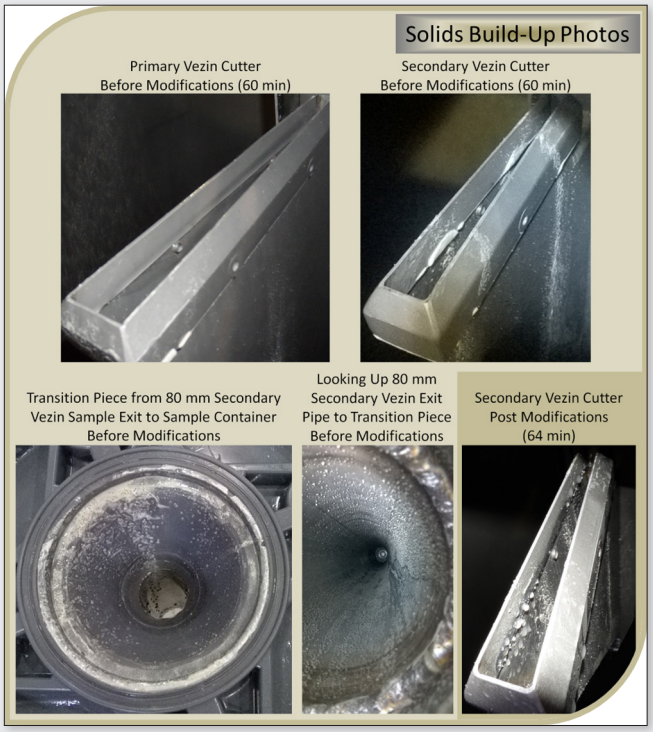

Figure 4. Vezin Inspection Photographs

addition of ~30 mL of a silicon based defoamer eliminated foaming in the high simulant and 3x that amount in the typical simulant.

During two formal test runs, 34 sample pairs were taken for each test — 30 (pairs 3 through 32) were analyzed for stainless steel and large sand. Parameters controlled during testing were flow rate, 530 ± 20 Lpm, and temperature 21 ± 1.7°C [3]. During first test, using the typical solids slurry, sample number 14 was mishandled and could not be submitted to the laboratory for analysis and the second sample pair was analyzed as a replacement. The only other issue occurring during the formal tests was increased Isolok® volume, from ~650 mL to over 800 mL, during the high simulant test. The root cause was found to be worn Isolok® surfaces (due to previous testing using harsh simulants) and worn O-rings. Components estimated to have been removed from the test were added back to the test loop, sampler O-rings were replaced, and the test was repeated. Only the results of the repeat high simulant test are reviewed here.

Results and data review

Data obtained for each sample pair was:

- Critical velocity of slurry.
- Density, sample mass/sample volume.
- Concentration of solids <710 µm and >180 µm, captured on a #80 mesh – primarily large sand.
- Concentration of solids <180 µm and >75 µm, captured on a #170 mesh – primarily stainless steel.
- Limited results on slow settling solids, <75 µm.

Analytical method

Five control sample pairs were sent to the laboratory mixed with test samples for each test. By pre-sieving solids with one full mesh size on each side of the analytical sieve, analytical error was very low. See Table 2. The low analytical error is also evident by the tight spread of data, percent relative standard deviation (%RSD), over the course of the 30 sample pairs analyzed for each test.

Typical and high slurry

Critical velocity was determined for each test simulant before and after testing to verify the simulants were within test parameters. This was determined by incrementally dropping the test loop flow rate and observing the solids flow along the bottom of the clear sections using a high resolution video camera. The flow rate at which a stationary bed was formed was designated the slurry's critical velocity. The typical simulant had initial and final critical velocities of 0.82 m/s, and the high simulant had a starting critical velocity of 1.25 m/s and a final critical velocity of 1.22 m/s.

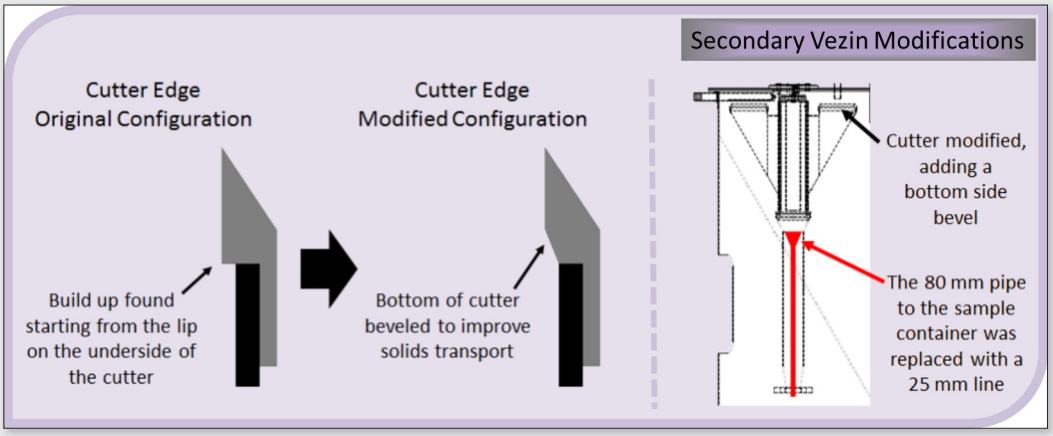

Figure 5. Modifications to Secondary Vezin Sampler

Table 2. Control Sample Data (for samples where slow settling solids were analysed)

Sample	Analysis By Sieve (g)			Prepared Mass (g)			% Recovered	
	<75 µm	75 µm	180 µm	<75 µm	M_{SS}	M_{LS}	<75 µm	% Total
Typical-Isolok® RSD-0804	108.1	7.3	4.8	109.7	7.3	4.9	98.5	98.5
Typical-Vezin RSD-0805	217.5	14.8	9.6	219.3	14.6	9.7	99.2	99.3
Typical-Isolok® RSD-0828	109.2	7.3	4.9	109.7	7.3	4.9	99.1	99.2
Typical-Vezin RSD-0829	217.9	14.6	9.7	219.3	14.6	9.7	99.4	99.4
High-Isolok® RSD-1023	53.9	13.6	8.4	58.0	13.3	8.4	93.0	95.3
High-Vezin RSD-1024	112.3	27.1	17.1	116.1	26.6	19.9	96.7	98.1

Note: SS = stainless steel and LS = large sand.

Sample pair densities and analytical data in terms of solids concentrations of material on each sieve are shown in Figure 6 for the typical slurry and Figure 7 for the high slurry. Both samplers were very consistent, sample to sample, without taking into account dynamic relationships (i.e., we assumed that the simulant did not change as material was removed and simply grouped all samples); see percent relative standard deviation data, Table 3.

Table 3. Sampler Consistency Review – % Relative Standard Deviation

Sampler	Sample Property	N	Typical Slurry % RSD	High Slurry % RSD
Isolok®	Volume	34	0.58%	0.61%
	Density	34	0.11%	0.12%
	[180 µm]	30	3.20%	2.23%
	[75 µm]	30	2.97%	3.21%
Vezin	Volume	34	0.26%	0.30%
	Density	34	0.06%	0.04%
	[180 µm]	30	2.21%	2.84%
	[75 µm]	30	2.54%	2.84%

As is quickly evident from review of Figure 6 and Figure 7, the accuracy for fast settling solids was highly biased for the Isolok® sampler, as shown in the figures. Although only three samples from each test were analyzed for particles less than <75 µm (particle density about the same as for large sand), the very good analytical performance allows the conclusion that the typical slurry may have a slight bias and the high slurry bias may be slightly higher, around 3.7%. These biases are much less than the bias found for the large sand in these two simulants.

Review of the data was also performed by using variogram technique,[4,5] further confirming Isolok® sampler performance – as it relates to over sampling particles based on size and density. The variograms are shown in Figure 8 and Figure 9. The patterns in the plots for all three parameters, density, 180 µm sieve, and 75 µm sieve, are different between the two samplers. Changes in the Vezin plots are more smooth and orderly. This means that the Isolok® see's patterns that are not there, but given the relative standard deviation of the samples this error is most likely acceptable.

From information in Figure 6 and Figure 7 we know that the Isolok® was removing material at rates different from the bulk flow concentrations. The Vezin sampler variogram review is key to understanding the resulting slurry changes and therefore providing

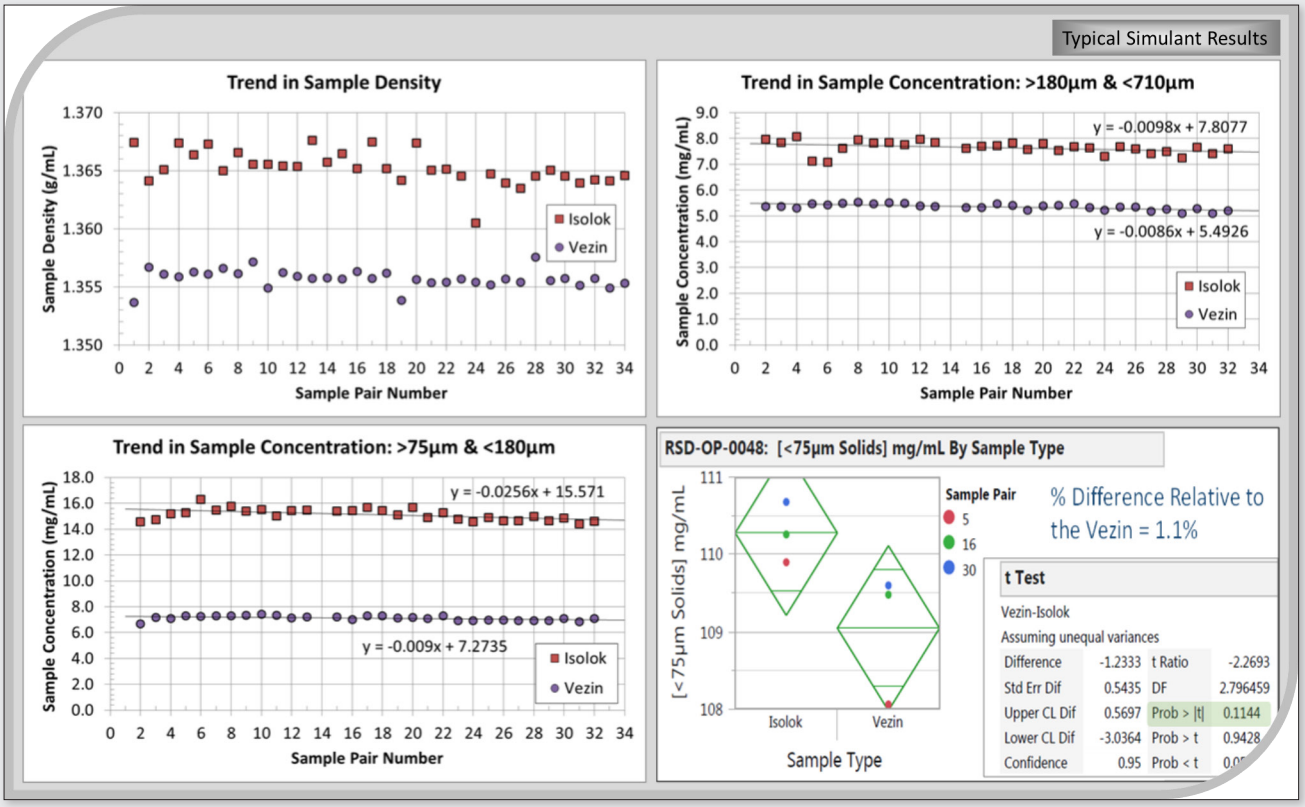

Figure 6. Typical Simulant – data Run Charts and Slow Settling Solids Analysis

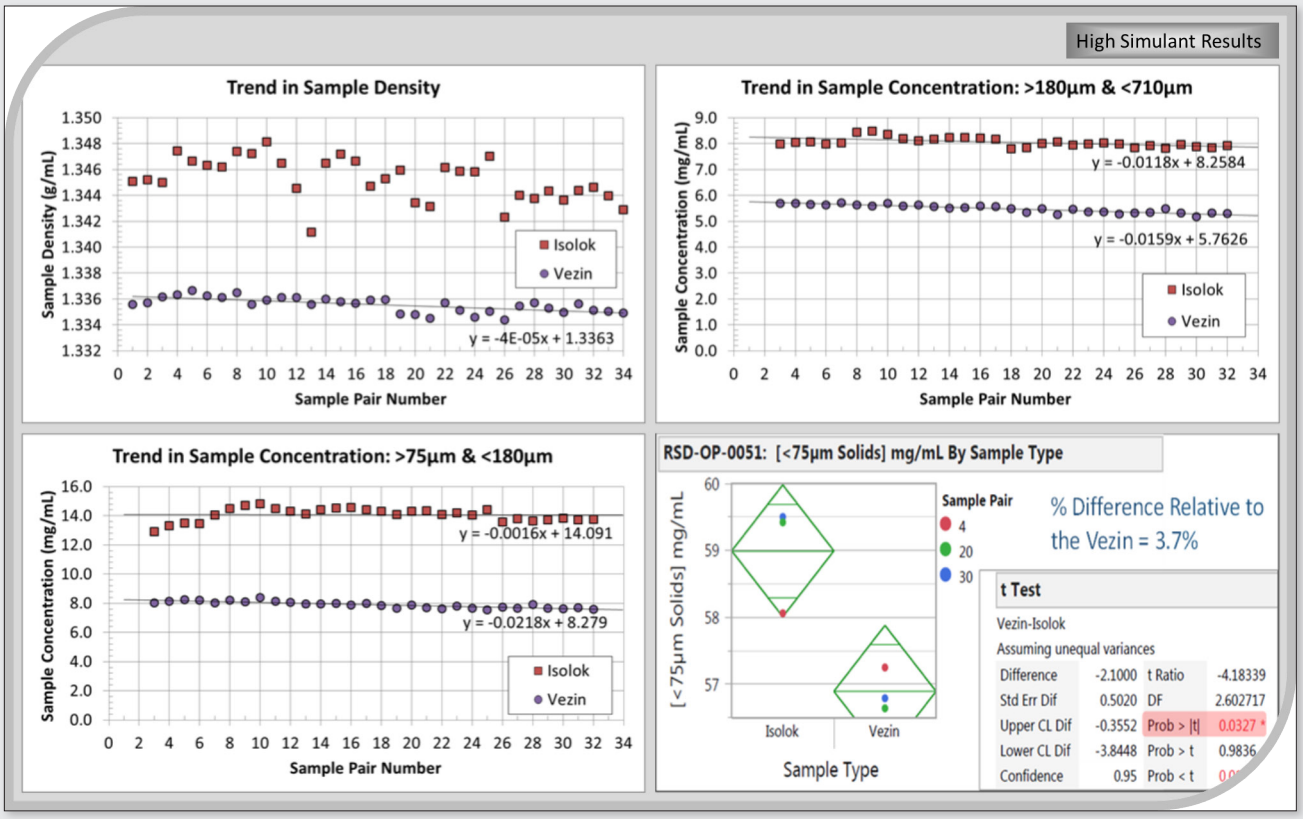

Figure 7. High Simulant – Data Run Charts and Slow Steeling Solids Analysis

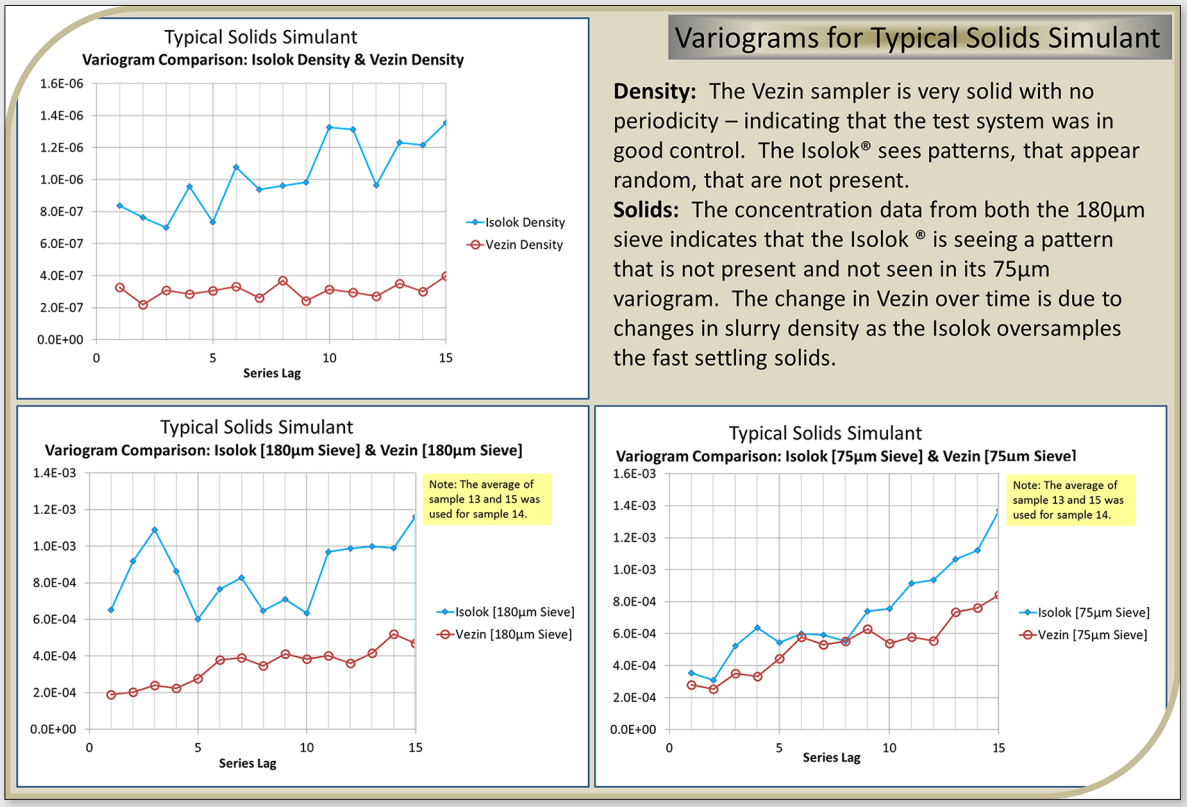

Figure 8. Typical Simulant – Variogram Review

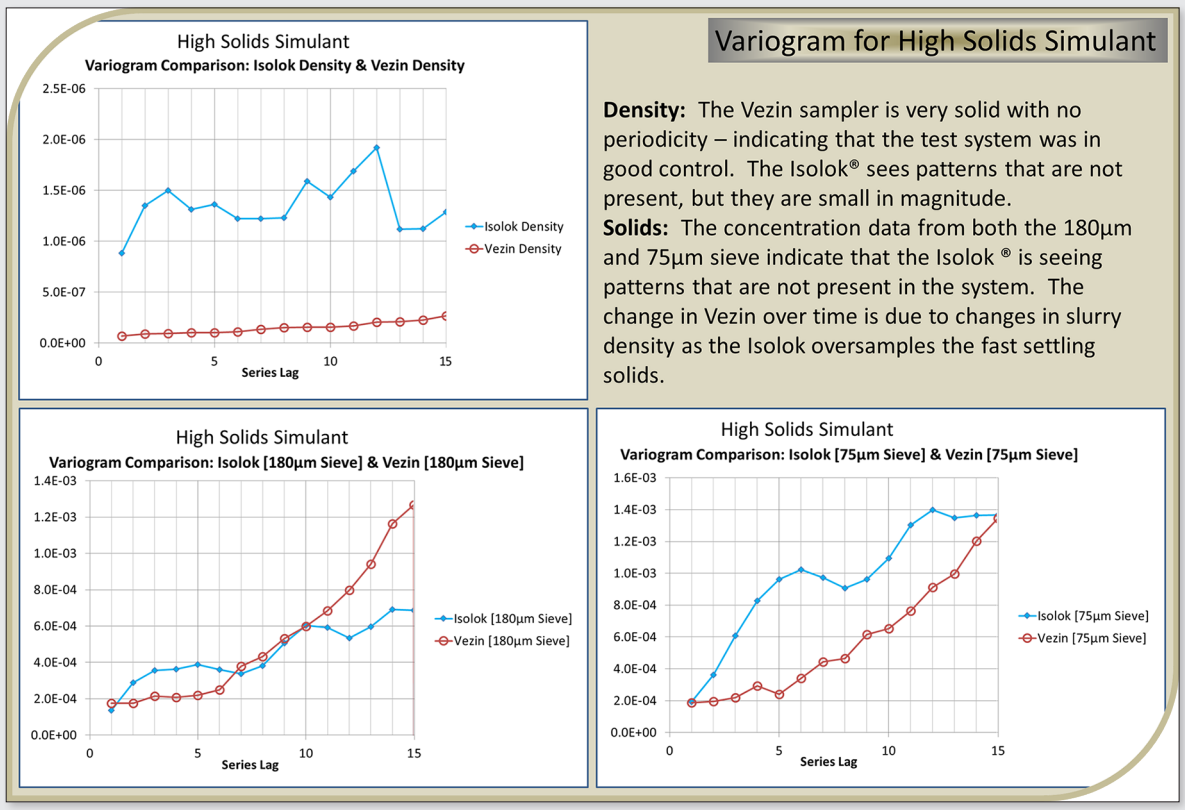

Figure 9. High Simulant – Variogram Review

Table 4. Isolok® Bias by Slurry Type

Sample Property	Typical Slurry (%Bias)	High Slurry (%Bias)
Density	0.7 ± 0.1%	0.7 ± 0.1%
[180 µm] (g/mL)	43.0 ± 4.4%	46.9 ± 3.6%
[75 µm] (g/mL)	112.6 ± 4.4%	78.2 ± 7.1%
[<75 µm] (g/mL)	Not statistically significant at the 95% confidence interval.	3.7%

more insight to Isolok® sampler performance. The Vezin typical slurry variograms have trends, but they are not strong or without the presence of noise. Slow settling solids make up 90 wt% of the solids in the typical slurry, and are 78% gibbsite (the smallest and lightest particles in the simulant). The lack of strong trends relative to sampling noise, and no measurable change in critical velocity from start to end of test shows there was little change in slurry properties over the course of this test.

The variograms for the high slurry Vezin samples show a different picture; trends are clear and with little noise. All three figures, slurry density as well as the 180 µm sieve, and 75 µm sieve concentrations, have very precise and predictable trends. The weight percent of fast settling solids between the two slurries was very similar, about 0.9 wt % for the typical and about 0.95 wt % for the high. The slow settling solids in the high slurry solids was primarily (76%) sand, larger and denser than the gibbsite used in the typical slurry. A slight drop in critical velocity was measured from start to end of the high slurry test. (If sampling was ideal, no change in simulant composition would occur and the critical velocity would be constant.)

Therefore, review of both the standard data analysis techniques and variograms show that the Isolok® oversamples particles at different rates based on particle size, particle density, and simulant component make up. This supports the <75 µm sample analysis results. The typical simulant showed no (or possibly a small) bias is present for the slow-settling solids. For the high simulant there was a marketable drop in the estimated sand bias from ~45% for the large sand to ~5% for the small sand.

Conclusions

Vezin samplers are well documented as being equiprobabilistic, proportional, and following good sampling protocol [4]. But more than just selection of the Vezin type should be considered during sampler design and installation. Results presented here show modification of features that can instigate particle accumulation should be performed during design and construction. Surface areas which are in excess of those needed to ensure a smooth flow path from the sampler's cutter to sample container should be minimized. Implementing modifications to mitigate these items allowed testing to be performed much more efficiently and most likely with less error. Review of Vezin data by standard run charts and variogram analysis showed that:

- The test loop was consistent throughout each test run.
- No spikes in slurry densities were observed from start to end of testing.
- The Vezin itself was telling the truth, i.e., it reflected what was in the test loop during any given sample pair.

The Sentry Liquid Isolok® MSE sampler, which does not follow good sampling protocol, was tested to determine its performance versus a two stage Vezin sampler for two relatively low weight percent solids slurries. Review of Isolok® data versus the Vezin data show that the Isolok® sampler oversamples undissolved solids based on particle size and density. See Table 4. As either particle size or density increase, so does the rate of over sampling. The rate of over sampling is also influenced by other particles and their concentrations in the slurry. The Isolok® also saw patterns in the test loop that were not there, however the error due to these signals were not significant compared to the sampling bias.

When reviewing the Isolok®, we should remember that it was designed for sampling of homogeneous liquids. See Table 5. However, due to its features (compact, enclosed, and easily automated), its use can easily be desired for applications outside its application; provided its limitations are understood and accounted for. The use of an Isolok® MSE sampler for obtaining Hanford's radioactive waste material will be based on its sampling performance (including data presented here) and its physical attributes as they relate to operational goals and data quality objectives to be applied to the sampled material. The data quality objectives have not been defined yet.

Table 5. Isolok® Bias by Slurry Type

Isolok®	Vezin
■ Cons	■ Cons
■ Not Equiprobabilistic	■ Handling
☐ Delimitation Error	☐ High Possibility of External Contamination
☐ Extraction Error	■ Pros
☐ Segregation Error	■ Handling
☐ Periodic Heterogeneity Fluctuation Error	☐ Preparation Error
■ Pros	■ Equiprobabilistic
■ Handling	☐ Delimitation Error
☐ Preparation Error	☐ Extraction Error
☐ Good Contamination Control	☐ Segregation Error
■ Size / Increment	☐ Periodic Heterogeneity Fluctuation Error
☐ Fundamental Error	■ Size / Increment
☐ Long-Range Heterogeneity Fluctuation Error	☐ Fundamental Error
☐ Periodic Heterogeneity Fluctuation Error	☐ Long-Range Heterogeneity Fluctuation Error
	☐ Periodic Heterogeneity Fluctuation Error

Acknowledgements

Kearn Pat Lee: Co-author of the test plan RPP-PLAN-51625 and final RSD Accuracy final report – currently in draft.

References

1. *Hanford Tank Farms Waste Feed Flow Loop Phase VI: PulseEcho System Performance Evaluation*, Pacific Northwest National Laboratory, Richland, Washington. PNNL-22029 Rev. 0 (2012).
2. *Waste Feed Delivery Mixing and Sampling Program Simulant Definition for Tank Farm Performance Testing*, Washington River Protection Solutions, LLC, Richland, Washington. RPP-PLAN-51625 Rev. 0 (2012).
3. *One System Waste Feed Delivery Remote Sampler Accuracy Test Plan*, Washington River Protection Solutions LLC, Richland, Washington. RPP-PLAN-56125 Rev 0 (2014).
4. F.F. Pitard, *Pierre Gy's Sampling Theory and Sampling Practice*, 2nd Edn. CRC Press (1993). ISBN 0-8493-8917-8.
5. P. L. Smith, *Primer for Sampling Solids, Liquids, and Gases: Based on the Seven Sampling Errors of Pierre Gy*, Alpha Stat Consulting Company (2001).

doi: 10.1255/tosf.64

Evaluation of sampling error sources in a multiple cutter metallurgical sampler

J. Loimi[a], P. Minkkinen[b], C. von Alfthan[a], J. Lohilahti[a] and T. Korpela[a]
[a]**Outotec, Rauhalanpuisto 9, P.O. Box 1000, FIN-02231 Espoo, Finland, E-mail: janne.loimi@outotec.com**
[b]**Lappeenranta University of Technology PO Box 20, FIN-53851, Lappeenranta, Finland. E-mail: Pentti.Minkkinen@lut.fi**

The head loss caused by metallurgical sampling for slurry streams can be significantly reduced by appropriate sampler design. When the process flow is sampled by vertical static cutters before an equal number of moving cutters, the installation requires less installation head space than other sampling arrangements and is easy to accommodate at suitable process locations. Low head loss reduces building costs for the processing plant and operational costs during the life time of the plant.

The presence of a possible systematic bias in the particle size distribution or the chemical composition between the vertical static cutters caused by segregation in the metallurgical sampler can be estimated by a designed sampling campaign where sub-samples are cut from each of the moving cutter sample streams simultaneously. The sub-sample assay results can be evaluated by an F-test to reveal if there exists significant variance between the cutter assays.

The Minimum Possible Error (MPE) caused by the sampling and analysis system can be estimated in another sampling campaign where spot samples are collected at equal intervals to perform a variographic experiment to characterise process heterogeneity and MPE by estimating the V(0) intercept. The V(0) is the variability of a single measurement and furthers an indication of the minimum sampling variance that can be expected in practice. MPE includes the Fundamental Sampling Error (FSE), the Grouping and Segregation Error (GSE), the Total Analysis Error (TAE) as well as preparation errors and the possible Incorrect Sampling Errors (ISE) perhaps not fully eliminated. In this paper we present an approach to evaluate the various sampling error sources and magnitudes in a multiple cutter metallurgical sampler.

Introduction

Outotec metallurgical sampler MSA 2/50 has a low head loss structure. A structural benefit is that installation is easier and operational costs are lower than with high head loss metallurgical sampler structures. Figure 1 shows the design of the sampler. The metallurgical sampler is composed of several parts. The first part consist of mixing tank where a flow gate regulates slurry mixing and the speed of the slurry to the second part, which is characterised by three static cutters. The third part houses three moving cutters.

The metallurgical sampler has been installed in a flotation feed process line in hydrocyclone overflow. The process flow rate was close to the maximum recommended level, indeed sometimes even higher, yet it was found to be able to work well under these conditions. In the first part of the study sub-samples were collected immediately behind the moving cutters, with a purpose to reveal if

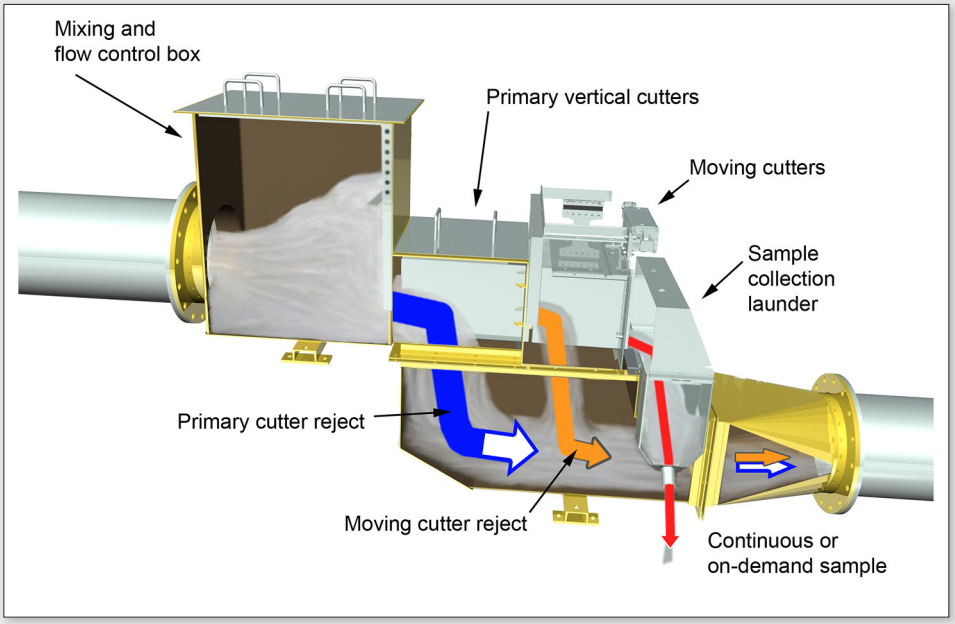

Figure 1. Metallurgical slurry sampler MSA 2/50. The cover of the sample collection launder was removed and three specially made boxes were placed in the launder for the taking the sub-samples used in this study. See Figure 10 for details of the moving cutters.

these show systematic differences with respect to chemical composition. If so, this would reflect an extraction error (IEE). Secondly, spot sample data were collected from a Courier on-line analyser and used in a variographic experiment to study process heterogeneity and to assess the Minimum Possible Error (MPE) by estimating the V_0 intercept. V_0 represents the short-range error variance of a single measurement.

Because sub-sample collection and variographic data collection was conducted as two different events, the ore fed to the process had changed in the particle size distribution and elemental content altering the scale of the fundamental sampling and, consequently, all analysis results of the studies are not directly comparable.

Sub-sample study

When sub-samples are taken simultaneously by the three moving cutters, the sampling error is caused by three error sources: long-range fluctuation in the process stream during the study, between cutters variation and short range variation consisting of the fundamental sampling error (FSE). If the error source variances are significantly larger than nil, their magnitude can be estimated from the experimental design shown in Figure 2 by using analysis of variance (ANOVA). In the following calculations σ^2 denotes theoretical variances and s^2 denotes estimated variances.

Due to the sample collection and preparation design used in this study the analytical error variance σ^2_a cannot be separated from the short term variance σ^2_{sh}. Instead, their sum can be estimated:

$$\sigma_0^2 = \sigma_{sh}^2 + \sigma_a^2 \tag{1}$$

Two other sampling variances, the between-cutter variance (σ^2_{bc}) revealing the local segregation, and the long-range variance (σ^2_{lr}) which includes all process changes during the experimental study, can be resolved from the four experimental variance estimates (s_1^2, s_2^2, s_3^2 and s_4^2) shown in Figure 2 (ANOVA). These are linear combinations of the three contributing error sources; they can therefore be used to calculate estimates for the individual error source variances (Equations 2–12). Here n = 10 is the number of primary samples from each cutter, j = 3 is the number of parallel cutters and df is the number of degrees of freedom for variance.

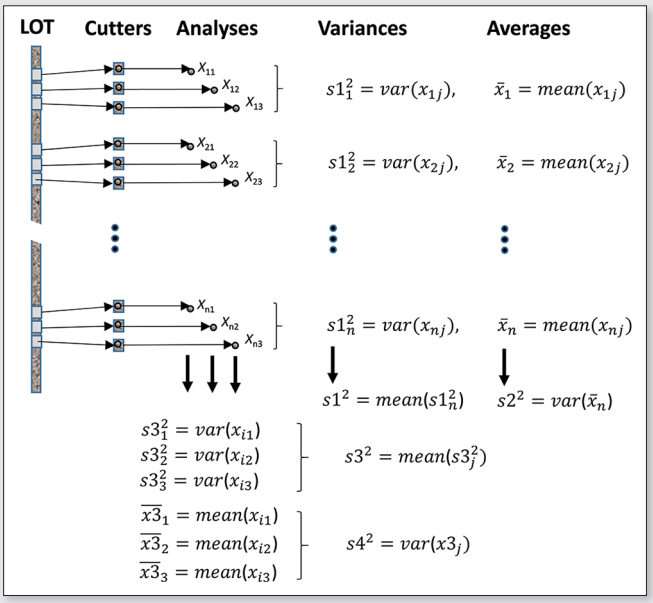

Figure 2. Experimental setup for ANOVA and calculation of four variances s_1^2–s_4^2 needed to estimate variances generating the total sampling error.

$$s_1^2 = \frac{\sum s_{1i}^2}{n} \approx \sigma_{bc}^2 + \sigma_0^2 , \qquad df = n(j-1) \tag{2}$$

$$s_2^2 \approx \sigma_{lr}^2 + \frac{\sigma_1^2}{j} = \sigma_{lr}^2 + \frac{\sigma_{bc}^2}{j} + \frac{\sigma_0^2}{j} , \quad df = n-1 \tag{3}$$

$$s_3^2 \approx \sigma_{lr}^2 + \sigma_0^2, \qquad df = j(n-1) \tag{4}$$

$$s_4^2 \approx \sigma_{bc}^2 + \frac{\sigma_3^2}{n} = \sigma_{bc}^2 + \frac{\sigma_{lr}^2}{n} + \frac{\sigma_0^2}{n} , \quad df = j-1 \tag{5}$$

The significance of the experimental variances was analysed by using an F-test with the ratio of the sample variance estimates as the test statistic. The significance of the long-range variance is tested with Eq. 6 and the between-cutters with Eq. 8.

$$F_1 = \frac{s_1^2}{s_2^2} = \frac{\frac{\sum s_{1i}^2}{n}}{s_2^2} = \frac{3s_2^2}{s_1^2} \approx \frac{3\sigma_{lr}^2 + \sigma_1^2}{\sigma_1^2} \tag{6}$$

In cases where the F test (6) is insignificant the long-range process variance does not differ significantly from zero and σ^2_{lr} can be assumed to be close to zero. In cases where the test results are significant, the estimate of long-range variance caused by long-range process fluctuation is:

$$s_{lr}^2 = s_2^2 - \frac{s_1^2}{j} \tag{7}$$

Similarly, the significance of the between-cutters variance can also be tested Eq. 8.

$$F_2 = \frac{ns_4^2}{s_3^2} \approx \frac{n\sigma_{bc}^2 + \sigma_3^2}{\sigma_3^2} \tag{8}$$

ANOVA showed that the between–cutter variance was insignificant, and consequently, the between-cutters variance can be assumed to be nil ($s^2_{bc} \approx 0$). The sum of the analytical error and short term process variance, s^2_0, and total variance of a single sample, s^2_{tot}, can also be estimated (Eqs. 10 and 11). The total variance is the sum of all error generating variances.

$$s_0^2 = s_1^2 - s_{bc}^2 \tag{9}$$

The total variance of a single measurement is the sum of all variances

$$\sigma_{tot}^2 = \sigma_{lr}^2 + \sigma_{bc}^2 + \sigma_{sh}^2 + \sigma_a^2 \approx s_{tot}^2 = s_{lr}^2 + s_{bc}^2 + s_0^2 = s_{lr}^2 + s_1^2 \tag{10}$$

If each j parallel cuts from n primary cuts are analysed the variance of the mean from the test period, excluding the possible autocorrelation discussed in the next chapter, is

$$s_{average}^2 = \frac{s_{lr}^2}{n} + \frac{s_{bc}^2}{n \cdot j} + \frac{s_0^2}{n \cdot j} \tag{11}$$

Because the sampling variance between cutters was not significant according this study (see above), the total observed variance is simply the sum of the long and short range process variances and the analytical variance. The design of feed box eliminates the horizontal segregation in the process stream and differences between the points of vertical cross cuts of the process stream were

Table 1. Anova variance components. Three replicate sub-samples were taken and analysed from ten primary process increments.

Measurement	Variance	Absolute standard deviation (%)	Relative standard deviation (RSD%)
A (%)	$s^2_{lr} = 0.00989$	0.099	0.88
	$s^2_{bc} \approx 0$	0	0
	$s^2_0 = 0.00872$	0.094	0.83
	$s^2_{tot} = 0.01867$	0.137	1.21
B (%)	$s^2_{lr} = 0.00586$	0.0024	2.30
	$s^2_{bc} \approx 0$	0	0
	$s_0^2 = 0.00024$	0.016	1.48
	$s^2_{tot} = 0.00083$	0.0040	2.74

insignificant, no systematic bias caused by the MSA 2/50 cutters could be observed in this study. The results of ANOVA are presented in Table 1. Because the data are confidential it was decided to denote the "analytes" as A and B without loss of generality.

Variographic experiment

The most complete theory on sampling for chemical analysis of particulate and solid matter in mineral processing industry that takes into account both the technical and statistical aspects of sampling, has been developed by Pierre Gy's and presented in two fundamental books[1,2] and in many later developments. Pitard[3] has also published a book based on Gy's sampling theory explaining variography in detail. A generic variogram is shown in Figure 3.

Gy has shown that the long-range Point Selection Errors, (PSE_1 and PSE_2), and the short term Point Selection Error (sum of Fundamental sampling error, FSE and Grouping and Segregation Error, GSE) can be estimated with a variographic experiment, in which N, a sufficient number of samples (minimum of 30 preferably more than 100) are collected systematically most often with equal time intervals. According to Gy's definitions the heterogeneity contribution is a structural property of the material. The heterogeneity contribution of every sample can be estimated,

$$h_i = \frac{a_i - a_L}{a_L}\frac{M_i}{M}, i = 1,2,\ldots,N \qquad (12)$$

in which i is the sample or increment number, a_i is the analysis result of sample i, a_L average of the process sequence, M_i is the weight of sample i and M is the average sample mass. If the sample size is proportional to the process flow or the flow rate correlates with the analysis result, the heterogeneity contributions and the average concentrations must be statistically weighted.

$$a_L = \frac{\sum M_i \cdot a_i}{\sum M_i} \qquad (13)$$

The heterogeneity contributions are the most often used format used as the basis for the variogram, V_j (as a function of sample lag interval j)

$$V_j = \frac{1}{2(N-j)}\sum_{i=1}^{N-j}\left(h_{i+j} - h_i\right)^2, j = 1,2,\ldots,\frac{N}{2} \qquad (14)$$

From the variogram variance and standard deviation estimates can be solved for the three principal sampling modes (systematic, random or stratified) thus providing useful information for optimising specific sampling plans[4,5].

Variographic analysis provides an estimate of the intercept V_0, also known as nugget effect, at zero lag. The intercept V_0 is a sum of several components, FSE, GSE and the variance of all the other components of the incorrect sampling errors, ISE, e.g. delimitation error and extraction error that potentially were not partially or fully eliminated. Because all the random errors of the sampling process are included in the intercept V_0, it provides an estimate of the precision of online sampling and analysis system. N.B. A proper variographic analysis must be made on accurate (unbiased) data.

The intercept V_0 is related to the zero point variability; it is the variance that would occur if the same sample could have been taken twice. It is the best obtainable estimate of the minimum sampling variance (minimum possible error, MPE) expected in process sampling in a one-dimensional lot such as process stream. The theory of sampling identifies this value as minimum practical error[6].

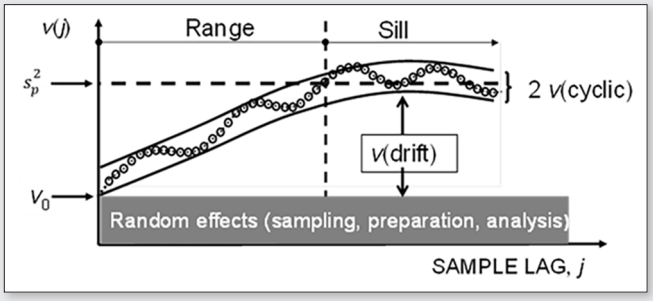

Figure 3. Generic variogram and its components. The variogram delineates the individual components of random and periodic process variances as well as the variance of a zero lag sampling point (plus the analysis error); s_p^2 is the long-range process variance, aka the sill, of a stationary process.

The variographic analysis of metallurgical sampler

The MSA 2/50 variograms were studied using two time series, each based on 10 or 15 minute intervals. The data used in the study were from a Courier XRF on-line elemental analyser data. Courier analyses the multiplexed sample streams at regular programmed intervals and provides elemental analysis data suitable for variographic study. Variograms calculated from the Courier data were used to extrapolate the V_0 intercept. Estimates of the relative standard deviations as a function of a sampling interval of systematic and stratified sampling modes were calculated by using Gy's method explained in detail in references 1 - 3. Figures 4 and 5 show the time

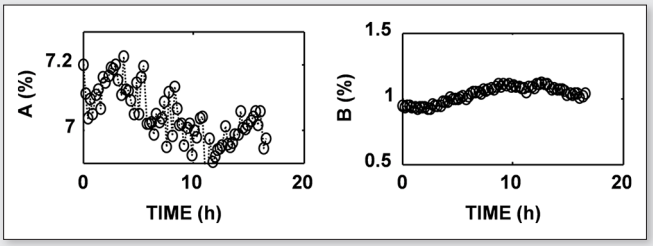

Figure 4. Time series plot of elements A and B, measurements at 15 minute intervals.

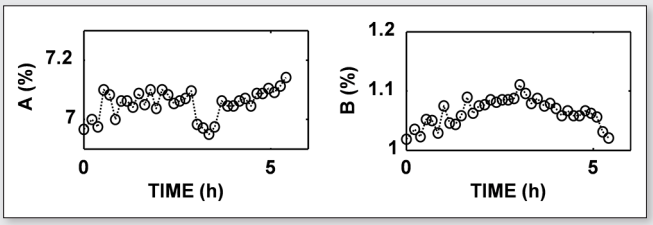

Figure 5. Time series plot of elements A and B, measurements at 10 minute intervals.

series of the elements A and B. Figures 6 and 7 show the corresponding variograms calculated together with the relative standard deviation graphs as function of a sampling interval. These values can be used to calculate standard deviations of, and confidence intervals for, point estimates and the average of several samples for the different sampling modes[5]. If n samples are taken with intervals j from a lot (systematic sampling), or one random sample from every consecutive substrata of length j (stratified sampling), the relative variance of the mean of the lot, a_L is

$$s^2_{a_L} = \frac{s^2_{sy/st}}{n} \quad (15)$$

where is $s^2_{sv/st}$ is the variance estimate of systematic or stratified sampling mode at lag j obtained from the variographic analysis.

Estimation of the Fundamental Sampling Error FSE

The fundamental sampling error gives an estimate of the relative sampling variance after all other error sources have been eliminated (if/when possible). FSE is caused only by the properties and of the sampled material.

$$\sigma^2_{FSE} = fgcld^3\left(\frac{1}{M_S} - \frac{1}{M_L}\right) \quad (16)$$

in which f is the particle shape factor, g is granulometric factor, c is mineralogical composition factor, $l = (d_l/d)^{1.5}$ is liberation factor (d_l is liberation size), d nominal top size of the sample, M_S mass of the sample and M_L mass of the lot, respectively. If the material is ground below the liberation size, as was done here, the liberation factor should be set as = 1. If the sampled lot is much larger than the sample, equation 17 simplifies to

$$\sigma^2_{FSE} = fgcld^3\left(\frac{1}{M_S}\right) \quad (17)$$

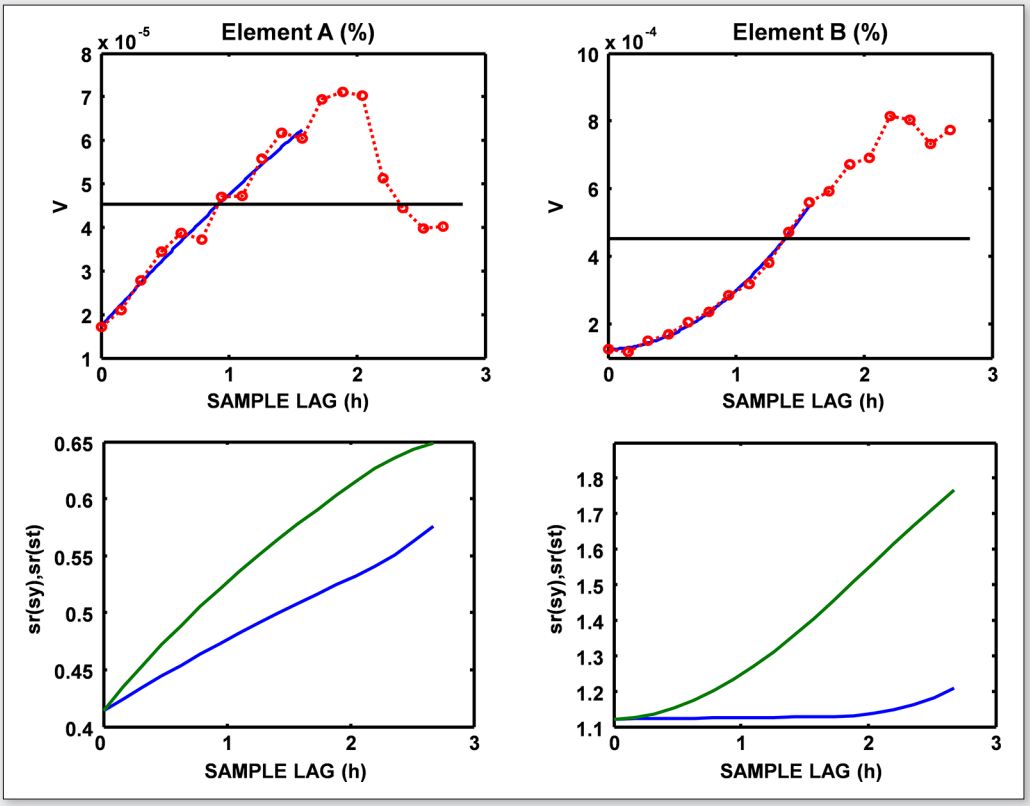

Figure 6. Flotation feed variograms of elements A and B instrumental analysis (Courier) in 10 min intervals (upper panels). Lower panels show estimated relative standard deviations for stratified (green) and systematic (blue) sampling modes.

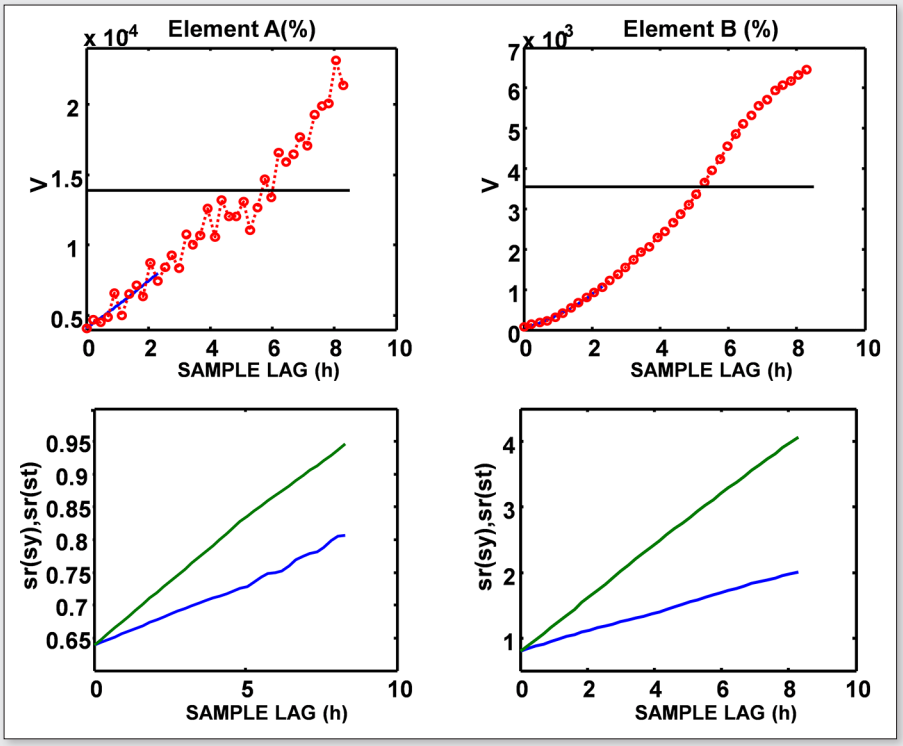

Figure 7. Flotation feed variograms of elements A and B instrumental analysis (Courier) in 15 min intervals (upper panels). Lower panels show estimated relative standard deviations for stratified (green) and systematic (blue) sampling modes.

The composition factor is estimated as

$$c = \frac{\left(1-\frac{a_L}{\alpha}\right)^2}{\frac{a_L}{\alpha}}\rho_c + \left(1-\frac{a_L}{\alpha}\right)\rho_m \qquad (18)$$

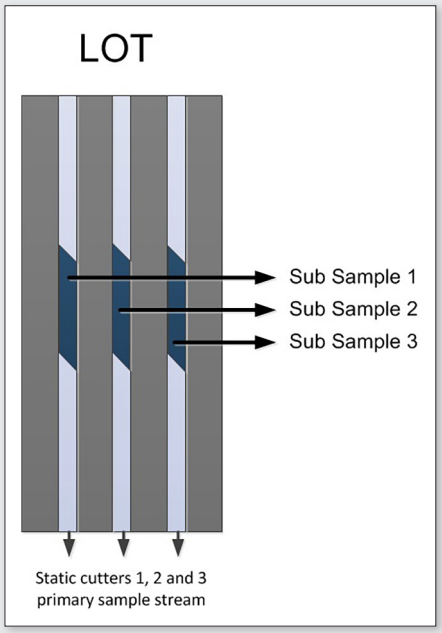

Figure 8. Schematic illustration of the experimental setup of the sub-sample study.

where a_L and α are the average concentration in the lot of and in the mineral that contains the element to be analysed, respectively and ρ_c and ρ_m are the densities of the mineral containing the analyte and the gangue (matrix).

Figure 8 shows schematically how the samples were cut with the moving cutters. In MSA 2/50 each of the three static cutters with equal width cut 8.3% from the process stream as the primary sample; in total the static cutters take one fourth of the process stream, in this case 600 m^3/h. The total flow-rate at the moving cutters is 150 l/min. The volume of the increments taken by cutters is 1.9 litres (5.6 l total sample). During the study the solids content of the slurry was 52% (m/m). Thus the individual sample mass was approximately 1.3 kg.

For estimating FSE for element B, some assumptions have to be made. The shape factor *f* is assumed to be 0.5 (meaning that particles are assumed to be spherical), and the granulometric factor *g* is set as 0.5 assuming that the material is classified. Element B concentration in dry slurry was 1%, and the density of the mineral containing it, α = 6 g/cm^3 while the density of gangue is 2.7 g/cm^3. Based on these data the composition factor *c* = 270 g/cm^3 can be calculated; the liberation factor *l* = 1 was used. FSE error estimates are based on 0.2 litre (180g) final increment size (taken with a secondary sampler), from which a 20 g laboratory analysis sample was finally extracted. The estimates of the relative standard deviation of the FSE at different sub-sampling stages and sample preparation were calculated and are presented in Table 3. As expected, a 20 g sample displays the largest sampling variance, 0.32% as relative standard deviation, while the primary increments only contribute 0.0035%. The reason for these small FSE is the small particle top size, which is about 150 µm only. The largest FSE for metallurgical sampling of elements with approximately 1/10% content in the

Table 2. Results of the variographic experiment for flotation feed elements A and B and Solids-%.

Estimated quantity	Lag (min)	Element A	Element B	Solids%
V_0	15	4.09E-05	6.47E-05	3.90E-05
	10	1.71E-05	1.26E-04	5.89E-05
Average, a_L (%)	15	7.05	1.03	40.99
	10	7.06	1.06	40.63
Relative Standard Deviation s_0 (%)	15	0.64	0.80	0.62
	10	0.41	1.12	0.77
Relative Long Range Standard Deviation of the process, s_p (%)	15	1.78	5.96	1.56
	10	0.67	2.13	1.13

flotation feed can be expected to be of the magnitude of relative standard deviation less than 0.1%. Much larger errors are caused during preparation of the analytical sample from the composite sample.

Discussion

Figure 9 shows Gy´s classification of the full complement of sampling errors. According to results of this study it is estimated is that the sum of the short term variation and analysis errors is responsible for the largest contributions to the total error for the flotation feed, in case of element B the relative standard deviation was estimated to be s_0 = 1.5% (ANOVA) and 0.8–1.1% (variographic experiment). These errors are caused by the short-range heterogeneity within the 1-D material flow, by the manual preparation of the analysis sample and by the laboratory analysis. In the variographic study s_0 was obtained by extrapolating the variogram to lag zero and it

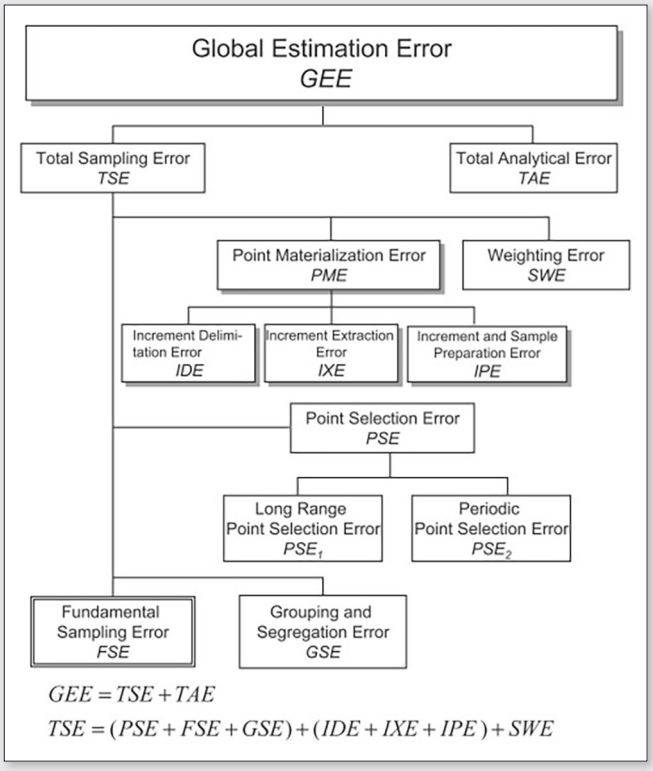

Figure 9. Gy's complete classification of sampling errors according to source[4].

includes the short-range and Courier analysis variations. The long range variation in the process caused by changes in the process feed in ANOVA study was s_{lr} = 2.3% and in the variographic study 6 and 2.1%, by comparison.

The main error sources in the sub-sampling study were likely operator errors during manual sub-sampling and manual sample preparation for laboratory analysis, and the actual analysis error, which could be estimated in this particular experiment. The FSE in the sub-sampling study is small due to small particle size S_{FSE} *(TOTAL)* = 0.34%.

According to the variographic experiment, the total element B measurement variance (15 min lag), V_0 = 6.47E-05, which includes the short term process variance and the variance caused by on-line XRF analyser. The intercept V_0 is the best possible estimate of the minimum practical (MPE) error for the present process sampling system[6].

MPE includes the fundamental sampling error, the grouping and segregation error, the analysis error and the point materialization errors. Therefore combined variance caused by fundamental sampling error, analysis error, grouping and segregation error and incorrect sampling error was during this study.

$\sigma^2_{MPE} = \sigma^2_{FSE} + \sigma^2_{TAE} + \sigma^2_{GSE} + \sigma^2_{PME} = 6.47 \times 10^{-5}$ for analyte B, which had on average 0.01052 mass fraction in a mineral form in the flotation feed. The relative error is thus: =1.12%.

The analysis of variance of sub-sampling study showed no significant bias between moving cutters, that is s^2_{bc} of elements A and B in Table 1 are nil. The difference between the dry solid material sampling from a conveyer belt and fine particle slurry sampling in flotation process is that even with a high solids fraction, e.g. 50% w/w, the volumetric solids fractions is about 25% v/v, which means that particle trajectories in slurries are also controlled by turbulent water flow and not only particle-particle interactions. Consequently, although the static cutters are not fully compatible with the theory of sampling in the sense that they do not cut a full cross-section from the process stream, the present results show that the mixing chamber before the static cutters is effective in randomising the slurry flow, essentially converting it into a fit-for-purpose 0-D sampling target at the time of cutting the primary increments before the moving cutters. For comparison, there has recently been developed an analogous full cross-section, vertical increment cutter sampler for pneumatically conveyed internally ducted two-phase (air/solid particles) aggregate sampling, Wagner & Esbensen[7]. In this solution the mixing is taken care of by the turbulent conducting transportation itself. Although addressing very different types of materials, both approaches share the prime objective of counteracting the

Table 3. Estimation of variance and relative standard deviation (%) of the fundamental sampling error (FSE) for element B assays at different stages of sampling and sub-sampling.

Source of variance	M_S (g)	σ^2_{FSE}	Relative Standard deviation (%)
σ^2_{FSE} static cutters	141120	1.20E-09	0.0035
σ^2_{FSE} moving cutters	3780	4.31E-08	0.021
σ^2_{FSE} sub sample	1260	8.93E-08	0.030
σ^2_{FSE} single increment	180	1.12E-06	0.11
σ^2_{FSE} laboratory analysis sample	20	1.00E-05	0.32
σ^2_{FSE} TOTAL		1.13E-5	0.34

bias-generation effects of vertical segregation in moving streams of matter.

PSE1 and PSE2, together with the analytical error, are the main contributors with the largest variation to the total measurement uncertainty. Increment and Sample Preparation Errors are largest sampling error sources, but it was impossible to estimate these individually for which reason they were included in the compound s^2_0 estimation. The fundamental error estimation shows how the total measurement uncertainty increases as sample mass is reduced; the only way to reduce the fundamental sampling error is to reduce the particle size and/or increase the composite sample mass. However the fundamental error is insignificant in the MSA 2/50 sample volumes and the Grouping and Segregation error (GSE) was also minimal according to the sub sample study.

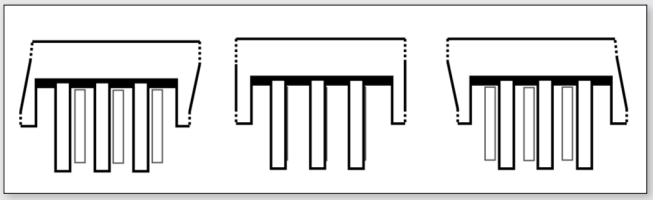

Figure 10. Operating principle of the MSA 2/50 Metallurgical sampler's moving cutters.

Conclusions

Based on this study the Outotec metallurgical sampler is able to represent the process variance reliably for elemental content and is able to substantiate timely process control actions. In the mineral beneficiation process the top particle size is very small, usually much less than 300 µm, and process flow velocities have to be sufficient effective to prevent the slurry particles from settling in the process piping, which reduces segregation in the sampled flow. The MSA sampler's feed box design controls the process stream flow velocity and randomizes the sample flow. According to the sub-sample study, when the process stream was cut by vertical static cutters no horizontal segregation could be observed.

If/when the total error budget estimates arrived at are acceptable for the operating company, this study has qualified the MSA 2/50 as a fit-for-purpose metallurgical sampler.

A complete cross section of the primary sample stream is cut by the moving cutter stage. The operating principle is shown in Figure 10. The moving cutters move at an adjustable velocity and frequency across the primary sample streams from the static cutters and thus provide the on-line analyser with a continuous sample by-pass flow that represents variations in the process validly and which can be sampled with a separate composite sampler for the metallurgical accounting purposes.

References

1. P.M. Gy, Sampling of Heterogeneous and Dynamic Material Systems, Elsevier, Amsterdam (1992).
2. P. M. Gy, Sampling for Analytical Purposes, John Wiley & Sons Ltd, Chichester (1998).
3. F.F. Pitard. Pierre Gy's Sampling Theory and Sampling Practice, 2nd Edn. CRC Press (1993).
4. P. Minkkinen. "Practical Applications of Sampling Theory", Chemom. Intell. Lab. Syst. **74,** 85–94 (2004).
5. P. Minkkinen. "Comparison of independent process analytical measurements – a variographic study", in Alfaro, M., Magri, E. and Pitard, F., Eds., 5th World Conference on Sampling and Blending, Gecamin Ltda, pp. 151-160 (2011).
6. L. Petersen, K.H. Esbensen. "Representative process sampling for reliable data analysis—a tutorial", J. Chemom. **19,** 625–647 (2005).
7. C. Wagner, K.H. Esbensen, "Final evaluation of 1/3-scale model sampler for horizontal pneumatic particulate material streams", Proceedings of World Conference of Sampling and Blending (WCSB 6). Peru (2013).

doi: 10.1255/tosf.56

Application of an integrated control system for continuous monitoring of sampling performance

C.S. Adams[a], K. Potts[b] and T. Neidel[c]
[a]**Craig Adams – Senior Technical Advisor, FLSmidth Pty Limited, 58-60 Dowd Street, 6106 Welshpool WA Australia.**
Email: craig.adams@flsmidth.com
[b]**Kenneth Potts – Design Engineer, FLSmidth Pty Limited, 58-60 Dowd Street, 6106 Welshpool WA Australia.**
Email: kenneth.potts@flsmidth.com
[c]**Tore Neidel – Engineering Manager, FLSmidth Pty Limited, 58-60 Dowd Street, 6106 Welshpool WA Australia.**
Email: tore.neidel@flsmidth.com

There is a need in the mineral processing industry for an integrated system to monitor and control ISO compliance of sample stations. This paper discusses development and application of a control system toolbox to meet this need and to deliver complete ISO compliant functionality. Traditionally, automated sampling systems rely on generic equipment control standards to operate the individual sampling components. The design of the sampling equipment in these systems may comply with ISO requirements, but does the integrated system also comply? This paper describes application of a standardized software library that integrates the requirements of ISO sampling standards with customized equipment control units via a supervisory control module, to bridge this gap. These libraries are based on many years of combined sampling, electrical and control engineering experience. This appropriate blend of expertise has enabled us to seamlessly integrate standalone, automated, sampling devices into ISO compliant sampling systems. All components have well-defined interfaces as well as common functional control and reporting mechanisms. The result is a fully integrated sample station that performs as an interconnected, ISO compliant quality system. The benefit of a standardized and integrated sample station is consistent production of reliable and accurate results. Trustworthy sample data gives Quality Assurance and Quality Control analysts, technicians and plant management a high degree of confidence that they have a full understanding of their material's properties and commercial worth. Confidence in sampling results is essential as the quality of the material is inexorably linked to a company's reputation as a reliable supplier of quality products and, ultimately, to their bottom line.

Introduction

Sampling systems can be designed, manufactured and installed so as to meet the requirements of ISO standards and Theory of Sampling (TOS).

However the operation and monitoring of these sampling systems is then left to the user to evaluate and monitor the performance of the sampling and to make changes as required to ensure continued unbiased performance. Too often the designers are asked to revisit installed systems to try to evaluate why the correct sampling protocol is not being achieved. The investigation often concludes that vital parameters have been altered and the installed control system no longer is able to produce the required primary or subsequent sampling.

In order to try to control the sampling process with continual monitoring of the necessary sampling parameters FLSmidth Pty Ltd embarked on a development program to integrate the various controls into a total control system which could provide the feedback necessary to instil operator confidence in the samples taken.

In 2014, the FLSmidth sampling development team designed and constructed a suite of software components that:

- Provided sample station control that follows TOS guidelines and complies with ISO standards
- Accesses software libraries modelled on the FLSmidth range of sampling products
- Ensures safe operation of the equipment
- Ensures robust and reliable performance of the equipment and system
- Provides user-friendly configuration and operation

The conceptual design of this software was presented at the Sampling 2014 conference in Perth, Australia, titled: "Control & Monitoring of International Organization for Standardization Compliance for Industrial Sampling Systems" – T Neidel, C Adams and R Shaw. This conceptual design has now been implemented in a fully automated Mineral Sampling System at a customer's iron-ore ship-loader installation. A second system has been constructed and waiting commissioning and another two systems are scheduled for completion later this year.

This paper presents and discusses the performance and operation of this Integrated Sampling Control System (ISCS) and demonstrates the advantages in its use.

Integrating the Sample Station and the Control System

The sample system mechanical layout and sampling process was designed in conjunction with the customer to provide a sampling protocol in accordance with *ISO 3082 Iron Ore – Sampling & Sample Preparation Procedure* (ISO 3082).

The sample system mechanical layout design followed acceptable sampling procedures selecting and integrating proven equipment into an ISO compliant process. The control system was built using function block libraries which allow station control system development to be simply a matter of selecting the function block components in a Lego® building block methodology, where a system is constructed by connecting pre-built building blocks. This minimises re-design and programming errors while promoting a well-defined structure with a consistent interface. In-built simulation functionality provided an excellent mechanism for off-line device and sequence testing providing a high degree of confidence before commissioning the system.

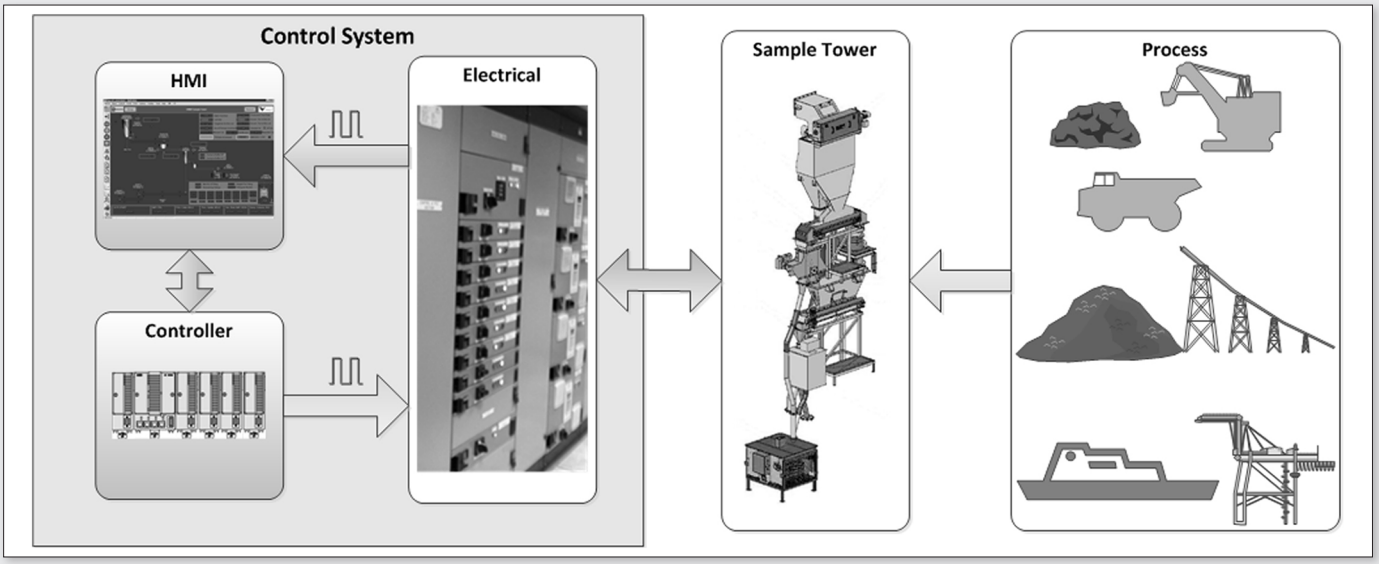

Figure 1. (a) Control system architecture (b) Sample tower and (c) Process schematics

Standard design principals were applied to the development of the ISCS using three standard FLSmidth products;

- ECS® (Expert Control and Supervision) – is a windows-based Human Machine Interface (HMI) for plant supervision and process control.
- Metis™ (Multi-Engineering Tool and Information System) is based on an object oriented control methodology especially designed for the cement and minerals industry. ACESYS is a standard library for consistent and reliable PLC programming.
- ACESys® (Adaptable Control Engineering System) – is a propriety tool for alignment of best practice engineering standards.

The control system uses a local, dedicated sub-control system to provide machine level control of sampling tasks. The system contains many advanced functions for trending, troubleshooting and remote reporting.

Emphasis was given to

- Safe operation
- Repeatable control

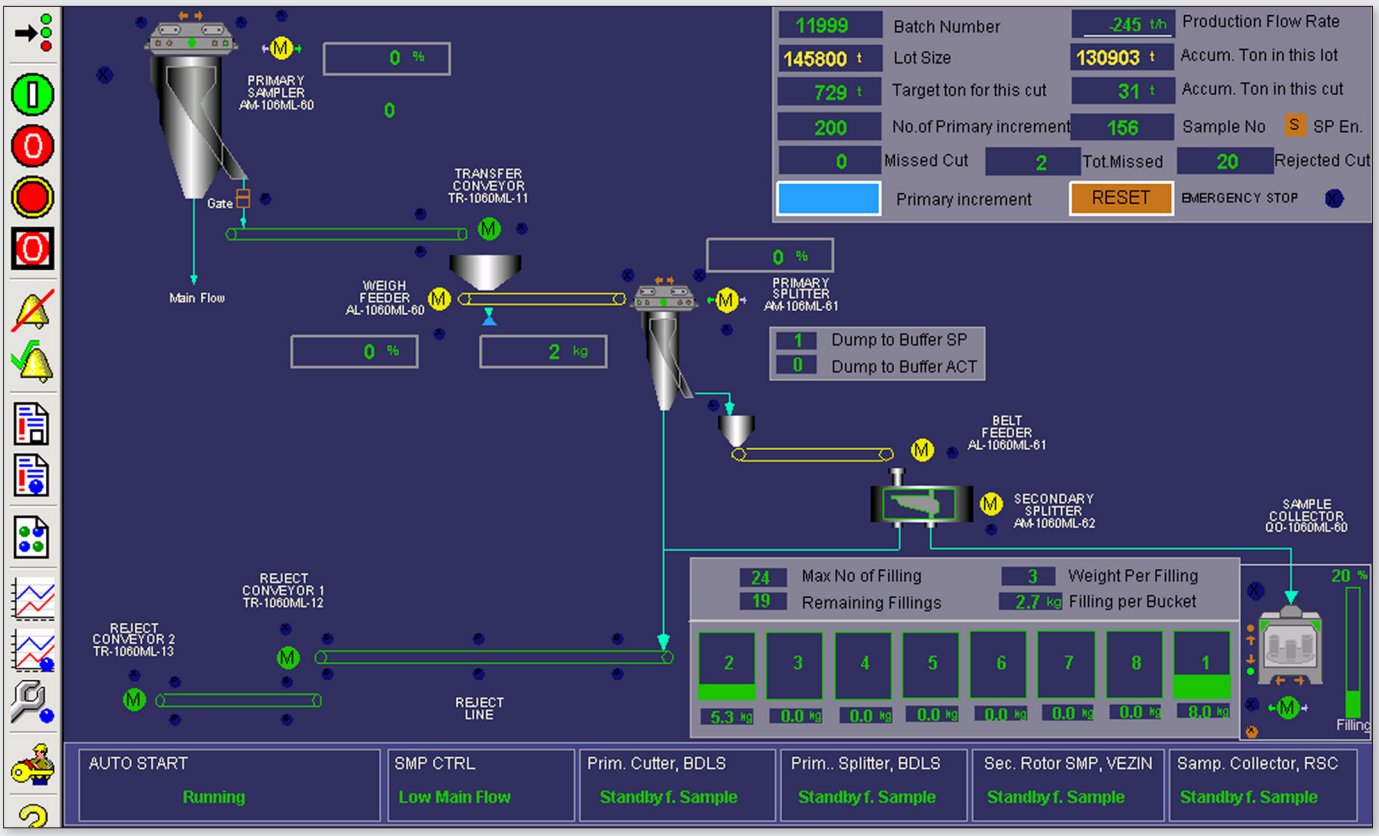

Figure 2. ISCS HMI graphical overview screen

- Adaptable to the customers process
- Ease of use and maintenance
- Full lifecycle support
- ISO 3082 Compliance

Figure 1 shows the relationship of the control system to the sampling station equipment and the ship loading process.

One of the features of the ISCS is the ability to provide transparency of the sample system activities. The Human Machine Interface (HMI) system is the window into the ISCS. It provides a series of real-time animated screens that display the current and historical status of the sample station. The benefits provided are;

- Monitor the operation and performance of the sampling system in real time – typical graphical overview screen is illustrated in Figure 2.
- Provide alarm and warning information – the notification can be related to;
  - ISO violations
  - Sampling equipment failures
  - Process events – such as a chute blockage
- Provide information on how to rectify faults

Alignment with ISO standards

While ISO standards mostly deal with the mechanical aspects of the collection and handling of a sample, there is other functionality that the control system must take into account. Therefore the software development must also consider the alignment to and application of ISO rules.

The ISCS control system we are describing in this paper is generic to the mineral sampling industry, but the discussion and examples relate to a system installed at an iron-ore ship-loader installation where the software was tailored to meet *ISO 3082 Iron Ore – Sampling & Sample Preparation Procedure*. The control system can be adapted to any other sampling standard.

The iron ore control system software has the following ISO 3082 monitoring and control features embedded in the code:

- Sampling methodology
- Cutter velocity control
- Safety of operations
- Robustness of sampling installation

Sampling Methodology

The top level function of the control system software is the selection of the appropriate sampling method.

The steps for establishing a sampling scheme are mostly decided by the sampling design group. However the control software uses ISO3082 to make decisions determining the number of increments and timing of the intervals between initiating a primary increment, based on QA/QC or production manager input of lot size and quality variation.

The design of the system is such that the initiation and handling of a sample lot is automated, eliminating operator-entry or lot- calculation errors.

For a customer specified lot, the lot information must be provided to the sample station control system. When the lot ID and size are transferred to the system (via the Plant Control System or a Laboratory Management System) a new lot/batch is initiated.

The number of primary increments and the tonnage target are automatically calculated by the system and then the tonnage accumulators are reset.

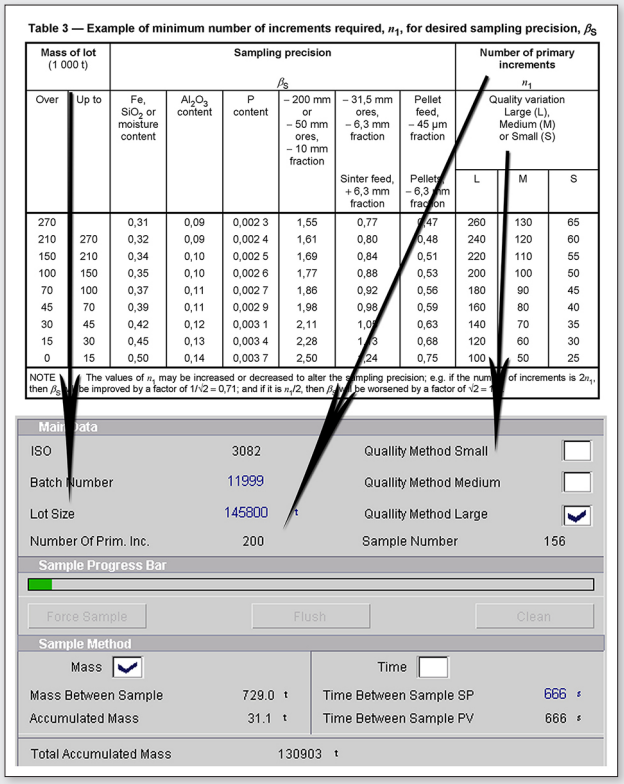

Table 3 — Example of minimum number of increments required, n_1, for desired sampling precision, β_S

Mass of lot (1 000 t)		Sampling precision β_S						Number of primary increments n_1		
Over	Up to	Fe, SiO_2 or moisture content	Al_2O_3 content	P content	– 200 mm or – 50 mm ores, – 10 mm fraction	– 31,5 mm ores, – 6,3 mm fraction Sinter feed, + 6,3 mm fraction	Pellet feed, – 45 µm fraction Pellets, – 6,3 mm fraction	Quality variation Large (L), Medium (M) or Small (S)		
								L	M	S
270		0,31	0,09	0,002 3	1,55	0,77	0,47	260	130	65
210	270	0,32	0,09	0,002 4	1,61	0,80	0,48	240	120	60
150	210	0,34	0,10	0,002 5	1,69	0,84	0,51	220	110	55
100	150	0,35	0,10	0,002 6	1,77	0,88	0,53	200	100	50
70	100	0,37	0,11	0,002 7	1,86	0,92	0,56	180	90	45
45	70	0,39	0,11	0,002 9	1,98	0,98	0,59	160	80	40
30	45	0,42	0,12	0,003 1	2,11	1,04	0,63	140	70	35
15	30	0,45	0,13	0,003 4	2,28	1,13	0,68	120	60	30
0	15	0,50	0,14	0,003 7	2,50	1,24	0,75	100	50	25

NOTE The values of n_1 may be increased or decreased to alter the sampling precision; e.g. if the number of increments is $2n_1$, then β_S will be improved by a factor of $1/\sqrt{2} = 0{,}71$; and if it is $n_1/2$, then β_S will be worsened by a factor of $\sqrt{2} = 1{,}41$.

Figure 3. Sampling Scheme – Main Data Screen

The control system calculates the number of primary increments based on Table 3 of ISO 3082 (Figure 3).

ISO 3082 defines three methods for sample collection:

- 6.1 Mass-Basis Sampling – where increments shall be taken at fixed mass intervals
- 6.2 Time-Basis Sampling – where increments shall be taken at fixed time intervals
- 6.3 Stratified Random Sampling within Fixed Mass or Time Intervals – where a randomized sampling interval is introduced to either the mass or time based schemes in 6.1 or 6.2

The client's preference was for Mass-Basis Sampling and the control system initiated the primary sampler from an upstream belt weigher (weightometer) to provide the ore mass flow rate required. Time-Basis sampling was also incorporated as a backup method for the Mass-Basis Sampling in case the upstream weightometer failure. The software provides the ability to switch from mass based sampling to a time based regime (and back) by the selection of a check box on an operator interface faceplate. All sample station tuning and configuration parameter changes are protected by a password control scheme.

The first increment of a new lot is taken at a randomly generated target tonnage after commencing the sampling operation (in accordance with 3082 – 6.1.4). Subsequent increments are taken at the fixed mass intervals until the entire lot has been processed.

The installation uses a variable speed cutter as required by the standard to match the cutter velocity to the mass flow rate. The system has provision to check the weight of the primary increment to determine if the increment is within the ISO 3082 specified 20% tolerance. If the primary increment is Out Of Specification (OOS), the sample is rejected and an immediate resample is initiated.

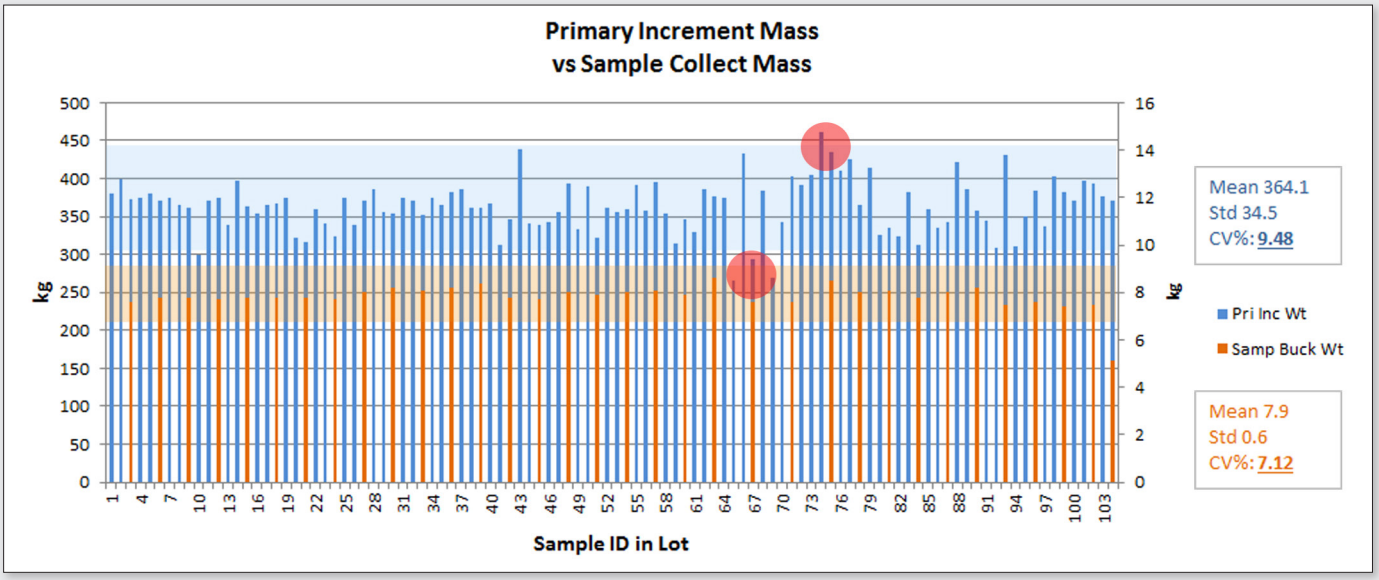

Figure 4. Primary increments vs. sample bucket mass – selected OOS samples highlighted

Figure 4 shows data from the installed site of the catch weights of 104 primary increments, with the 370 kg increment weight target, and the blue lines indicating the 20% tolerance level which was exceeded by the OOS samples that were rejected. Also displayed is comparative data showing the sample mass collected in the sample bucket, target mass 8 kg, the orange lines indicating the 20% tolerance level.

Cutter Velocity Control and Monitoring

The ISO standard defines in detail the design of the cutter geometry and its positioning for the collection of the primary increment. Details of the mechanical design and their meticulous application of the ISO standards are outside the scope of this paper. However section 5.1.4.1 of ISO 3082 covers the velocity of the primary cutter moving through the falling ore stream. The installed control system software provides a user interface screen (faceplate) for velocity control. The object is to minimise Delimitation Error (DE), hence eliminating bias in the sampling process. (Refer to "Sampling of Particulate Materials Theory and Practice" By Pierre Gy, Chapter 17, on Increment Delimitation Error).

The ISO standard also defines the mass of the increment to be taken (mechanically or manually) by a cutter-type sampler from the ore stream at the discharge end of the conveyer belt (ISO 3082:2009 – 5.1.4.1) by the following equation:

$$m_1 = \frac{q'1}{3{,}6v_c}$$

The relationship between cutter velocity and the production ore flow for a defined catch weight (in this case 370 kg) as is shown in Figure 5.

The actual velocity deviation through the ore stream can be monitored by a Linear Sampler monitoring system and it reports the

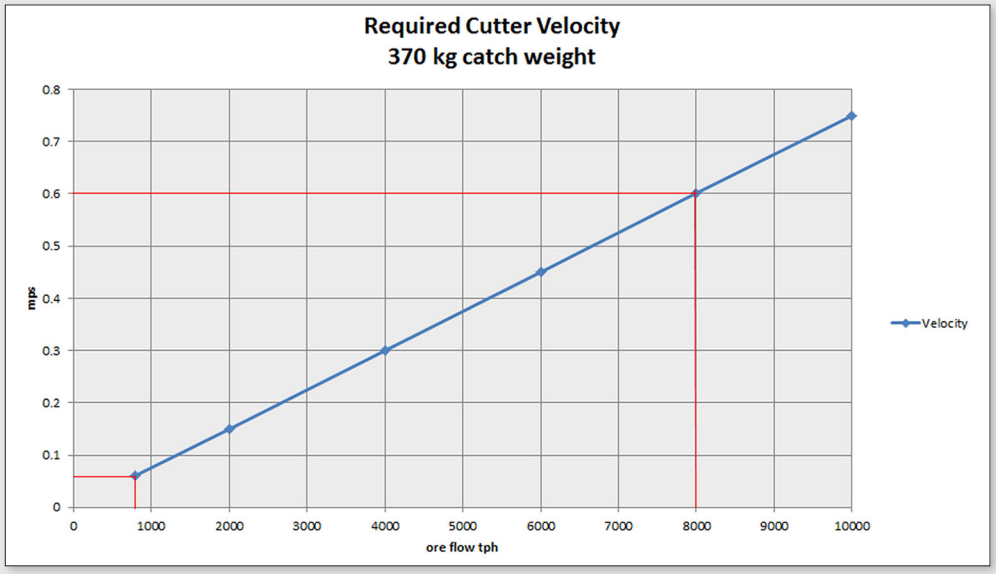

Figure 5. Proportional VSD speed vs. ore flow rate

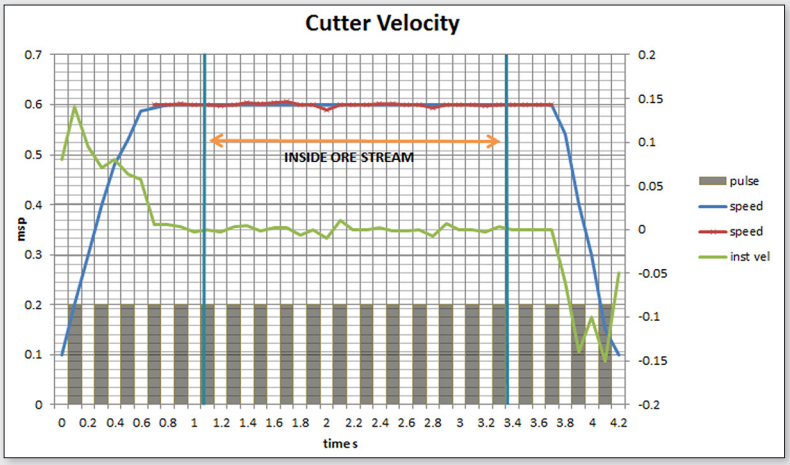

Figure 6. Cutter velocity vs. time

consistency of the cutter spoon's velocity through the ore stream and displays a reading of the sampler's motion (as a percentage of the average travel against the set point speed).

Figure 6 shows the cutter velocity over a period of 4.2 seconds (at 100 msec intervals).

Operational Safety and Standards

Operational safety is of critical importance to industrial operations and the control system allows observation, monitoring and control of the sample station from a safe environment. The ISCS aligns with ISO 3082 Section 7.2 Safety of Operations, and also incorporates all necessary safety standards as required by international regulations.

Robustness of the Sampling Installation

Failure of sampling systems is often a result of poor maintenance. Cutter blades are not replaced, cutter speeds not checked and sample masses not recorded. Bias tests on A and B primary samples are only checked at significant audits. While the ISO 3082 refers to the mechanical robustness of the sampling equipment and this should also be applied to the control and monitoring process.

Based on reliability data and experience the control system was strengthened by incorporating the following features:

- Redundant Central Processing Units and power supply
- Sampling equipment retry method (example – if a gate is blocked by a rock; retry to open and close the gate to dislodge the rock. These are common occurrences and should not cause the system to fail on the first attempt).
- Function to re-sample primary increment if OOS – in compliance with ISO 3082 6.1.1. Part C.
- Maintenance scheduling based on operation time.

Development Challenges

Bridging the gap between theory and reality presents challenges such as aligning the timing of the ore flow rate on the feed conveyor belt to the activation of the primary sampler. The production belt weightometer, being 53.7 meters before the primary sampler, with a belt speed of 3.72 meters/sec, resulted in a flow rate lag of 14.4 seconds.

$$t = \frac{53.7\ \text{m}}{3.72\ \text{mps}} = 14.4\ \text{seconds}$$

The inconsistent flow rate presented a problem for the mass based sampling method, raising the question of how to align the cutter velocity to the instantaneous flow rate. The challenge was

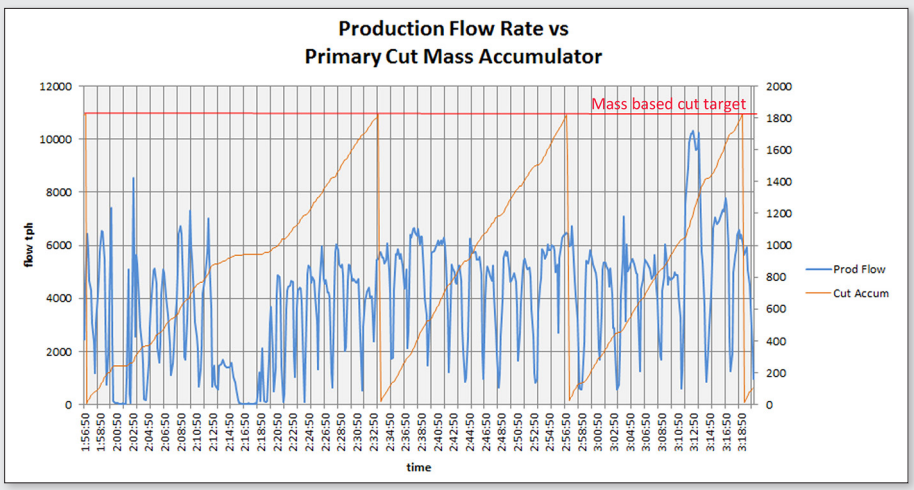

Figure 7. Production flow – note highly variable feed flow rate

Table 1. Device data blocks for sample tracking of primary sampler and splitter

Name	Data Type	Attributes	Description
MinSampleNo	Dint	retain hidden	Minimum Sample Number
MaxsampleNo	Dint	retain hidden	Maximum Sample Number
NoOfMainCuts	Dint	retain hidden	Number of Main Cuts
Weight_SP	Real	retain hidden	Weight Setpoint
Weight_PV	Real	retain hidden	Weight Actual
Weight_Tolerance	Real	retain hidden	Max Allowed Weight Tolerance (kg)
TotAccMass	Real	retain hidden	Total Accumulated Material Current Batch (kg)
BatchNo	Dint	retain hidden	Batch Number
AB_Cut	Bool	retain hidden	0 = A-cut, 1 = B-cut
LogType	Int	retain hidden	0 = OK, 1 = Weight Fault

resolved providing a consistent primary increment mass to meet the ISO standard CV requirement. Figure 7 shows the varying flow rate. As explained earlier timing is critical to ensure the cutter velocity is matched to the actual flow rate of ore, as it enters the cutter spoon, to ensure that the correct sample mass is collected in the increment as given by the following formula.

Sample Data Tracking

Event logs are an important requirement of any control system. The Integrated Sampling Control System provides an audit trail of sampling activities, sample masses and events. The software collects relevant sample data at every stage of the sampling process. The sampling process data is event driven and provided in real-time.

The ISCS also provides interpretive graphing of data so that trends can be monitored for sampling process analysis and diagnostic information.

Benefits of an Integrated Sampling Control System

Generally there are two common methods of programming and interfacing the vendor package to the plant a mineral handling or processing control system. They are:

- Typically during the construction of a mineral handling or processing plant, the principal contractor integrates the sampling system into the required area of the plant. Similarly the principal contractor integrates the control of the sample system into the plant control system; but this may introduces risk, due to the generic engineering integrator having limited sampling knowledge or functional understanding of sampling requirements.
- The sampling equipment designer provides an integrated packaged solution, where control is implemented with the sampling system. This methodology takes into account the complexities of sampling systems, conformance to sampling standards and the application of the manufactures expert knowledge.

The equipment designer is the expert in understanding and controlling the mechanical components and processes of their products. The operation of a sampling system and the control of the sampling equipment **is *not* a material handling application**. It is far more complex, as has been demonstrated in this paper. Generic control system engineers have, at best, a limited understanding of TOS and/or ISO requirements and therefore find it difficult to provide and integrated control system for the sample station.

A key benefit of correct integration of the sample station and control system is that the system designer is able to provide support (including remote support) over the life cycle of the system.

Conclusions

The Integrated Sampling Control System offers a reliable, safe and repeatable control system that allows operators to monitor and control the sampling parameters in accordance with TOS and ISO 3082 guidelines.

It provides the operator with:

- Security that the sampling system operates as it was designed and installed, and provides an integrated and accountable quality system.
- Detailed primary sample information.
- Correct sample increments for variable lot sizes.
- Monitoring of cutter velocity
- Advice to ensure programmed maintenance is performed.
- An audit trial of all sampling operations.

The ISCS can give the confidence when asked “Is your sampling system ISO 3082 compliant?”

Acknowledgements

Darryl Stevens, Global Product Manager – Sampling (FLSmidth), is the main sponsor through his sampling industry experience with practical application examples has had him initiate a process to ensure FLSmidth can offer an integrated system approach.

Rod Shaw, Senior Design Engineer – Sampling specialist (FLSmidth), responsible for design and consulting of sampling projects.

Finn Kousgaard Poulsen, Technical Manager (FLSmidth) & Johan Gajmark, Systems Engineers (FLSmidth), are responsible for the practical implementation of the sampling libraries into the FLSmidth standardized package.

References

1. SAI Global – 2009 – ISO 3082:2009 Iron Ores – Sampling & Sample Preparation Procedures.
2. Sampling 2014 – Control & Monitoring of International Organization for Standardization Compliance for Industrial Sampling Systems.
3. Gy, Pierre, 1979. Sampling of Particulate Materials Theory and Practice.

doi: 10.1255/tosf.60

Design advances and operational studies for the True Pipe® Sampler: A symmetry based unit for reliable sampling of pressurised particulate streams

A. Fouchee[a] and R.C. Steinhaus[b]
Multotec Process Equipment, P.O. Box 224, Kempton Park, 1620, South Africa. E-mail: [a] annelizef@multotec.com, [b] rolfs@multotec.com

Obtaining representative samples with minimised sampling errors, is critical for calculating accurate metallurgical mineral balances on process plants. A challenging situation exists, where no acceptable, robust or economically viable sampler has been commercialised for sampling of one-dimensional pressurised slurry pipelines yet. The design of the True Pipe® in-line sampler is based on the principle of symmetry, as described by Dominique François-Bongarçon[7], and also operates on a fail-safe principle for control on the synchronous opening and closing of identical valves for the sample chamber. Previous test work on the True Pipe® in-line sampler indicated that the prototype sampler is reliable within certain tolerances, initially indicating the concept could well be a viable design option. This paper presents the results from further test work, which mainly investigated three sampling phenomena in more detail, by examining classical one dimensional sampling, with the aid of an automated valve actuator. Firstly, the transient effect, which originates from the disruption in laminar particle flow. Secondly, the effect of split sampling, where the portion of the stream is sampled, as well as the full stream. Thirdly, the effect of symmetry is confirmed. The expected accuracy level of the True Pipe® in-line sampler is also evaluated for varied material conditions. Advances on the design include the ability to sample the entire pressurised particulate stream in a safe operating condition, by making use of a mechanical actuator for synchronous opening and closing of the sample chambers, as well as improved control on the valve opening and closing cycles.

Introduction

The need for increased accuracy of sampling in a mining process plant environment is driven by the reliability and confidence level that can be placed on the samples used for metallurgical accounting, official company reports and financial statements to comply with the increased requirements of corporate governance principles and guidelines as laid out in the AMIRA code[1]. Case studies[2] show that incorrect sampling protocols and equipment may have a crippling financial effect for the mine, but applying correct theory of sampling may save money. These studies underline the importance of installing correct sampling equipment on tailings streams.

Tailings streams are often pressurised horizontal one-dimensional pipe lines, which limit the application of conventional cross stream sampling equipment and for which there has to date not been a robust reliable TOS-compliant sampler solution presented. Some options available for sampling pressurised slurry streams are the t-piece bypass valve, poppet samplers and pressure pipe samplers. All of which fail to comply with TOS principals[3].

To honour the fundamental rule for correct sampling and sample processing, all parts of the ore, concentrate or slurry to be sampled must have an equal probability of being collected and becoming part of the final sample for analysis[4,5]. Poor precision may be improved by replicate samples or stringent control on sample preparation and analysis[6], but this will not eliminate bias once it is present. Correct design of sampling equipment and sampling systems can help to eliminate or at least minimise sources of bias to acceptably low levels.

Upholding the principle of symmetry[7], proposed by Dominique François-Bongarçon, where any biasing mechanism should affect the sample and its reject in exactly symmetrical ways, ensures sample correctness.

Design of the True Pipe® in-line sampler

The designed application for the True Pipe® in-line sampler is for sampling of high pressure particulate streams in the mining process plant environment, currently specifically focussing tailings pipe lines where flow velocity of 6ms^{-1} and line pressure of 1600 kPa or more is common. The True Pipe® in-line sampler, shown in Figure 1, allows for two parallel flow paths with diameters equal to that of the main feed pipe to the device, which is connected with a small angle Y-piece at each end. Two valves are present in each of the flow paths, delimitating specific sample captured volumes.

Previous True Pipe® in-line sampler test work

Initial exploratory test work conducted on the True Pipe® in-line sampler last year showed that at a 95% confidence interval, no statistically significant difference could be detected on the difference in mean between the reference sample and sample from each of the two sampler legs, when a synthesized ferrosilicon-silica ore was tested in the unit[3].

Drawbacks on the initial design included:

- Difficult manual operation of valves
- Insufficient control on valve closing time
- Unsafe operational condition for sampling a full cross stream cut
- Synthesized ore did not fully represent fluid rheology as present in mineral processing plants
- Manual sample draining and extraction

Design improvements on True Pipe® in-line sampler

The design optimisation of the True Pipe® in-line sampler calls for evaluation of certain theories associated with fluid born particle sampling. Transient effect recognition, in order to establish the final plant footprint required for the sampler, is where the actuating of the valves would cause an upstream disturbance of the particulate

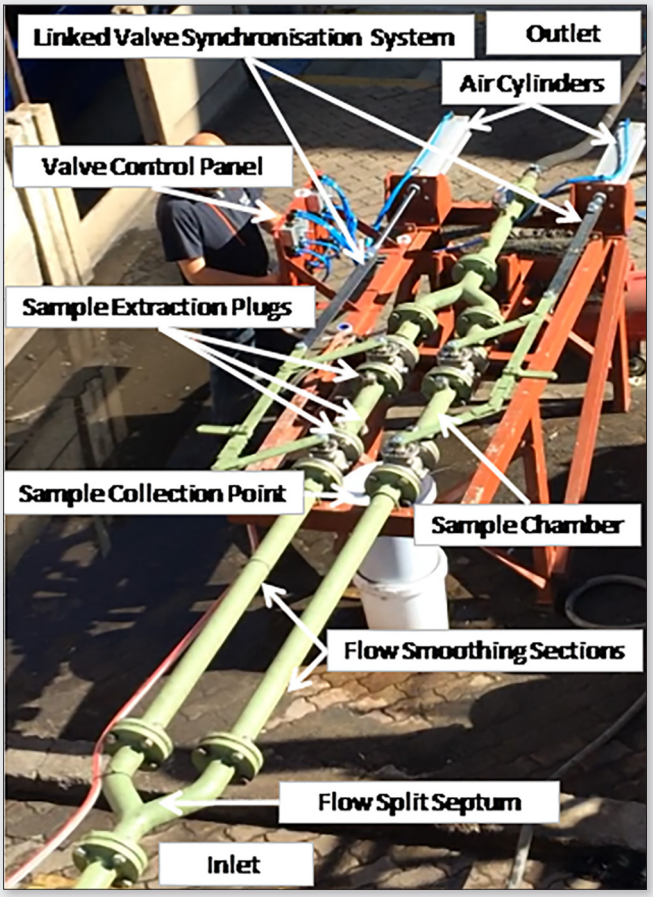

Figure 1. True Pipe® in-line sampler assembly

fluid stream at the septum of the Y-piece. Provided the valve closing time is faster than the time required for the disturbed particles to reach the first valve, the sample should be identical to the parent stream. This was to be evaluated by testing two different lengths of flow smoothing sections.

Another design consideration is identification of bias imposed on the particulate stream by split sampling. Inherent constitutional and distributional heterogeneities dismiss the theory of split sampling, where it is accepted that if a fluid stream is halved exactly, that each half of the stream is identical to the parent stream. Meticulous care was taken in the manufacturing of the device to ensure the best possible axial symmetry to halve the particulate flow.

The design of the True Pipe® in-line sampler respects the principle of symmetry by synchronous closing of actuated valves in the pipe line by means of a linked synchronising system. The principal is applied where the effect of any improperly delimitated particles misplaced into the sample chamber by the first valve would be identical to the effect of any particles improperly delimitated to the outside of the sample chamber by the second valve. One of the largest design improvements of the True Pipe® in-line sampler is the addition of actuators for automated control on consistent valve closing. The addition of the pneumatic actuators enables synchronous open and closing of either both valves in the same line (with the additional valves remaining open in the fail-safe position), or opening one set of valves and closing the other synchronously to enable cross stream sampling of the entire flow. Consistency of the valve closure speed was maintained by the addition of a pressurised air reservoir to constantly supply air to the control point where the air pressure to the valves is measured and monitored.

Methodology

A bias identification approach was followed in the design and operational assessment of the True Pipe® in-line sampler. This requires the sampler in question to be tested against a more recognised, reliable, correctly designed and unbiased sampling unit[8]. The integrity of the reference sample was ensured, by making use of an automated Multotec vezin sampler, which is TOS compliant, to obtain reference samples.

Test rig set-up

A closed re-cycle system as shown in Figure 2, consisting of a bottom discharge 5 m^3 feed tank and 6/4 AH slurry pump fitted with a variable speed drive, which was run at 850 rpm to achieve a measured in-line pressure of 300 kPa, which was the maximum pressure safely attainable with the test rig. Continuous mixing is established by aerating the feed tank with a Pachuca valve and recirculation of the particulate stream back into the feed tank. Class 10 2.5 inch industrial fibre reinforced rubber hose was used to connect the pump outlet to the sampler inlet and the sampler outlet to the vezin sampler feed chute. A special support structure, to which the sampler was secured with U-bolts, was manufactured to ensure level installation of the True Pipe® in-line sampler and to support the two additional 160mm air cylinder valve actuators attached to the synchronization linkage system for automated valve closure.

Material handling and sampling

Chrome tailings ore with a top size of 425 µm, from a chrome mineral processing plant discard line in the South African Bushveld Igneous Complex was sourced for this test work. Additional silica sand with a top size of 1mm was used for the test which required the ore composition to be synthetically altered. A slurry make up of approximately 45% solids by weight was maintained for all tests, except on the evaluation of this variable, where the solids were decreased to 25%.

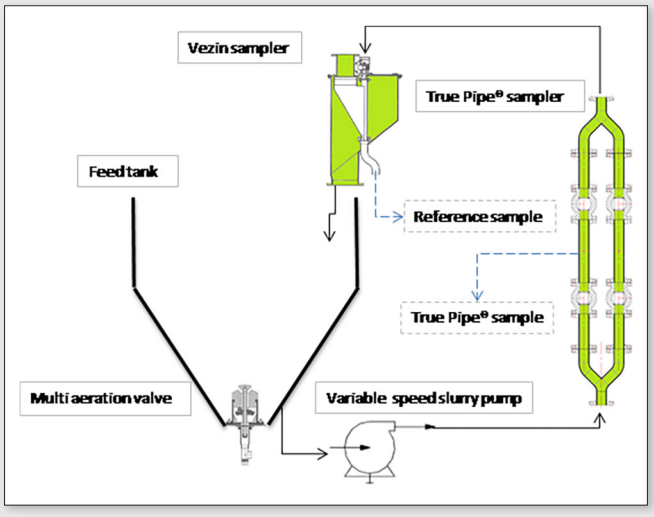

Figure 2. Schematic test rig setup for evaluating the True Pipe® in-line sampler

Samples are extracted from the sample chamber by washing particles out of the chamber and draining the sample into a container which is sealed immediately after sample extraction. Samples were dried at 90°C and the dry samples were dis-agglomerated and homogenised before being representatively split to a sample mass exceeding the prescribed minimum sample mass[3].

Representative sample splits were chemically analysed for major elements, specifically %Cr and %Si, by inductively coupled plasma atomic emission spectroscopy (ICP with OES), for which a certified reference material of similar matrix was used in the calibration of the instrument.

- For split sampling evaluation, a sample from the reference vezin sampler and each of the True Pipe® in-line sampler streams at 50% flow was taken. All other samples are collected from a full cross cut or slice of the particulate stream for each of the two legs.
- Transient effect recognition was enabled by fitting a 250 mm pipe extension before the sampling chamber and comparing this to a 1400 mm pipe extension where no transient fluid effects would be expected to be active.
- The application of the principle of symmetry was tested by introducing different valve closure speeds, all of which were synchronous and now automated.
- The operational effect of a change in solids concentration was evaluated by adding more water to the slurry make-up.
- Heterogeneity effects resulting from a change in ore type was tested by the addition of coarse silica sand to make up a synthesised ore.

Statistical methodology

The student's t-test is deemed satisfactory for obtaining 95% confidence limits on sampling data with reasonably consistent sample masses[8], when sample means or sample mean differences for two sample sets are compared. For comparison of three or more sample sets, repeated analysis of variance (rANOVA) is recommended. Both of these tests yield a two tailed p-value, which based upon a 95% confidence limit ($\alpha = 0.05$), is used to evaluate if the null hypotheses should be rejected.

Hypothesis tests[9] were conducted to evaluate the effect of design and operational variables on the %Cr mean difference between the reference vezin sample and the True Pipe® sample pair, (H_0: $\mu_{Reference} - \mu_{Sampler} = 0$; H_a: $\mu_{Reference} - \mu_{Sampler} \neq 0$). This test indicates whether the mean of the reference sample and the mean of the True Pipe® sample are statistically different.

An additional hypothesis test was conducted to evaluate whether the difference in sample mean between the reference vezin sample and the True Pipe® sample pair were statistically different under different design and operational conditions, (H_0: $[\mu_{ReferenceA} - \mu_{SamplerA}] - [\mu_{ReferenceB} - \mu_{SamplerB}] = 0$; H_a: $[\mu_{ReferenceA} - \mu_{SamplerA}] - [\mu_{ReferenceB} - \mu_{SamplerB}] \neq 0$). When the null hypothesis is accepted, the difference in mean between the reference and its corresponding True Pipe® sampler sample is not statistically different from the difference between another reference sample and its corresponding True Pipe® sampler sample. Thus accepting the level of uncertainty was not affected by the change in design, or operational variable for that test.

The use of rANOVA to test the equality of sample means is kept to analysis of split flow sampling means, where a vezin reference sample is compared to two samples from the True Pipe® sampler, each representing a 50% split of the original particulate stream. When a statistically significant difference exists between at least one of the True Pipe® sampler sample means and the vezin reference sample mean, the rANOVA hypothesis test should reveal this, (H_0: $\mu_{Reference} = \mu_{SamplerA} = \mu_{SamplerB}$; H_{a1}: $\mu_{Reference} \neq \mu_{SamplerA} = \mu_{SamplerB}$; H_{a2}: $\mu_{Reference} = \mu_{SamplerA} \neq \mu_{SamplerB}$; H_{a3}: $\mu_{Reference} \neq \mu_{SamplerA} \neq \mu_{SamplerB}$), although it is unable to identify which of the alternative hypothesis are valid.

Results and discussion

Flow 50% split sampling

The results from the split sampling rANOVA evaluation in Table 1 indicate that there exists a statistically significant difference between the sample means of the vezin sampler, True Pipe® Right sample and True Pipe® Left sample. The F-value of 9.05 exceeding the critical F-value of 3.19 and p-value of 0.00004, leads one to reject the null hypothesis of equality on sample means. The p-value of 0.044 on the paired t-test in Table 2, evaluating the mean difference in %Cr content between the vezin sample and the corresponding side

Table 1. Hypothesis rANOVA test on flow 50% stream splitting

Source of Variation	SS	df	MS	F	P-value	H_0: $\mu_{Reference} = \mu_{SamplerA} = \mu_{SamplerB}$
Between	0.51	2	0.26	9.05	0.00004	Reject Null Hypothesis
Within	3.97	72				
Subjects	2.61	24				
Error	1.36	48	0.03			

($\alpha = 0.05$, SS = sum of squares, df = degrees of freedom, MS = mean squares, F = F-statistic)

Table 2. Hypothesis paired t-test on flow 50% stream splitting

	Sample Size (N)	Mean %Cr (μ)	Sample Variance (σ)	Mean Difference ($\mu_{Reference} - \mu_{Sampler}$)	Variance (s^2)	P-value
Reference	25	11.69	0.061			
True Pipe® Right	25	11.62	0.047	0.073	0.043	0.044
True Pipe® Left	25	11.49	0.056	0.200	0.050	
H_0: $[\mu_{ReferenceA} - \mu_{SamplerA}] - [\mu_{ReferenceB} - \mu_{SamplerB}] = 0$				Reject Null Hypothesis		

($\alpha = 0.05$)

Table 3. Hypothesis t-tests on transient vs flow smoothing effect recognition

	Sample Size (N)	Mean %Cr (μ)	Sample Variance (σ)	P-value	Mean Difference ($\mu_{Reference} - \mu_{Sampler}$)	Variance (s^2)	P-value
Reference A	19	12.19	0.016	0.00000	0.517	0.033	0.013
True Pipe® Transient	19	11.67	0.014				
H_0: $\mu_{Reference} - \mu_{Sampler} = 0$		Reject Null Hypothesis					
Reference B	18	11.60	0.024	0.00001	0.341	0.050	
True Pipe® Non-Transient	18	11.94	0.022				
H_0: $\mu_{Reference} - \mu_{Sampler} = 0$		Reject Null Hypothesis					
H_0: $[\mu_{ReferenceA} - \mu_{SamplerA}] - [\mu_{ReferenceB} - \mu_{SamplerB}] = 0$					Reject Null Hypothesis		

($\alpha = 0.05$)

of the True Pipe® sample, indicates only a marginally statistically significant difference between the bias in True Pipe® Right and True Pipe® Left samples.

This indicates that the extreme effort to axially symmetrically split the particulate stream in two 50% flow streams does not help to eliminate a significant bias between the reference sample mean and the individual True Pipe® samples, but that this bias could be equal on each side of the True Pipe® sampler. This is a significant detail that should not be missed when one wishes to employ partial sampling techniques of plant process streams during process control operations.

Transient effect recognition

It is clear from both hypotheses tests in Table 3 that not only are there significant differences between the samples exposed to the transient disturbance and the samples which were subjected to a flow smoothing section prior to sampling with respect to their individual reference vezin samples, but also that there exists a statistically significant difference in the bias generated from each scenario. A p-value of 0.013 on the mean difference between the two design types shows that the non-transient True Pipe® sample, where a flow smoothing pipe of 1650mm was added before the sampling chamber, has a smaller bias than the transient True Pipe® sample, where there was no intentional flow smoothing.

Principle of symmetry

By throttling the main air valve to the system, the speed of automated valve closure was reduced consistently by a constant reduction in the air supply to the valve actuators from 8 bar to 4 bar. Table 4 indicates that again the means of the True Pipe® samples were not equivalent to the means of their paired reference vezin samples, but that the mean difference between the True Pipe® samples and vezin reference samples was not statistically significant, where a p-value of 0.441 does not reject the hypothesis, that the difference in sample means are equivalent.

These results validate the principle of symmetry, where the bias imposed by a disturbance in the particulate stream will be countered symmetrically if an identical disturbance is introduced at either end of the delineated sample.

Stream composition effect

A change in the particulate stream make-up, where the solids by weight concentration was changed from 45% to 25% did not improve the equality of True Pipe® sample means and vezin reference sample means in the 95% confidence limit hypothesis test results shown in Table 5, but with a p-value of 0.529 on the mean difference evaluation between the two True Pipe® sample sets, the bias in these two scenarios appeared to not be statistically significantly different. Thus the change in solids content of the fluid stream, did not affect the precision of the sampler.

Ore composition effect

The addition of silica sand with a top size of 1mm to the standard chrome tailings ore sourced for this test work highlighted the heterogeneity effect in sampling in this test. By measuring a statistically

Table 4. Hypothesis t-tests on principle of symmetry

	Sample Size (N)	Mean %Cr (μ)	Sample Variance (σ)	P-value	Mean Difference ($\mu_{Reference} - \mu_{Sampler}$)	Variance (s^2)	P-value
Reference A	18	11.94	0.024	0.00001	0.341	0.050	0.441
True Pipe® Slow Valves	18	11.60	0.022				
H_0: $\mu_{Reference} - \mu_{Sampler} = 0$		Reject Null Hypothesis					
Reference B	19	10.79	0.049	0.00000	0.399	0.050	
True Pipe® Fast Valves	19	10.39	0.018				
H_0: $\mu_{Reference} - \mu_{Sampler} = 0$		Reject Null Hypothesis					
H_0: $[\mu_{ReferenceA} - \mu_{SamplerA}] - [\mu_{ReferenceB} - \mu_{SamplerB}] = 0$					Do Not Reject Null Hypothesis		

($\alpha = 0.05$)

Table 5. Hypothesis t-tests on stream composition effects

	Sample Size (N)	Mean %Cr (μ)	Sample Variance (σ)	P-value	Mean Difference ($\mu_{Reference} - \mu_{Sampler}$)	Variance (s^*)	P-value
Reference A	9	12.31	0.017	0.00000	0.545	0.011	0.529
True Pipe® 45% solids	9	11.77	0.012				
H_0: $\mu_{Reference} - \mu_{Sampler} = 0$		Reject Null Hypothesis					
Reference B	9	13.18	0.037	0.00001	0.607	0.070	
True Pipe® 25% solids	9	12.57	0.099				
H_0: $\mu_{Reference} - \mu_{Sampler} = 0$		Reject Null Hypothesis					
H_0: $[\mu_{ReferenceA} - \mu_{SamplerA}] - [\mu_{ReferenceB} - \mu_{SamplerB}] = 0$					Do Not Reject Null Hypothesis		

($\alpha = 0.05$)

insignificant difference in the means of the True Pipe® Synthetic ore sample and its corresponding reference vezin sample a higher level of accuracy is attained with the True Pipe® sampler when this change in ore composition is made. A p-value of 0.986 for the synthesized ore means in Table 6 indicates that the means of the True Pipe® sample and vezin reference sample are not statistically different. The p-value of 0.003 rejecting the equality of the difference in sample means for the original standard and later synthetic ore, shows that the performance of the sampling unit will be effected by the ore type sampled.

The statistically significant difference in bias between the two different ores may be attributed to fluid rheology effects, where the fractional contribution of clay type minerals in the ore can easily increase the viscosity of the stream. When the viscosity of the particulate fluid is decreased, the effect of particle-particle interactions on the accuracy of sampling may also be decreased. The addition of silica to the original ore decreases the particulate fluid viscosity by surface chemical interactions between the silica particles and clay minerals. Positively charged ions from the wettened clay minerals will chemically bond to the negatively charged sites on silica particles, thus decreasing the concentration of dissolved ions in the fluid. Although this in turn will decrease the particle stability in the fluid, where coarser particles tend to settle faster, maintaining a particle line velocity of 4.5 ms^{-1} overcomes particle settling in the pipe column.

Conclusion

The design of the True Pipe® in-line pressurised particulate stream sampler, based on Dominique François-Bongarçon's principle of symmetry, strives to not only minimise sampler bias, but also achieve repeatable sampling results. The principle of symmetry inherently accepts a specific level of uncertainty, which is introduced in a symmetric fashion on either end of the delineated sample, such that a nett zero effect may be obtained. This design called for evaluation of certain theories associated with fluid born particle sampling to optimise future scale up of the prototype unit for industrial application. This test work confirms that the implementation of split sampling does not yield reliable sampling results from 50 percent cross stream cuts, no matter how careful the design tolerances and reliance on trying to control the particle lines of flow. One must rather design the unit to accommodate a full cross stream cut for meaningful results which once again validates and underpins TOS. It also identified that a difference in the magnitude of bias imposed by changing the pipe configuration for transient and flow smoothed, non-transient fluid conditions. The test work showed that a smaller bias was obtained when the particulate stream was subjected to a flow smoothing section before symmetric sampling. The principle of symmetry was confirmed by results showing no statistically significant difference in the magnitude of bias, when different synchronised valve closure speeds were implemented. The results of this test work also show that operational changes, such

Table 6. Hypothesis t-tests on ore composition effects

	Sample Size (N)	Mean %Cr (μ)	Sample Variance (σ)	P-value	Mean Difference ($\mu_{Reference} - \mu_{Sampler}$)	Variance (s^*)	P-value
Reference A	9	12.31	0.017	0.00000	0.545	0.011	0.003
True Pipe® Standard Ore	9	11.77	0.012				
H_0: $\mu_{Reference} - \mu_{Sampler} = 0$		Reject Null Hypothesis					
Reference B	9	8.97	0.036	0.986	-0.002	0.159	
True Pipe® Synthetic Ore	9	8.97	0.148				
H_0: $\mu_{Reference} - \mu_{Sampler} = 0$		Do Not Reject Null Hypothesis					
H_0: $[\mu_{ReferenceA} - \mu_{SamplerA}] - [\mu_{ReferenceB} - \mu_{SamplerB}] = 0$					Reject Null Hypothesis		

($\alpha = 0.05$)

as changes to the solids content of the particulate stream do not have a statistically significant effect on the sampling bias. Changes in the ore composition show a significant difference in the level of uncertainty. This phenomenon is attributed to the particle-particle interactions associated with the viscosity changes in the fluid.

The True Pipe® in-line sampler design investigations conducted to date, has sufficiently proven the concept of use for this patented sampler type as well as recognising certain effects to consider in the scale-up design. The next step is to manufacture a scale-up design of the True Pipe® sampler and also include an automated washing system, which will minimise operator interference during sample extraction.

Acknowledgements

The authors wish to express appreciation for the lifelong work on sampling theory conducted by Dominique François-Bongarçon; many thanks to Dr Paul Roberts for assisting in meticulous design of the prototype sampling unit and to the Multotec Research and Development team for their untiring commitment and patience during carefully supervised sample preparation.

References

1. Amira International Africa, "P754: Metal Accounting – Code of Practise and Guidelines", Release 3 (February) [online]. Registration No.2002/011077/08, (2007). Available from: http://www.amira.com.au
2. P. Carrasco, P. Carrasco and E. Jara, "The economic impact of correct sampling and analysis practices in the copper mining industry", *Chemometrics and Intelligent Laboratory Systems*, **74**, 209–213 (2004).
3. R.C. Steinhaus and G.J. Halstead, "True Pipe® Sampler – A Correct Design Utilising the Principle of Symmetry in Pressurised Slurry Particulate Streams", in *Sampling 2014 conference proceedings*, pp 127-134 (2014).
4. P.M. Gy, *Sampling of Particulate Materials—Theory and Practice*, 2nd edition, Elsevier, Amsterdam, (1982).
5. F.F. Pitard, *Pierre Gy's Sampling Theory and Sampling Practice*, 2nd edition, CRC Press, Florida, (1993).
6. R.J. Holmes, "Correct Sampling and measurement – the foundation of accurate metallurgical accounting", *Chemometrics and Intelligent Laboratory Systems*, **74**,7-24 (2004).
7. D. François-Bongarçon, "A fundamental principle for automatic sampler correctness", in *Proceedings 2nd World Conference on Sampling and Blending (WCSB2)*, AusIMM, pp.101-102 (2005).
8. P.W. Cleary and G.K. Robinson, "Analysis of Vezin sampler performance", *Chemical Engineering Science*, **66**, 2385-2397 (2011).
9. H. Kaltenbach, "Hypothesis Testing", in *A Concise Guide to Statistics*, Springer, Switzerland, (2012).

doi: 10.1255/tosf.54

PFTNA logging tools and their contributions to in-situ elemental analysis of mineral boreholes

C.P. Smith,[a] P. Jeanneau,[b] R.A.M. Maddever,[c] S.J. Fraser,[a] A. Rojc,[a] M.K. Lofgren[a] and V. Flahaut[b]
[a]**CSIRO Mineral Resources Flagship, Technology Court, Pullenvale, Australia. E-mail: craig.Smith @csiro.au**
[b]**Sodern, 20 av. Descartes 94451 Limeil-Brévannes, France. E-mail: philippe.jeanneau@sodern.fr**
[c]**BHP Billiton, 125 St Georges Terrace, Perth WA 6000, Australia. E-mail: Arthur.AM.Maddever@bhpbilliton.com**

Historically, the application of nuclear science to borehole logging began with the detection of the natural radioactivity emitted by rocks and soils. This simple and effective method found many applications, particularly in sedimentary, coal and uranium deposits. Whilst this technique is still widely used today, the industry quickly moved to more sophisticated logging techniques that activate rocks with neutrons and measure the induced radiation to infer characteristics of the material surrounding the hole. Neutrons, as primary particles, were found to be an excellent radiation source, which opened large opportunities for in-situ material analyses. Neutron based commercial instruments were introduced[1] for the first time in the 1940's. Early versions of neutron logging tools used isotopic neutron sources that primarily responded to the amount of hydrogen in the formation. These were adopted by the oil industry to identify zones of porosity. Common isotopic neutron sources, such as ^{252}Cf or ^{241}Am-Be, are environmentally problematic if, for any reason, the tool cannot be retrieved from the borehole. Tools using continuously-on isotopic sources also suffer from limited capacity to distinguish between water and oil. Pulsed sources were found to overcome this obstacle since, by exploiting differences in time response, they made it possible to distinguish water from oil beds. Thus, the need for switchable neutron generators was driven by the oil industry, which in turn prompted the development of compact industrial grade equipment suitable for the requirements of their logging tools. There is a variety of active logging techniques based on the use of pulsed neutrons. These can be classified according to the implementation of the neutron source and the type of induced particles that are detected. Among the latter, gamma photons are of considerable interest as they enable elemental analysis of rocks. Pulsed Fast and Thermal Neutron Activation (PFTNA) is one of the most commonly used techniques combining a neutron generator with a gamma scintillation detector. Application of PFTNA for borehole logging is not limited to the oil industry. Nevertheless, most commercial tools have been developed to withstand the severe pressure and temperature conditions inherent at great depths in oil wells and thus tend to be oversized and too costly for mining applications. Without the need to withstand high temperatures and pressures, the technology can be optimized to make it more cost effective. This article presents a new PFTNA tool developed for the mining industry.

PFTNA (Pulsed Fast and Thermal Neutron Activation)

Neutrons interaction for elemental analysis

Pulsed Fast and Thermal Neutron Analysis (PFTNA) is a technique that exploits several nuclear interactions of neutrons with matter in order to identify and quantify a large number of elements. Neutron energies are generally classified according to their kinetic energy into three categories: fast (E > 1 MeV), intermediate (1 keV < E < 1 MeV), and slow (E < 1 keV). This latter category is itself subdivided into epithermal (0.1 eV < E < 1 keV) and thermal (E<0.1 eV).

When neutrons penetrate the matter, they progressively lose their energy, mostly as results of successive elastic collisions. Each collision causes the transfer of a percentage of neutron kinetic energy from the incident to the target nucleus. This process is called *slowing down* or *thermalization*, which continues until the neutrons reach thermal equilibrium. Note that neutron particles have a mass nearly the same as hydrogen, making that element the most effective at slowing down neutrons following collision.

Apart from the elastic collision mechanisms, neutrons initiate three main types of interactions that results in the production of secondary particles:[2]

- Inelastic scattering: A neutron interacts with a nucleus to form a very short lived isotope in an excited state. This returns quickly to its ground state by emitting a gamma ray, then a neutron. The energy of the incident neutron needs to be above a threshold value specific of the element to initiate the reaction.
- Transfer reaction or Activation reaction: A neutron is absorbed by the nucleus which in turn releases one or more particles.
- Radiative capture: A neutron, once slowed down to thermal energy, is absorbed by a nucleus that reaches an excited state; that nucleus decays nearly instantaneously to the ground state by the emission of one or more gammas. The created isotope may be stable or may be itself radioactive.

Particles (gamma photons in particular) resulting from these interactions are characteristics of the target nuclei; and thus can be used for their identification. Neutron capture and inelastic scattering are the most common interactions exploited in neutron based borehole logging.

A large variety of elements found as constituents of common minerals, such as Si, Fe, Ca, Al and Mg can be measured using gamma rays resulting from neutron thermal capture reactions. Yet a few major elements, such as C and O display virtually no response to slow neutrons. Their direct measurement requires inelastic scattering interactions, which can only be initiated if the source can produce neutrons with sufficient energy to activate such reactions.

The use of energetic neutrons as produced by Deuterium-Tritium generators, for example, enables the excitation of surrounding material with a wide range of energies from thermal to fast, which opens up the opportunity to exploit the different types of reactions.

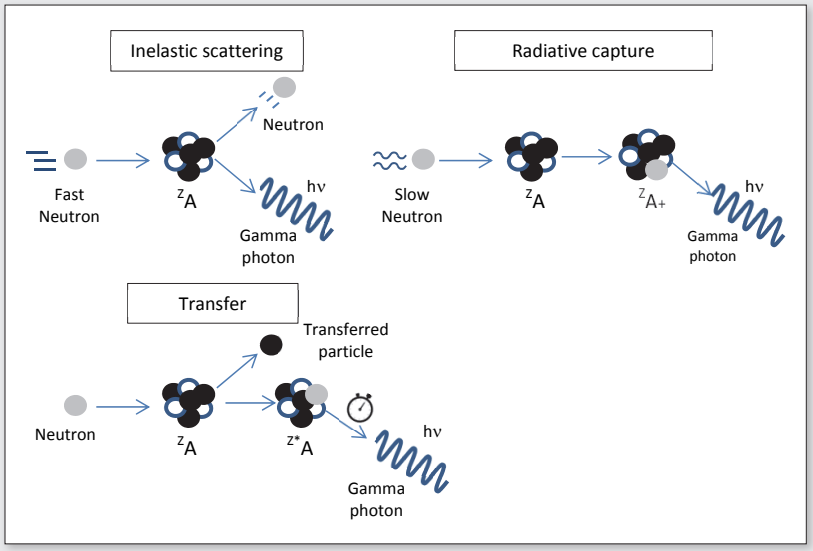

Figure 1. Neutron Interactions with matter

Pulsed electric neutron source

The PFTNA technique relies on a pulsed neutron generator (NG). The principal part of a neutron generator is a small linear particle accelerator, called a neutron tube. Neutron tubes have been built for more than 40 years; and they produce fast neutrons by fusion of hydrogen isotopes[3]. Two main nuclear reactions are used in standard neutron generators.

- Deuterium ^{2}H – Deuterium ^{2}H (D-D)

  $^{2}H + {}^{2}H \rightarrow {}^{3}He + {}^{1}n + 3.266\,MeV$ (neutron energy about 2.4 MeV)
- Deuterium ^{2}H – Tritium ^{3}H (D-T)

  $^{3}H + {}^{2}H \rightarrow {}^{4}He + {}^{1}n + 17.586\,MeV$ (neutron energy about 14.1 MeV)

The yield of the second reaction is about 100 times that of the first. Consequently, it is the DT fusion reactions, which creates high energy 14 MeV neutrons, that is more widely used of the two in the manufacture of borehole elemental logging tools.

A typical sealed neutron tube includes an ion source, an accelerating gap and a beam target; all these components are enclosed within a sealed vacuum enclosure. The high voltages for the accelerator and the ion source are provided by external power supplies. Tritium is impregnated on the target as solid hydride trapped in porous titanium. Deuterium is loaded similarly on a small resistor. A small quantity of gas is released on demand inside the tube by adjusting the current of the resistor. Plasma created inside the ion source produces ions which are accelerated onto the target to initiate DT fusion and neutron production.

The ability to interrupt neutron emission by turning off the power supply provides significant benefits for the use of electrical generators in borehole logging. The most notable is the absence of radiation when the tool is outside the borehole and handled by operators.

But this switchable capability may also be used to control the neutron pulse on a short time scale.[4] During the pulse of fast neutrons, the gamma ray spectrum is primarily composed of rays from the inelastic and transfer reactions. Between pulses, neutrons lose their energy and can initiate thermal capture reactions. With an appropriate gate circuit, it becomes possible to separate the gamma-ray spectra produced by neutron inelastic scattering from those excited in neutron capture reactions. By further encoding a

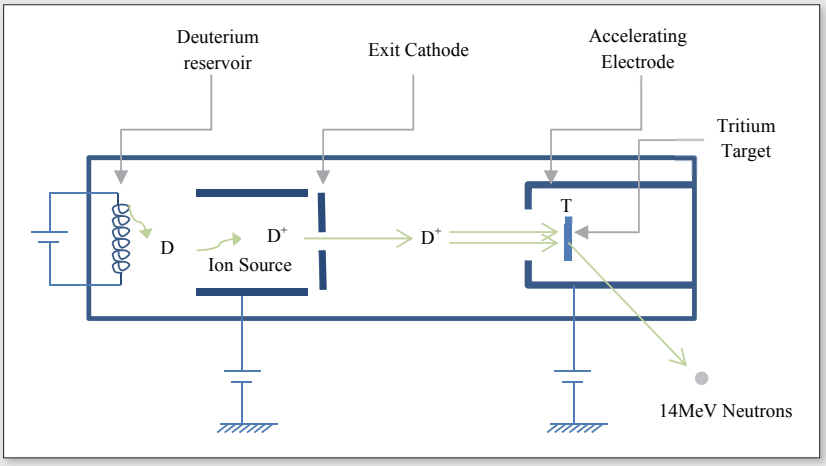

Figure 2. Neutron Tube Principle

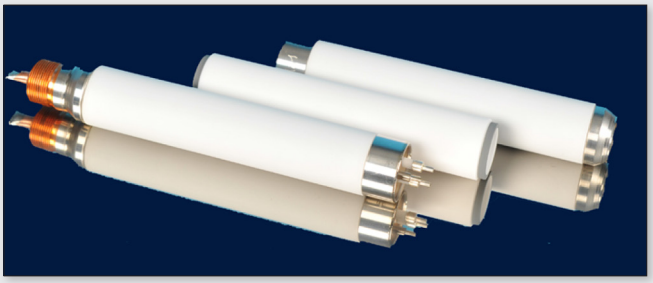

Figure 3. Ceramic body sealed neutron tube – Sodilog by Sodern

delay between the pulse waveforms, it is also possible to store in a separate memory events corresponding to decays of isotopes that may be created.

For some time, pulsed neutron generators have been widely used for oil logging. However, this application required them to be built to withstand high temperature and it is arguable that the associated high cost and reduced life time has limited their penetration into mining industry. Considering much less extreme conditions prevalent in most currently mined hard rock environments having boreholes that do not exceed a few hundreds of meters, commercial manufacturers have since gone to considerable efforts to propose reliable systems with extended life times of several thousands of hours, suitable for industrial mining applications.

High resolution gamma detectors

A spectrometric technique is used to record the energy of the gamma rays emitted by excited nuclei. Commonly found gamma rays detectors in logging tools are made of a scintillation material coupled with a photo multiplier tube (PMT). Incoming gamma particles are absorbed in the scintillator, which re-emits the energy in the form of light. This light is converted into electrons by the PMT photocathode. A series of amplification stages multiplies electrons to generate an electrical pulse having area or height that is proportional to the energy of the incident photons.

Specialized electronic circuits measure individual gamma photon energies, which build the population histogram. This is referred to as a *pulse heights spectrum*. The incoming gamma rays, originating from the different elements, have discrete and characteristic energies. However, noise and statistical effects in the pulse measurement introduce broadening of the corresponding peaks constructed in the spectrum. With respect to the various mechanisms of interaction between the gamma photons in the scintillator, the pulse heights spectrum is usually a rather complex structure.

Inorganic scintillators are typically used in borehole nuclear logging tools.[5] Well-known crystals such as NaI, CsI or BGO have been used for decades in both passive and active gamma logging techniques. Crystal choice results in several parameters that influence a tool's analytical performances and its operability. Spectral resolution is one parameter that plays a frequent role. Resolution is defined as the width of the peak at a given gamma energy. An ability to resolve narrow peaks decreases the risk of overlap between closely spaced gamma lines and helps in identification. Because manual processing is usually not sufficient, it also facilitates unfolding algorithms. This capability is of particular interest for the rich spectra composed of thermal capture gamma rays, which contain numerous and overlapping peaks.

Another property of the detector that needs to be taken into account is the scintillator stopping power, which corresponds to the efficiency of the crystal to interact with incoming photons. The higher the energy range of gamma photons, the more transparent will be the scintillator. Capture gamma rays produced by elements typically targeted in borehole logging, such as Si, Fe, Ca, Al and Mg, have energies above 3 MeV, and up to 10 MeV, which requires rather dense crystal to generate sufficient signal. Conversely, gamma rays created by inelastic scattering reactions with carbon and oxygen are rather sparse, and can be easily detected and identified by most crystals. However, for inelastic scattering reactions,

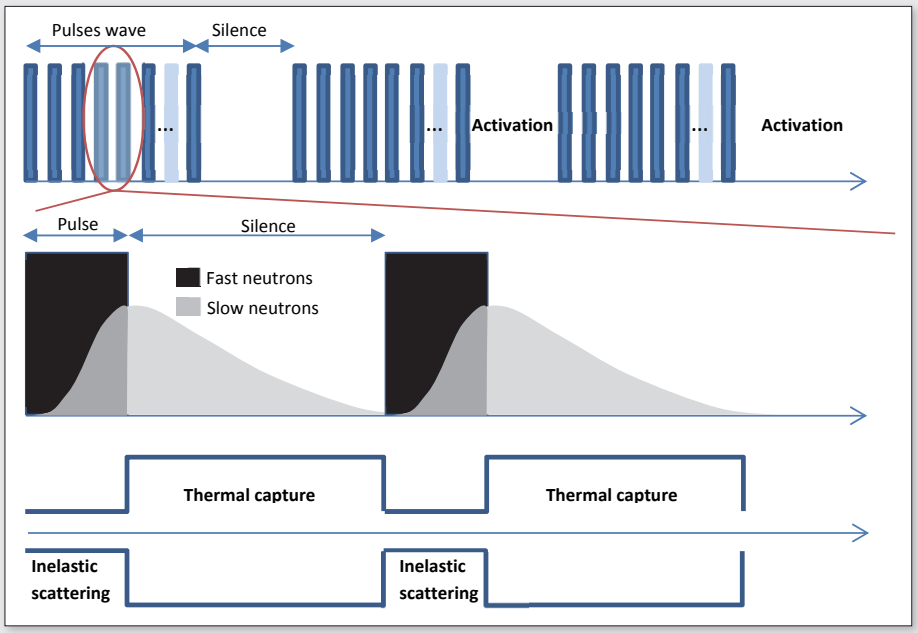

Figure 4. Pulse fast and thermal neutron analysis sequence

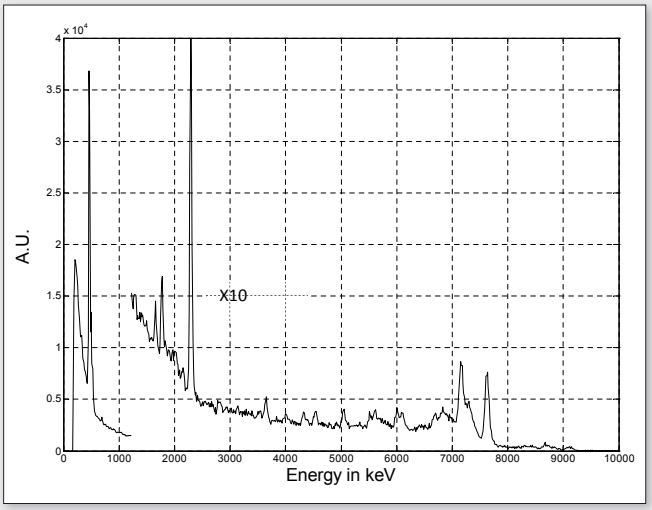

Figure 5. Spectrum from bromium lanthane detector $LaBr_3$ – iron ore – Thermal capture reactions

event-rates during the neutron burst are high, so scintillators exhibiting short durations of the pulses of light are preferred.

Beyond fundamental physical parameters, the sensitivity of the detector to operating conditions, including temperature and other environmental factors, plus economic considerations, are also usually taken into account. This leads the PFTNA logging tool designers to a trade-off that usually results in the adoption of BGO as a compromise; the down-side being relatively poor energy resolution and sensitivity to temperature, potentially limiting the performances of such systems.

A breakthrough has taken place since early 2000 with the market availability of a new crystal, Cerium-doped lanthanum bromide, LaBr3(Ce).[6] This crystal offers both excellent energy resolution and a fast response. Further, it has a density that makes it usable for high energy gammas and low sensitivity to temperature variation. Consequently, this crystal has now become a viable solution for PFTNA logging tools.

PFTNA logging tool development for mining industry

PFTNA logging tools have been used in oil logging for a long time, however, their use in the mining industry has remained quite limited until now. This is partly to do with the fact that oil logging tools are generally oversized and over-engineered for the mining application and partly because the high cost of development tends to be prohibitive, even for the larger mining corporations.

Hence the approach that we followed in developing a new PFTNA logging tool was to design it compatible with current operating procedures, field conditions and borehole characteristics common to ore extraction sites and, subsequently, through testing and analysis, to refine. A robust tool was designed based on these guidelines, so that it would be cost effective for implementation in coal and minerals mining activities. The development was undertaken jointly by three parties. Sodern, an Airbus company, having knowledge in design of compact sealed neutron tubes and neutron generators and how to incorporate them into neutron based industrial cross-belt analytical systems; the Commonwealth Scientific and Industrial Research Organisation (CSIRO) having deep experience in the

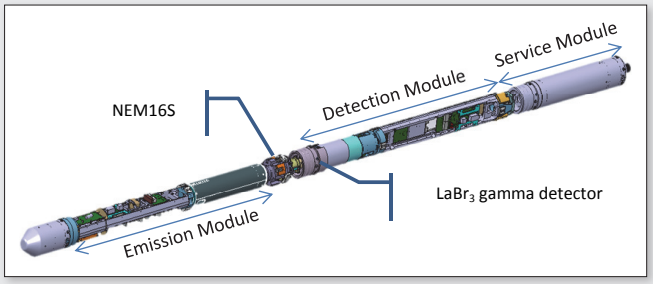

Figure 6. CAD view of the FastGrade™100 logging tool

design of nuclear logging tools,[7,8] who took responsibility for power, communications and overall implementation of the tool in the end user's logging environment; BHP Billiton, a mining company and the primary end user, who funded the development and provided the end-user specifications in addition to feedback and experience gained from thousands of kilometres of drilled and logged boreholes.

The new tool called FastGrade™100 (FG100) is primarily aimed at measuring boreholes drilled for exploration and resource estimations. This tool has been extensively tested in the Western Australian Pilbara iron ore mining district.

A diameter of 4 inches (101.6mm) was agreed for the logging tool, enabling it to fit with sufficient clearance inside 140mm diameter (and larger) holes commonly drilled on sites using reverse circulation (RC) drilling.

The overall length of the probe lowered inside the holes is about 3.3m. It is divided into 3 major sub modules:

- The Emission Module (EM)
- The Detection Module (DM)
- The Service Module (SM)
- The probe is connected to the surface using a regular 4 wires steel reinforced cable. The surface station is composed of:
- The Uphole Control Box
- The Uphole Control Computer and,
- A set of peripheral equipment used for radiation monitoring, geo-location and user-informative safety devices.

Each downhole module is individually housed in a steel metal barrel that connects them all together. Once assembled the tool can be used in dry, or water-filled boreholes and is certified for pressure up to 40bars.

Emission Module

The heart of the neutron emission subsystem is a Sodern sealed neutron tube called *Sodilog*[11]. The *Sodilog* tube is a miniature particle accelerator having a ceramic body. Originally designed by Sodern on request from oil logging companies, the *Sodilog* tube is now a proven technology that is produced in large quantities by Sodern for more than 15 years. The neutron tube is enclosed in a metal housing called Neutron Emitting Module (NEM), which is filled with SF_6 dielectric gas to insulate the high voltage elements of the tube from its surrounding.

The NEM is connected to a compact very high voltage (VHV) power supply providing up to 120kV for accelerating ions to the tritiated target. A separate pulsed power supply is connected to the ion source to create neutrons bursts with accurate and adjustable timing structure. Although the neutron timing must respect the

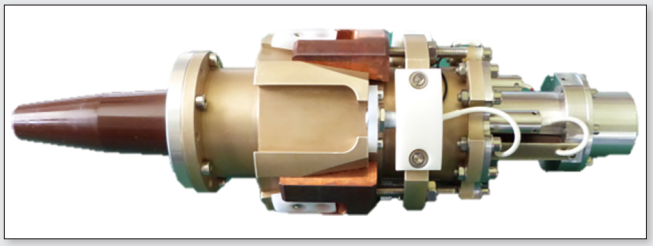

Figure 7. Compact Neutron Emitting Module – NEM16S

underlying physics, it has sufficient flexibility to allow optimisation of gamma rays scattering effects related to inelastic and thermal capture.

Detection module (DM)

The Detection Module accommodates a 3 x 4 inch $LaBr_3$(Ce) scintillation crystal. Selected for its intrinsic high performance, the detector is connected to a fully digitized acquisition and pulse-heights processing boards. The system is gated to measure individual timing windows synchronized with the neutron pulsing mechanism. The gamma rays from the different nuclear reactions are recorded in separate 1024 channels, one each for inelastic scattering, thermal capture and delayed activation. These are stored and made available to end users as well as being passed to the data processing module. Combining the fast response time of the crystal with the high speed FPGA processing components, minimizes dead time and enable acquisition times down to a few seconds.

Service Module (SM)

The Service Module was designed as the communication and power interface for the logging tool. Power is provided from the surface to the SM via a 240 VAC power link on two of the wireline conductors; communications are supplied on the other two. The power is converted into 12 V and 48 V before delivery to all downhole components.

Communication to the surface is based on VDSL digital communication over twin conductors. A proven technology largely deployed in industrial data network, VDSL easily covers the bandwidth requirements of the tool and allowed implementation of affordable commercial solutions. Communication from surface to tool was successfully tested down to depths of 650 m. Reliable and straightforward, it enables the set-up of an Ethernet network connecting all downhole and uphole modules. This approach exemplifies the design philosophy of building system components whenever possible using non-specific off-the-shelf technology.

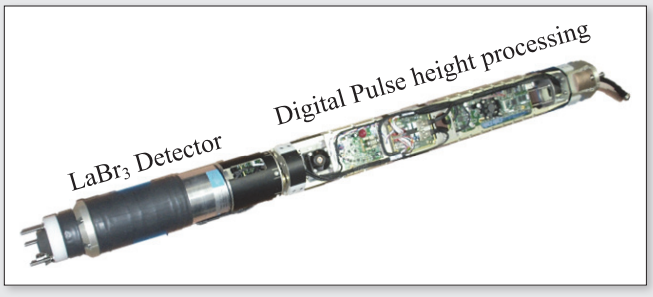

Figure 8. Detector Module – view $LaBr_3$ and digital processing electronic board

Uphole Control Box (UHCB)

The Uphole Control Box is the surface counterpart of the service module; it manages power, communication and data transfer. Beyond this, it also ensures safe operation of the equipment. Design protocols prevent it from allowing users to bypass any of the safety interlocks and, in the event of a hazardous situation, it will take advantage of the switchable nature of the neutron generator to turn off the probe in order to provide occupational safety for operators.

Cable connection and integrity to the tool is routinely tested before allowing any power to be applied. Loss of communication with the tool or the UCB will result in power to the tool being automatically disconnected, resulting in a complete shutdown.

The UCB provides interfaces to the logging vehicle, of particular importance being winch signals for depth, speed and directional information. The box supervises an on-board and independent radiation monitor and, in case of an alert, it will remove power from the tool and activate an alarm.

Uphole Control computer (UCC)

The Uphole Control Computer (UCC) is the user-interface to the logging tool. It enables the user to control and monitor all aspects of the tool operation such as depth, status of the safety loop, control of the neutron generator and acquired spectra.

The user interface has been defined in close cooperation with logging operators. In effect, this led to a single graphical page tailored to the strict minimum of necessary items to perform logging operations safely and reliably. More comprehensive diagnostic information on the tool status is available under various tabs on the interface.

The logging operation produces a file, written in HDF5 format. It contains, for each depth interval, the three different types of gamma spectra, as well as the detailed experimental conditions applying during the acquisition, such as voltages, currents, temperatures and GPS location. Elemental concentration as a function of depth may also be included provided a suitable calibration has been uploaded into the UCC.

Figure 9. Uphole Control Box

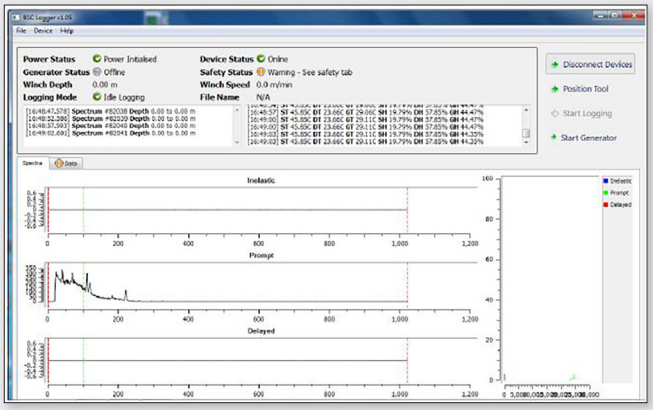

Figure 10. Logging software interface – Main page

An important requirement from miners is that, with these data, the end-user can recreate all aspects of the logging environment and be able to confirm, correct or update results later, when individual logs are merged and consolidated into 3D models using mine planning software.

Integrated System

The tool is integrated onto a dedicated logging vehicle. Handling operations have been mechanized and the tool can be taken out and positioned above a borehole, all by remote control. In this way, a single operator can drive the vehicle to the designated location and undertake a PFTNA log.

Figure 11. Equipped logging vehicle and FG100 handling

The tool is usually lowered to the desired lower depth of the targeted log section. The tool is then switched “on” to enable neutron emission. The tool is lifted and the system then automatically records gamma spectra. Operated at 2m/min, measurements are recorded every 6s, providing elemental data for each 20cm intervals.

With the intent to provide a new generation of logging tools suitable for the mineral industry, a PFTNA probe has been designed and manufactured. A neutron pulse generator from Sodern has been used on the basis of it being proven long life technology. To achieve optimum gamma spectrometry, the tool incorporates among the best industrial detectors. The remainder of the tool has been intentionally designed using purpose-built technology and off-the-shelf solutions suitable for the mining environment to strike the right balance between cost and reliability. Specifically designed with the end-user logging operator in mind, the software and electronics provides easy to use tools without any compromise in safety.

PFTNA and sampling methods

Neutrons and gamma rays exploited by PFTNA techniques are energetic particles. Consequently, neutrons are able to penetrate the surrounding material to considerable depth, following which the resulting gamma photons are able to reach the detector even through several tens of centimetres of bedrock. In a borehole logging configuration, the collected PFTNA signal, and the derived elemental composition, will be representative of a much larger volume of surrounding material than the delimited volume of the core material that is traditionally used to provide chemical analysis. This larger volume is the key that enables better sampling statistics and improved reliability in resource estimation using the PFTNA approach, especially when heterogeneous deposits are explored.

PFTNA provides several additional advantages that make it attractive when compared to the traditional approach based on material collected as part of a drilling operation followed by laboratory analysis:

- Whatever traditional sampling methods and equipment are used to sample borehole material, it is recognized that sample and core sample recovery is rarely complete, which limits it representativeness and introduces some level of sampling error.
- The PFTNA technique is also less sensitive to certain material physical parameters, such as density and mineralogical forms of rocks constituents. It therefore does not require the critical steps of material preparation that conventional laboratory techniques do.

Figure 12. Open holes RC drilling collected samples

- Even when applying sophisticated algorithms, modern computers are capable of processing PFTNA spectra within a few seconds and can provide analytical results as soon as they are received during logging. Rapidly available analytical data is a strong advantage compared with the conventional sampling and assaying approach that extends at best over days and more commonly over weeks.

As a consequence, the PFTNA technique, embodied in the FG100, seems to offer an excellent alternative solution for the mining industry, eliminating the well-known obstacles caused by sampling and sample preparation, while being affordable and leading to substantial reductions in cost and time. However, proposing PFTNA for in-situ measurements as an alternative to traditional chemical analysis may at times be overly-simplistic. For one thing, such a proposal ignores the fact that a laboratory can deploy several different techniques that not only provide elemental analysis, but also a variety of information that PFTNA alone will not be able to measure, such as hardness, grain distribution and crystalline structure.

For another, whilst PFTNA offers acceptable analytical detection limits for a large panel of elements of interest found in minerals, such as Si, Ca, Fe, Al, Mg, the base metals Cu and Ni and even light elements as H, C, and O, it will not necessarily achieve the required performance for trace elements. On occasions, these might be major indicators of ore quality, such as P in iron ore, or ppm levels of valuable elements, such as Au and Ag in some copper deposits. Consequently laboratory analysis of samples and PFTNA in-situ elemental logging should be considered complementary methods and implemented accordingly.

Of the two methods, the greater volume of material measured with PFTNA is an advantage, but it should not be idealized. At face value, it can be roughly assumed that the sample volume is a factor of 10 greater for the FG100 logging tool. However, the response function of the system is a complex convolution of the different nuclear phenomena that underlie the PFTNA theory. Neutrons emitted from the source will be spatially distributed in the material according to the slowing-down effect. To first order, this will define a population of neutrons that changes in quantity and energy with the distance from the source. This is modified by a second-order effect that takes account of local material characteristics. Similarly, the gamma photons subsequently created at each point in space will be measured by the detector according to a collection efficiency function that is also dependent on the distance to the detector and the characteristics of the material that the gamma rays traverse on their way to the detector. Thus, the signal produced by the collection of volume elements surrounding the tool results from the convolution of those effects and each volume element will be weighted differently in the sum spectra that is processed to infer an overall elemental composition.

During the development of the FG100 logging tool, the measured volume was investigated in details. Experimental evaluation (supposing that this would make sense) was not considered achievable for reasonable effort. Conversely, the use of Monte Carlo simulations was straightforward and allowed possibility of virtually inspecting the signal characteristics inside the material[9,10].

The simulation work has consisted of estimating how the tool spatial response function is influenced by variations in material physical properties as well as by specific operating parameters, such as rock density, moisture content and borehole diameter.

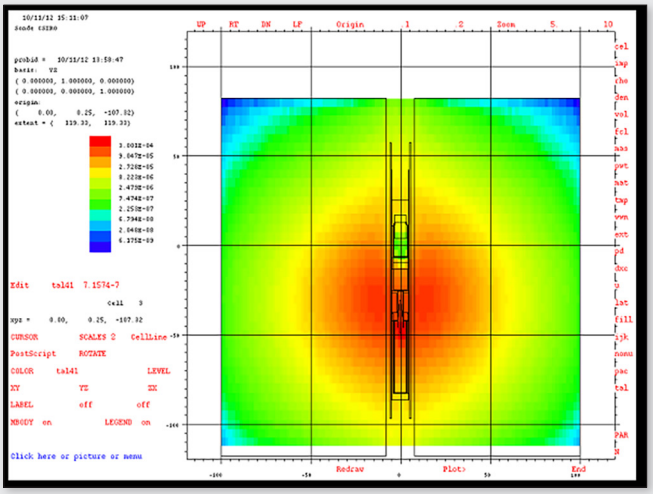

Figure 13. Thermal neutron distribution in the surrounding material obtained by Monte Carlo simulations

The framework for the simulation was a Western Australia iron ore deposit. The volume of material interrogated by the tool was found to vary significantly when the composition of the material varied widely. This was also the case when there was significant change in borehole characteristics along the few hundreds of meters of a typical log. For example, it was found that water-filled cavities in boreholes may reduce the penetration by up to a factor 2 compared to when dry.

To some extent, these " poor log recovery " events compare to and are similar to "core loss" or poor sample recovery during drilling programs with similar consequences and increased uncertainty that is then added to the compositional estimates for the corresponding depth interval. However, works undertaken during development of the FG100 PFTNA tool enabled toidentify some mitigation possibilities. Although calibration of the PFTNA tool is primarily intended to account for elemental variations, it was found that calibration could also incorporate algorithms that compensate for a variety of influencing effects. Multiple calibrations can also be established when conditions of use exhibit great difference, allowing optimized models to be developed that accommodate significant change of material or measurement conditions. This work remain exploratory, however, it is expected that Monte Carlo simulations can be used to refine the signal processing, offering the potential to extend the calibration base without requiring an intensive additional sampling campaign.

Conclusion

Pulsed Fast and Thermal Neutron analysis is a nuclear technique that can be applied to borehole logging. The technique is used for the in-situ and direct determination of elemental concentrations of material surrounding the hole. It takes advantage of a switchable pulsed neutron generator, overcoming the most significant limitation attached to traditional permanent isotopic sources. This makes PFTNA technique inherently safer and significantly improves occupational safety on site. Due to the deep penetration of neutrons and gamma rays, the technique is suitable for logging applications. Proven equipment is available for both emission of neutrons and detection of gamma rays. A next generation tool has been designed and produced with the aim of promoting it to industries such as

coal and other mineral commodities. The FG100 tool is built around the latest in technology for optimal spectrometric measurement. Notwithstanding this, the overall approach is intentionally oriented toward using components and technology widely established but specified for ore deposit logging conditions. All aspects have been considered for taking the instrument up to an industrial grade with the expected level of reliability and safety. The new tool has started making inroads in the iron ore industry where it can play a key role in the early phase of resource evaluation. The benefit of having in-situ, real time, chemical analysis will likely lead the industry to reconsider the current approach based on samples collection and laboratory analysis, although it is acknowledged that the latter will remain the method of choice for certain situations. We can expect future tactics will consider how the two methods could complement each other. Some improvements have been identified for future consideration. They primarily concern the calibration, particularly efforts to streamline this essential step. Also, further data processing work is foreseen to extract still underexploited information from the spectrometric data.

References

1. B. Pontecorvo, *Neutron Well Logging – A New Geological Method Based on Nuclear Physics,* Oil and Gas Journal 40: 32–33. 1941
2. P. Rinard, *Neutron Interactions with Matter, Los Alamos Technical Report* http://www.fas.org/sgp/othergov/doe/lanl/lib-www/la-pubs/00326407.pdf
3. *Neutron Generators for Analytical Purposes* IAEA RADIATION TECHNOLOGY REPORTS No. 1
4. Alexander P. Barzilov, Ivan S. Novikov and Phillip C. Womble (2012). *Material Analysis Using Characteristic Gamma Rays Induced by Neutrons, Gamma Radiation*, Prof. Feriz Adrovic (Ed.), ISBN: 978-953-51-0316-5, InTech, DOI: 10.5772/36372, http://www.intechopen.com/books/gamma-radiation/material-analysis-using-characteristic-gamma-rays-induced-by-pulse-neutrons
5 M. Borsaru, Selected topics in nuclear geophysics, Proceedings of the Romanian academy, Series A, Volume 6, Number 3/2005, http://www.acad.ro/sectii2002/proceedings/doc_2005_3/03-Borsaru.pdf
6. E. V. D. van Loef, P. Dorenbos, C. W. E. van Eijk, K. Krämer and H. U. Güdel, *High-energy-resolution scintillator: Ce3+ activated LaBr3*, Appl. Phys. Lett. 79, 1573 (2001)
7. M. Borsaru and J. Charbucinski, *Nuclear borehole logging techniques developed by CSIRO – Exploration and Mining for in situ evaluation of coal and mineral deposits,* Proceedings of the Second international conference on isotopes, 1997 http://www.iaea.org/inis/collection/NCLCollectionStore/_Public/29/057/29057219.pdf
8. K Trofimczyk, S Saraswatibhatla, C Smith, *Spectrometric Nuclear Logging as a tool for real-time, downhole assay – Case Studies using SIROLOG PGNAA*, 11th SAGA Biennial Technical Meeting and Exhibition Swaziland, 16–18 September 2009, pages 161–171
9. LANL X-5 Monte Carlo Team,MCNP-A General Monte Carlo N-Particle Transport Code, Version 5,2003.
10. Fusheng Li and Xiaogang Han, *Monte Carlo Numerical Models for Nuclear Logging Application*s, SYSTEMICS, CYBERNETICS AND INFORMATICS VOLUME 10 – NUMBER 3 – YEAR 2012
11 http://www.sodern.com/sites/docs_wsw/RUB_78/Fiche_Sodilog.pdf

doi: 10.1255/tosf.79

Introduction and first ever rigorous derivation of the liberation factor

Dominique M. Francois-Bongarcon, PhD
Agoratek International Consultants Inc., North Vancouver, Canada. E-mail: dfbgn2@gmail.com

A simplified approach to the demonstration of Gy's Theory of Sampling (TOS) sampling variance formula is proposed, with the added advantage that it clarifies the real assumptions that are necessary to lead the demonstration to its end. In the process, the introduction of the liberation factor in TOS is also clarified and, for the first time, a rigorous definition of that factor is offered, which naturally lead to its modelling in past years using geostatistical concepts. A generalised from for the mineralogical factor c is also proposed in an appendix.

Introduction

We will use the following notations and conventions:

Large lot L: Mass = M_L, made of N_L fragments $f_j(t_j, m_j)$ where t_j and m_j are the grades and masses of individual fragments
Sample S: Mass = M_S, made of N_S fragments $f_i(t_i, m_i)$

For the lot (summations on sub-index j by convention):

$$\bar{m}_L = M_L / N_L = \Sigma_j m_j / N_L$$

$$t_L = \Sigma_j m_j t_j / M_L = \Sigma_j (m_j t_j / \bar{m}_L) / N_L \quad \text{(grade of the lot)}$$

Similarly for a small sample (summations on sub-index i by convention):

$$\bar{m}_S = M_S / N_S = \Sigma_i m_i / N_S$$

$$t_S = \Sigma_i m_i t_i / M_S = \Sigma_i (m_i t_i / \bar{m}_S) / N_S$$

Important assumptions

We will assume sampling in number (the equivalence to sampling in mass was established by Matheron[1] (2015) so that N_S is a fixed number for all the samples.

$Var(m_i)$ is limited and N_S is a very large number, so that $Var(\bar{m}_S) = Var(m_i) / N_S$ is small. Additionally, if the sample is correct, $E(\bar{m}_S) = \bar{m}_L$. As a result:

$\bar{m}_S$ can be assimilated to $\bar{m}_L$ in "good approximation"

This FUNDAMENTAL approximation is equivalent to assuming exact representation in the sample of the average fragment mass in the lot. This, which includes the neglecting of the small variations in total mass M_S from sample to sample, is the origin of the mathematical difficulty of Gy's and Matheron's rigorous demonstrations, and of the first order approximation that characterises their result.

Relative sampling error

Under these conditions, the relative sampling error is:

$$\varepsilon_{RS} = (t_S - t_L) / t_L = \Sigma_i [(m_i / \bar{m}_L)(t_i - t_L) / t_L] N_S = \Sigma_i h_i / N_S$$
(i.e. the *arithmetic* mean of the independent h_i in S)

where $h_i = [(t_i - t_L) / t_L](m_i / \bar{m}_L)$ (see TOS terminology in Appendix 1)
Properties of h_i:

$$\bar{h}_L = \Sigma_j (m_j t_j / \bar{m}_L) / (t_L N_L) - t_L / t_L = 1 - 1 = 0, \text{ therefore}$$

$$Var(h_i) = \Sigma_j [(t_j - t_L) / t_L]^2 (m_j / \bar{m}_L)^2 / N_L = CH_L$$
(see TOS terminology in Appendix 1)

Relative sampling variance

Since: $\bar{\varepsilon}_{RS} = 0$

$$\sigma_R^2 = Var(\varepsilon_{RS}) = Var(h_i) / N_S = CH_L / N_S = (\bar{m}_L / M_S) CH_L$$

And as: $CH_L = \Sigma_j [(t_j - t_L) / t_L]^2 m_j^2 / (\bar{m}_L M_L)$:

$$\sigma_R^2 = (1 / M_S) \Sigma_j [(t_j - t_L) / t_L]^2 m_j^2 / M_L \text{ (for large lots)}$$

For smaller lots, because (in geostatistical notations):

$$D^2(M_S \mid \infty) = D^2(M_S \mid M_L) + D^2(M_L \mid \infty)$$

in all cases, we have:

$$\sigma_R^2 = (1 / M_S - 1 / M_L) \Sigma_j [(t_j - t_L) / t_L]^2 m_j^2 / M_L$$

This is Gy's and Matheron's first order approximation of the sampling variance.

Below liberation, by separating mineral and gangue fragments in the summation, this formula can easily be transformed into the fully calculable quantity (see demonstration in Appendix 2):

$$\sigma_R^2 = (1 / M_S - 1 / M_L) c f_G g d_{NG}^3 = (1 / M_S - 1 / M_L) C d_N^3$$

where C is a calculable constant in which **c is a *generalized* mineralogical constant**, and $d_{NG} = d_N$ is the comminution size of the lot.

Above liberation, it is not calculable, but somewhat smaller than if liberation had been achieved, so, introducing a number ℓ between 0 and 1, we can write:

$$\sigma_R^2 = (1 / M_S - 1 / M_L) c f_G \ell d_N^3 \text{ with } 0 < \ell < 1$$

Gy's well-known theory ends here, with no status given to ℓ, unfortunately precluding its (necessary) modelling.

We need to go further and:
- uncover the physical meaning of ℓ
- find the factors affecting it
- find a model for its variations

Important note:
One should mention there was one valuable attempt by Gy at modelling ℓ using the maximum grade achievable by a fragment at nominal size (Pitard, 2015).[2] This work was of theoretical interest, but it was not practical and only established (therefore valid) under very restrictive conditions.

However, in Francis Pitard's words, this method *"...showed quite well the relation of the liberation factor with mineralogy. For example, the liberation curve may look completely different if it is individual and isolated gold particle that liberate, or if it is a cluster made of many particles side by side, or if you prefer an aggregate of many particles."*

This said, full, general modelling of ℓ calls for geostatistical concepts that were simply not available at the time Gy was publishing TOS.

True definition of the liberation factor

In the liberated case, for a given, correct sample S, from a much larger, liberated lot:

$$\text{Rel.Var.}[S] = c\ f\ g\ d_N^3 / M_S$$

As we stated above, reasoning shows that when the ore is NOT liberated, the sampling variance is necessarily somewhat lower. As a result, for a given, sample S, from a large, non-liberated lot, by introducing a number ℓ between 0 and 1, Gy wrote:

$$\text{Rel.Var.}[S] = [c\ f\ g\ d_N^3 / M_S]\ \ell \quad \text{with } \mathbf{0 < \ell < 1} \qquad (1)$$

Now, let S_{Lib} be a correct sample, taken the same way, in the LIBERATED lot, with the same average number of fragments N as in S, i.e. with mass M_{Lib} such that:

$$M_{Lib} = N\ \bar{m}_{Lib} \quad \text{with } N = M_S / \bar{m}_L$$

$\bar{m}_{Lib}$ and $\bar{m}_L$ being the average fragment masses in the liberated and non-liberated lots.

$$\text{Rel.Var.}[S_{Lib}] = c\ f\ g\ d_\ell^3 / M_{Lib} \qquad (2)$$

In our model:

$$\bar{m}_{Lib} / \bar{m}_L = f\ g\ d_\ell^3 / f\ g\ d_N^3 = (d_\ell / d_N)^3 = M_{Lib} / M_S$$

So that we can replace M_{Lib} by $M_S\ (d_\ell / d_N)^3$ in (2):

$$\text{Rel.Var.}[S_{Lib}] = c\ f\ g\ d_\ell^3 / M_{Lib} = c\ f\ g\ d_\ell^3 / [M_S\ (d_\ell / d_N)^3]$$

Or:

$$\text{Rel.Var.}[S_{Lib}] = c\ f\ g\ d_N^3 / M_S \qquad (3)$$

Therefore, dividing (1) by (3):

$$\mathbf{\ell = \text{Rel. Grade Var.}[S] / \text{Rel. Grade Var.}[S_{Lib}]} \qquad \mathbf{(4)}$$

This new equation, *ratio of the sample variance to the variance of the liberated sample with the same average number of fragments*, is valid and constant for any sample (or sample mass), and provides us with a precise, rigorous and *objective* definition of factor ℓ.

Models for ℓ based on this characterisation have been the objects of numerous papers by the author. Equation (4) amounts to a ratio of variances of two different fragment sizes (in the lot being sampled and in the liberated one), and this ratio could only be modeled by drawing from geostatistical considerations.

References

1. G. Matheron, "Comparison between samples with constant mass and samples with constant fragment population size (and calculations of their sampling variances)", Translated from French to English, clarified and further commented by D. François-Bongarçon and F. Pitard, in *Proceedings of the 7th International Conference on Sampling and Blending*, Ed by K.H. Esbensen and C. Wagner, *TOS forum* **Issue 5,** in press (2015). doi: http://dx.doi.org/10.1255/tosf.80
2. F.F. Pitard, *Pierre Gy's Sampling Theory and Sampling Practice*, 2nd Edn. CRC Press (1993). ISBN 0-8493-8917-8

Appendix 1

Some TOS Classical Definitions

RELATIVE HETEROGENEITY carried by fragment f_i in lot L:

$$h_i = [(t_i - t_L) / t_L]\ (m_i / \bar{m}_L)$$

CONSTITUTION HETEROGENEITY of lot L:

$$CH_L = \Sigma_j\ [(t_j - t_L) / t_L]^2\ (m_j / \bar{m}_L)^2\ (\bar{m}_L / M_L)$$
$$= \Sigma_j\ [(t_j - t_L) / t_L]^2\ m_j^2 / (\bar{m}_L\ M_L)$$

It is a characteristic (weighted variance) of the "average fragment" in the lot and it measures the intrinsic variability of the lot.

HETEROGENEITY INVARIANT of lot L:

$$H_L = CH_L\ \bar{m}_L$$

Appendix 2
At liberation size and below

$$\sigma_R^2 = (1 / M_S - 1 / M_L)\, c\, f_G\, g\, d_{NG}^3 = (1 / M_S - 1 / M_L)\, C\, d_N^3$$

Summing on Mineral (M) and Gangue (G) with respective sub-indices i and j:

$$\sigma_R^2 = (1 / M_S - 1 / M_L)\{{}^M\Sigma_j\, [(t_j - t_L) / t_L]^2\, m_j^2 / M_L + {}^G\Sigma_i\, [(t_i - t_L) / t_L]^2\, m_i^2 / M_L\}$$

For the mineral, $t_j = 1$ and for gangue $t_i = 0$, so, introducing the densities ρ_M and ρ_G and fragment volumes v_i and v_j:

$$\sigma_R^2 = (1 / M_S - 1 / M_L)\, \{[(1 - t_L) / t_L]^2\, {}^M\Sigma_j\, m_j^2 / M_L + {}^G\Sigma_i\, m_i^2 / M_L\}$$

$$\sigma_R^2 = (1 / M_S - 1 / M_L)\, \{[(1 - t_L) / t_L]^2\, \rho_M\, {}^M\Sigma_j\, v_j\, m_j / M_L + \rho_G\, {}^G\Sigma_i\, v_i\, m_i / M_L\}$$

Now:

$${}^M\Sigma_j\, v_j\, m_j / M_L = (M_M / M_L)\, {}^M\Sigma_j\, [(m_j / M_M)\, v_j]$$

$M_M / M_L = t_L$ and ${}^M\Sigma_j\, [(m_j / M_L)\, v_j]$ is the mass-weighted average mineral fragment volume $\bar{v}_M$ in the lot, so that:

$${}^M\Sigma_j\, v_j\, m_j / M_L = t_L\, \bar{v}_M$$

Similarly:

$${}^G\Sigma_i\, v_i\, m_i / M_L = (1 - t_L)\, \bar{v}_G$$

where $\bar{v}_G$ is the mass-weighted average gangue fragment volume in the lot.
So now:

$$\sigma_R^2 = (1 / M_S - 1 / M_L)\, \{[(1 - t_L) / t_L]^2\, \rho_M\, t_L\, \bar{v}_M + \rho_G\, (1 - t_L)\, \bar{v}_G\}$$

finally:

$$\sigma_R^2 = (1 / M_S - 1 / M_L)\, [(1 - t_L) / t_L]\, [(1 - t_L)\, \rho_M\, \bar{v}_M + t_L\, \rho_G\, \bar{v}_G]$$

Let us introduce the volume ratio $k = \bar{v}_M / \bar{v}_G$:

$$\sigma_R^2 = (1 / M_S - 1 / M_L)\, [(1 - t_L) / t_L]\, [(1 - t_L)\, k\, \rho_M + t_L\, \rho_G]\, \bar{v}_G$$

In this expression,

$$\mathbf{c = [(1 - t_L) / t_L]\, [(1 - t_L)\, k\, \rho_M + t_L\, \rho_G]}$$

is the "**generalised** mineralogical factor" and

$$\sigma_R^2 = (1 / M_S - 1 / M_L)\, c\, \bar{v}_G$$

This is a very important formula, which actually is the **true** variance formula. It shows the lot behaves, in terms of sampling it, exactly as a hypothetical lot with all fragments having the same size corresponding to the average gangue fragment volume.

Calculation of constant k in factor c

Introducing Gy's classical granulometric factor g, liberation size d_ℓ, the shape factors f_M and f_G and the nominal comminution sizes $d_{NM}\ \sigma\ d_\ell$ and $d_{NG}\ \sigma\ d_\ell$ of mineral and gangue:

$$\bar{v}_M = f_M\, g\, d_{NM}^3 \quad \text{and} \quad \bar{v}_G = f_G\, g\, d_{NG}^3$$

$$k = \bar{v}_M / \bar{v}_G = (f_M / f_G)\, (d_{NM} / d_{NG})^3$$

Particular cases:

- Mineral and gangue comminute together and have the same shape factors:
  then k = 1
- Mineral and gangue comminute together and have different shape factors:
  then $k = f_M / f_G$
- Mineral does not comminute below liberation size (e.g. gold grains) while gangue is comminuted to size d_N:
  then: $k = (f_M / f_G) (d_\ell / d_N)^3$ in general,
  or: $k = (d_\ell / d_N)^3$ if $f_M = f_G$
- Special cases can be calculated as well. For instance, if the mineral has a unique size instead of a size distribution, one can take g = 1 for mineral grains in the definition of $\bar{v}_M$.

In all cases, the relative variance then becomes:

$$\sigma_R^2 = (1 / M_S - 1 / M_L)\, c\, f_G\, g\, d_{NG}^3 = (1 / M_S - 1 / M_L)\, C\, d_{NG}^3$$

where C is a calculable constant.

Note: in the case of non-comminutable gold (third bullet above), this expression reduces to the following approximation:

$$\sigma_R^2 = (1 / M_S - 1 / M_L)\, (\rho_M / t_L)\, f_M\, g\, d_N^3$$

which is why, in that case, the shape factor to be used is that of the gold grains.

doi: 10.1255/tosf.76

A multivariate approach for process variograms

Q. Dehaine[a] and L. Filippov[b]
[a, b] Université de Lorraine, CNRS, CREGU, GeoRessources lab., 2 rue du Doyen Marcel Roubault, F-54518, Vandœuvre-lès-Nancy, France.
[a]E-mail: quentin.dehaine@univ-lorraine.fr
[b]E-mail: lev.filippov@univ-lorraine.fr

In the theory of sampling, variograms have proven to be a powerful tool to characterise the heterogeneity of 1-dimensional lots. Yet its definition and application in sampling for mineral processing have always been limited to one variable, typically ore grade. However this definition is not adapted to sampling for mineral processing where samples contain multiple properties of interest, i.e. variables, such as multiple element grades, grain size, etc. For such cases, the multivariable variogram, originally developed for spatial data analysis, can be used to summarise time variation of multiple variables (e.g. ore characteristics which are important for the process) and highlights the multivariate time auto-correlation of these variables. A case study of low-grade kaolin residue sampling for gravity processing shows that the multivariogram summarises the overall variability and highlights a periodic phenomenon when all variables are taken into account. This example illustrates the potential of the multivariable variogram compared to the classical approach.

Introduction

In every mining project, economic improvement goes through metallurgical assessment by means of series of metallurgical tests performed on the so-called process samples. Process samples are typically extracted from flowing stream, the so-called one-dimensional (1D) lots, at regular interval to obtain representative samples regarding the grade, mineralogical or physical characteristics. The metallurgical tests allow settling the best operating parameters which will allow reaching the desired recoveries and grades, and therefore improve the process. The effectiveness of these process improvements will depend directly on the representativeness of the samples initially collected for the tests.

The Theory Of Sampling (TOS) developed by Pierre Gy[1] gives a simple set of rules to eliminate sampling biases and minimises the sampling error (variance).TOS introduced the semi-variogram (referred as variogram in the text) adapted to sampling purpose as a way to characterise the autocorrelation between the units of a process and the heterogeneity of 1D lots. This tool provide critical information on[2,3]:

- process variability over time and the magnitude of the different variability components,
- the lot mean and the uncertainty of a single measurement with respect to the autocorrelation phenomenon,
- the optimal design and scheme (*i.e.* random, stratified or systematic) for the sampling protocol.

In a typical variographic experiment, a set of N discrete units (*i.e.* increments) is collected from a one-dimensional flowing stream along a time period, representing the 1D lot. The relative heterogeneity associated with a property of interest, A, in a single unit of mass M_i, expressed in the proportion a_i, is defined as:

$$h_i = \frac{a_i - a_L}{a_L}\frac{M_i}{\bar{M}_i},\ i = 1,\cdots,N \qquad (1)$$

where $\bar{M}_i$ is the average mass increment and a_L the proportion of component A in the lot. This relative heterogeneity is dimensionless and hence the component A can describe any intensive property that characterise the material, *e.g.* grade, size distribution, hardness or specific gravity. The variogram v_j is calculated for a sufficient number of units (up to a maximum of *N/2*) using the equation:

$$v_j = \frac{1}{2(N-j)}\sum_{i}^{N-j}\left(h_i - h_{i+j}\right)^2,\ j = 1,\cdots,N/2 \qquad (2)$$

where j is a dimensionless lag-parameter, defining the distance between two increments. Thus, the variogram describes the variation, due to component A, between units as a function of the distance between them. An extensive description of the variographic technique and its practical application can be found in reference papers[2–4].

However, in the field of mineral processing, results from metallurgical tests often depends on several characteristics of the sample. Thus the samples need to be representative not only for one property (*i.e.* component) but for a certain range of properties. In these situations the practical approach is to identify the property with the most heterogeneous distribution and to take only this property into account. The main difficulty of this approach is that it doesn't account for the multivariate nature of heterogeneity, which can lead to underestimation of significant heterogeneity between close neighbours[5]. The importance of taking into account the multivariate character of the heterogeneity is well-known in geostatistics and particularly for spatial data analysis. The first solution to this problem was proposed by Oliver and Webster[6], who suggested to perform a Principal Component Analysis (PCA) on the data and to study the variogram of the first few principal components. While only a few studies have recently applied this approach to chemometrics, they show the usefulness of a variographic modelling based on PCA scores[7,8].

The purpose of this paper is to introduce the multivariate variogram, originally developed for spatial data analysis by Bourgault and Marcotte[9], which is defined in a way similar to that of the traditional variogram but in a multi-dimensional space. This new tool could be more adapted to process sampling of one-dimensional lots as it takes all properties of interest into account. To illustrate this, a variographic study is performed on a process stream from a kaolin mining plant which has been sampled for metallurgical testing.

Multivariate variogram applied to process sampling

We now assume that the heterogeneity contribution is a multivariate measure. If a material is characterised by a number p of parameters, the heterogeneity could therefore be represented as a vector of p individual heterogeneity contributions:

$$H_i = \left[h_1,\cdots,h_k,\cdots,h_p\right]_i \ , \ i=1,\cdots,N \tag{3}$$

The univariate definition of the variogram is thus no longer adapted and need to be improved. G. Bourgault and D. Marcotte were the first to formalise the principle of a multivariate variogram[9] and it has been widely used for spatial data analysis and mapping since[5,10]. For every metric M it is possible to calculate the multivariate variogram V_j by analogy to the univariate case using the equation:

$$V_j = \frac{1}{2(N-j)}\sum_i^{N-j}\left(H_i - H_{i+j}\right)M\left(H_i - H_{i+j}\right)^t \ , \ j=1,\cdots,N/2 \tag{4}$$

where ^{t} symbolise the transpose and M is positive definite $p \times p$ matrix which defines the metric in the calculation of the "distance" between the units. This metric defines the relation between the variables, such metrics are the identity matrix (Euclidian distance). The multivariate variogram is therefore simply the sum of the univariate variograms, or the inverse of the variance-covariance matrix (Mahalanobis distance)[9].

In contrast to variographic analysis of PCA scores, this approach captures all variables in a single variogram. Thus it is possible to calculate the auxiliary functions and consequently the error generating functions for each sampling scheme using classical point-by-point calculation[3], with the exception of the random selection scheme. Indeed the error generating function associated to this sampling scheme is equal to the constitutional heterogeneity of the lot (CH_L) which is defined as the variance of the (multivariate) heterogeneity contribution of all units making up the lot L:

$$CH_L = s^2\left(H_i\right) = \frac{1}{N}\sum_i^N H_i M H_i^t \tag{5}$$

Material and methods

Material sampling

The samples used in this work were collected with the help of Imerys Ltd., UK. The primary objective of this sampling exercise was to design a protocol which allows collecting a representative sample of a shift (of approximately 2 h) for metallurgical testing. A total of 50 samples (of approximately 25 kg) were collected from the secondary hydrocyclones underflow stream of a kaolin dry mining plant operating at an approximate flow rate of 15 tons/hours corresponding to a micaceous residue which is studied as a potential source of metals[11]. Note that the increments are manually extracted every 2 minutes systematically using a by-pass which diverts the whole stream into the sample collector. This sample extraction protocol may lead to an Increment Extraction Error (IEE) which is difficult to assess.

All increments were weighted then dried directly without dewatering to avoid fine particles loss. Once dried the samples were weighted to estimate their initial pulp density and then riffled to obtain subsamples for particle size analyses. The remaining samples were then crushed and riffled alternatively in accordance with the theory of sampling to obtain representative subsamples for chemical analysis[12].

Analytical methods

The studied material has been sampled with the objective of metallurgical testing by gravity concentration. Thus the analytical methods chosen for the representativeness study must be adapted to this objective. In addition to classical chemical analysis, the critical characteristic of a material for gravity concentration is its size distribution[13].

Chemical Analysis. A set of 18 elements/ oxides were analysed, among which LREE (La, Ce, Nd), Nb and Sn. Representative 10 g aliquots were mixed with Cereox wax (Fluxana® GmbH & Co. KG) and pressed into pellets. Chemical analyses were carried out by Energy Dispersive X-Ray Fluorescence spectroscopy (ED-XRF) using a S2 Ranger (Bruker Corporation) at the GeoRessources laboratory (Vandoeuvre-lès-Nancy, France). The calibration of the XRF used results from Inductively Coupled Plasma Atom-Emission analysis (ICP-AES) for major elements and mass spectral analysis (ICP-MS) for the trace elements realised at the Service d'Analyses des Roches et des Minéraux (SARM-CNRS, Nancy, France).

Particle size analysis. A range of 4 parameters have been retained to describe the particle size distribution of the material: the D10, D50, D90 and Rosin R ammler (RR) slope which represent the particle sizes below which 10%, 50% and 90% of the particles are distributed respectively. And the slope of the size distribution using the Rosin-Rammler model[13]. Particle size analysis has been performed by laser light scattering using a Helium-Neon Laser Optical System MASTERSIZER 3000 (Malvern instruments Ltd.) coupled with a Hydro Extended Volume (EV) sample dispersion unit.

Case study

Experimental individual variograms

The analytical results of 7 selected variables (LREE, Nb, Sn, D10, D50, D90 and RR slope) for 50 micaceous residue samples are presented in Figure 1. The variation illustrates the stream material heterogeneity with time. The results show that, for variables (D10, Nb, Sn, and LREE), the variability expressed by the entire profile is equal to the global variation interval represented by the mean ±2σ interval, whereas for variables (D50, D90, and RRslope), the variability seems associated with slight trends. However, there are no significant outliers in the profiles. Thus the analytical results can be used directly without any pre-treatment.

It is difficult to interpret from these different scales profiles which variable contributes most to the heterogeneity of the lot. One can thus compare the individual heterogeneity contribution, calculated using equation (1) for each variable (Figure 2). It is observed that the LREE content has the largest overall variability.

From these individual heterogeneity contributions the individual variograms are calculated using equation (2) and the nugget effects V_0 are estimated by backward extrapolation (Figure 3A). The auxiliary functions noted w_j and w'_j are shown in Figure 3C and D. The individual variograms distinguish two main groups, a high-sill variables group (LREE, D90 and Sn) and a low-sill variables group (D10, D50, RR Slope and Nb). The overall range is difficult to estimate using directly the variograms, but the auxiliary functions suggest an overall range around 5-7. The variograms of the low-sill groups

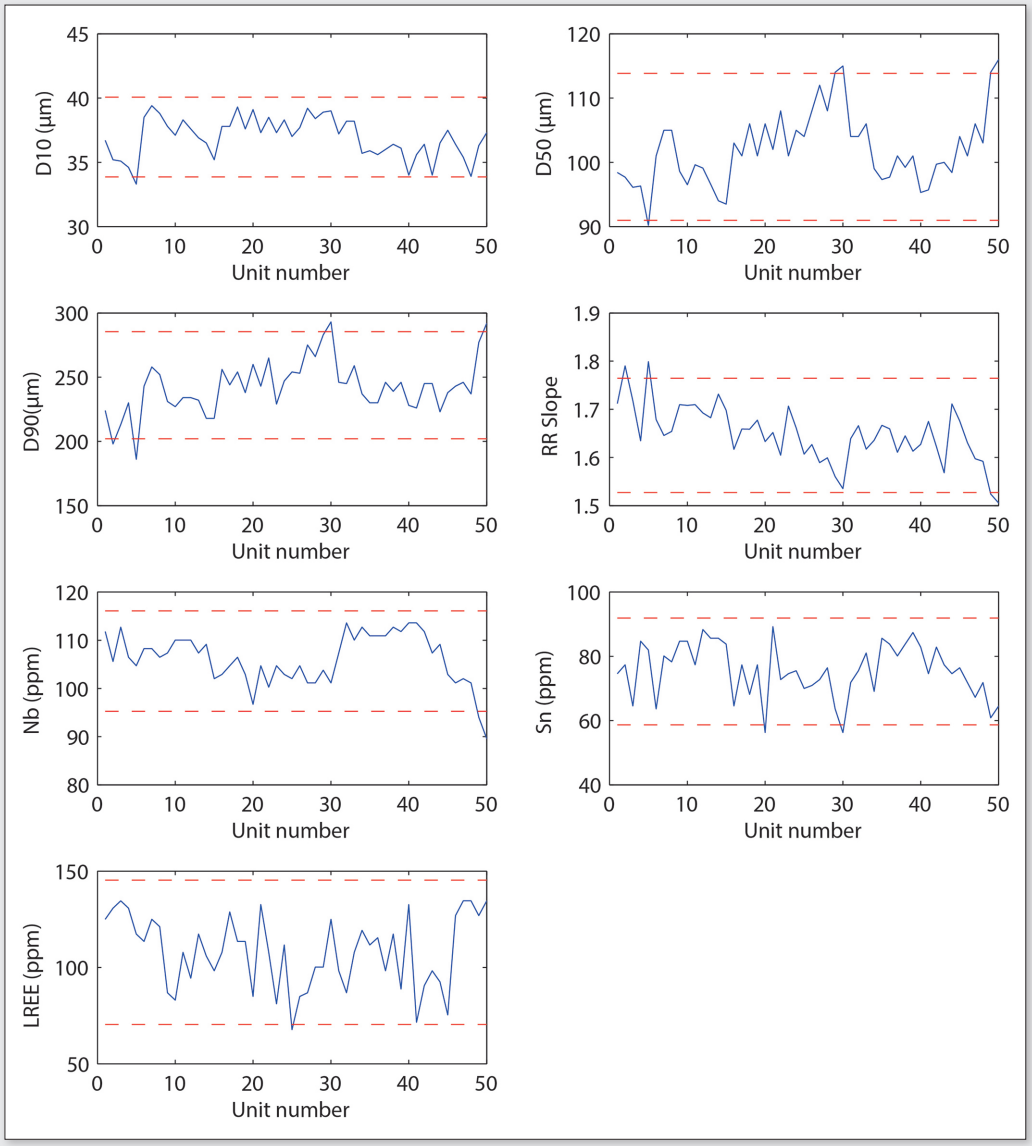

Figure 1. Analytical results characterising the variations of the geochemical compositions (Nb, Sn, and LREE) and size distributions (D10, D50, D90, and RR slope) during time, each unit being extracted at 2 min intervals. The dashed lines represent the mean ±2σ of the analytical results. It can be seen that there is no significant outliers.

appear to 'flat' as well as the variogram of Sn. A minimum can be observed in the variogram of LREE at j = 15 indicating the existence of a possible cyclic fluctuation with a too long period of (*i.e.* j = 15 = 30 min) to see another minimum in the variogram. A similar observation is observed for the D90 variogram (Figure 3B). Indeed, a local minimum is observed at j = 7-9 and a tentative repetition at j = 20 (this can also observed for w_j but not for w'_j since the curve is too smooth). This suggests the existence of some periodic phenomenon for the D90 with a rather short period of approximately 9 lags (*i.e.* j = 9 = 18 min).

The classical conclusion at this point will be to focus the sampling protocol on the LREE content taking care of the periodic phenomena.

Figure 4 show the error generation functions for LREE according to the sampling scheme which is used to choose a protocol with the lowest sampling variance. It can be seen that the 3 sampling schemes are quite close but the systematic sampling stay the sampling scheme with the lowest variance. The recommended sampling protocol is thus hard to define it could be recommended to use a stratified random sampling or systematic sampling with at least 5 or 10 increments with a sampling frequency higher than two per period of 18 min and 30 min. Since the average shift duration is around 3h this would imply to sample not 5 or 10 but at least 20 increments.

Experimental multivariograms

A multivariate analysis highlights the relationships between the variables which are not taken into account in classic variographic studies. Table 1 presents the correlation matrix for the selected 7 variables. As predicted all the variables referring to the size distribution are strongly to moderately correlated with the exception of D10 which only display moderate correlations (with D50 and D90) or no correlation at all (with RRslope). Sn and Nb are both moderately correlated with the D50 whereas LREE display a clear independency.

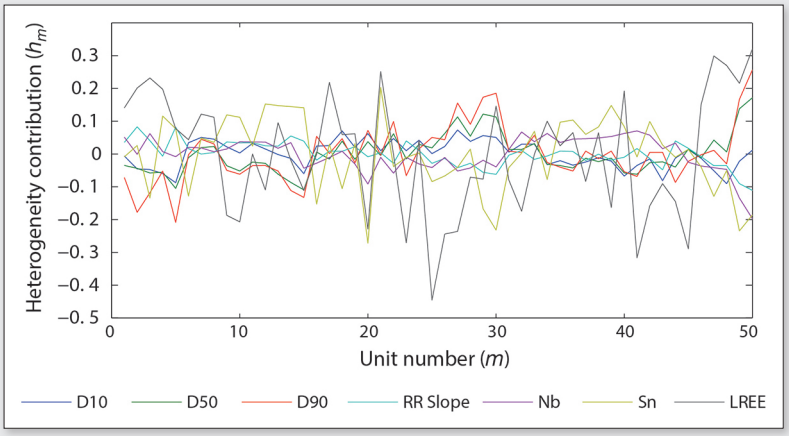

Figure 2. Individual heterogeneity contributions h_m of the 7 variables of interest for the 50 units.

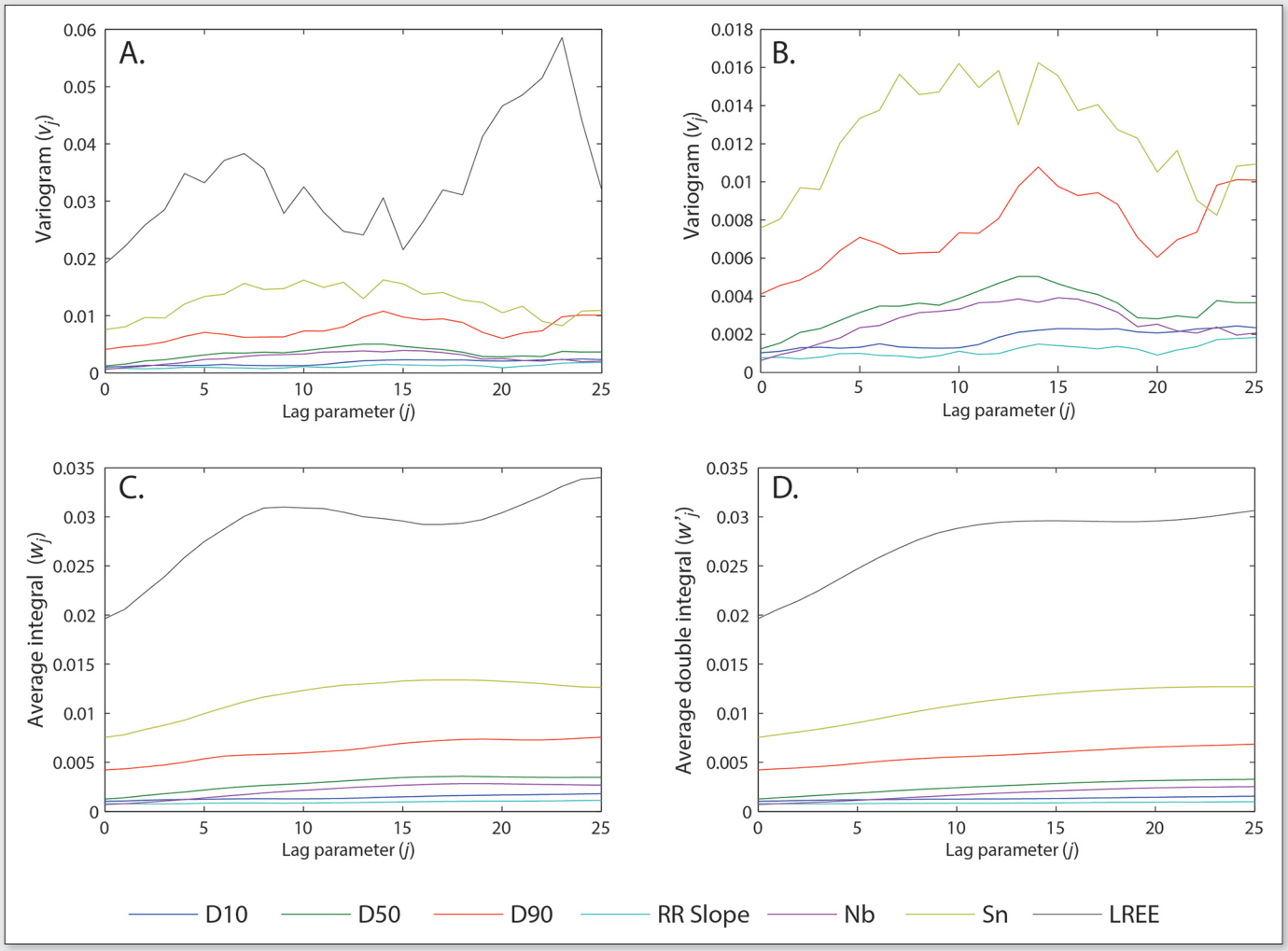

Figure 3. (A) Experimental variograms V_j of the 7 variables of interest. (B) Experimental variograms V_j of 6 of the variables of interest without LREE. (C) Average first order integral w_j and (D) Average second order integral w'_j. A common range of approximately 5-7 lags (10-14 min) is observed.

The multivariogram is computed using formula (4) with Mahalanobis metrics (Figure 5). The general shape of the multivariogram is approximated by a smoothed curve with a spherical model[14]:

$$V_j = \begin{cases} s\left[\frac{3j}{2r} - \frac{1}{2}\left(\frac{j}{r}\right)^3\right], & j \le r \\ s, & j > r \end{cases} \quad (6)$$

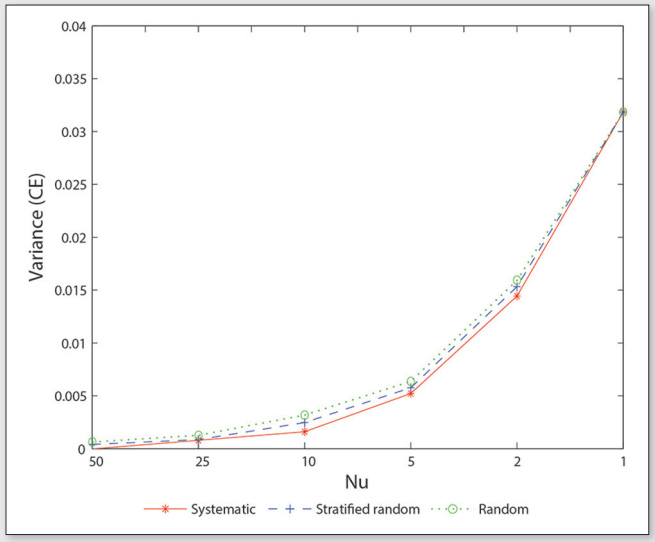

Figure 4. Plot of the error generating functions associated to the LREE content for the 3 sampling schemes as a function of the number of units/increments collected to make the final sample (Nu).

where s represent the sill of the variogram and r the range. The range suggested by the spherical model is around 11, which is twice the general range observed for the individual variograms. Two minimums at j = 9 and j = 20 on the multivariogram curve suggest a periodic phenomenon with a period of approximately 10 lags (j = 10 = 20 min) which is a results of the periodic phenomena observed in the individual variograms. The multivariogram also displays a high sill of approximately 7, which is due to the metric used in the computation of the multivariogram. Hence the sampling variance is much more important too, and with 5 increments to make the final sample, the sampling variance is still about 0.67 and 0.25 if 10 increments are collected (Figure 6). Based on this multivariogram a sampling protocol could be to take at least 10 increments with a sampling frequency higher than two per period of 20 min.

The multivariogram has allowed proposing a more adapted sampling protocol which takes into account a periodic phenomenon. However the estimated global variance with this approach is very high and implies a large number of increments should be sampled to achieve a reasonably lower sampling variation. This is a direct consequence of the choice of the variables of interest for the variographic study which all contribute at various degrees to the heterogeneity. Note that their importance for the process tested could be completely different from one variable to the other. Thus the sampler must pay attention to the choice of the variables of interest to avoid overestimation of the sampling variance. Another way to have a sampling variance more adapted to the tests for which the samples are collected would be to weight the variables by the mean of an adapted metric.

Table 1. Correlation matrix for all the variables of interest. The high correlation coefficients (>|0.75|) are noted in italic.

Variables	D10	D50	D90	RR Slope	Nb	Sn	LREE
D10	**1.00**	0.61	0.62	-0.20	-0.24	-0.30	-0.25
D50	0.61	**1.00**	0.93	-0.78	-0.64	-0.64	0.02
D90	0.62	0.93	**1.00**	-0.88	-0.54	-0.54	-0.02
RR Slope	-0.20	-0.78	-0.88	**1.00**	0.48	0.45	-0.09
Nb	-0.24	-0.64	-0.54	0.48	**1.00**	0.52	-0.14
Sn	-0.30	-0.64	-0.54	0.45	0.52	**1.00**	-0.09
LREE	-0.25	0.02	-0.02	-0.09	-0.14	-0.09	**1.00**

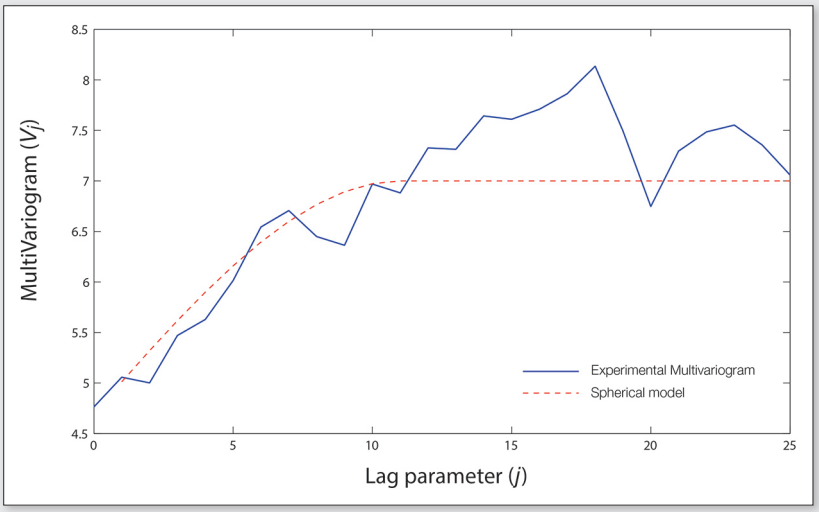

Figure 5. Multivariogram for the 7 variables of interest and fitted spherical model. The range given by the spherical model is approximately 11 with a sill around 7. However two minimums at j = 9 and j = 20 suggest a periodic phenomenon with a period of approximately 20 min.

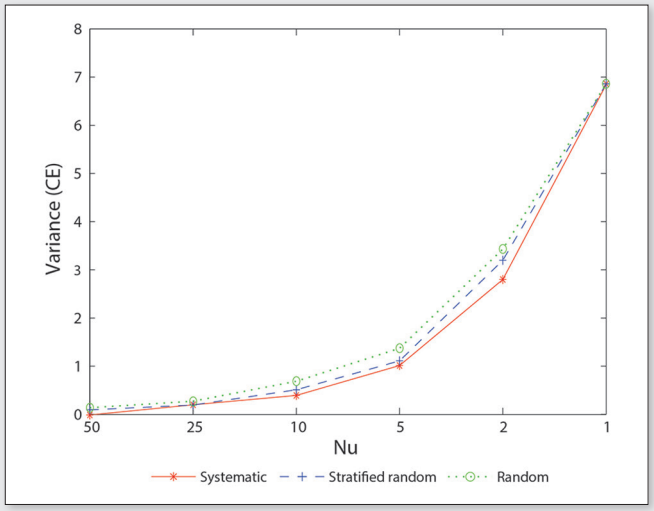

Figure 6. Plot of the error generating functions of the multivariogram for the 3 sampling schemes as a function of the number of units/increments collected to make the final sample (Nu).

Conclusions

The multivariate approach of process variograms described in this work has allowed a better description of the heterogeneity of a material taking into account all the variables of interest simultaneously. This approach give to the sampler the opportunity to choose all the parameters that characterise the material for a given objectives and to use the multivariate variogram as a summarising tool to describe the variability of this material and to design an adapted sampling protocol.

Acknowledgments

The authors wish to thank the Imerys Ltd., UK, and especially S. Moradi, P. Chauhan and A. Coe for their help during the sampling exercise. We are also grateful to S. Lightfoot and P. Budge for their advices and technical support. We thank C. Gauthier for its help in the sample preparation process. T.M.K. LE is also thanked for her work during her master project. This work has been financially supported by the European FP7 project "Sustainable Technologies for Calcined Industrial Minerals in Europe" (STOICISM), grant NMP2-LA-2012-310645.

References

1. P. Gy, *Sampling for Analytical Purposes*. John Wiley & Sons, Chichester (1998).
2. P. Gy, "Sampling of discrete materials III. Quantitative approach—sampling of one-dimensional objects". *Chemometrics and Intelligent Laboratory Systems*. **74**, 39–47 (2004). doi: http://dx.doi.org/10.1016/j.chemolab.2004.05.015
3. L. Petersen, K.H. Esbensen, "Representative process sampling for reliable data analysis—a tutorial". *Journal of Chemometrics*. **19**, 625–647 (2005). doi: http://dx.doi.org/10.1002/cem.968
4. P. Minkkinen, "Practical applications of sampling theory". *Chemometrics and Intelligent Laboratory Systems*. **74**, 85–94 (2004). doi: http://dx.doi.org/10.1016/j.chemolab.2004.03.013
5. G. Bourgault, D. Marcotte, P. Legendre, "The multivariate (co)variogram as a spatial weighting function in classification methods". *Mathematical Geology*. **24**, 463–478 (1992). doi: http://dx.doi.org/10.1007/bf00890530
6. M.A. Oliver, R. Webster, "A geostatistical basis for spatial weighting in multivariate classification". *Mathematical Geology*. **21**, 15–35 (1989). doi: http://dx.doi.org/10.1007/bf00897238
7. P. Minkkinen, K.H. Esbensen, "Multivariate variographic versus bilinear data modeling". *Journal of Chemometrics*. **28**, 395–410 (2014). doi: http://dx.doi.org/10.1002/cem.2514
8. Z. Kardanpour, O.S. Jacobsen, K.H. Esbensen, "Soil heterogeneity characterization using PCA (Xvariogram) - Multivariate analysis of spatial signatures for optimal sampling purposes". *Chemometrics and Intelligent Laboratory Systems*. **136**, 24–35 (2014). doi: http://dx.doi.org/10.1016/j.chemolab.2014.04.020
9. G. Bourgault, D. Marcotte, "Multivariable variogram and its application to the linear model of coregionalization". *Mathematical Geology*. **23**, 899–928 (1991). doi: http://dx.doi.org/10.1007/bf02066732
10. R. Kerry, M.A. Oliver, "Variograms of Ancillary Data to Aid Sampling for Soil Surveys". *Precision Agriculture*. **4**, 261–278 (2003). doi: http://dx.doi.org/10.1023/a:1024952406744
11. Q. Dehaine, L.O. Filippov, "Rare earth (La, Ce, Nd) and rare metals (Sn, Nb, W) as by-product of kaolin production, Cornwall: Part1: Selection and characterisation of the valuable stream". *Minerals Engineering*. (2014). doi: http://dx.doi.org/10.1016/j.mineng.2014.10.006
12. L. Petersen, C.K. Dahl, K.H. Esbensen, "Representative mass reduction in sampling—a critical survey of techniques and hardware". *Chemometrics and Intelligent Laboratory Systems*. **74**, 95–114 (2004). doi: http://dx.doi.org/10.1016/j.chemolab.2004.03.020
13. B.A. Wills, T. Napier-Munn, *Wills' Mineral Processing Technology*. Elsevier (2005).
14. R. Webster, M.A. Oliver, *Geostatistics for Environmental Scientists*. John Wiley & Sons, Ltd, Chichester, UK (2007).

doi: 10.1255/tosf.63

Comparison of sampling methods by using size distribution analysis

P. Minkkinen[a*], I. Auranen[b], L. Ruotsalainen[c] and J. Auranen[d]
[a]Lappeenranta University of TechnologyPO Box 20, FIN-53851, Lappeenranta, Finland. E-mail: Pentti.Minkkinen@lut.fi
[b]IMA Engineering, Luoteisrinne 4A, FIN-02270, Espoo, Finland. E-mail: ilpo.auranen@ima.fi
[c]Mine On-Line Service, Luoteisrinne 4A, FIN-02270, Espoo, Finland. E-mail: lari.ruotsalainen@mols.fi
[d]Mine On-Line Service, Luoteisrinne 4A, FIN-02270, Espoo, Finland. E-mail: jesse.auranen@mols.fi

Pierre Gy has derived an equation, which can be used to estimate the relative variance of the fundamental sampling error of size distribution results given as mass fractions for each size class. This theory is used in this study. The Heterogeneity Invariant, *HI*, is the relative variance of the fundamental sampling error extrapolated to a sample size of a unit mass (usually 1 g). *HI* can be estimated from a sieve analysis for each size class *i* from Eq. 1.

$$HI_i = \left(\frac{1}{a_i} - 2\right) v_i \rho_i + \sum_{i=1}^{n} \rho_i a_i v_i \quad (1)$$

Here a_i is the mass fraction of size class *i*, v_i the average particle size in class *i* and ρ_i the density of particles in size class *i*. Given HI_i, the relative variance of the fundamental sampling error, S^2_{FSE} can be estimated for different sample sizes to be sieved from the test material:

$$s^2_{FSE} = HI_i \left(\frac{1}{m_s} - \frac{1}{m_L}\right) \quad (2)$$

Here m_s is the sample size to be sieved and m_L the size of the lot from which the sample is taken.

If the sampling methods performs correctly (unbiased) and is able to minimize the segregation effects, always present when material consisting of fragments or particles having a wide size distribution, the observed variance of replicate samples should be close to that obtained by using the above equations. It is also possible to calculate a confidence intervals for a given size distribution.

In this study a newly developed sampler was tested by sampling blast hole chippings from Northland Resources' Kaunisvaara Iron Ore Mine in northern Sweden and the results were compared to other sampling methods currently in use. A number of the samples were also sent for chemical analysis to see if the analytical results correlate with the size classes. A convenient way to summarize and compare size distribution results and analytical results is to carry out Principal Component Analysis (PCA) on both the size data and the analytical data.

Introduction

Blast hole sampling, especially from large rotary drill holes, is challenging. While the final circumstances depend on the material density and the diameter and depth of the hole, the mass of drill cuttings coming up from the hole is often counted in tons. Once the drill cuttings have settled on the ground, correct sampling is nearly impossible due to segregation and delimitation error. After the cuttings have settled, depth information is lost making sampling per meter impossible. Especially in vein type ores the grade can vary greatly as a function of depth, and sampling each meter would provide more detailed information. In the past, sampler cutters of different types including sectorial samplers and tube samplers have been applied with varying success. Often the practically useful methods does not provide representative samples and the ones that could give correctly cut samples need so much work and preparation that it is not feasible in practice. Above all, the working environment for someone taking samples near the drill is very poor due to excessive noise and dust, and significant health hazards are present in form of heavy moving machinery.

A newly developed sampling device, RAS – Rotary AutoSampler, was designed by IMA Engineering Oy Ltd. (Figure 1). This is an automatic sampling system that collects a sample continuously while drilling and subsequently splits the sample into an adjustable and pre-selected sample size. Depth information is also recorded for each sample. The sampler consists of two main parts, a primary sampling belt and a rotating cone splitter. The basic operation is simple: the primary sampling belt takes a continuous sectorial sample from the original flow of drill cuttings which is then delivered to the cone splitter, which divides the final samples that are collected

Figure 1. RAS – Rotary Autosampler installed in a rotary drill

MOLS Sampled Hole		Hole Number 465100		Iron mine Hole Average
3.55	4	0 -> 1 m	37	
9.14	9	1 -> 2 m	37	
14.60	15	2 -> 3 m	37	
23.50	24	3 -> 4 m	37	
24.90	25	4 -> 5 m	37	
32.30	32	5 -> 6 m	37	
50.21	50	6 -> 7 m	37	
50.21	50	7 -> 8 m	37	36.79275842
54.10	54	8 -> 9 m	37	
40.40	40	9 -> 10 m	37	
40.40	40	10 -> 11 m	37	
42.10	42	11 -> 12 m	37	
30.90	31	12 -> 13 m	37	

Figure 2. Iron content per meter vs. iron content from single pile sample

in transparent plastic sample bags, which are then processed and analysed. This kind of sampling method is new and never been fully tested before. Therefore this research was necessary to examine if the sampling technology is correct, if the samples taken are representative of the original lot and if the method can be applied in practice. Testing was carried out in Northland Resources' Kaunisvaara Iron Ore Mine in northern Sweden and IMA Engineering premises in Espoo, Finland. A certified commercial laboratory Labtium Oy was used to process and analyse the samples obtained.

According to the results, the primary sampling belt collects on average 10% of the total cuttings blown out of the drill hole. The total mass of cuttings from each hole varies greatly and is seldom the theoretical amount calculated from material density and hole dimensions. Often the cuttings also spread unevenly around the hole, which adds to the size variation of the sample. Moreover, the first 1-3 drill meters that penetrate the previous sub-drill yield very little sample which is often originating from the filling material used to level the blast benches for easier drill rig movement. The mass of collectable sample material increases as a function of depth. The last few meters yield the usually the largest sample, so significant part of the lot comes from sub-drilling which represents the next bench instead of current bench (Figure 2).

Design of sampling experiments

Equipment

Sampling Belt

The primary sampling belt is essentially a conveyor belt, which collects drill cuttings as they fly out of the blast hole during drilling (Figure 3). Minor modifications (Figure 6) were made to the dust curtains of an Atlas Copco Pit-Viper 271 (Figure 4) rotary blast hole drill in order to fit the sampler belt next to the drill rod to collect cuttings. The drill was drilling 12-14 meter long blast holes using 251 mm (9 7/8 inch) diameter tricone drill bit.

The collected drill cuttings fall from the conveyor belt through a splitter capable of splitting the feed into samples with the following ratios: 1/8, 1/8, 3/4 (Figure 5). To summarise, drill cuttings flying out from the blast hole would be carried by the conveyor belt and dropped through the splitter, and the final sample is collected in a bucket underneath the splitter (Figure 7).

Figure 3. Primary sampling belt conveyor used in this study. Conveyor width was 400 mm and length 3 meters.

Autosampler

The Autosampler is a rotating cone splitter which divides the drill cuttings feed from the RAS primary sampling belt into 2 samples and a reject pile (Figure 8). The splitting ratio and sample size can

Figure 4. Atlas Copco Pit Viper 271 Rotary drill at Kaunisvaara iron ore mine

Figure 5. A Metzke model MFS 3T32 3C 3-tier splitter was used at the end of the conveyor belt to split collected drill cuttings at ratios 1/8 , 1/8, 3/4, as shown above right.

Figure 6. Modification in Pit Viper's dust curtain for RAS conveyor belt entry.

be adjusted. Autosampler was tested independently of the primary sampling belt test. (Figure 9)

Detailed testing procedures

Primary sampling with belt conveyor (3m samples)

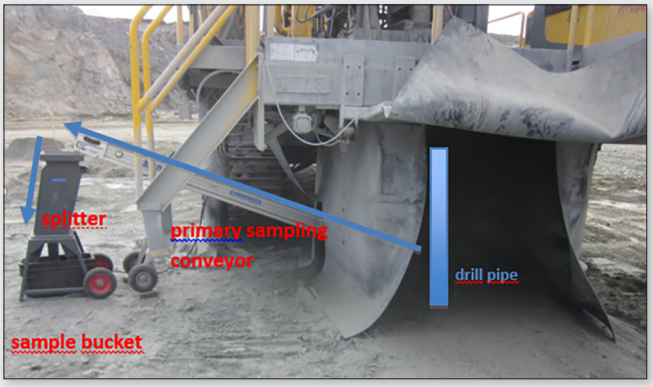

Figure 7. Drill cuttings flow chart

Figure 8. Autosampler system with Softcore™ sample socks attached.

The experiment is designed to collect samples of borehole cuttings from 3 drill meters and compare grain size distribution and chemical properties against the discarded cuttings:

Figure 9. Testing the Autosampler by pouring drill cuttings through it. Two samples are collected in buckets on opposite sides and the reject in the centre.

Figure 10. Tarp laid on the ground around the concrete ring, which surrounds the blast hole.

- Pit Viper 271 drills to 4 m depth. The drill pipe and drill bit is then lifted from the hole, drill cuttings cone already accumulated around the hole is cleared, and a 6m^2 tarpaulin is laid on the ground to surround the drill hole. The tarpaulin prevents contamination of the accumulated cuttings from the ground underneath. A concrete ring is placed around the drill hole on top of the tarpaulin cover to prevent any drill cuttings from being lost under the cover (Figure 10).
- The conveyor belt is then brought through the opening in the helm, to the edge of the drill hole. Drilling is continued. A Sample is continuously collected by the primary sampling conveyor and the drill cuttings from the 3 m drilling from 4–7 m depth accumulate on top of the tarpaulin (Figure 11).

Figure 11. Primary sampling conveyor is pushed through the opening in the dust curtain and placed next to the mouth of the blast hole.

Figure 12. A drill cuttings cone as viewed from under the dust curtain, with the RAS conveyor belt in place.

- The Pit Viper drills for 3 meters. Meanwhile, most of the drill cuttings accumulate as a cone on the tarpaulin. The rest of the drill cuttings are carried out by the conveyor, through the splitter (splitting them at 1/8) and collected in buckets (Figure 12).
- After 3 m has been drilled, the entire cuttings cone left on the tarpaulin is also split with 1/8 ratio, into sample buckets. This was done by shovelling all the drill cuttings from the heap on to the conveyor belt. From the belt the material falls through the splitter, and is collected in buckets beneath the splitter. For practical reasons, splitting was continued until a sample of around 6-10 kg was achieved. This sample is used for comparison with the conveyor sample collected during drilling (Figure 13).
- Samples taken with the sampling belt and the sample collected from the rest of the pile (Figure 14) are sent to a laboratory for sieving and chemical analyses in order to compare the results.

Autosampler (rotating cone splitter)

The Autosampler was tested as follows:

- A bucket of drill cuttings was originally collected from a drill cuttings cone in the Kaunisvaara mine.
- These were then poured through the Autosampler (Figure 9).
- As they fall through, the Autosampler splits the poured bucket of drill cuttings into 3 parts: 2 samples, actual sample and duplicate) (white buckets) and 1 reject pile (pink bucket) in the centre.
- All 3 samples from each pour were sent to a certified laboratory for further analysis (grain-size distribution and elemental contents).
- Grain-size distributions and elemental contents of all the samples were compared and analysed.

Additional testing methods

Some sectorial samples were also taken for comparison. The sectorial sampling boxes shown in Figure 15 were placed next to the hole at the same time than sampling belt, and removed after 3 meters was drilled. The sample was split with riffle splitter until a practical sample size was achieved.

Figure 13. Drill cuttings flow

Estimation of sampling variance from sieve analysis

Pierre Gy[1,2] has derived an equation, which can be used to estimate the relative variance of the fundamental sampling error of size distribution results given as mass fractions for each size class. This theory is used in this study. The Heterogeneity Invariant, *HI*, is the relative variance of the fundamental sampling error extrapolated to a sample size of a unit mass (usually 1 g). For each size class i from a sieve analysis, *HI* is estimated from Eq. 1.

$$HI_i = \left(\frac{1}{a_i} - 2\right) v_i \rho_i + \sum_{i=1}^{n} \rho_i a_i v_i \qquad (1)$$

Here a_i is the mass fraction of size class i, v_i average particle size in class i and ρ_i the density of particles in size class i. Average particle size can be estimated from the upper, d_{iu} and lower d_{il} openings

Figure 14. Visual comparison of primary sampling belt collected drill cuttings pile on the left vs. the remainder of the blast hole cone after 14m drilling.

Figure 15. Triangular sampling trays next to the blast hole prior to drilling 3 meters.

of the sieves:

$$v_i = f_i \frac{d_{iu}^3 + d_{il}^3}{2} \quad (2)$$

f = particle shape factor, which is 1 for cubic particles, 0.524 for spherical particles. For most crushed and ground materials, the factor is close to 0.5 which was used in this study as the default value. If a sample of size m_s is taken from a lot m_L, which is much larger than the sample, the constitution heterogeneity, CH, or relative variance of the fundamental sampling error for each size class is

$$CH_i = s_{FSE}^2 = \frac{HI_i}{m_s}, m_L >> m_s \quad (3)$$

If the sample forms a significant part of the lot from which it is taken, then a correction has to be made in estimating the sample variance

$$CH_i = s_F SE^2 = HI_i(1/m_s - 1/m_L) \quad (4)$$

Often the primary sample is so large that the sample size has to be reduced before sieving. If, e.g., the primary sample m_{s1} is taken from a lot by size m_L, and sample m_{s2} is taken from the primary sample and sample m_{s3} taken from the secondary sample is then sieved the variance of this 3-step process is, if the size distribution is not changed:

$$CH_{TOT} = HI_i\left(\frac{1}{m_{s1}} - \frac{1}{m_L}\right) + HI_i\left(\frac{1}{m_{s2}} - \frac{1}{m_{s1}}\right) + HI_i\left(\frac{1}{m_{s3}} - \frac{1}{m_{s2}}\right) = HI_i\left(\frac{1}{m_{s3}} - \frac{1}{m_L}\right) \quad (5)$$

Constitution heterogeneity is converted to relative standard deviation follows:

$$s_{ri} = \sqrt{CH_i} \quad (6)$$

If the relative standard deviation is given in percentages s_{ri} should be multiplied by 100. Fundamental sampling variance gives the variance of an ideal sampling process, i.e., the material of the lot is a random mixture of its constituents and the sampling process is correct. If there is segregation in the lot or sampling devices are not correctly designed or operated, experimental variances are larger than those calculated from Eq. 1.

Confidence intervals

When HI values from the sieving are available approximate confidence intervals for the size fractions can be estimated. Absolute standard deviations for the size fractions i are, given the sizes of the lot (m_L) and the sample (m_{si}):

$$s_i = \sqrt{HI_i\left(\frac{1}{m_{si}} - \frac{1}{m_L}\right)} \cdot a_i \quad (7)$$

Approximate confidence intervals ci for the size fractions are

$$ci_i = a_i \pm k \cdot s_i \quad (8)$$

The coverage factor $k = 2$ gives theoretically 95% confidence interval, i.e., if the lot is a truly random mixture of fragments and the sampling system is correctly designed and operated, as an average only one value in 20 replicate samples taken from the same lot shows results outside the confidence interval. If the standard deviations are multiplied with a factor of 3, it gives 99.7% confidence interval corresponding as an average to one outlier in 300 observations. In practise, the fragment shape and density values used in calculations are approximate values, not exact. Consequently, the confidence levels are also approximate values. However, significant deviations from these values indicate either a deficient sampling system or material segregation that the sampling system cannot eliminate.

Note: If the sample is so small that only a few fragments, say less than 16, from the coarsest fraction are included in the sample symmetric confidence intervals obtained from Eq. 8 are not valid for this size fraction. Relative standard deviation estimate larger than 25% is an indication that number of these fragments in the sample is smaller than 16.

Minimum sample size for a given precision requirement

Given the lot size and precision requirement, i.e., the required relative standard deviation, , Equation 9 gives the minimum sample size (for an ideal mixture and sampling system)

$$m_s \geq \frac{HI}{s_{r(req)}^2 + \frac{HI}{m_L}} \quad (9)$$

In interpreting experimental results one should remember that the results obtained from FSE calculations are valid for ideal mixtures and sampling equipment designed and operated according to the principles of TOS. In practice parameters, like shape factors and size class densities, are not exact but only approximates. As safety factor it is recommended that the theoretical minimum sample sizes are doubled. In addition, if the sample size needs to be reduced for analysis each new sample should consist of several increments, ideally from as many as is possible without introducing increment *delimitation and extraction* errors. Increasing the number of fragments in the samples reduces the grouping and segregation errors defined in TOS.

Experimental results

Example of calculations

Tables 1 and 2 show the sieve results obtained from one of the experimental drill holes. The sample, 6.053 kg, was taken with the RAS sampler from a 3 m section of the drill hole. Table 1 gives the results of the fundamental sampling error calculations as explained in the previous section. Table 2 gives the average fragment mass, total mass of fragments and the average number of fragments in each of the six size classes sieved from the sample.

Sampling variance of a particle mixture is a function of the number of the analyte particles in the sample. As Table 2 shows, the number of fragments rapidly increases when the particle size is reduced and, consequently, HI decreases. If a reliable result of the coarsest fraction in sample is necessary, then it determines the minimum sample size that should be used. Table 3 shows the confidence intervals for the mass fractions in each size class for 1 kg and 5 kg samples calculated using the experimental HI values (Eqs. 7 and 8). The confidence intervals for the coarsest size fraction are: from 1 kg sample a_i = 5% ± 3.52% and from 5 kg sample a_i = 5% ± 1.50%

Table 4 shows how the theoretical minimum sample size depends on the required uncertainty of sampling given as the relative standard deviation: 1%, 5% and 10%. Sample sizes were calculated for

Table 1. Results from calculating the heterogeneity invariant (*HI*), constitution heterogeneity (*CH*) and relative standard deviation (s_r) from sieving results of 6053 g sample from a 50 kg lot. Shape factor $f = 0.5$ and density 3.2 g/cm^3 were assumed.

Size class d1 (cm)	Size class d2 (cm)	d(nominal)	v_i (cm^3)	a_i	*HI* (g)	*CH*	s_r (%)
1.5	0.8	1.248	0.972	0.050	56.18	0.00816	9.03%
0.8	0.2	0.638	0.130	0.123	2.757	0.0004	2.00%
0.2	0.1	0.165	0.002	0.076	0.288	4.18E-05	0.65%
0.1	0.05	0.0825	0.000281	0.111	0.214	3.1E-05	0.56%
0.05	0.025	0.0413	0.0000352	0.181	0.208	3.02E-05	0.55%
0.025	0.01	0.0203	0.00000416	0.451	0.207	3.01E-05	0.55%

Table 2. Average fragment mass, total mass and number of fragments in each size class in 6053 g sample.

d (nominal)	v_i (cm^3)	fragment mass (g)	Total mass in size class (g)	Av. No. of fragments
1.248	0.972	3.1096	303	97.3
0.638	0.130	0.416	745	1790
0.165	0.002	0.0072	460	63893
0.083	0.000281	0.0009	672	746537
0.041	0.0000352	0.0001125	1096	9738604
0.020	0.00000416	0.0000133	2730	205255865

two different lot sizes: 200 kg (sample taken from a pile) and from a lot much larger than the sample (primary sample taken from a large target). The minimum sample size depends strongly on the required standard deviation: if the uncertainty is reduced by factor 10 the sample size has to be increased by factor of 100 in case the lot is much larger than the sample size. In case that the lot size is 200 kg in order to reduce the sampling standard deviation of the coarsest fraction to 1% 147 kg sample is needed.

Comparison of samples taken from the same lot

In most of the experimental drill holes 3-m sections were taken and sampled with the methods currently in use and with the new test

Table 3. 3 *s* confidence intervals calculated for 1 kg and 5 kg sample sizes from the experimental results.

HI (g)	*s* (mass fraction) m_s = 1 kg	*s* (mass fraction) m_s = 5 kg	a_i	3 *s* conf. interv. (m_s = 1 kg) lower	3 *s* conf. interv. (m_s = 1 kg) upper	3 *s* conf. interv. (m_s = 5 kg) lower	3 *s* conf. interv. (m_s = 5 kg) upper
56.18	0.01173	0.00503	0.050	0.0148	0.0852	0.035	0.065
2.757	0.00639	0.00274	0.123	0.1038	0.1422	0.115	0.131
0.288	0.00128	0.00055	0.076	0.0722	0.0798	0.074	0.078
0.214	0.00161	0.00069	0.111	0.1062	0.1158	0.109	0.113
0.208	0.00258	0.00111	0.181	0.1733	0.1887	0.178	0.184
0.207	0.00643	0.00276	0.451	0.4317	0.4703	0.443	0.459

Table 4. Minimum sample sizes calculated for three different relative standard deviation targets for sampling error; lot sizes m_L = 200 kg and $m >> m_s$.

HI (g)	Minimum sample size (g) s_r = 1% $m_L >> m_s$	s_r = 1% m_L = 200 kg	s_r = 5% $m_L >> m_s$	s_r = 5% m_L = 200 kg	s_r = 10% $m_L >> m_s$	s_r = 10% m_L = 200 kg
56.18	562000	147500	22500	20200	5620	5460
2.757	27600	24230	1100	1100	276	275
0.288	2880	2840	115	115	29	29
0.214	2140	2120	86	86	21	21
0.208	2080	2060	83	83	21	21
0.207	2070	2050	83	83	21	21

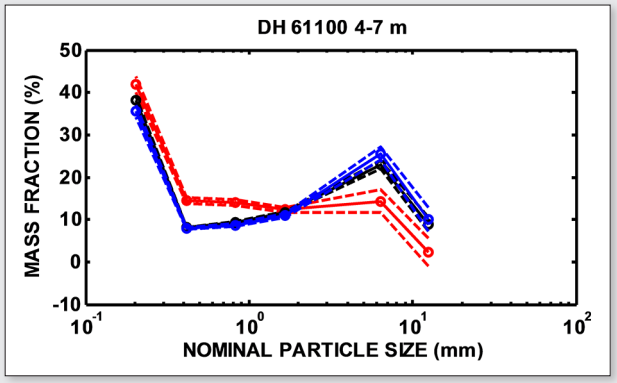

Figure 16. Size fractions with 3 s confidence intervals calculated from data of the test method (red) and from two sampling methods currently used (black and blue). 4–7 m section of the drill hole was sampled.

method. The remaining pile was split in two or three steps using riffle splitter type sampler in order to obtain pile sample weighing less than 10 kg. If necessary, other primary samples taken from the pile were also split. Sample sizes sieved varied from 2 to 9 kg. From the sieve results *HI* values were calculated for each six size fractions obtained in sieve analysis. *HI* values available confidence intervals of the size fractions can be calculated for the used sample sizes. Confidence intervals calculated for the samples obtained by using different sampling methods should overlap, if the sampling methods are correct and can eliminate the effects of segregation. Segregation is caused by variation in the rock that the drill has penetrated and segregation in forming the pile. Significant differences indicate that segregation errors play a significant role, and samples taken with different methods are not comparable. Figure 16 shows an example, where the test method (RAS) was compared with two samples taken with a sectorial boxes, which do not extract a complete sector from the pile. The box samples are comparable but differ significantly from the test sample which has lower concentration of coarse and higher concentration of finer fragments. It is obvious that incomplete extraction of a sample sector increases the risk of segregation error in results.

When all samples taken from the lot (drill section in this case) and the sample taken from the remaining pile are analysed it is possible to calculate reference values for the size distribution as weighted

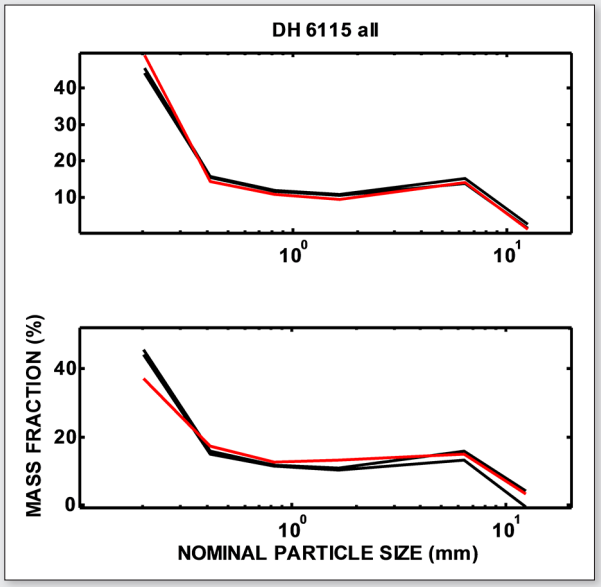

Figure 17. 3 s confidence intervals (black lines) calculated from the weighted averages of the size distribution from all samples for sample sizes of the conveyor and pile sample. Red line shows the observed size distribution of RAS sample (upper panel) and pile sample (lower panel).

average from the analysed samples. The lot mass is the sum of the sample masses (m_j) and the mass of remaining part of the pile (m_R).

$$m_L = \sum_j^n m_j + m_R \tag{10}$$

The reference value for each size class i of this lot thus is:

$$a_i\,(ref) = \frac{\sum_j^n m_j \cdot a_{ij} + m_R \cdot a_{Ri}}{m_L} \tag{11}$$

With these reference values HI_i of each size class of the lot can be calculated. Applying Eqs. 7 & 8 the confidence intervals for each experimental sample size can be estimated. If the experimental results are within confidence interval the sampling method/process can be regarded unbiased. As an example from one of the test

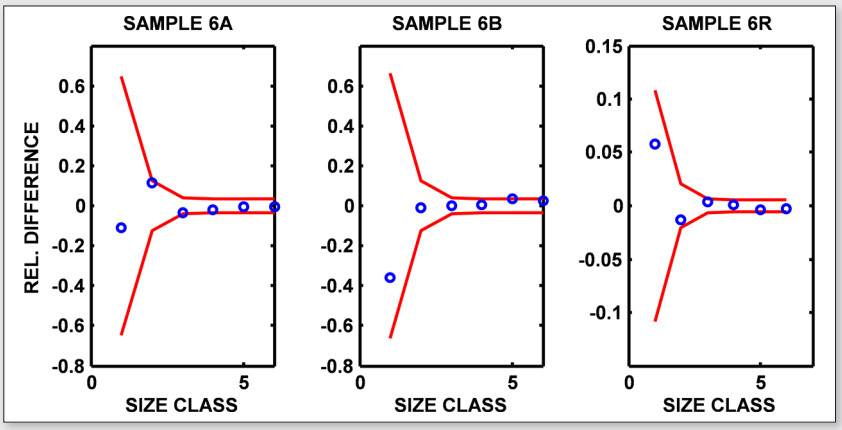

Figure 18. Relative differences (o) of the sieve results from the weighted size class mass fraction values. A and B are duplicates taken with the RAS sampler and R is the sample from the remaining pile. Red lines give the 3 s_r confidence intervals. Size class1 is the coarsest and 6 the finest.

drillings Figure 17 shows the confidence intervals and experimental results of the sample taken from the pile and test method (RAS).

From some of the test piles duplicate samples were taken with the test method (RAS). Pile samples were also analysed, consequently, the reference *HI* values of the lot, and relative deviations of the experimental size distribution from the reference could be calculated. Relative differences of size class *i* in sample *j* from the reference are:

$$dr_{ij} = \frac{a_{ij} - a_i(ref)}{a_i(ref)} \quad (12)$$

Expected confidence intervals of the relative differences are

$$cf_{ij} = 0 \pm k\, s_{ri} \quad (13)$$

and s_{ri} is calculated applying Eq. 6. Figure 18 shows an example from one of the experimental drillings, where duplicate samples were taken with RAS sampler. In general, results of RAS method agreed well with the reference values of the whole pile.

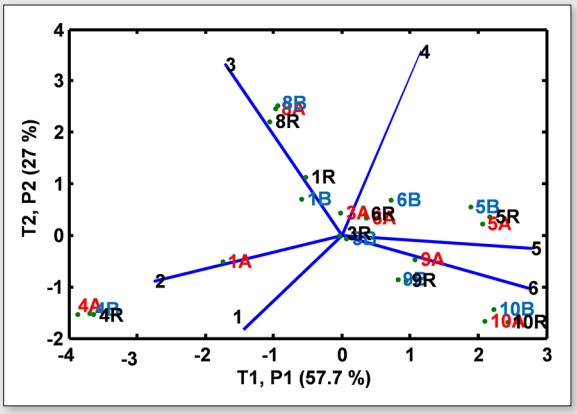

Figure 20. Score and loadings biplot of the two first components of the PCA model. Blue lines show the loadings of the size fractions (1 coarsest, 6 finest) and dots the sample scores. First component explains 57.7% of the total variance of size data (X) and second 27%.

Multivariate analysis of the experimental results

Information available in large data sets consisting of several variables measured on a large number of objects can often conveniently be extracted by using a mathematical tool called principal component analysis (PCA)[3,4]. The principle of the PCA is presented in Figure 19. The data matrix **X** is organised so that the variables (size fractions or analytical results) are on columns of **X,** while objects (samples in this case) are on rows. **X** is usually first auto-scaled, i.e., from each column of **X** its mean value is subtracted and divided by its standard deviation. The first principal component finds the direction of the highest spread of the objects in the multivariate space. The second PC finds an orthogonal direction where the spread of the objects is next highest, etc. *Variable loadings* define the directions of the PC axes and *object scores* are objects projected on these axes. In ideal case the residual matrix **E** contains only noise. Often only a few PC's are needed to extract the useful information contained in **X**. Plotting the scores of two PC's gives a projection of objects from the original multivariate space onto a 2-D plane. Plotting loadings shows which variables are important on these components. Objects grouping close to each other have common features and variables having high correlation have loadings with similar values. Plotting scores and loadings superimposed as so called bi-plots show how objects and variables are related.

PCA was calculated from the size fraction data of the samples as **X** matrix. Figure 20 shows as a bi-plot the two first components of the PCA model. Duplicate RAS samples (A and B) are compared with the pile samples (R). The samples taken from the same drill sections form tight clusters indicating high similarity between samples from the same lot (drill section). The only exception is sample 1A which is far from 1B and 1R and thus an outlier in this group. Samples 10 and 5 have high concentrations in two of the coarsest size fractions and samples 4 are high in finest fraction. Samples 8 have high in middle fractions. The other samples are close to the average sample.

Chemical analyses vs. size distribution

Most of the samples collected in this study were analysed for major and minor elements in a laboratory by using XRF. From one experimental drill hole only composite samples from 1–2 metre sections were analysed and from other hole samples also the size fractions. How the rock breaks in concussion drilling depends on the type and mineral composition of the rock penetrated by the drill. So there is a correlation between size distribution and chemical composition. This is clearly seen in Figure 21. Fe, Al, Ti, V and K show a similar pattern (concentration decreases with increasing fragment size) whereas Mg, Si and to some degree also Ca and Mn show opposite behaviour.

Figure 22 shows the variation of chemical composition of major constituent with increasing depth in one of the drill hole, from which composite samples representing 1 or 2 metre sections were analysed. It is obvious that this kind of variation causes severe segregation (stratification) in the pile. If the sample is taken from the pile it is difficult to eliminate the segregation error. It is easier to eliminate

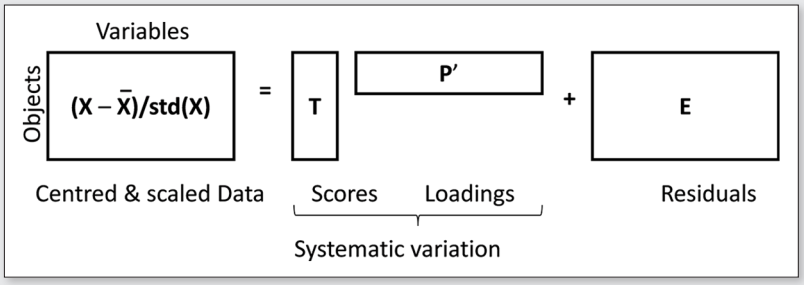

Figure 19. In PCA the original data matrix, which is usually autoscaled, is decomposed into two smaller object score and variable loading matrices and residual matrix.

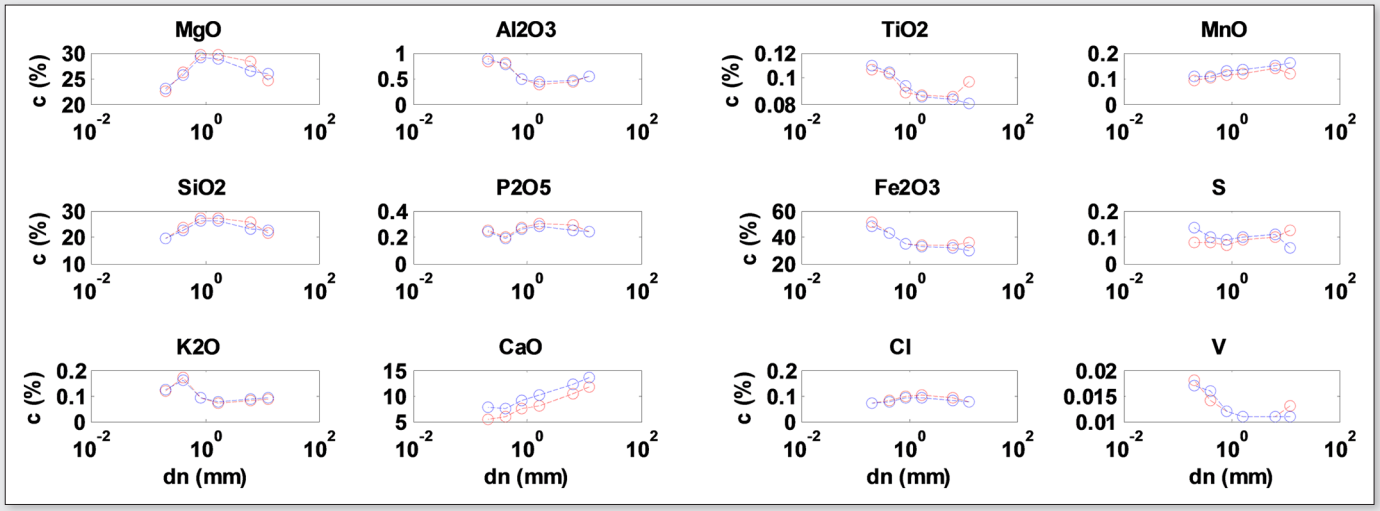

Figure 21. Chemical composition vs. nominal particle size of the size fractions in a 3 metre section of one experimental drill hole. Red dots are RAS samples and blue dots sample taken from the remaining pile.

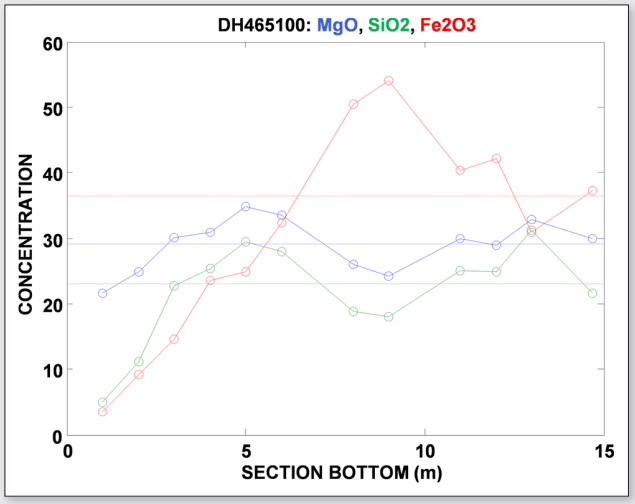

Figure 22. Variation of chemical composition in composite samples with increasing depth.

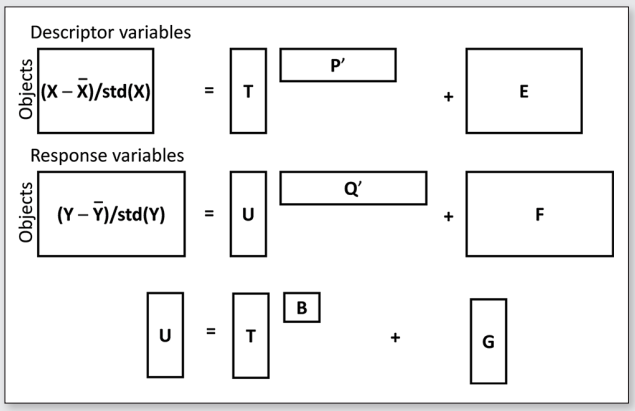

Figure 23. Principle of PLS regression: Descriptor and response variable matrices are decomposed into object and variable score matrices so that when columns of U are regressed on T the fit is optimised (sum of squared residuals G minimised). When descriptor variables on new objects are available T, U and predictions of Y can be calculated.

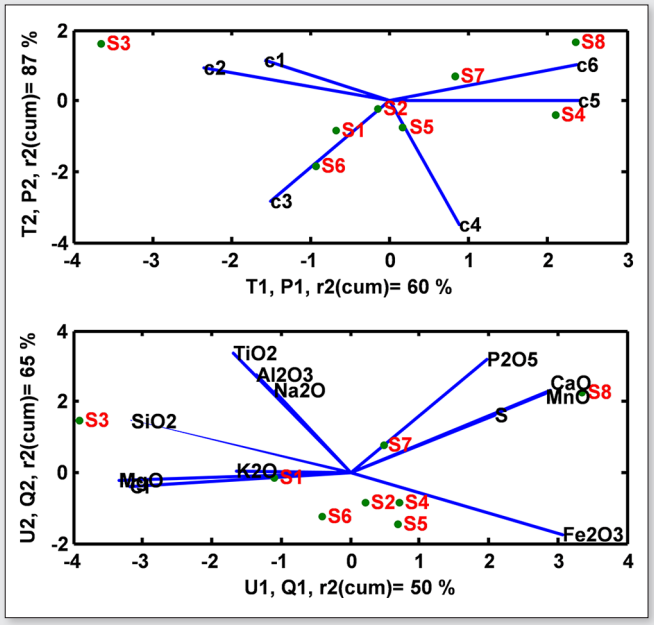

Figure 24. Result of PLS as biplots. Upper panel shows loadings of the size fractions c1 (coarsest) – c6 (finest) and scores of the samples (S1–S8). Lower panel shows s variable loadings of the Y matrix (chemical composition).

segregation error if the composite sample is collected continuously with a correctly designed sampling device, when the drilling progresses.

If two types of variables, descriptor variables **X** and response variables **Y** are measured on the same objects their relationship can be modelled by using Partial Least Squares regression (PLS). PLS is a standard method used in chemometrics[3,4]. The principle of PLS is given in Figure 23. Just like in case of PCA the main features of the data sets can be presented as informative projections. Figure 24 shows an example. Mean values of the size distribution from 8 samples (drill core sections) were used as **X** and chemical composition as **Y**. Two first components explain 87% and 65% of the total variance of **X** and **Y**, respectively. This means that the chemical

composition of the drill sections could be approximately predicted from the sieve results. The plot also shows at a glance the relationship between samples, size distribution and chemical analysis.

Conclusions

Taking representative samples from a pile of blast hole drill chippings is a very difficult task. Variations in mineral composition in the ore body inevitably cause stratification in the pile. Also the pile accumulation process segregates fragments depending on the particle size, shape and density. Here the performance of a new design of a blast hole sampler was tested by comparing the results with samples taken by other sampling methods and also with results obtained by splitting the whole remaining pile (reference). The Theory of Sampling was used to analyse the estimation uncertainty of an ideal (random) mixture of material consisting of particles of different sizes. The results of this study showed that the new design largely eliminates the effect of segregation and gives reliable results.

Acknowledgements

We should like to thank Northland Resources for letting us to do the experimental work at their Kaunisvaara iron ore mine site. We would also like to thank Kaunisvaara mine staff for being helpful and providing us with everything we needed during the in-situ work.

References

1. P.M. Gy, *Sampling of Heterogeneous and Dynamic Material Systems*, Elsevier, Amsterdam (1992).
2. P. M. Gy, *Sampling for Analytical Purposes*, John Wiley & Sons Ltd, Chichester (1998).
3. H. Martens and T. Næs, *Multivariate Calibration*, John Wiley and Sons Ltd., Chichester (1992).
4. A. Höskuldsson, *Prediction Methods in Science and Technology*, Thor Publishing, Copenhagen (1996).

doi: 10.1255/tosf.51

Geostatistical comparison between blast and drill holes in a porphyry copper deposit

Serge Antoine Séguret
MINES ParisTech, Center for Geosciences/Geostatistical team, 35 rue Saint Honoré, 7730 Fontainebleau, France.
E-mail: serge.seguret@mines-paristech.fr

Diamond drill-hole grades are known to be of better quality than those of blast holes; is this true? We present a formal study of a porphyry copper deposit in Chile where the variogram of 3-meter long drill hole samples is compared to 15-meter long blast hole ones and we show that the blast holes can be assumed to regularizing the point information deduced from the drill holes, except for a nugget effect specific to the blast samples. Complementary analyses based on migrated data show that the drill holes also have their own errors. After a brief description of the first steps in the blast sampling protocol, we show, by using extension variance concepts, that the blast error is not due to the arbitrary removal of material from the sampling cone produced by drilling.

Introduction

The present study establishes a formal link between blast and drill holes which leads to linear systems:

- Removal by kriging of the blast (or the drill) error;
- Deconvolution of the blast measurements to transform them into point ones;
- Block modeling where drill and blast holes are used together.

In the following, we thought it useful to detail some calculations and give some key formulas so that the reader can eventually adapt to other comparisons such as diamond drill holes compared to reverse circulation drill holes. Overall, this study shows how to combine measurements known on two different supports, a very complex challenge.

Data

The data comes from an open-pit copper mine in Northern Chile of which a 600 × 400 × 125 m^3 sub domain is analysed (Figure 1) as it is almost homogeneously covered by around 3,000 drill-hole samples (3 m long) and 13,000 blast-hole samples (15 m long).

Over this sub domain, the averaged copper grades of the blast and the drill holes are almost identical (around 0.6%). The variograms of blast and drill holes have similar behaviours (Figure 2), a high percentage of nugget effect (around 40%) and they differ mainly by their sills (0.12 for drill holes, 0.8 for blast holes), a comprehensible property as the blast support is larger.

Methodology

The geostatistical comparison between the two types of measurements is decomposed into two steps:

Deconvolution & convolution

- Starting from the drill variogram, identifying the basic structures that model its behavior and deducing the underlying "point" variogram by deconvolution;
- Making the theoretical convolution of the point variogram on 15-meter long supports and checking that it correctly fits the vertical and horizontal blast variograms, except for an additional nugget effect of 0.2.

Migration & cross variogram

- As there is no point where both drill and blast measurements are known, we make some blast holes migrate to drill hole locations and calculate the cross variogram;
- The objective is to measure the nugget effect shared by the two types of measurements.

There are not enough drill samples to distinguish between horizontal and vertical drill variograms (they are drilled along many different

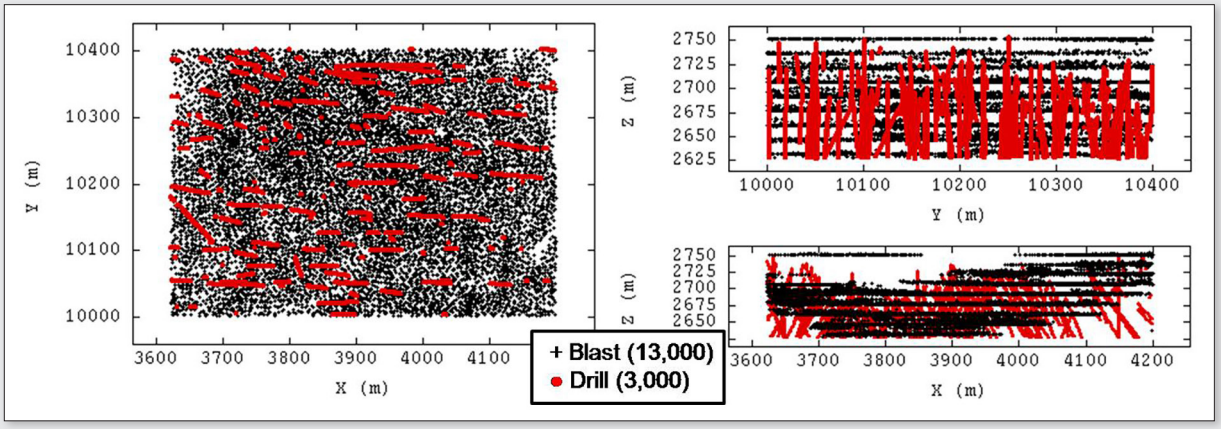

Figure 1. Base maps of blast (black) and drill (red) measurements.

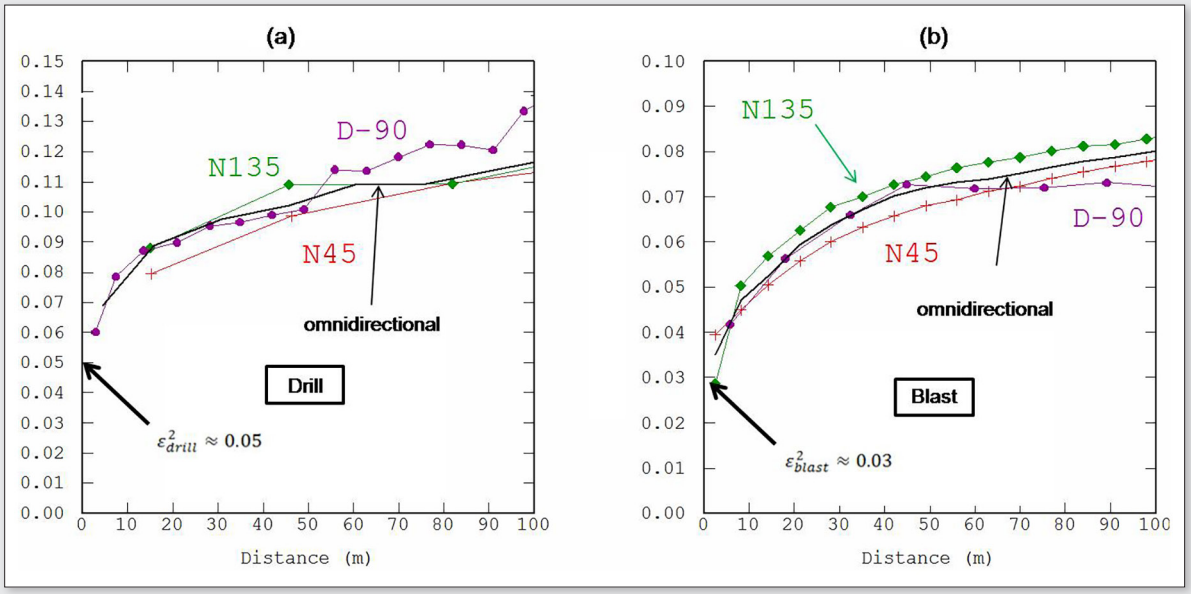

Figure 2. (a) Drill hole copper grade variogram; (b) Blast copper grade variogram. Three directions are represented, 45° North (N45), 135° North (N135), and vertical (D-90). Black continuous line is the isotropic variogram.

directions). This is the first reason why an omnidirectional variogram will be considered for the drill samples, the second one is that all the formulas at our disposal require isotropy. Consequently, we make two comparisons between:

- An omnidirectional drill variogram and a vertical blast one;
- An omnidirectional drill variogram and a horizontal blast one.

The distinction is important because the formulas differ between the two cases.

General formulas

All the formulas have been known for a long time in the literature, but in different places, and some are not even published. For the convolution charts, the most useful reference is probably reference 1; for the complete fundamental formulas, refer to reference 2 and concerning the extension formulas, refer to reference 3.

In the following we apply a procedure illustrated in reference 4 where we use the following approximation of a variogram regularized over a support "*l*" (the distance "*h*" being large in comparison with the dimension of the support):

$$\gamma_l(h) \simeq \gamma(h) - \bar{\gamma}(l,l) \tag{1}$$

with

$$\bar{\gamma}(l,l) = \frac{1}{l^2}\int_0^l \int_0^l \gamma(u-v)dudv \tag{2}$$

$\bar{\gamma}(l, l)$ is the average of the point variogram when both extremities of vector *h* describe the support independently. In (2), 1D integrals are used because the core diameters are small compared to the lengths. The way this formula is applied depends on the structure of the point variogram (spherical, exponential, linear, etc.) but also on the calculation direction compared with the regularization direction. In the following, we consider two situations:

- The calculation direction is parallel to the regularization direction, notation $\gamma_l^{\parallel}(h)$;
- The calculation direction is perpendicular to the regularization direction, notation $\gamma_l^{\perp}(h)$.

For the structures with a range, whether asymptotically (Exponential, Gaussian) or real (Spherical), we have:

$$\text{range of } \gamma_l(h) = \text{range of } \gamma(h) + l \tag{3}$$

Note that (3) is not compatible with approximation (1) which amounts to assigning to the regularized model the same range as that of the point model. So (1) is essentially useful for *comparing the sills* of regularized structures.

Step 1: deconvolution & convolution

Fitting the drill-hole variogram

Three basic structures are necessary: nugget, exponential, linear:

$$\gamma_{drill}(h) = \varepsilon^2_{drill} + C_{drill}(1 - e^{-\frac{|h|}{a_{drill}}}) + b_{drill}\,|h| \tag{4}$$

with:

$$\varepsilon^2_{drill} = 0.05,\ C_{drill} = 0.05,\ 3a_{drill} = 35m,\ b_{drill} = \frac{0.015}{100}$$

Nugget effect (or small-range structure) deconvolution & convolution

The attenuation of the nugget effect, whether "pure" or associated with a microstructure which reaches its sill long before the first variogram lags, is proportional to the ratio of the supports. In the present case study, the diameters of drill holes and blast holes are considered to be equal and we ratio the lengths but generally speaking, one has to consider the ratio of the volumes:

$$\varepsilon^2_{blast} = \frac{l_{drill}}{l_{blast}}\varepsilon^2_{drill} \tag{5}$$

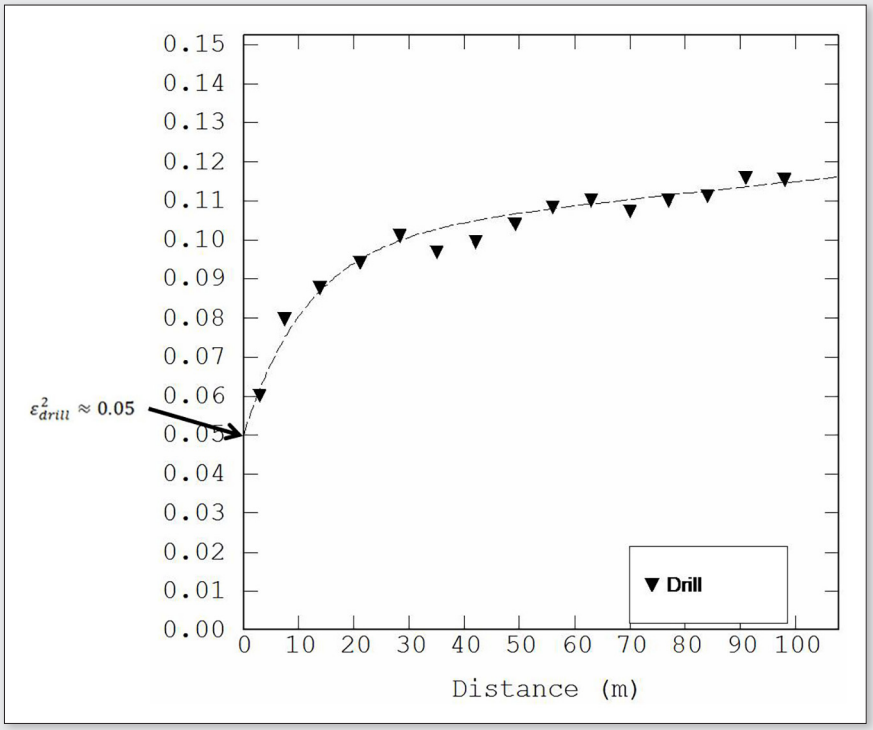

Figure 3. Drill hole variogram fitting. Dotted line, the experimental curve; continuous line, the model.

With $l_{drill} = 3$, $l_{blast} = 15$, the nugget effect of the blasts must be five times smaller than that of the drills. For $\varepsilon^2_{drill} = 0.05$ (Figure 2a) we obtain $\varepsilon^2_{blast} = 0.01$, a value three times smaller than the 0.03 value deduced from the blast variogram (Figure 2b). If one takes the blast nugget effect as a reference, the drill nugget effect should be 0.15, a quantity above the local sill of the variogram and not realistic.

Conclusion: the support cannot explain the differences between the nuggets of the blasts and of the drills. The blast nugget is too large.

Vertical variograms—deconvolution & convolution

The calculation direction is parallel to the blast regularization direction (i.e. vertical).

Exponential structure

If the practical drill range is 35 m, the parameter associated with the underlying point exponential structure is expressed by (3):

$$3a_0 = 35 - 3 \rightarrow a_0 = 10.7$$

If $\gamma(\,)$ denotes a variogram normalized by its sill, the underlying point sill C_0 of the exponential structure is produced by (1):

$$C_{drill} = C_0(1 - \bar{\gamma}(3,3))$$

For the exponential structure, the charts in[1] yield:

$$\bar{\gamma}(3,3) = 0.087 \rightarrow C_0 = 0.055$$

For $l = 15$ m, we deduce:

$$C_{15} = C_0(1 - \bar{\gamma}(15,15))$$

and we obtain:

$$\bar{\gamma}(15,15) = 0.34 \rightarrow C_{15} = 0.036$$

We will see later if these results correspond to the experimental blast variogram, but we must first look at the linear structure which completes the model (4).

Linear structure

For $h > l$ we have, where b is the slope of the structure[1]:

$$\bar{\gamma}(l,l) = b\frac{l}{3} \tag{6}$$

The slope b, which does not change with the support, is given by the drill samples and the difference between two supports l and l' equals:

$$\bar{\gamma}(l,l) - \bar{\gamma}(l',l') = b\frac{l - l'}{3} \tag{7}$$

When $l = 0$ m and $l' = 3$ m, and with $b_{drill} = 0.015/100$ obtained by (4), the attenuation is 0.00015, a negligible quantity. When $l = 3$ m and $l' = 15$m, the attenuation is 0.0006, still negligible. In any case, the effect of the regularization on the linear structure is negligible. This is due to the weak slope of the linear structure.

The combination of all the regularizations is shown in figure 4a where the dotted line represents the actual model and the red line the model we should obtain with a more realistic nugget effect. One can see that apart from the problem of the nugget effect, the variation range is acceptable, even if the linear part of the theoretical structure does not appear in the vertical experimental blast variogram.

Horizontal variograms—deconvolution & convolution

The calculation direction is perpendicular to the blast regularization direction (i.e. horizontal).

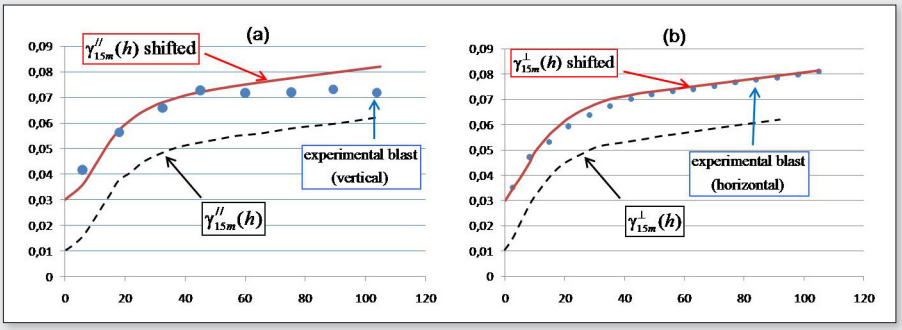

Figure 4. In blue, the points of the experimental blast variogram; dotted line, the theoretical model for the blasts deduced from the drills; in red, the theoretical model with a more realistic nugget effect. (a) Theoretical regularization parallel to the vertical blast variogram. (b) Theoretical regularization perpendicular to the horizontal blast variogram.

The same procedure is followed, the only difference is that approximation (1) is not acceptable and we have to use charts that produce the exact calculation (see[1], chart number 11).

We obtain figure 4b where the dotted line represents the actual model and the red line the model we should obtain with a more realistic nugget effect. The fit is good.

First conclusions

If we omit the problem of the nugget effect, we see that both blast and drill holes can be considered as a regularization of the same reality according to their respective supports. This result, which we did not dare to hope, surprised us pleasantly and shows that the measurements from the blast holes are not as bad as people often think, anyway the case for this company. But the approach followed up to now suffers from two uncertainties:

- The analyses are done independently. Imagine that all the blast locations have been shifted from a constant equal to the range (around 100 m). In that case, the correlation between blast and drills will be zero while the same coherence properties are maintained when making individual regularizations as previously;
- The analyses refer to the drill nugget assumed to be a "natural" micro structure; is this true?

To answer these questions, cross variograms must be calculated but we do not have any location with both measurements, so a migration is necessary.

Step 2: migration & cross variogram

Migration

In order to obtain a significant number of measurements at the same location, around 1,000 blasts samples were migrated to drill locations when the migration distance did not exceed 10 meters. Figure 5a presents the scatter diagram between the migrated values and the drill ones. The correlation coefficient is low (0.4) because the nugget effects are large.

On Figure 5b, points (resp. triangles) present the migrated blast (resp. drill) variograms. They differ slightly from the previous ones because the number of samples is smaller and the migration affects the results. In the same figure, the stars represent the cross variogram which does not show a significant nugget effect, possibly a small negative one without any magnitude in common with the effects encountered on the individual variograms.

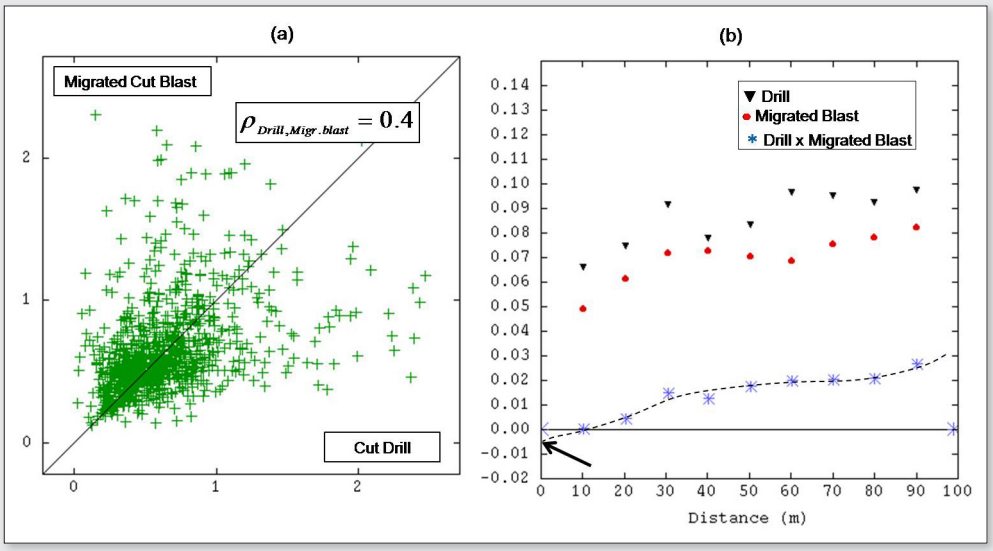

Figure 5. (a) Scatter diagram between migrated blasts and drills; (b) Direct variogram of migrated blasts (black triangles), corresponding drills (red points) and cross-variogram of both (blue stars). The cross variogram reveals a tiny negative nugget effect with no comparison with the drill or blast ones.

Conclusions

It seems that the drill-holes have their own errors too, independent of the blast ones, and the two measurements share only the structured parts of the variogram: the exponential and linear structures.

Analyse of the blast error

Description of the blast sampling

Up to now the theoretical blast support has been set to 15 m but in fact the blast drilling length is approximately 17 m, producing a large cone from the floor of which around 5 cm of material is removed by hand across the entire surface, the idea being to restore an overall volume of 15 m. Without any consideration of the numerous sampling procedures, we stay at this stage and ask the question: could the error specific to the blasts be due to the arbitrary removal of material and the blast length variability?

Randomization of the blast support

Let l and l' be two different supports. One finds in[3] the formula which expresses the variance of the difference between the two grades Y over l and l', called "extension variance from l to l', also equal to twice the variogram between the grades averaged over the two supports:

$$D^2(Y_l(x)-Y_{l'}(x+h)) = E[(Y_l(x)-Y_{l'}(x+h))^2]) \\ = 2\gamma_{ll'}(h) = 2\bar{\gamma}(l,l'_h)-\bar{\gamma}(l,l)-\bar{\gamma}(l',l') \quad (8)$$

In (8), l'_h represents the translation of the support l' by a vector h. $\bar{\gamma}(l, l)$ and $\bar{\gamma}(l', l')$ represent the averaged variogram when two points move independently along both the supports involved.

Suppose that l and l' are randomly and independently selected uniformly in an interval, for example equal to [12.5 m, 17.5 m]. Then one has to calculate the mathematical expectation of (8) to obtain the resulting variogram. We have:

$$E[\bar{\gamma}(l,l)] = E[\bar{\gamma}(l',l')] \quad (9)$$

$$E[\gamma_{ll'}(h)] = E[\bar{\gamma}(l,l'_h)] - E[\bar{\gamma}(l,l)] \quad (10)$$

(10) is the theoretical variogram that we want to compare to the actual experimental variogram in order to verify if the blast nugget could be associated with some support-length uncertainty.

$E[\bar{\gamma}(l, l'_h)]$ is a continuous function, complex to calculate as it depends on the mutual configuration of l and l', but about which we know that for h greater than the range plus l, it reaches and stays at the sill of the underlying point variogram. In practice, the only structure that we consider is the exponential; its point sill is 0.055. For the interval of support-length uncertainty [12.5 m, 17.5 m], we deduce from (10) that the sill is reduced by a quantity obtained by:

$$E[\bar{\gamma}(l,l)] = \frac{1}{l}\int_{12.5}^{17.5}\bar{\gamma}(l,l)dl \quad (11)$$

To evaluate the range of variations, the integral (11) is approximated by a finite sum:

$$E[\bar{\gamma}(l,l)] \approx \frac{1}{5}\sum_{l=13,14,15,16,17}\bar{\gamma}(l,l) \quad (12)$$

We use the same charts as previously to calculate the values of $\bar{\gamma}(l, l)$ involved and finally (12) yields:

$$E[\bar{\gamma}(l,l)] \approx 0.055\frac{1}{5}(0.295+0.305+0.325+0.337+0.352) \\ = 0.055 * 0.323 \quad (13)$$

Notice that even if we randomize the blast support over a larger interval still centered around 15 m, the variance reduction does not change and stays approximately equal to the sill multiplied by 0.325. If we suppose that the support fluctuation is not symmetric around 15 m, but around 13 m for example, the multiplicative factor for the sill reduction decreases to 0.295. In any case, we conclude that:

- The uncertainty on the support length does not produce a nugget effect but a variance reduction;
- This variance reduction represents approximately 30% of the underlying variogram sill;
- The arbitrary removal of the material, as well as the uncertainty on the blast length, cannot explain an error specific to the blasts and necessarily linked to the subsequent sampling procedures.

Summary: a formal link between blast and drill holes

Formal link

Finally, we have:

$$Y_{blast}(x,y,z) = Y(x,y,z) * p_{15m}(z) + R(x,y,z) \quad (14)$$

with

$Y(x,y,z)$, the point grade assumed to be isotropic and devoid of any measurement error;
"$*$" denotes a convolution product;

$$Y(x,y,z) * p_{15m}(z) = \int_{-\infty}^{+\infty} Y(x,y,u)p_{15m}(z-u)du$$

$$p_{15m}(z) = \frac{1}{15}1_{[0,\frac{15}{2}]}(|z|)$$

$1_{[0,\frac{15}{2}]}(|z|)$ the indicator function equal to 0 outside the interval and 1 inside it;

$R(x,y,z)$, a "white noise" residual statistically and spatially independent from $Y(x,y,z)$ and representing the blast error

The variogram of $Y_{blast}(x,y,z)$ becomes:

$$\gamma_{blast}(h) = \gamma_{15m}(h) + \gamma_R(h) \quad (15)$$

with

$\gamma_R(h)$ the nugget effect due to the blast error;

$\gamma_{15m}(h) = \gamma * \mathcal{P}_{15m}(h)$

$\gamma(h)$, the point variogram, assumed to be isotropic;

$\mathcal{P}_{15m}(h) = p * \dot{p}(h) = (-|h|+15)1_{[0,15]}(|h|)$

The model supposes that the blasts and the drills have the same average because the independent residuals are of zero mean. It must be verified when using this model. It is approximately the case here (0.63 for the drills, 0.69 for the blasts).

Removing the blast error by kriging

Model (14) can be used to remove the blast error by "Factorial Kriging" estimation[5]. One can easily build a linear system applicable to each blast measurement, choosing a local neighborhood of surrounding blast samples. The system is presented symbolically by using matrix formalism:

$$\begin{pmatrix} \gamma * \mathcal{P}_{15m} + \gamma_R & 1 \\ 1 & 0 \end{pmatrix} \begin{pmatrix} \lambda \\ \mu \end{pmatrix} = \begin{pmatrix} \gamma * \mathcal{P}_{15m} \\ 1 \end{pmatrix}$$

In this system, $\gamma_{|R}$ disappears from the second member of the linear system whereby we remove, from the estimation, the part associated with the measurement error. It does not mean that in the remaining part $\gamma * \mathcal{P}_{15m}$ there is no nugget effect; it means that only the "natural" part remains. In our case, the complete nugget effect has to be removed because blasts and drills do not share any micro-structure.

Deconvolution by kriging

It may be interesting to remove the effect of regularization on the blast using a kriging system which estimates, for each blast measurement, a "point" value while simultaneously removing the part of the nugget effect associated with blast errors:

$$\begin{pmatrix} \gamma * \mathcal{P}_{15m} + \gamma_R & 1 \\ 1 & 0 \end{pmatrix} \begin{pmatrix} \lambda \\ \mu \end{pmatrix} = \begin{pmatrix} \gamma * p_{15m} \\ 1 \end{pmatrix}$$

The difference with the previous system is that in the second member, $\gamma * \mathcal{P}_{15m}$ (capital "$\mathcal{P}$") is replaced by

$$\gamma * p_{15m}(h_x, h_y, h_z) = \int_{-\infty}^{+\infty} \gamma(h_x, h_y, u) p_{15m}(h_z - u) du \qquad \text{(small "p")}.$$

Block estimate by cokriging drill and blast measures

Finally, one can imagine locally renewing the mine planning block model by using blasts and drills together through a cokriging system *with a linked mean* (same average for both measurements):

$$\begin{pmatrix} \gamma * \mathcal{P}_{3m} & \gamma * p_{3m} * p_{15m} & 1 \\ \gamma * p_{15m} * p_{3m} & \gamma * \mathcal{P}_{15m} + \gamma_R & 1 \\ 1 & 1 & 0 \end{pmatrix} \begin{pmatrix} \lambda \\ \lambda' \\ \mu \end{pmatrix} = \begin{pmatrix} \gamma * \mathcal{P}_{3m} * p_V \\ \gamma * p_{3m} * p_{15m} * p_V \\ 1 \end{pmatrix}$$

These systems were tested on a realistic simulation where the truth is known; they produce good results which will be published in the near future.

Conclusion

In this deposit—and more generally, in this company (other test have been done), diamond drill hole grades and blast hole grades are consistent in the sense that, apart from the nugget effect, the structured part of their respective variograms follow the theoretical laws of regularization.

Concerning the nugget effects, we discover, by cross-analyses, that there is no natural micro-structure in the underlying point grade and the large nugget effects encountered on the variograms (approximately 50% of the variance for blasts and drills) are due to blast and drill measurement errors, independent of either measurement type.

The analysis of the blast error leads to the conclusion that the error is not due to the first step of the sampling procedure, it has to be found later in the process.

As a conclusion, some linear systems are proposed for removing the nugget effects from the data, reducing the effect of convolution and, more importantly, using blasts and drills together for the short-term mine planning. These systems, among numerous different potential ones, easy to demonstrate, result directly from the formal link established here between blast and drill holes. Before using these systems, the link must be verified by adhering to the methodology presented here.

Acknowledgements

The author would like to thank CODELCO Chile, for its strong support in the implementation of good geostatistical practices along the copper business value chain. I warmly thank the Editor for excellent recommendations which improved the manuscript. Many thanks to Sebastian de La Fuentes and the complete team of R&T. Without them, nothing would have been possible.

References

1. A.G. Journel, Ch. J. Huijbregts, "*Mining Geostatistics*", 5nd Edn. The Blackburn Press (1991).
2. J. Serra, «*Echantillonnage et estimation locale des phénomènes de transition miniers*». Doctoral thesis, Faculté des Sciences de Nancy (1967).
3. G. Matheron, «*Les Variables Régionalisées et leur estimation*». Masson et Cie Editeurs (1965).
4. S. A. Séguret, "*Spatial sampling effect of laboratory practices in a porphyry copper deposit". Proceedings of the 5th world conference on Sampling and Blending, Santiago, Chile (October 2011).*
5. J. P. Chilès, P. Delfiner, *Geostatistics*. 2nd edition, Willey (2012).

doi: 10.1255/tosf.52

Estimating granite roughness using systematic random sampling for the evaluation of radon gas emanation from ornamental granite rocks

T.M. El Hajj,[a] I. Tertuliano,[b] T. Vieira,[c] A.C. Chieregati[a] and H. Delboni Jr.[a]
[a]Dept. of Mining and Petroleum Engineering, University of Sao Paulo, Av. Prof. Mello Moraes 2373, 05508-030, Sao Paulo, Brazil. E-mail: thammiris.poli@usp.br, ana.chieregati@usp.br, hdelboni@usp.br
[b]Dept. of Mechanical Engineering, University of Sao Paulo, Av. Prof. Mello Moraes 2231, 05508-030, Sao Paulo, Brazil. E-mail: iramar@usp.br
[c]Dept. of Civil Engineering, University of Sao Paulo, Av. Prof. Almeida Prado 83, 05508-070, Sao Paulo, Brazil. E-mail: tiagovr@gmail.com

There are three natural radioactive families according to their decay, which are: the uranium series (^{238}U decreasing to stable ^{206}Pb), the actinium series (^{235}U decreasing to stable ^{207}Pb) and the thorium series (^{236}U → ^{232}Th decreasing to stable ^{208}Pb). The three series all have radon gas as an intermediary element, but each with a different atomic mass (^{222}Rn, ^{219}Rn and ^{220}Rn). The three isotopes are inert gases at ambient conditions and all are alpha particles emitters. Soils naturally emanate these radioactive gases in variable concentrations depending on composition and location. The radon radioactive emanation is a mass flow composed of radionuclides emitted to the atmosphere from the surface of the material, or transported to it. Emanation depends on the amount of radon atoms formed from the decay of radium and on the surface roughness of the material. Treatment such as polishing can be used to decrease radon gas emanation by closing open surface pores and reducing the specific surface area. This study aims at evaluating granite roughness of experimental plates of ornamental rocks using a systematic random sampling approach in order to minimise analysis time. To validate the systematic minimum area sampling results these were compared to measurements made over the whole reference area. It is concluded that measurements can be conducted in just a few locations using systematic random sampling, significantly reducing the time for obtaining estimates of the granite's roughness by factors 150–200.

Introduction

This study addresses development of a fast method to obtain a granite plate's roughness using systematic random sampling as a tool to minimize the measurement time without quality loss. Granite roughness is an important parameter for a correct evaluation of radon gas emanation. Estimating granite roughness is part of test regimens for characterizing gas emanation. This test is by far the slowest of all characterisation tests. It takes 16 days to obtain relevant data from a 20 × 20 cm plate. This motivated the authors to use a sampling method to reduce the time needed for estimating granite roughness.

Among the available surface treatments aiming to decrease radon gas emanation, there is granite polishing which is a cheap and efficient method since it reduces the specific area and closes open surface pores. Figure 1 shows the difference of emanation between polished and rough surfaces measured by a radon meter, which has a scintillation cell as operating principle.

The EU (European Union) published a Council Directive in December of 2013 (2013/59 EURATOM) that compels all member states to present a national action plan to address long-term risks from radon exposures by February of 2018. Guidance on methods and tools for measurements, identification of building materials with significant radon emanation are on the list of items to be considered in preparing this action plan. In view of this EU document, the authors feel that methodological studies in this field are well motivated.

Radon emanation

There are three radon isotopes (^{222}Rn, ^{219}Rn and ^{220}Rn) which are alpha particles emitters, all of which are inert gases at ambient conditions. The radioactive emanation is a mass flow composed of radionuclides transported to the atmosphere from the material, depending on the amount of radon atoms formed from decay from radium and the physical characteristics e.g. surface roughness[1]. The amount of gas that reaches the surface is directly proportional to the specific area of the material.

Inhalation of radon gas and its decay products is a health risk to humans. Alpha particles from the radioactive decay may reach lung tissue and cause damage that can lead to lung cancer. Most of radon gas exits the human body by exhalation before the decay process however, so most of the radioactive dose comes from the decay products that are inhaled as dust and become lodged in the lung tissue. These radionuclides decay quickly which results in further damage of the lung tissue[2].

Surface metrology – Interferometry

Surface metrology is a branch of engineering related to measurement of roughness, sharpness, waviness and other surface parameters, which are dependent on a given engineering application. Methods available to characterize surface texture can be classified as contacting and non-contacting[3]. While contacting methods demand physical contact to assess the surface topography, non-contacting methods, as the name implies, do not require any such. Surface interferometry is a non-contacting technique, based on a superposition principle. Two waves with no phase shift, identical w.r.t. amplitude and frequency, when combined, will result in a wave with the same frequency but the amplitude will be doubled. This effect is known as constructive interference. Two waves with a phase shift of 180° will result in a wave with zero amplitude. This effect is known as destructive interference. The interaction between different waves in general results in patterns, known as fringes, showing constructive and destructive interference. Figure 2 shows

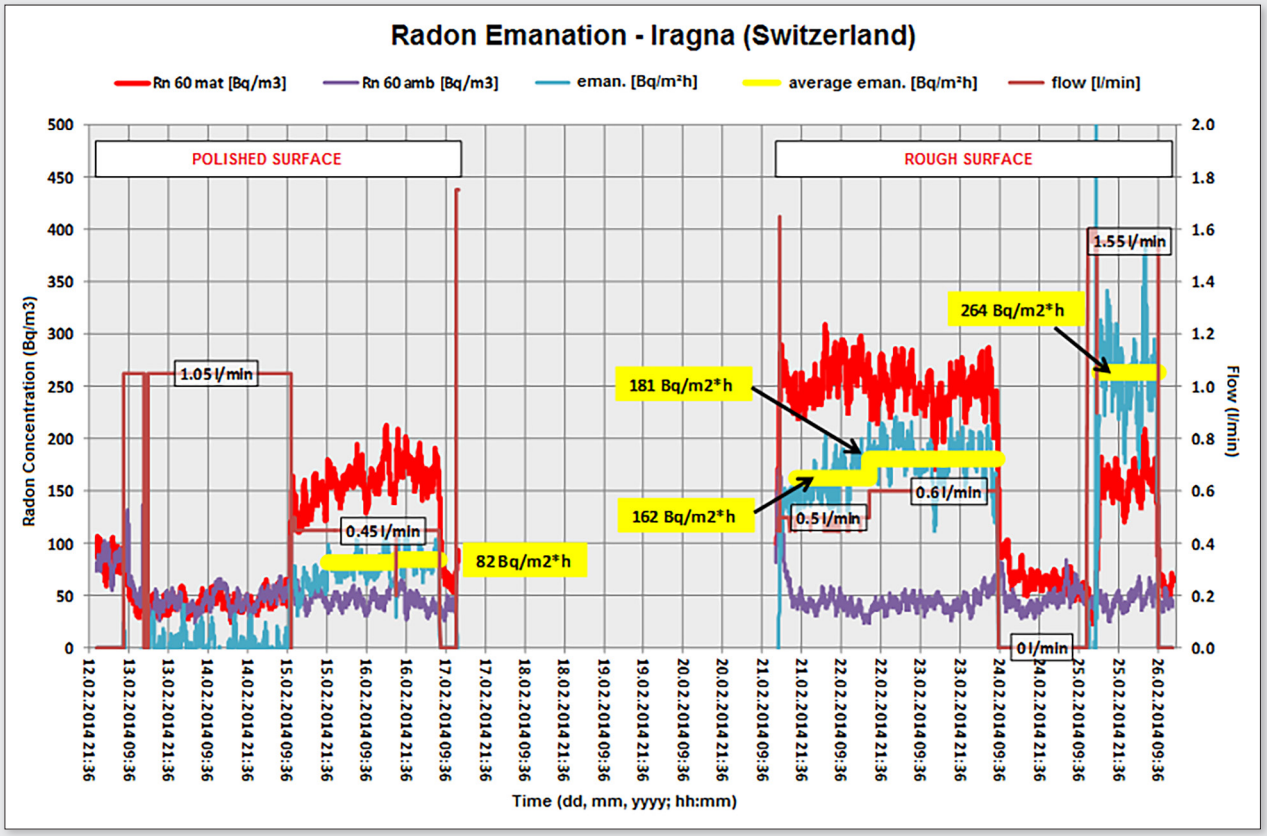

Figure 1. Difference of radon gas emanation from polished (left) and rough (right) surfaces as measured by a radon meter (based on a scintillation cell).

the reference and test beams combined, resulting in constructive interference[4].

An interferometer emits a single light beam which is split into two by a beam splitter. The two beams are destined to interact with each other resulting in the mentioned fringe pattern *after* interaction with the surface whose texture is to be characterised. One light beam is directed to the sample surface, the test beam. The other beam will be directed to a reference mirror. The two beams are reflected and reach the detector. The device then analyses the coherence of the resulting signal, which is a measure of the correlation of two beams in the resulting wave, separated by a given delay. The device finds the proper height at which the coherence value for each pixel reaches a maximum and the resulting fringe pattern is used to calculate the surface height. Figure 2 also shows the interferometer scanning process, which finds the surface height by analysing the fringe patterns[4].

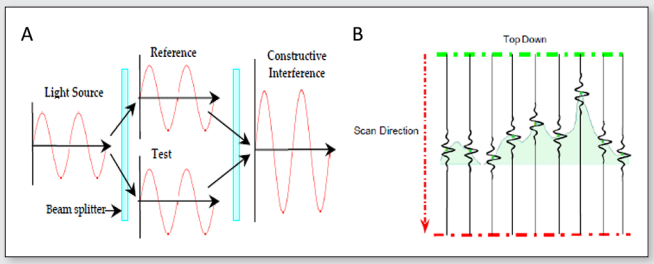

Figure 2[3]. (A) Superposition principle on an interferometer showing the combination of reference and test beams, resulting in constructive interference[4] (B) Interferometer scanning process, which finds the surface height by analysing the fringe patterns.

Systematic Random Sampling (SRS)

This sampling method is probabilistic and involves a regular, pre-established pattern for selecting sampling locations. The sampled area was divided into sectors, strata and substrata, where[5]:

- Sector: is a fraction of the total area, whose size could e.g. be based on recommendation from statisticians. Or, as in this study, based on reverse calculation to define this size, using the attainable substrata (explained bellow) size.
- Stratum: each sector is submitted to the preselected sampling mode (random systematic). This is performed by dividing each sector into a systematic grid.
- Substratum: each stratum must be divided into a certain number of basic units called substrata. It is suggested that division of each stratum in a number of substrata must be at least 20 times the number of measurements that should be collected within one sector.

The location of the initial sampling point is randomly selected in one preselected stratum of an area which is divided into smaller equal size substrata. In general, data acquisition and data analysis for each substratum should be managed independently. Figure 3 illustrates this kind of systematic sampling.

Methodology

The test sample was a granite from the city of Iragna, Switzerland. The material is commonly commercialised in plates, which have one polished surface and one natural surface (this is the 'rough surface'

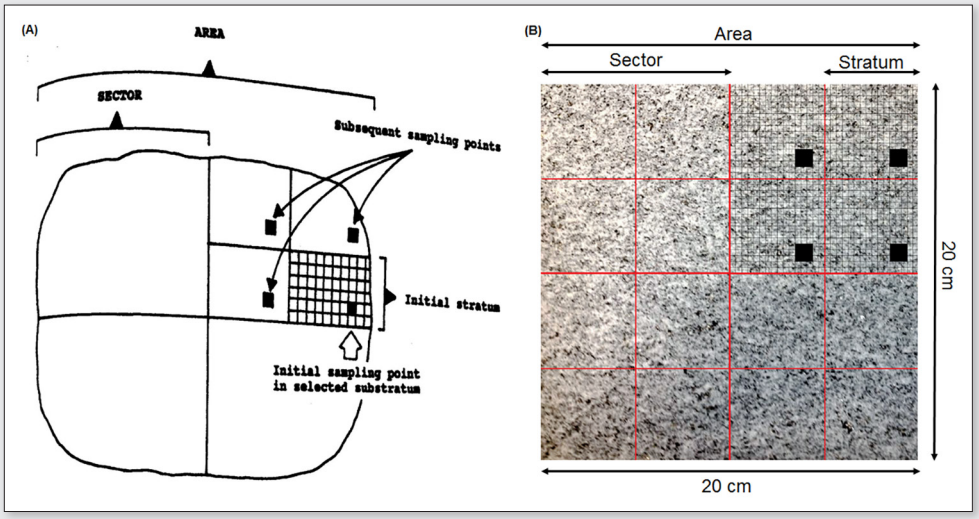

Figure 3. (A) Diagram showing initial selection of one random substratum in the initial stratum of one sector (SRS)[5] (B) Grid used to guide roughness assessment of Iragna's granite plate, the location of the initial sampling point is randomly selected in one preselected strata of an area which is divided into smaller equal size sectors, called substrata.

in this study). Both sides were tested to evaluate the accuracy of the data obtained by SRS. The whole area measurement was taken as reference. In this case, the sectors were set as a systematic grid following an adapted interpretation of the Theory of Sampling for contaminated areas[5].

In order to achieve good measurements we setup our study to fulfil these three pre-requirements[5]:

- Each sector must have a surface smaller than the local limit. In this study, the local limit is one 20 × 20 cm granite plate.
- The number of strata per sector must be at least four.
- Each sector must be characterized by their average and variances.

Figure 3 shows the grid used to stratify the granite plate surface (20 × 20 cm). The original sample was cut in 16 smaller pieces (5 × 5 cm) so that each stratum would fit in the object holder for the optical interferometer, used for the surface measurements from which 3D surface parameters were obtained (Figure 4).

Three strata from the 16 were randomly chosen to be tested (sample 1, 2, 3) both rough and polished surfaces, six tests total. The estimated time for measuring a 5 × 5 cm surface is one day using the interferometer (16 days to measure the whole 20 × 20 cm granite plate). This is considered too long and consequently too resource demanding for obtaining this crucial parameter to evaluate emanation correctly, especially since the interferometer is rented by the hour. Furthermore, estimating roughness is only one of many tests (e.g. porosimetry, permeability, X-ray diffraction) that should be performed in order to characterise the sample fully before the radon emanation measurement. It is currently the slowest test and it delays the final result of the radon emanation analysis seriously.

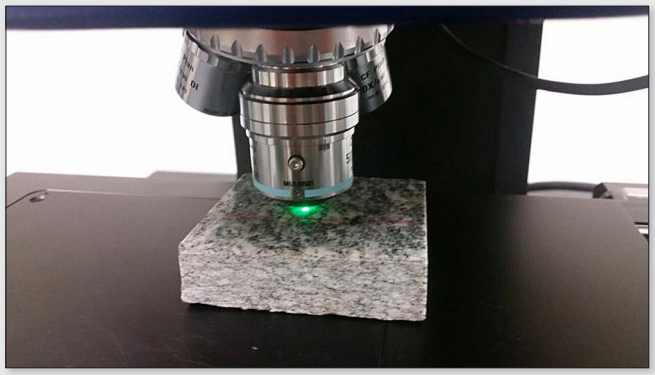

Figure 4. Interferometer in active measuring, also showing object holder.

The statistical analysis (Wilcoxon Signed Rank Test) of the results was conducted using SPSS for Windows statistical software (version 22).

Results and discussion

The three samples analysed were obtained by randomly choosing three strata of the granite plate. The area of each sample was analysed completely (whole area) and was subsequently partitioned to apply Systematic Random Sampling on a much smaller area to assess the same roughness manifestation. Figure 5 illustrates the SRS applied for one of the 5 × 5 cm plates (sample 1). The schematic drawing covers only a half plate but measurements were conducted in full, thus totalling 16 substrata on each surface. [Figure 5]

The output parameters of the interferometer software are:

- Height parameters (ISO 25178): Sq (root mean square height - µm); Ssk (skewness) and Sku (kurtosis).
- Volume functional parameters (ISO 25178): Vm (material volume – $\mu m^3/\mu m^2$); Vv (void volume – $\mu m^3/\mu m^2$); Vmp (peak material volume - $\mu m^3/\mu m^2$); Vmc (core material volume – $\mu m^3/\mu m^2$); Vvc (core void volume – $\mu m^3/\mu m^2$); Vvv (pit void volume – $\mu m^3/\mu m^2$).
- Functional parameters (ISO 25178): Smr (area material ratio - %); Smc (inverse area material ratio - µm).
- Hybrid parameters (EUR 15178N): Sdr (developed interfacial area ratio - %).

It is difficult to select a most suitable parameter for roughness characterisation and it is therefore common to use a combination of two or three, dependent on the material type.

Tables 1 and 2 show the results from a relative error analysis between the SRS data and data based on the whole area (reference).

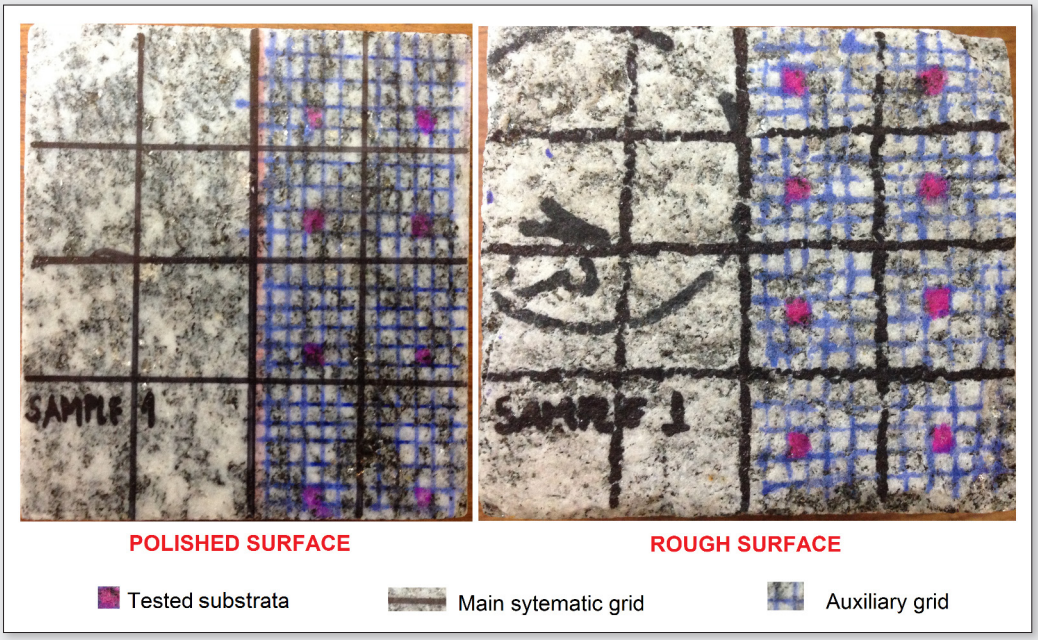

Figure 5. SRS applied to 5 × 5 cm plates of both polished and rough surfaces – Sample 1. Schematic drawing covers only half plates but the measurements were conducted in full, totalling 16 substrata on each surface.

The results show that:

- There is, not surprisingly, a consistent roughness difference between the polished and the rough surface (Figure 6). The parameter used for this comparison is Sq, the one displaying the smallest relative error for both surface type.
- Some height and volume parameters are to be used with caution as they are sensitive to isolated peaks and pits which may not be significant. They could be used if extreme peaks and valleys are removed or a threshold is applied[6]. Therefore, considering the high interference from small distortions in the analysis, it can be concluded that there is a small systematic error (bias) between whole area analysis and SRS for some parameters, such as Sq, Vv and Vvv.
- The other parameters tend to show a higher systematic error (bias) between the two analyses because they are more sensitive to small distortions that usually are averaged out when analysing a bigger area.

Figure 7 illustrates small distortions of this kind.

Method validation

To validate the SRS approach a Wilcoxon Signed Rank Test was used (for paired samples) to determine whether there were

Table 1. Analysis of surface data for polished surfaces.

	Polished surfaces								
Parameter	Whole Area Sample 1	SRS Sample 1	Relative Error Sample 1	Whole Area Sample 2	SRS Sample 2	Relative Error Sample 2	Whole Area Sample 3	SRS Sample 3	Relative Error Sample 3
Sq	5.6315	6.254	-11%	3.1155	3.102	0%	4.264	4.318	-2%
Ssk	-7.1535	-4.264	40%	-1.492385	-1.25	16%	-0.095	-0.105	-1%
Sku	47.83	60.234	-26%	21.79	22.015	-1%	15.012	16.04	-5%
Vm	0.05677	0.016	72%	0.18275	0.182	0%	0.654	0.54215	61%
Vv	2.7395	2.84	-4%	1.51385	1.235	18%	2.661	2.4065	21%
Vmp	0.05677	0.063	-11%	0.18275	0.152	17%	0.778	0.54215	155%
Vmc	1.00055	1.121	-12%	0.64605	0.524	19%	1.75	0.8487	172%
Vvc	1.2945	1.125	13%	0.7887	0.624	21%	1.523	1.60435	-13%
Vvv	1.4447	1.332	8%	0.72515	0.654	10%	0.745	0.80185	-9%
Smr	0.000080365	0.0005042	-527%	0.000066345	0.00006624	0%	0.00004032	0.000008035	49%
Smc	2.6825	2.745	-2%	1.331	1.223	8%	1.564	1.864	-25%
Sdr	13.796	12.052	13%	142.24	145.321	-2%	646.21	332.9	216%

Table 2. Analysis of surface data for rough surfaces.

Parameter	Rough surfaces								
	Whole Area Sample 1	SRS Sample 1	Relative Error Sample 1	Whole Area Sample 2	SRS Sample 2	Relative Error Sample 2	Whole Area Sample 3	SRS Sample 3	Relative Error Sample 3
Sq	27.67	25.21	9%	27.4	31.7	-16%	36.36	42.21	-18%
Ssk	0.028265	0.1120215	-296%	0.052936	0.023549	56%	0.04564	0.03215	57%
Sku	2.436	2.315	5%	2.6115	1.5362	41%	2.452	3.111	-43%
Vm	1.0685	1.5445	-45%	1.1662	1.3641	-17%	1.428	0.987	32%
Vv	37.485	35.046	7%	37.58	39.24	-4%	49.365	53.321	-10%
Vmp	1.0685	2.354	-120%	1.1662	1.3214	-13%	1.428	1.564	-10%
Vmc	26.965	27.165	-1%	25.775	27.664	-7%	35.37	37.35	-7%
Vvc	34.845	36.011	-3%	34.79	36.21	-4%	45.92	47.36	-4%
Vvv	2.6385	2.7892	-6%	2.7945	2.654	5%	3.447	3.664	-8%
Smr	0.00003764	0.001214	-3125%	0.000020098	0.000032151	-60%	0.0001084	0.000632	-1629%
Smc	36.415	36.154	1%	36.415	39.215	-8%	47.935	42.635	14%
Sdr	18594.5	18596.5	0%	7041.5	7951.3	-13%	31870.5	36321.5	-56%

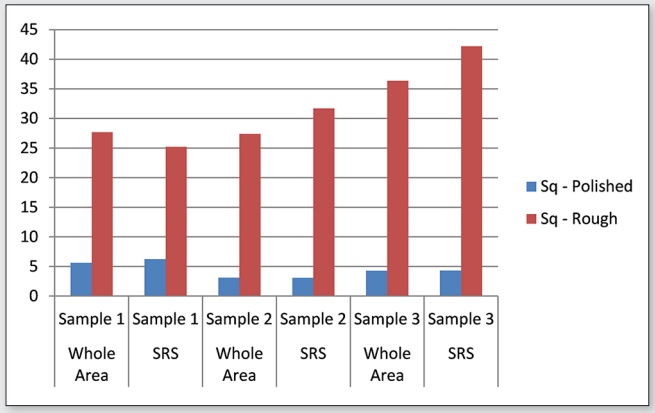

Figure 6. Root mean square height (Sq parameter) for rough and polished surfaces showing data consistency. This parameter was chosen because it displays the smallest relative error for both rough and polished surfaces

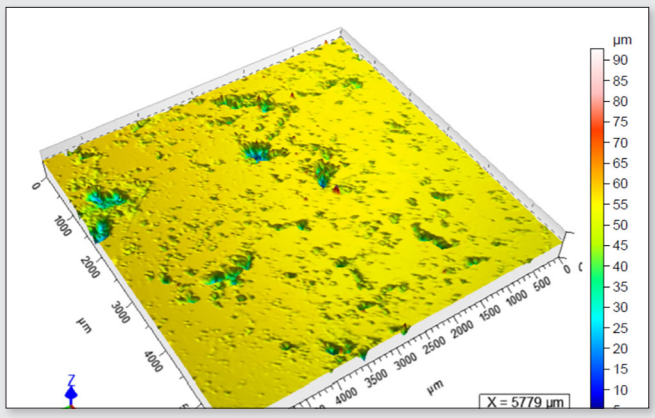

Figure 7. Surface morphology image obtained through the interferometer software. Note "small distortions".

significant differences between the whole area and the 6SRS measurements. The signed rank test compares the median of the values with a hypothetical population median (represented as the reference whole area in this study). Both the difference between these two values and the confidence interval of the difference are compared. The test leads to accepting the null hypothesis when there is no significant difference between the two values. Since the nonparametric test works with ranks, it is usually not possible to get a confidence interval with exactly 95% confidence[7].

Out of six Wilcoxon Signed Rank Tests, five retained the null hypothesis and one test rejected the null hypothesis. It is however believed that this is due to an experimental error and it is currently being re-measured.

The tests refers to three selected strata measured both rough and polished surfaces. The main results are:

- There is no significant difference between the whole area analysis and Systematic Random Sampling analysis (84% adherence) despite having one rejected case. In order to confirm this result more tests are currently being carried out amongst others varying number of sampled points in the SRS design.
- Thus it is possible to validate the method, at a first stage. The SRS approach will be very useful to reduce the time needed for estimating granite roughness. The new method provides the final result for one 20x20 cm granite plate in less than one hour, unbelievably fast compared to 16 days with the current approach.

Conclusions

Radon gas is formed from natural materials that have one of its natural precursors as part of its compositional make up. Granites tend to have a high radon gas emanation rate and since they are used as ornamental rocks inside and outside buildings it is important to assess the concentration reliably. This study presents a method that substantially decreases the time and resources needed to perform these important assessments. Analysis of the experimental results demonstrates the feasibility of a Systematic Random Sampling approach to obtain reliable estimates of granite roughness,

an approach that is much faster than analysing the entire target area (factor of 192). As a consequence of the reduced measurement time, the cost of the test also decreases substantially since the interferometer is expensive when rented by the hour.

Acknowledgments

The authors kindly thank Professor Mauro Gandolla (Università della Svizzera Italiana) for supporting our work, the laboratory LFS (*Laboratório de Fenômenos de Superfícies*) of the Polytechnic School, University of São Paulo for use of the interferometer, and André Kazuo Kuchiishi from LTP (*Laboratório de Tecnologia de Pavimentação*) of the Polytechnic School, University of São Paulo for his help with the data analysis. The Editor is thanked for substantive help in preparing this manuscript.

References

IAEA – International Atomic Energy Agency. "Measuring Radionuclides in the Environment. Argonne National Laboratory", USA (2010).

EPA – Environmental Protection Agency. Washington, D.C. Radiation Protection – Radon. Available at: <http://www.epa.gov/radiation/radionuclides/radon.html#affecthealth>.

HUTCHINGS, I. M. Tribology – "Friction and Wear of Engineering Materials". Arnold, Butterworth-Heinemann, London (1992).

LEACH, R.; BROWN, L.; JIANG, X.; BLUNT, R.; MAUGER, M. "Measurement Good Practice Guide No.108: Guide to the Measurement of Smooth Surface Topography using Coherence Scanning Interferometry". National Physical Laboratory. London, United Kingdom (2008).

PITARD, F. F. "Pierre Gy's sampling theory and sampling practice: heterogeneity, sampling correctness, and statistical process control". Florida, CRC Press, (1993). 2nd ed.

LEACH, R., Characterization of Areal Surface Texture, DOI: 10.1007/978-3-642-36458-7_2, Springer-Verlag Berlin Heidelberg (2013).

D.J. Sheskin, Handbook of Parametric and Nonparametric Statistical Procedures, fifth edition (2011).

doi: 10.1255/tosf.67

Proper sampling for archeometric discrimination of Bronze-age fields on Bornholm, Denmark – Archaeology meets TOS meets Chemometrics

Bastian Germundsson[1,3], Anders Pihl[2] and Kim H. Esbensen[3,4]
[1]Department of Geosciences and Natural Resource Management (IGN), Copenhagen University, Denmark.
E-mail: bgermundsson@gmail.com
[2]Bornholm Museum, Rønne, Denmark Email: ap@bornholmsmuseum.dk
[3]Geological Survey of Denmark and Greenland (GEUS). Copenhagen. Denmark. Email: ke@geus.dk Phone: +45 20214525
[4]ACABS Research Group, Aalborg University, Denmark

In archaeology it is of interest to ascertain whether a particular Bronze-age field has been cultivated or not based on traditional archaeological evidences, but these often deal with one chemical element only, Phosphorous. We here augment this endeavour to include multi-element geochemistry characteristics. A pilot study sampling campaign was carried out (2014) on the island of Bornholm with the objective to discriminate between well-documented cultivated and un-cultivated Bronze-age agricultural fields based on multivariate data analysis (chemometrics) of soil chemistry (metal concentrations, ICP-MS). All samples originate from the same soil depth corresponding to the paleo-cultivated layer, or the equivalent depth in uncultivated fields. The experimental design focused on proper field sampling (Theory of Sampling), including replicate sampling at two levels. Applying Principal Component Analysis (PCA), the first three components corresponds to 68 % of the most discriminative variance in the 15 variable/41 sample array. The first and third PC-component reveals a complete discrimination of un-cultivated vs.3 cultivated fields; it is likely that general soil chemistry features are compensated for by the second component in the PCA solution. We present the specifics pertaining to the field sampling procedure, including the hierarchical two-level experimental design, which allow assessment of the local vs. field-wide heterogeneities in order better to understand the successful discrimination achieved. Five elements appear to be particularly involved in the discrimination [P, Fe, Mn, Zn, Pb], currently undergoing paleo-agricultural/geochemical interpretation. Based on these first results we plan a full test-set validation campaign in 2015 which will be the ultimate performance test for this type of archeometric discrimination. This contribution illustrates the versatility and power of multivariate data analysis (chemometrics) applied to data with a substantial proportion of potential sampling errors, in need of effective management (TOS).

Introduction

Bornholm is a minor Danish island in the Baltic Sea known for a diverse, interesting geology – and a magnificent archaeological venue with a great number of Celtic (Bronze age) agricultural fields, which date back to the first century BC. The Celtic field systems have been recognized and documented for more than 100 years, but little is known to how the fields were cultivated and what crops were grown. The primary knowledge is related to different indirect evidence in the form of Agricultural tools, and crops, found on secondary locations, typically settlements. The aim of this pilot project was to gain information from the primary sources, the cultivated fields themselves. By introducing geochemical fingerprinting of the subsoil from both cultivated and pristine fields, and applying Multivariate Data Analysis (MVDA), this project entertains whether it is possible to discriminate between cultivated and uncultivated fields of Celtic age on this basis. It is hoped that this may contribute to increased insight into the different agricultural methods and strategies that were used in Late Bronze Age and Early Iron Age. For this purpose Bornholm is an obvious location due to a comprehensive documentation of Celtic fields and due to the geomorphology, which allows archaeologists to distinguish between cultivated and uncultivated areas with ease and certainty, which is important classification information to be used in training a data analytical discrimination facility.

Data analysis – from univariate to multivariate

Traditional archeological data analysis in this context has overwhelmingly been an univariate approach, i.e. a directed focus on just one element, Phosphorous, which has been used extensively as a 'signal element' due to its increased concentration in manure that has been used as fertilizer. In the present study this univariate approach shows severe limitations however, for which reason a multivariate approach may act better in discriminating between fields based on a full series of 15 geochemical elements. General knowledge as to which elements might correlate with Phosphorous in cultivated fields is sparse however; Nielsen et al. (2014) showed in a similar multivariate study that Sr conceivably correlate with cultivated fields due to addition of bone fragments and household waste. Information is also scanty regarding how the geochemical fingerprints of uncultivated fields might appear in this context. We have therefore adopted a multivariate data analysis approach (Chemometrics) without any prerequisites or assumptions, letting the data speak for themselves. The archeological field use discrimination is an important piece of the puzzle.

Theory of Sampling (TOS)

TOS is also a critical agent in this endeavor: The validity of analytical results is exactly as good, or bad, as the validity of the primary sampling, as well as of all sub-samples produced in the laboratory on the pathway to the analytical aliquots. The primary – and

secondary sampling in this project was in complete TOS-control, DS 3077 (2013), with a strong emphasis on unbiased field sampling and subsequent mass-reduction (riffle-splitting). The tertiary sampling consisting of spatula extraction of the analyte (0,5-1,0 gram) was carried out in and by the analytical laboratory involved (interesting minor sampling error effects were detected here, fully reported elsewhere in the first authors M.Sc. thesis; luckily these were detected early and were not of a magnitude to interfere with the first order conclusions reported below).

In order to quantify the Total Sampling Error (TSE) and to evaluate the magnitude of the soil heterogeneity on different levels, two experimental designs were embedded in the field sampling plan.

Methods

Primary sampling was conducted in August 2014, where mild weather resulted in dry soils, giving optimal conditions to distinguish between different soil horizons, and in general making field sampling easier. Due to the need for comparison between the final data, the entire sampling campaign was carried out under identical conditions.

Two cultivated fields, A & B and one uncultivated field, X were sampled on the same day, in which a total of 41 samples were collected. The three fields are located in the now forested area "Vestre Indlæg", Figures 1 and 2a, and have never been involved in previous studies. The stratum of interests, according to archeological experiences, manifests itself as a yellow quartz-rich sand underlying a purple heather-rich sandy topsoil, which was found just under the contemporary O horizon. The purple, heather-rich topsoil was used as an upper boundary demarcation due to its marked, recognizable characteristics, while the lower boundary of the target stratum was not identified (generally located 45-55 cm below the surface in the area).

The fields were prepared with 9 sampling locations for the uncultivated field X and 10 sampling locations for each of the two cultivated fields A & B. For the latter two, different sampling plans were chosen: Cultivated field A was sampled along a transect while the cultivated field B was sampled in a random grid within the archeologically delineated boundary. The uncultivated field X was also sampled along a transect which constituted an extension of the transect for field A, Figure 1. The experimental design thus totals 29 samples. Each single sample was collected as a 4-increment composite sample as explained below.

Figure 2 a,b. Line transect (left) and expanded local embedded sampling ("box") (right), see text for details.

Primary sampling

Each cross in Figure 1 denotes a sample location, approx. 20 × 20 × 20 cm. The vertical dimension of the sample dug outs was constant in order not to incur unnecessary Increment Delimitation Error (IDE). A four-increment composite sample was manually collected from each box with a combined use of a garden shovel and a trowel, Figure 2b. Each increment was composed of an equal volume scrape-off material from one side of the box. In the field, when aggregated these four increments were deemed to constitute a representative, Incorrect Sampling Error (ISE)-eliminating and Correct Sampling Error (CSE)-minimizing composite sample. Identical use of the sampling tools allowed a minimum Increment Delimitation Error, Increment Extraction Error (IEE) & Increment Preparation Error (IPE) (the precise trowel was used to scrape off material into the garden shovel which was used to allow all the scraped-off material to be carefully collected – eliminating spillage and/or contamination). This sampling procedure also honors the Fundamental

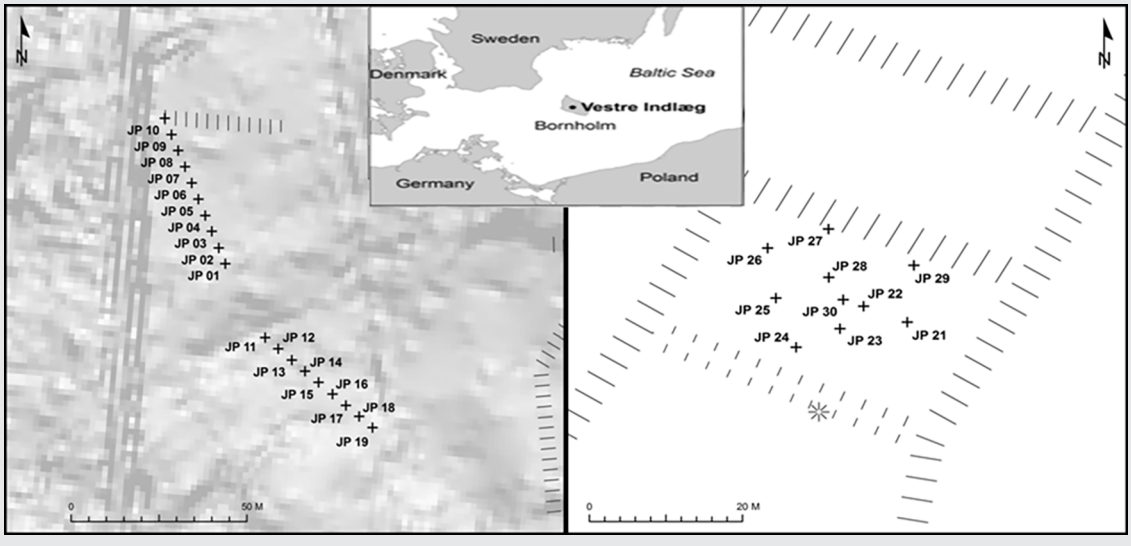

Figure 1 a,b. Location and pilot study area on the Danish island of Bornholm (Baltic Sea)

Sampling Principle (FSP) because the soil underlying the entire location has an equal possibility to end up as a part of the sample (the edge direction of the sample dug out was chosen at random; there should always be some random element in all good sampling procedures).

Local embedded sampling

In order to be able to quantify the heterogeneity at different field scales, an additional experiment was embedded in the overall experimental plan described above. For each of the three fields (at a randomly selected location along the transects or within the grid), a small-scale replication experiment, DS 3077 (2013) was carried out in the form of four additional field samples arranged in a "box-like" pattern, Figure 2b.

The standard dugout was here expanded in size to approx. 100 × 100 × 40 cm which allowed improved pedological characterization as a basis for a larger sample size. These special samples were collected using the same general protocol as previous, but all four sides were now specifically not combined to form a composite sample. Instead each side was sampled separately along the entire wall face. This resulted in four individual 'parallel' samples (designated w, x, y and z) + the existing composite sample (c) belonging to the transect (or grid). This set up allow quantification of the local heterogeneity for each field commensurate with dimensions 100 × 100 cm (termed embedded "boxes"). This replication scheme added 12 samples, the entire pilot project now totaling 41 samples.

Laboratory sample processing

Laboratory sample preparations comprised drying, homogenization and sieving through a 2 mm sieve. The sieving process was carried out with an effort to minimize spillage (IPE). After sieving, the samples were mass reduced using a RAKO Riffle Splitter (32 chutes) to a sample size of 2-3 gram. Laboratory mass reduction meets all the requirements for representative mass reduction as laid out by Petersen et al. (2004). Finally the samples were analyzed for 15 geochemical elements by Inductively Coupled Plasma analysis (ICP), courtesy of Aalborg University, campus Esbjerg.

Lot characterization

Field heterogeneity

Traditionally it has been argued, that for comparison between the geochemistry of different fields, only one single 'representative' sample is needed from each. There are countless examples in the literature where 'representativity' is only assumed for a single grab sample however, very often without proper documentation. But from even a cursory examination of this approach, in the light of TOS' understanding of heterogeneity, it is extremely likely that this can never result in reliable conclusions. A single sample is a grab sample w.r.t. the field it is supposed to represent; there is no way this can express both the local as well as the "global" field heterogeneity in a valid fashion; such an approach is therefore not to be considered trustworthy. Any singular grab sample from any one field cannot be representative hereof without specific proof.

Therefore the primary field sampling constitutes a replication experiment with respect to the full heterogeneity within each field. The overall heterogeneity can be regarded as a specific signature, characteristic of the scale pertaining to cultivated as well as uncultivated fields, but it cannot necessarily be assumed to be identical between fields, Figures 3 and 5. Thus 9 (or 10) composite samples from each field constitutes a replication experiment allowing reliable aggregated results, and also to detect, and remove, outliers, whether defined by the heterogeneity or TSE (one analytical outlier was detected only because of this type of inter-leaved replication experiments in the ultimate laboratory stage). Each field is at the outset considered as a unique sampling target characterized by 9(10) samples covering the specific lot geometry. 9/10 were chosen based on the available logistical constraints (this number could alternatively had been higher, e.g. 20 if no economical, practical, or logistical sampling limitations had existed).

The sample plans were laid out at random – either as a randomly selected transect direction, or as a randomly oriented grid. Replicate samples from each field are hypothesized to correlate stronger within-group than with respect to between-group (between-fields). The two cultivated fields A & B are also assumed to correlate stronger between themselves contra the uncultivated field X. Such relationships would be expected if the geochemical discrimination hypothesis is to be substantiated. But does this hold for all geochemical elements analyzed for? Or just for a few?

Local embedded replicate experiment

The sampling process of the "local" box replication experiment was described above, allowing quantification of the heterogeneity pertaining to this local scale. It is a fair assumption that with five samples it should be possible to express the local heterogeneity with reasonable resolution; these samples should be correlated stronger with each other than with respect to the whole field data, see Figure 5 below.

Univariate data analysis

A traditional univariate data analysis, visualized as a box plot, Figure 3, is carried out for Phosphorous based on data from the three local replication experiments and full field data, allowing to characterize and compare the local and global heterogeneity of each field. Figure 3 will also show to which degree it is possible to distinguish between cultivated and uncultivated fields within this traditional univariate regime.

Table 1 presents the relevant averages and standard deviations. Comparing the three sets of "Box characterizations" it is not

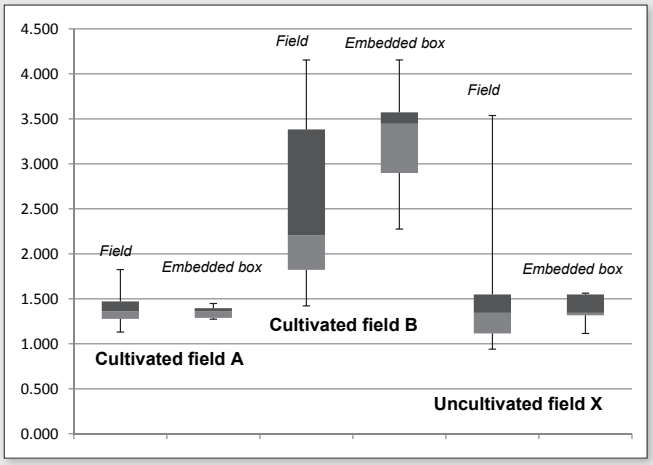

Figure 3. Box-plots of field vs. box heterogeneity characteristics for the element Phosphorous

Table 1. Phosphorous data characterisation (ICP)

ICP results for the three boxes					
Cultivated field A					
	9	9w	9x	9y	9z
Phosphor (mg/L)	1,396	1,288	1,448	1,360	1,274
Average	1,353				
Std. Deviation	0,073125				
Cultivated field B					
	30	30w	30x	30y	30z
Phosphor (mg/L)	2,275	3,573	2,898	4,155	3,446
Average	3,269				
Std. Deviation	0,713165				
Uncultivated field X					
	13	13w	13x	13y	13z
Phosphor (mg/L)	1,344	1,548	1,563	1,317	1,115
Average	1,377				
Std. Deviation	0,185182				

possible to conclude that fields A & B are in fact both cultivated. On the contrary, if this approach is used one would probably conclude that field B was cultivated (because of its elevated P levels) while field A and field X represent uncultivated areas. This is manifestly incorrect however – and the univariate approach fails. The box plot evidence also pictures the difference between the local and global phosphor heterogeneity and, as assumed a priori, the local heterogeneity constitutes but a fraction of the global field heterogeneity.

From the standard deviations one can conclude that the variability for phosphor is largest in cultivated field B.

Multivariate Data Analysis (MVDA)

Clear limitations and attending misinterpretations were found by the univariate approach. This is due to the fact that cultivated fields apparently do not have the same levels of elevated phosphor concentration. But even though the P concentration is low, field A is actually cultivated as shown by irrefutable archeological evidences. Perhaps such relationships can be better appreciated from a multivariate approach when considering a range of 15 elements simultaneously?

MVDA is an approach in which the covariance structure of different datasets is modeled and visualized based on the correlations between the variables included. MVDA contains different methods that can handle different data analysis objectives. One of the powerful tools is Principal Component Analysis (PCA), which reveals data structures (exploratory data analysis) in two complementary plots, the so-called scores and loadings plots (Esbensen (2010), Martens & Næs (1989)). Results of PCA carried out on soil metal concentrations are depicted in Figures 4–6 (41 objects and 15 variables). PCA on this data set will also allow to survey heterogeneity in the different fields due to the two different experimental designs.

Field characterization

Figure 4 is a first PCA visualization of the overall structure (score plot t1-t3), which depicts the variance-maximized relationships between the three fields. Based on the information modeled by PC 1 and

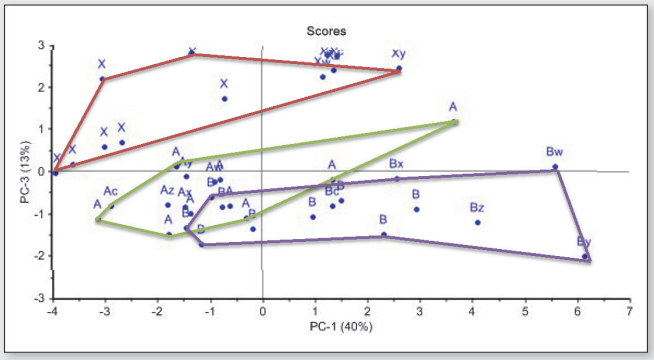

Figure 4. PCA score plot t_1-t_3 of the complete data set. Convex polygons surround data from each of the three fields (X, A, B), see text for details.

PC 3, three clear data groupings (data classes) can be identified, helped along with the known archeological field assignment annotation (A, B, X), which is used to draw convex polygons enveloping the fields. The three fields outline a trend from the uncultivated field X to the two cultivated fields A and B. The latter two fields are only very slightly overlapping due to their distinct geochemistry fingerprints. Based on this simple score plot it is possible to discriminate fully between these two agricultural groups with ease and certainty, but no information about the geochemistry and which elements are causing the between-group trend has been identified – yet. For this the complementary loading plot is needed, in which is depicted the correlation relationships between all the variables involved in the data analysis.

The loading plot, Figure 6, reveal that the strong mutual correlation between [P, Zn, Fe, Mn] is the defining feature for the two cultivated fields A & B, allowing one to conclude that the levels of these elements are elevated in these fields. Due to the group trend from uncultivated to cultivated, which is most pronounced in the vertical direction along PC 3, Mn would appear to be the element that correlates strongest with the cultivated group. Conversely Pb is correlating strongest with the uncultivated field X along PC 1 and B along PC 3.

The multivariate approach is clearly useful for distinguishing between cultivated and uncultivated fields employing 15 geochemical elements instead of one.

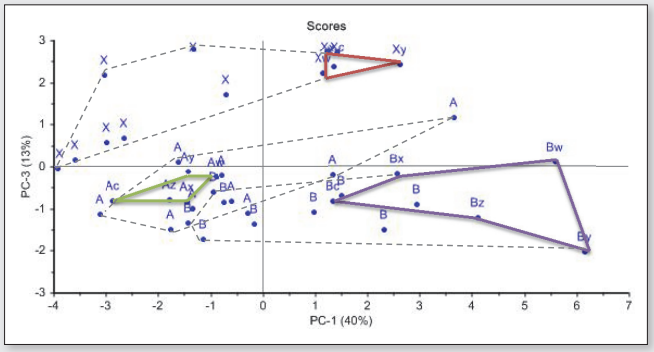

Figure 5. PCA score t1-t3 plot, annotated with convex polygons for the three local box experiments only (heavy lines). Relationships to field-wide classifications (in Fig. 4) indicated by stippled lines

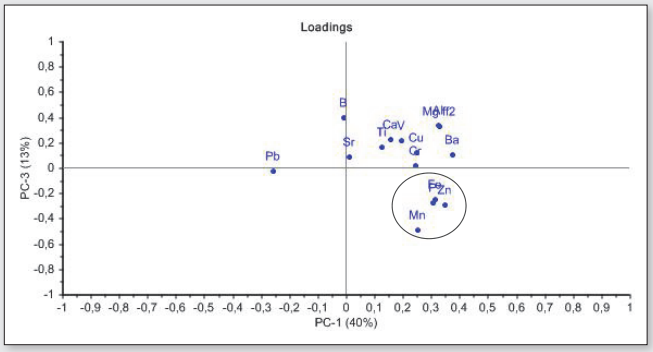

Figure 6. PCA loading plot t_1-t_3 (all data). The most influential correlated elemental group relative to the discriminations seen [Fe, Zn, Mn] in Figures 4 and 5 is indicated (circle); see text for details.

The field replicate experiment also allows a display of the global heterogeneity variations within each field. By use of "connecting lines" one can direct attention to the convex heterogeneity envelope for each field and compare them, which is the annotation used in Figure 4. From this one can argue that they are displaying almost the same degree of field heterogeneity but with different elements as the largest contributors, which can be studied by a more detailed interpretation of Figure 6.

Local heterogeneity characterization

To illustrate the 'local' embedded replicate experiment, the same score plot, Figure 5, can be used again but for this purpose the connecting lines now only frame the sample subsets from the three embedded boxes, emphasizing the local heterogeneity. It is observed that the largest local heterogeneity is indeed found within field B, with much smaller variabilities for field A and X, which show somewhat similar local heterogeneities. From this plot it is also possible to point out potential outliers.

Interestingly the convex polygon that pictures the heterogeneity of uncultivated field X is found as an end-member of the entire field heterogeneity – without the embedded replicate experiment one could perhaps have been led to conclude that this sample could be an outlier.

The above first interpretations from a simple PCA shows the strength of replication experiments on both field and local scales and that the local heterogeneity can vary among, and between fields of different status even. Though small, the present data set is complex to a non-trivial extent, precluding meaningful data analysis based on only one, traditional parameter (P). The complexity is easily and effectively delineated in full measure however when based on the chemometric multivariate approach, PCA[1,4].

The present pilot study data set is not large enough to make a reasonable validation of the strength of PCA solutions calculated. For this it is necessary to invoke a test set, a new data set from similar fields, also taking in at least one of the present fields for re-sampling as well (to be carried out in the summer 2015). Test set validation forms an essential part of proper chemometric data analysis[1,4].

Conclusion

Based on a chemometric multivariate discrimination along PC 3, it is fully possible to distinguish between cultivated and uncultivated Celtic fields on the island of Bornholm – a task for which the traditional P-based univariate approach fails (in the areas investigated here). The present results can therefore be of significant help for archeologists, who until recently would have classified cultivated field A and perhaps many others also, as uncultivated using the traditional univariate P-approach. The multivariate approach is able to yield much more reliable and trustworthy results.

This holds true if – and only if – sampling is done in a representative fashion however, eliminating the majority of all ISE and minimize CSE. Geochemical data typically can contain up to 50% or so random data variance ('data analytical noise'), so PCA decomposition is essential ('shredding data structure from noise').

In this pilot project four elements showed the strongest correlation with the cultivated fields and especially Mn was found to be of pronounced influence. Sparse knowledge as to why Mn, Fe and Zn behave in this correlated fashion with P is raising interest in further geochemical and/or agricultural studies. These relationships could only have been discovered using the chemometric PCA. It will almost always be of interest to increase the number of elements analyzed and e.g. Cobalt should be an element that are of significance in the archeological world.

Through two different experimental designs it was found that each field is characterized by quite similar overall heterogeneities, and that the local heterogeneity (embedded box experiments) was indeed significantly less extensive, Figure 5. The largest heterogeneity was found in cultivated field B, which also had the largest levels of Fe, Zn, P and Mn, Figure 4-6. Geochemical multi-element signatures successfully define different data classes (fields) outlining their internal structures and variable correlations. Why the uncultivated field is particularly strongly correlated with Pb and B is not fully understood at present, an issue that is incorporated in the planned follow-up studies (2015).

All the above findings could only have been discovered using MVDA: Archeology meets TOS meets Chemometrics.

Biography

Bastian Germundsson is a M.Sc. student at IGN & GEUS, currently engaged in different projects with primary focus on sampling issues and with special interests in environmental – and urban geochemistry. Anders Pihl is an archaeologist at Bornholm's Museum with primary interest in Celtic agriculture. Kim H. Esbensen is research Professor at GEUS and AAU, particularly interested in applying TOS and Chemometrics in all of science, technology and industry

References

1. K. H. Esbensen, Multivariate data analysis: in practice: an introduction to multivariate data analysis and experimental design. 5.th Ed. 598 p. CAMO Publ. (2010). ISBN 82-993330-3-2
2. L. Petersen, C. K. Dahl, & K.H. Esbensen, Representative mass reduction in sampling—a critical survey of techniques and hardware.Chemometrics and Intelligent Laboratory Systems, 74(1), 95-114 (2004).
3. DS 3077 (2013). Representative Sampling – Horizontal Standard. Danish Standardisation. www.ds.dk
4. H. Martens, & T. Næs, Multivariate Calibration. Wiley. (1989). ISBN 0-471-90979-3
5. N.H. Nielsen, & S.M. Kristiansen, Identifying ancient manuring: traditional phosphate vs. multi-element analysis of archaeological soil. Journal of Archaeological Science, 42, 390-398 (2014).

doi: 10.1255/tosf.69

Counteracting soil heterogeneity sampling for environmental studies (pesticide residues, contaminant transformation) – TOS is critical

Z. Kardanpour[a,b], O.S. Jacobsen[b] and K.H. Esbensen[a,b,c]
[a]ACABS Research Group, Aalborg University, Denmark. E-mail: zk@bio.aau.dk
[b]Geological Survey of Denmark and Greenland (GEUS). Copenhagen. Denmark
[c]ACRG Research Group, Telemark University College, Norway

This Ph.D. project aims at development of an improved methodology for soil heterogeneity characterization for 'next generation' sampling/monitoring and spatial modeling practices a.o. allowing more realistic pesticide variability in environmental contaminant assessment studies. Such studies typically take place in the laboratory. The key question therefore is: Are current sampling techniques able to counteract the inherent soil heterogeneity met with in the field? Analysis of traditional soil sampling approaches from a Theory of Sampling perspective, the answer is a resounding negative. This contribution summarises the extensive sampling aspects involved in the overall project context, also involving chemometric data analysis with a special twist.

Soil heterogeneity

Soil heterogeneity characteristics in the natural environment do not follow normal statistical distributions and most certainly not regular spatial distributions. There is a need for scientifically based procedures and principles for parameterisation of the intrinsic variability in many types of agricultural, urban and natural soil systems. Conventional computer simulations are critically dependent on the specific choices of model and statistical distribution characteristics, not necessarily always realistic. To a large extent, knowledge in these fields of research is based on laboratory-scale batch experiments involving either soil 'as is' and often with samples of only a few grams of the soil matrix, Figure 1.

Even when procedures for species transport, kinetic studies and analysis follow established scientific and international standards, it is increasingly recognised that small scale experiments do not fully reflect the effective variability and heterogeneity of the salient soil and geological formations at larger, more relevant and more realistic fields scales.[1,2] This will unavoidably cause problems for the later scaling-up to field scale of the processes and effects studied, especially regarding the possibility for valid *volume generalisation*.

The soil matrices involved are in fact often significantly heterogeneous, and a number of the subsequent soil model and interpretation issues are critically related to the empirical variability at scales larger than the laboratory samples (both in vertical and horizontal dimensions). Also taking into account the time scales involved in dynamic studies only add further to system complexity. Within the environmental sciences there is a strong need for an integrated understanding of chemical contaminant transformations (e.g. pesticide degradation), spatial modeling and multivariate data analysis.[3–5] All critical soil characterizing parameters are in need of *effective counteraction* of the variability related to inherent soil heterogeneity when securing valid soil pots for laboratory experimentation, i.e. how to secure representativity of individual pots? Not only that, but how to guarantee that multiple pots containing soil sampled in nature are as identical as possible for replicate laboratory studies?

The main motivation for this Ph.D. has been to develop generic procedures to map the effective heterogeneity of soils *at all relevant scales*. The present paper describes a comprehensive approach

Figure 1. Traditionally "experimental pots" to be used in the laboratory (e.g. pesticide residue, pollutant characterisation or contaminants transformation studies) are 'sampled' directly in the field (*grab sampling*). Ignoring inherent soil heterogeneity leads to compositional differences between pots of an unknown magnitude due to uncontrolled FSE, GSE, ISE. Pots are all too often simply *assumed* to be identical. Observe the drastic mass-reduction from field, sample, pot, often of the order of magnitude 1:1000.

for this purpose, here applied on typical clayey soils with a focus on intrinsic parameters (minerogenic variables, 'soil framework variables'). Clayey soils serve as an exemplar medium, chosen because of the typical non-trivial practical sampling problems and limitations encountered for this type of soil. The main focus is on characterising and comparing grab vs. composite sampling in a full-scale experimental study based on both a short range 2-D design (cm-dm) and a large scale linear profile (dm - ~100m scale). The methodological principles developed are completely general for all soil types however. Results from parallel sandy soil studies are also be presented—together these two soil types cover a significant range of temperate region soil types.

Field experiments—field sampling

This study evaluates a series of experiments testing improved designs of field and laboratory sampling, Figures 2-3, at all stages from the primary field sampling to the final analytical sample preparation, Figures 3-5. The effect of soil heterogeneity at different scales critically affects the validity of the sampling/monitoring procedures involved.

Field samples were collected from the topsoil (A-horizon; 0-25 cm) of a typical clayey soil. For a short range experiment a 50 × 50 cm square of top soil was exposed by carefully removing the uppermost grass layer (approx. 5 cm), Figure 3A. Within this square a total of 68 'standard' soil samples, each of 30-40 g, were collected with the shortest practically possible in-between distance (less than 2 cm) in the pattern shown in Figure 3A. Primary soil samples were extracted using a conventional cut plastic syringe (diameter 1.5 cm, length 10 cm, Figure 3B) and immediately sealed in airtight containers; these samples make up the S-Set samples to be used for '2-D heterogeneity visualisation' (see below). The remaining soil of the square "box" (Figure 3 A) down to 10 cm depth was extracted as a "primary bulk sample", also sealed in a moisture tight plastic bag and transported to the laboratory for further sub-sampling experiments. For a *large scale* variographic characterization, soil samples were collected in identical fashion in the same field with an equidistance of 1 m along a 85 m long profile. A parallel study on sandy soil included a *short scale* replication experiment,[6] is presented in Figure 2.

Contemporary sampling approaches in environmental/soil sciences makes little or no allowance for soil heterogeneity, resulting in significant between-pot heterogeneity which impacts on the discriminating power in laboratory experiments. This is not unavoidable however. Variographic analysis (below) shows the advantage of using increment locations for composite sampling with a distance below the range for both organic and inorganic compounds based on empirical soil sample variograms.

Analytical methods

Field samples were 300-400 gram, while laboratory samples were 20-30 gram moist soil after careful TOS-compliant sub-sampling.[7,8] A focused mass reduction experimental design employed a suite of 16 natural soil parameters including: moisture, organic matter (loss on ignition), pH, soil cations and anions (clayey soil). In addition a large suit of 38 inorganic parameters plus a set of 9 natural and anthropogenic compounds including moisture, organic matter, bacteria counts (CFU), carbon-14 measurement of MCPA sorption and mineralization and glucose respiration were analysed in the sandy soil. Analytical parameters were selected with an aim

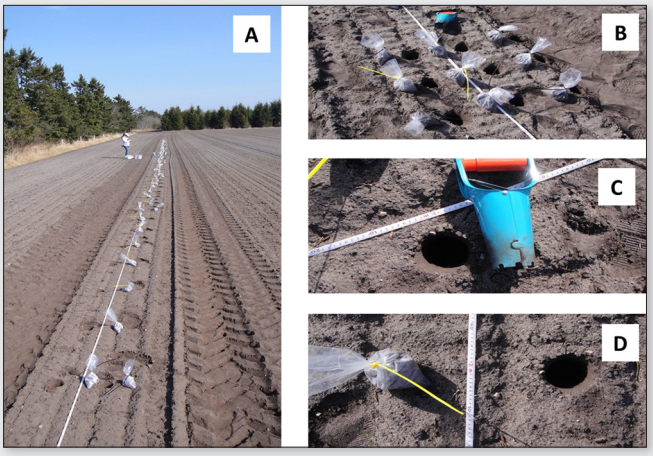

Figure 2. Sandy soil sampling. a) Long range profile for variographic characterisation (~100 m) parallel to the recent ploughing direction; b) Local "grid replication design" (9 samples covering 1 × 1 m); c) Conventional soil sampling hand tool; d) Sample excavation and airtight sample bag.

Figure 3. Laboratory mass reduction for clayey soil samples, A) "Small scale 2-D experiment" (50 × 50 cm), B) Single syringe sample; C) Primary bulk grab sample, D) Single grab sub-sample taken from C); E) Remaining bulk sample laid out for composite sub-sampling, F) Increment size, G) Single composite sample (15 increments); H) Single sample after grinding, entering a bespoke laboratory splitter. Identical procedures were applied to all samples in this study. I) Two sub-samples obtain after splitting.

to study soil heterogeneity with different natural (sandy, clayey), anthropogenic (sandy) and minerogenic (sandy, clayey) parameters with an aim to develop suitable sampling methods for these and similar matrix types.

Laboratory sub-sampling

A general framework is needed for dealing with all operative scale-interdependencies when establishing representative sampling procedures for specific soil types, instead of traditionally having to rely on a universal, standardized sample size and a conventional sampling plan, *supposed* to be able to work well for all soil types as is today's tradition in many fields.

The primary field sample size (200-300 gram) must be reduced to the analytical sample size (1-2 gram), not a trivial mass-handling issue under significant heterogeneity. In order to provide representative sub-samples, TOS principles were applied scrupulously to all mass reduction steps.[7,8] In this project a comparison was directed at grab vs composite sampling, in which two sub-sample sets, a.o. obtained by alternative methods for grinding/splitting, are compared. An embedded 2-D heterogeneity study was finally used for small scale spatial correlation characterisation, supported with a data analytical correlation study (chemometrics). All practical sub-sampling stages are illustrated in Figures 3-5.

Variographic profile characterisation

The cm-dm scale heterogeneity was studied by the '2-D small scale experiments' illustrated above, while the m-100m transect scales were studied by variographic characterisation[6,9] to provide an understanding of how the individual elements are distributed spatially in the field along the 100 m long baseline profile. All data were inspected for possible outliers or trends; outliers have been excluded and in case of a variable trend (possibly to be expected as samples are distributed along the shallow trend incline, Figure 2), de-trended profiles were subjected to variogram characterisation.[9]

Chemometric data analysis

Synoptic overviews of the correlation data structure between 40+ chemical parameters and of the relationships between all variograms were analysed by multivariate data analysis (chemometrics).[11] In here each variogram contributes to a special type of X-matrix in which the objects correspond to the set of variograms, all of which are characterized by a joint set of special variables, 'lag variables' [1, $N_U/2$]. This array is termed the $X_{variogram}$ matrix. The number of 'objects' (N_{obj}) is equal to the number of elements.

Figure 4: Fresh soil mass-reduction steps for clayey soil. A procedure, identical to riffle splitting, was developed for sub-sampling in the laboratory for this type of mildly sticky, non-flowing material.

Figure 5. Manual 'riffle-splitting' simulation for representative sub-sampling in the laboratory. This technique is also known as bed-blending, scaled-down and adapted to both dried, but still cohesive primary sandy soil samples (top) as well as to fine-crushed, dried powder (bottom). This procedure can be described as 'linear bed blending/transverse thin-slice reclaiming'.

Decomposing $X_{variogram}$ results in score plots in which each variogram is depicted in relation to all other variograms, i.e. to which degree variograms are *similar* or *dissimilar* in their characterization of the spatial structures. Whereas standard PCA displays the behavior between correlated variables,[10] the loading plot of the $X_{variogram}$ matrix visualizes the relationships between the variogram lags i.e. which *scales* behave in a coherent fashion, and which display different behaviors. For PCA($X_{variogram}$) the scores and loadings plots render a synoptic characterization of the spatial characteristics for all chemical parameters involved.[11]

According to the nature of the variogram, V(j) values represent squared heterogeneity differences, which means the $X_{variogram}$ data are all expressed in the same 'measurement unit' ('lag distance'). The analogy to ordinary spectral data is clear as conventional spectral values (transmittances, absorbances or otherwise transformed original radiometric data) are also expressed in the same 'measurement units'. This will make interpretation of the $X_{variogram}$ PCA solutions more familiar for those in-the-know regarding multivariate data analysis. Note that these special types of spectra may be in need of auto-scaling, or that may not – which will depend on the empirical variance differences between the variables (or 'lag-variables'). This issue is problem-dependent and cannot be resolved by a general imperative; different data set structures may require specific solutions.

Results and discussion

Aiming for a general approach to exemplify and quantify the effectiveness of heterogeneity characterisation in soil, a set of relevant geochemical parameters was studied at scales from cm to 100 m. In this context both small scale (2-D) and large scale (1-D) variability studies were conducted on different soil types (clayey and sandy soil). This study includes all scales from field sample to analytical aliquot and primary sampling w.r.t. soil type, secondary sub-sampling comparison, further subsampling procedure and evaluation.

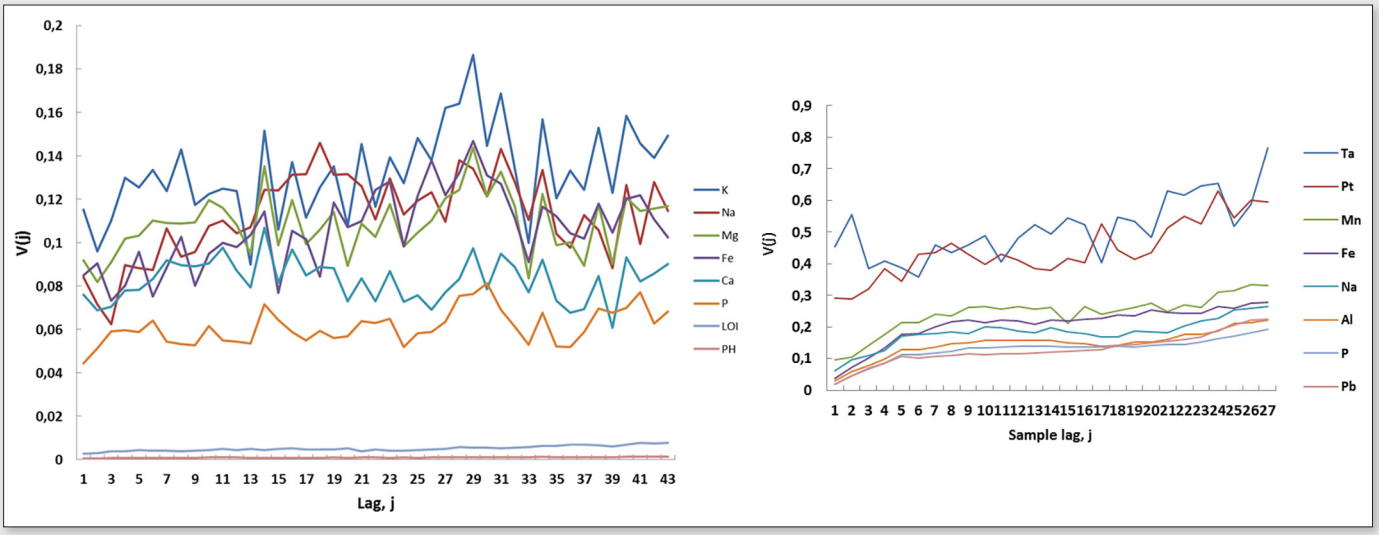

Figure 6. (left) Synoptic variogram plot for eight selected parameters in clayey soil (LOI after de-trending). Two clear groupings can be observed, i.e. two parameters with extremely low and stable variograms and six parameters which show distinctly more irregular variograms at higher sill levels (signifying distinctly larger heterogeneities). All variograms are essentially flat without a clear range for this soil type. (right) Synoptic variogram (sandy soil) for eight selected parameters (Ta, Pt, Mn, Fe, Na, Al, P, Pb) comprising both the highest and the lowest sills encountered (Ta, Pt) vs. (P, Pb) respectively. There would appear to be a general average range of approx. 5 meters. Weak variogram trends do not distrub conventional interpretation.

Evaluation and comparison of subsampling stages were conducted for clayey soil only, the most complex soil type (because of both structural properties and logistics), including a characterisation of different mass reduction (sub-sampling) procedures. Assessing the reproducibility of laboratory grinding/splitting, the TOS-optimized grinding and homogenization step was found to be acceptable for the current purpose. Furthermore, as expected from comparing grab and composite sampling (TOS), for 2/3 of the geochemical soil parameters sub-sampling methods show significant differences when based on grab sampling.

A large scale variability study was directed at two fields with different soil properties with the aim of showing a general comprehensive soil heterogeneity characterization approach wholly based on TOS principles. Figures 6 show variographic characterisation of selected variables for both clayey and sandy soils. These studies are reported in full in the first author's Ph.D. thesis.

It may occasionally be of interest to apply a multivariate approach in order to include all soil parameters simultaneously. A PCA ($X_{variogram}$) approach has been developed that simplify all variogram relationships in conventional scores and loadings plots.[10,11] As one example, Figure 7 shows how it is easy to estimate a general (average) variogram range. This approach is generic and can be applied to any set of parameters in any type of soil. It is only necessary to have enough data (samples) to be able calculate proper variograms.

Combining results of natural organic and anthropogenic parameters with minerogenic parameters from two soil types, the optimal procedure for securing *comparable* field samples (for 'identical' pot samples) for environmental pollutant experiments (samples with minimum inter-sample variability) must be by systematic deployment of *composite sampling* with increment distances less than half the range, Figure 6 - always with a number of increments as high as practical and logistically possible (depending on the total

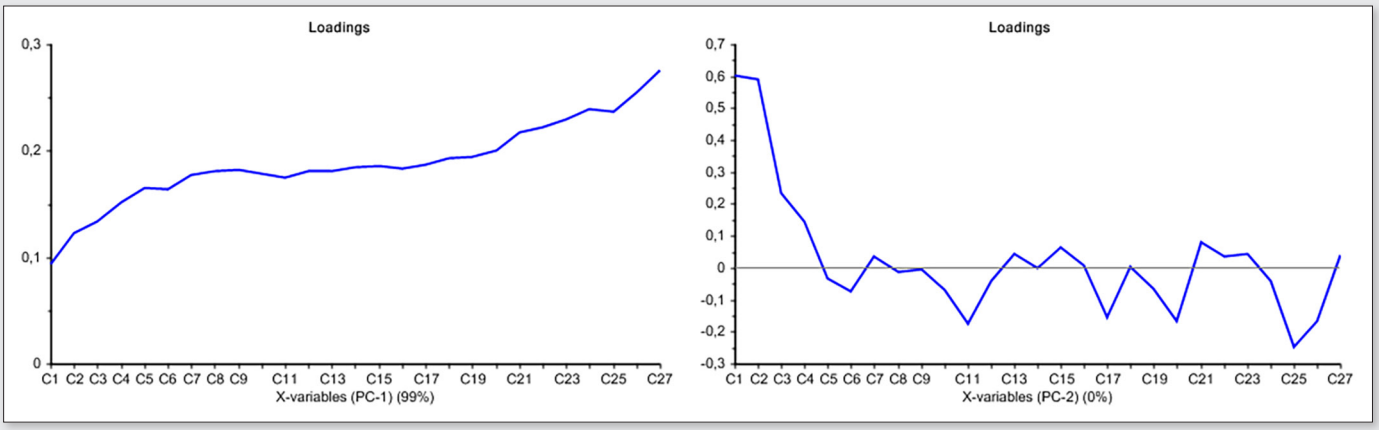

Figure 7. (left) PCA ($X_{variogram}$) loading plot PC-1 (sandy soil, all parameters), and PC-2 (right). The $X_{variogram}$ matrix has not been subjected to pre-treatment (no centering, no scaling), see text for details. The range of the average variogram shape (PC-1 loading spectrum, at left) is ca. 5 meters.

mass required for experimentation). This conclusion strictly speaking only applies to the specific soils investigated here, one of which happens already to be somewhat well mixed (the sandy soil). Other soil types may display much shorter ranges, much higher heterogeneities that is. The general lesson is that increments for composite sampling have to originate only from areas with scale a parameter less than half the range of the salient empirical soil variogram. A heterogeneity-characterising pilot study variogram is sine qua non.

Conclusions

Empirical heterogeneity description is a critical success factor in soil, contamination, pollution and environmental science studies a.o. when natural variability effects are to be reliably managed. The Theory of Sampling (TOS) is a versatile generic framework that is able to deliver the tools for heterogeneity counteraction in the sampling stage(s), which is necessary for designing an unbiased and reproducible sampling procedure.[12]

A pilot experiment focusing on intrinsic heterogeneity characterization will always be advantageous. Different approaches for scale characterization were evaluated: embedded small-scale experimental designs in combination with larger scale 1-D transect sampling can reveal the inherent heterogeneity at scales from sampling volume up to the maximum experimental length scale studied. Thus e.g. for collecting experimental soil samples for laboratory pesticide fate studies based on *realistic* soil samples, this purpose would be served the worst by samples having inter-distance larger than the range. Emphasis should be on securing realistic, representative soil pot samples with the most *similar* characteristics, especially when deploying duplicate or replicate pot samples for such studies. It has also been demonstrated how to use representative mass reduction to get sample sizes down from field to aliquot scales in a fully representative fashion and how to counteract and manage soil heterogeneity in this process.[11,12]

Results from the various replication sampling approaches reveal considerable heterogeneities at scales from 3 cm to 100 meter. The heterogeneity in 1-D profiles can be visualized by a variogram description, the statistics of which (nugget effect, sill, range) offers a full description of all necessary and sufficient spatial characteristics of the heterogeneity. PCA score plots of the special $X_{variogram}$ matrix offer an effective overview of similarity vs. dissimilarity between variograms (especially in the case of many elements), which in the present case mainly reflect different sill levels (in general cases this will also encompass range difference).

We have developed a comprehensive approach to reach all the stated project objectives and evaluated their performances with realistic field and laboratory experiments.[11,12] The methods presented and illustrated in this Ph.D. project have a substantial carrying-over potential to geochemistry and in environmental science, as well as other application areas.

References

1. Boudreault, J.-P., Dubé, J.-S., Sona, M. & Hardy, E. Analysis of procedures for sampling contaminated soil using Gy's Sampling Theory and Practice. *Sci. Total Environ.* **425,** 199–207 (2012).
2. De Zorzi, P. *et al.* Estimation of uncertainty arising from different soil sampling devices: the use of variogram parameters. *Chemosphere* **70,** 745–52 (2008).
3. Barbizzi, S. *et al.* Characterisation of a reference site for quantifying uncertainties related to soil sampling. *Environ. Pollut.* **127,** 131–135 (2004).
4. Dubus, I. G., Brown, C. D. & Beulke, S. Sources of uncertainty in pesticide fate modelling. *Sci. Total Environ.* **317,** 53–72 (2003).
5. Chappell, A. & Viscarra Rossel, R. a. The importance of sampling support for explaining change in soil organic carbon. *Geoderma* **193-194,** 323–325 (2013).
6. DS3077. in **44,** 1–38 (Danish Standard Authority, 2013).
7. Petersen, L., Dahl, C. K. & Esbensen, K. H. Representative mass reduction in sampling—a critical survey of techniques and hardware. *Chemom. Intell. Lab. Syst.* **74,** 95–114 (2004).
8. Wagner, C. & Esbensen, K. H. A critical assessment of the HCGAgrain sampling guide. in *TOS Forum* 16–21 (2014).
9. Esbensen, K. H., Friis-Petersen, H. H., Petersen, L., Holm-Nielsen, J. B. & Mortensen, P. P. Representative process sampling — in practice: Variographic analysis and estimation of total sampling errors (TSE). *Chemom. Intell. Lab. Syst.* **88,** 41–59 (2007).
10. Esbensen, K. H. *Multivariate Data Analysis – in practice.* 597 (CAMO Software, 2010).
11. Z. Kardanpour, O.S. Jacobsen, K. H. E. Soil heterogeneity characterization using PCA (Xvariogram) – Multivariate analysis of spatial signatures for optimal sampling purposes. *Chemom. Intell. Lab. Syst.* (2014).
12. Z. Kardanpour, O. S. Jacobsen, R. K. Juhler, K. H. E. Scale-dependent Soil Heterogeneity Characterization Theory of Sampling(TOS) and Variograms. *Eur. J. Soil Sci.* (2014).

doi: 10.1255/tosf.74

Distributional assumptions in food and feed commodities: how to develop fit-for-purpose sampling protocols?

C. Paoletti[a] and K.H. Esbensen[b]
[a]European Food Safety Authority (EFSA), Parma, Italy. E-mail: claudia.paoletti@efsa.europa.eu
[b]National Geological Surveys of Denmark and Greenland, Copenhagen and Department of Biotechnology, Chemistry and Environmental Engineering, Aalborg University campus Esbjerg (AAUE), Denmark. E-mail: ke@geus.dk

Bulk food and feed sampling is a multi-step procedure in which typically a composite sample is first produced by pooling primary increments, thoroughly mixed and then mass-reduced (possibly in several steps) to obtain an ultimate laboratory sample of suitable size for analysis: the test portion, or the analytical aliquot. Among all sampling steps involved in this pathway, application of composite sampling is the most critical. If the primary sample cannot be proven to be representative, all ensuing steps of mass-reduction, sample preparation and analysis are in vain, for reasons recently explained in full in the horizontal standard DS 3077[1], where the specific requirements for ensuring representativeness, are addressed in full.

Although it is well known that material heterogeneity influences the effectiveness of sampling procedures, most guidelines defining sampling strategies specific for, or routinely applied to, food and feed products are based on stringent distributional assumptions, seldom justified or discussed in sufficient detail, if at all. Indeed most are based on classical statistical distribution requirements – foremost the normal, binomial and Poisson distributions - and almost universally rely on the assumption of randomness[2, 3, 4]. This is an unrealistic and suboptimal state of affairs at best however. Does the supposed randomness relate to constitutional heterogeneity or to distributional heterogeneity for example? How are the unavoidable irregular spatial distributions accounted for? The scientific and industrial communities actually recognizes a strong preponderance of non-random distribution within commodity lots[5, 6, 7, 8], which therefore should be the more realistic pre-requisite for definition of effective sampling protocols. Heterogeneity issues are too often overlooked, instead allowing non-scientific considerations to determine sampling protocols, focusing financial, time, equipment and personnel constraints instead of mandating acquisition of documented representative samples under realistic heterogeneity conditions. We show how the principles promulgated in the Theory of Sampling (TOS), e.g. as practically tested in an EU study on soybean materials[9], actually apply universally in the food and feed realm and should be considered as an *exemplar* for development of valid sampling protocols free from distributional constraints. TOS provides a framework within which identification and development of unbiased sampling plans is driven by empirical observations made on a case-by-case basis and calibrated upon the *specific* heterogeneity characteristics of the material under assessment. Under the guidance of TOS' Fundamental Sampling Principle, systematic application of stratified random sampling will suffice to always 'cover' the entire lot. The appropriate number of increments is not scalable with the size of the lot, contrary to many standard myths perpetuated *ad infinitum*, but only with the degree of heterogeneity in the lot and the a priori chosen degree of confidence, i.e. the acceptable level of risk.

Food and/or feed products constitute no special case in this context: if sampling is not carried out correctly (if biased), subsequent analytical efforts in the laboratory are completely futile[1,5,6,7,10,11,12]. Much work still needs to be done in order to prevent continued use of non-representative sampling protocols that are prevalent in international standards and guidelines, sometimes limited by unsubstantiated distributional assumptions. If providing correct sampling recommendations is a priority for both the scientific community and regulators responsible for consumers' protection, it is necessary to contribute towards a unanimous acceptance of the position that evaluation of the total sampling error (TSE – including laboratory handling errors) is equally important as the evaluation of the analytical error[13]. So far, far too much attention has been devoted only to estimates of the total analytical error (TAE) and many, very specific, and therefore only ad hoc experimental designs, with or without a sufficient number of increments and replicates, has been evaluated only as a function of the specific properties of the analytical method involved. Applying TOS principles allows development fit-for-purpose TSE criteria based on of empirical lot heterogeneity characterisation[5, 6, 7] with which to enter into e.g. risk analysis or compliance testing, on a fully realistic basis.

References

1. DS 3077- Horizontal Standard: Representative Sampling, Esbensen, K.H., "DS 3077 Horizontal—a new standard for representative sampling. Design, history and acknowledgements", *TOS forum* **Issue 1,** 19–22 (2013). doi: 10.1255/tosf.7
2. K. Remund, D. Dixon, D. Wright, & L. Holden, Statistical considerations in seed purity testing for transgenic traits. *Seed Science Res.* 11, 101-120 (2001).
3. M. R. Binns, J. P. Nyrop, & W. van der Werf, *Sampling and monitoring crop protection. The theoretical basis for developing practical decision guides*. CABI Publishing, Oxon, UK (2000).
4. G. W. Cochran, *Sampling Techniques*. 3rd Edition. J. Wiley & Sons Inc., NY, USA (1977).
5. K.H. Esbensen, C. Paoletti and P. Minkkinen, Representative sampling of large kernel lots I. Theory of sampling and variographic analysis. *TrAC* 32, 154-164 (2012).
6. P. Minkkinen, K.H. Esbensen and C. Paoletti, Representative sampling of large kernel lots II. Application to soybean sampling for GMO control. *TrAC* 32, 165-177 (2012).
7. K.H. Esbensen, C. Paoletti and P. Minkkinen, Representative sampling of large kernel lots III. General considerations on sampling heterogeneous foods. *TrAC* 32, 178-184 (2012).
8. C. Wagner, Critical Practicalities in Sampling for Mycotoxins in Feed. *J. AOAC Int*. 98 (2015).
9. C. Paoletti, A. Heissemberger, M. Mazzara, S. Larcher, E. Grazioli, P. Corbisier, N. Hess, G. Berben, P.S. Lübeck, M. De Loose, G. Moran,

C. Henry, C. Brera, I. Folch, J. Ovesna, G. Van den Eede, Kernel lot distribution assessment (KeLDA): a study on the distribution of GMO in large soybean shipments. *Eur. Food Res. Technol.* 224, 129-139 (2006).

10. P. Lischer, Sampling procedures to determine the proportion of genetically modified organisms in raw materials Part I: correct sampling, good sampling practice. *Mitt Lebensm Hyg*. 92, 290-304 (2001).
11. P. Gy, Sampling for Analytical Purposes. Wiley. ISBN 0-471-97956-2 (1998).
12. K. H. Esbensen, C. Wagner, Theory of Sampling (TOS) versus measurement uncertainty (MU) – A call for integration. *TrAC* 57, 93-106 (2014).
13. C. Paoletti and K.H. Esbensen, Distributional assumptions in food and feed commodities – development of fit-for-purpose sampling protocols. *J. AOAC Int*. 98 (2015).

doi: 10.1255/tosf.78

Representative sampling for a full-scale incineration plant test—how to succeed with TOS facing unavoidable logistical and practical constraints

Peter Bøgh Pedersen[a] and *Jan Hinnerskov Jensen[b]
[a]Danish Technological Institute, Kongsvang Allé 29, 8000 Aarhus C, Denmark. E-mail: pbbp@dti.dk
[b]Danish Technological Institute, Kongsvang Allé 29, 8000 Aarhus C, Denmark. E-mail: jhje@dti.dk

Danish Technological Institute is a self-owned and not-for-profit institution. We develop, apply and disseminate research and technologically based knowledge for Danish and international business sectors. As such, we participate in development projects, which are of use to society in close collaboration with leading research and educational institutions in Denmark and abroad.

Introduction

Impregnated wood waste comprises a significant part of all waste produced in Denmark. All impregnated wood waste is gathered at recycling centres. According to Danish law, combined heat and power plants are not allowed to incinerate this type of wood waste, and therefore all impregnated wood waste is exported to Germany for incineration. This is very expensive and not at all an intelligent way to treat wood waste: harmful emission is not avoided and a lot of transportation is involved. In order to consider a more environmentally friendly method for incineration of impregnated wood waste, the Danish Environmental Protection Agency needed additional knowledge. Danish Technological Institute was commissioned to execute a full-scale test at an already existing combined heat and power plant. Together with Renosyd I/S (a heat and power plant near Aarhus) Danish Technological Institute planned and measured all waste streams regarding the incineration of impregnated wood waste. The impregnated wood waste came from five different recycling centres from the area surrounding the heat and power plant involved. The wood waste consisted of railway sleepers, telephone poles, fence posts, boards, window frames and some fractions were in the metre size range, some smaller.

Considerations before practical execution

Renosyd I/S collected and accumulated an estimated amount of 600 tons of impregnated wood at its disposal site 5 km from the incineration plant – see Figure 1. During normal operations, the wood waste will pass a shredder at the incineration plant. However, for this present study sampling behind the shredder was not an option due to physical conditions and safety aspects. Size and mass reduction consequently had to be performed off-line, but these operations could not be made at the incineration plant due to the limited space. Therefore, the sampling campaign had to be performed at the disposal site.

A representative sample of the 600 ton lot was needed for chemical analysis before the incineration tests in order to follow and give a reliable characterisation of all waste streams[3-7]. With the present type of inhomogeneous wood waste in mind, it was of utmost importance first of all to mass and size reduce the lot, Figure 2. The task was to reduce a 600 ton potential, very heterogeneous lot to a laboratory sample of approximately 10 kg; i.e. a sampling rate of 60,000 to 1. Laboratory techniques for further sample reduction were already well established and known to industry.

It was not possible to place the large amount of wood waste on a concrete foundation, but it was found acceptable to place the impregnated wood on the frozen mid-January ground in an isolated pile with no risk of being mixed with other types of wood or waste. The pile was approximately 75 metres long and 15 metres wide, Figure 2. The logistical constraint was that there had to be room enough for lorries to unload the wood waste.

For size reduction, a shredder with a nominal capacity of 40 tons/hour was chosen. The shredder had to be able to size reduce, e.g., large telephone poles to a particle size of 30 cm. The number of increments would be adjusted to the shredder capacity with respect to the total sample mass opted for. Further size reduction in one step was not possible, as the heat and power plant was not able to handle pieces of material smaller than 30 cm. Therefore, a second size reduction step was needed later in the process.

In close cooperation with the workforce at the waste deposit, it was decided that mass reduction could be performed via the one-dimensional stream throw-off from the shredder, Figure 4.2. Increments of a minimum of 100 kg could be taken by using a front loader. The increments were all placed in a separate pile for later additional size and mass reduction treatment, Figure 5.1. The importance of strip mixing (bed blending) should be emphasised

Figure 1. Overview of deposit site (Google maps). The area where the wood waste was placed and handled is marked with blue. The lot comprised the red area.

Figure 2. The original wood waste lot as received at the deposit.

and clearly described to the workforce responsible for taking the increments. A shredder capacity of 20 tons/hour with increment removal every fifteen minutes would result in 120 increments and a total primary sample mass of 12 tons. If the capacity had been only 15 tons per hour and increments were taken, e.g., every thirty minutes, approx. 80 increments corresponding to eight tons of material would have been gathered.

After a second chopping, wood shards of an expected particle size of 10-30 cm were to be further size reduced in a wood chip cutter. An amount of wood waste of 8-12 tons was too large for this equipment, so a further mass reduction was needed for practical reasons. The degree of mass reduction depended on the exact size of the wood pieces. The final procedure in this step was therefore postponed until after the second pass through the shredder in order to make a more qualified decision regarding the amount and specific procedure.

Recommendations for making qualified decisions have to be based on the European Standard EN 14780: *Sampling and sample reduction of solid biofuels.* The standard prescribes a sample amount of at least 120 kg when the pieces are up to 20 cm and of at least 400 kg when the pieces are up to 30 cm. It is worth mentioning that the new DS standard 3077: *Representative Sampling (2013)* explains how scaling the amount of increment with the total lot mass is obsolete – the amount of increment needed scales according to the degree of heterogeneity encountered. Due to the

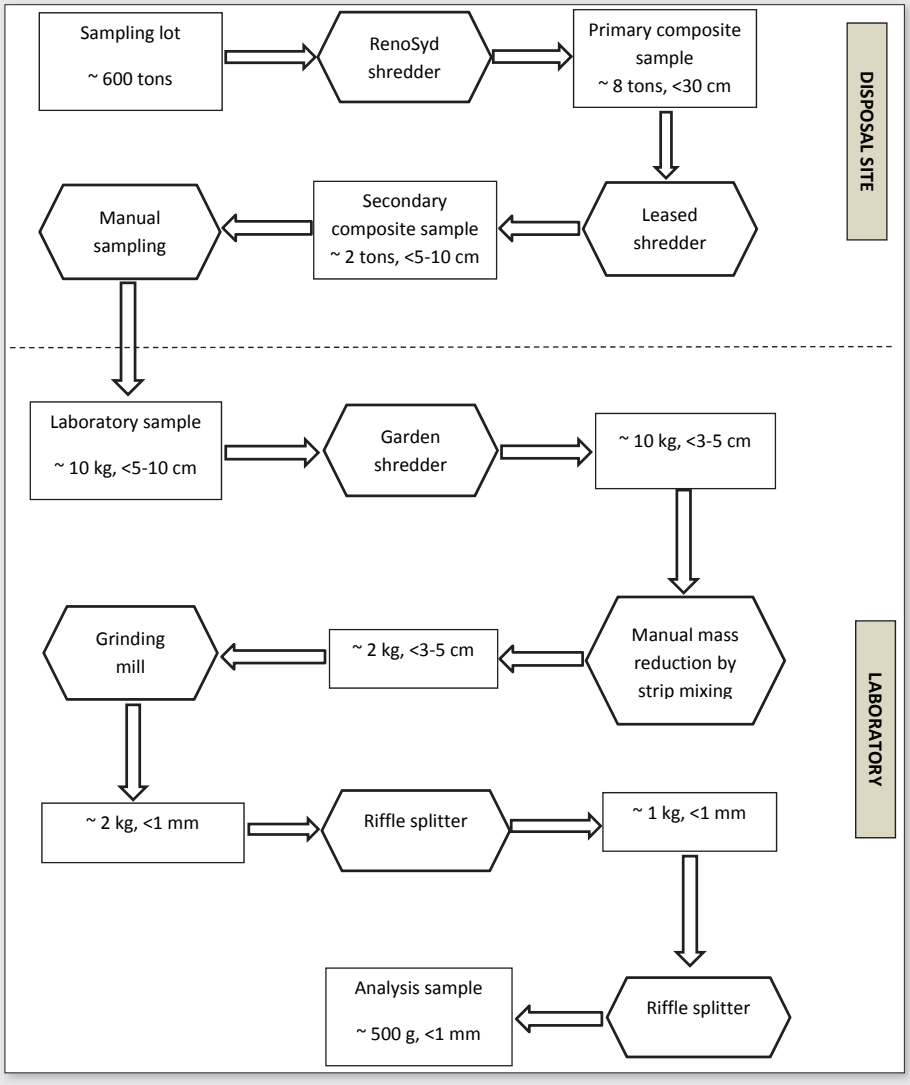

Figure 3. Planned flow diagram of the process described in the present contribution.

expected inhomogeneity of the wood waste compared to wood chips and wood pellets it was decided to do better than the EN standard prescriptions - it was decided that the amount should be at least 4,000 kg before the wood chip cutter-step.

After mass reduction, the sample amount would be cut in the wood chip cutter. Another mass reduction step would then be necessary before ending up with a sample of 10 kg to be handled in the laboratory – see Figure 3.

Sampling Plan

A sampling plan was designed based on the following preliminary considerations that contain the following elements:

- Composite sampling is a must.
- Successive steps of particle size reduction.
- The total lot is moved to secure that all parts are accessible and to make it possible to carry out one dimensional sampling from a free falling stream.
- The heterogeneity of the material, and hence the increment variance, was not known a priori. It was unfortunately not possible to make an estimation (a replication experiment (DS 3077:2013)) within the project budget. The number of increments is therefore a result of a realistic survey of prevailing conditions and based on "good practice and experience".
- Practical execution of on-site sampling

For the incineration trial, a volume of 600 tons was estimated to be necessary, and therefore the total pile made up the sampling lot – see Figure 1. The lot was not divided into sub-lots.

The waste wood consisted mainly of large pieces of telephone poles, fences and building residues and some of them contained metal. When laying up the pile, the material was "pre-crushed" with a "compacter". Sampling from the present pile was not possible for two reasons: large parts of the pile were not accessible, and the large "particle" size could lead to a bias and it would require too large sample volumes. Therefore, the 600 tons of wood waste was size reduced in a shredder, model Arjes VZ 750. That type of shredder was suitable for handling the metal pieces that were found in some of the wood waste. The shredder was placed beside the pile and loaded continuously by a front loader. The feeding of the shredder and the size reduction of the wood waste went smoothly, so the full capacity of 40 tons per hour could be observed most of the time. The estimated effective time used was 15-20 hours, Figure 4.1.

Composite sampling took place as a front loader collected a number of primary increments from the falling discharge from the shredder (one-dimensional process sampling); increments were continuously accumulated in a separate pile at a new location. The first campaign day, an increment was taken every fifteen minutes. This frequency was increased to every 10-12 minutes for the remaining time. It is acknowledged that that gives a sampling bias as the frequency was altered during the process. Based on the practical experience from day one, it was found that improved frequent sampling was desirable, see Figure 4.2.

The total number of increments was *estimated* to be more than 100. The weight of each increment is estimated to approx. 75 kg resulting in a total primary sample of about 8,000 kg. Given a bulk density of approx. 400 kg/m^3 this gives a pile of 20 m^3 consisting of pieces below 30 cm, which can be seen in Figures 5.1 and 5.2.

A front loader bucket-full of the already size-reduced wood waste was tentatively loaded into the shredder for a second pass, but no significant size reduction was found. Another solution was needed, since further size reduction was essential before continuing. After some searching, a smaller shredder was rented to reduce the size of the primary sample to below 5-10 cm, Figure 6.2. The procedure using a front loader to feed the shredder and to extract increments from the falling material stream out of the shredder was a copy of the one used in the first reduction step, again making one-dimensional process sampling possible, Figure 6.1. A secondary sampling was designed on that basis, which consisted of more than 200 increments each of just less than 10 kg. The composite secondary sample was laid up as a longitudinal pile by strip mixing (bed blending) and subsequently flattened to a height of less than 50 cm, Figure 7.

From this pile, a final composite sample of 50 litres was extracted, manually extracting 50 increments with a shovel. All 50 increments were taken at randomly chosen locations and depths. The final

Figure 4. (a) Loading the shredder at step 1. (b). Extraction of increment at step 1. Each increment is approx. 75 kg, extracted every 10-15 minute.

Figure 5. (a) The accumulated primary sample lot (approx. 20 m^3). (b) Particle size distribution after primary shredding at step 1 (see Figure 3). A 20 cm folding ruler for scale.

Figure 6. (a) Extraction of increment at step 2 (size reduction to a particle size below 5-10 cm). (b) Particle size after size reduction step 2. A 20 cm ruler for scale.

sample was placed in a large plastic bucket, sealed and marked before further handling in the laboratory.

Laboratory sample preparation

The final 10 kg (50 litres) sample was particle size reduced in a garden shredder in the laboratory to less than 3 - 5 cm. Manual mass reduction was also performed by strip mixing, resulting in a sample mass of 2 kg, on which another particle size reduction step was made, this time using a laboratory grinding mill. Finally, this 2 kg sample was split (in two steps) into two parallel sub-samples of 500 gram, by using a riffle splitter[8]; the 1 kg sub-sample was discarded after step one. These two parallel samples were then delivered to the analytical laboratory: one for chemical analysis, the other as a backup archival sample.

Potential error sources

Placing the pile on the frozen ground was not optimal. Possible errors in later chemical analyses could for example originate from material in the dirt, giving rise to detection of certain extraneous trace elements. However, this project is decidedly of the "art-of-the-possible" type, a project that simply has to be performed in the real world. In any case, the available funding and time were issues that gave us the possibility to operate as described in this paper.

It was not possible to traverse the free falling stream from the shredder with the front loader completely as prescribed in the TOS literature[6]. However, it is believed that it did not have any important effects, mainly because no segregation was found in this highly non-flowing type of material, Figures 2, 5.1, 5.2, 6.2, 7.

From the minor shredder, a loss of fines was observed from the outgoing stream during operation due to a light wind. The loss is considered negligible as it was *very* low in mass percentage compared to the total mass, and we have no reason to believe that any chemical component was over-represented in this fraction based on visual inspection.

A minor mass loss also occurred in shredder-step 1 due to the removal of metal parts. Small amounts of wood were attached to some of the metal parts after the shredder step, but only a few kg of wood waste out of the total of 600 tons were lost that way.

Figure 7. The composite secondary sample lot flattened to a maximum height of 50 cm. 50 increments were taken at randomly selected locations and depths (using a shovel), making up the final composite sample of 10 kg.

It could probably always be discussed whether the number and size of increments in relation to "particle size" are adequate. In this case, they were considered *appropriate* based on experience, knowledge from EN 14780[1] and a sound judgement on site.

It is emphasised that a perfunctory "replication experiment", DS 3077:2013, unfortunately was out of reach relative to the project budget and time available. It is considered imperative to include such approaches in future projects.

Results

While writing this proceeding, the final report for the Danish Environmental Protection Agency was finalized. Until the Danish Environmental Protection Agency has read and approved the report, it is not possible to conclude whether or not this case study has contributed to change Danish legislation on incineration of impregnated wood waste in Denmark.

Conclusion

It is emphasised that this was not a study in representative sampling. To a high degree, it is a case with severe logistical constraints but it demonstrates the practical application of the underlying theory. Specialized equipment for size and mass reduction, e.g., conveyer belts equipped with proper cross-stream cutters were not an option. However, proper process sampling could still be implemented thanks to the workforce at the deposit site where the sampling campaign was conducted. The local workforce performed the task with enthusiasm and appreciation of the goal and offered many useful suggestions. In addition, it accepted to spend the extra time required. The workforce was also willing to adapt to changes during the process, e.g., renting a smaller shredder when needed within hours.

From a practical point of view, a reasonable solution for downsizing and mass reduction was accomplished. Years of practical experience and underlying knowledge of sampling theory have had a significant impact on the solutions that were exercised.

References

1. EN 14780 Sampling and sample reduction of solid biofuels
2. G.H.Rubæk and P.Sørensen, "Jordanalyser – kvalitet og anvendelse", *DCA report no. 002*, (2011)
3. P. Thy, K.H. Esbensen and B.M. Jenkins, "On representative sampling and reliable chemical characterization in thermal biomass conversion studies", *Biomass Bioenerg.* **33,** 1513–1519 (2009). doi: http://dx.doi.org/10.1016/j.biombioe.2009.07.015
4. H.S. Møller and K.H. Esbensen, "Representative sampling of wood chips", in *Proceedings 2nd World Conference on Sampling and Blending (WCSB2)*. AusIMM, pp. 255–208 (2005).
5. Esbensen, K.H. & Julius, L.P. (2009). Representative sampling, data quality, validation – a necessary trinity in chemometrics. *in* Brown, S, Tauler, R, Walczak,R (Eds.) COMPREHENSIVE CHEMOMETRICS, Wiley Major Reference Works, vol. 4, pp.1-20. Oxford: Elsevier
6. Wagner, C., Esbensen, K., H., 2011. *A critical review of sampling standards for solid biofuels – Missing contributions from the Theory of Sampling (TOS)*. Renewable and Sustainable Energy Reviews, 16 (2011), 504-517.
7. DS 3077 (2013) Esbensen, K.H. (chairman taskforce F-205 2008-2013). "DS 3077. Representative sampling – Horizontal Standard". Danish Standards. www.ds.dk
8. L. Petersen, C. K. Dahl and K. H. Esbensen, "Representative mass reduction in sampling—a critical survey of techniques and hardware", Chemometrics and Intelligent Laboratory Systems 74, 95– 114, (2004)

doi: 10.1255/tosf.70

Representative sampling for food and feed materials: a critical need for food/feed safety

N. Thiex*[a], C. Paoletti[b] and K.H. Esbensen[c]
[a]Thiex Laboratory Solutions LLC, Brookings, SD, USA. E-mail: nancy.thiex@gmail.com
[b]European Food Safety Authority, Parma, Italy E-mail: claudia.paoletti@efsa.europa.eu
[c]Geological Survey of Denmark and Greenland, Copenhagen, Denmark, E-mail: ke@geus.dk
[c]ACABS Research Group, University of Aalborg,Campus Esbjerg, Denmark.

Journal of AOAC INTERNATIONAL (JAOAC) Special Guest Editor Section: "Representative Sampling for Food and Feed Materials: A Critical Need for Food/Feed Safety"

A special collection of papers on all aspects of food and feed safety sampling - to be used in risk assessment, process control in a food/feed manufacturing environment, foodborne disease outbreaks, and regulatory compliance - is now available as an open access publication on the Journal of AOAC INTERNATIONAL's (JAOAC's) website. Visit http://aoac.publisher.ingentaconnect.com/content/aoac/jaoac to find 11 fully refereed papers in the March/April 2015 issue.

These papers are the result of a ground-breaking trans-Atlantic collaboration between researchers, samplers, and regulators from Europe and the United State, a true first within the sampling world. The authors gathered in Windsor, Colorado in October 2014 to collaborate and write. The authors brought strong opinions to the meeting and worked hard to reach a consensus, but met with success in the end (this process jokingly referred to as the 'shootout'.)

The papers in this Special Guest Editor section introduce the Theory of Sampling (TOS) as relevant for all aspects of food and feed safety sampling, as the principles governing representative sampling apply universally. The papers are not independent; they were written and composed to integrate with each other, thus providing a comprehensive, yet very compact overview of the criteria that must be followed to ensure representative sampling in this realm.

Figure 1. Transatlantic Special Section taskforce, October 2014, Windsor, Colorado (left to right): Nancy Thiex, Thiex Laboratory Solutions; Kim H. Esbensen, Geological Survey of Denmark and Greenland and ACABS Research Group, University of Aalborg; Charles Ramsey, EnviroStat, Inc.; Claas Wagner, Wagner Consultants; and Claudia Paoletti, European Food Safety Authority, Parma, Italy. (insert: the only feasible way for harmonisation of terminology – a shootout)

The guest editors were: **Kim H. Esbensen**, Geological Survey of Denmark and Greenland, and Aalborg University, Denmark; **Claudia Paoletti**, European Food Safety Authority Parma, Italy; and **Nancy Thiex**, Thiex Laboratory Solutions, and Agricultural Materials section editor for the Journal.

The target audience for this SGE section includes all food/feed protection personnel: field sampling operators, academic and industrial scientists, laboratory personnel, companies, organizations, regulatory bodies and agencies that are responsible for sampling, as well as their project leaders, project managers, quality managers, supervisors, and directors. In the United States alone, there are an estimated 45,000 federal, state and local food/feed regulatory personnel, not including industry or laboratory personnel. The situation in Europe is similar.

"We hope to trigger a scientific discussion and awareness towards the need for global harmonization of representatitive sampling approaches for food and feed commodities," it is stated in the section's introduction. "As a collection, these papers represent a leap forward with respect to a valid sampling-plus-analysis approach for the entire food and feed area."

The SGE section includes the following contributions:

- "Food and Feed Safety Assessment: The Importance of Proper Sampling' by **Harry Kuiper** and **Claudia Paoletti**.
- "Towards a Unified Sampling Terminology: Clarifying Misperceptions" by **Nancy Thiex**, **Kim H. Esbensen**, and **Claudia Paoletti**.
- "A Systematic Approach to Representative Sampling" by **Claas Wagner** & **Charles Ramsey**
- "Sample Quality Criteria" by **Charles Ramsey** & **Claas Wagner**
- "Materials Properties: Heterogeneity and Appropriate Sampling Modes" by **Kim H. Esbensen**
- "Theory of Sampling—Four Critical Success Factors Before Analysis" by **Claas Wagner** & **Kim H. Esbensen**
- "Quality Control of Sampling Processes—A First Foray; From Field to Test Portion" by **Kim H. Esbensen** & **Charles Ramsey**
- "Considerations for Inference to Decision Units" by **Charles Ramsey**
- "Distributional Assumptions in Agricultural Commodities—Development of Fit-for-Decision Sampling Protocols" by **Claudia Paoletti** & **Kim H. Esbensen**
- "Critical Practicalities in Sampling For Mycotoxins in Feed" by **Claas Wagner**

- "Considerations for Sampling Contaminants in Agricultural Soils" by **Charles Ramsey**
- "Considerations for Sampling of Water" by **Charles Ramsey**

The Special Guest Editor Section is available online at http://aoac.publisher.ingentaconnect.com/content/aoac/jaoac

About AOAC INTERNATIONAL

AOAC INTERNATIONAL is a global scientific association dedicated to the development and validation of analytical methods, improvement of quality assurance procedures in laboratories and professional development of analytical scientists around the world. AOAC INTERNATIONAL members include leading decision-makers from government, academia, and industry working in the areas of foods and beverages, feeds, fertilizers, soil and water, pharmaceuticals, and cosmetics. J. AOAC Int.'s reputation for excellence is based on nearly 100 years of publishing top papers in the analytical field. For more information on AOAC INTERNATIONAL, please visit www.aoac.org - The Journal of AOAC INTERNATIONAL publishes 6 issues per year of fully refereed contributed papers in the fields of chemical and microbiological analysis: original research on new techniques and applications, validation studies, studies leading to method development, and invited reviews. Manuscript topics include foods, drugs, agriculture, and the environment.

Acknowledgements

This work was supported, in part, by the Association of American Feed Control Officials (AAFCO), the Association of Public Health Laboratories (APHL) and by Grant No. 1U18FD004710 from the U.S. Food and Drug Administration (FDA). Its contents are solely the responsibility of the authors and do not necessarily represent the official views of AAFCO, APHL or FDA.

Claudia Paoletti is employed by the European Food Safety Authority (EFSA). The positions and opinions presented in this special session are those of the author alone and do not necessarily represent the views or scientific works of EFSA.

doi: 10.1255/tosf.55

A European standard for sampling of waste material: EN 14899

Philippe Wavrer,*[a] Bernard Morvan[b] and Sebastien Louis-Rose[c]
[a]Caspeo, 3 avenue Claude Guillemin, 45060 Orléans Cedex 2, France. E-mail: p.wavrer@caspeo.net
[b]Traidema, 36, rue Albert Briand, 35200 Rennes, France. E-mail: bmorvan.traidema@numericable.fr
[c]Afnor Normalisation, 93571 La Plaine Saint-Denis Cedex, France. E-mail: sebastien.louisrose@afnor.org

Introduction

Management of waste streams requires knowledge of their intrinsic characteristics, especially with respect to evaluating their response to various treatments, and their potential impacts on the environment. Testing and characterization of wastes allows informed decisions to be made on the appropriate way in which they should be treated, (or not), recovered or disposed. In order to undertake valid tests, it is a requirement that this is based only on representative samples.

Wastes arise in a wide variety of types (e.g. pastes, liquids, granular materials, mixes of different materials) and sampling situations (e.g. during a waste production process, from stockpiles, tanks, drums). Because of the variability, instability, and their widely contrasting compositions, it is often difficult to make measurements directly at their production and the problem of sampling becomes particularly prominent. Moreover, there can be a variety of sampling objectives within each of the three broad categories, i.e. basic characterization, compliance testing and on-site verification.

In 2005, the European Committee for Standardization (CEN) and one year later AFNOR, the French Standardization Association, published the standard EN 14899[1] which deals with the general waste sampling problem. This European Standard, prepared by the Technical Committee CEN/TC 292 "*Characterization of Waste*", specifies the procedural steps to be taken in the preparation and application of appropriate sampling plans. It takes into account waste specific features resulting from:

- Strong heterogeneities;
- Occasional complex behaviours during the sampling and preparation stages, due to instability or other physicochemical characteristics;
- The result of a specific production process, which may be necessary to consider for a proper sampling strategy.

Thus, it provides a framework that can be used to produce standardised sampling plans for use under routine circumstances, with a view also to be able to incorporate specific sampling requirements demanded by European or national legislations, and finally to design and develop sampling plans for use on a case-by-case basis.

Presentation of standard EN 14899

To achieve the objectives of a waste testing program, appropriate sampling methods need to be selected or designed, that will ensure representative samples. For this purpose, the European Standard EN 14899 "Characterization of Waste – Sampling of waste materials: Framework for the preparation and application of a sampling plan", largely based on the concepts of the Theory of Sampling (TOS)[2-5] which represents the only comprehensive approach to representative sampling, provides a framework for how to prepare a sampling plan, in which the elements of the sampling process are defined. It is the first of the following seven program testing steps (see also Figure 1):

- Definition of sampling plan.
- Field sample extraction.
- Delivery to laboratory.
- Test sample preparation.
- Extraction.
- Analysis.
- Measurement report.

The standard EN 14899 aims to provide a list of issues which must be considered when establishing a waste sampling protocol; in particular, it is intended as a guide for writing standards applied to sampling of specific waste (daughter/derived standards).

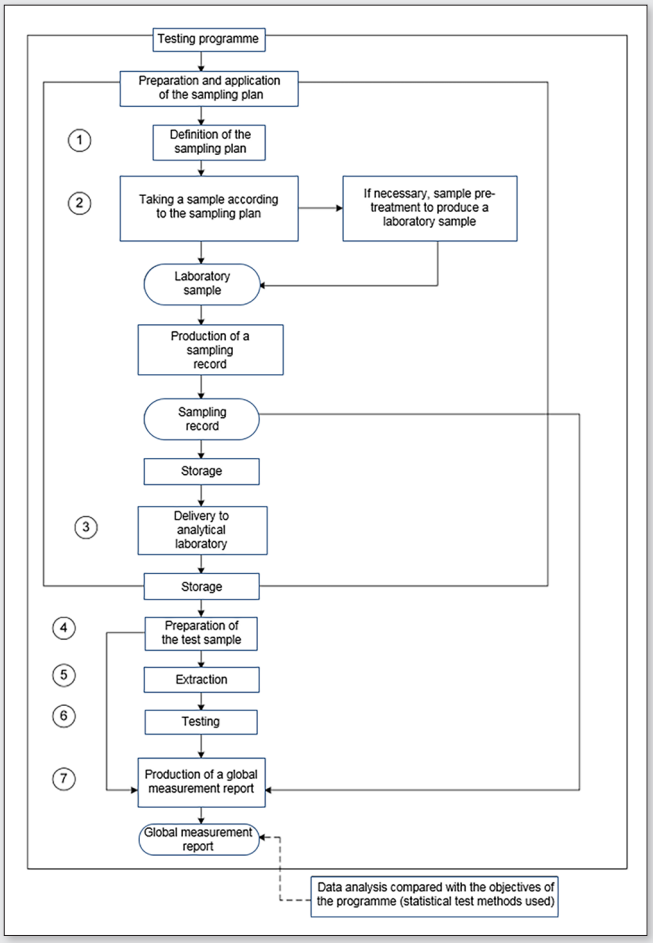

Figure 1. Links between the essential elements of a testing program following EN 14899. NOTE: Key Steps define the 7 overall steps that make-up a testing program.

To facilitate its implementation and enforcement, the standard EN 14899 is accompanied by the following five informative technical reports:

- CEN/TR 15310-1, Characterization of Waste – Sampling: Part 1 – Information on the selection and application of a basic statistical approach to sampling under various conditions[6].
- CEN/TR 15310-2, Characterization of Waste – Sampling: Part 2 – Information on sampling techniques[7].
- CEN/TR 15310-3, Characterization of Waste – Sampling: Part 3 – Information on procedures for subsampling in the field[8].
- CEN/TR 15310-4, Characterization of Waste – Sampling: Part 4 – Information on procedures for sample packaging, storage, preservation, transport and delivery[9].
- CEN/TR 15310-5, Characterization of Waste – Sampling: Part 5 – Information on the process of defining the sampling plan[10].

These technical reports contain procedural options that can be selected to match the sampling requirements of all testing program. By contrast, the five technical reports are not normative documents; rather they provide illustrative examples of potential approaches and tools allowing a project manager to design a customized sampling plan for a given test scenario.

The rest of the present contribution gives a brief overview of the main components of standard EN 14899. This cannot replace the official normative document, which remains the reference for any question of waste sampling plan definition.

Design of a sampling plan

The standard EN 16457:2014 "Characterization of waste – Framework for the preparation and application of a testing program – Objectives, planning and report"[11] describes requirements for a waste testing program regarding objectives, planning and reporting with the intent to ensure reliable and comparable results when using the reference methods that have been developed and/or adopted by CEN/TC 292. This defines the sampling plan as "all the information pertinent to a particular sampling activity" and specifies also that "Note 1: The sampling plan includes the taking of the sample, the production of a laboratory sample, and the transport (to the laboratory), and may include the storage of the laboratory sample" and "Note 2: In case the measurement can be done directly in the field, transport and storage might not be necessary and then will not be elaborated further in the sampling plan".

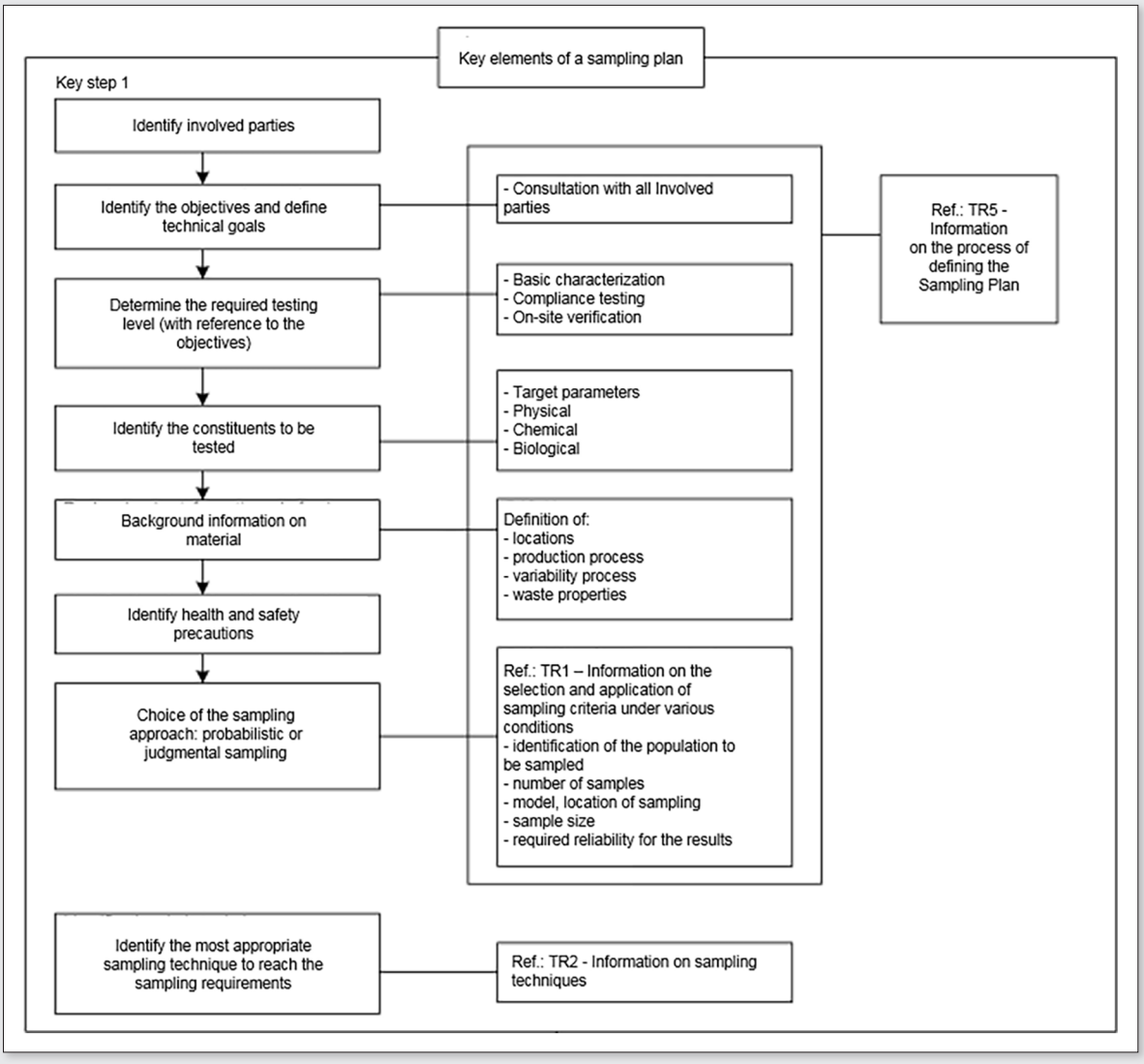

Figure 2. Key elements of a sampling plan following EN 14899.

In others words, a sampling plan shall be completed prior to undertaking any sampling and shall provide the sampler with detailed instructions on how sampling should be carried out. In the process of defining a sampling plan the key elements of the testing program, shown in Figure 2, shall be addressed.

When defining a sampling plan, the following points must be systematically addressed.

Identification of involved parties

The parties involved may as a minimum be the waste producer, but usually also the waste manager, the sampler, the laboratory analyst, etc. The process shall be guided by the need for all involved parties to participate fully, with the objective of improving the quality of the testing program.

Definition of the objectives of the testing program

The objectives of the testing program define what the involved parties want to achieve by the planned waste charaterisation project. Thus they determine the desired level of information (basic characterization, compliance testing or on-site verification) and the desired reliability of the sampling results. Examples of possible objectives of a testing program are:

- To compare the quality of the test material with quality levels defined in national or international legislation;
- To characterise the test material following a change in ownership;
- To determine the re-usability of the test material;
- To determine the leachability of the test material;
- To assess the human health and / or environmental risks posed by the test material.

In the majority of cases, the initial objective of the testing program is too general and non-specific for it to lead directly to the detailed instructions necessary for a proper sampling plan. It is therefore necessary to translate the objective into one or several practical and achievable technical goals. Since the technical specifications for the required samples and the quality level desired are not the same for different objectives, usually one sampling plan is needed for each objective. In some circumstances, it is possible to meet several objectives through a single sampling plan however.

Definition of the required testing level

The sampling plan shall identify the level of testing required to meet the technical goals of the testing program. These will dictate the different types and frequency of investigation to be performed. Examples of testing levels could include basic (or comprehensive) characterization, compliance testing or on-site verification.

Identification of constituents to be tested

The sampling plan shall identify the characteristics or components to investigate, taking into account all known information, such as:

- Origin of the material;
- Intended end-use of the material;
- Total volume of material (in the case of identical units: the population) to be assessed;
- Information from knowledge of process or material involved;

At this point, it is important to collect background information on the material, in order to identify details of the site location or to define the production process, the variability of the process and the waste properties (at least type and dimensions). The sampling plan shall list all known physical and chemical characteristics of the material, including all known potential hazards. In the absence of sufficient information, a 'preliminary investigation' should be instigated, a pilot study.

Selection of the most suitable sampling approach

The sampling plan shall take into account the variability within the lot, or the population and/or sub-population. In addition, the sampling plan shall identify when, where, by whom and how samples shall be taken and collected to ensure that the sample is appropriate to meet the sampling objectives.

At this stage, it is important:

- To define the lot/population to be sampled.
- The lot/population is defined as the total amount (volume or mass) of material about which information is required through sampling (see also technical report CEN/TR 15310-5:2006).
- To identify the scale that defines the volume or the mass of waste material that a sample shall represent. Depending on the nature and the objective of a testing program, scale can also be defined in terms of time. Because of heterogeneities of waste (following TOS, distributional heterogeneity and constitutional heterogeneity have to be considered), defining the scale is important, as heterogeneity is a scale dependent characteristic. As a consequence of the direct relation between scale and heterogeneity, sampling results will be only valid for the scale that is equal to the scale of sampling or higher scales (see also technical report CEN/TR 15310-5:2006).
- To choose the desired reliability of the sampling approach, mainly in terms of "confidence interval" and precision. This reliability strongly depends on the heterogeneities of the considered material, the chosen number of samples, the assumed statistical probability distribution followed by the population, etc. In most cases, it is suggested that the reliability should be as high as possible and representative samples are requested (according to the TOS, a sampling process is representative only when it is both accurate and precise)[12].

Depending on the sampling objective, the sampling plan shall specify either 'probabilistic' sampling, which ensure that each unit within the population being sampled has an equal chance of being sampled, or 'judgmental' sampling.

The sampling approach should at least include:

- The increment size, representing the amount of material (mass or volume) that is obtained through one single sampling action. An increment is not analysed as an individual unit, but is combined with other increments to form a composite sample.
- The sample size.
- The use of composite or individual samples (the latter is known as 'grab samples').
- The required number of samples.
- The sampling location.
- The sampling frequency.

Table 1 summarizes the main steps in defining a sampling plan for a testing program. This table summarizes one of the most important points to consider in establishing a sampling plan as consideration and appropriate choice of statistical criteria are of key importance in the production of a sampling plan.

All information relating to the choice of sampling approach, but also the determination of the size of the increment and of the

Table 1. Main steps in defining a sampling plan for a testing program.

Step	Subject
Specify the objectives of the testing program	
1	Specify the objectives of the testing program
Develop the Technical Goals from the objective	
2	Define the lot/population to be sampled
3	Assess variability
4	Select the sampling approach
5	Identify the scale
6	Choose the required statistical approach
7	Choose the desired reliability
Determine the practical instructions	
8	Choose the sampling pattern
9	Determine the increment/sample size
10	Determine the use of composite or individual samples
11	Determine required number of samples
Define the sampling plan	
12	Define the sampling plan

sample, as well as the number of samples associated with a specified level of uncertainty are given in the technical report CEN/TR 15310-1:2006.

Identify the most appropriate sampling technique

The sampling plan shall identify the technique(s) selected to collect the sample, and shall identify the consequences of deviation from the designated sampling technique or equipment.

Information on the type and use of sampling techniques are given in the technical report CEN/TR 15310-2:2006 and technical report CEN/TR 15310-3:2006 gives information on methods to reduce the sample size for presentation to the laboratory.

Conclusion

Wastes arising in a wide variety of types and sampling situations. Because sampling objectives may vary, a single standard cannot provide definitive instructions for each and every potential case. The European Standard 14899 prepared by the Technical Committee CEN/TC 292 is in fact an umbrella standard that defines minimum requirements on the program, objective, sampling plan and report for the execution of a testing program for waste characterization.

Since its release, it has been applied successfully many times in France, on different types of waste and for different objectives. Examples include:

- Sampling of municipal solid wastes during the last French national household waste characterization survey in 2007. The household waste of a representative sample of hundred municipalities randomly selected to represent the country as a whole was characterized and analysed in order to ascertain the composition of household waste on a national basis.
- Sampling of end-of-life tyres granulate. Aliapur, a Public Limited Company and the leader company in the field of recovering used tyres in France, implemented the standard to define sampling protocols with the objective of characterizing granulate. The resulting protocols have been transformed into standards which can be considered as daughter/derived norms of the EN 14899.

References

1. CEN/TC292/WG1, EN 14899:2005, *Characterization of Waste – Sampling: Framework for the preparation and application of a Sampling Plan* (2005).
2. P.M. Gy, *Sampling for Analytical Purposes*, John Wiley & Sons Ltd, Chichester (1998).
3. K.H. Esbensen, L.J. Petersen, *Representative sampling, data quality, validation – a necessary trinity in chemometrics*, in: S. Brown, R. Tauler, R. Walczak (Eds.), Comprehensive Chemometrics, vol. 4, Elsevier, Oxford, pp. 1–20 (2010).
4. L. Petersen et al., *Representative sampling for reliable data analysis. Theory of sampling*, Chemometr. Intell. Lab. Syst. 77 (1–2) 261–277 (2005).
5. F.F. Pitard, *Pierre Gy's Sampling Theory and Sampling Practice*, second ed., CRC, Press, Boca Raton (1993).
6. CEN/TC292/WG1, TR 15310-1:2006, *Characterization of Waste – Sampling: Part 1 – Information on the selection and application of a basic statistical approach to sampling under various conditions* (2006).
7. CEN/TC292/WG1, TR 15310-2:2006, *Characterization of Waste – Sampling: Part 2 – Information on sampling techniques* (2006).
8. CEN/TC292/WG1, TR 15310-3:2006, *Characterization of Waste – Sampling: Part 3 – Information on procedures for subsampling in the field* (2006).
9. CEN/TC292/WG1, TR 15310-4:2006, *Characterization of Waste – Sampling: Part 4 – Information on procedures for sample packaging, storage, preservation, transport and delivery* (2006).
10. CEN/TC292/WG1, TR 15310-5:2006, *Characterization of Waste – Sampling: Part 5 – Information on the process of defining the Sampling Plan* (2006).
11. EN 16457:2014, *Characterization of waste. Framework for the preparation and application of a testing programme. Objectives, planning and report* (2014).
12. K.H. Esbensen, C. Wagner, *Theory of sampling (TOS) versus measurement uncertainty (MU) – A call for integration*, Trends in Analytical Chemistry 57, 93–106, (2014).

doi: 10.1255/tosf.82

Innovative sampling solutions for the mining industry

Maurice Wicks
IMP Group Pty Ltd, PO Box 1183, Osborne Park, Perth WA 6916, Australia. E-mail: maurice@impgroup.com.au

While online analytical systems are continuously improving, the mine site laboratory remains the benchmark. The laboratory is expected to produce high quality information, so the sampling process is critical. Process managers demand high quality, timely produced results. Mine managers and shareholders are demanding that the process, analytical results and productivity is optimized to maximize return on investment. These demands conflict with traditional sampling and laboratory routines which are frequently slow, labour intensive and commonly involve potentially dangerous, not to mention unscientific methods and work practices. For more than a quarter of a century, IMP has teamed with partners and like-minded customers, to challenge conventional sample collection and processing techniques. In doing so innovative automated sampling and laboratory solutions have been developed for the mining industry. This paper introduces a selection of IMP's automated sampling and laboratory solutions by presenting project examples including a time-based and a mass-based solution for iron ore lump and fines, powder sampling and analysis as well as a slurry sampling and analysis solution.

Introduction

Manual sampling methods and laboratories can involve unsafe working practices, are prone to error and produce historical results rather than timely results. Thus, many modern mines have automated the sampling and laboratory processes, or are in the process of considering automating the laboratory. An automated sampling/laboratory, which usually involves the use of robots and/or utilizes the latest technologies offer the following advantages:

- Improved health and safety as workers are not exposed to dust, repetitive lifting and noise;
- Provides higher quality data as the possibility of human error, such as the switching of sample identification tags and operator bias, is minimized as all samples are handled in exactly the same way improving the overall quality of data produced;
- Increased productivity. Less people are required to operate an automated laboratory than a traditional laboratory. Additionally, automation reduces the need for boring and repetitive tasks to be completed manually – which inevitably leads to mistakes and time wasted due to re-working of samples;
- Laboratory operating costs are more easily managed and automated laboratories usually cost less to operate than traditional laboratories; and
- Sample throughput is considerably quicker. This is because samples are processed sequentially rather than in batches.

However, while laboratory automaton can produce great results in a timely fashion, without a representative sample, that is collected and analysed in a timely way, the laboratory efforts are meaningless. Thus, focus must be on "End to End" solutions – from the point of sampling to final analysis. In doing so IMP has pioneered and/or been involved with the several sampling and associated laboratory innovations, summarized below.

Discussion – Case Studies

Innovative Port Laboratories

IMP's customers include the world's leading Iron Ore exporters. In Australia and South Africa IMP has designed and built several integrated port laboratories where the entire process – from sampling to analysis and cargo certification is fully automated. Thus, all procedures which include sample collection, sample transport, sample drying, sample splitting, particle size determination, moisture determination and chemical analysis are automated. Bulk composite samples can be produced and sampling can be mass or time based.

Each sampling and laboratory solution is tailored to the customer's technical and budgetary requirements while always complying with the relevant ISO standard, usually ISO3082. An Iron Ore port laboratory is illustrative. Frequently when sampling iron ore, primary cuts of up to one ton are taken. This cut is passed through secondary (and often tertiary) cutters to achieve a constant mass division from each primary cut. This constant mass division is typically achieved in one of two ways; this can be performed by collecting the entire cut (which is of a variable mass) in a weigh hopper and using this weight to calculate the size and number of increments that need to be taken from this cut to achieve the constant mass sample output which is sent to the automated laboratory, alternatively, the flow rate of the variable mass cut, onto the sample cutter feeder, is controlled, the sample "slug" length is determined (using belt weightometers together with the belt speed) and using this information the cutter speed and cut frequency is set to achieve the desired constant mass output sample to be sent to the automated laboratory. A portion representing each primary cut is transported automatically to the robotic laboratory via a conveyor system or using IMP's "Monorail Sample Transport System". These aliquots are composited then divided into sub-lots. Particle size analyses and moisture are determined on each sub-lot. Some clients carry out sub-lot chemical analysis while others analyze the final composite.

At the 2014 Sampling Conference in Perth RioTinto presented a paper that discussed the building, design and operation of their new Cape Lambert Iron Ore Port Facility (CLB)[1]. This facility is the world's largest automated iron ore port laboratory (Figures 1–2). The turnkey solution comprises of a fully automated sampling and analysis system that uses time-based sampling methodology. The facility has the ability to sample iron ore products "of medium quality variation as defined in ISO 3082 (ISO, 2009)." [1]. In this instance, there was a need to design a sampling procedure that would collect a representative sample at the required precision and provide full load-port analysis while cargo was being loaded at flow rates of between "6000t/h to 10440t/h. This sampling procedure was

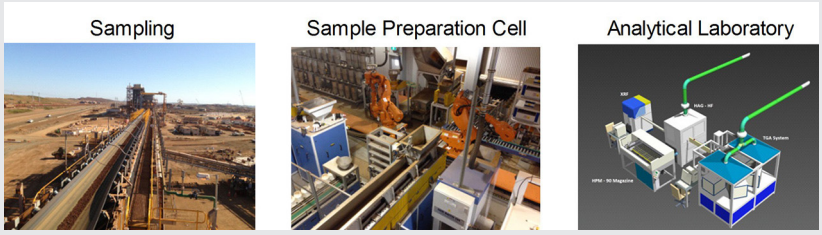

Figure 1.The three components of the Cape Lambert Port B automated sampling and analysis facility [1].

designed in terms of the ISO 3082 specification as a guideline for aspects such as the minimum amount of cuts to be taken from a primary cut and acceptable precision limits for sampling, sample preparation and measurement. Various TOS components were also used in the design of aspects of the sampling solution such as the maximum cutter speed of 0.6m/s, orientation of cutting plane normal to the material flow, minimum cutter aperture of 3x max particle size, distance of cutter park position from material flow to ensure no cross contamination. The sampling approach is to proportionally extend primary increments (of varying mass relative to ship-loading rate) to a standard length using variable speed aerobelt conveyor systems. This enables a fixed number of secondary cuts to be achieved for all primary increment masses and to be delivered to the automated cell. The cell is required to be capable of concurrently processing four individual shipments, each containing multiple cargoes." [1]. To achieve the specified scope, a robotic sample preparation system was designed which incorporates two robots working together on a linear track in effect creating a horizontal sampling tower.

Detailed in this paper [1], during commissioning a bulk sampling campaign was carried out to externally verify all results from the CLB automated laboratory and to check for potential bias in the sample preparation through the automated cell. In addition to this, in order to get an assessment of the sampling, division and measurement precision, the overall precision for this CLB laboratory was compared to a nearby laboratory that processes the same products with similar quality variability. "Precisions are calculated as per ISO 3085 (ISO, 2002), and, in all cases, the precision for each element exceeds the requirements of the standard" [1]. An extract from these results showed the β_{SPM} for Fe % at the CLB sampling system to be 0.102% compared to 0.138% calculated for the other laboratory. Although both systems exceeded the requirements of the ISO 3082 standard and the calculated β_M was only slightly better at the CLB laboratory compared to the other laboratory, the author of this paper discussed that "what is clearly evident at the CLB automated cell are superior precisions for sample preparation and also sampling itself."[1]. Space does not permit to explain the system fully, but the authors conclude that while the challenges of implementing this innovative project were significant, "the success of this system is clearly demonstrated by the improvement in the sampling precision, reliability of the sampling components and quality of the results produced by the system, all of which have been verified externally."[1].

Integrated Automated Mine Site Sampling and laboratory Systems

Increasingly, mine sites require fast timely information that will allow the process to be optimized. While tremendous progress has been made with online analytical systems, sampling stations and onsite laboratories still provide the benchmark for analysis. IMP has risen to the challenge by integrating sampling stations with robotic automated laboratories. In several instances IMP has done so with the aim to determine particle size, and to perform automated chemical analysis along with moisture and density testing. Samples can also be prepared for manual jigging tests and other physical tests (Figure 3). As the entire end to end system is close to the sample collection point and being fully automated, precise results can be transmitted immediately via IMP's "Control Track Lims" software to the

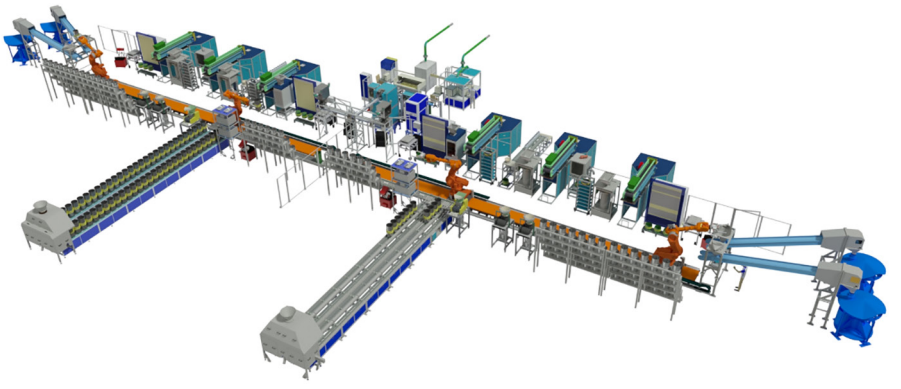

Figure 2. Schematic of dual sample preparation cells, at RioTinto's Cape Lambert Port B (CLB) Laboratory, showing an equipment layout for a "horizontal" sampling, division and measurement system.

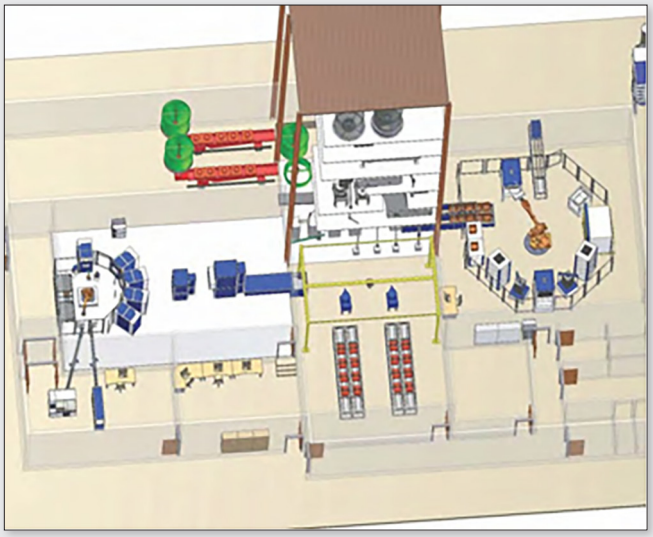

Figure 3. Automated sampling integrated with an automated laboratory.

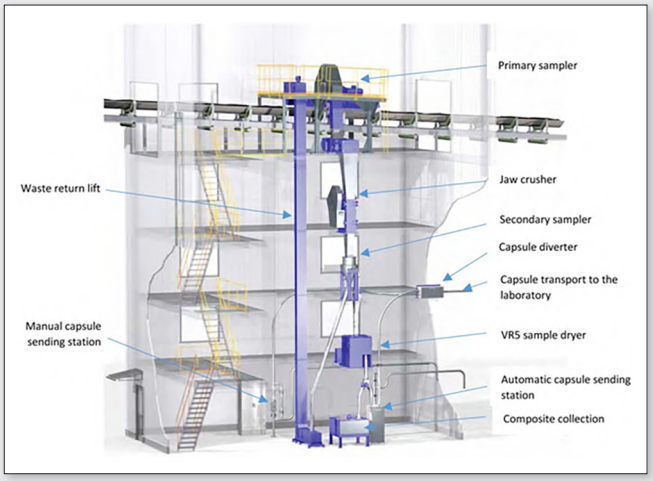

Figure 4. Integrated Sampling Station.

plant control system: allowing the complete "end to end" analytical process to be optimized – transforming the laboratory into a true "Process Optimization Centre".

In another instance, as shown in Figure 4, sample splitting, crushing and drying occurs in the sample station. This allows a dry aliquot to be sent directly to the laboratory using a pneumatic capsule transport system. This is made possible because the entire drying process happens in a few minutes, integrated into the sampling tower. This is achieved using an innovative "IMP vibro dryer", which combines infrared drying with a vibrating oil heated base-plate. As the base-plate vibrates the sample is forced to move in a circular direction. This motion releases trapped moisture while continually exposing fresh surfaces to the infrared lamps – which allows rapid drying to occur. A built-in pyrometer monitors the surface temperature and controls the heat within the predefined limits. This bespoke drying system ensures that samples are dried rapidly without compromising integrity. After drying, the direction of vibration is changed which discharges the sample. The discharged sample is automatically placed into a capsule and sent directly to the laboratory via an air tube system. After the sample is received in the laboratory, it is automatically removed from the capsule for further processing.

Integrated Automated Slurry Sampling and Laboratory Systems

Historically, slurry samples are collected automatically into a bucket and manually transferred to the laboratory. In these instances it is typical for automated slurry stream samplers to direct the sample through one or more Vezin splitters so eventually a correct amount of slurry sample accumulates in a bucket. Normally this occurs once each shift, or a pre-determined number of times during the day but usually two or three samples per 24 hour period are collected in the bucket (Figure 5). Once or twice a day the bucket is transported manually to the laboratory which may be some distance from the sampling point. Therefore it is not uncommon for the first sample to reach the laboratory some hours (often 24 hours) after accumulation of the sample commenced. Because of the manual filter-pressing, drying and sample preparation, typical analysis processing times are 1–2 days for the first composite. These systems may provide high quality data for metal-accounting and good statistics on plant performance but offer no added value to the immediate

Figure 5. Typical bucket sampling system with manual filter presses.

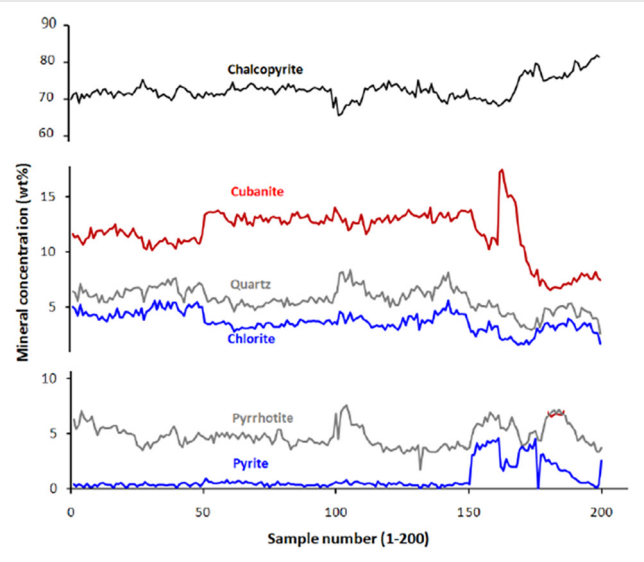

Figure 6. Variation in the concentration of the main mineral phases using XRD.

running of the process. It is because of this that laboratories are frequently seen as an overhead rather than a valued Process Optimization Centre.

IMP has responded to this challenge by developing an automated slurry sampling system and laboratory. By employing a novel solution to transport the slurry aliquots from the various plant sampling points to the laboratory results can be available in minutes rather than hours or days. For example, from time of sampling to getting a finished result, automated X-ray fluorescence and/or mineralogical data can be available in around 20 minutes. Automated fire assay results, using IMP's patented Fast (FIFA) inline fire assay techniques, can be available in under an hour. Thus, many more samples can be processed than in a manual system described above – meaning the plant's processes can be optimized because of the timely data received from the laboratory or the now valued "Process Optimization Centre".

To achieve these analytical times slurry aliquots are automatically filtered and prepared using a robotic sample cell. If required, the liquor can also be captured for analysis. An alternative to this system is to dry the slurry by "trickle feeding" onto a continuous belt infrared drier. When dried the sample is scrapped off the belt and fed into

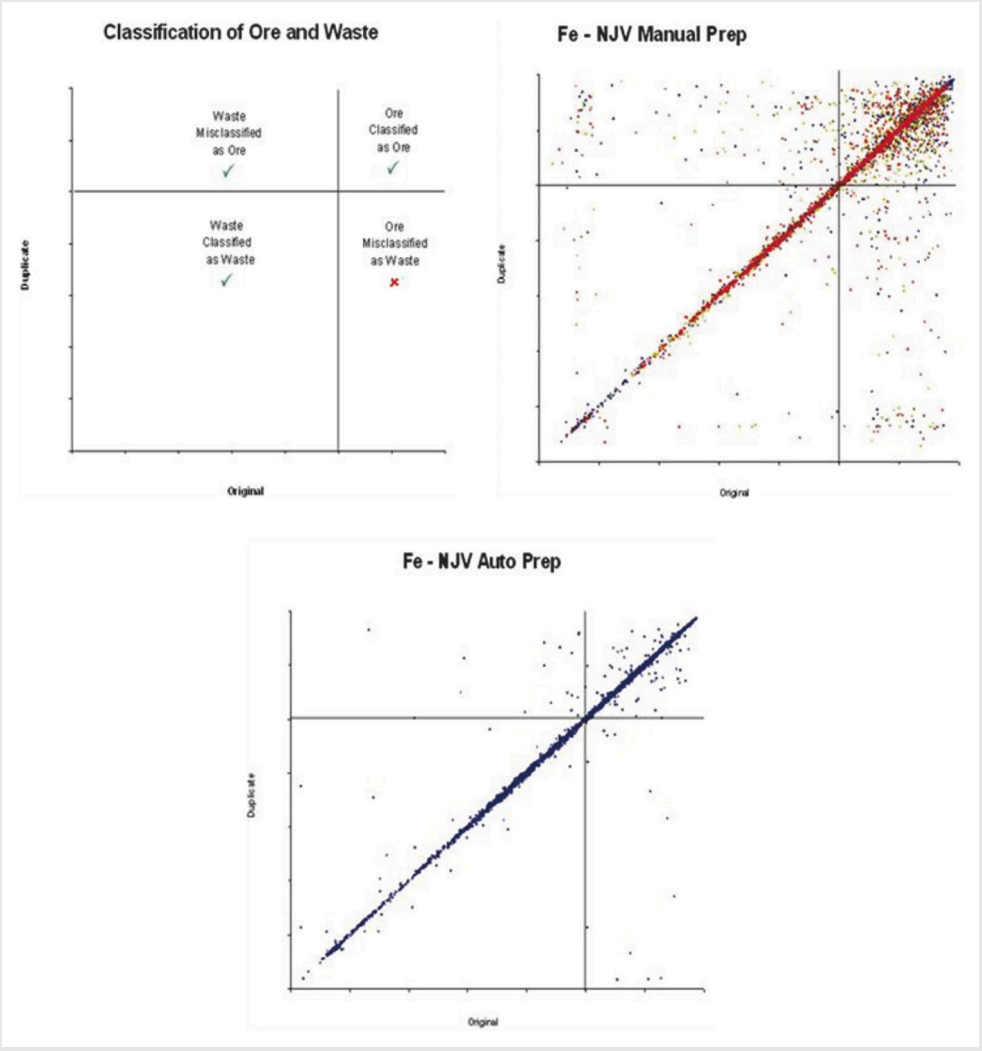

Figure 7. Results from BHPBilliton.

a capsule for transporting to the laboratory. It is essential that the samplers (typically cross-stream) comply with good sampling practice such as cutting the whole stream at 90° and not just part of it. The vezin type cutters should also be radial and cut the full stream at 90° and the slot width of the cutter should be at least three times the nominal particle top size of the solids.

The value of rapid analysis was demonstrated by an experiment undertaken by a copper mine in Australia. During these tests the customer took 200 samples over 32 hours from the concentrator, to replicate an automated rapid "End to End" sampling/analytical system. For the first 150 samples the mineralogy did not change but around the 150 sample mark results showed that the pyrite values had increased (Figure 6). If the operators had known that abnormal proportions of pyrite were floating, a depressant could have been used to benefit the operation. In this case it is predicated that an extra 0.25% of copper could have been extracted, over the 32 hours, which is significant when applied to the life of the mine.

Quality – A Key Benefit of End to End Automation

RioTinto identified significant improvements to precision when using an automatic end to end system that incorporated a time-based sampling methodology with a fully automated analytical facility. This improvement in quality is supported by BHP. At a conference in 2011 BHP Iron Ore gave a presentation [2] that compared the analytical results obtained using an automated system and a manual system. When building the new Mt Whaleback automated laboratory in Newman, Western Australia, duplicates were run through the manual laboratory versus the automated laboratory. Duplicates were used to classify ore into four groups based on a cut-off grade:

- ore classified as ore – a good outcome;
- waste classified as waste – a good outcome;
- waste misclassified as ore – a marginally acceptable outcome as it is a dilution of the ore body and;
- ore misclassified as waste – the worst possible outcome, the equivalent of throwing money away!

Automated preparation of samples clearly demonstrates an improvement in precision and a corresponding reduction in ore being incorrectly misclassified as waste. The difference is dramatic and the questions have to be asked – how much did the manual analytical system really cost in lost revenues? How does one quantify the revenue lost to a company because ore was classified as waste?

In addition to these analytical improvements BHP Billiton were able to quantify a significant reduction in occupational health and safety hazards as workers were not exposed to as many repetitive tasks, heavy lifting and were exposed to less dust and noise level than when working in conventional/manual sampling stations laboratories.

Conclusion

Automating the entire process, from sampling to analysis, results in the fastest possible turnaround times of precise analytical data. This turns the laboratory into a valued process tool, or Process Optimization Centre as data becomes available in minutes rather than hours or days. Quicker results enable production personnel to improve plant control resulting in increased plant efficiencies and improved beneficiation.

Additionally, IMP's customers have published results confirming that with "End to End" automation systems the data obtained improves significantly. This impacts the bottom line, improves decision making, and has the added advantage of improving occupational health and safety.

Finally, automated "End to End" sampling analytical systems are not confined to one particular commodity, laboratory or sample form. Samples can be bulk or large samples, have varying particle sizes, be solid or in the form of a slurry. Across the industries, from aluminum to zinc, IMP has successfully implemented innovative automated "End to End" sampling analytical solutions for ports, at the mine and in mineral processing plants.

Acknowledgments

IMP's customers are thanked for making data available for this paper. Additionally colleagues from IMP, especially Pierre Hofymeyr are acknowledged. Pierre's input contributed significantly to this paper as did discussions with Trevor Bruce, IMP's Engineering manager and Boyne Hohenstein, IMP's Managing Director.

References

1. Brunning R., Andringa-Bate, C., Graham, M. & Westergren S. (2014) Cape Lambert Port B Shiploading, Sampling and Analysis, Sampling 2014 Conference Perth
2. BHP Billiton (2011) Presentation Harnessing the benefits of laboratory automation coming from a manual based operation, Laboratory Managers' Conference, Melbourne. 2011

doi: 10.1255/tosf.80

Comparison between samples with constant mass and samples with constant fragment population size

(and calculations of their sampling variances)

G. Matheron (Author)
Dominique François-Bongarçon[a] and Francis F. Pitard[b] (Translators/Editors)
[a]**Agoratek International Consultants Inc., North Vancouver, Canada. E-mail: dfbgn2@gmail.com**
[b]**14800 Tejon Street, Broomfield, CO 80023 USA. E-mail: fpsc@aol.com**

Dominique is the founder of Agoratek International Consultants Inc., a consulting practice that includes sampling services in its palette, along with reconciliations and all related disciplines. An active and passionate researcher in the theory of sampling, he is a recipient of Pierre Gy's gold medal for excellence in promoting and teaching the Theory of Sampling (WCSB3). Francis is the founder of Francis Pitard Sampling Consultants (FPSC) and has provided professional sampling consultation services and educational programs to many of the world's leading companies. *Pierre Gy's Sampling Theory and Sampling Practice*, 2nd Edition, CRC Press (1993) is one of his many publications. He is a recipient of Pierre Gy's gold medal for excellence in promoting and teaching the Theory of Sampling (WCSB4).

A short introduction from the "Revue de l'Industrie Minerale"

In the 1960s the "Revue de l'Industrie Minerale" took the delicate task to publish several special editions in its journal to expose the Theory of Sampling suggested by Pierre Gy. They wrote:

"In these documents Pierre Gy suggests an equi-probabilistic Theory of Sampling based on samples with a constant number of fragments; in other words, considering samples that are all made of the same number of fragments. Nevertheless, results from his theoretical analysis lead to the justification that formulas that are suggested in practice are applicable to samples with constant mass or constant volume as well. It should be underlined that similar American studies seem to support Pierre Gy's opinion."

G. Matheron, through a careful review of Pierre Gy's work, has demonstrated, by means of a rigorous mathematical analysis that both samples with a constant number of fragments and samples with a constant mass lead to a dispersion of possible grades for the lot to be sampled that have similar variances.

The mathematical level of this study may prove to be difficult to many readers. However, the importance of the argument is critical for the validity of the Theory of Sampling; it is an argument that has been approached by many authors over the years leading to frustration and failure. As a consequence, Pierre Gy's theory generated passionate controversies.

The "Revue de l'Industrie Minerale" is proud to bring to this important discussion the contribution of an authority as famous as G. Matheron."

This document was published 55 years ago and still endures the challenges of time. During that long period of time it became clear that the fact that such an important document was written in French was a huge handicap, especially for reaching the Anglo-Saxon audience effectively. We hope the present translation made by two recipients of Pierre Gy's Gold Medal for excellence in teaching the Theory of Sampling will help to fill that gap. Complementary explanations are also inserted where appropriate, so the reader can progress in a more friendly way, and better appreciate the subtle foundations of the Theory of Sampling.

Abstract

In his essay "l'echantillonnage des minerais en vrac" that could be translated as "sampling of particulate ore" published in 1967 in France by the *Revue de l'Industrie Minerale*, Pierre Gy suggests a calculation of the variance associated with samples with a constant number of fragments. In practice, samples with a constant mass are instead collected, which may seem at first like a contradiction. In this mathematical development it is clearly demonstrated that these two kinds of samples lead to variances that are similar within well-established mathematical limits.

[Translators' Note (T.N.): To make the translation easier to read, the structure and the logical articulation of Matheron's long and tedious paper need to be understood first:

1. *The introduction first establishes the difference between "sampling in number" and "sampling in mass", to ready the mathematical background.*
2. ***Sampling in Number** is then studied.*
   - *This first calls for specific developments aimed at calculating first order approximations to* $E(1/Y)$, $E(1/Y^k)$ *and, for Gy's formula,* $E(X^k/Y^k)$ *for a random variable* Y. *There are no ready-made formulas in statistics, and no exact formulas for this task.*
   - *A rather tedious demonstration using the Laplace transform indeed shows that in the case of* $E(1/Y)$, *for any random variable* Y *that can be interpreted as the mean of "*n*" independent, identically distributed (i.d.d.) random variables, even a divergent serial development can be actually used as a limited development near the value of "*n*" considered. The result is then generalized to* $E(1/Y^k)$.
   - *Having set up these mathematical tools, then Gy's formula is established for sampling in number and the result is formally identical to Gy's findings, thus validating it.*
3. ***Sampling in Mass** is then tackled:*
   - *The necessary approximations are again established for* $E(N)$ *and* $E(N^2)$, N *being the number of fragments (now a random variable) in the sample of a given mass* p.
   - *Then approximations are also needed for* $E(X;p)$ *and* $E(X^2;p)$, *i.e. the mathematical expectations of the sample metal*

quantity X at a given mass p, and of its square. This time, the Fourier transform helps establish, like before, usable limited developments.

- *The same formula as for sampling in number is finally reached in the case of a given mass, and the paper concludes that Gy's formula is formally and fully validated for both types of sampling.]*

1. Matheron's introduction

In his fundamental document published in 1967 dedicated to "l'echantillonnage des minerais en vrac" (i.e. the sampling of bulk ores) Pierre Gy demonstrated that the variance associated with a sample made of a given number of fragments n (i.e., sample made of a preset number n of elementary fragments) follows an asymptotic tendency when the number n is large and when the sampling mode that is used is equi-probabilistic (i.e., correct, which means all possible samples with n fragments have the same probability of being selected by the sampling tool). The theoretical path followed by Pierre Gy has been the object of severe criticism over the years that can be summarized by the two following arguments:

1. As far as the calculation of the variance is concerned, the validity of some of Gy's developments has been contested.
2. Furthermore, in daily practice, the collection of samples with a constant number of fragments n predetermined in advance is never done that way, but rather samples with a predetermined mass or volume are indeed collected; the number of fragments in these real samples is then necessarily unknown. Then, consequently, it is apparently justified to doubt that conclusions reached for samples with a constant number of fragments are also valid for samples with a constant mass or a constant volume.

The objective of this study is to carefully investigate these objections and demonstrate the full legitimacy of Pierre Gy's results *[T.N.: in other words it is a corner stone to confirm the legitimacy of the Theory of Sampling]*. From a mathematical standpoint it is relatively easy to demonstrate the legitimacy of a theory based on samples with a constant number of fragments. However, to legitimately transfer these results to a theory based on samples of constant mass or constant volume requires the use of far more difficult mathematical tools. In a way this explains why Pierre Gy in his search for a pragmatic tool chose to use the simplest approach. For the sake of simplicity and to avoid unnecessary mathematical developments the assumption is made that the original number of fragments in the lot to be sampled is practically infinite, which is most of the time almost exactly the case. To get straight to the point the two following hypotheses are made:

The mass $\bar{\omega}$ of one ore fragment and its metal content q can be considered as two random variables that are not independent. Furthermore, to simplify notations, the assumption is made that their distribution function $F(q \cdot \bar{\omega})$ carries a probability density function $f(q,\bar{\omega})$.

1. The sample collection mode is such that the selected sample can be considered as the reunion of fragments following the same probability law $f(q,\bar{\omega})$ (i.e., collected one by one at random and making sure they are independent from one another). In other words:
   a. For a sample with a given number of fragments n, its mass and its metal content can be written as follows:

$$X_n = \sum_{i=1}^{n} q_i \qquad [1]$$

$$Y_n = \sum_{i=1}^{n} \bar{\omega}_i \qquad [2]$$

It is understood that each q_i is independent of q_j and $\bar{\omega}_j$ for $j \neq i$ (but it is also understood that q_i and $\bar{\omega}_i$ are not independent), and each pair $(q_i,\bar{\omega}_i)$ follows the same probability law $f(q,\bar{\omega})$.

   b. If, on the contrary, we consider a sample of a given mass p defined by the following condition:

$$\sum_{i=1}^{N} \bar{\omega}_i < p \quad \text{and} \quad \sum_{i=1}^{N+1} \bar{\omega}_i \geq p \qquad [3]$$

its number of fragments N appears to be a random variable. The mass Y_n and the quantity of metal X_n of this sample are then defined as sums of a random number N of variables $\bar{\omega}_i$ or q_i.

In a first part we will calculate the mathematical expectation and the variance of the metal concentration X_n/Y_n of the sample carrying a number of fragments n when n is a large number. In the second part the same calculations are repeated for the metal concentration X_N/p of a sample of a given mass p, when p is a large number. It is intended to demonstrate that their variances for both cases are asymptotically equivalent when p is large.

2. Case of a sample with a constant number of fragments

Assuming the number of fragments in the sample is n let us introduce:

$$X = \frac{1}{n} X_n = \frac{1}{n} \sum_{i=1}^{n} q_i \qquad [4]$$

$$Y = \frac{1}{n} Y_n = \frac{1}{n} \sum_{i=1}^{n} \bar{\omega}_i \qquad [5]$$

When n is large, variances of X and Y are in $1/n$, and the centered moments of superior orders are at least in $1/n^2$. The metal concentration X/Y of the sample appears then like the ratio of two random variables having very small variances. To calculate its mathematical expectation and its variance, it is convenient to write:

$$Y = m_y + \varepsilon \quad \text{with} \quad m_y = E(Y) \qquad [6]$$

and then getting started from the following formal development in series:

$$\frac{X}{Y} = \frac{X}{m_y}\left[1 - \frac{\varepsilon}{m_y} + \frac{\varepsilon^2}{(m_y)^2} + \ldots + (-1^n)\frac{\varepsilon^n}{(m_y)^n} + \ldots\right] \qquad [7]$$

which can be used if $|\varepsilon/m_y| < 1$.

If there is a probability of "one" that the inequality $|\varepsilon/m_y| < 1$ be verified, it is possible then to take the mathematical expectation one term at a time, and then deduce from a complete serial development what the expression of the average and the variance of X/Y should be. Of course, if the inequality $|\varepsilon/m_y| < 1$ is not verified with a probability of "one", this mode of calculation would no longer be valid, plus the serial developments that could be obtained would generally diverge anyway. Nevertheless, as a limited development (as opposed to a formal serial development) the results obtained by this process would conserve their validity.

2.1 Mathematical expectation $E(1/Y)$

To prove it without useless mathematical developments, let's focus only on the mathematical expectation $E(1/Y)$ of a variable Y characterized by a density $f(y)$. In this case indeed:

$$E\left(\frac{1}{Y}\right)=\int_{-\infty}^{+\infty}\frac{1}{y}f(y)dy \qquad [8]$$

If $f(0) \neq 0$, this integral is divergent and therefore $1/Y$ cannot have a mathematical expectation: for example, if Y is a normal variable, its inverse can never have a mathematical expectation. Therefore it is critically important not to assume that the law of $f(y)$ is close to a Gaussian law. In fact, Y representing a mass, $f(y)$ is different of *0* only for $y \geq 0$, and the integral [8] will exist provided the density $f(y)$ is of a very small order $\varepsilon > 0$ for $y = 0$. It is easy to demonstrate that this condition is always satisfied in the case where Y is the sum of at least two independent variables that themselves follow continuous laws. In the problem that is investigated in this study $E(1/Y)$ therefore always exists *(T.N.: because of equation [5])*.

To evaluate $E(1/Y)$ it is convenient to introduce the Laplace transform of the law $f(y)$:

$$\Phi(\lambda)=\int_0^{\infty}e^{-\lambda y}f(y)dy \qquad [9]$$

As a matter of fact $\Phi(\lambda)$ always exists for $\lambda \geq 0$ and the following integral as well:

$$\int_0^{\mu}\Phi(\lambda)d\lambda=\int_0^{\infty}\frac{1-e^{-\mu y}}{y}f(y)dy \qquad [10]$$

If μ tends toward the infinite in relation [10] it can be noticed that the mathematical expectation of $1/Y$ exists at the same time as the integral

$\int_0^{\mu}\Phi(\lambda)d\lambda$, and that:

$$E\left(\frac{1}{Y}\right)=\int_0^{\infty}\Phi(\lambda)d\lambda \qquad [11]$$

(T.N.: i.e. the integral of the Laplace transform on [0,∞].)

Let's call m the mean, σ^2 the variance and μ_n the centered moment of order n of the variable Y (that we will assume *to* exist); let's also call $\Phi_c(\lambda)$ the Laplace transform of the law of the centered variable $Y-m$:

$$\Phi_c(\lambda)=E\left[e^{-\lambda(Y-m)}\right]=e^{\lambda m}\Phi(\lambda) \qquad [12]$$

Then also:

$$E\left(\frac{1}{Y}\right)=\int_0^{\infty}e^{-\lambda m}\Phi_c(\lambda)\ d\lambda \qquad [13]$$

Now, in some cases $\Phi_c(\lambda)$ can be developed into a formal series of the following form:

$$\Phi_c(\lambda)=1+\frac{\lambda^2\sigma^2}{2!}+\ldots+(-1)^k\frac{\lambda^k\mu_k}{k!}+\ldots \qquad [14]$$

Taking this expression into [13] and if it is integrated term by term, the following expression is obtained *(T.N.: after quite some calculus):*

$$E\left(\frac{1}{Y}\right)=\frac{1}{m}+\frac{\sigma^2}{m^3}+\ldots+(-1)^k\frac{\mu_k}{m^{k+1}}+\ldots \qquad [15]$$

In other words, it is exactly the result that should be expected from the development [7] *[T.N.: with* X = *1 and* Y – m = *ε]*.

However:

- It is possible that the series [14] may not be convergent; this is the case when Y is, for instance, a lognormal variable.
- It is also possible that even if the series [14] is convergent, it may not be uniformly convergent, making the term by term integration invalid; it is what happens, for instance, when f is a gamma law:

$$f(y)=\frac{b^{\alpha}}{\Gamma(\alpha)}y^{\alpha-1}e^{-by} \qquad [16]$$

For $\alpha > 1$, $E(1/Y)$ exists and [14] converges. However, the convergence is not uniform and it is easily shown that the formal mathematical development written in [15] is diverging (μ_k/m^k tends toward an infinite value with k).

Therefore, in general, it is not possible to use the full development written in [15] as a formal series.

However, as we are going to see, it is always possible to use it as a limited development within the domain of variations that is of interest to us, provided we can show the rest of the development behaves as a negligible remainder in that domain.

As a matter of fact let's write:

$$\Phi_c(\lambda)=1+\lambda^2\frac{\sigma^2}{2!}+\ldots+\frac{(-1)^k}{k!}\lambda^k\mu_k+R_k(\lambda) \qquad [17]$$

The remainder $R_k(\lambda)$ of this development is:

$$R_k(\lambda)=\int_0^{\infty}\left[e^{-\lambda(x-m)}-1-\lambda^2\frac{(x-m)^2}{2!}-\ldots-\frac{(-1)^k\lambda^k}{k!}(x-m)^k\right]f(x)dx \qquad [18]$$

By taking [17] into [13] the following expression is obtained:

$$E\left(\frac{1}{Y}\right)=\frac{1}{m}+\frac{\sigma^2}{m^3}+\ldots+(-1)^k\frac{\mu_k}{m^{k+1}}+R'_k \qquad [19]$$

The remainder R'_k of this development is:

$$R'_k=\int_0^{\infty}e^{-\lambda m}R_k(\lambda)d\lambda=\int_0^{\infty}\frac{1}{x}\left(1-\frac{x}{m}\right)^{k+1}f(x)dx \qquad [20]$$

To find an upper bound for this remainder let's take a number $\alpha > 1$ (that we will soon define) and let's write:

$$R'_k=\int_0^{\frac{m}{\alpha}}\frac{1}{x}\left(1-\frac{x}{m}\right)^{k+1}f(x)dx+\int_{\frac{m}{\alpha}}^{\infty}\frac{1}{x}\left(1-\frac{x}{m}\right)^{k+1}f(x)dx \qquad [21]$$

For $x \geq (m/\alpha)$ we have:

$$\left|\frac{1}{x}\left(1-\frac{x}{m}\right)^{k+1}\right|\leq\frac{\alpha}{m^{k+2}}|m-x|^{k+1} \qquad [22]$$

so that an upper bound for the second integral is:

$$\frac{\alpha}{m^{k+2}}E\left[\ |Y-m|^{k+1}\right] \qquad [23]$$

But, if Y can be written like

$\frac{1}{n}\sum_{i=1}^{n}Y_i$

the centered absolute moment

$E\left[\,|Y-m|^{k+1}\right]$

tends toward *0* when *n* tends towards infinity (generally it is an infinitesimally small value of order $h+1<k+1$ in $1/n$).

What is left to do is finding an upper bound for the first integral of remainder R'_k.

If the density of Y_i has a number *B* as upper bound, the density of *Y* verifies:

$$f(x)\le (nB)^n\frac{x^{n-1}}{(n-1)!} \qquad [24]$$

[T.N.: this upper bound can be difficult to establish. First, one must show the density function of the sum of the n *variables* X_i *has*

$$\left\{B^n\frac{x^{n-1}}{(n-1)!}\right\}$$

as upper bound. This is obtained by recurrence, remembering the density function g(t) *of the sum of two independent random variables with positive values is the convolution product of their densities (summed between 0 and* t*). The upper bound for the average of the* X_i *is then only derived, remembering the density function* h(t) *of variable "*X/n*" can be derived from the density* f(t) *of* X *as* h(t) = n f(nt)*.]*

Then, the following expression is obtained:

$$\int_0^{\frac{m}{\alpha}}\frac{1}{x}\left(1-\frac{x}{m}\right)^{k+1}f(x)\,dx\le (nB)^n\int_0^{\frac{m}{\alpha}}\frac{x^{n-2}}{(n-1)!}\,dx=\frac{(nB)^n}{(n-1)(n-1)!}\left(\frac{m}{\alpha}\right)^{n-1} \qquad [25]$$

If *n* is sufficiently large the Stirling formula can be used to replace factorials in [25] by a term such as

$$(Be)^n\left(\frac{m}{\alpha}\right)^{n-1}$$

that tends exponentially toward *0* when $n\to\infty$ **as long as the selected value for** α is superior to *Bme* (e.g., $\alpha = 3Bm$).

Therefore, finally, the last part R'_k is an infinitesimally small number in $1/n$ in the order of

$$\frac{1}{m^{k+2}}E\left[|Y-m|^{k+1}\right]$$

(an order generally smaller than $k+1$). It is not important if R'_k tends toward 0 or not for $k\to\infty$. If, for any given value of *k,* it is possible to verify that R'_k is in the order of $h+1$ in $1/n$, it is then possible in the approximation of order *h* (generally $< k$) to utilize the development [19] and stop at the term in μ_k.

2.2 Mathematical expectation $E(1/Y^k)$

Similarly it is possible to demonstrate that the mathematical expectation $E(1/Y^k)$ exists at the same time as the integral

$$\int_0^\infty\frac{\lambda^{k-1}}{(k-1)!}\Phi(\lambda)\,d\lambda$$

and then:

$$E\left[\frac{1}{Y^k}\right]=\int_0^\infty\frac{\lambda^{k-1}}{(k-1)!}\Phi(\lambda)\,d\lambda \qquad [26]$$

It is then sufficient to replace $\Phi(\lambda)$ with $e^{-\lambda m}\Phi_c(\lambda)$ to obtain, as above [see (13)], the formal development of $E(1/Y^k)$ which is most of the time divergent; however, it is possible to use it as a limited development. For example, for $k = 2$, it becomes:

$$E\left(\frac{1}{Y^2}\right)=\frac{1}{m^2}\left(1+\frac{3\sigma^2}{m^2}-4\frac{\mu_3}{m^3}+\ldots\right) \qquad [27]$$

from which (by subtracting the square of $E(1/Y)$ in (19), it is possible to obtain the principal part of the variance of $1/Y$:

$$D^2\left(\frac{1}{Y}\right)=\frac{\sigma^2}{m^4}+\ldots \qquad [28]$$

2.3 Establishing Gy's formula

If *X* and *Y* are two random variables of law *f(x,y)* we can start by introducing the Laplace transform:

$$\Phi(\lambda,\mu)=\int_0^\infty\int_0^\infty e^{-\lambda x-\mu y}f(x,y)\,dxdy \qquad [29]$$

And, as above, the following relation is obtained:

$$E\left[\frac{X^k}{Y^k}\right]=(-1)^k\int_0^\infty\frac{\mu^{k-1}}{(k-1)!}\cdot\frac{\partial^k\Phi(\lambda,\mu)}{\partial\lambda^k}d\mu\;\Big|_{\lambda=0} \qquad [30]$$

[T.N.: To see it, one first calculates:

$$\frac{\partial^k\Phi(\lambda,\mu)}{\partial\lambda^k}d\mu\;\Big|_{\lambda=0}=\int_0^\infty\int_0^\infty(-1)^k\,x^k e^{-\mu y}f(x,y)\,dxdy$$

So that the right-hand side of [30] is:

$$I=\int_0^\infty\frac{\mu^{k-1}}{(k-1)!}\cdot d\mu\int_0^\infty\int_0^\infty x^k e^{-\mu y}f(x,y)\,dxdy$$

Noting that:

$$E\left[\frac{1}{Y^k}\right]=\int_0^\infty\frac{f(y)}{y^k}\,dy=\int_0^\infty\frac{\mu^{k-1}}{(k-1)!}\cdot d\mu\int_0^\infty e^{-\mu y}f(y)\,dy$$
$$=\int_0^\infty\int_0^\infty\int_0^\infty\frac{\mu^{k-1}}{(k-1)!}e^{-\mu y}f(x,y)\,dx\,dy\,d\mu$$

One can see that:

$$I=\int_0^\infty\int_0^\infty\frac{x^k}{y^k}f(x,y)\,dxdy=E\left[\frac{X^k}{Y^k}\right]$$

(Q.E.D.)]

Then, calling Φ_c the transform of the centered variables law:

$$\Phi_c(\lambda,\mu)=E\left[e^{-\lambda(X-m_x)-\mu(Y-m_y)}\right]=1+\frac{\lambda^2\sigma_x^2+2\lambda\mu\sigma_{xy}+\mu^2\sigma_y^2}{2!}+\ldots \qquad [31]$$

Suffice substituting Φ for $e^{-\lambda m_x-\mu m_y}\Phi_c$ in equation [30], as before, to obtain some formal developments, generally divergent, that can be used as limited developments. So that, from:

$$-\frac{\partial}{\partial\lambda}\Phi(\lambda,\mu)\big|_{\lambda=0}=\left[m_x\left(1+\frac{\mu^2}{2}\sigma_y^2+\ldots\right)-\mu\sigma_{xy}+\ldots\right]e^{-\mu m_y} \qquad [32]$$

$$\frac{\partial^2}{\partial\lambda^2}\Phi(\lambda,\mu)\big|_{\lambda=0}=\left[m_x^2\left(1+\frac{\mu^2}{2}\sigma_y^2\right)-2\mu m_x\sigma_{xy}+\sigma_x^2+\ldots\right]e^{-\mu m_y} \qquad [33]$$

one obtains without difficulty the first terms of the developments of $E(X/Y)$ and $E(X^2/Y^2)$:

$$E\left(\frac{X}{Y}\right)=\frac{m_x}{m_y}\left[1+\frac{\sigma_y^2}{(m_y)^2}-\frac{\sigma_{xy}}{m_x m_y}+\ldots\right] \qquad [34]$$

$$E\left(\frac{X^2}{Y^2}\right)=\left(\frac{m_x}{m_y}\right)^2\left[1+3\frac{\sigma_y^2}{(m_y)^2}-4\frac{\sigma_{xy}}{m_x m_y}+\frac{\sigma_x^2}{(m_x)^2}+\ldots\right] \quad [35]$$

as well as the principal part of the variance of X/Y:

$$D^2\left(\frac{X}{Y}\right)=\left(\frac{m_x}{m_y}\right)^2\left[\frac{\sigma_x^2}{(m_x)^2}-\frac{2\sigma_{xy}}{m_x m_y}+\frac{\sigma_y^2}{(m_y)^2}+\ldots\right] \quad [36]$$

which can also be written:

$$D^2\left(\frac{X}{Y}\right)=\left(\frac{m_x}{m_y}\right)^2 E\left[\left(\frac{X}{m_x}-\frac{Y}{m_y}\right)^2\right] \quad [37]$$

Coming back to the original notations shown in [1] and [2], it is easy to see that the metal content $X/Y = X_n/Y_n$ of the sample with n fragments has a mathematical expectation and a variance that can be written as follows [when ignoring the terms in $1/n^2$ and letting $x_0 = E(q)$ and $y_0 = E(\bar{\omega})$]

$$E\left(\frac{X}{Y}\right)=\frac{x_0}{y_0}+\frac{1}{n}\cdot\frac{x_0}{y_0}E\left[\frac{\bar{\omega}}{y_0}\left(\frac{\bar{\omega}}{y_0}-\frac{q}{x_0}\right)\right] \quad [38]$$

$$D^2\left(\frac{X}{Y}\right)=\frac{1}{n}\left(\frac{x_0}{y_0}\right)^2 E\left[\left(\frac{q}{x_0}-\frac{\bar{\omega}}{y_0}\right)^2\right] \quad [39]$$

These are indeed the formulas obtained by Pierre Gy and in particular formulas obtained in Chapter IV of his January 15, 1967 publication. The validity of these formulas is therefore no longer questionable. It can be seen that the mathematical expectation $E(X/Y)$ of the metal content of the sample made of n fragments (for all the possible choices of the sample in the lot) does not exactly coincide with the real mean of the lot, which is x_0/y_0, but the difference is extremely small and in $1/n$. Therefore there is indeed always a small bias. The variance is, as expected, as the inverse of size n.

3. Case of a sample with constant mass

In daily practice it is clear that collected samples have either a constant mass, or volume, pre-selected in advance, rather than a constant number n of fragments. Then it is not obvious that the sampling variances for these two sampling modes are the same. Because the variable

$$\frac{1}{n}\sum_{i=1}^{n}\bar{\omega}$$

almost surely converges toward $E(\bar{\omega})$ when n tends toward an infinite value, one would certainly suspect they are, but it would be wiser to demonstrate this property more rigorously.

Let's assume that in the collected sample, everything is like randomly collecting successive fragments with average masses $\bar{\omega}_i$ and metal contents q_i, and that each one of these two quantities obeys the same probability law for all the fragments. Then, when n fragments have been collected, a sample is obtained with the following characteristics:

$$X_n=\sum_{i=1}^{n}q_i \quad [40]$$

$$Y_n=\sum_{i=1}^{n}\bar{\omega}_i \quad [41]$$

When n changes the vector (X_n,Y_n) is a stochastic process (i.e., a vectorial process with two components X_n and Y_n defined within the discrete set of positive integers n. Because of the independence of the successive fragment selections, it constitutes a Markov process with independent and stationary increments.).

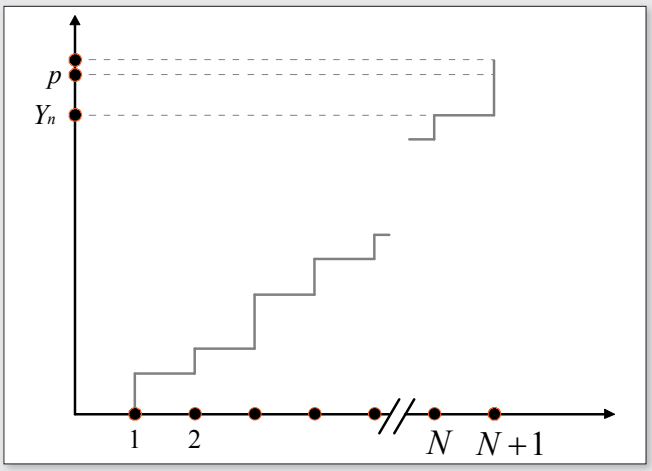

Figure 1. Illustration of the Markov process.

Each of the two components X_n and Y_n can be represented by a random steps process as illustrated in Figure 1. The sample with a number of fragments k pre-selected in advance, and studied in the former section, is defined by (X_k,Y_k), which is the value of the process (X_n,Y_n) for the particular value $n = k$.

The sample of mass p selected in advance can be defined in two different ways, either by default or by excess. As a matter of fact if N is the random time (the value of n) for which we have:

$$Y_N < p, \qquad Y_{N+1} \geq p \quad [42]$$

then it can be said that N is the random number of fragments of the sample of pre-selected mass p. Indeed, the two inequalities [42] mean that the N first fragments consist of a sample of mass smaller than p, and that the total mass of the $N + 1$ first fragments reaches or surpasses p. The sample itself can be defined either by default with characteristics X_n and Y_n or by excess with characteristics X_{n+1} and Y_{n+1}. These two definitions can be considered as equivalent; indeed both samples usually made of many fragments are different only by one fragment which is the fragment selected at a $(N + 1)^{th}$ time.

In the following developments we opted for the definition by excess (X_{N+1},Y_{N+1}). In the first step, the law of the random number of fragments N of the sample of pre-selected mass p is investigated, then in a second step, the law of the metal content of the same sample is investigated, or, in other words the law of X_{N+1}. The given mass p of the sample being assumed large, relative to the average mass $y_0 = E(\bar{\omega})$ of the individual fragments, we will be mainly searching for the asymptotic expressions of the mean and the variance of these different variables.

3.1 Law of the number of fragments *N* in the sample of pre-selected mass *p*

Let's call $P_n(p)$ the probability of having $N = n$, or, in other words, a number n *of* fragments in the sample. The event "$N = n$" coincides by definition with the event "$Y_n < P$ and $Y_{n+1} \geq p$".

Let's define $f_n(y)$ as the density of probability, and $F_n(y)$ the cumulative distribution function of the Y_n distribution. Therefore, the probability of the event "$Y_n < P$" is $F_n(p)$ and the probability of the

event "$Y_{n+1} < p$" is $F_{n+1}(p)$. Since the event "$Y_n < p$" is the logical sum of events "$N = n$" and "$Y_{n+1} < p$" that are incompatible (i.e. we have "$N = n$" OR ELSE "$Y_{n+1} < p$"), we obtain:

$$F_n(p) = P_n(p) + F_{n+1}(p) \quad [43]$$

from which the following expressions can be deduced:

$$P_n(p) = F_n(p) - F_{n+1}(p) \quad [44]$$

$$P_0(p) = 1 - F_1(p) \quad [45]$$

It is then convenient to introduce the generating function $G(s;p)$ of the $P_n(p)$ probabilities, which, according to [44] and [45] lead to:

$$G(s;p) \equiv \sum_{n=0}^{\infty} s^n P_n(p) = 1 + \sum_{n=1}^{\infty} s^{n-1}(s-1)F_n(p) \quad [46]$$

As is well known, suffices deriving the generating function and taking $s = 1$ to obtain the successive moments of the discrete law of $P_n(p)$. The two first interesting moments are:

$$E(N) = G'(1) \quad [47]$$

$$E[N(N-1)] = G''(1) \quad [48]$$

Taking into account the expression of the generating function [46] we obtain:

$$E(N) = \sum_{n=1}^{\infty} F_n(p) \quad [49]$$

$$E[N(N-1)] = 2\sum_{n=1}^{\infty}(n-1)F_n(p) \quad [50]$$

We therefore need to evaluate both sums $\Sigma F_n(p)$ and $\Sigma n F_n(p)$ when p is large. This is made possible introducing the Fourier transform and by using the following rule:

> *If* h(x) *is a function, and if* H(u) *is its Fourier transform (generally taken in its distributional expression), it is known that the continuity properties of* H(u) *give an image of the regularity of* h(x) *toward the infinite. In particular, if the distribution of* H(u) *is identified with a continuous function growing slowly,* h(x) *tends toward zero when* x *tends toward the infinite.*

Then, let $h(x)$ be a function worth zero for $x < 0$, and $H(u)$ its Fourier transform, which generally is a distribution. If the distribution

$$H(u) + \frac{a_0}{iu} - \frac{a_1}{(iu)^2} + \frac{a_2}{(iu)^3}$$

is identified with a continuous function growing slowly, then:

$$\lim\left[h(x) - a_0 - a_i x - \frac{a_2}{2}x^2\right] = 0 \quad \text{when} \quad x \to +\infty \quad [51]$$

In other words $h(x)$ is then asymptotically equal to the polynomial function

$$a_0 + a_1 x + \frac{a_2}{2}x^2 .$$

In what follows let's make $\lambda = -iu$ which is formally equivalent to using the Laplace transform. We should ignore some mathematical difficulties that are of no consequences in the following study, especially the summation of geometric series of the type $\Sigma[\Phi(u)]^n$, where $\Phi(u)$ is a characteristic function: in fact it is necessary to assume the inequality $|\Phi(u)| < 1$ is strict as soon as u is not nil. This condition is indeed verified for all usual laws, with the exception of discrete laws such as the Poisson law, for which the random variable cannot admit other values than integer multiples of a same quantity: these laws have characteristic functions that are periodic and the equality $\Phi(u = 1)$ is indeed possible for $u \neq 0$.

To find the asymptotic expression:

$$h(x) \approx a_0 + a_1 x + \frac{a_2}{2}x^2 \quad [52]$$

of a function $h(x)$ (identically nil for $x < 0$), suffice taking its Laplace transform $\Phi(\lambda)$, and then determining constants a_0, a_1 and a_2 in such a way that

$$\Phi(\lambda) - \frac{a_0}{\lambda} - \frac{a_1}{\lambda^2} - \frac{a_2}{\lambda^3}$$

is a continuous function in $\lambda = 0$.

Calculation of E(N) *and* E(N^2)

Then, let $F_1(y)$ be the function representing Y_1 (i.e. the mass of a fragment) and $\Phi(\mu)$ its Laplace transform:

$$\Phi(\mu) = \int_0^{\infty} e^{-\mu y} dF_1(y) \quad [53]$$

The variable Y_n which is the sum of n independent variables from the distribution law F_i, follows a law for which the Laplace transform is $[\Phi(\mu)]^n$. The transform of $F_n(p)$ is then $(1/\mu)[\Phi(\mu)]^n$, and the sum

$$\sum_{n=0}^{\infty} F_n(p)$$

has the following transform:

$$\frac{1}{\mu}\sum_{n=0}^{\infty}[\Phi(\mu)]^n = \frac{1}{\mu[1-\Phi(\mu)]} \quad [54]$$

[T.N.: by summation of the series].

Let $y_0 = E(Y_1)$ and σ_y^2 be the mean and the variance of the fragment mass.

[T.N.: Replacing $e^{-\mu y}$ *in [53] by its development in series* $e^{-\mu y} = 1 + (-\mu y)/1! + (-\mu y)^2/2! = \ldots$ *and integrating]* we obtain the limited development:

$$\Phi(\mu) = 1 - y_0\mu + \frac{1}{2}\mu^2(y_0^2 + \sigma_y^2) + \ldots \quad [55]$$

from which we derive:

$$\frac{1}{\mu[1-\Phi(\mu)]} = \frac{1}{y_0\mu^2} + \frac{1}{2\mu}\left(1 + \frac{\sigma_y^2}{y_0^2}\right) + \ldots \quad [56]$$

Applying the rule described above, the following asymptotic expression is deduced:

$$\sum_{n=0}^{\infty} F_n(p) \approx \frac{p}{y_0} + \frac{1}{2}\left(1 + \frac{\sigma_y^2}{y_0^2}\right) \quad [57]$$

Go back to [49] and [50] remembering that $F_0(p) = 1$. The mathematical expectation $E(N;p)$ of the number of fragments in the sample of mass p, then admits the following asymptotic expression:

$$E(N;p)=\frac{p}{y_0}+\frac{1}{2}\left(\frac{\sigma_y^2}{y_0^2}-1\right) \quad [58]$$

Its principal part coincides, as expected, with the ratio of the selected sample mass p to the average mass y_0 of individual fragments. *(T.N.: but it is not equal to it exactly, and there is a first, small bias. To understand why this surprising bias exists, one needs to go back to the definition of the sample of mass* p*, i.e. to formula [42].)*

Now, let's go to the sum $\Sigma nF_n(p)$ for which the Laplace transform relative to p is:

$$\frac{1}{\mu}\sum_{n=1}^{\infty} n\left[\Phi(\mu)\right]^n=\frac{1}{\mu}\cdot\frac{\Phi(\mu)}{\left[1-\Phi(\mu)\right]^2} \quad [59]$$

Taking the limited development, now pushed to the third order, and calling a_3 the moment of order 3 of the law Φ (i.e. F_1), we obtain:

$$\Phi(\mu)=1-y_0\mu+\frac{1}{2!}\mu^2\left[y_0^2+\sigma_y^2\right]-\frac{1}{3!}a_3\mu^3+\ldots \quad [60]$$

From which we easily obtain:

$$\frac{1}{\mu}\cdot\frac{\Phi(\mu)}{\left[1-\Phi(\mu)\right]^2}=\frac{1}{y_0^2\mu^3}+\frac{1}{\mu^2}\cdot\frac{\sigma_y^2}{y_0^3}+\frac{1}{\mu}\left[\frac{1}{4}+\frac{\sigma_y^2}{y_0^2}+\frac{3}{4}\cdot\frac{\sigma_y^4}{y_0^4}-\frac{1}{3}\cdot\frac{a_3}{y_0^3}\right]+\ldots \quad [61]$$

By applying the rule used earlier we obtain the following asymptotic expression:

$$\sum_{n=1}^{\infty} nF_n(p)\approx\frac{1}{2}\cdot\frac{p^2}{y_0^2}+p\cdot\frac{\sigma_y^2}{y_0^3}+\frac{1}{4}+\frac{\sigma_y^2}{y_0^2}+\frac{3}{4}\cdot\frac{\sigma_y^4}{y_0^4}-\frac{1}{3}\cdot\frac{a_3}{y_0^3} \quad [62]$$

In fact (for p large) we only need the terms in p and p^2 and we can ignore the constant term. Transposing this result into [49] and [50], and taking into account expression [58] for $E(N)$, we obtain:

$$E\left(N^2\right)=\frac{p^2}{y_0^2}+\left(2\cdot\frac{\sigma_y^2}{y_0^2}-1\right)\frac{p}{y_0} \quad [63]$$

Then by elevating [58] to a square and subtracting it from the above expression [63], we finally find the asymptotic expression of the variance of the number of fragments in the sample of mass p:

$$D^2(N;p)=\frac{p}{y_0}\cdot\frac{\sigma_y^2}{y_0^2} \quad [64]$$

This expression is proportional to p/y_0 therefore proportional to $E(N;p)$ at the first order.

3.2 Law for the metal content X_{N+1} of the sample with a given mass

Now, let's call $f(x,y)$ the density of probability of the (X_n,Y_n) characteristics of a single fragment, and let $\Phi(\lambda,\mu)$ be its Laplace transform:

$$\Phi(\lambda,\mu)=\int_0^{\infty}\int_0^{\infty} e^{-\lambda x-\mu y}f(x,y)\,dxdy \quad [65]$$

We must determine the density $g(x;p)$ of the metal content X_{N+1} of the sample (by excess) of a given mass p and random number of fragments N.

[T.N.: $g(x,p)=\int_0^{\infty} f(x,y)\,dy$*]*

To express this law, and in particular to find the asymptotic expressions of the mean and variance of X_{N+1} we shall use the Laplace transform $\Gamma(\lambda,\mu)$ of the function $g(x;p)$, relative to the two variables x and p:

$$\Gamma(\lambda,\mu)=\int_0^{\infty}\int_0^{\infty} g(x;p)\,e^{-\lambda x-\mu p}dxdp \quad [66]$$

We will take advantage of the fact that the process (X_n,Y_n) is made of stationary and independent increments, and more precisely that for all $n>1$, the vector (X_n-X_1,Y_n-Y_1) is independent of (X_1,Y_1) and follows the same probability law that of (X_{n-1},Y_{n-1}). The sample of a given mass p has a number of fragments $N=0$ if the first fragment has a mass $Y_1\geq p$. On the contrary if the first fragment has a mass $Y_1=\eta<p$ and a metal content $X_1=\varepsilon$ the conditional probability law of the sample of given mass p (tied by conditions $X_1=\varepsilon$ and $Y_1=\eta$) has a density $g(x-\varepsilon;p-\eta)$. We then deduce the integral equation:

$$g(x,p)=\int_p^{\infty} f(x,y)\,dy+\int_0^{x} d\varepsilon\int_0^{p} g(x-\varepsilon;p-\eta)\,f(\varepsilon,\eta)\,d\eta \quad [67]$$

If we apply the Laplace Transform (in x and p), to both members of equation [67], the convolution products they contain are replaced by ordinary multiplicative products and we obtain:

$$\Gamma(\lambda,\mu)=\frac{1}{\mu}\left[\Phi(\lambda,0)-\Phi(\lambda,\mu)\right]+\Gamma(\lambda,\mu)\,\Phi(\lambda,\mu) \quad [68]$$

From [68] we immediately deduce the expression of the Laplace transform $\Gamma(\lambda,\mu)$ of the density $g(x;p)$:

$$\Gamma(\lambda,\mu)=\frac{1}{\mu}\cdot\frac{\Phi(\lambda,0)-\Phi(\lambda,\mu)}{1-\Phi(\lambda,\mu)} \quad [69]$$

By deriving this transform in λ and by making $\lambda=0$ we obtain the Laplace transforms for the mathematical expectation $E(X;p)$ and the variance $E(X^2;p)$, which are functions of the only variable p. To write this in a concise way we will call the metal content of the sample by excess X, instead of calling it X_{N+1}. By using the Laplace transforms, the rule already used earlier will then allow us to calculate the asymptotic expressions representing these two mathematical expectations, and, as a result, the variance of the sample with a given mass p.

Calculation of E(X;p)

By deriving [69] once in λ and by making $\lambda=0$ we obtain the transform of $E(X;p)$ under the following form:

$$-\frac{1}{\mu}\cdot\frac{\Phi'\lambda(0,0)}{1-\Phi(0,\mu)}=\frac{x_0}{\mu}\sum_{n=0}^{\infty}\left[\Phi(0,\mu)\right]^n \quad [70]$$

where designates the mathematical expectation $E(X_1)$ of the metal content of a given fragment. In the same way σ_x^2 will designate the variance of X_1.

Since $(1/\mu)[\Phi(0,\mu)]^n$ is the transform of $F_n(p)$ according to [49] and [50] we obtain:

$$E(X;p)=x_0\left[1+E(N;p)\right] \quad [71]$$

Then, the by-excess sample, with a number of fragments $N+1$ instead of N, contains, on average, a metal content proportional to its size. As far as the mathematical expectations are concerned, the condition that we imposed to the sample by fixing its mass p does

not generate any effect: everything remains as if it was the collection of a given number of fragments $n = 1 + E(N;p)$.

Taking into account [58] we also obtain:

$$E(X;p) = \frac{x_0}{y_0}p + \frac{1}{2}x_0\left(1+\frac{\sigma_y^2}{y_0^2}\right) \quad [72]$$

The mathematical expectation $(1/p)E(X;p)$ of the metal concentration X/p of the sample of given mass p is different than the real concentration x_0/y_0 by a quantity that is always positive, but very small (in x_0/p).

This tiny, positive bias is easily explained if we recall that we are dealing with a sample by excess with a real mass Y_{N+1} that is always slightly superior to p (see [42]).

Calculation of $E(X^2;p)$

We obtain the Laplace transform of the order 2 moment by deriving $\Gamma(\lambda,\mu)$ twice in λ before making $\lambda = 0$, which according to [69] gives:

$$\frac{1}{\mu}\cdot\frac{\Phi_\lambda^{''}2(0,0)}{1-\Phi(0,\mu)} + \frac{2}{\mu}\cdot\frac{\Phi_\lambda^{'}(0,0)\Phi_\lambda^{'}(0,\mu)}{\left[1-\Phi(0,\mu)\right]^2}$$
$$= \frac{1}{\mu}\cdot\frac{x_0^2+\sigma_x^2}{1-\Phi(0,\mu)} - \frac{2x_0}{\mu}\cdot\frac{\Phi_\lambda^{'}(0,\mu)}{\left[1-\Phi(0,\mu)\right]^2} \quad [73]$$

The first term is different from the one that we used to calculate $E(X;p)$ only by a constant factor. Then, it corresponds to a term with a principal part in p in expression $E(X^2;p)$, which is $(x_0^2 + \sigma_x^2)(p/y_0)$.

Developing the second term, we easily obtain:

$$-\frac{2x_0}{\mu}\cdot\frac{\Phi_\lambda^{'}(0,\mu)}{\left[1-\Phi(0,\mu)\right]^2} = \frac{2x_0^2}{\mu^3 y_0^2}\left[1+\mu\left(\frac{\sigma_y^2}{y_0}-\frac{\sigma_{xy}}{x_0}\right)+\ldots\right] \quad [74]$$

The corresponding asymptotic expression is then (limiting ourselves to the first two main terms in p and p^2):

$$\frac{x_0^2}{y_0^2}p^2 + 2\frac{x_0^2}{y_0^2}\left(\frac{\sigma_y^2}{y_0}-\frac{\sigma_{xy}}{x_0}\right)p$$

By grouping these two results together we finally obtain:

$$E(X^2;p) = \frac{x_0^2}{y_0^2}p^2 + x_0^2\frac{p}{y_0}\left(1+\frac{\sigma_x^2}{x_0^2}+2\frac{\sigma_y^2}{y_0^2}-2\frac{\sigma_{xy}}{x_0y_0}\right) \quad [75]$$

Calculating the variance of the sample of given mass p

It is only necessary to square equation [72] to make this calculation, of course limiting the calculation to the terms p and p^2, and then subtracting it from equation [75] which leads to the principal part of the variance:

$$D^2(X;p) = p\frac{x_0^2}{y_0}\left[\frac{\sigma_x^2}{x_0^2}+\frac{\sigma_y^2}{y_0^2}-2\frac{\sigma_{xy}}{x_0y_0}\right] \quad [76]$$

The expression between brackets can be replaced by:

$$E\left[\left(\frac{X_1}{x_0}-\frac{Y_1}{y_0}\right)^2\right] = E\left[\left(\frac{q}{x_0}-\frac{\bar{\omega}}{y_0}\right)^2\right] \quad [77]$$

since $Y_1 = \bar{\omega}$ is the average mass of one elementary fragment and $X_1 = q$ is the metal content of that fragment. Therefore the concentration X/p of the sample of a given mass p has a variance equal to:

$$\frac{1}{p^2}D^2(X;p) = \frac{y_0}{p}\cdot\frac{x_0^2}{y_0^2}E\left[\left(\frac{q}{x_0}-\frac{\bar{\omega}}{y_0}\right)^2\right] \quad [78]$$

Finally, in a first order in $1/p$ according to [58] we can replace y_0/p by $1/E(N;p)$ and obtain:

$$\frac{1}{p^2}D^2(X;p) = \frac{1}{E(N;p)}\left(\frac{x_0}{y_0}\right)^2 E\left[\left(\frac{q}{x_0}-\frac{\bar{\omega}}{y_0}\right)^2\right] \quad [79]$$

Now, let's go back to equation [39]. We find that the sample of a given mass p has the same variance as the sample with a given number of fragments n, on the condition, of course, that we select for n the mathematical expectation $E(N;p)$ of the random number of fragments in the sample of a given mass p. This result is valid if p or $E(N)$ are large enough in order to ignore the terms in $1/p^2$ or $1/[E(N)]^2$.

4. Conclusion

We finally reach the point where the full justification of the calculation mode selected by Pierre Gy has been achieved once and for all. As far as we are concerned, we are satisfied to have, through this study, so arid for many, brought our own contribution to this fundamental piece of work, so critically important for the foundation of the Theory of Sampling. Also, and but not the least, this work has allowed us to refute without appeal the many criticisms unfairly made over the years to Pierre Gy's work.

Acknowledgements

We are most grateful to the Société de l'industrie minérale for permission to publish our translation of Matheron's paper: G. Matheron, "Comparaison entre les échantillonnages à poids constant et à effectif constant", *Revue de l'Industrie Minérale* **Août,** 609–621 (1966). Dr Marco Alfaro of the UCV (Universidad Católica de Valparaiso, Chile) is gratefully acknowledged for his help in showing the most elegant way (probably the same as Matheron's) in the calculation of upper bound [24].

Recommended reading

1. Gy, P.M., "L'Echantillonage des Minerais en Vrac (Sampling of particulate materials). Volume 1", *Revue de l'Industrie Minerale*, St. Etienne, France. Numero Special (Special issue, January 15, 1967).
2. Gy, P.M., "L'Echantillonage des Minerais en Vrac (Sampling of particulate materials). Volume 2", *Revue de l'Industrie Minerale*, St. Etienne, France. Numero Special (Special issue, September 15, 1971).

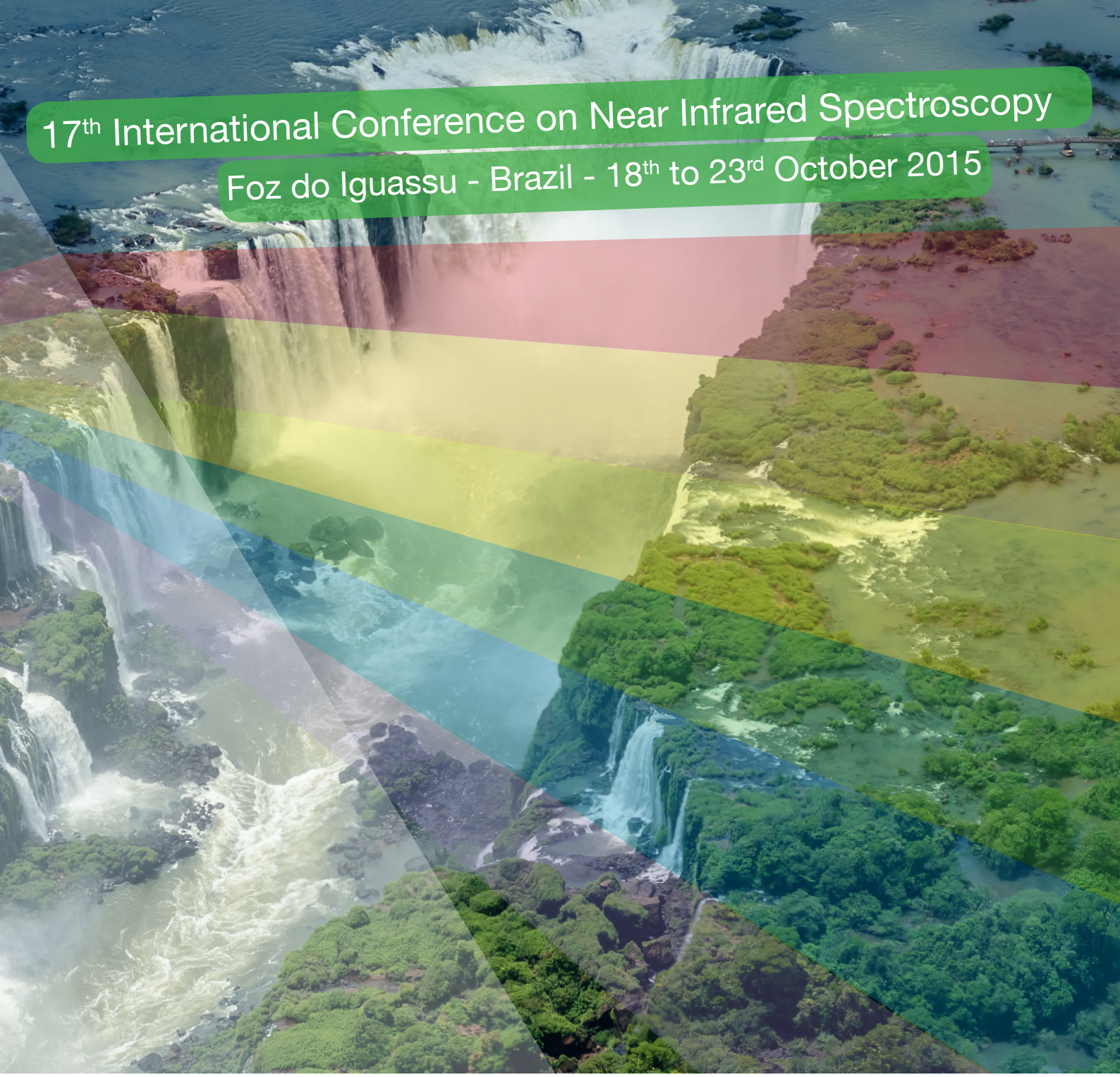

17th International Conference on Near Infrared Spectroscopy

Foz do Iguassu - Brazil - 18th to 23rd October 2015

NIR 2015 Brazil

Highlighting South America

DEADLINE EXTENDED

ABSTRACT SUBMISSION **31 MAY**

EARLY-BIRD REGISTRATION **31 JULY**

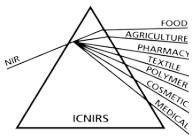

NIR 2015 is held under the auspices of the International Council for Near Infrared Spectroscopy

nir2015.com.br

WCSB7 Proceedings kindly supported by CGDAS and ACABS Research Groups

www.cgdas.eu

The Editors and Publisher thank the following organisations for their help in the publication of the Proceedings

ACABS – Aalborg University, campus Esbjerg
CGDAS – Geological Survey of Denmark and Greenland (GEUS)
CSIRO— Commonwealth Scientific and Industrial Research Organisation
IMP Group